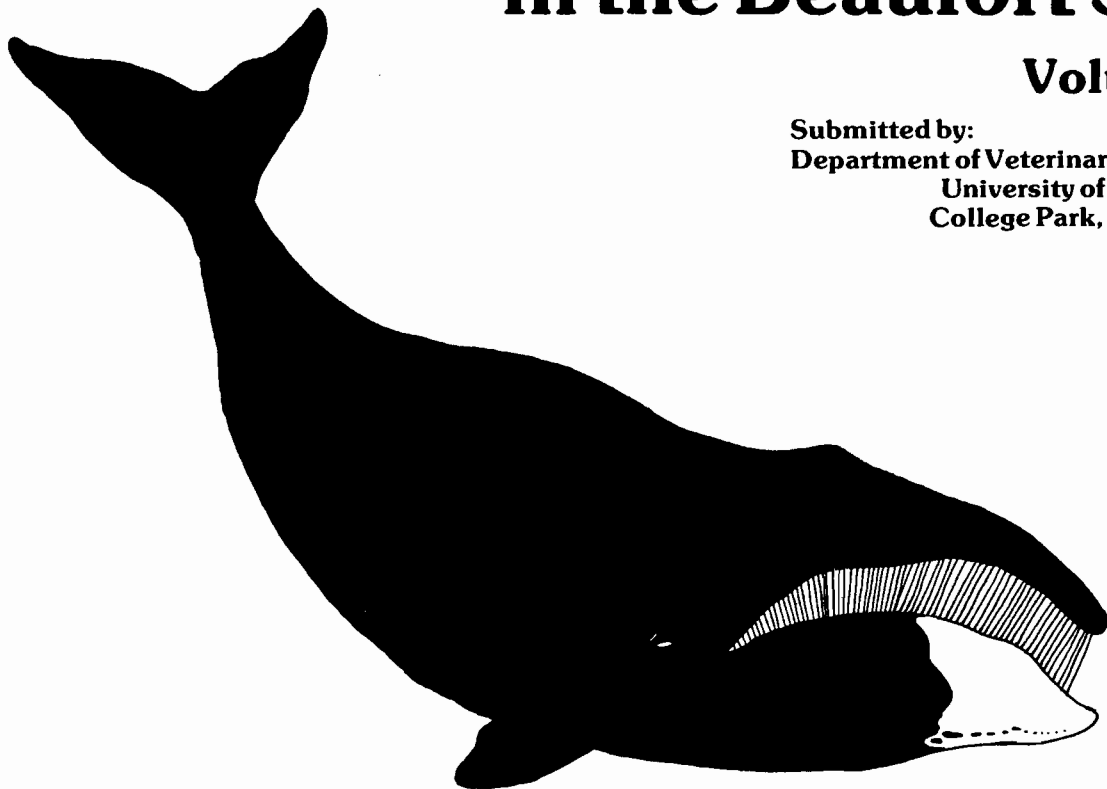


# **Tissue Structural Studies and Other Investigations on the Biology of Endangered Whales in the Beaufort Sea**

**Volume I**

Submitted by:  
Department of Veterinary Science  
University of Maryland  
College Park, Maryland  
20742



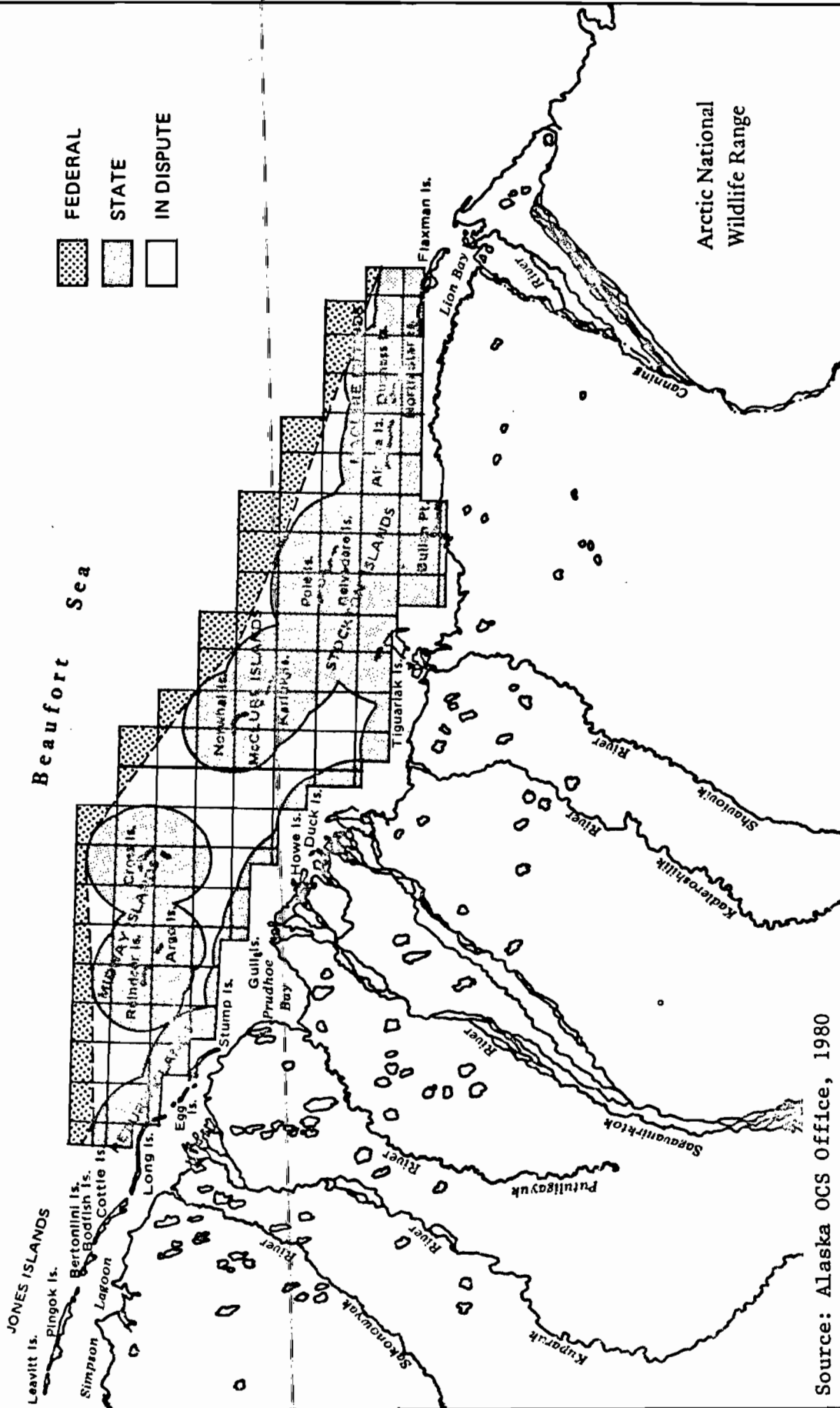
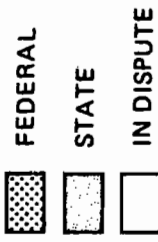
**Final Report for the Period April 1, 1980 through June 30, 1981.**

**Prepared for:**

**U.S. Department of the Interior   Bureau of Land Management   Alaska OCS Office   Anchorage, Alaska**

ARCTIC OCEAN

Beaufort Sea



Source: Alaska OCS Office, 1980

Joint Federal/State Beaufort Sea Lease Area.

TISSUE STRUCTURAL STUDIES AND OTHER INVESTIGATIONS  
ON THE BIOLOGY OF ENDANGERED WHALES IN THE  
BEAUFORT SEA

Volume I

Edited By

Thomas F. Albert  
Department of Veterinary Science  
University of Maryland  
College Park, Maryland 20742

Prepared for  
U.S. Department of the Interior  
Bureau of Land Management  
Alaska OCS Office  
Anchorage, Alaska

Final Report for the Period  
April 1, 1980 through June 30, 1981

Contract No. AA851-CTO-22

The opinions, findings, conclusions, or recommendations expressed in this report/product are those of the authors and do not necessarily reflect the views of the U.S. Department of the Interior, nor does mention of trade names or commercial products constitute endorsement or recommendation for use by the Federal Government.

It is suggested that sections of the report and the entire report be cited as follows.

Dubielzig, R. and G. Aguirre. 1981. Morphological studies of the visual apparatus of the bowhead whale, Balaena mysticetus. In: Tissue Structural Studies and Other Investigations on the Biology of Endangered Whales in the Beaufort Sea, T.F. Albert (ed.), pp. 157-172. Report to the Bureau of Land Management from the Department of Veterinary Science, University of Maryland, College Park, MD, 20742. 953 pp.

Albert, T. (ed). 1981. Tissue Structural Studies and Other Investigations on the Biology of Endangered Whales in the Beaufort Sea. 953 pp. Report to the Bureau of Land Management from the Department of Veterinary Science, University of Maryland, College Park, MD, 20742.

This report contains the results of a major research effort concerning the basic tissue structure of the bowhead whale, Balaena mysticetus. Tissue samples were collected from Eskimo harvested bowhead whales during the spring of 1980. Specimens were distributed to the various investigators associated with the project. By utilizing many investigators, each expert in their own field, it was felt that the greatest amount of information could be generated in the shortest practical time. As can be seen by the great amount of information contained within this report, the project investigators took their tasks very seriously. I am indeed grateful to my fellow investigators for their cooperation.

As a project report we have attempted to document our findings for the funding agency in great detail. We realize that the detail presented here is in excess of that seen presented in anatomical journals. Findings will be presented at appropriate meetings and published in appropriate journals. It is anticipated that the large number of specimens collected will continue to provide a basis for anatomic study long after the conclusion of this project.

This study was a continuation and expansion of research begun as part of "Project Whales." "Project Whales" was a research program\* conducted by the Naval Arctic Research Laboratory (NARL) for the Bureau of Land Management. During the early phase of that study critical support was provided by Dr. Arthur B. Callahan of the Office of Naval Research, to whom I am indebted.

The present study would not have been possible without the cooperation of the Alaska Eskimo Whaling Commission, the Barrow Whaling Captains Association and the many individual whalers who have directly assisted us. It is indeed a pleasure to acknowledge the help of the whalers that have assisted us, in particular; Jacob Adams, Eugene Brower, Harry Brower, Sr., Arnold Brower, Sr and Joseph Kaleak.

During the spring 1980 whaling season, the NARL Animal Research Facility served as a logistical base for those concerned with the collection of specimens.

---

\* Kelley, J. and G. Laursen, (eds). 1979. Investigation of the Occurrence and Behavior Patterns of Whales in the Vicinity of the Beaufort Sea Lease Area. 753pp. Final Report to the Bureau of Land Management from the Naval Arctic Research Laboratory, Barrow, Alaska.

It is a pleasure to acknowledge the assistance rendered by NARL personnel and in particular that provided by; LCDR Maria Kazanowska, Dr. John Kelley, Dr. Gary Laursen and Mr. George Selby.

A major contribution to this research effort was made by the tissue collection team which included; Dr. L. M. Philo, Dr. L. Dalton, Dr. J. Everitt and Mr. J. George. Needless to say, I am deeply indebted to these individuals for their assistance in the field.

The compilation of this report would not have been possible without the secretarial support of Barbara Rolleston and the proofreading skills of Marnie Albert.

Financial support was provided by Bureau of Land Management Contract AA851-CT0-22 to the University of Maryland.

Thomas F. Albert  
Department of Veterinary Science  
University of Maryland  
College Park, Maryland

TABLE OF CONTENTS

---

TITLE PAGE .....	i
PREFACE .....	iii
GENERAL SUMMARY .....	1
PROJECT MANAGEMENT, COORDINATION OF RESEARCH EFFORTS AND COLLECTION OF TISSUE SPECIMENS FROM THE BOWHEAD WHALE, <u>BALAENA MYSTICETUS</u> AND THE GRAY WHALE, <u>ESCHRICHTIUS</u> <u>ROBUSTUS</u> (RU 180) .....	19
DETERMINATION OF THE INCIDENCE OF WHALE STRANDINGS IN THE VICINITY OF THE LEASE AREA (RU 280) .....	43
DETERMINATION OF LEVELS OF TOXIC SUBSTANCES IN SELECTED TISSUES OF THE BOWHEAD WHALE, <u>BALAENA MYSTICETUS</u> , AND THE GRAY WHALE, <u>ESCHRICHTIUS ROBUSTUS</u> (RU 380) .....	47
DETERMINATION OF THE GROSS AND MICROSCOPIC STRUCTURES OF SELECTED TISSUE AND ORGANS OF THE BOWHEAD WHALE, <u>BALAENA MYSTICETUS</u> , WITH EMPHASIS ON BONE, BLUBBER AND THE LYMPHOIMMUNE AND CARDIOVASCULAR SYSTEMS (RU 480) .....	51
THE BIOLOGY OF THE REPRODUCTIVE AND ENDOCRINE SYSTEMS OF THE BOWHEAD WHALE, <u>BALAENA MYSTICETUS</u> , AS DETERMINED BY EVALUATION OF TISSUES AND FLUIDS FROM SUBSISTENCE- KILLED WHALES (RU 580) .....	89
MORPHOLOGICAL STUDIES OF THE VISUAL APPARATUS OF THE BOWHEAD WHALE, <u>BALAENA MYSTICETUS</u> (RU 680) .....	157
THE MICROSCOPIC EXAMINATION OF THE BOWHEAD WHALE, <u>BALAENA MYSTICETUS</u> AND THE GRAY WHALE, <u>ESCHRICHTUS</u> <u>ROBUSTUS</u> FOR CHANGES DUE TO TOXIC SUBSTANCES AND INFECTIOUS AGENTS (RU 780) .....	173
THE CYTOLOGICAL AND CLINICAL EVALUATION OF BLOOD AND URINE OF THE BOWHEAD WHALE, <u>BALAENA MYSTICETUS</u> (RU 880) .....	201
CYTOGENETIC AND MORPHOLOGICAL INVESTIGATION OF VARIABILITY IN THE BOWHEAD WHALE, <u>BALAENA MYSTICETUS</u> (RU 980) .....	213
INVESTIGATIONS OF THE SERUM ANTIBODIES AND VIRUSES OF THE BOWHEAD WHALE, <u>BALAENA MYSTICETUS</u> (RU 1080) .....	233

TABLE OF CONTENTS (continued)

BACTERIOLOGICAL STUDY OF THE BOWHEAD WHALE, <u>BALAENA MYSTICETUS</u> (RU 1180) .....	255
PARASITOLOGICAL STUDY OF THE BOWHEAD WHALE, <u>BALAENA MYSTICETUS</u> (RU 1280) .....	275
DETERMINATION OF THE GROSS AND MICROSCOPIC STRUCTURE OF THE LUNG, KIDNEY, BRAIN AND SKIN OF THE BOWHEAD WHALE, <u>BALAENA MYSTICETUS</u> (RU 1380) .....	305
 (See Volume II)	
<hr/>	
DETERMINATION OF THE GROSS AND MICROSCOPIC STRUCTURE OF THE STOMACH AND SMALL INTESTINE OF THE BOWHEAD WHALE, <u>BALAENA MYSTICETUS</u> (RU 1480) .....	663
HEARING IN THE BOWHEAD WHALE, <u>BALAENA MYSTICETUS</u> , AS ESTIMATED BY COCHLEAR MORPHOLOGY (RU 1580) .....	745
APPENDIX I    CURRENT PROCEDURE FOR ALLOCATING THE BOWHEAD WHALE, <u>BALAENA MYSTICETUS</u> , BY THE ESKIMO WHALERS OF BARROW, ALASKA .....	789
APPENDIX II    OBSERVATIONS ON THE HEART OF THE BOWHEAD WHALE .....	805
APPENDIX III    RESEARCH MEETING .....	829
APPENDIX IV    SOME BRAIN MORPHOMETRICS OF THE BOWHEAD WHALE ...	837
APPENDIX V    LISTING OF COLLECTED BOWHEAD WHALE SPECIMENS WITH OBSERVATIONS MADE DURING INITIAL EXAMINATION .....	845
APPENDIX VI    OBSERVATIONS ON THE RADIOGRAPHIC ANATOMY OF THE PECTORAL LIMB OF THE BOWHEAD WHALE .....	917
APPENDIX VII    STATEMENT OF WORK .....	937
APPENDIX VIII    PUBLICATIONS AND PAPERS PRESENTED .....	943
APPENDIX IX    SOME THOUGHTS REGARDING THE POSSIBLE EFFECTS OF OIL CONTAMINATION ON BOWHEAD WHALES, <u>BALAENA MYSTICETUS</u> .....	945



## GENERAL SUMMARY

### BACKGROUND

In 1953 the Outer Continental Shelf (OCS) Lands Act (67 Stat. 462) was passed establishing Federal jurisdiction over the submerged lands of the continental shelf seaward of State boundaries. The Act charged the Secretary of the Interior with the responsibility for the administration of the mineral exploration and development of the OCS. It also empowered the Secretary to formulate regulations so that the provisions of the Act might be met.

Subsequent to the passage of the OCS Lands Act of 1953, the Secretary of the Interior designated the Bureau of Land Management (BLM) as the administrative agency for leasing submerged Federal lands and the Geological Survey for supervising exploration and production.

The National Environmental Policy Act of 1969 requires that all Federal agencies shall utilize a systematic approach which will insure the integrated use of the natural and social sciences in any planning and decision-making which may have an impact on man's environment. The BLM efforts in this direction are Environmental Impact Statements (EIS), environmental assessment teams, marine environmental data acquisition and analysis, literature surveys, socio-economic analyses, public conferences, and special studies.

The Marine Mammal Protection Act (MMPA) of 1972 (16 U.S.C. 1361-1407) indicates that certain species and populations of marine mammals are, or may be, in danger of extinction or depletion as a result of man's activities and establishes a national policy that marine mammal populations shall be protected and encouraged to develop to the greatest extent feasible commensurate with sound policies of resource management. The Secretaries of the Interior and Commerce are charged with all responsibility, authority, funding, and duties under the Act.

The Endangered Species Act of 1973, as amended in 1978, provides for the conservation of all animal and plant species which are determined to be endangered or threatened. The Act requires that all major Federal actions do not jeopardize the continued existence of endangered species and threatened species or result in the destruction or modification of their habitats. Section 7 of the Act requires that BLM consult with other Federal agencies to determine if a potential jeopardy may exist.

OCS Lands Act amendments of 1978 (92 Stat. 629) were passed establishing "a policy for the management of oil and natural gas in the Outer Continental

Shelf" and for protecting "the marine and coastal environment". The amendments authorize the Secretary of the Interior to conduct studies in areas or regions of lease sales to ascertain the "environmental impacts on the marine and coastal environments of the Outer Continental Shelf and coastal areas which may be affected by oil and gas development" (43 U.S.C. 1346).

In order to address these managements mandates, particularly those of the Endangered Species Act, the BLM recognized that it was necessary to conduct further studies to fill existing data gaps on endangered cetaceans. As part of its environmental studies program, BLM has contracted with the University of Maryland to conduct tissue structural studies of endangered whales which inhabit the lease area (see lease area map on inside of front cover). The two whales are the bowhead whale, Balaena mysticetus and the gray whale, Eschrichtius robustus. Because of availability of specimen material and local abundance the bowhead whale was the major topic of study. This present study was a continuation of research begun as part of an earlier bowhead research program\* conducted for BLM by the Naval Arctic Research Laboratory.

## OBJECTIVES

Under the continuation of the project, the following major objectives were addressed:

1. Determine the structure of the major tissues and organ systems of the bowhead whale, especially those which are likely to be affected by oil or other contaminants in order to provide a basis for detecting and monitoring changes that may occur as the result of offshore oil and gas development in the Beaufort Sea.
2. Identify present microbiological and parasitological burdens, tissue pollutant levels and incidence of pathology in order to provide a basis for detecting and monitoring changes in whales that may occur as a result of offshore oil and gas development in the Beaufort Sea.
3. Gather biologic information which may resolve the question of whether the Ingutuk is a separate species of whale or a morphological variant of the bowhead whale.

---

\*Kelley, J. and G. Laursen (eds.). 1979. Investigation of the Occurrence and Behavior Patterns of Whales in the Vicinity of the Beaufort Sea Lease Area. 753 pp. Final Report to the Bureau of Land Management from the Naval Arctic Research Laboratory, Barrow, Alaska.

4. Determine the incidence of whales stranded on shores in the vicinity of the Beaufort Sea lease area in order to provide a basis for detecting and monitoring changes that may occur as a result of offshore oil and gas development in the Beaufort Sea.

#### PROJECT MANAGEMENT AND COORDINATION

The entire research effort was designed to gather specimen materials from harvested and/or stranded whales and to then evaluate the materials to achieve the objectives listed above. In order to accomplish this, one research unit (RU 180) was given responsibility for overall project management and for the collection and distribution of the specimens. Figure 1-6 illustrates the overall plan for specimen collection and distribution. Major aspects of project management and coordination are summarized below.

Coordination with Eskimo Hunters. Examination of individual whales was limited to those which were either hunter-killed or stranded. Hunter-killed whales were potentially available during the spring from Barrow, Wainwright and Point Hope to the west of the lease area and during the fall from Barrow to the west and Kaktovik to the east. There could be no collection of tissues from harvested bowhead whales without the cooperation of the individual Captain and his crew at the butchering site. It was therefore essential that personal contacts be made with individual Captains as well as officers of the Alaska Eskimo Whaling Commission and the Barrow Whaling Captains Association. Such personal relationships were developed over the past 3 1/2 years.

Tissue Collection Team. The transport of large quantities of formalin (tissue preservative), cutting implements, cameras, etc., over long distances of rough ice required special planning and logistic management. Similarly the careful handling of specimens at the butchering site and then returning the heavily laden sled to the logistical base of operation required unique approaches. The tissue collection team included three veterinarians in order to assure that appropriate collecting, tissue handling, and preserving techniques were utilized. A fourth member of the team possessed needed additional skills, including experience in cold weather survival techniques, snowmachine maintenance, carpentry and knowledge of ice conditions.

Logistical Base of Operation. The logistical base was the Animal Research Facility of the Naval Arctic Research Laboratory (NARL). The NARL, located just north of the village of Barrow, provided food, lodging, laboratory space, tools for snowmachine repair, sleds, communications (phone and CB radio), trucks, and both warm and cold storage.

Field Logistics. When monitoring of Citizen Band transmissions indicated a whale had been taken, the two sleds and snowmachines were quickly loaded and headed out onto the ice. Increased snowmachine and sled traffic from Barrow and the other whaling camps toward the camp of the crew which had just taken the whale indicated where it was located.

The trails that led out to the whaling camps were hacked out of the jumbled ice by the Eskimo hunters. The whaling camps were spread out along the edge of the lead (an open water area extending like a channel through the ice). During the 1980 spring whaling season the nearshore lead was usually 2-15 km wide with the whaling camps 4-10 km from shore. Camps were located from approximately 8 km above Barrow to at least 30 km below Barrow.

Specimen Collection. Although this study concerned itself with endangered whales that may inhabit the Beaufort Sea lease area (bowhead whales and gray whales), the vast bulk of samples obtained were from bowhead whales. The only gray whale material available for examination was that obtained earlier from an animal found stranded near Barrow in 1978.

Bowhead whales are harvested for food purposes and the hunt and butchering process are important cultural events. Thus the entire butchering process occurs according to a rather precise schedule. This scheduled dismemberment of the animal as well as the severity of the weather were the major factors limiting the completeness of the sampling for any given whale. In order to appreciate the constraints within which samples can be collected, a description of the butchering process is given in APPENDIX I.

The low ambient temperatures (-20-0°C) presented problems particularly when dealing with very small samples and small quantities of preservatives because they could freeze during or just after collection if not handled properly.

Specimens collected were labeled at the butchering site and appropriate descriptions entered onto hand held tape recorders. Numerous photographs were taken to record where small samples originated from, to provide gross anatomical

information, and to describe the physical appearance of the butchering site. Collected materials were returned to the logistical base (NARL) for further evaluation. Specimens were logged into a record book, subsampled as necessary, and stored as appropriate until being distributed to the other Research Units.

Specimen Distribution. As mentioned above, specimens were distributed to Research Units 380 through 1580 in the manner represented in Figure 1-6.

## RESULTS

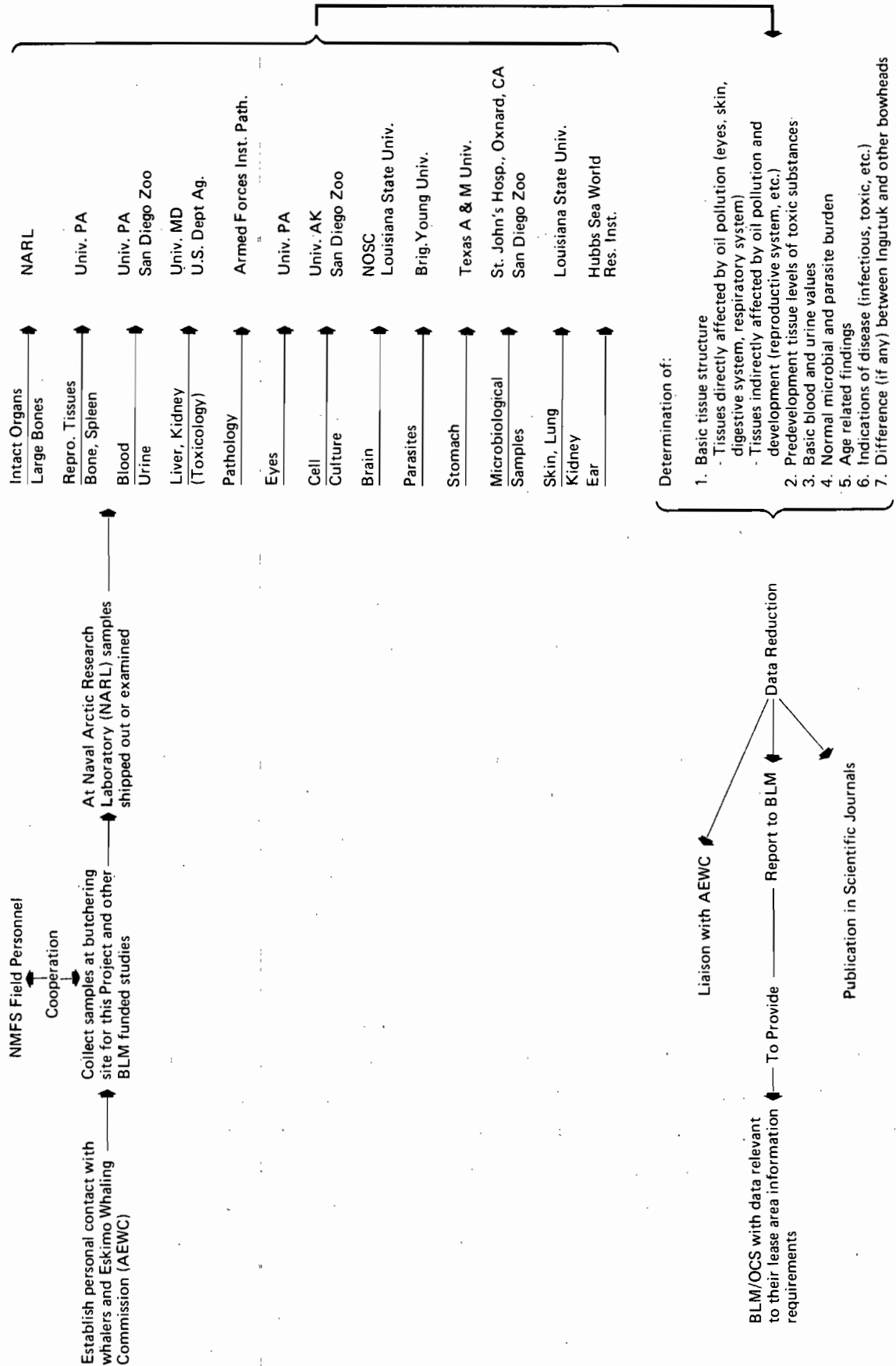
Specimen Collection (RU 180). During the spring of 1980 more than 550 specimens were collected from the nine bowhead whales taken at Barrow, Alaska.

Strandings (RU 280). One bowhead whale was seen stranded between Barrow and Barter Island, however no specimens were obtained from the animal.

Toxic Substances (RU 380). Tissue samples were collected, however, no examinations for heavy metals, etc. were performed due to difficulty in obtaining suitable analytical services.

Ingutuk. Comparisons were made between an animal identified as an Ingutuk and those identified as regular bowheads regarding blubber structure (RU 480), bone structure (RU 480), and cytogenetic evaluation (RU 980). The Eskimo hunters identify an Ingutuk by virtue of its greater girth, thicker blubber, shorter baleen and denser bones as compared to those regarded as regular bowheads. In both, there seem to be two distinct layers of adipose tissue beneath the skin over much of the body. The outer layer (blubber) contained much dense collagenous connective tissue. The inner layer, where seen, was composed of a very oily adipose tissue devoid of the thick collagenous strands seen in the outer layer. The demarcation between the outer and inner layers was well marked. In several instances bundles of skeletal muscle were seen between the two layers. The basic histological structure of the blubber was similar in the Ingutuk and the regular bowhead. The gross and microscopic structure of bone specimens from six regular bowhead whales, one gray whale and one Ingutuk were evaluated. Bones from the regular bowhead and gray whale resembled bones which have been described for other cetaceans. The bones from these whales differed significantly from

FIGURE 1-6 TISSUE COLLECTION AND HANDLING FLOW CHART



those of the Ingutuk. Grossly, bones from the animal identified as an Ingutuk were somewhat shorter and thicker (wider) than those from the regular bowhead. Microscopically, the number and caliber of the trabeculae of spongy bone were much greater than in regular bowheads, giving the bone a solid appearance similar to compact bone. In this respect, the bones of the Ingutuk resembled the pachyostotic bones of certain marine mammals, e.g., the manatee and dugong. However, the spongy (cancellous) bones of the Ingutuk had persistence of central cartilage cores, a feature not present in the pachyostotic manatee and dugong. This unique feature of the Ingutuk is remarkably similar to the bone lesion in terrestrial mammals with congenital osteopetrosis and humans with Albers-Schonberg disease. Therefore, these histological studies support the concept that a defect in skeletal remodeling exists in the Ingutuk which is not present in the regular bowhead.

There seem to be no genetic differences between Ingutuks and regular bowheads that can be demonstrated by conventional cytogenetic evaluation. G- and C-banding of chromosomes reveal no consistent differences between the Ingutuk and regular bowheads. Technical limitations precluded definitive falsification of the hypothesis that C-band heteromorphism is correlated with phenotypic polymorphism. The distribution of some clearly identified heteromorphic chromosome pairs in both forms of whale suggests a single freely-interbreeding population.

Based on available evidence, Ingutuks clearly seem to be bowheads. They also evidence a defect in skeletal remodeling not seen in other bowheads. Whether this is a congenital defect or is related to rapid growth in certain young bowheads is still not clear.

Reproduction (RU 580). Intact, complete organs were not available from any given individual but a reasonably complete picture of the bowhead, particularly the prepuberal bowhead, can be drawn. There was a substantial muscle in the region between the teat and milk cisterns which may play a role in withholding and ejection of milk. The cervix was an interesting structure and four to seven elongated annular folds separated by empty "compartments". The first part of the cervix was lined by a stratified epithelium similar to that of the vagina except that it was not keratinized. The anterior portion of the cervix was characterized by having a typical simple columnar epithelium and bountiful crypts. These crypts extended about 5 cm into the body of the uterus at which point typical endometrial glands commenced. It was hypothesized that the

cervical rings serve as valves which serve to enable sperm to ascend while keeping seawater out and the bountiful cervical crypts serve as sperm storage compartments enabling release over a prolonged period of time.

The uterus was bicornuate with a long body and two rather straight (uncoiled) horns. The endometrium was thrown into prominent longitudinal folds and lacked caruncles although it had typical branched tubular glands.

The ovaries were large, oval organs in the prepuberal individuals and very elongate in the postpuberal ones. The surface of the ovary was characterized by a random network of grooves which were more prominent on one pole than the other. The mesovarium was attached to the ovary at a prominent hilus. Histologically the ovary was covered by a serosa and a tunica albuginea beneath which was a typical mammalian cortex surrounding a very vascular medulla. Two types of follicular atresia were noted - cystic and obliterative. The processes were reminiscent of the process in the cow. The corpus luteum was very large and grossly had a scalloped or convoluted cut-surface. This was due to trabeculae which served to divide the organ into lobules. Histologically the parenchyma contained numerous granulosa lutein cells.

In the prepuberal testicles there were numerous seminiferous tubules lined by Sertoli cells and a scattering of spermatogonia. There were no identifiable Leydig cells. The epididymis was remarkable because of its large size macroscopically and its very complicated structure microscopically. At this time it appears unique among mammalian epididymides. The complicated microscopic structure may be related to sperm maturation. The structure of the epididymis carried over into the initial segment of the ductus deferens but then became a single nonglandular duct. Macroscopically the ductus deferens was tortuous in contrast to the nontortuous organ of other mammals.

Eye (RU 680). The eye is basically similar to that described for other cetaceans. It was noted that the cornea was thinnest centrally, the conjunctival sac extended 3/4 of the way back toward the posterior of the eye, and there were only two extrinsic ocular muscles. The eye is likely to be very mobile within the orbit due to the extent of the conjunctival sac and the finding of several tendinous attachments to the globe for each of the two extrinsic muscles.

Disease and Disease Resistance. Efforts to monitor disease and the likelihood of disease onset in the bowhead included an examination of: obvious sites of



pathology (RU 780), the lymphoimmune system (RU 480), the blood and urine (RU 880), and the normal microbial (RU 1080, RU 1180) and parasitic (RU 1280) burdens.

Pathological findings (RU 780) included skin scars, elevated and cystic areas in the rear of the mouth (likely due to trauma by baleen), parasitic nodules in the submucosa of the esophageal portion of the stomach, a lipoma in the liver, ulcers in the anorectal canal, cutaneous encapsulation of bomb fragments, and areas of localized epidematitis (particularly on the head).

An interesting variation in the lymphoimmune system (RU 480) was that in the bowhead, lymph node structure was inverted in appearance similar to that in the domestic pig. In this type of arrangement, the cortical and medullary tissues are reversed with the lymphatic nodules occupying a central position and medullary sinus area peripheral.

Morphologic examination of the lymphoid structures allowed several important conclusions to be made. All lymph nodes from regions of the body not associated with the alimentary canal revealed hyporeactive morphologic states. One can infer from this structural appearance that the animal was relatively quiescent immunologically. This seems likely when one considers that the whale resides in a relatively clean Arctic environment and has few known disease problems. It was readily apparent that lymph nodes centered around the alimentary tract show numerous follicles with large germinal centers thereby indicating reactivity. Similarly, the activity of the gut-associated lymphoid tissue and lymph nodes along the alimentary tract make it apparent that the majority of the antigenic exposure of the bowhead is by the oral route. Thus, ingestion of toxicants could lead to immunological effects.

The bowhead spleen showed very little white pulp activity. No information on splenic structure in other baleen whales could be found. Spleens from small odontocetes have been reported to have a high malpighian corpuscle content.

An examination of the blood (RU 880) revealed the presence of the normal cellular constituents, however, hemolysis precluded detailed hematological studies. An interesting finding was the presence of large numbers of spermatozoa in a urine sample from a whale harvested during the fall of 1979 (RU 880).

Virological and serological studies (RU 1080) showed that the bowhead has antibodies to several viruses known to be pathogenic for other animals. Of 12 marine calicivirus serotypes tested, three of the four bowhead tested

were serologically positive for SMSV-5 (SMSV=San Miguel sea lion virus), two were positive for SMSV-8 and two were positive for SMSV-10. All three of these virus types had been previously isolated from marine mammals in the Bering Sea. In addition, two of the bowheads had antibodies against two of twelve serotypes of exotic calicivirus (vesicular exanthema of swine virus). A finding of significance was the isolation of two adenoviruses from the bowhead. At the present time there is no evidence to indicate their infectivity for the bowhead whale. Additional effort is needed to resolve their status.

Bacteriological studies (RU 1180) involved eighteen specimens, each containing one or more bacterial isolates. Most of the samples were from the respiratory passages. At least nine species of bacteria isolated are known to be pathogenic or potentially pathogenic.

Parasitological studies (RU 1280) have expanded the list of known parasites of the bowhead. New finds include: two protozoans (one is a previously undescribed species); four genera of diatoms; and a nematode. Another significant finding was that diatoms are 5-10 times more numerous in the eroded areas of skin than on areas of undamaged skin.

Lung (RU 1380). The orifices of the external nares are regulated by a narial sphincter composed of specialized blubber and skeletal muscle fibers. In addition, the nasal septal cartilages were paired rather than single as has been reported in other cetacea. In the laryngeal region of the covering of the epiglottis and arytenoids was composed of keratinized stratified squamous epithelium with dermal papillae containing encapsulated nerve end organs; the arytenoid cartilages were not fused caudally, and lymphatic tissue occurred only at the laryngotracheal junction.

In the airways the tracheal cartilages were C-shaped and open ventrally. This opening was filled by skeletal muscle which also encircled the laryngeal sac. The primary and segmental bronchi branched at obtuse angles, as did their accompanying arteries and nerves. The pulmonary veins did not follow this pattern. Mucous glands occurred continuously in the large airways but were seen only between cartilage rings in smaller bronchi and were absent in the bronchioles. Myoelastic sphincters which are found in some other cetaceans were absent but smooth muscle was present in the bronchioles. Hyaline cartilage was found in all bronchi and bronchioles down to the level of the terminal and respiratory bronchioles. Cartilaginous rings were seen in bronchioles as small

as 0.3 mm diameter. The bronchial epithelium contained cells with only microvilli on their surface as well as cells which contained both cilia and microvilli. The degree of ciliation of the bronchial lining appeared to vary with the bronchial diameter. At the ultrastructural level the pseudo-stratified epithelium of the primary bronchus was similar to that seen in other cetaceans. Desmosomes were found between adjacent cells in the basal region and hemidesmosomes were seen between the basal cells and the basal lamina. Plasma cells occurred beneath the basal lamina. Apparently encapsulated nerve endings were seen in the submucosa of bronchioles only. The respiratory bronchioles were lined by a typical respiratory epithelium composed of both type I and II pneumocytes.

In the air exchange system the alveolar ducts, sacs, and alveoli were lined by respiratory epithelium. Only elastic laminae and sphincters were found in these walls. No myoelastic sphincters were seen, although they are reported at this level in other cetaceans. The type II pneumocytes of the respiratory epithelium contained typical multilamellar bodies which were also seen free in the airspaces as was the tubulomyelin they produce. Few alveolar macrophages were observed.

No internal septa were seen in the lung and no external or internal lobulation was seen. The pleura was composed of a thick, highly elastic dense connective tissue with a mesothelium covering.

Kidney (RU 1380). Several anatomical differences were noted between the kidney of the bowhead and those other cetaceans. A major difference was the absence of any smooth muscle in the sporta perimedularis (at the corticomedullary junction) and the calyx walls. Another difference was the presence of the arcuate vessels in the sporta as opposed to their reported location some distance from it in other cetaceans. A unique morphological finding that has not been described in other cetaceans was the presence of large thin-walled veins that filled the spaces between renicules and intimately surrounded calyces and ureteral branches. Other findings included the presence of thin segments of Henle's loop deep in the renal papilla which indicate long looped nephrons, and the presence of a well developed juxtaglomerular apparatus.

Brain (RU 1380 and APPENDIX IV). As in other cetaceans, the cerebral hemispheres presented deep sulci and gyri, the hippocampus and some other "limbic"

structures were relatively small, the pineal body was probably absent, the cerebellum was large, and all structures associated with the auditory system were very large. The paleocortex (olfactory lobe) was rather large. As in other cetaceans the most prominent feature was the large olfactory tubercle, which underlines the head of the corpus striatum. An interthalamic adhesion (massa intermedia) was not present.

The rhomencephalon appeared to be wide and shallow. It curved up around the caudal aspect of the cerebellum. The transverse fibers of the pons formed a massive structure. The trigeminal nerve (fifth cranial nerve, mediates sensation from the head) was the largest cranial nerve and was large compared to that of other cetaceans. It exited through the transverse fibers of the pons. The next largest cranial nerve was the vestibulocochlear (VIII) nerve seen at the lateral border of the well developed trapezoid body which was visible caudal to the transverse pontine fibers.

The bowhead brains examined were less convoluted than odontocete brains and are in the same size range as those of much smaller odontocetes (Grampus, Globicephala, Delphinapterus). The mentioned odontocetes have cortical surface area to volume ratios about one-third greater than the bowhead. In general, the brain of the bowhead whale resembles that of the southern right whale more closely than it resembles the brain of the humpback, fin or sei whale.

Skin (RU 1380). Skin samples from a variety of body regions of the bowhead whale were examined. The epidermis was determined to be as much as 24 mm thick, up to 8 times thicker than that reported in other whales. Regional variations in thickness occurred with the thinnest areas observed occurring on the eyelids and inner lips. A distinctive parakeratotic stratum corneum and the underlying stratum spinosum extend over the entire body surface varying in thickness in different regions. Several diatom species resided in/on the stratum corneum producing a rougher surface in many areas. In thick areas, the stratum basale cells capping the distal ends of the dermal papillae gave rise to a circularly arranged array of spinosal cells which maintained this configuration through the stratum spinosum. These dense concentrations of spinosal cells were best described as epidermal rods which extended toward the surface surrounded by the more typical larger polyhedral spinosal cells. All of the spinosal cells gradually became flatter and reduced in volume as they approached the epidermal surface. This process concentrated the keratohyaline granules within their

cytoplasm so that the final 12-60 cell layers of the epidermis from a normal parakeratotic stratum corneum of squamous cells that retained recognizable, but pyknotic nuclei.

The dermal papillae extended into the very thick epidermis to within 5 mm (flipper, fluke), 10 mm (general body), or, in thinner regions, within 0.1 mm of the outer surface of the parakeratotic stratum corneum. In thin epidermal areas of the lips and inner lips, large dermal papillae with encapsulated nerve end organs were detected.

Vibrissae which emerge from the skin only in specific regions inserted into a modified tactile hair follicle with an associated nerve net.

The use of the term "hair" in reference to baleen is misleading despite the general gross appearance of these structures. Two distinct types of baleen "hairs" develop in bowheads, simple and compound. Each type develops from the deep stratum basale cells encircling the bases of the long dermal papillae that interdigitate with the very thick gingival epidermis. The tubular structures produced in the horns of cattle and hooves of many animals. In general, the origin and structure of baleen hairs more closely resembled the origin and structure of horn and hooves in terrestrial animals than hair. A major difference was that the stratum spinosum cells between the growing horn tubules of baleen did not form intertubular horn as the hooves and horns of terrestrial mammals. The tissue between the baleen horn tubules became only slightly firmer than the thick stratum spinosum of the body skin, possibly permitting the horn tubule to elongate more rapidly, emerge through the gingival surface, and extend down as hairlike structures. The organization of the baleen horn tubules after emergence from the gums was a direct function of the depth of the gingival epidermis. The greater the depth of epidermis, the greater the number of horn tubules that became fused forming compound baleen "hairs" or baleen plates. The shallowness of the gingival plate adjacent to the hard palate yielded individual (simple) baleen "hairs". As the stratum spinosum thickened laterally, the individual horn tubules became fused into groups emerging as larger, darker, compound baleen "hairs". Finally, from the thickest (most lateral) part of the gingival plate, laterally elongated fusion groups emerge as the baleen plates. The fringe of "filaments" on the medial surfaces of the baleen plates is merely the result of the fusion layer holding individual horn tubules together becoming worn which releases the distal ends of the horn tubules to hang free and increases the filtering effectiveness of the baleen apparatus.

Six morphologically different types of epidermal lesions were seen on skin samples studied. Histological analysis showed that each morphological type tends to have a somewhat different population of microflora. Each lesion type was an example of restricted epidermatitis which affected the stratum corneum and may affect the more superficial layers of the stratus spinosum.

In a preliminary study involving formalin-fixed skin samples raised through a crude oil "slick" at 3°C and resubmerged through the oil with limited agitation for three cycles, it was noted that the oil stuck to the skin surface to varying degrees. Vibrissae from both the blowhole and the chin became partially coated with definite globules of oil remaining on the shafts themselves. The amount of oil adhering to the preserved skin in this laboratory situation appeared to be directly proportional to the degree of "roughness" of the skin surface.

Stomach and Small Intestine (RU 1480). The alimentary canal of the bowhead shares many similarities with that of other cetaceans. The esophagus was a thick-walled but narrow tube lined by a stratified squamous mucosa with a tendency for keratinization. Both mucoserous glands and lymphoid nodules were frequent in its walls, especially at the cranial end. The stomach itself was comprised of four chambers, the first of which was the largest and was non-glandular. The lining of this first chamber, the forestomach, differed from that of the esophagus only by more extensive infolding, a greater tendency for keratin production and the apparent absence of both subepithelial glands and well-developed lymphoid collections.

The remaining three compartments of the stomach were glandular in appearance and consisted of the fundic chamber, connecting channel and pyloric chamber. The entire lining of the fundic chamber was distinguished by a multitude of gastric pits which were lined by columnar mucous cells and which lead into the glands themselves. In the initial portion of the fundic chamber these glands were mucous, thus forming a cardiac region. For the mysticetes a cardiac region has been previously reported only for the blue whale. The remaining glands of the fundic chamber contained cells of chemical digestion, the parietal and chief cells. Mucous neck cells were also identified in the proximal portions of the glands. The connection channel was a narrow tubular structure leading from the fundic chamber and was characterized by a glandular appearing mucosa. After making a "U" shaped bend it emptied into the final, or pyloric, chamber. The

pyloric chamber, whose lining was also glandular in appearance was tubular but had a larger diameter than the connecting channel. It communicated with the small intestine through a narrow pyloric sphincter.

The small intestine began as a dilated sac termed the duodenal ampulla. This sac tapered rather abruptly into the duodenum proper which has a more narrow but consistent diameter. The small intestine ended abruptly where a sudden enlargement in intestinal diameter marked the start of the colon. No cecum was present. The mucosal lining changed abruptly to a stratified squamous epithelium upon junction of the large intestine with the anal canal. Numerous crypts lead into well developed subepithelial aggregations of lymphoid nodules in this region.

The bowhead pancreas consisted of both exocrine and endocrine fractions which were structurally similar to that of other mammals. The liver contained an abundant deposition of yellowish brown granules (possibly hemosiderin) in its hepatocytes. In other mammals the presence of these granules would indicate a pathologic process. A melanin-like pigment was also observed in the hepatic sinusoids, especially in the Ingutuk. However, the significance of the pigment and the granules in the bowhead is unknown at this time. A cell type, apparently corresponding to the lipocyte, was seen randomly and abundantly scattered throughout the hepatic parenchyma in the regular bowhead. Although this cell could not be identified in the Ingutuk, a lack of cytoplasmic filling may have obscured its presence. Further study is required to define the nature and significance of these "lipocytes".

Ear (RU 1580). The auditory response capabilities of the bowhead whale were estimated based on examination of the middle and inner ear morphology of ten individuals. Observed ossicular mass ratios were intermediate between mean ratios for representative delphinids and phocoenids, both of which have been demonstrated to have high frequency hearing abilities. Basilar membrane length was 61.25 mm; width was 120  $\mu$ m basally; widening to 1.67 mm apically. An apical to basal stiffness gradient was described in the spiral laminae. These values and descriptions were compared to other cetaceans and indicated that the bowhead whale possesses several unique auditory morphological characteristics, particularly at the hook — the area of the cochlea where highest frequency audition takes place — and at the helicotrema, the area of lowest frequency audition. Whether or not other mysticetes possess similar morphologies has not

been assessed. Available evidence supports the tentative conclusion that the auditory response capabilities of the bowhead whale range from high infrasonic or low sonic to high sonic or low ultrasonic frequencies (sonic is here used as 20Hz to 20kHz).

Allocation of Whale Tissue by Eskimo Hunters (APPENDIX I). Bowhead whaling is a central aspect of the Inupiaq culture and requires the successful coordination of many people within a village. When a whale is captured, it is divided equally among active whaling crews, which in turn will divide it further among community members. Thus, the successful crews will get essentially the same share as the others.

The successful captain directs the butchering of the whale under precise traditional rules. He is also responsible for saving certain pieces for the three village festivals — Thanksgiving, Nalukataq and Christmas.

Heart (APPENDIX II). A single, poorly preserved bowhead heart was available for gross anatomical observation. Revealed was a large globular shaped heart with similar structure to other large mammalian species. The aortic valve orientation was similar to that of the pig heart. Two fenestrative lesions near the margin of the left cusp of the aortic valve were similar to normal fenestrations reported in semilunar valves of man and horses. Three firm nodular to cylindrical thickenings on each of three chordae tendinae of the mitral valve were composed of fibrous connective tissue with foci of calcification. Similar chordae lesions have not been described in other cetacean hearts or in hearts of other mammals. The coronary vascular pattern resembled that which has been described in hearts from sei and gray whales. Histologic studies were not possible due to decomposition of the specimen prior to fixation.

Listing of Specimens With Initial Observations (APPENDIX V). The numerous specimens (over 550) are listed by animal of origin with their destination (Research Unit) indicated. Also included are brief descriptions of the samples with appropriate photographs to provide for proper orientation of samples.

Radiographic Examination of Flippers (APPENDIX VI). Flippers (intact or partial) were examined from nine bowhead whales. The number of carpals seen ranged from



zero to four. The number of metacarpal bones seen was either four or five with the variation due to the presence or absence of the first. There were four digits with digits two through five present. The second digit had three phalanges, the third digit four phalanges, the fourth digit three phalanges and the fifth digit two phalanges. The total number of bones in each of the bowhead flippers examined ranged from 19-24, due to variation in the number of carpals and metacarpals.

#### Possible Effects on Bowheads Migrating Through Oil Contaminated Waters

(APPENDIX IX). In APPENDIX IX are presented some thoughts as to the possible effects on bowheads migrating through oil contaminated waters. It is felt that the most likely adverse effects of oil contact will be: 1) conjunctivitis and corneal inflammation leading to reduced vision and possibly blindness; 2) development of skin ulcerations from existing eroded areas on skin surface (possibly due to direct irritant effect of oil on already damaged epithelium, and/or possibly due to increased activity by bacteria already present in eroded areas) with subsequent possibility of bacteremia; 3) compromising of tactile hairs as sensory structure; 4) development of bronchitis or pneumonia as result of inhaled irritants.

## RESEARCH UNIT 180

### PROJECT MANAGEMENT, COORDINATION OF RESEARCH EFFORTS AND COLLECTION OF TISSUE SPECIMENS FROM THE BOWHEAD WHALE, BALAENA MYSTICETUS AND THE GRAY WHALE, ESCHRICHTIUS ROBUSTUS

THOMAS F. ALBERT, V.M.D., Ph.D.  
Department of Veterinary Science  
University of Maryland  
College Park, Maryland 20742

#### INTRODUCTION

This study concerns endangered whales occurring in the proposed Beaufort Sea lease area, the bowhead and gray whales. The lease area is depicted in the illustration on the inside of the cover of this report. This Research Unit dealt with the overall management of the various aspects of the research effort as well as the collection of tissue samples. The entire research effort was an expansion and continuation of a study begun in the fall of 1978 (Albert, 1980; Albert and Philo, 1978). A major effort involved determination of the normal structure and function of critical tissues of these whales. Emphasis was placed upon those tissues most likely to evidence adverse effects, either direct or indirect, as a result of offshore oil and gas development.

#### OBJECTIVES

1. To provide management of the overall research program particularly to assure coordination of the Research Units (Table 1-1). Data gathered by the Research Units will be assembled into the appropriate reports as required by the funding agency.
2. To provide the necessary personnel and logistical support for the collection of tissue specimens from Eskimo harvested whales. Such collected specimens were distributed to personnel associated with the various Research Units.

#### METHODS

Examination of individual whales was limited to those which were either hunter-killed or stranded. Hunter-killed whales were potentially available during the spring from Barrow, Wainwright and Point Hope to the west of the

TABLE 1-1. INVESTIGATORS, CONSULTANTS AND RESEARCH UNITS ASSOCIATED WITH THE PROJECT

Investigator	Research Unit #	RU Code Name
T. F. Albert,* Univ. of Maryland	180	Management/Tissue Collection
T. F. Albert, Univ. of Maryland	280	Strandings
T. F. Albert, Univ. of Maryland	380	Toxic Substances
A. Fetter, J. Everitt, Univ. of Pennsylvania	480	Lymph/Bone
R. Kenney, M. Garcia, J. Everitt, Univ. of Pennsylvania	580	Reproduction
G. Aguirre, R. Dubielzig, Univ. of Pennsylvania	680	Eye
G. Migaki, Armed Forces Institute of Pathology	780	Pathology
W. Medway, Univ. of Pennsylvania	880	Blood/Urine
G. Jarrell, G. Shields, Univ. of Alaska	980	Cytogenetics
A. Smith, K. Benirschke, San Diego Zoo	1080	Virus/Serology
D. Johnston, St. John's Hospital Oxnard, California	1180	Bacteria
R. Heckmann, Brigham Young Univ.	1280	Parasites
J. T. Haldiman, Y. Z. Abdelbaki, F. K. Al-Bagdadi, D. W. Duffield, W. G. Henk, R. W. Henry, Louisiana State Univ.	1380	Skin/Lung
R. Sis, R. Tarpley, Texas A&M Univ.	1480	Stomach/Intestine
S. Leatherwood, J. Norris, Hubbs Sea World Research Institute	1580	Ear
Consultants	Area of Effort	
J. Burns, Alaska Dept. of Fish & Game	Program Structure	
L. Dalton, Naval Arctic Research Laboratory	Tissue Collection	
J. Everitt, Univ. of Pennsylvania	Tissue Collection	
J. C. George, Chappaqua, NY	Tissue Collection	
C. Jones, Univ. of Pennsylvania	Cardiology**	
L. M. Philo, Univ. of Alaska	Tissue Collection	
S. H. Ridgway, Naval Ocean Systems Center	Brain Morphology***	

\* Principal Investigator

\*\* See APPENDIX II

\*\*\*See APPENDIX IV

the lease area and during the fall from Barrow to the west and from Kaktovik to the east.

It must be kept in mind that although the bowhead travels through much of the western and northern Alaskan coastal waters (and thereby through proposed and potential lease areas), the animal is available for sampling only at the whaling villages. Such sites represent unique opportunities for the collection and examination of critical tissues from this far-ranging whale.

Coordination with Eskimo Hunters. There could be no collection of tissues from harvested bowhead whales without the cooperation of the individual Captain and his crew at the butchering site. It was therefore essential that personal contacts be made with individual Captains as well as officers of the Alaska Eskimo Whaling Commission (AEWK) and the Barrow Whaling Captains Association (BWCA). Such personal relationships were developed over the past 3 1/2 years. These relationships were strengthened by consulting with AEWK and BWCA prior to each whaling season and seeking their support. In addition, research findings (verbal presentations, copies of earlier reports) were shared with AEWK, BWCA and interested individuals (including the successful whaling Captains) in the Eskimo community. Such communication was vital to the success of the study.

Tissue Collection Team. During an earlier study (spring 1979) the collections were done by a team of two veterinarians (T. Albert and M. Philo) utilizing one snow machine and one sled with an attempt made to reach each whale taken (Albert and Philo, 1979). The transport of large quantities of formalin (tissue preservative), cutting implements, cameras, etc. over the many km of rough ice was not simple. Even more difficult was the careful collection, labeling, photography, etc. of specimens at the butchering site and then returning the heavily laden sled to the Animal Research Facility at the Naval Arctic Research Laboratory. The specimens were then transferred to new formalin, labeled in more detail and the sled readied for the next whale. In retrospect this was just too much for two people to do in view of the expanded requests for tissues. During this spring (1980) it was decided to take more people to the butchering site and spend more time there collecting critical tissues. It was felt that more was to be gained by doing a more intensive job on a given whale rather than trying to examine every whale. This especially

applied when more than one whale was taken in the same day. It was felt that in order to have a reasonable chance of obtaining the various required samples, the tissue collection team should consist of four individuals. The team included three veterinarians\* by virtue of their knowledge of comparative anatomy, tissue handling and preserving techniques, general mammalian pathology and ability to take suitable microbiological samples from the seemingly amorphous masses of tissue produced during the butchering process. The fourth member of the team (J. C. George) possessed needed additional skills, including experience in cold weather survival techniques, snow machine maintenance, carpentry and some knowledge of ice conditions.

Logistical Base of Operation. The logistical base was the Animal Research Facility of the Naval Arctic Research Laboratory (NARL). The NARL (Fig. 1-1), located just north of the village of Barrow provided food, lodging, laboratory space, tools for snow machine repair, sleds, communications (phone and CB radio), trucks, and both warm and cold storage. Other critical items available at NARL for the initial handling and examination of tissues included: large tubs in which to preserve major samples such as intact lungs (Fig. 1-2); a saw capable of cutting bone into thin slabs (1 cm); a radiographic capability ("X-ray" machine) to examine large bones and intact flippers (Fig. 1-3); large freezers (Fig. 1-4); basic carpentry supplies and wood to construct the numerous shipping crates required.

Unfortunately, the NARL was undergoing closure during the spring season and support was indeed diminished. Carpentry and snow machine repair services had to be supplied by our group although the tools were still available. NARL science support diminished steadily and ceased on 30 September 1980. No logistical support from NARL would have made tissue collection far more difficult during the fall season (September and October).

Preparation Prior to Tissue Collection. Prior to the spring whaling season a letter was sent to each member of the Barrow Whaling Captains Association requesting their support should they capture a whale. In a similar manner support was sought from the Alaska Eskimo Whaling Commission.

---

\*T. Albert, L. Dalton, J. Everitt, L. M. Philo (J. Everitt and L. M. Philo worked during different parts of the spring 1980 whaling season).

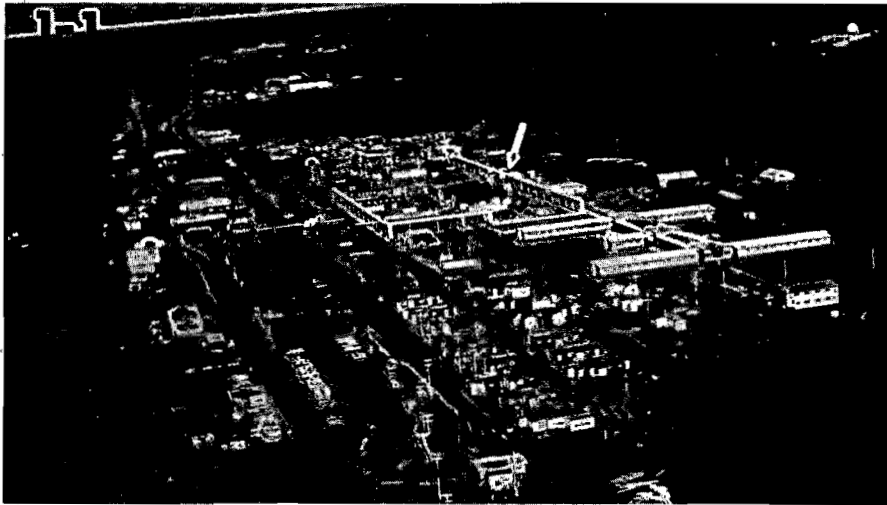


Figure 1-1. Naval Arctic Research Laboratory (NARL) as it appeared in July, 1977. The Animal Research Facility (arrow) served as the logistical base for specimen collection efforts. NARL located approximately 5 km north of Barrow, Alaska ceased all science support as of September 30, 1980. Visible in the upper right is the POW-Main DEW Line Site.

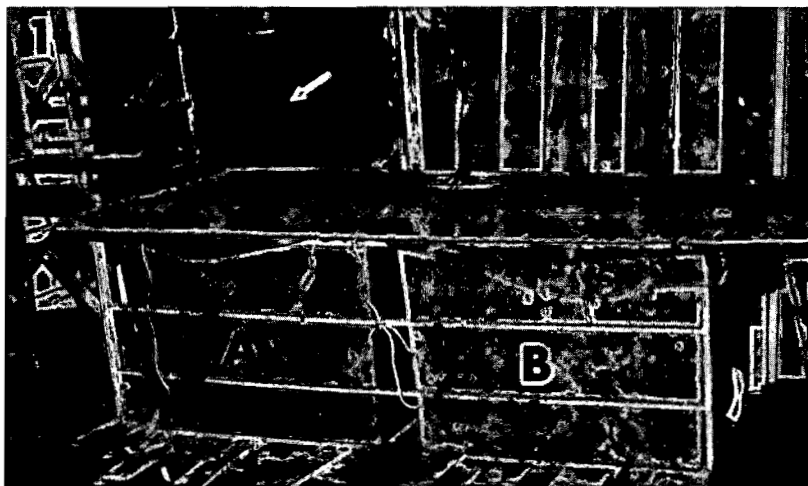


Figure 1-2. Large containers (A, B) of 10% formalin for the preservation and storage of large specimens such as intact heart, lung, stomach, etc. Each container was approximately 1 x 1 x 1 m. Note the heater (arrow) necessary for warm storage.

Various members of the tissue collection team were at NARL from mid-April through mid-June. By arriving prior to the likely time of the first whale being taken, equipment was taken from storage and tested, preservatives prepared, visits made to whaling camps on the ice, and the major ice trails located. An unexpected problem developed during the equipment preparation period when it was noted that the engines of the snowmachines had been damaged during the prior year's use. The cause of the damage was not clearly established, however it was probably due to having used an improper fuel mixture and/or a less than optimum spark plug along with the pulling of heavy loads during the past year. The damaged engines were replaced and the obtaining of proper advice concerning fuel mixture and spark plugs resulted in snowmachines which functioned very well in spite of the pulling of heavy loads over very rough ice.

The basic pieces of equipment were the two snowmachines and two wooden sleds. One sled had two large styrofoam insulated plywood boxes securely fastened to it (Fig. 1-5). Into one of these boxes were placed four large plastic containers (approximately 11 l each) of preservative and a CB radio. Into the other insulated box were placed 4-6 plastic specimen bottles (approximately 3 l each) of preservative. Also included in this box were the blood and microbiological sampling materials as well as a smaller insulated box containing preservative for electron microscopy samples and sampling instruments for specimens for tissue culture and for electron microscopy. Also on this sled was placed a box containing the various cutting instruments (from scalpels to saws). On the second sled were placed an additional box of cutting instruments, ropes, webbing to wrap large specimens, survival gear, chain saw and extra fuel. Unless otherwise specified the "preservative" was 10% buffered formalin.

The snowmachines, sleds and fuel were kept just outside the Animal Research Facility while the other gear mentioned was kept indoors in one area.

Basic Procedures for Collecting and Distributing Specimens. The overall scheme for collection and distribution of specimens is depicted in Figure 1-6. Procedures were developed to facilitate field logistics, specimen collection, and specimen distribution.

Field logistics. Word that a whale was taken reached us through the CB radio. Although nearly all transmissions were in the Inupiat language, the frequency of transmissions rose sharply when a whale was taken. When this happened, the two sleds and snowmachines were quickly loaded and headed out onto

the ice. By getting onto the major ice trail running along the coast one could detect in which direction the camp that took the whale was located. This was due to the "heavy" (but brief) snowmachine and sled traffic heading from Barrow and the other whaling camps toward the camp of the crew which had just taken the whale. If one did not respond quickly and this brief rush of traffic were missed, rapid location of the proper camp would not be possible. Reliance upon the previously known positions of the various crews was not possible as the locations changed depending upon weather conditions and the decisions of the Captains and their crews.

The trails that led out to whaling camps were hacked out of the jumbled ice (Fig. 1-7) by the Eskimo hunters. The whaling camps were spread out along the edge of the lead. A camp consisted of a tent for the Captain and crew and their skin boat with associated supplies. Members of the crew kept watch (Fig. 1-8) for whales moving up the lead. The leads varied in width from a few meters to 30 km or more, depending upon wind and currents. The location of the "near shore" lead can be just a km or so offshore (Fig. 1-9) or can be many km from shore. The usual situation during the 1980 whaling 'season was a lead 2-15 km wide from approximately 8 km above Barrow to at least 30 km below Barrow. When the weather became particularly bad and shifted the ice, crews would sometimes relocate or pull their skin boats back onto more stable ice.

Specimen collection. When the camp of the successful crew was reached, it was essential to locate the Captain and inform him of our desire to collect specimens. In each instance to date the Captain had given his permission for us to sample their whale during butchering. Several Captains have been especially supportive of our efforts and went to much trouble to accomodate our needs during the butchering process.

It must be remembered however that the whales were harvested for food purposes and that the hunt and butchering processes are important cultural events. The entire butchering process occurred according to a rather precise schedule. This scheduled dismemberment of the animal, as well as the severity of the weather, were major factors limiting the completeness of the sampling for any given whale. In order to appreciate the constraints within which samples were collected, a description of the butchering process is given in APPENDIX I.

The low ambient temperatures (-20 to 0°C) presented obvious problems particularly when dealing with very small samples and small quantities of



Figure 1-3. Flipper from bowhead whale 80B8 being readied for radiographic examination by Dr. L. Dalton at NARL Animal Research Facility. The articular surface of the humerus (A) is visible. The small arrow indicates two thumbtacks (radiographic markers) at a site approximately 61 cm from the proximal end of the humerus. The large arrow locates the hole cut through the distal portion of the flipper by Eskimo hunters in order to tie the two flippers together over the animal's chest. (see also Fig 1-11 and 21-12).

Figure 1-4. Large bone samples being placed into one of four freezer units that were available for long term storage at NARL.

Figure 1-5. Sleds being unloaded after returning to NARL. Sled in foreground has large insulated box while other sled has smaller boxes of cutting instruments and containers of preservative. (Photo by G. Selby).

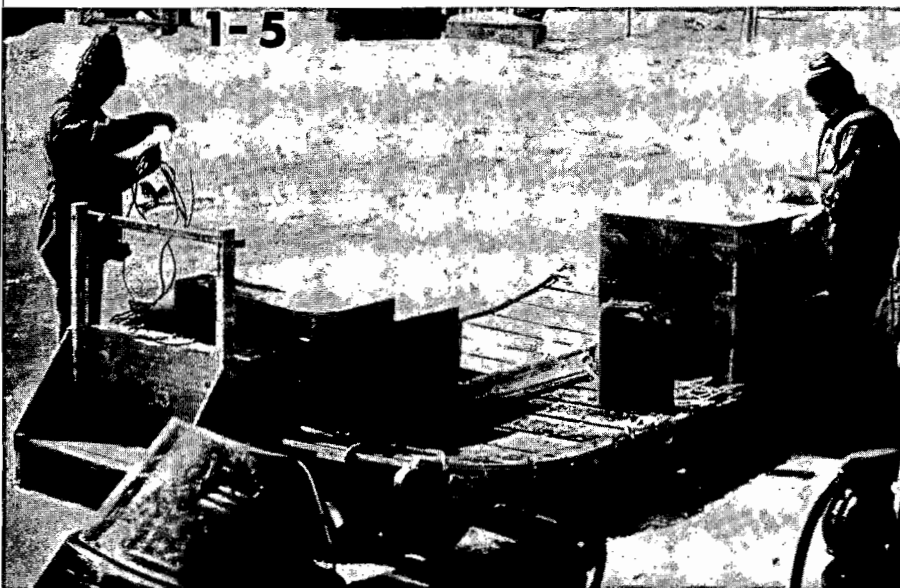
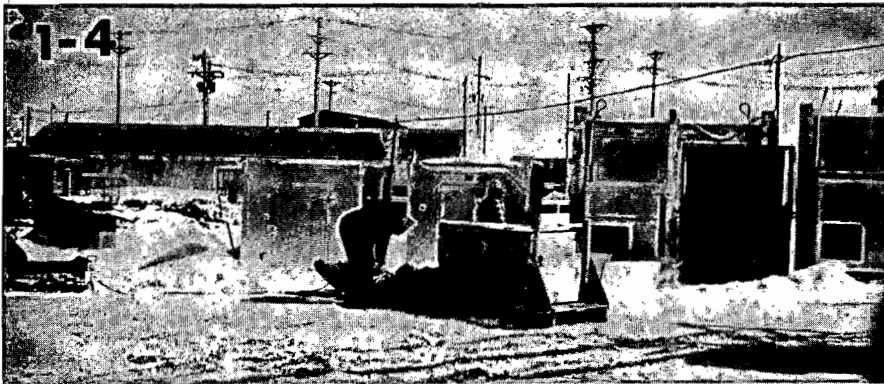
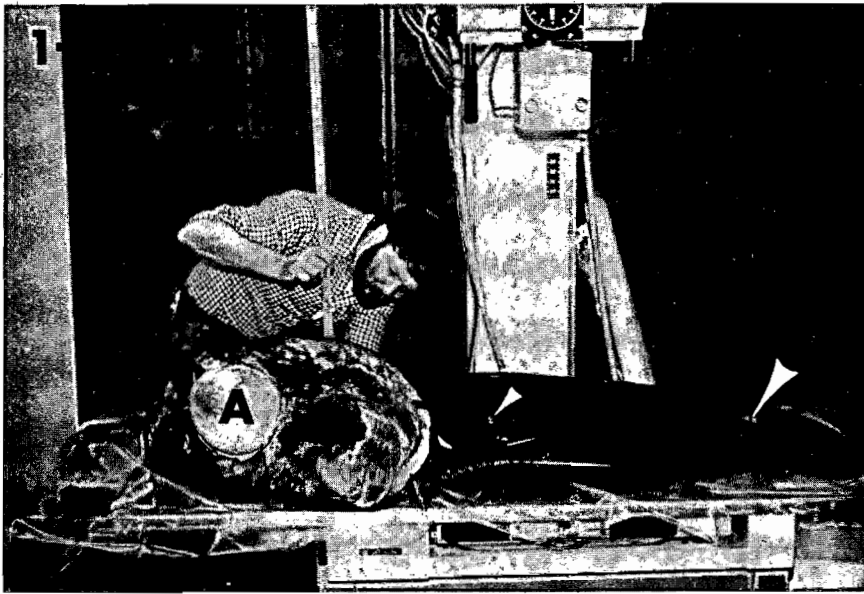
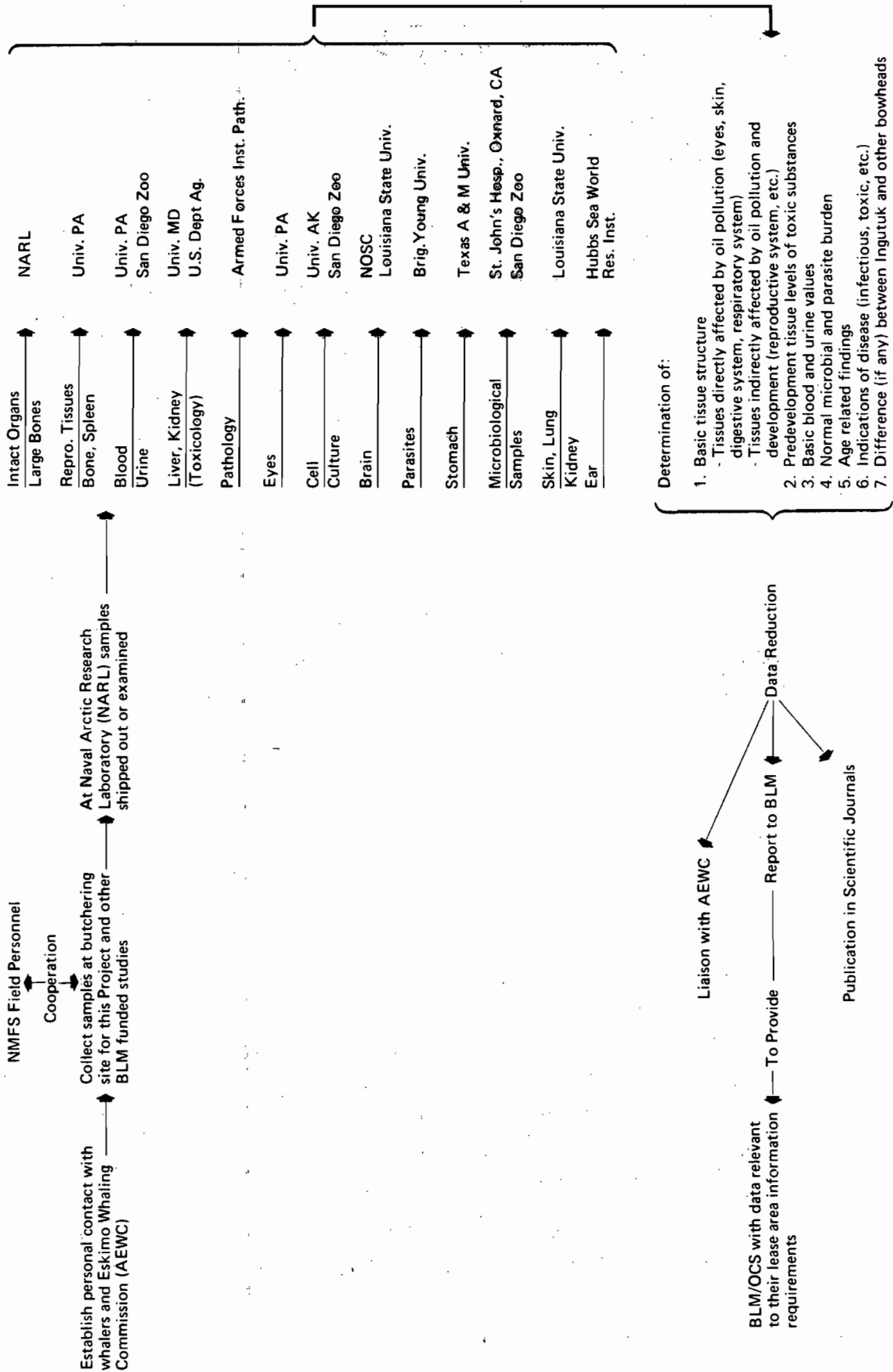


FIGURE 1-6 TISSUE COLLECTION AND HANDLING FLOW CHART



preservatives. Freezing of the small samples during or just after collection was indeed a problem.

During the specimen collection process, samples were collected according to a predetermined schedule to the extent possible. If we arrived in time (before the butchering had begun) (Fig. 1-11, 1-12); the skin was sampled first as well as microbiological sampling of the body orifices. As the skin and blubber were removed, additional samples could be taken. Then the abdominal cavity usually was opened with the abdominal viscera (liver, kidney, stomach, intestines, internal reproductive structures, etc.) quickly cut loose and dragged a few meters away by the crew. This resulted in some orientation problems with great caution having to have been exercised in tissue and microbiological sampling. The thoracic viscera (heart, lungs) were also quickly removed by the crew. The heart, an important food item, was usually difficult to sample. The only time that a complete heart could be collected would be when the internal organs had undergone decomposition due to an inadvertent delay in landing the animal. Such an instance pertaining to the heart is detailed in APPENDIX II.

Specimens collected were labeled at the butchering site and appropriate descriptions entered onto hand held tape recorders. Particularly helpful items were the small clip-on tags\* which could be readily applied to tissue samples. Numerous photographs were taken to record where small samples originated to provide gross anatomical information, and to describe the physical appearance of the butchering site. Collected materials were returned to the logistical base (NARL) for further evaluation. Specimens were logged into a record book, subsampled as necessary, and stored as appropriate until being distributed to the other Research Units.

The largest single specimen to be examined was a flipper. When possible a flipper was taken to NARL for gross measurement and radiographic evaluation. The radiographic examination allowed for a determination of the boney make-up of the limb. The flipper was returned to the whaling Captain after the brief examination (APPENDIX VI).

Specimen distribution. It was recognized that no one individual could properly respond to the objectives of the Work Statement (APPENDIX VII). As illustrated previously in Table 1-1, a research team involving 15 Research

---

\*Daily Delivery Tags, Pittsburgh Tag Co., Pittsburgh, PA (see Fig. 20-27).

Figure 1-7. Ice trail leading out to whaling camp. Trails are cut through jumbled ice by Eskimo hunters in order to reach lead which may be several km from shore.

Figure 1-8. Whaling camp near ice edge. Tent (A) provides shelter for hunters. Skin boat is visible just to left of tent and CB radio antenna (solid triangle) is located to right of tent. Whaling Captain Eugene Brower standing on ice pile maintains watch for whales in lead.

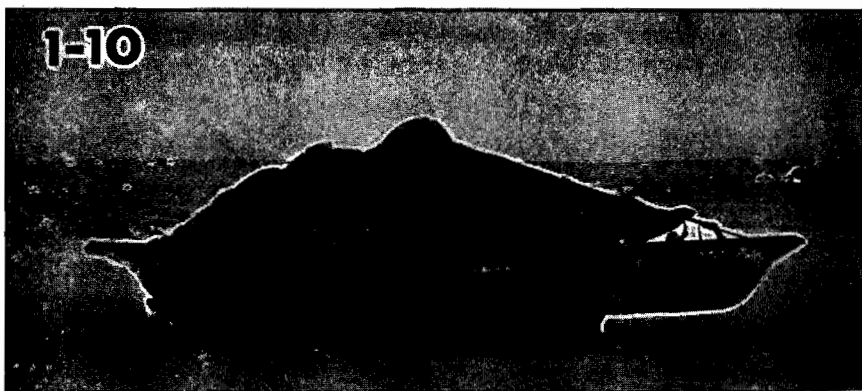
Figure 1-9. Narrow lead (white arrow) very near shore, just off Naval Arctic Research Laboratory (black arrow). POW-Main DEW Line Site is barely visible just above and to left of NARL. Dark structure in upper left is engine of NARL aircraft.



Figure 1-10. Skin boat on sled which has been pulled back to safe ice when ice further out is shifting. Whaling gear is stored in covered boat.

Figure 1-11. Whaling Captains Harry Brower, Sr. (1) and Arnold Brower, Sr. (2) examine bowhead whale 80B7 while determining how best to pull whale up onto ice. Whale is lying in water at ice edge with ventral aspect uppermost. Small white arrowhead locates white skin on ventral aspect of lower jaw. Larger arrowhead points to right flipper which is tied by rope (barely visible just above water) to left flipper over animal's chest. Skin boat is partially visible on ice at extreme lower right.

Figure 1-12. Bowhead whale 80B8 (an Ingutuk) lying on right side. Butchering just beginning. Note irregular patches of white skin on ventral aspect.





Units was assembled. Table 1-2 depicts how the various Research Units relate to the objectives of the Work Statement. Collected specimens were distributed by the project manager to the appropriate Research Units, as illustrated in Figure 1-6 and Table 1-1.

## RESULTS

An extensive ice jam in the Bering Straits delayed the northward migration of the bowhead whales during the spring of 1980. When the ice conditions became more favorable, large numbers moved northward so that the whales arrived at Barrow later than usual.

Specimens Collected from Whales at Barrow. Nine bowhead whales were taken by Eskimo hunters at Barrow during the spring of 1980 whaling season (Table 1-3). All nine whales were taken between 24 and 27 May.

It should be noted, that during one 24 hour period (May 25) there were five whales (80B2-80B6) on the ice being butchered at approximately the same time. We were only able to get to one of these (80B2) during that day. This was consistent with our planning as it was felt that more could be gained by staying with one whale and doing a more thorough examination rather than moving from one butchering site to the next and obtaining only a few samples from each whale.

In another instance two whales were being butchered during the same 24 hour period (May 27) and we stayed at the first of these (80B8) until finished. This animal (80B8) was an Ingutuk and represented a unique chance to obtain a large number of samples. The second animal taken that day (80B9) was not reached until after the butchering process was well underway.

A good selection of tissue samples were obtained from five whales (80B1, 80B2, 80B7, 80B8, 80B9). An excellent selection of tissues was obtained from one of these whales (80B8, an Ingutuk). Only reproductive tissue or bone was obtained from three whales (80B3\*, 80B4, 80B5\*). No tissues were obtained from one whale (80B6).

---

\*Only reproductive tissue was obtained from these animals and it was obtained by National Marine Fisheries Service Field personnel whose cooperation was appreciated.

TABLE 1-2. RELATIONSHIPS OF RESEARCH UNITS TO OBJECTIVES OF WORK STATEMENT\*

Research Unit # and Code Name	Work Statement Objective # and Topic						Multi-Year Res. Plan
	#1 Morphology	#2 Micro/Parasite/ Toxic/Pathol.	#3 Ingutuk	#4 Strandings	#5 Section 7	#6	
180 Management/ Tissue Collection	X	X	X	X	X	X	
280 Strandings				X	X	X	
380 Toxic Substances		X			X	X	
480 Lymph/Bone	X		X		X	X	
580 Reproduction	X				X	X	
680 Eye	X				X	X	
780 Pathology		X			X	X	
880 Blood/Urine	X				X	X	
980 Cytogenetics			X		X	X	
1080 Virus/Serology		X			X	X	
1180 Bacteria		X			X	X	
1280 Parasites		X			X	X	
1380 Skin/Lung	X				X	X	
1480 Stomach/ Intestine	X				X	X	
1580 Ear	X				X	X	

\* The Work Statement is presented in APPENDIX VII

There were no gray whales taken by Eskimo hunters. Gray whales are seldom hunted and none were harvested in the Barrow area. The only gray whale specimen was available for study had been obtained from an animal found stranded in 1978 (Albert and Philo, 1978).

A complete listing (with related observations) of the various specimens obtained from the harvested whales is presented in APPENDIX V. This listing also indicates the Research Unit to which each sample was sent.

Heart from Bowhead Whale 78KK1. A nearly intact heart was obtained during the fall of 1979 from whale 78KK1 taken in Kaktovik. Severe weather had resulted in a delay in beaching that animal (Albert, 1979) so that the heart was not useful for food. We had been able to transport the damaged heart (Fig. 20-40) to NARL and store it in a large container of formalin (Fig. 1-2). This unique specimen was examined in detail during the summer of 1980 with the findings presented in APPENDIX II.

Examination of Flipper from Bowhead Whale 79B4. A large bowhead whale (15.2 m) was found in October 1979 frozen into the ice along a barrier island approximately 13 km southeast of Point Barrow (Albert, 1979). Through the efforts of Harry Brower, Sr., a major portion of the left flipper was made available for radiographic examination (Table 21-1). The flipper remnant was cut into smaller pieces with a chain saw and then into slabs approximately 4 cm thick (similar to that in Fig. 21-8). This sectioning allowed for the visualizing of bones and cartilage seen radiographically (Fig. 21-5 through 21-12). Much of the subcutaneous portion of the flipper was composed of bone and cartilage.

Bone samples from this flipper consisted of the following 8 pieces:

- Metacarpal, carpal, distal ulna, 1 cm thick slab
- Metacarpal, carpal, distal ulna, 1 cm thick slab
- Metacarpal, carpal, distal ulna, 1 cm thick slab
- Metacarpal, carpal, distal ulna, 1 cm thick slab
- Metacarpal, carpal, distal ulna, 2 cm thick slab
- Cartilage and metacarpal, 1 cm thick slab
- Cartilage and metacarpal, 1 cm thick slab
- Metacarpal #1, 2 cm slab.

Unfortunately, these bone samples had been long frozen, however, they were forwarded in 10% buffered formalin to RU 480 for gross examination.

TABLE 1-3. BOWHEAD WHALES TAKEN DURING SPRING 1980 HUNT AT BARROW, ALASKA

Whale Number	Length (m)	Sex	Date Taken	Captain of Successful Crew
80B1	10.9	F	May 24	A. Brower, Sr.
80B2	10.8	M	May 25	M. Nageak
80B3	8.5(approx)	M	May 25	P. Nusunginya
80B4	10.4	M	May 25	R. Aveoganna
80B5	10.4	M	May 25	B. Itta
80B6	8.5	M	May 25	S. Patkotak
80B7	10.0	F	May 26	G. Ahmaogak
80B8	8.7	M	May 27	H. Brower, Sr.
80B9	13.6	F	May 27	P. Tukle

Bowhead Whale 80G1. This whale was taken on 4 May 1980 at Gambell (St. Lawrence Island). It was examined by National Marine Fisheries Service (NMFS) personnel at the butchering site (K. Hazard, B. Kelly, A. Gifford). The animal had been struck at sometime in the past as a healed bomb wound was located (Hazard, 1980; Sylvester, 1980). Samples from the healed wound site and one ovary were collected by NMFS field personnel. The wound site material was forwarded to RU 780 and the ovary to RU 580.

Bowhead Whale 80WW1. This whale (7.8 m length) was taken on 23 May 1980 at Wainwright. It was examined by National Marine Fisheries Service (NMFS) personnel (B. Lawhead). Both testicles were collected by NMFS personnel. Gross measurements for one testicle were 206 mm in length and 70 mm in width while the other testicle was 205 mm in length and 65 mm in width. Both were forwarded to RU 580.

Specimens Collected for Other BLM Supported Research Groups. Two pieces of frozen blubber were supplied to L. Hobbs, National Marine Mammal Laboratory, National Marine Fisheries Service, Seattle, Washington. The two samples (each approximately 30 x 30 x 15 cm) were obtained from bowhead whales 80B1 and 80B2.

Baleen, including 81 plates in two intact segments of gum was supplied to Dr. L. Braithwaite, Department of Zoology, Brigham Young University, Provo, Utah. These were obtained from bowhead whale 80B8, an Ingutuk.

Miscellaneous Specimens from Other Bowhead Whales. At least eight specimens from several other bowhead whales were sent to the appropriate Research Units. All were stored (Fig. 1-2 and 1-4) at the Naval Arctic Research Laboratory since having been collected during 1978 and 1979. With the closure of the laboratory (30 September 1980) such specimens would have been discarded. An intact humerus from whale 78KK2 was sent to RU 1380. The blowhole area (including external nares) from 79KK1 was sent to RU 1380. The spleen from 78KK1 was sent to RU 1480. From whale 79B1 a lung was sent to RU 1380 and a portion of the stomach to RU 1480.

Several specimens collected in 1979 and in storage could not be positively identified as to exact whale origin. These specimens included; a stomach sent to RU 1480, a stomach (likely from 79B2) sent to RU 1480 and a colon segment (approximately 1.2 m) sent to RU 1480.

Radiographic Examination of Bowhead Whale Flippers. This effort is described in more detail in APPENDIX VI. Some brief findings include the presence of what seemed to be numerous vascular channels within the cartilage (Fig. 21-6), variability in the number of carpals and metacarpals, and stability in the boney structure of the digits (Fig. 21-14).

Examination of Distributed Specimens. The specimens were distributed to the appropriate investigators (Table 1-1) and their findings are included as subsequent sections (by Research Unit) of this report. In addition to the data presented by the separate Research Units, some related findings are presented in the various Appendices.

Fall (1980) Whaling Season. There was no field effort mounted to collect specimens during the fall (September-October) whaling season. This decision was made by BLM in consultation with the principal investigator. It was felt to be unwise for the BLM to collect specimens from what the National Marine Fisheries Service (NMFS) regarded as illegally harvested whales. Any whales that might have been taken during the fall season would have been in excess of the number set as a maximum for 1980 by NMFS.

Research Meeting. A research meeting involving project investigators and consultants was held 18-20 December 1980. The meeting served to bring investigators together for individual research presentations, group discussions and aspects of report preparation. A listing of research topics presented and those in attendance are given in APPENDIX III.

## DISCUSSION

Specimen Collection and Distribution. The procedure for tissue collection and distribution worked well. Contributing most to this success were a good working relationship with Eskimo hunters, an adequate logistical base, reasonable communications, and field personnel with a good knowledge of comparative anatomy and microbiological sampling techniques. The working relationship with Eskimo hunters was established over a 3 1/2 year period and aided by attendance of project personnel at meetings, visiting individual whaling captains, and dissemination of previous research findings to the whalers. The logistical base as provided by the Naval Arctic Research Laboratory was excellent. It is now

difficult to imagine how such a large scale effort could continue after the laboratory's closing on 30 September 1980. Communications in the field were through personal visits to the whaling camps and the use of the CB radio. Specimen collection was always subordinated to the butchering process. Due to the rapidity of the butchering process, individuals collecting samples had to be able to quickly sample large and often disoriented structures. Specimen labeling and record keeping were facilitated by the use of small "clip on" tags and small hand held tape recorders.

The collection and examination of tissues from Eskimo harvested bowhead whales provided the means whereby the detailed structure of a large baleen whale could be partially determined. Hopefully these efforts will provide a standard of comparison for subsequent research. Although the detailed structure of a large whale has never been determined, a major effort toward that goal was begun.

Recovery of Previously Struck Bowhead Whale. The whale (80G1) taken in Gambell during the spring whaling season is definitive evidence of a bowhead having survived an earlier strike (Hazard, 1980; Sylvester, 1980). A similar but less well documented case has also been described (Albert and Philo, 1978; Albert et al., 1980). In another instance a partially healed triangular scar thought to be due to an Eskimo "Bomblance" harpoon was noted on a small bowhead captured in Osaka Bay, Japan (Nishiwaki and Kasuya, 1970). It seems clear that some bowhead whales survive which are struck and lost. However, the available evidence is so sparse that it is still not possible to give an accurate estimate of what portion of such whales survive.

#### SUMMARY

A working relationship was established with Eskimo hunters whereby harvested bowhead whales could be sampled during the butchering process. The on site specimen collection team consisted of four individuals and the Naval Arctic Research Laboratory served as the logistical base. More than 550 specimens were collected from the nine bowhead whales harvested by Eskimo hunters during the spring 1980 whaling season. The samples were distributed to the 22 investigators associated with the other Research Units for examination. Research findings were preliminarily examined and discussed at an investigator's

meeting 18-20 December 1980. The results of the specimen examinations are presented in the findings of Research Units 280 through 1580.

#### ACKNOWLEDGMENTS

It is a pleasure to recognize the support that has been given by all those who helped to make this study a success. The help and cooperation of the Alaska Eskimo Whaling Commission and Barrow Whaling Captains Association is greatly appreciated as is that rendered by the individual Whaling Captains who (mentioned in the text) took whales during the spring of 1980. Special thanks are due to Whaling Captains Jacob Adams, Arnold Brower, Sr., Eugene Brower and Harry Brower, Sr. for their cooperation and advice.

It is also a pleasure to recognize the assistance provided by those involved in collecting the specimens, namely; Les Dalton, D.V.M., Jeff Everitt, D.V.M., John C. George and L. M. Philo, V.M.D. The cooperation of NMFS field personnel (mentioned in text) is also appreciated. The logistical support provided by the staff of the Naval Arctic Research Laboratory especially Dr. John Kelley, formerly NARL Technical Director and George Selby, formerly Animal Research Facility Supervisor is greatly appreciated.



## REFERENCES

- Albert, T. F. 1979. Tissues (structure/function) (RU 280). In: Investigation of the Occurrence and Behavior Patterns of Whales in the Vicinity of the Beaufort Sea Lease Area, J. Kelley and G. Laursen (eds.), pp 297-329. Final Report to the Bureau of Land Management from the Naval Arctic Research Laboratory, Barrow, Alaska.
- Albert, T. F. 1980. Tissue structure studies of the bowhead whale. Arctic Coastal Zone Management Newsletter. No. 28:15-19.
- Albert, T. F., G. Migaki, H. W. Casey and L. M. Philo. 1980. Healed penetrating injury of the bowhead whale, Balaena mysticetus. Marine Fisheries Review. 42:92-96.
- Albert, T. F. and L. M. Philo. 1978. Tissues (RU 578). In: Investigation of the Occurrence and Behavior Patterns of Whales in the Vicinity of the Beaufort Sea Lease Area, J. Kelley (ed.), pp 15-30. Final Report to the Bureau of Land Management from the Naval Arctic Research Laboratory, Barrow, Alaska.
- Albert, T. F. and L. M. Philo. 1979. Tissues (structure/function) (RU 579). In: Investigation of the Occurrence and Behavior Patterns of Whales in the Vicinity of the Beaufort Sea Lease Area, J. Kelley and G. Laursen (eds.), pp 187-212. Final Report to the Bureau of Land Management from the Naval Arctic Research Laboratory, Barrow, Alaska.
- Hazard, K. 1980. Personal communication.
- Nishiwaki, M. and T. Kasuya. 1970. A greenland right whale caught at Osaka Bay. Sci. Rep. Whales Res. Inst. No. 22:45-62.
- Sylvester, B. 1980. Old bomb wound found in bowhead. Arctic Coastal Zone Management Newsletter. No. 30-11.

## RESEARCH UNIT 280

### DETERMINATION OF THE INCIDENCE OF WHALE STRANDINGS IN THE VICINITY OF THE LEASE AREA

THOMAS F. ALBERT, V.M.D., Ph.D.  
Department of Veterinary Science  
University of Maryland  
College Park, Maryland 20742

#### INTRODUCTION

This Research Unit involved surveys of beaches in the vicinity of the lease area for stranded whales. It seems reasonable to determine the predevelopment levels of whale strandings to provide a baseline against which future findings can be compared as development proceeds.

#### OBJECTIVE

To determine the incidence of whale strandings in the vicinity of the lease area to provide a basis for detecting and monitoring changes that may occur in association with offshore development in the Beaufort Sea.

#### METHODS

The coastline to be examined by aerial survey was that from Point Lay (southwest of Barrow) to Kaktovik (southeast of Barrow) in a manner similar to last summer. The coastline was to be examined twice during the ice free period (early to mid August and late August) utilizing a twin engine aircraft under contract to BLM.

## RESULTS

The coastline from Point Lay to Kaktovik was examined once for stranded whales. Poor flying weather and difficulties in coordinating the use of the BLM chartered twin engine aircraft resulted in single engine aircraft charter on August 31. Between Barrow and Point Lay no stranded whales were seen.

The beach between Kaktovik and Barrow was examined by a cooperating BLM supported individual (M. Platter-Rieger) returning to Deadhorse and then Barrow on September 5. The badly decomposed remains of a stranded whale were sighted on a barrier island (part of the McClure Islands) approximately 350 km to the east of Barrow. This was the same carcass (primarily skeletal remains) located in early July by other members (D. Ljungblad and F. Ship) of the above mentioned BLM supported group while conducting aerial surveys in and around the lease area. On July 16, the carcass was examined from the air (Fig 2-1) by a consultant to this project (L. Dalton). Beach conditions were such that a landing was not possible, however, the animal seemed to be a bowhead whale. The animal had been examined earlier and it was noted (Ljungblad 1980) that the animal was approximately 7.6 m in length and possessed "black baleen".

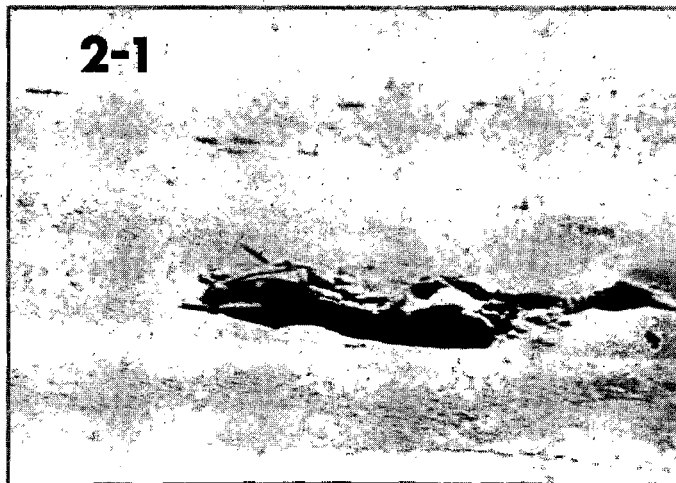


Figure 2-1. Skeletal remains of bowhead whale located on the shore of a barrier island approximately 350 km to the east of Barrow. (Photo by L. Dalton).

## DISCUSSION

One stranded bowhead whale was noted this year on a barrier island to the southeast of Barrow (between Barrow and Kaktovik). During 1979, another bowhead whale was stranded on a barrier island to the southeast of Barrow (Albert 1979), as was a gray whale during 1978 (Albert and Philo 1978).

To the southwest of Barrow (between Barrow and Point Lay) no stranded bowhead whales were noted during surveys in 1979 and 1980. A stranded gray whale was noted to the southeast of Barrow in the fall of 1978 (Albert and Philo 1978) as was another gray whale and an unidentified whale, Balaenoptera sp. during the summer of 1979 (Albert 1979).

It, therefore, seems (on this limited evidence) that it is "normal" for one stranded bowhead to be located per year between Barrow and Kaktovik and one or two gray whales to be found stranded in the vicinity of Barrow and to the southwest.

## SUMMARY

One stranded bowhead whale was noted this year on examining the coastline between Point Lay and Kaktovik. This is the sixth whale (second bowhead) found stranded in the mentioned area since the fall of 1978. In no instance was the cause of death determined.

## ACKNOWLEDGMENTS

It is a pleasure to acknowledge the cooperation of Dr. Les Dalton as well as that of Donald Ljungblad and his associates, Mary Platter-Rieger and Frank Shipp, in this study.

## REFERENCES

- Albert, T.F. 1979. Tissues (structure/function, RU 280).  
In: Investigation of the Occurrence and Behavior Patterns of Whales in the Vicinity of the Beaufort Sea Lease Area. J. Kelley and G. Laursen (eds.), pp. 297-329, Report to Bureau of Land Management from Naval Arctic Research Laboratory.
- Albert, T.F. and L. M. Philo. 1978. Tissues (RU 578).  
In: Investigation of the Occurrence and Behavior Patterns of Whales in the Vicinity of the Beaufort Sea Lease Area. J. Kelley (ed). pp. 15-30, Report to Bureau of Land Management from Naval Arctic Research Laboratory.
- Ljungblad, D.K. 1980. Personal communication.



## RESEARCH UNIT 380

### DETERMINATION OF LEVELS OF TOXIC SUBSTANCES IN SELECTED TISSUES OF THE BOWHEAD WHALE, BALAENA MYSTICETUS, AND GRAY WHALE, ESCHRICHTIUS ROBUSTUS

THOMAS F. ALBERT. V.M.D., Ph.D.  
Department of Veterinary Science  
University of Maryland  
College Park, Maryland 20742

#### INTRODUCTION

Since the bowhead whale is a major food item for the Eskimo people, monitoring the accumulation of toxic substances in whale tissues as off-shore development progresses is a reasonable approach to avoid the potential risks to human health. Such toxicants would include heavy metals, organochlorines and hydrocarbons of petroleum origin.

Heavy metals such as lead, mercury, cadmium, and zinc are commonly recognized to be potentially harmful. Although such metals are more concentrated in the marine sediments as opposed to the water column, they enter the food chain and are frequently found in seal tissues (Holden 1978). It is reasonable to expect them to be also found in tissues of the bowhead and gray whales frequenting the Beaufort Sea. It is also reasonable to expect that both the bowhead and gray whales in the Beaufort Sea contain detectable tissue levels of toxic compounds such as certain chlorinated hydrocarbons and heavy metals. Organochlorine toxicants such as DDT and polychlorinated biphenyls ( PCBs ) have been reported to occur at low levels in pinnipeds from the Beaufort Sea (Galster and Burns 1972). DDT has also been reported in beluga whales (Delphinapterus leucas) in the Beaufort Sea (Addison and Brodie 1973). Unfortunately, offshore development also brings with it the potential for the release of hydrocarbons of petroleum origin into the water and their subsequent accumulation in marine animals.

## OBJECTIVES

Examination of whale tissues for toxic substances had three objectives: 1) to establish baseline levels for such substances in critical tissues prior to offshore development; 2) to monitor the tissue levels of such substances as development progresses; and 3) to assess the effects of such substances on the well-being of bowhead and gray whales.

## METHODS

In view of that mentioned above, the methodology should include at least a determination of the following toxic substances: chlorinated hydrocarbons, such as DDT (including its breakdown products) and PCBs; and metals including lead, mercury, zinc, and cadmium. As a minimum, the blubber was to be examined for chlorinated hydrocarbons and the liver, spleen, kidney and skeletal muscle for heavy metals.

Specimens were received from four Eskimo harvested bowhead whales by way of Research Unit 180.

## RESULTS

Samples from bowhead whales 80B1 and 80B2 consisted of spleen, liver, blubber and skeletal muscle. From whale 80B7 samples of spleen, liver, blubber, skeletal muscle and kidney were obtained. From whale 80B8 samples of spleen, liver, blubber, skeletal muscle, diaphragm and kidney were obtained. In each instance duplicate samples were obtained, each approximately 0.5 kg.

No chemical determinations have yet been conducted due to difficulty in obtaining suitable analytical services. The specimens remain frozen in storage.

## SUMMARY

A total of 19 duplicate samples were collected from four bowhead whales. Specimens remain frozen at the University of Maryland.

#### REFERENCES

- Addison, R.F. and P.F. Brodie. 1973. Occurrence of DDT residues in beluga whales (Delphinapterus leucas) from the Mackenzie Delta, N.W.T. J. Fish. Res. Board Can., 30:1733-1736.
- Galster, W. and J. Burns. 1972. Accumulation of pesticides in Alaskan marine mammals. In: Proceedings of the Twenty-Third Alaska Science Conference, p. 50, Alaska Division American Association for Advancement of Science, Fairbanks, AK.
- Holden, A.V. 1978. Pollutants and seals - a review. Mammal Review, 8:53-66.



## RESEARCH UNIT 480

# DETERMINATION OF THE GROSS AND MICROSCOPIC STRUCTURES OF SELECTED TISSUES AND ORGANS OF THE BOWHEAD WHALE, BALAENA MYSTICETUS, WITH EMPHASIS ON BONE, BLUBBER AND THE LYMPHOIMMUNE AND CARDIOVASCULAR SYSTEMS

A. W. FETTER, D.V.M., M.S., Ph.D.

J. I. EVERITT, D.V.M.

Department of Pathology

School of Veterinary Medicine

University of Pennsylvania

New Bolton Center

382 West Steet Road

Kennett Square, Pennsylvania 19348

## INTRODUCTION

Bone. This study concerned the gross and microscopic evaluation of the humerus, radius, ulna and vertebrae in four bowhead whales; three regular (80B1, 80B2 and 80B4) and one Ingutuk (80B8). Vertebral specimens also were available from two additional bowheads (80B7 and 80B9), while specimens of the humerus, radius and ulna were available from bowhead 78KK2. The only bowhead in which carpals and metacarpals were available was from 79B4. Particular emphasis was placed on determining the differences between the bone structure in the regular bowhead whales compared to the Ingutuk.

Most reports in the literature that describe the skeleton of the whale have been on macerated specimens (Omura et al., 1970; Nishiwaki and Kasuya, 1971; Omura et al., 1971; Omura, 1972; Omura, 1975; Omura and Kasuya, 1976). A more detailed study of the structural and developmental characteristics of the humerus in the finback, beluga and pilot whales and of the radius in the beluga, small white and pilot whales, has been reported by Felts and Spurrell (1965, 1966).

The histologic features observed in the bones of the bowhead whale compared to the pachyostotic bone observed in the manatee and penguin are discussed.

Blubber. The gross and microscopic structure of the blubber of regular bowhead whales, Balaena mysticetus, as well as of an Ingutuk variant, was studied to determine morphologic differences which might lead to further understanding of the relationship between the two forms.

Lymphoimmune System. The study performed was to determine the gross and microscopic structure of the lymphoid system of the bowhead whale, Balaena mysticetus. The purpose of the study was to establish the normal structure of the major lymphoid organs in an effort to assess normal baseline status of the immune system. An assessment of this system will be of crucial importance for future environmental toxicologic evaluation of whales in the Beaufort Sea.

In both terrestrial and aquatic mammals, the lymphoid system governs the immune response which is of major significance as a disease defense mechanism. Insults to the lymphoid system of Balaena mysticetus by pollutants could adversely affect the health status of the entire bowhead population. Presently, a morphologic assessment of the lymphoid system is the only practical method of determining the immune status of the bowhead population.

Cardiovascular System. See Appendix II.

#### OBJECTIVES

1. To determine the gross and microscopic structure of several of the major tissues and organ systems of the bowhead whale. Emphasis is to be placed upon the lymphoimmune tissues, bone, baleen, cartilage, blubber, cardiovascular structures and tissues of the mouth.

2. To determine the structure and density of bone and baleen in bowhead whales.

3. To determine the extent (if any) to which the Ingutuk and other bowhead whales differ regarding the density of bone and baleen and with regard to basic tissue structure.

4. To search for histological evidence of aging based upon such changes seen in better studied mammals.

#### METHODS

Bone. Specimens of the humerus, radius, ulna and vertebrae, approximately 2-4 cm in thickness and fixed in 10% buffered formalin were received from RU-180. Following gross evaluations, samples were further reduced approximately 50% in thickness on a Hobart band saw. Where complete longitudinal sections of the humerus and vertebrae were available, successive sections of these bones measuring approximately 2 cm long x 1 cm wide x 0.5 cm thick were made in duplicate through the center of the bone slab from the articular surface on one

end to the articular surface on the opposite end. This insured that bone tissue throughout the entire length of the specimen was available for histological evaluation.

The bone specimens were held in a fresh supply of 10% phosphate buffered formalin. One set of specimens was decalcified in formic acid - HCl prior to processing through ascending concentrations of alcohol, embedding in paraffin, and sectioning at 6  $\mu\text{m}$ . The second set of specimens was held in reserve for possible preparation of undecalcified sections, the need for which was to be determined by the results obtained in the decalcified sections.

Bone density was to have been determined by photodensitometry; however, acquisition of the photodensitometer unit by the University of Pennsylvania was delayed so that bone densities were unable to be determined.

Blubber. Full-thickness cores of skin and blubber from four hunter-killed whales were analyzed for gross and microscopic characteristics. Specimens were cut into (2-4 cm in diameter) cores and preserved in 10% phosphate-buffered formalin by collection personnel of RU-180. All cores were measured, photographed and examined to ascertain gross structure. Selected sections were cut into 5 mm slabs, dehydrated through ascending concentrations of alcohol, embedded in paraffin, sectioned at 5  $\mu\text{m}$ , and stained with hematoxylin and eosin as well as Masson's trichrome.

Lymphoimmune System. Selected lymphoid tissues and organs from both the 1979 and 1980 Eskimo bowhead harvest were examined, measured and photographed. Tissues were cut into 5 mm thick sections, fixed in 10% phosphate-buffered formalin, dehydrated through ascending concentrations of alcohol, embedded in paraffin, sectioned at 5  $\mu\text{m}$  and stained with hematoxylin and eosin. Selected sections were stained with Weigert's elastic stain, Masson's trichrome stain and Wilder's reticulum stain.

Cardiovascular System. See Appendix II.

## RESULTS

Bone. Grossly, long bones of the bowhead whales were characterized by the presence of articular cartilage at both the proximal and distal ends. Small cavities interpreted to be vascular canals were present throughout the entire

thickness of the articular cartilage on both the proximal and distal surfaces. Growth plates were present in all bones examined. While they were relatively uniform in thickness from whale to whale, the growth plates in whale 78KK2 was much narrower than those in the other whales. In some areas of the growth plate in this whale, bone bridging had occurred. This suggested that the growth plate was undergoing closure in this individual and provided evidence that it was an older animal than the other whales. The epiphysis (area between the growth plate and the articular cartilage) consisted of dense spongy (cancellous) bone. A dense band of bone, the subchondral plate, was present immediately beneath the articular cartilage and a terminal bone plate was present adjacent to the growth plate.

The humeral and radial bone shafts were devoid of a medullary cavity and were instead filled by dense spongy bone. Usually, a large vascular plexus was observed in the midshaft region (Fig. 4-1). The cortices consisted of compact bone and were readily discernible from the spongy bone of the shaft at the junction of the two.

All vertebrae consisted of a vertebral body separated from the proximal and distal secondary centers of ossification by a growth plate. The entire vertebra consisted of dense spongy bone in which a large vascular plexus was present in the center of the vertebral body. A dense band of compact bone was present on the concave dorsal and ventral surfaces of the vertebral body (Fig. 4-2).

The vertebrae and long bones of the Ingotuk grossly were similar to those of the bowhead whales except that they were somewhat shorter and thicker with a marked increase in the quantity of spongy bone. This resulted in a marked decrease in the tissue spaces between the closely set bone trabeculae. This can be observed in Figures 4-2 and 4-3, which are paired radiographs of regular bowhead (80B7 and 78KK2) whales compared to the Ingotuk (80B8). In the long bones, the line of demarcation between the compact bone of the shaft and the cancellous bone in the medullary area was much less well defined in the Ingotuk, both grossly and radiographically, than in the regular bowhead whales (Fig. 4-4).

The articular surface of the proximal humerus was smooth and glistening with no evidence that there had been cartilaginous connections with adjacent or surrounding tissues. In contrast, the elbow and carpal joints were synchondroses in which the joint space separating two adjacent bones were bridged by cartilaginous connections (see Figs. 4-5 and 4-6). The carpal

bones in whale 79B4 contained a central, solitary ossification center surrounded by hyaline cartilage, in which there were numerous vascular canals (Figs. 4-7 and 4-8). In some areas, the proximity of the vascular canals to the cartilaginous bridges suggested that the vascular canals crossed the joint space. In the Ingotuk (80B8), four such ossification centers were observed in the carpal bones of the flipper. In addition, an irregular, solitary, radiopaque nidus of bone was present immediately adjacent to the ossified ulna (Figs. 21-10 and 21-11, See Appendix VI).

Histological evaluation of bone sections revealed numerous vascular canals in the articular cartilage overlying the bone of the epiphysis. The bone of the epiphysis was separated from the bone of the metaphysis by a cartilaginous growth plate (Fig. 4-9). It was similar in thickness in all bowheads except 79KK2 where it was either absent (proximal humerus) or considerably narrowed, (distal humerus) with focal areas of bone bridging between the epiphysis and the metaphysis (Fig. 4-10). The cartilage of the growth plate contained a central zone in which the chondrocytes were randomly arranged and few in number relative to the amount of matrix. However, the epiphyseal and metaphyseal surfaces of the growth plate contained large hypertrophic chondrocytes arranged in columns in a proximal-distal direction, with the largest cells near the bone surface. This latter feature was more prominent on the metaphyseal side of the growth plate (Fig. 4-11).

The spongy (cancellous) bone of the epiphysis and metaphysis in the regular bowhead whales and the gray whale consisted of broad trabeculae of bone whose trajectories were randomly arranged, i.e. oriented in both proximal-distal and medial-lateral directions (Fig. 4-12). The trabeculae consisted of solid bone in most areas. In the areas immediately beneath the articular cartilage and adjacent to the growth plate on the metaphyseal side, the trabeculae contained central cores of cartilage. A very dense subchondral plate was present immediately beneath the articular cartilage, and similarly, a terminal bone plate was present adjacent to the growth plate on the epiphyseal side.

The spaces between the trabeculae (intertrabecular spaces) frequently were empty or contained hemolyzed red blood cells, fat cells and connective tissue. It was not uncommon to observe one or more islands of hyaline cartilage in the intertrabecular spaces in either the epiphysis or metaphysis. Osteoblasts and osteoclasts were rarely observed on bone surfaces, and the osteocytic lacunae within the bone usually were empty. A large vascular plexus usually was present

in the medullary cavity in the midshaft region of the long bones and within the body of the vertebrae. The plexus contained arterioles, venules and loosely arranged connective tissue.

Histologic evaluation of bone sections from the Ingutuk (80B8) consisted of closely set trabeculae so that the appearance was more like that of compact bone than of spongy bone. The intertrabecular spaces were considerably reduced in size due to the broad caliber of the trabeculae of spongy bone. The tissue elements in the intertrabecular spaces were similar to those in regular bowhead whales. The subchondral and terminal plates of the epiphysis were broader and denser than in the regular bowheads. As in the regular bowhead whales, islands of hyaline cartilage occasionally were observed in the epiphysis and the metaphysis. Also, the growth plate of the Ingutuk was similar in morphology and width to that observed in regular bowhead whales.

In addition to their broader caliber, the trabeculae of the Ingutuk contained central cores of cartilage which were present in trabeculae from the subchondral plate beneath the articular cartilage to the growth plate. Similarly, these cores were also present in the trabeculae of the metaphysis and extended all the way to the midshaft region (Figs. 4-13 and 4-14). The cartilage cores gradually disappeared in the center of the vertebral body.

Radiographically, grossly and histologically, bone sections from whale 80B4 resembled those from the Ingutuk (80B8) more than those of the regular bowhead whales (Figs. 4-1, 4-15 and 4-16).

Baleen was evaluated by Research Unit 1380, and therefore was eliminated as an objective of this study.

Blubber. Measurements were carefully made to determine the extent and existence of skeletal muscle within the subcutaneous adipose tissue. A special effort was made to note any differences between 80B8, the Ingutuk, and the three regular bowhead whales.

A firm blubber layer was present beneath the thick epidermis. Histologically, this layer was comprised of a significant amount of dense collagenous connective tissue (Fig. 4-17). Beneath the blubber layer was an additional layer of adipose tissue seen in many of the core samples. This "second blubber layer" commonly referred to by Eskimo hunters appeared to be grossly a very oily adipose tissue devoid of the thick collagenous strands of the layer above it (Fig. 4-18, Tables 4-1 and 4-2).

The demarcation between the fibrous blubber and underlying adipose tissue was clearly demonstrated in all cores where both layers existed. The lack of the inner layer of adipose tissue on some cores most likely reflected a sample which was not full-thickness. A single sample from an unknown location on whale 80B1 revealed a continuous layer of fibrous blubber down to the level of skeletal muscle. This may be indicative of the lack of a two-layer adipose tissue distribution throughout the entire body of the bowhead.

The difficulty of sampling uniformity and on-site measuring made generalizations of blubber thickness between whales difficult to assess. In several samples small bundles of striated skeletal muscle fibers were present at the demarcation between the blubber layer and underlying adipose tissue (Figs. 4-19, 4-20). This is believed to be the cutaneous muscle. The direction of muscle fibers could not be determined from the limited specimens obtained.

Lymphoimmune System - Thymus. The thymus was examined from two bowhead whales. In each case, 79B1 and 80B8, the animal was an Ingutuk variant. The thymus appears as a lobulated gray parenchymal organ within the anterior mediastinum (Fig. 4-21). It is not known how many of the harvested bowheads actually possessed thymic tissue due to difficulty in finding this organ. Thymic tissue could be dissected free of associated mediastinal adipose tissue and mediastinal lymph nodes. Microscopically the thymus appeared to be made up of lobules partially separated by thin septa of collagenous connective tissue. Distinct cortical and medullary regions could be identified (Fig. 4-22). The cortex consisted of densely packed lymphocytes. Medullary regions contained lymphocytes as well as large epithelial reticular cells. Characteristic hyalinized thymic corpuscles were scattered throughout medullary areas.

Lymphoimmune System - Lymph Nodes. The gross and microscopic structure of lymph nodes from three 1980 (80B1, 80B2, 80B7) and three 1979 (79B1, 79B2, 79KK2) bowhead whales were studied. Gross observation showed that the nodes had a typically mammalian appearance with readily discernible gray cortical and darker medullary regions (Figs. 4-23 and 4-24). A tough fibrous capsule with black melanotic pigment was present in a colonic lymph node from 80B1.

Observations of the structure of lymphatic distribution in the bowhead whale were limited. It was readily apparent that the largest lymph nodes were associated with the mesentery of the alimentary tract especially the colon.

Lymph nodes which were sampled included mediastinal, periaortic, bronchial, mesenteric, colonic and perirectal.

Microscopically the bowhead lymph nodes had a typical mammalian pattern with cortical and medullary regions (Fig. 4-25). A connective tissue capsule surrounded the node and was made up of dense collagenous tissue and reticular fibers. Trabeculae extend from the capsule into the lymph node parenchyma. An interesting variation in the bowhead lymph node structure was the inverted appearance similar to the domestic pig. In this type of architectural arrangement the cortical and medullary tissues are reversed with the lymphatic nodules occupying a central position and medullary sinus areas peripheral.

It was extremely difficult to locate the hilar region in the bowhead lymph node and thus the vascular pattern through the organ is not known. In many nodes the capsule was thick with large lymphatic vessels and nerves penetrating the structure. There have been few reports of lymphatic structure of cetaceans and very few on baleen whales. For these reasons, it is difficult to compare the bowhead with other species of cetaceans and whales.

The histologic appearance of the bowhead lymph node was similar enough to domestic mammals to allow generalizations concerning the degree of antigenic exposure. It has been shown that lymphoproliferative states occur in diseased cetaceans (Simpson and Gardner, 1972). Germinal follicles, paracortical regions, and plasma cell differentiation were easy to visualize in many specimens which were studied. It was readily apparent that lymph nodes centered around the alimentary tract show numerous follicles with large germinal centers indicating reactivity. Similarly, lymph node specimens from other regions of the body had a cortical region devoid of germinal centers and little activity along the sinusoids indicating a relatively quiescent immune status.

No evidence of extramedullary hematopoiesis was present in any lymph nodes examined. The degree of lymphopoiesis which takes place within the node could not be determined but is probably similar to other mammals.

Lymphoimmune System - Spleen. Splenic samples have been studied from nine bowhead whales including two Ingotuks. Grossly there was variability in shape and size (Table 4-3). In general, cetaceans have small spleens (Arvy, 1970) and the bowhead whale was no exception. The spleen appeared to have a concave and convex surface with the concave side containing a hilar region where large vessels enter (Fig. 4-26).



Microscopic examination revealed the splenic capsule to be moderately thick compared to domestic mammals. It was comprised of collagenous connective tissue and reticular fibers. The amount of smooth muscle was not determined. Numerous vascular structures were present within the capsule and extending down into the trabecular network. Trabeculae were not particularly numerous in the bowhead spleen.

The vast majority of splenic parenchyma in Balaena mysticetus was made up of red pulp (Fig. 4-27). Light microscopic study revealed the spleen to be a venous, non-sinusoidal type similar to domestic ruminants. Primary capillaries were not apparent nor were marginal zones. White pulp regions were not prominent and germinal centers were not present in most specimens. This seems to indicate relative immunologic quiescence in the whale although splenic physiology in cetaceans is not well studied.

The splenic red pulp contained a similar cellular and reticular structure to well studied terrestrial mammals. Lymphoid and reticular cells predominated. No hemosiderophages or megakaryocytes were noted in any specimen examined. Similarly, no evidence of extramedullary hematopoiesis was found.

Lymphoimmune System - Gut-associated Lymphoid Tissue (GALT). No specimens were examined from the 1980 whale harvest but earlier 1979 specimens revealed a very marked amount of subepithelial lymphoid activity along all levels of gastrointestinal tract. Many lymphoid follicles with germinal centers were seen underlying modified epithelial surfaces (Fetter and Everitt, 1979).

The bowhead whale had a gut-associated lymphoepithelial organ (tonsil) at the colon-anal canal junction (Fetter and Everitt, 1979). Similar structures have been reported in the sperm whale, Physeter catodon (Uys and Best, 1966) and the gray whale, Eschrichtius robustus (Cowan and Brownell, 1974). Grossly, the anal tonsil appeared as irregular, slightly raised elevations (2-3 mm) with small crypt openings. Microscopically there was extensive lymphoid follicular activity with downgrowth of squamous epithelium.

A single specimen (79B1) revealed ulceration of the overlying epithelial surface and perivascular inflammation extending around the anal tonsil region (Fetter and Everitt, 1979). This ulceration was similar to reports in other cetaceans (Cowan and Brownell, 1974). The significance of the anal lymphoepithelial organ is unknown. It may play a significant role as a mammalian equivalent to the bursa of fabricius and be of major importance to the humoral immune response of the bowhead.

TABLE 4-1. EXAMINATION OF BLUBBER CORE SAMPLES TAKEN FROM VARIOUS SITES ON FOUR BOWHEAD WHALES

Sample Identification	Cutaneous Muscle	Origin of Sample	Whether Sample Extended To Underlying Musculature
80B1 #76	Not present	Unknown	Only a single blubber layer Full-thickness
80B7 1/2V	Present	Ventral midline halfway between flipper and fluke	Full-thickness
80B7 1/2MBH	Not present	1/2 meter caudal to blowhole	Not full-thickness
80B7 x 15	Present	Ventral midline near umbilicus	Full-thickness
80B8 #29	Not present	Mid-body lateral line	Not known if full-thickness
80B8 #97	Not present	Ventral midline one-third distance between flipper and flukes	Not known if full-thickness
80B8 #33	Present	1.2 meter caudal to left flipper on lateral line	Full-thickness
80B8 #1	Present	Unknown	Full-thickness
80B8 #8	Not present	4.5 cm above left eye	Full-thickness
80B8 #36	Present	Behind flipper	Full-thickness
80B8 #55	Present	Unknown	Not full-thickness
80B9 #13	Not present	61 cm behind blowhole	Full-thickness

TABLE 4-2. THICKNESS (cm) OF EPIDERMIS AND FIBROUS BLUBBER LAYER IN SAMPLES FROM FOUR BOWHEAD WHALES

Sample	Epidermis	Fibrous Blubber
80B1 #76	2	17
80B7 1/2V	2	22
80B7 1/2MBH	1.5	21
80B7 #15	2	16
80B8 #29	2	20
80B8 #97	2	20
80B8 #33	2.3	15.5
80B8 #1	2	17
80B8 #8	1.8	18
80B8 #36	2	16
80B8 #55	2	18
80B9 #13	2	28

TABLE 4-3. SPLENIC MEASUREMENTS FROM THREE BOWHEAD WHALES

Whale	Body Length (m)	Splenic Weight (kg)	Length* (cm)	Width* (cm)	Height* (cm)
79KK3	10.3	4.2	31	21	7
79KK4	10.2	4.6	33	24	8
80B9	13.6	5	48	25	9

\*Greatest measurement is indicated.

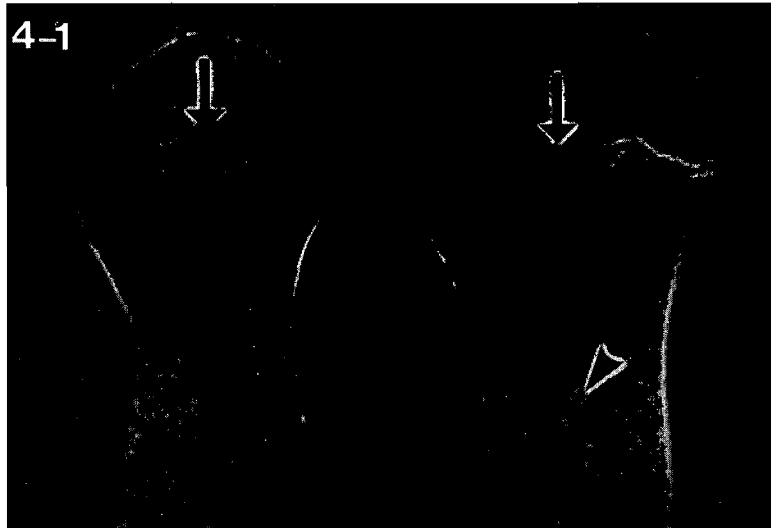


Figure 4-1. Radiograph of the proximal humerus from 80B4, considered to be a regular bowhead and an Ingotuk (80B8). Note the vascular plexus (arrowhead) in the shaft of the Ingotuk. Also, note the similarity in overall bone density of the two specimens. The growth plates (arrows) are similar in thickness in both bones.

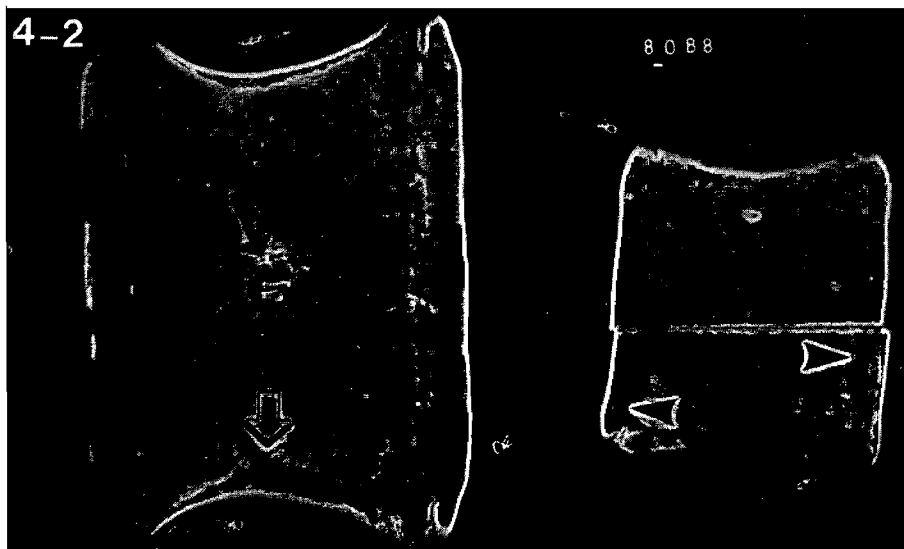


Figure 4-2. Radiograph of the vertebral body of a bowhead (80B7) compared to an Ingotuk (80B8). Note the anterior and posterior growth plates (arrowheads) and the alternating lines of radiopacity and radiolucency in both whales. Cortices of compact bone are present on the dorsal and ventral surfaces (open arrows). A central vascular plexus is identified in the regular bowhead (arrow).

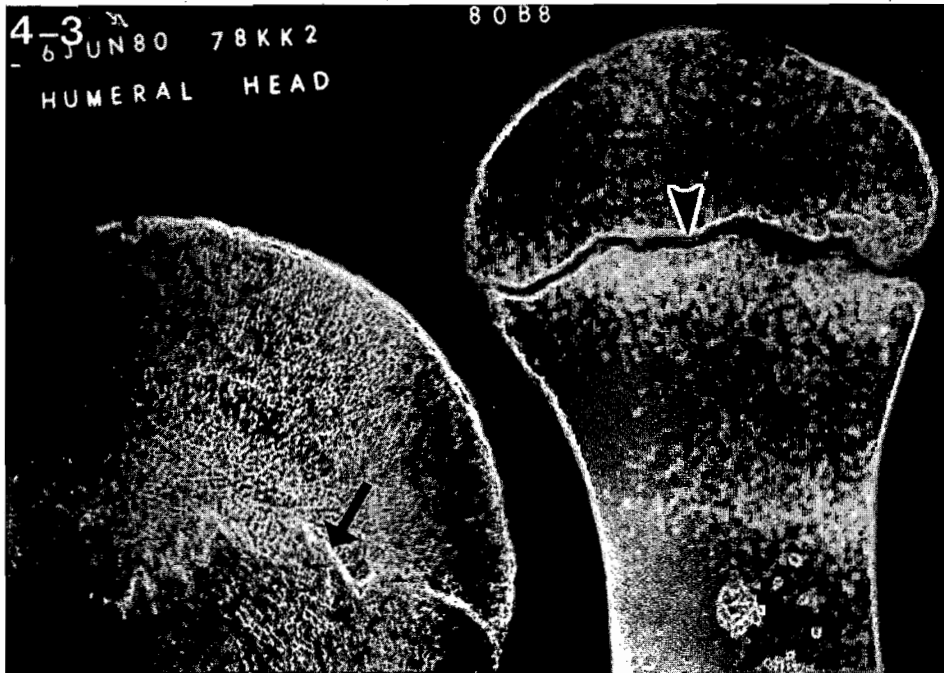


Figure 4-3. Radiograph of the humeral head in a bowhead (78KK2) compared to an Ingutuk (80B8). The bone of the Ingutuk is much denser than that of the bowhead, as indicated by the marked radiopacity of the humerus in the Ingutuk. The growth plate is present in the Ingutuk (arrowhead) but has closed in the bowhead with only a radiopaque line still present (arrow) which represents the terminal epiphyseal plate.

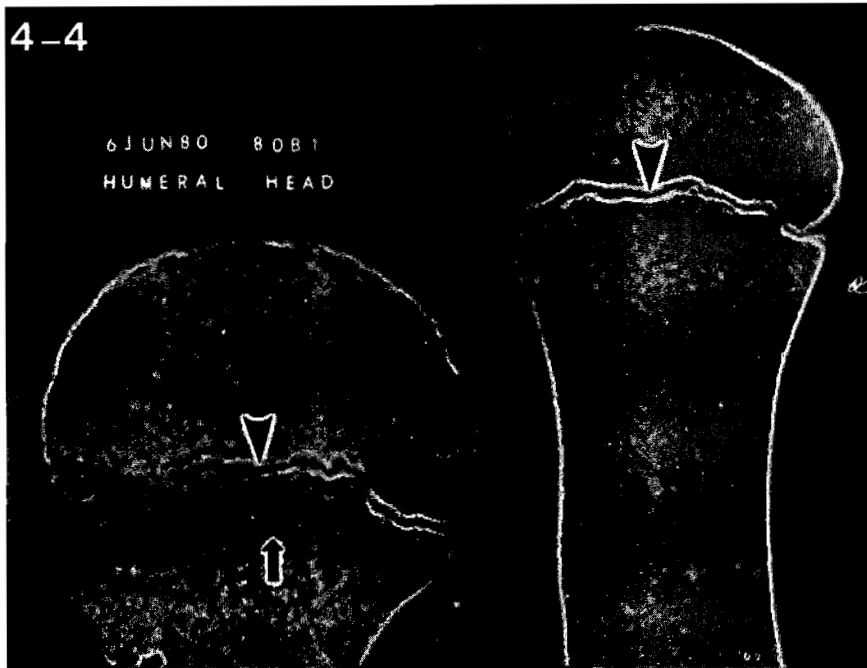


Figure 4-4. Radiograph similar to Figure 4-3 comparing the Ingotuk (80B8) to a bowhead (80B1). The growth plates are present in both whales (arrowheads). The line of demarcation between cortex and the spongy bone of the metaphysis is discernible in the bowhead (short arrow) but not in the Ingotuk. Note the layer of articular cartilage on the surface of the bones (C) and the line of radiopacity in the metaphysis, which represents a period of reduced growth with interconnections of the bone trabeculae (long arrow).



Figure 4-5. Photomicrograph of the synchondrosis of the carpal-metacarpal joint in a regular bowhead (79B4). Bands of hyaline cartilage extend into the joint space (J) between the cartilage of the two bones. H&E, 1.6X.

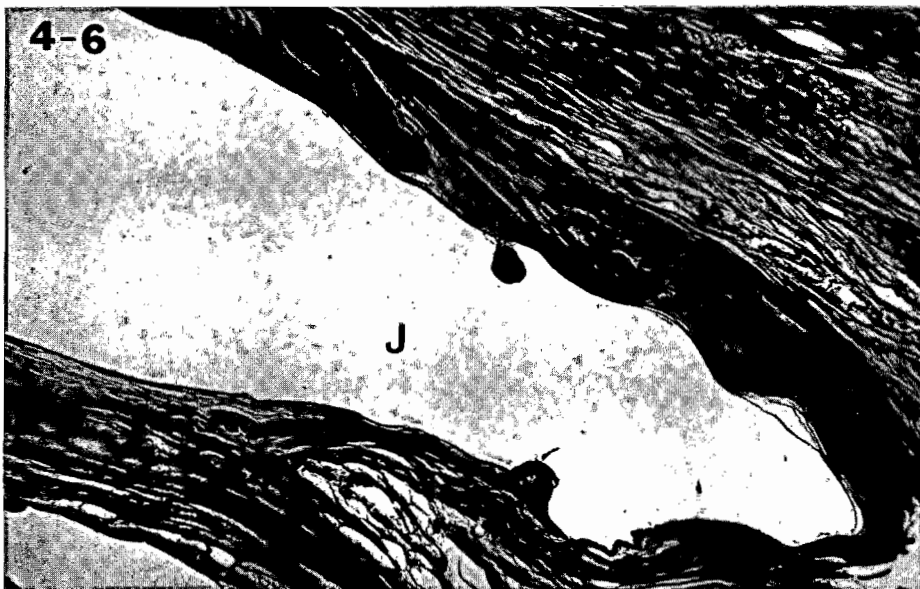


Figure 4-6. Higher magnification of a cartilage band extending across the joint space (J) between the distal ulna and carpal bone of bowhead 79B4. H&E, 10X.

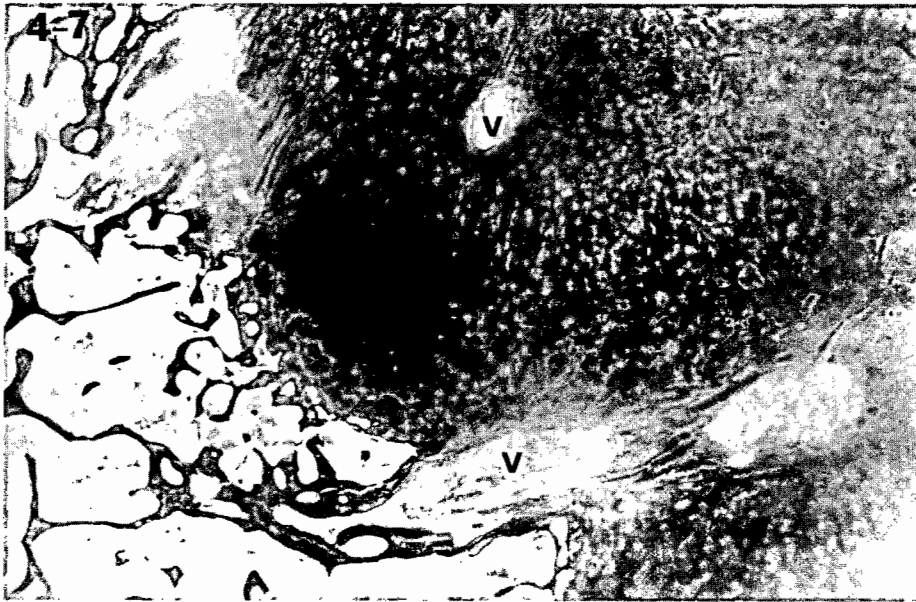


Figure 4-7. Junction of the secondary ossification center and hyaline cartilage in the carpal bone of bowhead 79B4. Vascular canals (V) are present within the cartilage and at the junction of cartilage and bone. H&E, 1.6X.

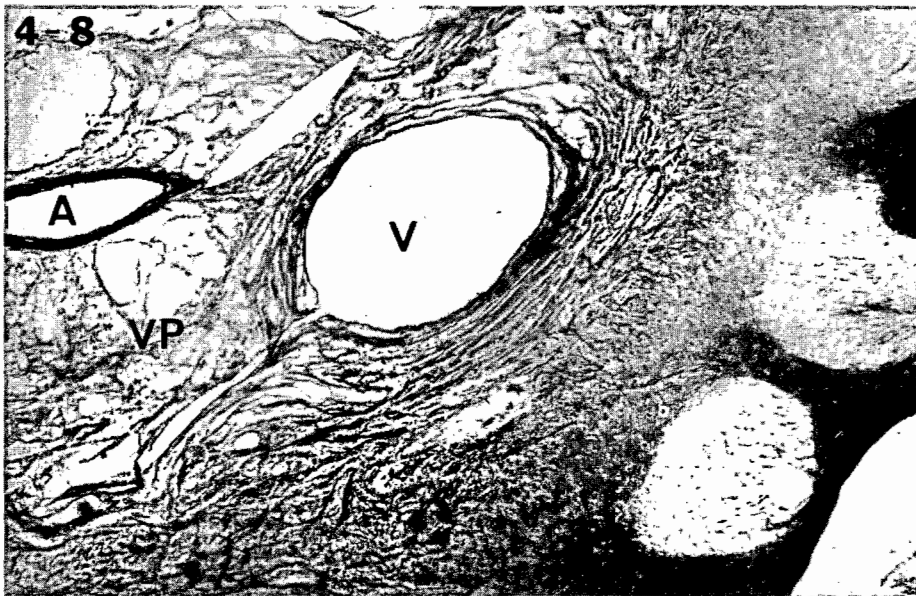


Figure 4-8. Vascular plexus (VP) consisting of arterioles (A) and venules (V) at the margin of a secondary ossification center in the carpal bone of bowhead 79B4. H&E, 10X.





Figure 4-9. Growth plate (arrow) separating the spongy bone of the epiphysis and the body (M = metaphysis) of the vertebra in bowhead 80B2. Note the delicate trabeculae of bone (arrowheads). H&E, 10X.

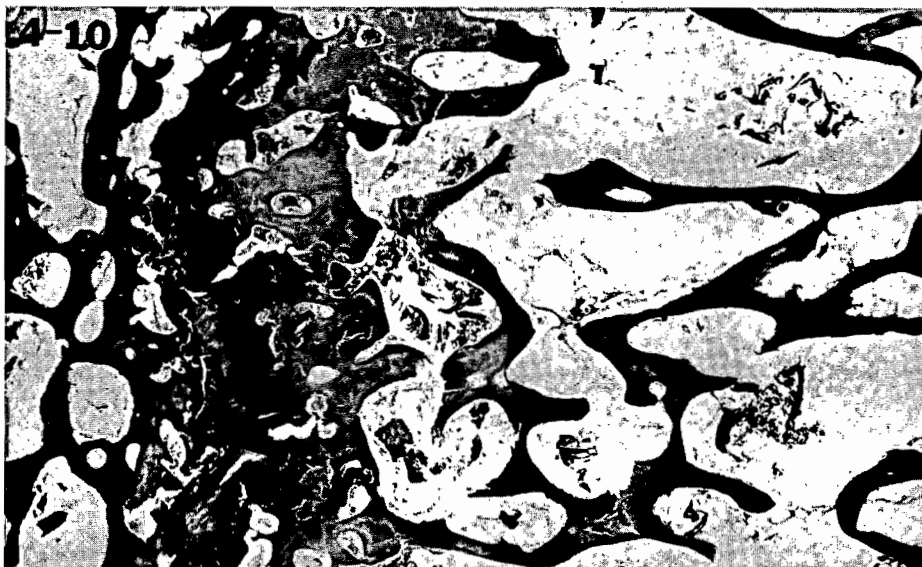


Figure 4-10. Distal humeral growth plate in bowhead 78KK2 in which there is bone bridging (arrowheads) indicating early closure of the growth plate. H&E, 10X.

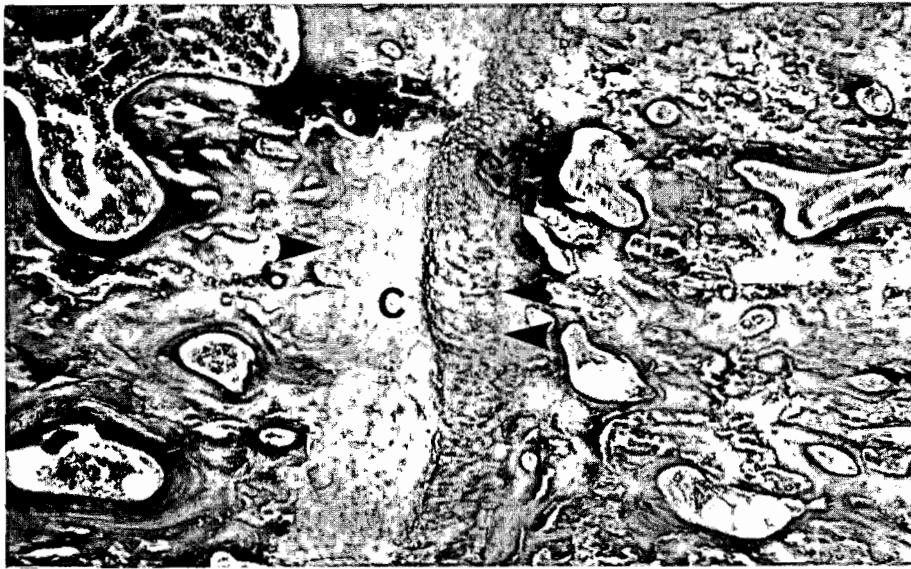


Figure 4-11. Growth plate of the Ingotuk (80B8) in which there is a central zone of chondrocytes (C) with a zone of hypertrophied chondrocytes on the epiphyseal side (arrowhead) and an even larger zone on the metaphyseal side (double arrowheads). H&E, 10X.



Figure 4-12. Spongy bone of the vertebral body in bowhead 80B2. Scattered central cores of cartilage (arrowheads) are present in the bone trabeculae adjacent to the growth plate. Note the prominent intertrabecular spaces (IT) and the hypertrophied chondrocytes of the growth plate (HC). H&E, 10X.

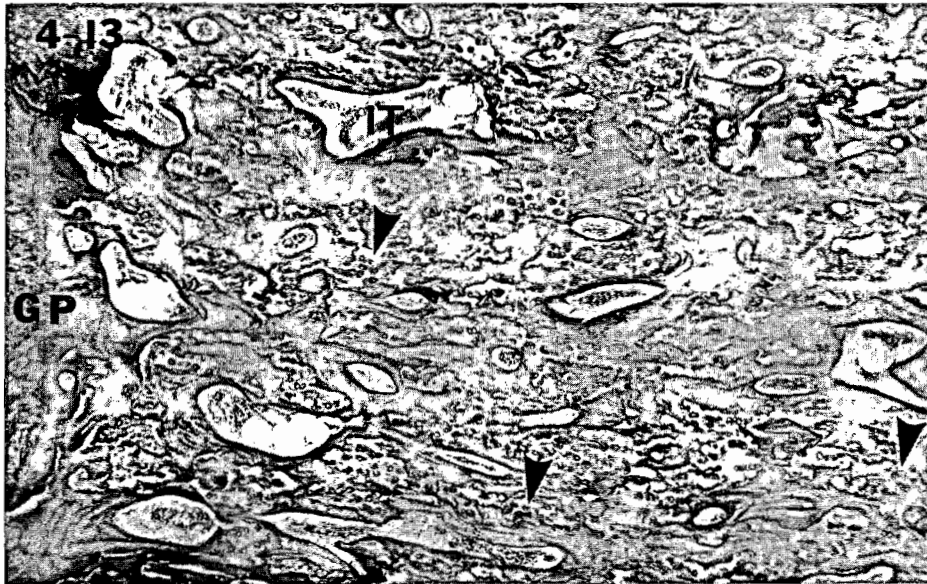


Figure 4-13. Spongy bone of the vertebral body immediately adjacent to the growth plate (GP) in the Ingotuk 80B8. Note the persistence of central cartilage cores (arrowheads) and the small number of intertrabecular spaces (IT).

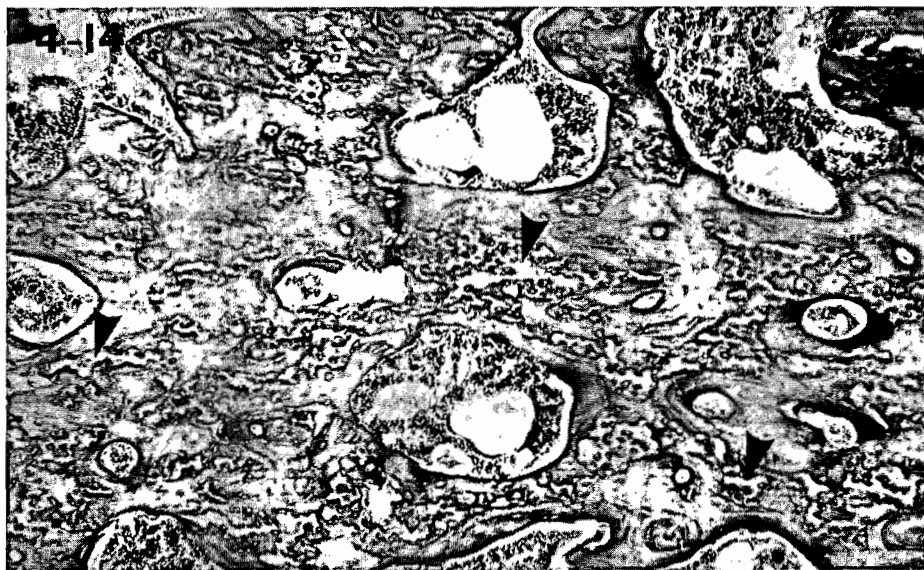


Figure 4-14. Same as Figure 4-13, but the section was taken further from the growth plate toward the center of the vertebral body. Again, note the numerous central cores of cartilage in the bone trabeculae (arrowheads). H&E, 10X.



Figure 4-15. Spongy bone of the metaphysis away from the growth plate and toward the midshaft of the humerus in bowhead 80B4. Note the compact appearance of the bone and the persistence of central cores of cartilage (arrowheads). H&E, 10X.



Figure 4-16. Spongy bone of the vertebral body adjacent to the growth plate (GP) in bowhead 80B4. The close-set trabeculae of bone give the appearance of compact bone. Note the central cores of cartilage (arrowheads). H&E, 10X.

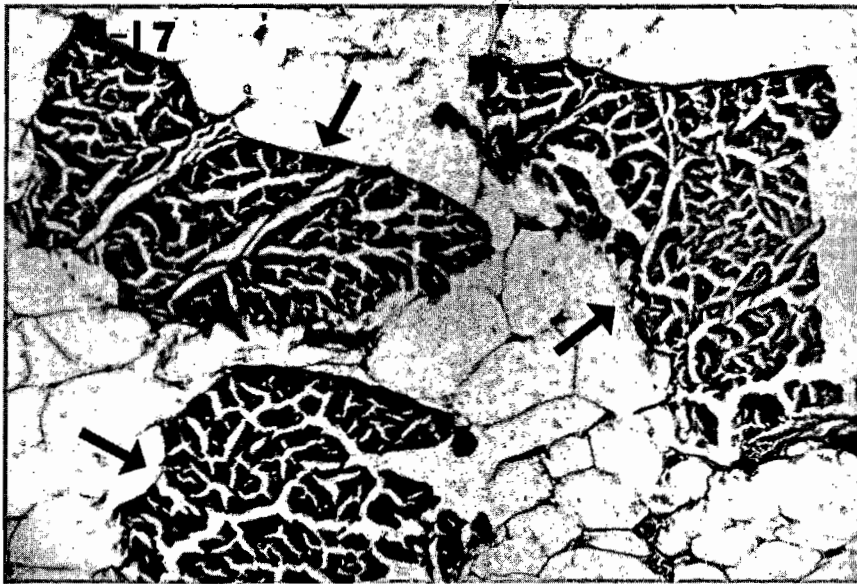


Figure 4-17. Several areas of dense collagenous connective tissue (arrows) within the fibrous blubber layer. Trichrome, 120X.

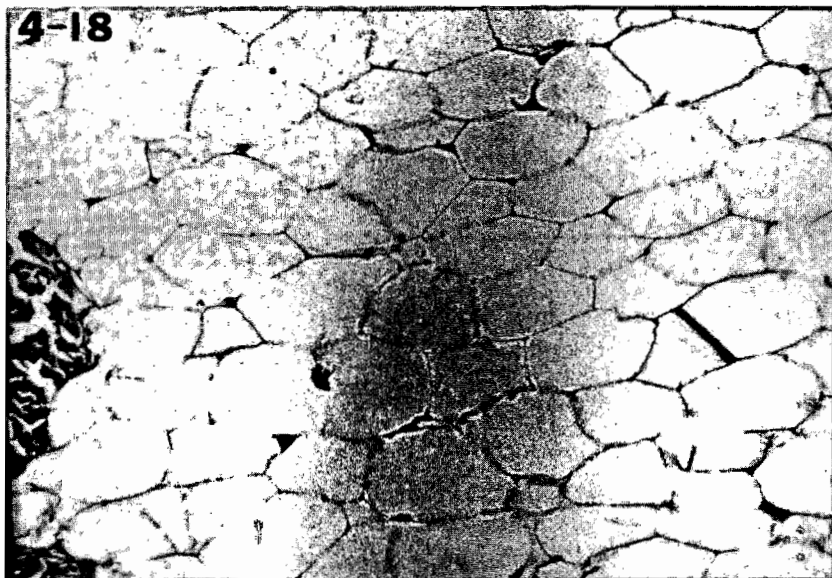


Figure 4-18. Mature adipose tissue which makes up the lower blubber layer in both the regular bowhead whale and the Ingutuk variant. H&E, 120X.

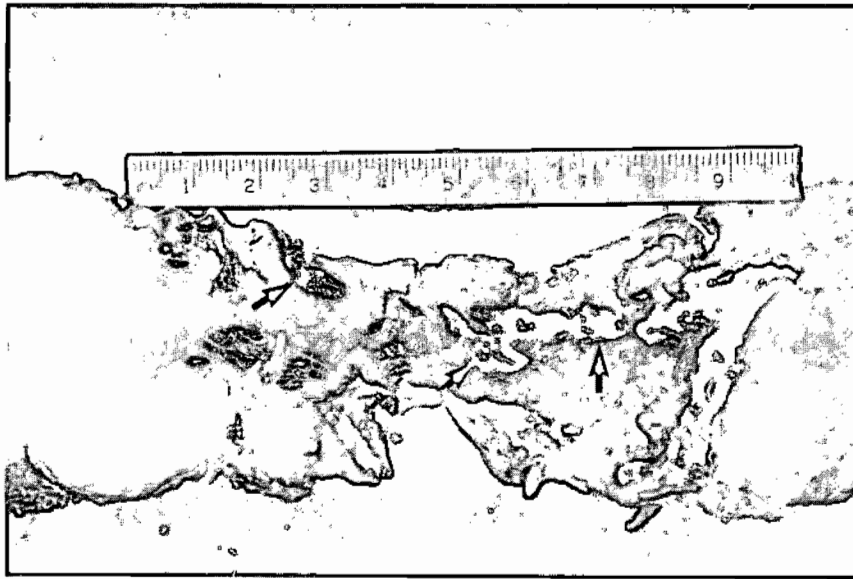


Figure 4-19. Gross photograph of the panniculus muscle of the Ingotuk 80B8. Arrows show skeletal muscle bundles.

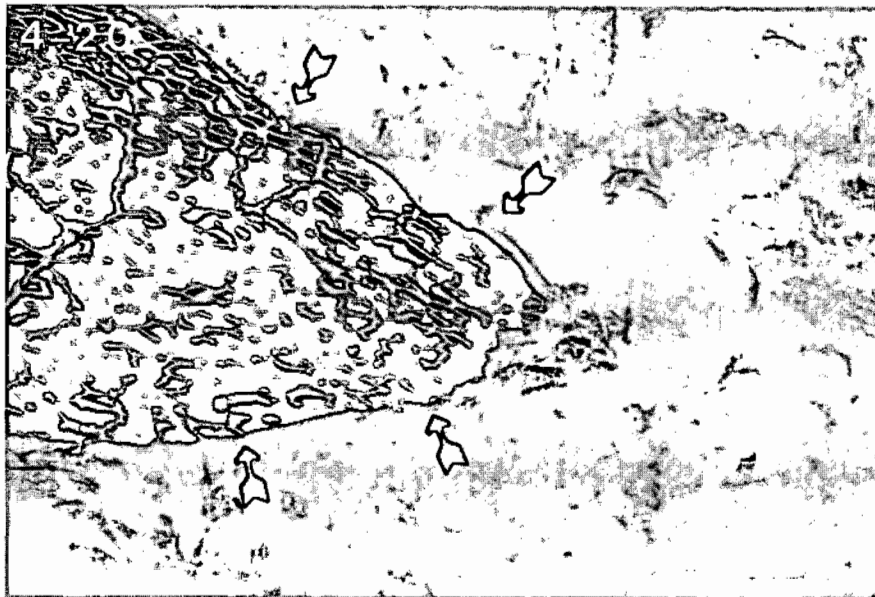


Figure 4-20. Photomicrograph of a striated skeletal muscle bundle from the panniculus muscle of the Ingotuk 80B8. H&E, 120X.

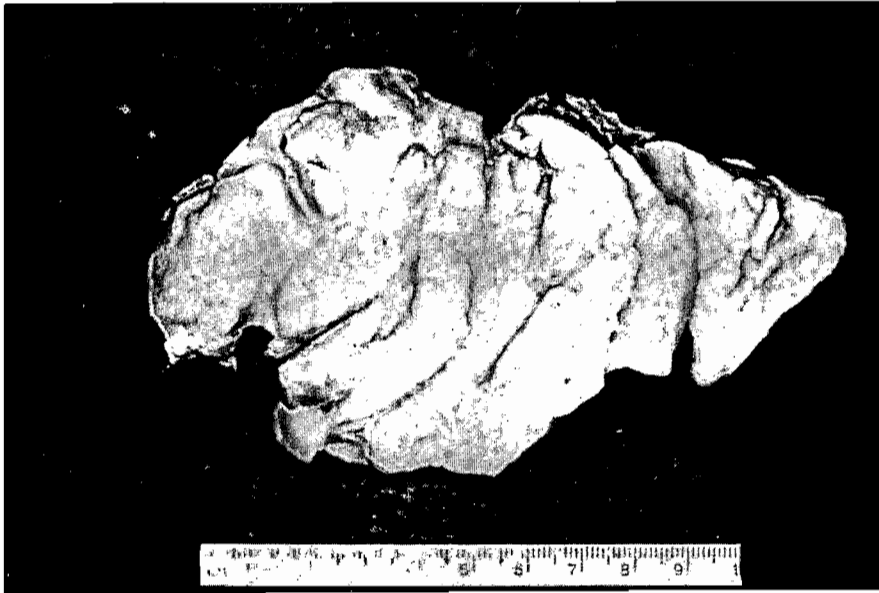


Figure 4-21. Thymus of the Ingotuk 80B8.

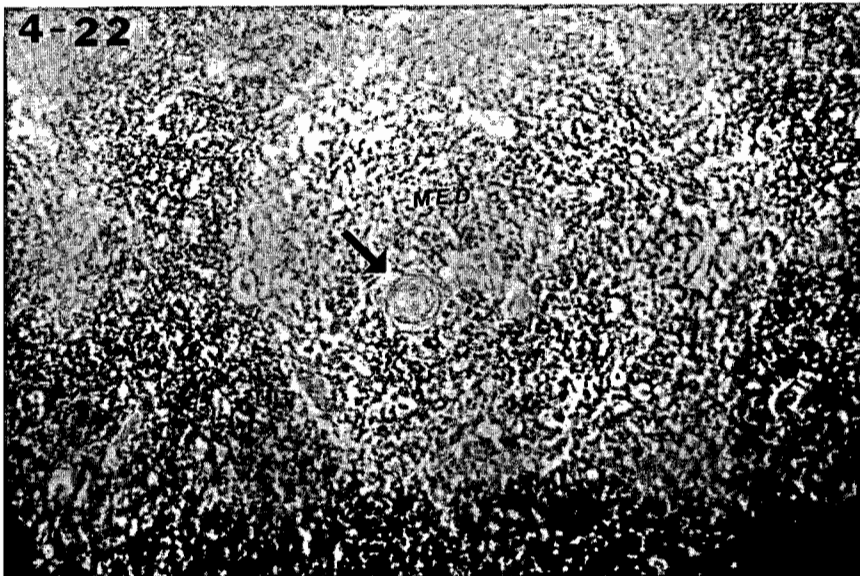


Figure 4-22. Photomicrograph of the thymic parenchyma which shows both cortical and medullary (MED) regions. The arrow demonstrates a Hassall's corpuscle.

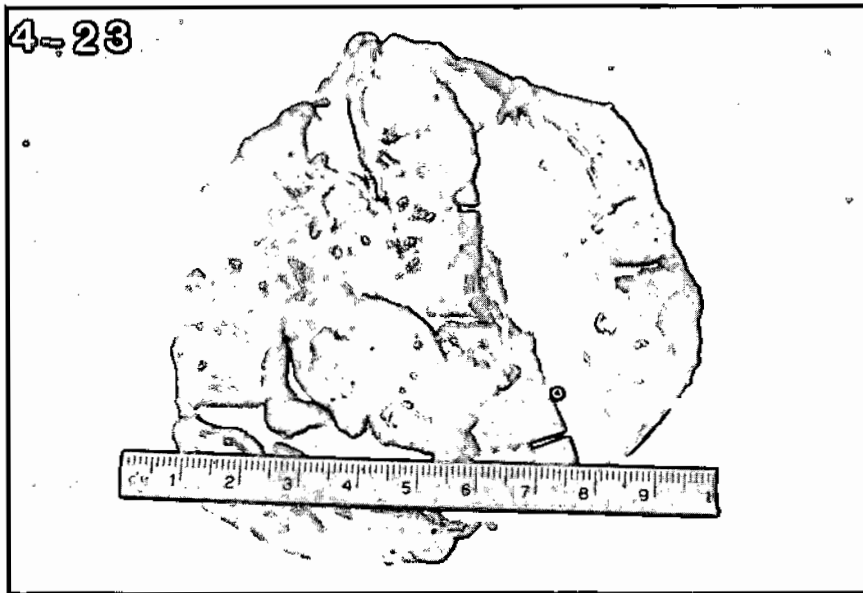


Figure 4-23. Lymph node from the gastric region of 80B7. Note the light gray cortical regions (arrows) which bulge on the cut surface. These represent follicular activity in a reactive lymph node. Darker surrounding tissue represents the medullary region.



Figure 4-24. Lymph node along the lower alimentary tract of 80B1. A reactive cortical region (dark arrow) and melanin pigment in the capsule (white arrow) are present.



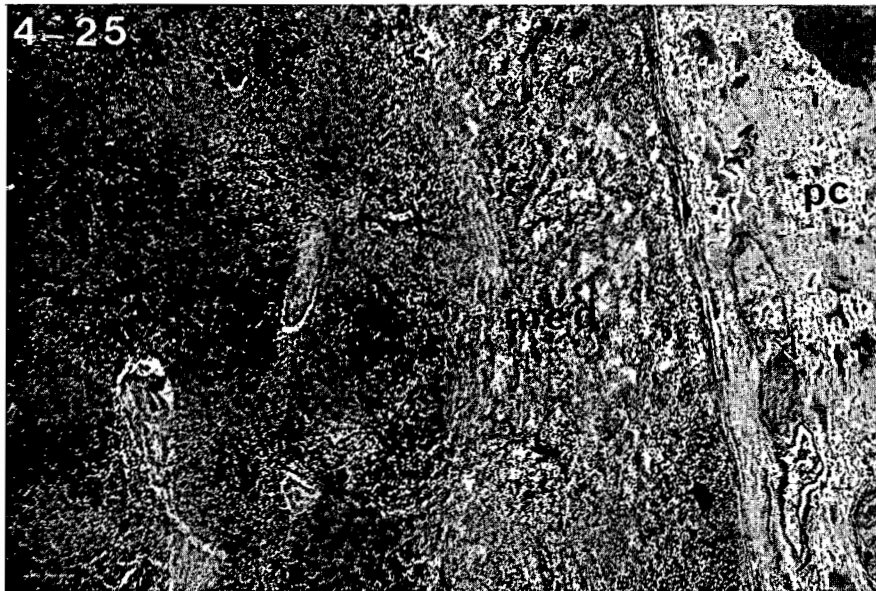


Figure 4-25. Lymph node depicting general nodal architecture. Loose connective tissue containing large vessels is present in the pericapsular (PC) region. Medullary sinuses (MED) are present in a subcapsular position. Follicular structures are present in the cortical region (COR). H&E, 40X.

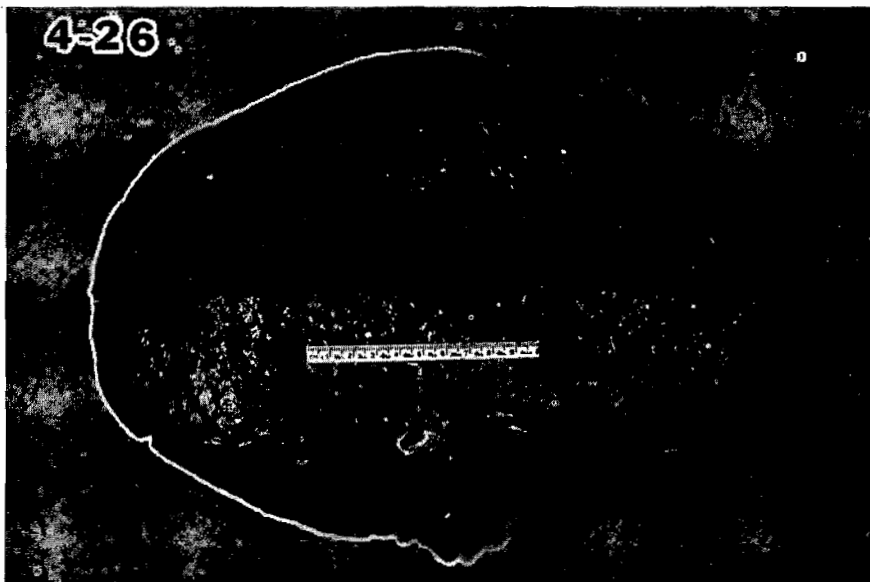


Figure 4-26. Convex face of the spleen of 79KK3.



Figure 4-27. Photomicrograph of the spleen of the Ingotuk 80B8. The arrows demonstrate white pulp regions. Note that the fibrous trabeculae are relatively sparse and contain vascular structures. H&E, 40X.

Cardiovascular System. See Appendix II.

Tissues of the Mouth. No tissue from the oral cavity was received by Research Unit 480.

#### DISCUSSION

Bone. The results of this study indicated that the gross and microscopic structure of bone in the regular bowhead whale resembles that described for other cetaceans (Felts and Spurrell, 1965; Felts and Spurrell, 1966). The enarthrodial shoulder articulation appears to be the only freely moveable joint in the flipper of the bowhead. The articulation of the radius and ulna with the distal humerus at the elbow and the articulation of the distal radius and ulna with the carpal bones are synarthroses. This form of articulation is capable of only limited motion, the opposing surfaces of bone being in almost direct contact and united by intervening connective tissue or hyaline cartilage.

The variability of the number of carpal bones reported in Appendix VI is consistent with previous reports in the literature for other mysticetes and odontocetes (Felts and Spurrell, 1965). The carpal bones in all of the bowhead whales in this study resembled those described in Appendix VI, i.e., they consisted of a small, central, discrete round to ovoid osseous component surrounded by hyaline cartilage. Thus, the carpal bones consisted predominantly of cartilaginous tissue. This suggests that either the carpal bones in the bowhead never completely ossify or that the bowheads in this study all were immature individuals with the central core of bone representing a secondary ossification center. Felts and Spurrell (1965) reported that the maturation of carpal centers was irregular and that the secondary bipolar phalangeal centers rarely were complete in older beluga and pilot whales.

The irregular radiopaque structure observed in Appendix VI, Fig. 21-10, is indicative of focal ossification in the cartilage immediately adjacent to the ulna. Similar structures in this location have been observed in other cetaceans (Ogden et al., 1981; Omura et al., 1970; Omura, 1975). Like Ogden's (1981) interpretation of a similar structure in this location in an immature fin whale, we concluded that this irregular, elongate bone represented a focal center of epiphyseal ossification.

Microscopically, the articular cartilage resembled that in other adult mammalian species except for the numerous vascular canals which were present from the articular surface to the subchondral region. The canals, which measured approximately 0.5-1.0 mm in diameter, contained arterioles, venules and loosely arranged connective tissue. They resembled vascular canals which have been described in the cartilage of the epiphysis of terrestrial mammals prior to the development of a secondary ossification center. Cartilage in all species is avascular in terms of capillary-sized vessels, nourishment being derived from diffusion of nutrients from the synovial fluid or vessels in the adjacent bone. However, when large masses of cartilage exceed the distance over which nutrients can diffuse, vascular canals then persist to provide sufficient nutrients to the cartilage. This appears to be the explanation for these structures in the articular cartilage of the bowhead, since the overall thickness of the articular cartilage is much greater than in terrestrial mammals.

The observation of columns of hypertrophied chondrocytes on both the epiphyseal and metaphyseal sides of the growth plate differs from that described in other mammals where this feature is limited primarily to the metaphyseal side. This finding in the bowhead suggests that the epiphyseal side of the growth plate makes a substantial contribution to longitudinal growth as well as the metaphyseal side. In other mammals, longitudinal growth is primarily due to enchondral bone formation on the metaphyseal surface with the epiphyseal contribution to longitudinal growth being minimal. The narrowed growth plate with focal areas of bone bridging in bowhead 78KK2 suggested that this whale was the oldest of any of the bowheads examined. This finding suggests that the growth plates of the bowhead do in fact close at a certain age and that the remaining bowheads were less mature than bowhead 78KK2.

The presence of islands of hyaline cartilage in the epiphysis and metaphysis of bowhead whales and the Ingutuk, as well as "tongues" of cartilage extending from the growth plate into the epiphysis or metaphysis resembled osteochondrosis, an abnormality of enchondral ossification described in dogs, pigs and horses (Olsson, 1976). Similar changes were observed in bowhead whales and in the Ingutuk in previous studies (Fetter and Everitt, 1979). Further, a similar condition has been described by Riser (1965) in fast-growing large breed dogs where elongated islands of cartilage persist in the metaphysis after closure of the growth plate. The cause of this condition is unknown, but genetic, nutritional, endocrinological and metabolic factors have been

incriminated. Although this interesting finding warrants further investigation in a larger number of whales, its definitive interpretation will be difficult without determination of the age of the whales investigated.

Histologic evaluation of the bone was essentially limited to the bone matrix, since the marrow elements were destroyed in virtually all specimens, apparently due to the combination of postmortem autolysis and freezing during specimen collection. Therefore, evidence of formation or resorption of bone was based on the appearance of bone surfaces, i.e. smooth surfaces indicative of bone formation and irregular scalloped surfaces indicative of resorption, rather than identification of osteoblasts and osteoclasts on the surfaces. Except for the cells within, the osseous and cartilaginous matrix were relatively unaffected by these adverse conditions.

The histologic features of the spongy (cancellous) and compact bone of the long bones and vertebrae in the regular bowhead whales and the gray whale were not remarkably different from that found in terrestrial mammals. The major difference was lack of proximal-distal orientation of the cancellous trabeculae in the bowhead compared to land mammals. This is undoubtedly due to the more uniform distribution of mechanical stresses in an aquatic environment compared to the mechanical stress which occurs in ambulatory mammals. Ambulation also produces resonance which influences the overall structure of bone. These differences are best summarized by Wolff's Law, which states that "the internal architecture and the external form of a bone are related to its function, and change with altered function." This may also explain the smaller number of Haversian systems in the compact bone of the cortices in the long bones of the regular bowhead compared to terrestrial mammals.

The absence of a medullary cavity in regular bowhead whales and the Ingotuk is consistent with previous findings that all whale bones are without open medullary cavities. This feature apparently is related to full aquatic adaptation, since the bones of partially terrestrial sea lions, seals and walruses have some internal cavitation. Distinction definitely can be made, however, between the heavy solid bones of the Sirenia (manatee, dugong) (Fawcett, 1942) the penguins (Meister, 1962) and the rather lighter spongy bones of the bowhead and other cetaceans.

In spite of the absence of marrow elements and bone cells, close examination of the surfaces of the trabeculae of cancellous bone and the Haversian canals and vascular spaces in the compact cortical bone, revealed a striking

absence of remodeling. Bones in terrestrial mammals are characterized by constant turnover, i.e. osteoclastic removal of bone, and this in turn is followed by bone formation by osteoblasts. The resorption phase is characterized by concavities on the surface of the bone referred to as Howship's lacunae. Thus, even in the absence of the cells, the "footprint" of their former activity remains. Such features were much less common in the bones of the bowhead and Ingutuk than would be expected in other mammalian species, regardless of age. This suggests that the need for remodeling or reconstruction of the bone, as occurs in ambulatory mammals, is either not required or is absent in the aquatic bowhead.

The alternating lines of radiopacity and radiolucency observed in some long bones and in the vertebrae radiographically, were not readily apparent in histologic sections. This is most likely due to the small area encompassed in histologic section compared to the larger, thicker specimens in the radiographs. Further, although such lines of alternating density are readily recognized in mammals with their proximal-distal orientation of cancellous trabeculae, they are much less easily identified in the randomly arranged trabeculae of the bowhead. Their presence in man and domestic animals is indicative of growth "spurts", i.e. the dense lines correlate to decreased growth rate with broad, dense, interconnecting trabeculae, and the lucent lines correlate to periods of rapid growth with thin, delicate, longitudinally oriented trabeculae. Whether these findings are related to variation in the rate of growth due to the self-imposed starvation of the bowhead, or other factors, is speculative but warrants further investigation.

It is noteworthy that the bone specimens from bowhead 80B4 were similar to those of the Ingutuk. Although only the flipper was made available to RU-180 for this whale, there was no report that it had been an Ingutuk. Yet radiographically, grossly and microscopically, the bones from this whale were nearly identical in appearance to those in 80B8, suggesting that it too may have been an Ingutuk.

Histologically, the long bones and vertebrae of the Ingutuk (80B8) were remarkably different from those of the regular bowhead whales. The cancellous trabeculae were of broader caliber, resulting in increased bone mass, with decrease in the area of the intertrabecular spaces, giving the sections the appearance of compact rather than spongy bone. Based on these features, the bones of the Ingutuk resembled the pachyostotic bone of the manatee and dugong (Fawcett, 1942) and the penguin (Meister, 1962).

One very significant difference was present in the Ingotuk compared to the other species with pachyostosis, however. In the Ingotuk, the cancellous (spongy) trabeculae of the epiphysis and metaphysis virtually all contained central cartilage cores. This finding is evidence for a failure of skeletal remodeling during enchondral bone formation, which occurs beneath the articular cartilage at the subchondral plate, on the epiphyseal side of the growth plate at the terminal plate, and most importantly, on the metaphyseal side of the growth plate where most longitudinal growth of bone occurs. In order to fully understand the development of such a lesion, one must understand the normal process of enchondral bone formation at the growth plate. A brief review of this process follows.

The cartilaginous matrix between the columns of hypertrophied chondrocytes undergoes mineralization. Concurrently, the hypertrophied chondrocytes degenerate and die, with the space previously occupied by the cells now vacated to permit the ingress of capillary tufts from the metaphysis. These capillaries bring with them pluripotential mononuclear cells capable of differentiating into either osteoblasts, osteoclasts or chondroclasts. Chondroclasts normally resorb approximately three out of every four spicules of mineralized cartilage that extend from the growth plate into the metaphysis. In those remaining, osteoblasts then deposit bone (osteoid) on the surface of the remaining spicules of mineralized cartilage, which in effect serves as a scaffold for the new bone formation. The new bone trabeculae containing the central cores of cartilage extend into the metaphysis a short distance where a second wave of osteoclastic remodeling cuts them off, and new trabeculae of solid bone are formed which extend on toward the diaphysis of midshaft region. Thus, the cartilage-containing trabeculae are converted to trabeculae of solid bone.

Persistence of cartilage cores in either the epiphyseal or the metaphyseal trabeculae is not a normal feature of any mammalian species. Furthermore, there are no known reports in the literature that retention of cartilage cores occurs normally in any mammalian species postnatally. However, it is characteristic of congenital osteopetrosis (osteo=bone; petrosis=marble- or stone-like) in domestic mammals and mutant laboratory rodents (Greene, 1974; Marks Jr. 1973; Murphy, 1969; Walker, 1973) and Albers-Schönberg disease in man (Albers-Schönberg, 1904). In most of these species, the lesion has been found to be the result of a defect in osteoclastic remodeling. In some species the

osteoclasts are markedly decreased in number and/or are defective in their production or release of enzymes. Morphologic abnormalities also frequently are present in the osteoclasts from these species. Due to the defective osteoclastic remodeling, the cancellous trabeculae contain central cartilage cores which persist even into the midshaft region of the long bones. These animals may become anemic due to obliteration of the marrow spaces, which are essential in the postnatal period for hematopoietic activity. In some species, the bone defect is self-limiting with the bone returning to normal after a brief period of osteopetrosis.

The presence of such a bone "lesion" in the Ingutuk strongly suggests that the Ingutuk may be congenitally osteopetrotic. Defective enchondral bone formation in congenital osteopetrosis results in bones which are shorter, thicker and denser than normal. Thus, congenital osteopetrosis is a dwarfing disease. Affected animals are small in stature due to the abnormality in enchondral bone formation in the long bones, and usually have rounded, domed craniums as a result of the defective enchondral bone formation of the bones of the skull. The conformation of the Ingutuk, which is described to be shorter and "fatter" or more rounded than the regular bowhead whale, supports this tenet. The absence of central cartilage cores in the trabeculae in the central region of the vertebral bodies suggests that if such an osteoclast defect was present, it occurred after a period of normal remodeling, since the oldest bone of the vertebrae is that which is in the center of the vertebral body. Confirmation of the alterations in matrix was prevented by the severe postmortem autolysis and freezing which precluded evaluation of the number and morphology of bone cells.

Zangerl (1935) suggested that the pachyostosis of the Sirenia and penguin was a means of compensating for lung volume and overall buoyancy in the early stages of the return by mammals to marine life. Early marine reptiles had extremely dense limb bones but later fossil examples from the same lines possessed a less dense, even spongy, bone structure. Alternative theories in explanation of pachyostosis have implicated anoxia, and the state and function of the thyroid gland (Fawcett, 1942). However, retention of cartilage cores in the spongy bone is not a feature of any of these conditions. Therefore, the Ingutuk appears to be unique and distinct from other marine mammals which have been reported to be pachyostotic.



Recently, Braham et al. (1980) reported the Ingutuk to be a morphologic variant of the regular bowhead. Because a clear distinction between the Ingutuk and bowhead could not always be made, these authors suggested that the Ingutuk might be a developmental stage which would grow to become a "normal" bowhead. They also suggested that the Ingutuk may be a sex-related, i.e. female, trait.

We agree that the morphological features of the Ingutuk could be sex-linked genetic defect, perhaps with incomplete penetrance which would explain the variability in size and characteristics. However, the Ingutuk in this study was a male, which thereby discredits the female sex-linked theory. Further, the results of our study do not support, and in fact contradict, the suggestion that Ingutuks represent immature or developing bowheads.

Skeletally, there was no evidence that the Ingutuk was an early postnatal individual. Furthermore, it seems reasonable that, based on the number of regular bowheads examined, a variety of ages must have been included. This is supported by evidence for closure of the growth plate in bowhead 78KK2. However, all the bone sections from these whales were remarkably similar in their lack of central cartilage cores. Determination of the expected age for closure of the growth plates would certainly be advantageous in both the regular bowheads and the Ingutuk. For example, the sequence of epiphyseal fusion in other cetaceans has been found to be: distal humerus, proximal radius and ulna, proximal humerus, and then distal radius and ulna, in that order (Felts and Spurrell, 1965).

Based on the findings in this study, we concluded that a defect in skeletal remodeling exists in the Ingutuk which is not present in the regular bowhead. Further, this defect resembles that in terrestrial mammals with congenital osteopetrosis. For future investigations, and in order to confirm these findings, the single most valuable contribution that could be made would be acquisition of well-fixed bone specimens with minimal postmortem autolysis, i.e. specimens obtained within two to three hours of death and fixed in 10% buffered formalin, with little or no freezing. This is essential if detailed histologic evaluation of the bone marrow and bone cells is to be made, thereby allowing correlation of cellular changes with alteration in remodeling of the bone matrix.

Blubber. Blubber cores from regular bowheads and an Ingutuk variant were carefully examined to note similarities in structure from a gross morphologic and histologic viewpoint. The samples from four whales allowed one to determine that the regular bowhead and Ingutuk both have a two-layer subcutaneous depot of adipose tissue as well as a cutaneous skeletal muscle layer. No microscopic differences could be found in either the fibrous blubber layer or the underlying adipose layer.

Further work and many additional samples will have to be studied to determine if there are differences in the distribution of the blubber layers or orientation of the cutaneous muscles. Previous reports (Braham et al., 1980) have indicated the possibility of a thicker two-layer "blubber" in the Ingutuk variant. The two-layers of adipose tissue appear identical grossly and microscopically in the cores from three regular bowhead whales and the single Ingutuk which was sampled.

Lymphoimmune System. The bowhead whale had a typical mammalian thymus. It is of interest that in many species the thymus involutes with age and both thymic specimens which have been examined are from Ingutuks. This is probably a coincidence since a mediastinal structure is difficult to study at the harvest area and no special effort was undertaken to note the presence or absence of the organ. The interesting point concerns the belief of some people that the Ingutuk represents a young animal (Braham et al., 1980). Further observations concerning the absence or presence of the thymus in various sized animals are needed before conclusions can be drawn.

Morphologic examination of the lymphoid structures allowed several important conclusions to be made. All lymph nodes from regions of the body not associated with the alimentary canal revealed hyporeactive morphologic states. One can infer from this structural appearance that the animal was in a relative state of immunologic quiescence. This makes perfect sense when one considers that the whale resides in a relatively clean Arctic environment and has few known disease problems.

The activity of the gut-associated lymphoid tissue and lymph nodes along the alimentary tract make it apparent that the majority of the antigenic exposure of the bowhead is by the oral route. One must view with caution the oral ingestion of any possible toxicological insults to the lymphoid system for fear that it might jeopardize the immune status of the individual.

Thoracic lymph nodes appeared relatively inactive yet there was no reason to think that this part of the immune defense system could not respond to environmental insults to the respiratory system. Information concerning pulmonary immune mechanisms are lacking in cetaceans but appear important in disease states, as in terrestrial mammals (Simpson and Gardner, 1972).

The bowhead spleen as in other cetaceans was small and did not allow for "reservoir" function. The small spleen and large rete mirabilia make it probable that the bowhead whale blood pressure regulation takes place in the retes (Arvy, 1970). This would explain the splenic size and lack of well developed blood sinusoids.

Previous work describing the spleens of small Odontoceti including Delphinus delphis, Grampus griseus and Stenella styx (Arvy, 1970) demonstrated high malpighian corpuscle content. It is not known whether this is a species difference, a difference between Mysticeti and Odontoceti, or a difference in general antigenic exposure. This study demonstrated that in the bowhead whale in unpolluted waters there is little white pulp activity. No descriptions of the microscopic structure of Mysticeti spleens could be found in the literature.

Examination of the lymphoid organs did not reveal differences between the regular bowhead whale and the Ingutuk variant except for the thymic findings described above. This was particularly interesting concerning lack of extra-medullary hematopoiesis since the Ingutuk with osteopetrotic bones might have less red marrow reserve.

Cardiovascular System. See Appendix II.

#### SUMMARY

Bone. The gross and microscopic structure of bone specimens from six regular bowhead whales, one Ingutuk and one gray whale were evaluated. Bones from the regular bowhead and gray whale resembled bones which have been described from other cetaceans. Although age determination based on the appearance of the growth plate was not possible, the finding of early closure in the growth plates of one regular bowhead provided evidence that closure of the growth plates in fact does occur. However, the bones from these whales differed significantly from those of the Ingutuk. Grossly, bones from the Ingutuk were somewhat shorter and thicker (wider) than those from the regular bowhead. Microscopically, the number and caliber of the trabeculae of spongy bone

were much greater than in the regular bowheads, giving the bone a solid appearance similar to compact bone. In this respect, the bones of the Ingutuk resembled the pachyostotic bones of certain other marine mammals, e.g. the manatee and dugong. However, the spongy (cancellous) bone of the Ingutuk had persistence of central cartilage cores, a feature not present in the pachyostotic manatee and dugong. This unique feature of the Ingutuk is remarkably similar to the bone lesion in terrestrial mammals with congenital osteopetrosis and humans with Albers-Schönberg disease. Therefore, the skeletal changes in the Ingutuk appear to be unique and distinct from those in the regular bowhead as well as other marine mammals with pachyostotic bones.

Blubber. No differences were noted grossly or microscopically in blubber cores examined from three regular bowheads and a single Ingutuk. This gives additional circumstantial evidence that the Ingutuk is a morphologic variant of the bowhead whale Balaena mysticetus. Both forms have a double layer of subcutaneous adipose tissue with evidence of a cutaneous muscle.

Lymphoimmune System. The morphologic appearance of the lymphoid system of Balaena mysticetus indicated relative immunologic inactivity. This was a reflection of both good health and a relatively clean environment. The microscopic anatomy had a typical mammalian pattern which would allow "immunologic monitoring" for disease and pollutant-induced effects in the future.

The fact that the major lymphoid activity in the bowhead was centered around the alimentary tract makes one wary of any ingested intoxicant which might cause damage to the lymphoimmune system. The lack of lymphoid activity surrounding the respiratory system may imply an inability of the whale to cope with pathologic insults to the system.

The nature of the lymphoimmune system within the overall defense mechanism of mammals, makes toxic effects important and often difficult to assess. Lymphoid depletion with compromise of the immune system could cause increase in disease of the individuals affected and the population as a whole. These effects are often subtle and not direct toxic effects.

## REFERENCES

- Albers-Schönberg, H. 1904. Rontgenbilder einer seltenen Knochenerkrankung, Munchen. Med. Wschr. 51:365-376.
- Arvy, L. 1976. The unknowns of the lymphatic system in cetacea. In: Investigations on cetacea. G. Pilleri (ed.), Vol. 2, pp. 169-178, Berne.
- Arvy, L. and G. Pilleri. 1970. Some characteristics of the cetacean spleen. In: Investigations on cetacean. G. Pilleri (ed.), Vol. 2, pp. 165-177, Berne.
- Braham, H. W., F. E. Durham, G. H. Jarrell and S. Leatherwood. 1980. Ingutuk: A morphological variant of the bowhead whale, Balaena mysticetus. Marine Fisheries Review, 42(9-10):70-73.
- Cowan, D. F. and R. L. Brownell, Jr. 1974. Gut-associated lymphoepithelial organ ("anal-tonsil") in the grey whale. In: Functional Anatomy of Marine Mammals. R. J. Harrison (ed.), Vol. 2, pp. 321-327, Academic Press, London, New York and San Francisco.
- Fawcett, D. W. 1942. The amedullary bones of the Florida manatee. Am. J. Anat., 71:271-309.
- Felts, W. J. L. and F. A. Spurrell. 1965. Structural orientation and density in cetacean humeri. Am. J. Anat., 116:171-204.
- Felts, W. J. L. and F. A. Spurrell. 1966. Some structural and developmental characteristics of cetacean (odontocete) radii. A study of adaptive osteogenesis. Am. J. Anat., 118:103-134.
- Fetter, A. W. and J. I. Everitt. 1979. Tissues structure/function (RU-280A). In: Investigations of the occurrence and behavior patterns of whales in the vicinity of the Beaufort Sea lease area. J. Kelley and G. Laursen (eds.), pp. 351-358. Final report to the Bureau of Land Management from the Naval Arctic Research Laboratory, Barrow, Alaska.
- Greene, H. J., H. W. Leipold, C. M. Hibbs and C. A. Kirkbride. 1974. Congenital osteopetrosis in angus calves. J.A.V.M.A., 164(4):389-395.
- Marks, S. C. Jr. 1973. Pathogenesis of osteopetrosis in the ia rat: reduced bone resorption due to reduced osteoclast function. Am. J. Anat., 138: 165-190.
- Meister, W. 1962. Histological structure of the long bones of penguins. Anat. Rec., 143:377-388.

- Murphy, H. M. 1969. A review of inherited osteopetrosis in the mouse. *Clinical Orthopaedics and Related Research*, 65:97-109.
- Nishiwaki, M. and Kasuya, T. 1971. Osteological note of an Antarctic Sei whale. *Sci. Rep. Whales Res. Inst.*, 23:83-89.
- Ogden, J. A., G. J. Conlogue, T. R. Light and T. R. Sloan. 1981. Fractures of the radius and ulna in a skeletally immature fin whale. *J. Wildlife Diseases*, 17(1):111-116.
- Olsson, S. 1976. Osteochondrosis - a growing problem to dog breeders. *Progress* (a journal of summary and comment published quarterly by the Gaines Dog Research Center, New York), P. Davis (ed.).
- Omura, H. 1972. An osteological study of the Cuvier's Beaked Whale, Ziphius cavirostris, in the northwest Pacific. *Sci. Rep. Whales Res. Inst.*, 24:1-34.
- Omura, H. 1975. Osteological study of the minke whale from the Antarctic. *Sci. Rep. Whales Res. Inst.*, 27:1-36.
- Omura, H. and T. Kasuya. 1976. Additional information on skeleton of the minke whale from the Antarctic. *Sci. Rep. Whales Res. Inst.*, 28:57-68.
- Omura, H., T. Ichihara and T. Kasuya. 1970. Osteology of pygmy blue whale with additional information on external and other characteristics. *Sci. Rep. Whales Res. Inst.*, 22:1-27.
- Omura, H., M. Nishiwaki and T. Kasuya. 1971. Further studies on two skeletons of the black right whale in the north Pacific. *Sci. Rep. Whales Res. Inst.*, 23:71-81.
- Riser, W. H. and J. F. Shirer. 1965. Normal and abnormal growth of the distal foreleg in large and giant dogs. *J. Am. Vet. Rad. Soc.*, VI:50-64.
- Simpson, J. G. and M. R. Gardner. 1972. Comparative microscopic anatomy of selected marine mammals. In: *Mammals of the Sea*. S. H. Ridgway (ed.), pp. 298-418, Charles C. Thomas Co.
- Uys, C. J. and P. B. Best. 1966. Pathology of lesions observed in whales flensed at Saldanha Bay, South Africa. *J. Comp. Path.*, 76:407-412.
- Walker, D. G. 1973. Experimental osteopetrosis. *Clinical Orthopaedics*, 97:158-174.
- Zangerl, R. 1935. IX. Pachypleurosaurus edwardsi, Cornalia sp. Ostelogie, Variationsbreite - Biologie. In: B. Peyer: *Dis Triasfauna der Tessiner Kalkalpen Abh. Schweiz. Pal. Ges.*, 56:1-80.

## RESEARCH UNIT 580

# THE BIOLOGY OF THE REPRODUCTIVE AND ENDOCRINE SYSTEMS OF THE BOWHEAD WHALE, BALAENA MYSTICETUS, AS DETERMINED BY EVALUATION OF TISSUES AND FLUIDS FROM SUBSISTENCE HARVESTED WHALES

ROBERT M. KENNEY, D.V.M., Ph.D.  
MAROLO C. GARCIA, D.V.M., Ph.D.  
JEFFREY I. EVERITT, D.V.M  
Departments of Clinical Studies and Pathology  
School of Veterinary Medicine  
University of Pennsylvania  
New Bolton Center, 382 W. Street Road  
Kennett Square, PA 19348

## INTRODUCTION

Reproductive function is essential to the survival of any species and is especially important to understand the effect of changes proposed in the environment of an endangered animal. This study involved the examination and assessment of various reproductive and endocrine tissues from Eskimo harvested bowhead whales in an effort to better understand the reproductive biology of the bowhead whale.

## OBJECTIVES

1. To determine the gross and microscopic structure of reproductive tract tissues and the major endocrine glands.
2. To relate reproductive hormone levels (blood, follicular fluid) to the histological structure of appropriate structures (uterine mucosa, testicles, ovary, etc.).
3. To determine the reproductive status (prepuberal, estrus, senile, etc.) of harvested whales.
4. To assess the function and status of the various reproductive tissues in the light of their determined structure and by comparison with better studied mammals.
5. To search for histological and hormonal changes that are age related in better studied mammals.

## METHODS

Intact reproductive organs in 10% phosphate-buffered formalin were received from RU 180 and represented eight Eskimo harvested bowhead whales from

the 1980 season. In addition, several important samples of the female reproductive tract were received from personnel of the National Marine Fisheries Service. Fixed reproductive samples were carefully examined grossly, measured, and photographed. Portions of these tissues and organs were cut into 5 mm thick slabs, embedded in paraffin and sectioned at 5  $\mu$ m. Most tissues were stained routinely with hematoxylin and eosin with selected specimens stained with Masson's trichrome or periodic acid-Schiff stains.

Frozen serum samples were received from four bowhead whales including an Ingutuk. Gonadal and adrenal steroids were quantitated with a single antibody method using charcoal dextran to separate the bound from the free hormone. Free steroids were extracted from the plasma samples with diethyl ether or hexane/ethyl acetate. All values were corrected for percent recovery and final values were expressed on a per milliliter plasma basis.

Total triiodothyronine and thyroxine levels were quantitated with a solid-phase radioimmunoassay procedure using  $^{125}\text{I}$  as the tracer.

## RESULTS

Mammary Glands, Nipples, and Genital Slit - Macroscopic Findings. Macroscopic examinations of the genital slit, nipple and mammary region were conducted on specimens from prepuberal bowhead whales 80B7 and 80B9 (Figs. 5-1, 5-3). Examination of the tissues from whale 80B9 revealed two supernumerary slits 20 cm and 35 cm lateral to a mammary slit (Fig. 5-2). One nipple each was enclosed within paired symmetrical, paravulvar, posterior abdominal mammary slits (Figs. 5-4, 5-5).

A nipple from 80B9 measured 4 cm in diameter at its base and was 4.5 cm in length. It was covered by a 5 mm thick epithelium. The lining of the teat cistern was made up of approximately 10 longitudinal folds which were 1-2 mm thick at the base. In the region between the teat and milk cistern were bundles of muscle fibers (Fig. 5-6) whose direction of orientation was impossible to determine.

Mammary Glands, Nipples, and Genital Slit - Microscopic Findings. No mammary tissue was detected in the specimens examined.



Microscopic examination of the nipple revealed the outer portion to be a thick, stratified squamous epithelium (Fig. 5-7) with well vascularized and extremely well-innervated subepithelial connective tissue (Fig. 5-8). The teat cistern was extremely interesting from a comparative anatomical viewpoint because it was characterized by numerous (10-12) primary longitudinal folds which were covered with secondary folds (Fig. 5-9). All foldings were covered with stratified cuboidal to simple columnar epithelium (Fig. 5-10) beneath which were well vascularized pegs of submucosa. Polymorphonuclear leukocytes could be seen within the epithelial layer while aggregates of plasmacytes were present in the submucosal region (Fig. 5-11). Bundles of smooth muscle fibers were present in the connective tissue between the skin and the teat cistern.

Vagina and Vulva - Macroscopic Findings. The vagina of 76B11 was 70 cm long. It is not certain that this specimen included the entire vagina. The organ consisted of a series of longitudinal folds.

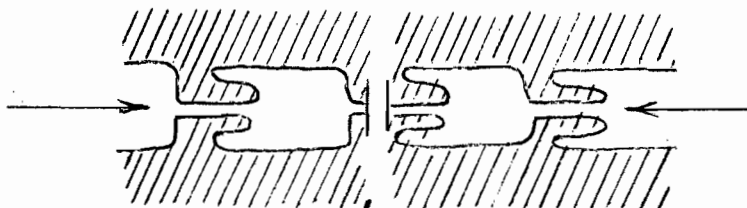
A single specimen (80B9) was available for examination of a large portion of the genital slit, vulva and clitoris. Both pigmented and non-pigmented stratified squamous epithelium covered the surface of the genital slit region. The vaginal compartment was completely pigmented. An 8 cm elongate, pigmented clitoris (Fig. 5-1) was at the end of the genital slit and covered the region believed to be the urethral swelling. It should be noted that there was no evidence of a vaginal band as has been described for several Balaenopterid whales (Ohsumi, 1969).

Vagina - Microscopic Findings. Microscopically the vaginal lumen was lined by stratified squamous epithelium 1 mm thick. Beneath the epithelium was an extremely dense collagenous connective tissue containing numerous thick-walled blood vessels and nerves. A distinct plasma cell infiltration directly below the epithelial covering indicated that the genital area is an area receiving antigenic stimulation. No evidence of mucus-secreting activity could be found in the sections of vagina examined from 80B1. Oblique smooth muscle bundles resided deep to the lamina propria.

Cervix - Macroscopic Findings. Several intact cervical samples were examined (76B11, 80B1, 80B9) and varied in size with the overall length of the whale as did other reproductive specimens. All of the specimens were from prepuberal females. The cervix in the two intact specimens appeared to have six separate

annular rings (Figs. 5-12, 5-13) each of which contained a variable number (approximately 20) of longitudinal folds up to 1 cm thick (Fig. 5-14).

The cervical rings are remarkable structures in that they are not merely raised annular folds. Rather they are very substantial structures which protrude posteriorly in the cervical canal for 5 cm. Their unique structure is represented diagrammatically in a mid-sagittal section.



The orifices of the cervical rings appeared oriented posteriorly towards the vagina. Macroscopically 80B1 cervical ring specimens possessed small, lucent structures 1-5 mm in diameter (Fig. 5-14).

Cervix - Microscopic Findings. Microscopic examination of cervical specimens revealed a stratified squamous epithelial lining without a transition to a mucus-secreting columnar epithelium (Fig. 5-15). There were numerous foci of inflammation in the cervix of 80B1 characterized by neutrophils in the epithelium (Fig. 5-16) as well as lymphocytes and plasmacytes in the connective tissue papillae (Figs. 5-17, 5-19). The circumscribed lucent regions noted macroscopically were large lymphoid nodules indicating the antigenic reactivity of this region (Fig. 5-18). A prominent muscularis mucosae was present. Both the lamina propria and muscular layers were well vascularized with thick-walled arterioles.

Uterus - Macroscopic Findings. The uterus grossly resembles that of a sow rather than that of a cow as has been previously reported (Kenney, 1979). Specimens studied from 76B11 and 80B9 (Fig. 5-20) indicated a relatively long uterine body and straight uncoiled uterine horns. Macroscopically it was readily apparent that there were no caruncles but there were prominent longitudinal linear folds (Fig. 5-21). Whale 80B1 had a uterine horn approximately 4 cm in diameter (Fig. 5-22) with an inner myometrial layer of circular smooth muscle fibers approximately 5 mm thick, a very prominent stratum vasculare, and a thin 1-2 mm thick longitudinal muscle layer.

As has been previously reported (Kenney, 1979) the bowhead has an extremely vascular uterus with numerous large veins running from the mesometrial

attachment through the broad ligament. Uterine horn size was equal bilaterally in both specimens examined.

Macroscopically there were approximately 15 longitudinal uterine folds (Fig. 5-21) which tapered from 4 mm wide at the base to 2 mm at the periphery. Each primary fold was subdivided into smaller secondary folds.

Uterus - Microscopic Findings. The folds noted on gross examination were evident microscopically as were the small secondary folds (Fig. 5-23). The folds consisted of a connective tissue core covered by the limina propria and cuboidal to columnal luminal epithelium (Figs. 5-24, 5-25). Figures 5-24 and 5-25 were chosen because they exhibit the above features while also showing gland-free areas. The luminal epithelium was simple columnal while the marked feature of the lamina propria was branched tubular glands (Fig 5-26).

What appeared to be uterine body 5 cm anterior to the cervix on gross examination had microscopic features of cervix with crypts rather than glands (Fig. 5-27). Just about at this level glands begin to appear (Fig. 5-28).

Oviduct - Macroscopic Findings. The oviduct in four prepuberal whales was about 25 cm long and 1 cm in diameter at the ovarian end and 0.3 cm in diameter at the uterine end. There was neither a bursa nor an infundibulum evident in the intact specimen examined. It is probable that the infundibulum was removed during collection. The opening to the oviduct appeared to be directly into the ampulla and is readily apparent in the specimen from 80B1 (Figs. 5-35, 5-36).

Oviduct - Microscopic Findings. The oviduct demonstrates thick longitudinal mucosal folds covered by a simple cuboidal epithelium. Inner circular and outer longitudinal smooth muscle layers are present (Figs. 5-29, 5-30).

Ovary - Macroscopic Findings. The ovaries were examined from three prepuberal (80B1, 80B7, 80B9) and one post-puberal animal (80G1) from the 1980 bowhead harvest. The size of the ovaries is presented in Table 5-1 and appears related to body length and sexual maturity. Figures 5-31 and 5-32 clearly reveal the difference in size between the pre and postpuberal ovaries.

The surface of the bowhead ovary is characterized by a series of irregular, randomized, frequently interconnected grooves which tended to be more prominent in one pole than the other (Fig. 5-35).

In cross-section the ovary is seen to consist of a richly vascularized medulla of 2-4 cm (Figs. 5-33, 5-34) covered by a cortex of 1-2 cm containing many follicles in both the pre and postpuberal animals. In the prepuberal ovaries, the antral follicles were up to 5 mm in diameter, but most were smaller. Covering the cortex is a tunica albuginea 1 mm thick which, in turn, is covered by a monolayer of squamous to cuboidal serosal cells as in other mammals.

One ovary of whale 80G1 had a corpus luteum with dimensions of 17 x 11 x 7 cm (Fig 5-46). In the fixed specimen this was pale yellow. It was characterized by radially arranged trabeculae.

Ovary - Microscopic Findings. The cortex contains very large numbers of typical mammalian primary follicles (Fig. 5-37). They consist of a monolayer of cuboidal follicular (granulosa) cells surrounding the oocyte which generally contained an active nucleus (Fig. 5-38). Many follicles exhibited some degree of autolysis. Ten primary follicles from 80B1 and 80B9 had the following measurements in microns.

<u>Follicle Diameter</u>	<u>Oocyte Diameter</u>	<u>Nucleus Diameter</u>
1. 60 x 50	40 x 20	20 x 10
2. 60	30	15
3. 40	25	15
4. 50	25	20 x 10
5. 60	25	10
6. 60	25	20
7. 60 x 50	35	10
8. 80	40	25 x 30
9. 50 x 60	30	20 x 15
10. 80	45	20

These fall in the same size range as reported for the sperm whale by Best (1972).

Once primary follicles begin to grow as indicated by hypertrophy and hyperplasia of the follicular (granulosa) cells they are called growing follicles (Rajakoski, 1960). Such follicles were very infrequent in these ovaries. When a growing follicle develops a fluid-filled space amongst the follicle (granulosa) cells and epithelioid cells appear adjacent to the basement membrane (theca interna) the follicle is called a Graafian (or antral) follicle (Rajakoski, 1960). These are characterized by a basement membrane which is lined by stratified

granulosa cells on the inside and is surrounded on the outside by a mixture of cells, the principal one being epithelioid cells, i.e. the theca epithelioid cells (Fig. 5-39). Both the granulosa and theca epithelioid cells are producers of gonadal steroids. Such a follicle is shown in Figure 5-40. Along with these primary follicles, most of the follicles in these ovaries were either primary ones or a mixture of viable and atretic antral follicles with only rare growing follicles in evidence. Viable antral follicles are those which have the potential to grow to maturity and ovulate. Atretic follicles are those which for unknown reasons undergo regression.

Basically two types of atresia were observed in these whales. Most common was cystic atresia wherein the granulosa and theca cells degenerate and disappear while the antrum remained distended with fluid. A low power view of such a follicle is shown in Figure 5-41. In a higher power view it is evident that most of the granulosa cells have degenerated and lysed and that no theca lutein cells are evident. In some such follicles there occasionally develop hyalin patches in the region of the former theca (Fig. 5-42).

The second type of atresia is termed obliterative (Rajakoski, 1960) since the antrum is filled-in with connective tissue rather than remaining fluid-filled (Fig. 5-43). Simultaneously with degeneration of the parenchymal cells a hyalin membrane develops in the former theca interna (Fig. 5-44). Eventually the space occupied by both types of atretic follicles is essentially returned to normal stroma. Occasionally the only remnant of the existence of a former follicle is a patch of convoluted hyalin membrane (Fig. 5-45).

Histologically the corpus luteum was divided into pseudolobules with trabeculae radiating inwards from the surface (Fig. 5-47). Parenchymal cells were granulosa lutein cells typical of the mammalian corpus luteum (Fig. 5-48). Admixed are atrophic and pyknotic cells which could have been caused by inadequate fixation or a corpus luteum in the early stages of involution. The cells typical of active mammalian luteal cells are large oval cells with abundant eosinophilic cytoplasm and a large relatively open-faced nucleus. There are abundant capillaries (Fig. 5-49) along with the active and atrophic, large luteal cells with cytoplasmic vacuoles (Fig. 5-50). Such changes are probably of a degenerative nature and lend support to the idea that the pyknotic cells are of a degenerative nature rather than autolytic.

Testicles and Efferent Tubules - Macroscopic Findings. The testicles, or portions of the testicles, were available from four prepuberal individuals from the 1980

harvest (80B3, 80B5, 80B8, 80WW1). The dimensions of the testicles are presented in Table 5-2. The prepuberal testicle with attached epididymis of 80WW1 as well as their relative sizes can be seen in Figure 5-51. The uniformity of the cut surface (Fig. 5-52) indicates the lack of mediastinum and rete testis. A very large vascular plexus was evident entering and leaving the testicle between the head of the epididymis and adjacent testicle (Figs. 5-53, 5-54).

Exiting the cephalic end of the testicle small tubules - probably efferent tubules - were found wrapped in circumferential connective tissue (Fig. 5-55). The bundles vary from 1-4 mm in diameter.

Testicles and Efferent Tubules - Microscopic Findings. Microscopically the parenchyma of the testicle is dominated by the prepuberal seminiferous tubules (Fig. 5-56) which are 45  $\mu$ m in diameter. The tubules are lined largely by Sertoli cells with a scattering of spermatogonia (Fig. 5-57). There is a remarkable lack of identifiable Leydig cells as evident in both of the above photographs.

It appears that after sperm leave the seminiferous tubules they would enter "collecting tubules" which appear randomly distributed throughout the parenchyma. Each convoluted seminiferous tubule probably leads into a "collecting tubule" which promptly enters a connective tissue trabecula (Fig. 5-58) which is connected to the tunica albuginea. By this means the "collecting tubules" are conducted to the tunica albuginea at the cephalad end of the testicle (Figs. 5-59, 5-60) through which they course toward the head of the epididymis (Fig. 5-61). They are simple channels lined by cuboidal epithelium (Fig. 5-60). As they course toward the end of the testicle they coalesce into nests of tubules encircled by a connective tissue "wreath" (Fig. 5-62). These are the efferent tubules seen leaving the cephalad end of the testicle in the gross specimen.

Epididymis and Ductus Deferens - Macroscopic Findings. The size of the epididymis of the prepuberal bowhead whale is remarkable for a mammalian epididymis. Its size relative to the testis is evident in Figure 5-63. The mass of convoluted, knobby tubules is not only longer than the respective testicle, but is almost as wide while only half as thick. It commences at the cephalad end of the testicle where the efferent tubules exit the tunical albuginea (Fig. 5-55).

The ductus deferens continues the excurrent duct system for sperm. It tends to be twisted, as can be seen in Figure 5-63. In terrestrial mammals it is not tortuous.

Epididymis and Ductus Deferens - Microscopic Findings. The efferent tubules from the testicle connect the collecting tubules to the epididymal duct. They are apparent in the region of the head of the epididymis still in the wreaths of connective tissue in which they left the testicle yet adjacent to epididymal tubule (Fig. 5-62). Once they have left the tunica albuginea of the testicle and crossed over to the head of the epididymis they can be differentiated from the epididymal tubules (Fig. 5-64).

The epididymal duct is remarkable for a mammal in that instead of consisting of a simple, single lumen duct it consists of a central duct from which branched glands or crypts extend to form "nests" each with their own circumferential connective tissue. An example of the configuration in the head is in Figure 5-66. The channels are lined by a simple columnar epithelium with a vacuolated cytoplasm (Fig. 5-67).

The same pattern is evident in the body (Fig. 5-68) as well as the tail (Fig. 5-69) of the epididymis where the individual locules are more prominent. The simple columnar epithelium remains the same throughout (Fig. 5-70).

The ductus deferens continues the pattern of a central channel with multiple glands or crypts seen in the epididymis (Fig. 5-71). It eventually became a single channel.

Pituitary - Macroscopic Findings. Pituitaries were available from a male (80B8) and a female (80B1). That from 80B1 was in the best state of preservation. In the mid-sagittal section there were two large, sharply demarcated areas (Figs. 5-72, 5-73) and a third smaller one. The pituitary was surrounded by a vascular rete (Fig. 5-74). The more anterior portion (part A) appears to correspond to the pars distalis. A sharp line of demarcation separated it from the portion termed part B. The third smaller portion appeared to cap the posterior aspect and is designated part C.

No evidence of a cleft or neurohypophysis was found.

Pituitary - Microscopic Findings. The portion labeled part A is the pars distalis and can be divided into a cortex rich in acidophils (Fig. 5-75) and a medulla which was more vascular and had fewer but still numerous acidophils (Fig. 5-76).

Histologically there was no evidence of either a neurohypophysis or intermediate lobe.

Figure 5-1. Portion of the genital slit of 80B9 showing a view of the pigmented clitoris (arrow).

Figure 5-2. Mammary slit of 80B9 showing nipple (central arrowhead) within fold. Supernumerary mammary slits medially and laterally (arrows).

Figure 5-3. Genital slit of 80B9 demonstrating relationship of mammary slits and supernumerary mammary slits.

Figure 5-4. View of teat of 80B7 showing the unpigmented surface epithelium around the teat orifice.

Figure 5-5. Nipple, which has been transected longitudinally, and underlying connective tissue of 80B9.



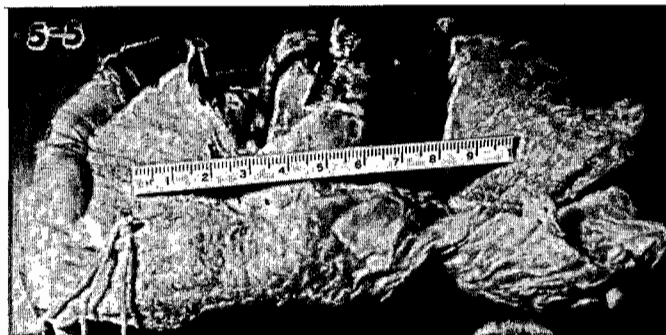
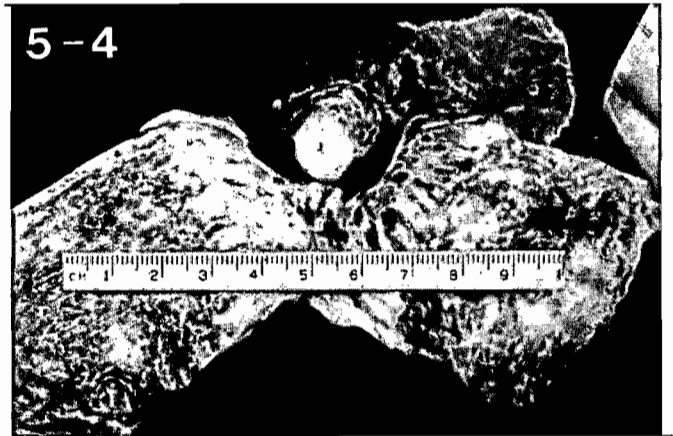
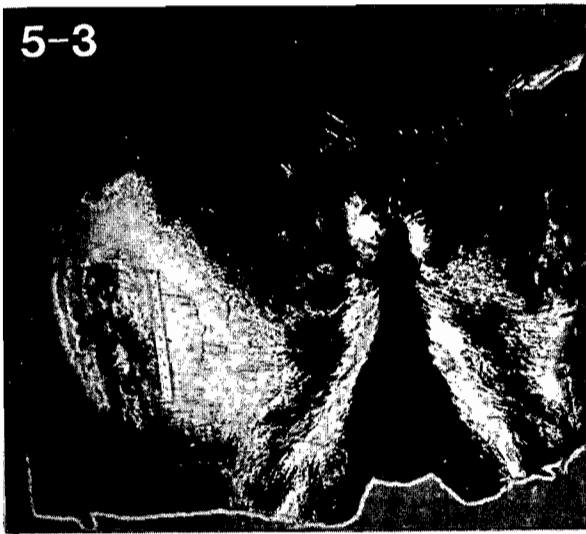
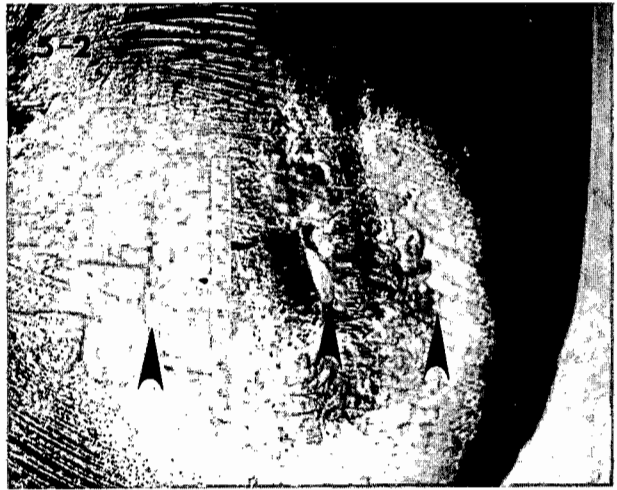


Figure 5-6. Photo depicts the muscle bundles (white arrow) surrounding the base of the teat cistern (black arrow) of 80B9.

Figure 5-7. Photomicrograph of the stratified squamous epithelium which overlies the nipple. (H&E, 30X)

Figure 5-8. Nerve bundles (n) within the subepithelial connective tissue of the teat cistern from 80B9. (H&E, 120X)

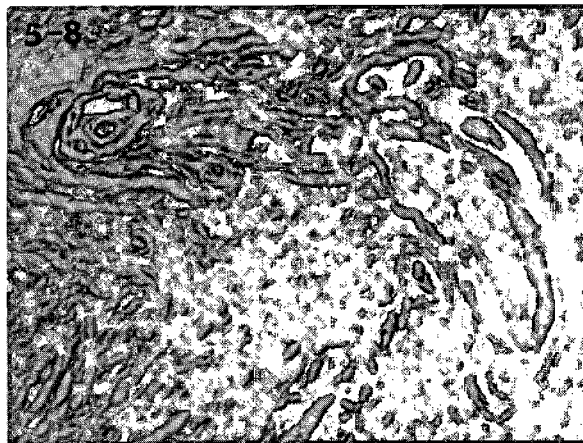
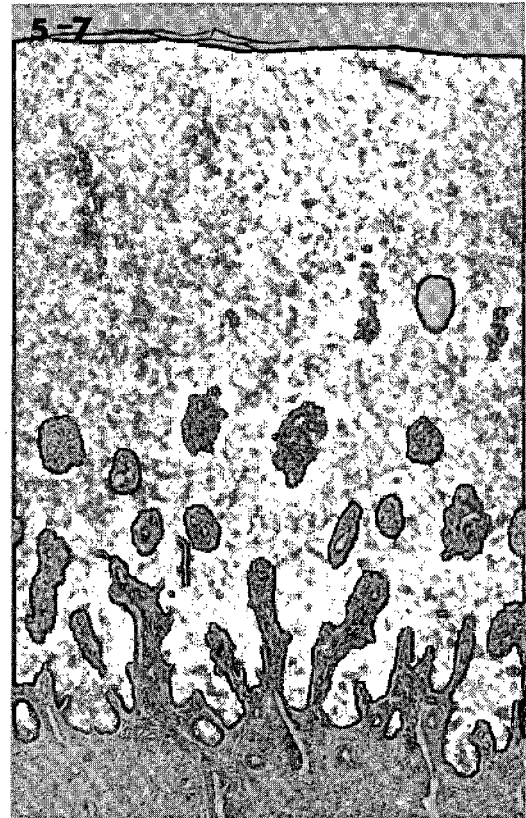


Figure 5-9. Photomicrograph shows the extensive folding pattern lining the teat cistern. (H&E, 30X)

Figure 5-10. Photomicrograph demonstrates the stratified cuboidal to columnar epithelium lining the teat cistern of 80B9. (H&E, 480X)

Figure 5-11. Photomicrograph shows a round cell focus adjacent to a venule (ven) in the subepithelial tissue of the teat of 80B9. (H&E 480X)

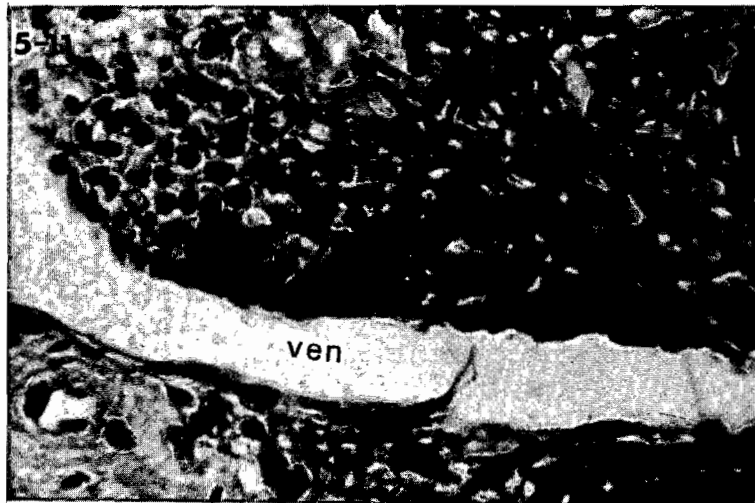


Figure 5-12. The cervix and genital slit (single arrow) of 76B11. Note the three annular rings oriented posteriorly (demonstrated by the double arrows).

Figure 5-13. Cervix of 80B1 at the vaginal junction. An opened annular ring is represented (the small arrows). A closed annular ring is present (arrowhead). Note the longitudinal folds on the cervical rings.

Figure 5-14. A portion of an annular cervical ring showing lucent regions which histologically represented lymphoid follicles.

Figure 5-15. Photomicrograph of the stratified squamous cervical epithelium of 80B1. Note the nuclei in all cellular layers, and the inflammatory cells in the subepithelial connective tissue. (H&E, 120X)

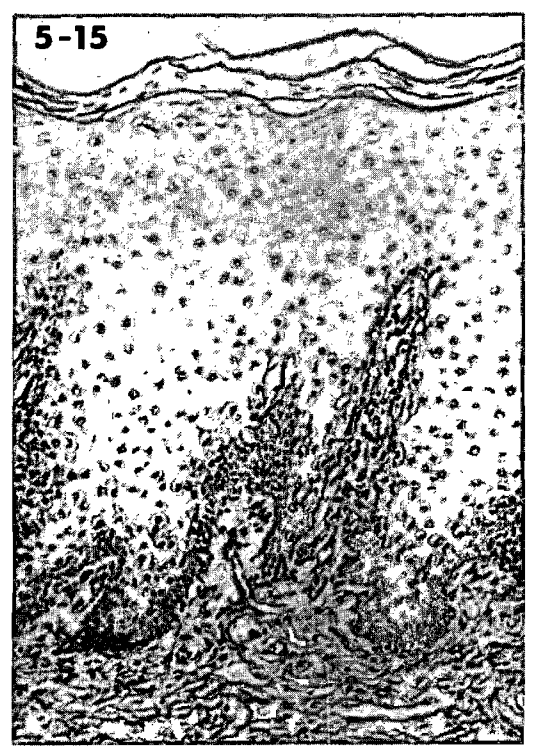
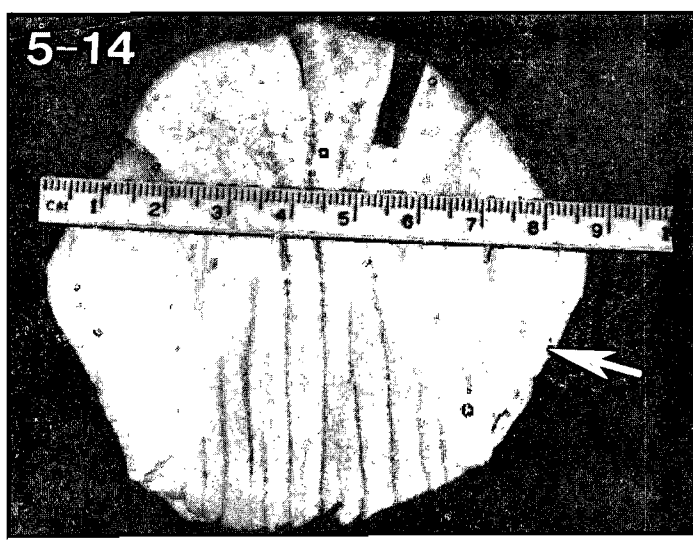
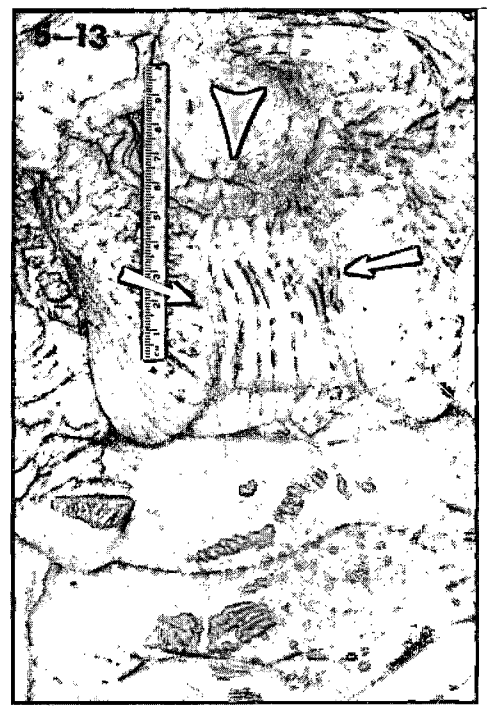
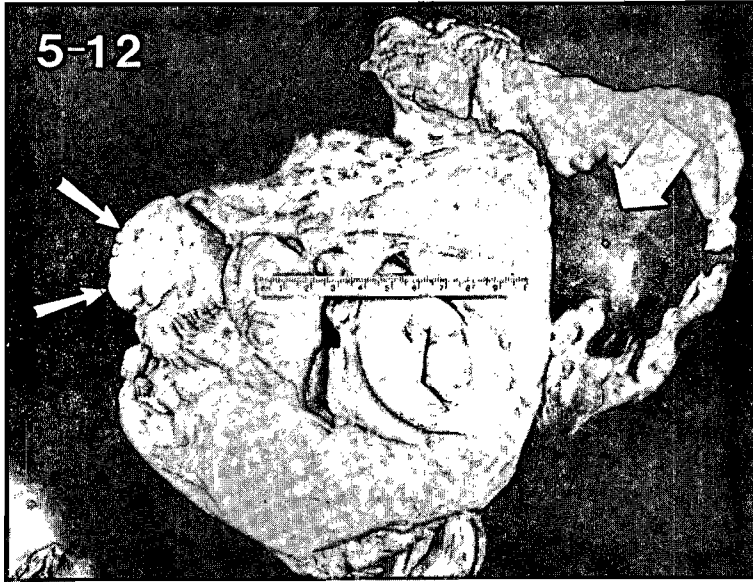


Figure 5-16. Photomicrograph depicts a region of cervix from 80B1 which has acute inflammatory changes. Numerous polymorphonuclear leukocytes are present through all layers of epithelium while lymphocytes are in subepithelial connective tissue. (H&E, 120X)

Figure 5-17. Photomicrograph shows numerous polymorphonuclear leukocytes (arrows) in the stratified squamous epithelium of the cervix of 80B1. This is an acute cervicitis. (H&E, 480X)

Figure 5-18. Photomicrograph demonstrates a lymphoid nodule from the cervix of 80B1. This region corresponds to a lucent region on the surface of the cervical ring shown in Figure 5-14. (H&E, 45X)

Figure 5-19. Photomicrograph from the vagina of 80B1 which demonstrates the numerous subepithelial lymphoid cells and plasma cells. (H&E, 480X)



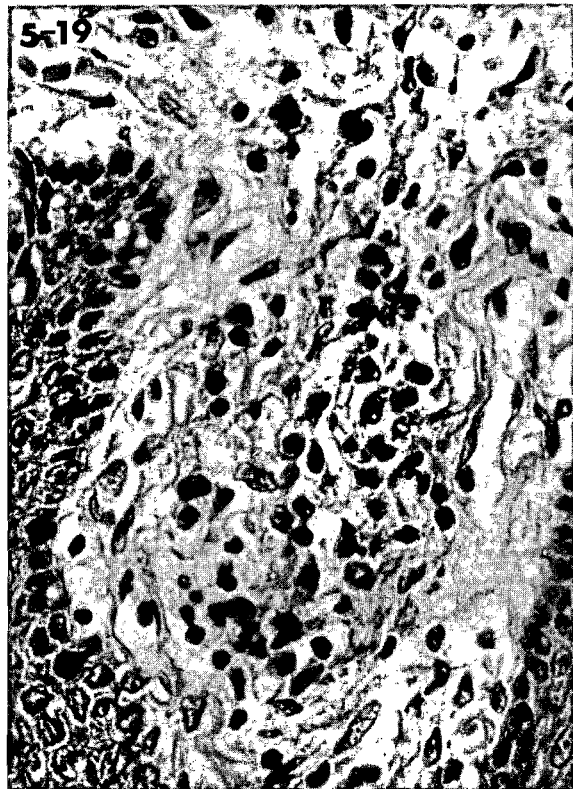
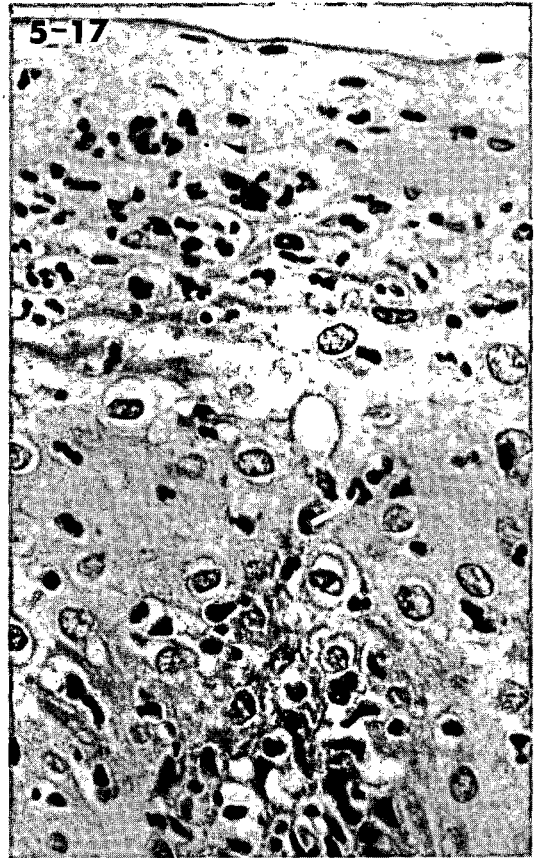
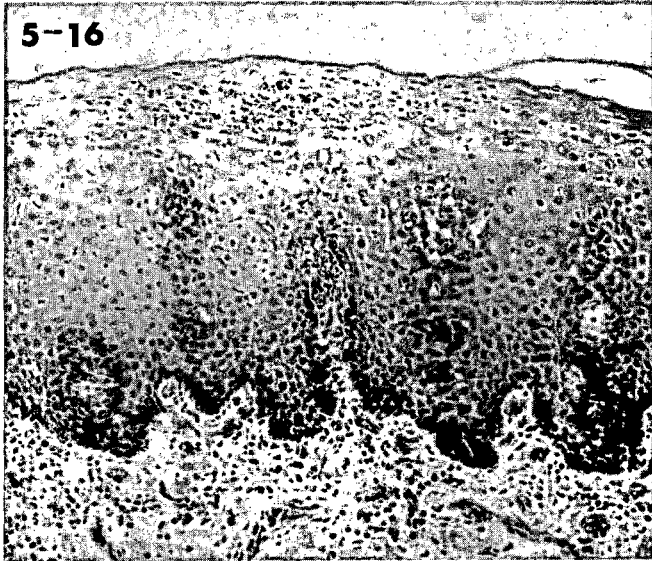


Figure 5-20. Opened uterus of 76B11 demonstrating the prominent linear folds.

Figure 5-21. Cross-section of the uterine horn of 80B1 demonstrating the longitudinal folds and the prominent stratum vasculare (arrows).

Figure 5-22. Cross-section of the uterus of 80B1 showing the prominent mucosal folds and the relatively thin myometrial layers (myo).

Figure 5-23. Portions of two endometrial folds with numerous glands within the lamina propria. (H&E, 30X)

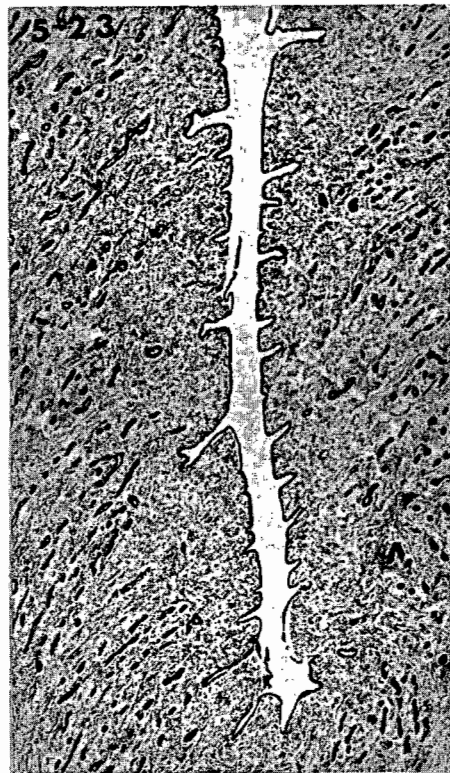
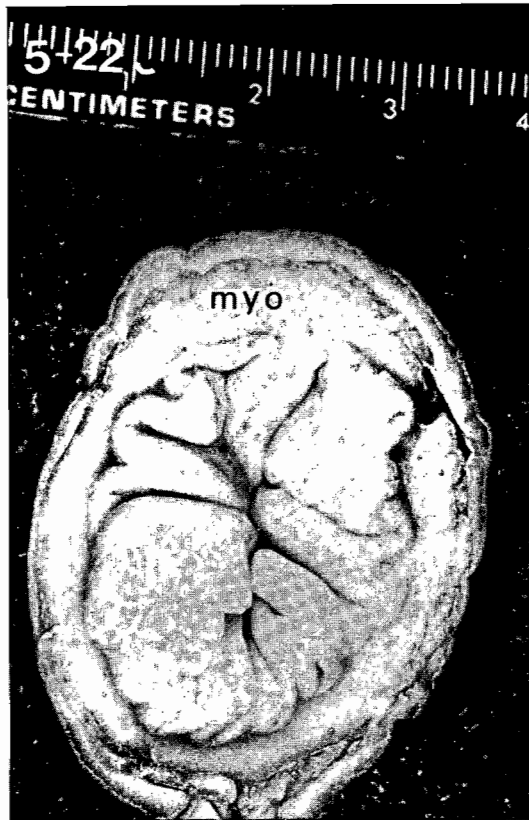
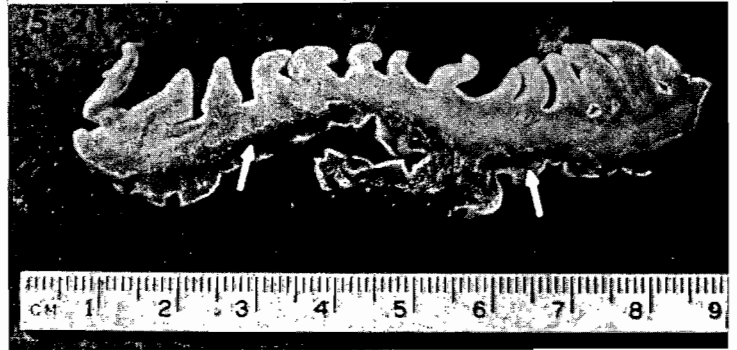


Figure 5-24. Photomicrograph shows the inactive low cuboidal epithelium lining the endometrial lumina and glands (80B1). (H&E, 120X)

Figure 5-25. Photomicrograph depicts an extensive glandular-free region of endometrium in the uterus of 80B1. (H&E, 30X)

Figure 5-26. Endometrial fold of 80B1 showing a gland-free region (gf).

Figure 5-27. Photomicrograph of the region just anterior to the cervix of 80B1. No glandular elements are present. Cervical crypts (cc) are evident and the region appears cervical rather than uterine. (H&E, 30X)

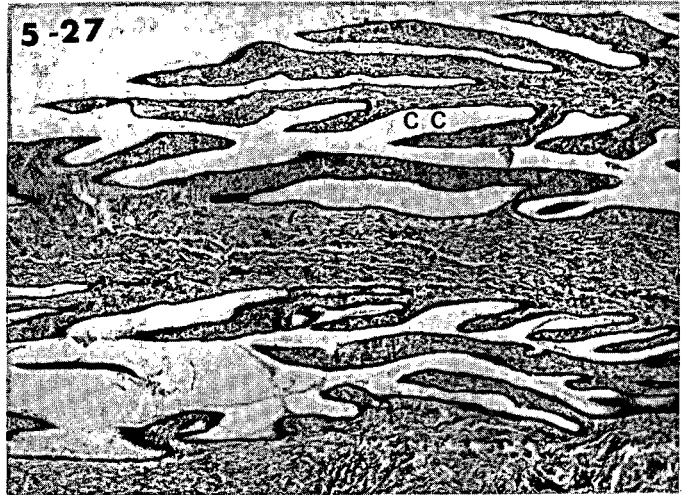
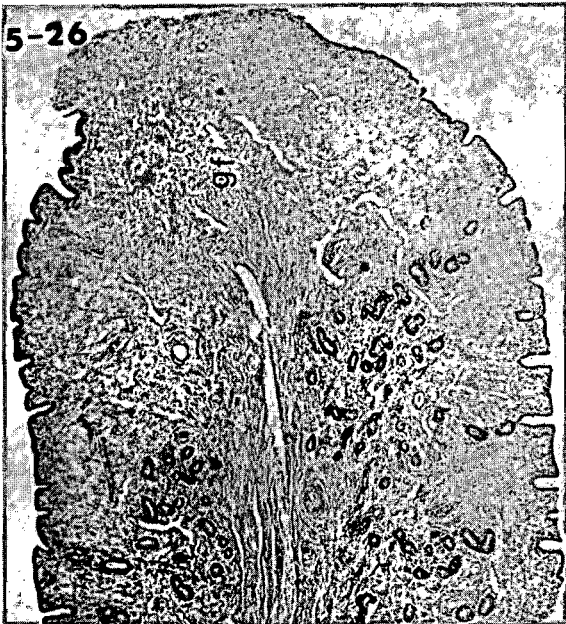
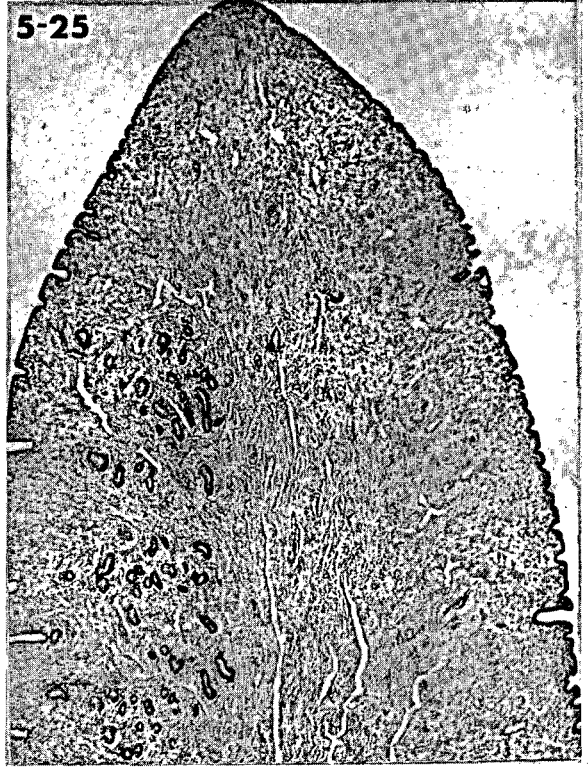
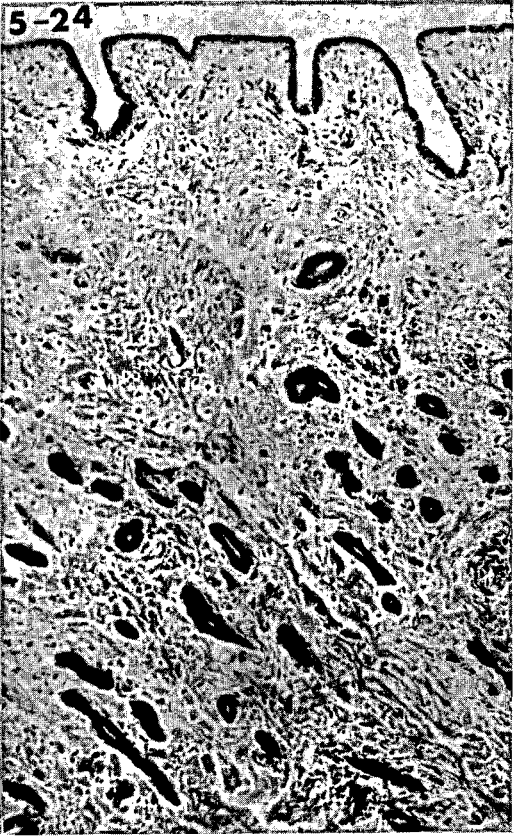


Figure 5-28. Photomicrograph of the region anterior to the cervix of 80B1 which demonstrates the junctional zone. Both cervical crypts (cc) and endometrial glands (arrows) are present. (H&E, 30X)

Figure 5-29. Photomicrograph of cross-section of oviduct of whale 80B1. Note thickness of folds. (H&E, 30X)

Figure 5-30. Thick oviductal folds of whale 80B1 showing gland-like crypts rather than thin folds. (H&E, 30X)

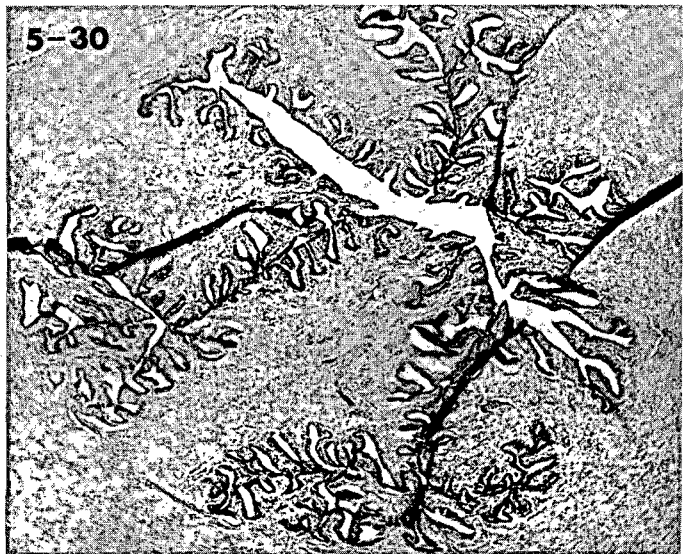
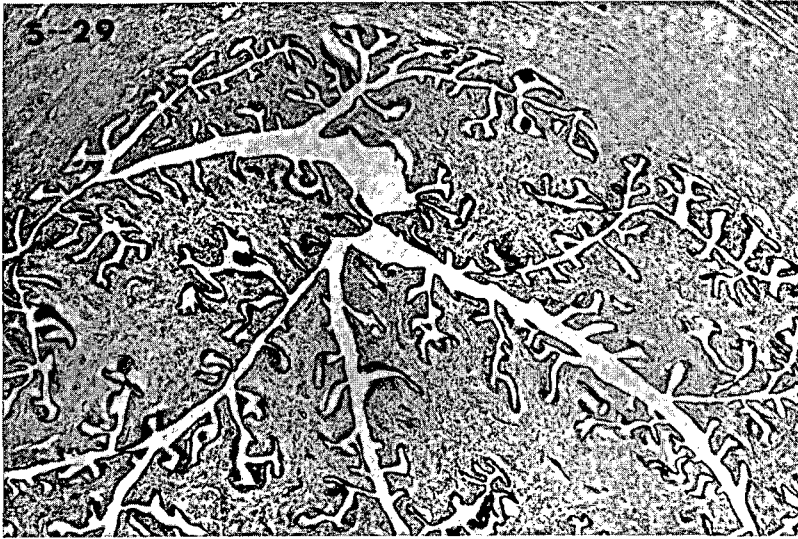


Figure 5-31. Gross photograph showing size disparity between ovaries of a postpuberal bowhead (80G1) and prepuberal animal (80B1).

Figure 5-32. Cross-sections of a postpuberal ovary (80G1) and a prepuberal ovary (76B11). Note the corpus luteum (CL) on the postpuberal specimen.

Figure 5-33. Cross-section of ovary of 76B11 demonstrating the distinct cortical (COR) and medullary (MED) regions in a prepuberal animal. The arrow depicts the hilus where the mesovarium attaches. Note the large blood vessels in the medulla.



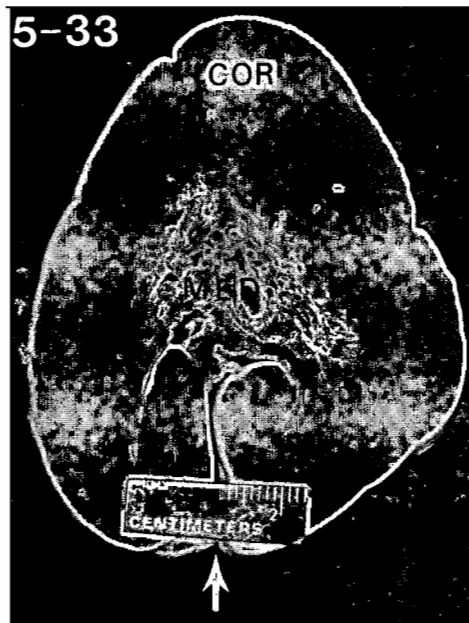
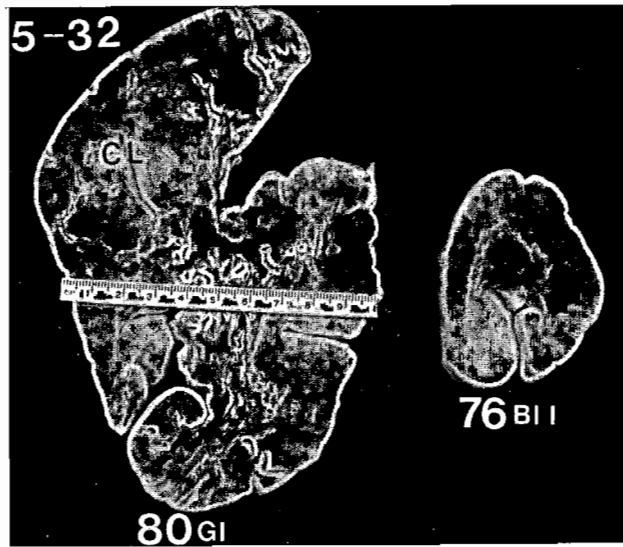
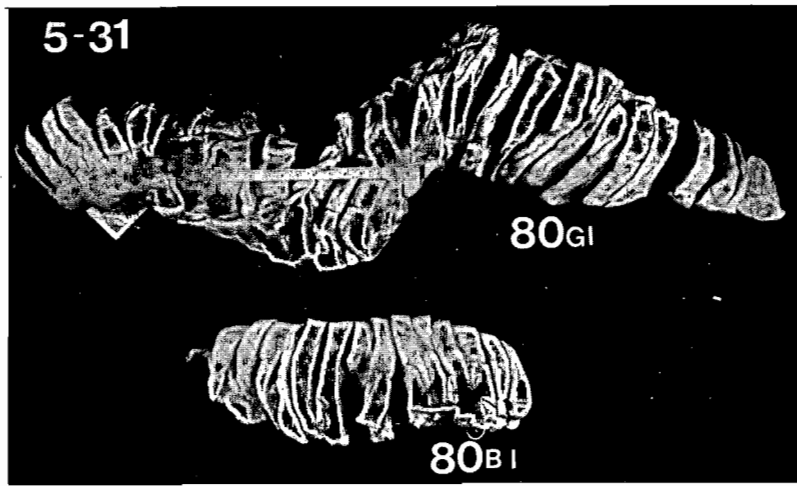
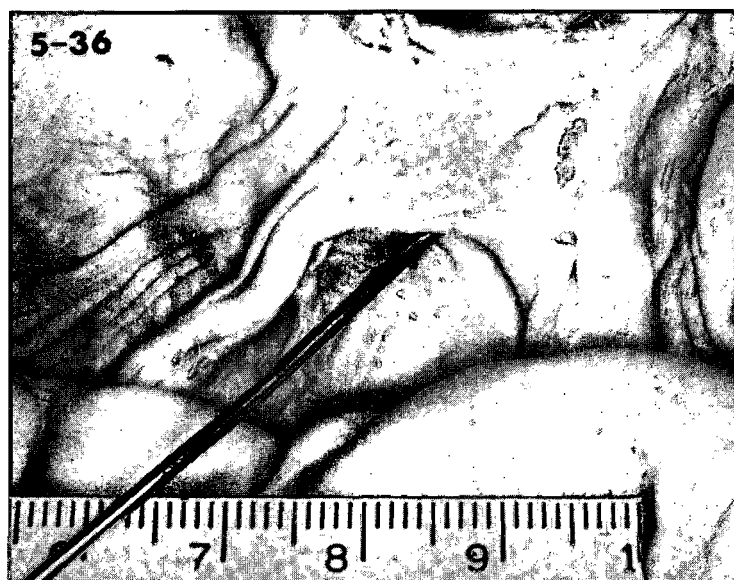
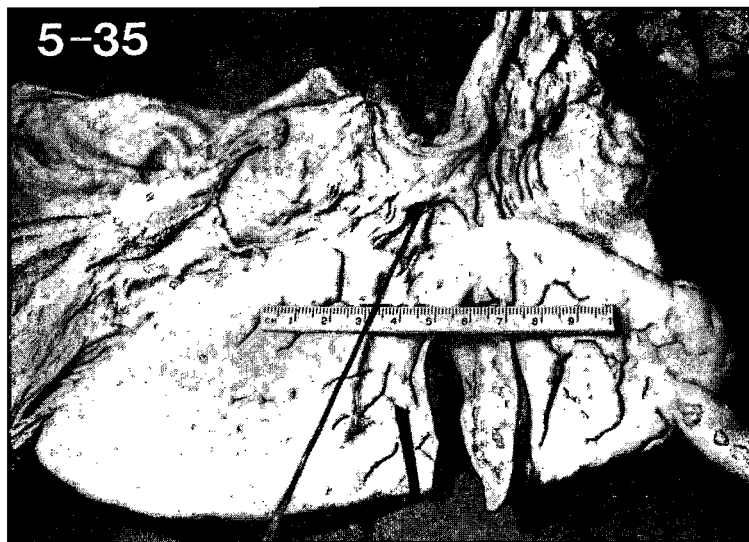
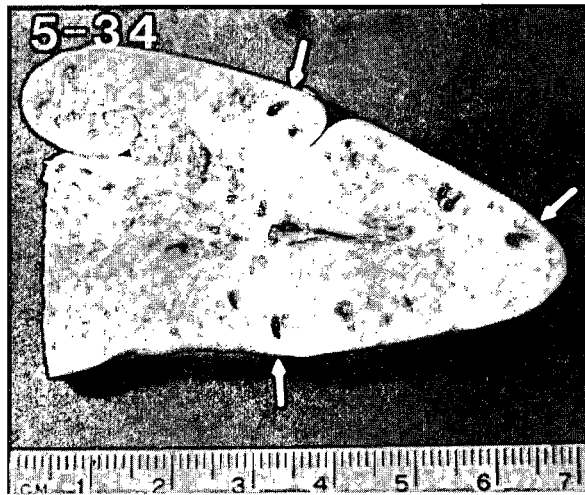


Figure 5-34. Cross-section of the ovary of 80B1 demonstrating numerous small follicles within the cortex (arrows).

Figure 5-35. Ovary of 80B1 with probe in the very attenuated infundibulum which was probably lost during collection, or the ampulla itself. Note the grooves on the ovarian surface which are more pronounced on one pole.

Figure 5-36. Closeup view of the attenuated infundibulum which was probably lost during collection, or ampulla of 80B1.



- Figure 5-37. Photomicrograph of cortex of whale 80B1 showing the serosa, tunica albuginea and particularly the multitude of primary follicles. (H&E, 30X)
- Figure 5-38. Primary follicle of whale 80B1. The follicle measures 60 x 50  $\mu\text{m}$ , the oocyte 30  $\mu\text{m}$  and the nucleus 20 x 15  $\mu\text{m}$ . (H&E, 480X)
- Figure 5-39. Wall of antral (Graafian) follicle of whale 80B9 showing the multilayered mural granulosa and the theca epithelioid cells (arrow) of the theca interna. (H&E, 360X)
- Figure 5-40. A small antral (Graafian) follicle (gf) (600 x 480  $\mu\text{m}$ ) of whale 80B9 with two primary follicles. Very few theca epithelioid cells were present. (H&E, 120X)
- Figure 5-41. Photomicrograph of 3 x 2 mm follicle of whale 80B9 undergoing obliterative atresia. (H&E, 30X)

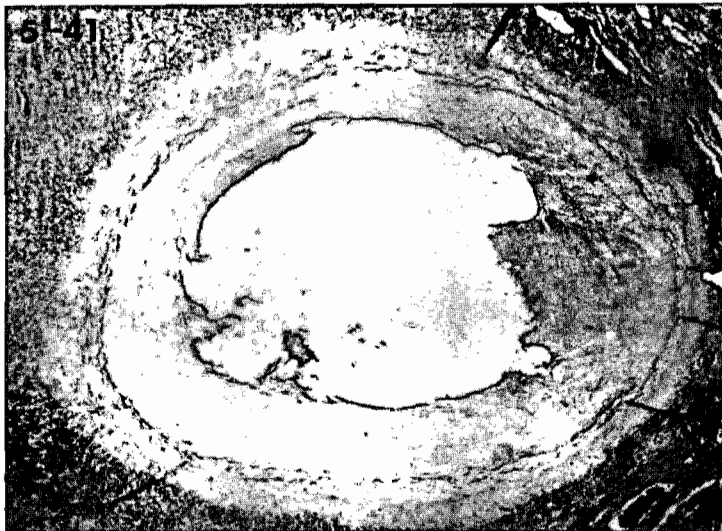
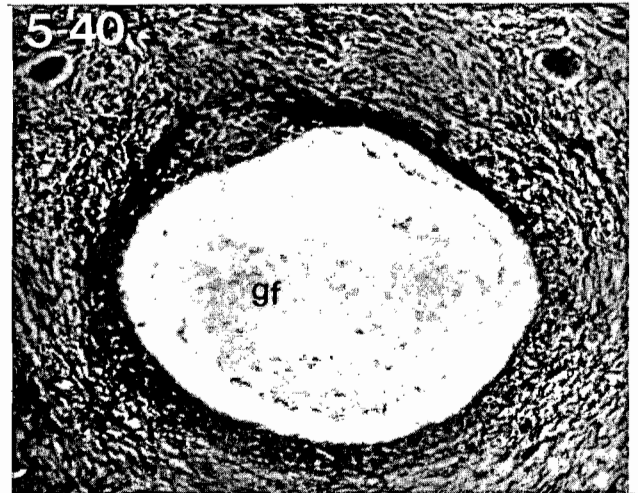
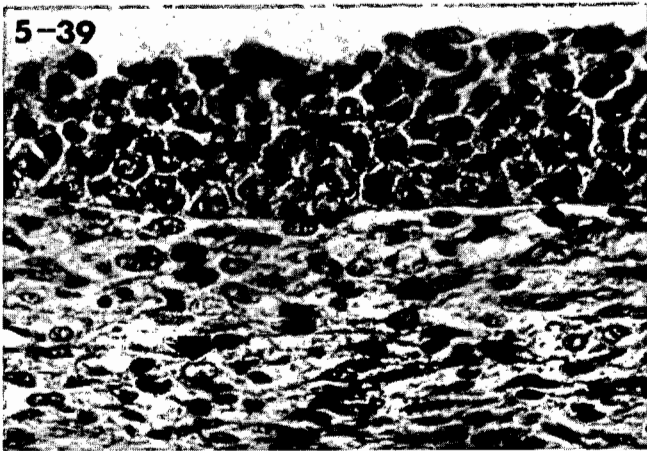
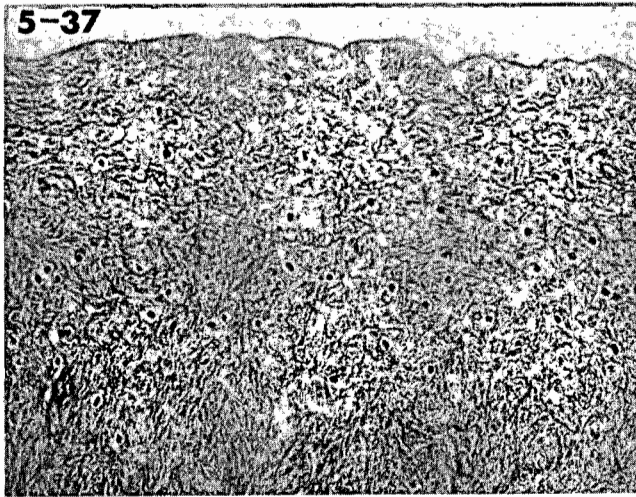


Figure 5-42. Wall of follicle of whale 80B9 undergoing cystic atresia with patch of hyalinization of theca interna. (H&E, 120X)

Figure 5-43. Obliterative atresia in 1.5 mm follicle of whale 80B9. Note antrum being filled-in with polysaccharide and connective tissue. (H&E, 30X)

Figure 5-44. Early obliterative atresia in 3 x 2 mm follicle of whale 80B9. Note hyalinization of former theca interna. (H&E, 120X)

Figure 5-45. Remains of atretic follicle in ovary of whale 80B9. This 500 x 320  $\mu\text{m}$  mass is the hyalinized former theca (arrow) interna. (H&E, 120X)

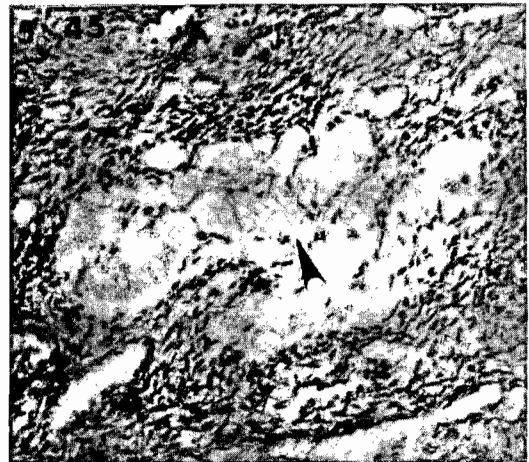


Figure 5-46. Macroscopic cross-section of ovary of whale 80G1 through the large, pale yellow corpus luteum (cl).

Figure 5-47. Photomicrograph of corpus luteum of whale 80G1 showing trabeculum formed by infolding of collapsed follicle. (H&E, 30X)

Figure 5-48. Photomicrograph of parenchyma of corpus luteum of whale 80G1. Mixture of active, shrunken and vacuolated granulosa lutein cells. (H&E, 120X)

Figure 5-49. Granulosa lutein cells of corpus luteum of whale 80G1. The cytoplasm of many of the cells are markedly vacuolated. (H&E, 480X)

Figure 5-50. Active and vacuolated granulosa lutein cells in corpus luteum of whale 80G1. (H&E, 480X)



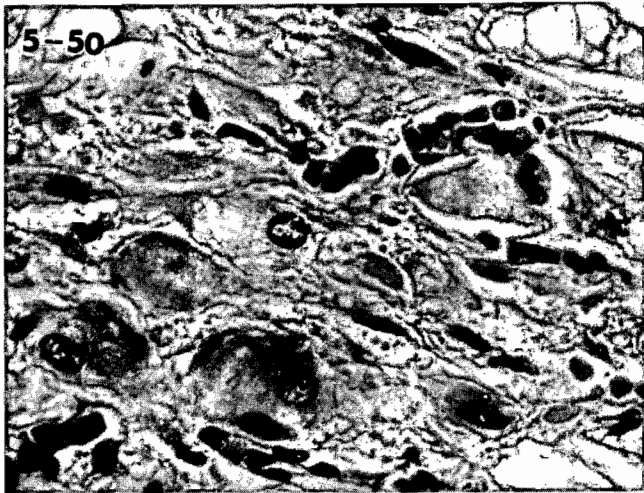
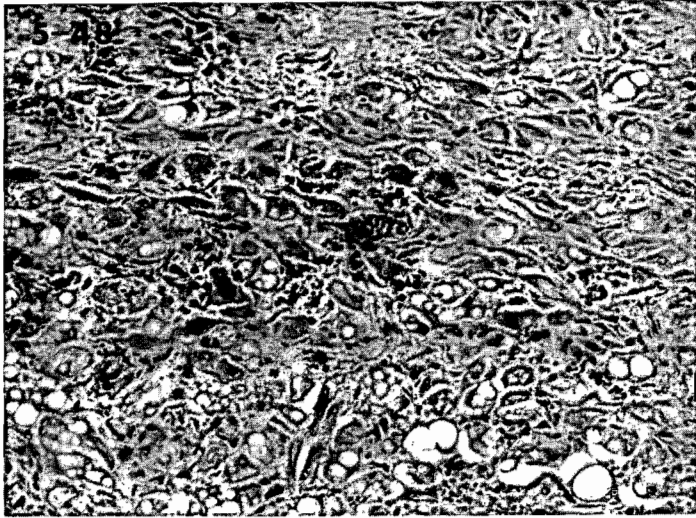
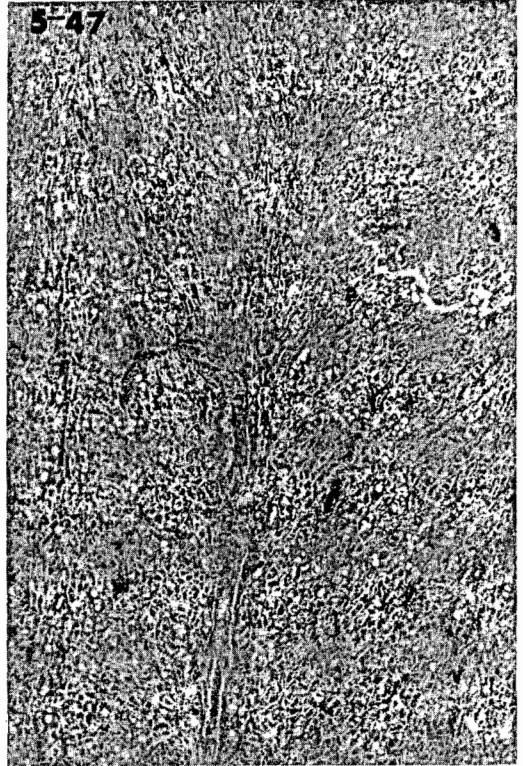
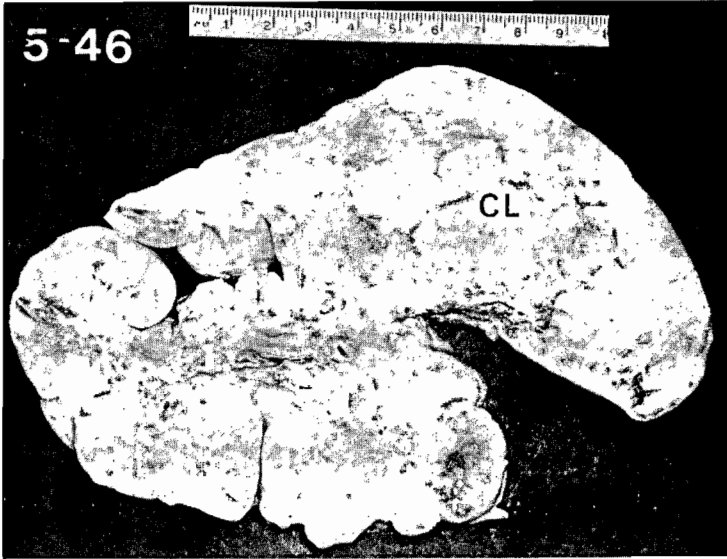


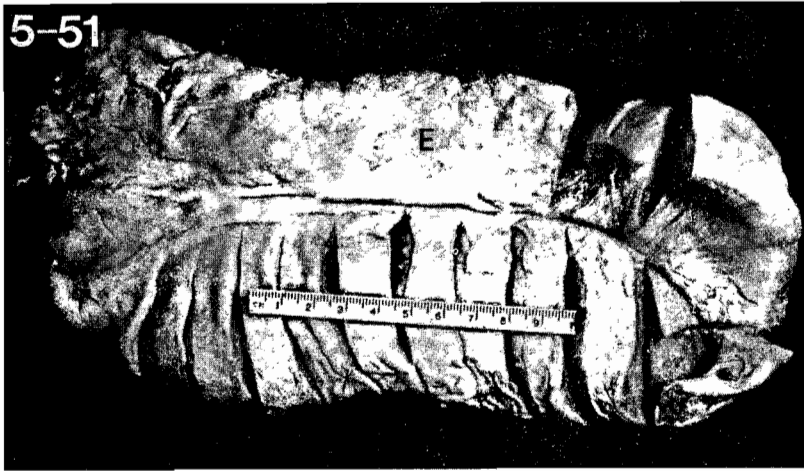
Figure 5-51. Prepuberal testicle and epididymis (E) of 80WW1. Ruler is on testicle. Note epididymis is longer and almost as wide as testis.

Figure 5-52. Cross-section of testicle of 80B5. Note lack of mediastinum.

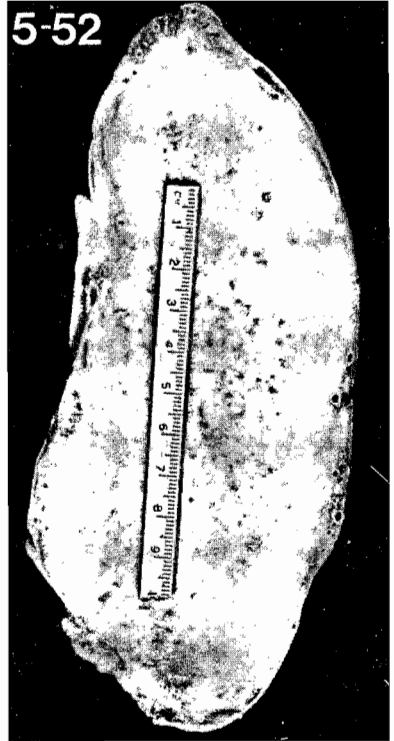
Figure 5-53. Substantial vascular plexus (between arrows), between testis and epididymis of 80WW1.

Figure 5-54. Close-up of vascular plexus of 80WW1 entering testicle and epididymis (between arrows).

5-51



5-52



5-53



5-54



Figure 5-55. Cut-edge of testicular-epididymal ligament of 80WW1. Note bundles of efferent tubules (arrows).

Figure 5-56. Photomicrograph of prepuberal seminiferous tubules of 80WW1 which are about 45  $\mu\text{m}$  in diameter. (H&E, 120X)

Figure 5-57. Seminiferous tubule of 80WW1 lined by Sertoli cells and occasional spermatogonia (arrow). (H&E, 480X)

Figure 5-58. Photomicrograph of testicular trabecula of 80B3 containing collecting tubules (arrows). (H&E, 30X)

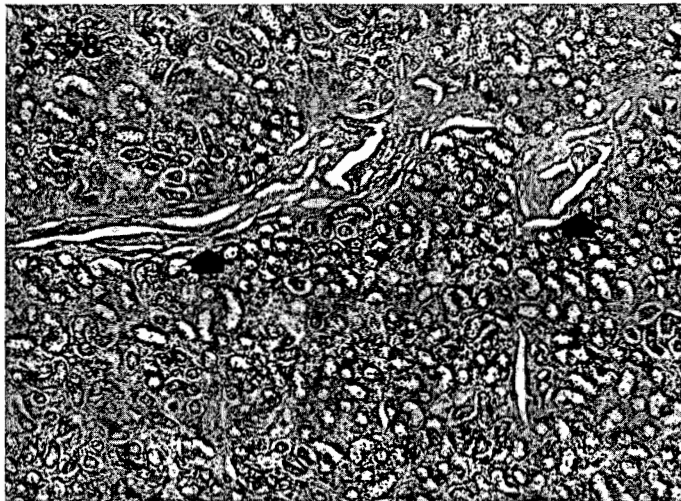
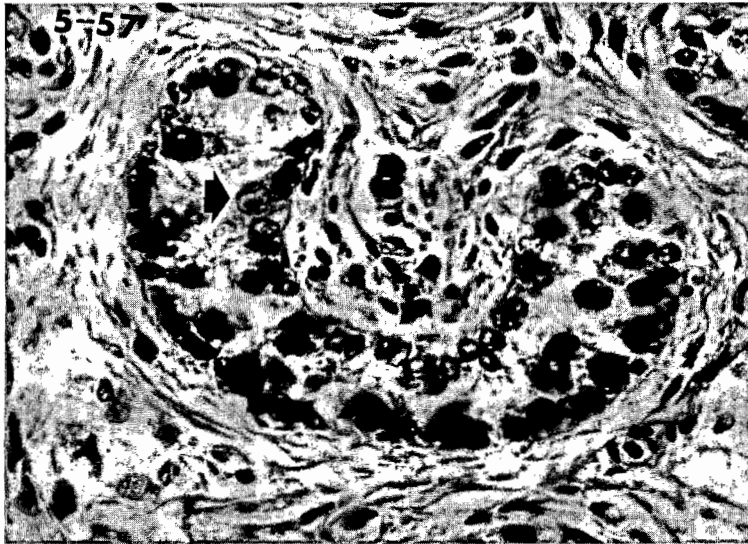
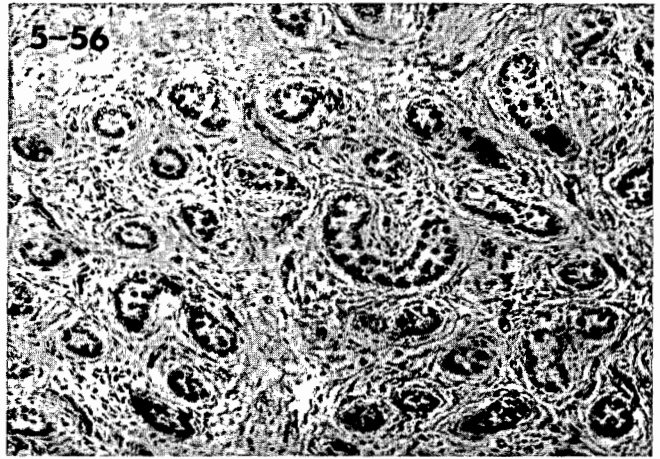
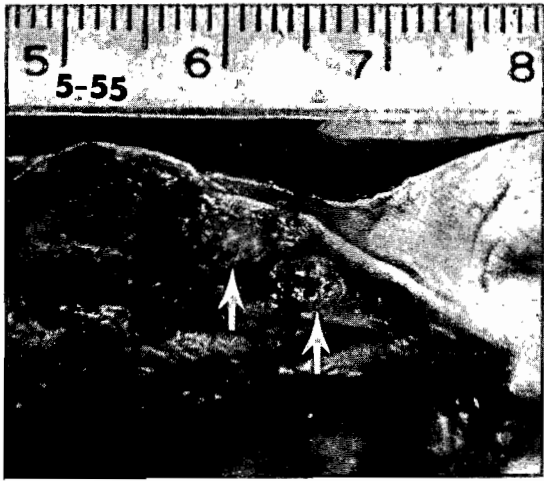


Figure 5-59. Photomicrograph of tunica albuginea of testicle of 80B3 with collecting tubules entering from trabecula (arrow). (H&E, 30X)

Figure 5-60. Close-up of testicular collecting tubules (arrows) of 80B3 entering tunica albuginea from trabecula. (H&E, 30X)

Figure 5-61. Multitude of collecting tubules passing through tunica albuginea of 80B3 adjacent to epididymis (H&E, 30X)

Figure 5-62. Photomicrograph of bundle of efferent tubules in testicle of 80B3. (H&E, 30X)

Figure 5-63. Testicle (T), epididymis (E) and ductus deferens (arrow) of 80WW1. Note large size of epididymis and tortuosity of ductus.

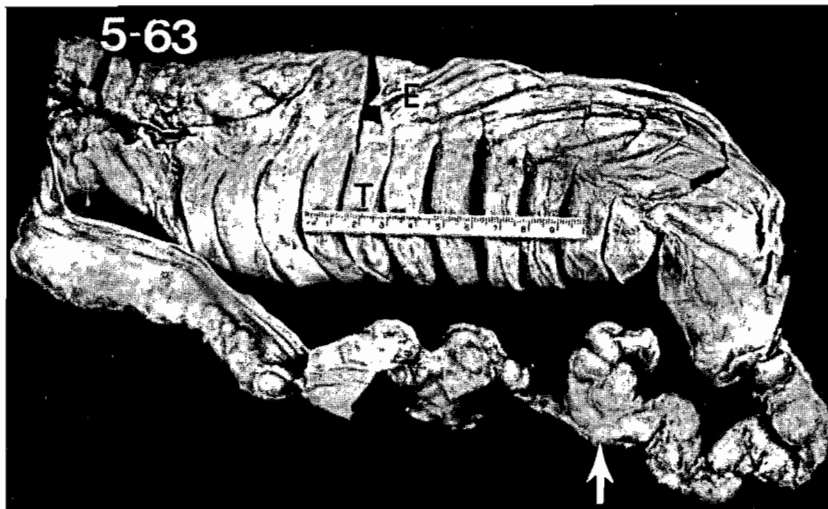
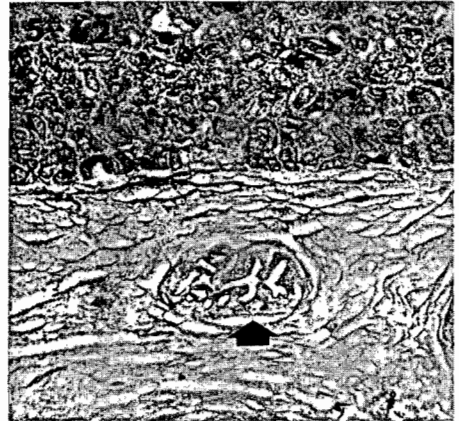
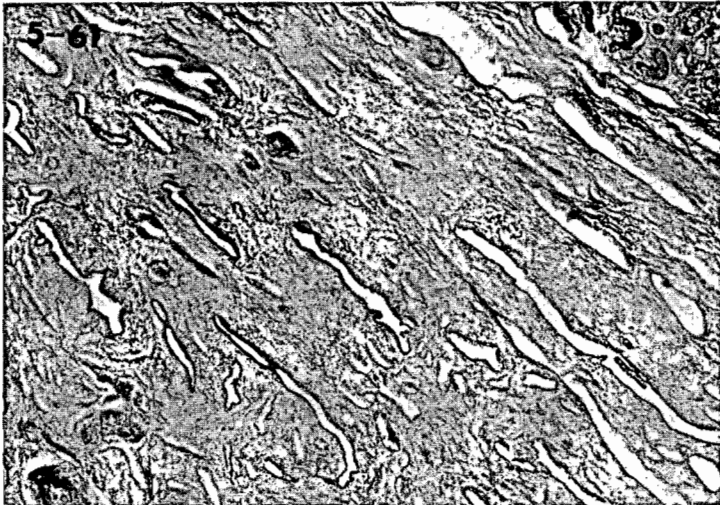
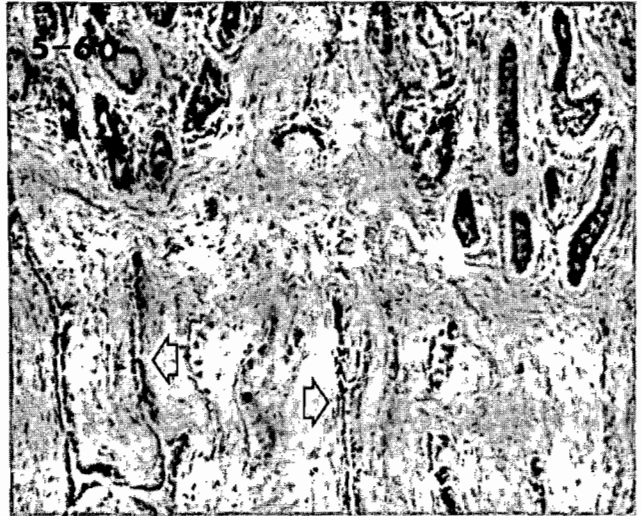
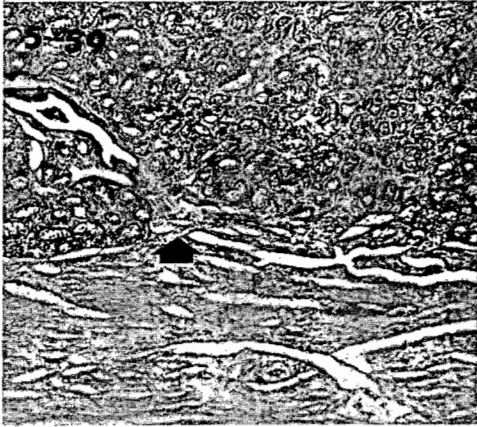


Figure 5-64. Efferent tubules (arrow) and tubules of head of epididymis of 80WW1. (H&E, 30X)

Figure 5-65. Close-up of efferent tubules adjacent to epididymal tubules which are not pictured. Notice simple columnar epithelium. (H&E, 120X)

Figure 5-66. Photomicrograph of head of epididymis of whale 80WW1 showing central duct (arrow) and multiple crypts. (H&E, 30X)

Figure 5-67. Close-up of central channel of head of epididymis with multiple crypts of whale 80WW1. (H&E, 120X)



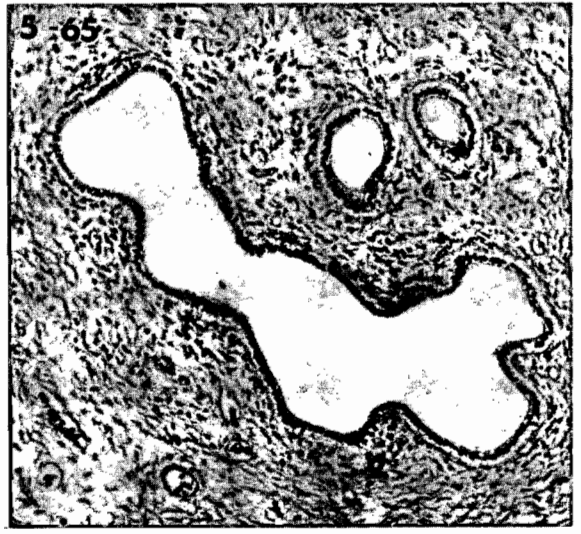
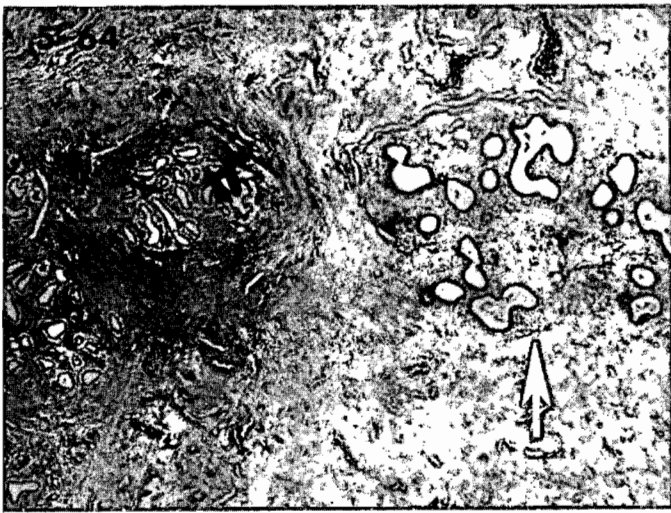


Figure 5-68. Body of epididymis of whale 80B3 showing central duct (arrow) and bundles of crypts. (H&E, 30X)

Figure 5-69. Tail of epididymis of whale 80B3 showing the continuation of the pattern of a central duct and multiple bundles of crypts. (H&E, 30X)

Figure 5-70. Close-up of central channel of epididymal duct of whale 80W11 lined by simple columnar epithelium. Note also the numerous attached crypts. (H&E, 120X)

Figure 5-71. Photomicrograph of ductus deferens of whale 80WW1 showing central duct still with multiple crypts and abundant muscle. (H&E, 30X)

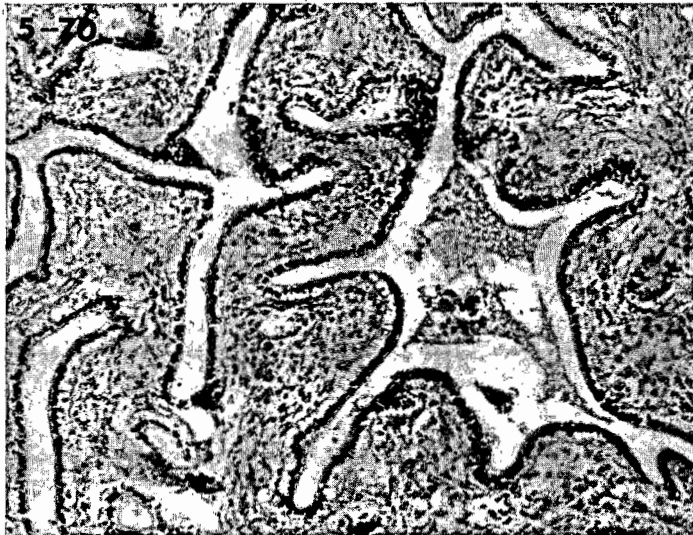


Figure 5-72. Pituitary of whale 80B1. Note three regions (A, B, C).

Figure 5-73. Pituitary of whale 80B3 wrapped in choroid plexus.

Figure 5-74. Pituitary of whale 80B1 still attached to choroid plexus.

Figure 5-75. Photomicrograph of cortical portion of portion A (pars distalis) of pituitary of whale 80B1. The darker cells are acidophiles. (H&E, 480X)

Figure 5-76. Medulla of portion A (pars distalis) of pituitary of whale 80B1. There are fewer cells and more vessels than in the cortex. (H&E, 480X)

Figure 5-77. Photomicrograph of characteristic cells of portion B of pituitary of whale 80B1. (H&E, 480X)

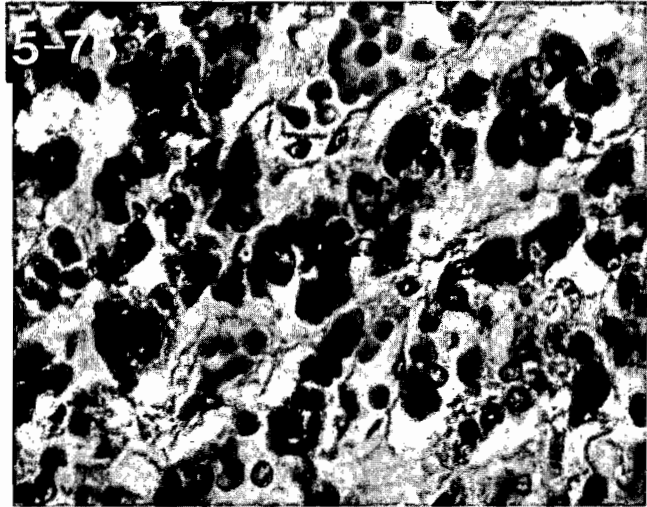
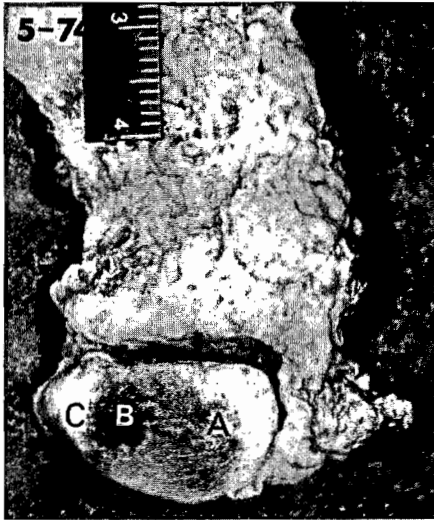
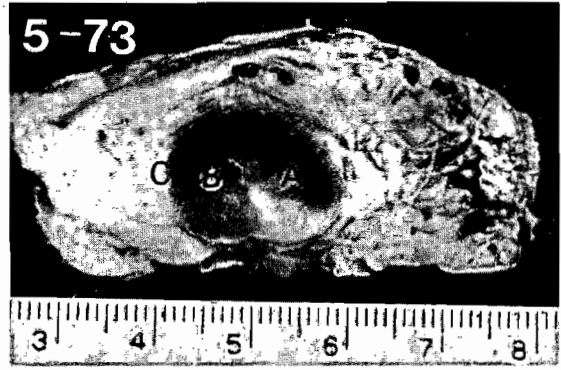
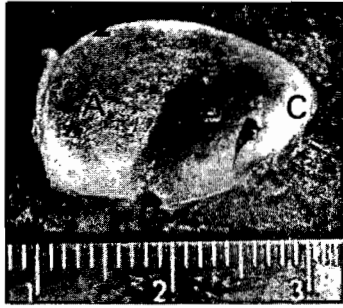


Figure 5-78. Typical cells of portion C of pituitary of whale 80B1. (H&E, 480X)

Figure 5-79. This photomicrograph reveals the line of demarcation between portions A and B of the pituitary of whale 80B1. The white arrows point to the line. (H&E, 30X)

Figure 5-80. Higher power view of sharp line of demarcation shown in Figure 5-79. White arrows on side of portion A and black arrows on side of portion B. (H&E, 120X)

Figure 5-81. Still higher power view of line of demarcation shown in Figures 5-79 and 5-80. Arrows point toward portion A (pars distalis). (H&E, 480X)

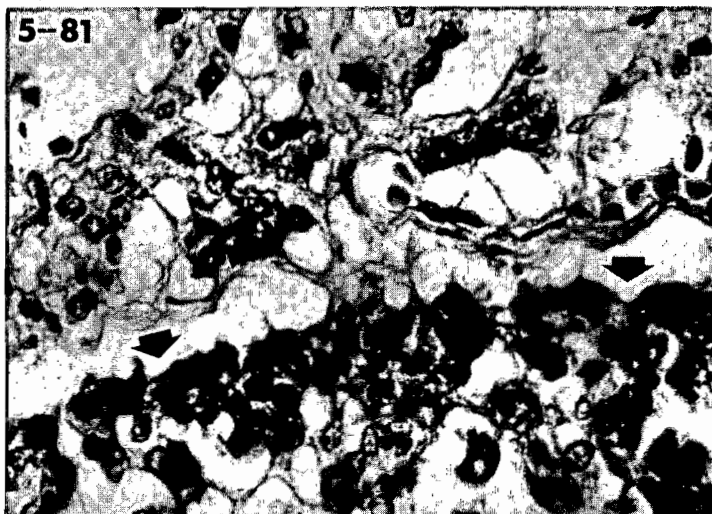
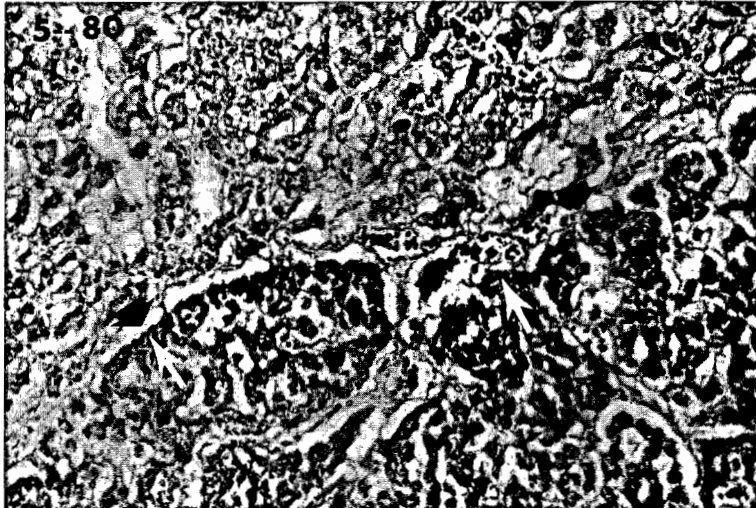
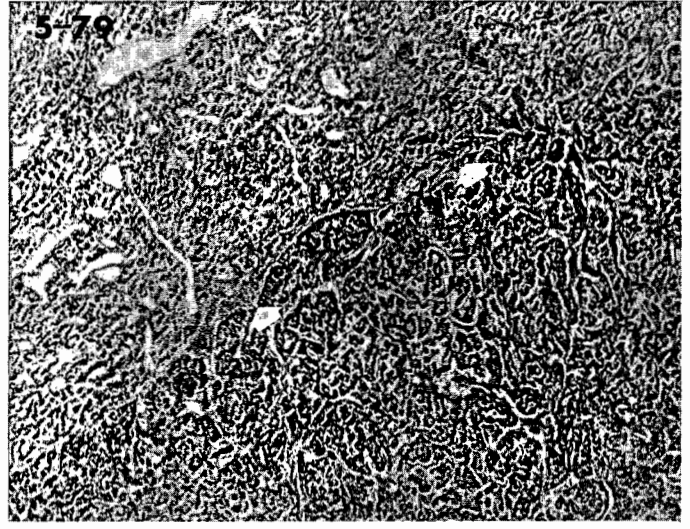
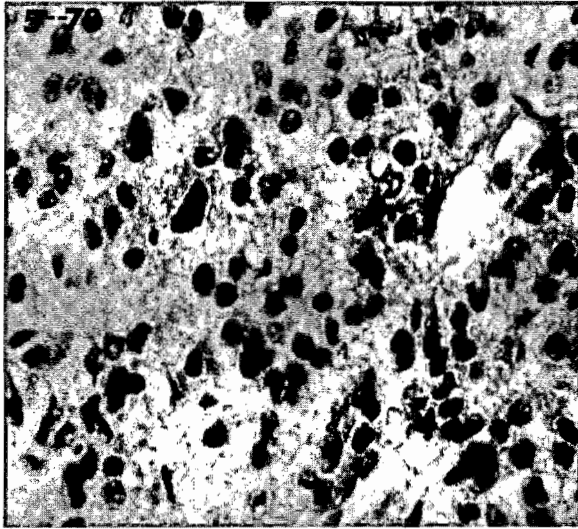


Figure 5-82. Cross-section of adrenal gland of bowhead 80B8 showing the scalloped appearance to the cortex (white arrowhead).

Figure 5-83. Portion of the adrenal gland of 80B8 demonstrating the "hook-like" portion of one pole. (Under the 6).

Figure 5-84. Photomicrograph of a cortical fold of the adrenal gland of 80B1 which shows the fibrous connective tissue (ct) giving the pseudolobulated appearance of the bowhead adrenal cortex. (H&E, 30X)



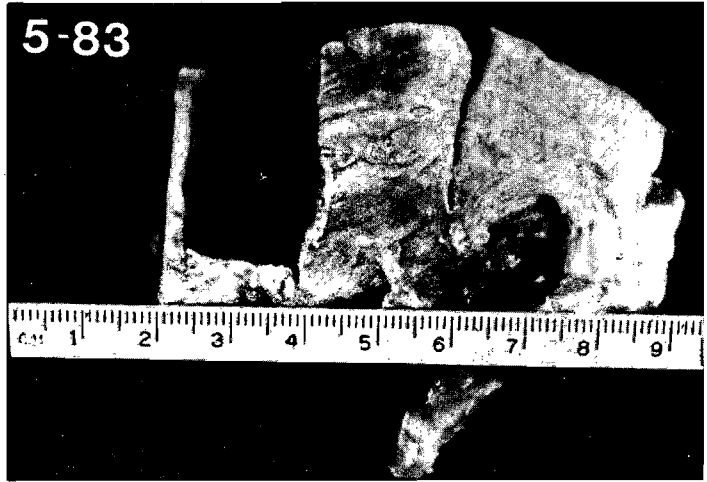
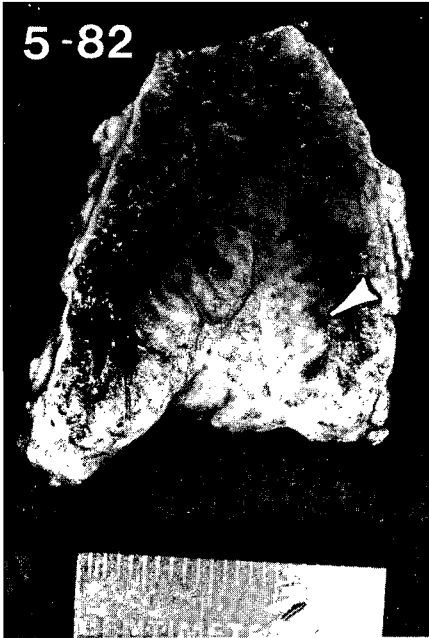


Figure 5-85. Photomicrograph of the adrenal cortex of 80B1 showing the zona glomerulosa (zg) and the zona fasciculata (zf). Note the arcuate arrangement in the zona glomerulosa. (H&E, 120X)

Figure 5-86. Photomicrograph of the adrenal cortex of 80B1 showing the arcuate arrangement of the zona glomerulosa. (H&E, 120X)

Figure 5-87. Photomicrograph of the adrenal medulla of 80B1 demonstrating basophilic granules. (H&E, 480X)

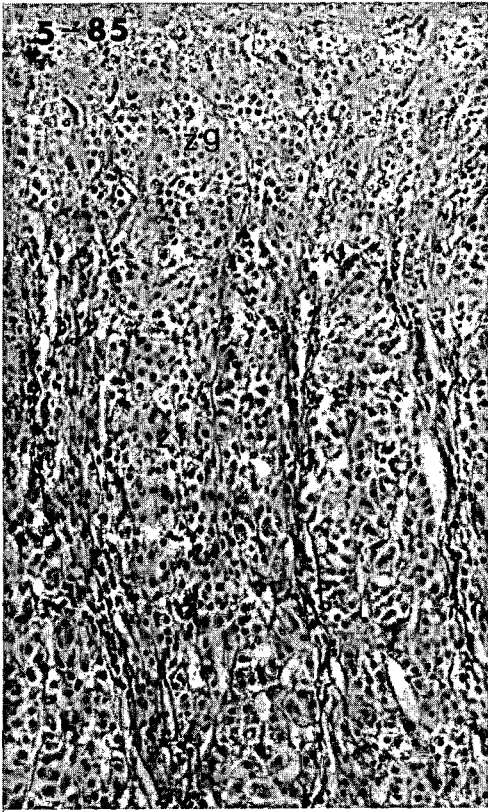


TABLE 5-1. MEASUREMENTS OF PREPUBERAL FEMALE REPRODUCTIVE ORGANS

Specimen Identification	Body Length (m)	Ovary (cm) <sup>1</sup>	Oviduct (cm) <sup>2</sup>	Uterus (cm) <sup>3</sup>	
80B1	10.9				
L		22 x 4 x 7.7	6.5 Straight	64	30
R		20.5 x 3.4 x 8.7	*		
80B7	10.3				
L		19.5 x 4 x 7.3	*		
R		19 x 5.5 x 7	*		
80B9	13.6				
L		27.8 x 8.4 x 11.7	*	69	32
R		*	*		
76B11	*		25	27.5**	20
#1		21 x 6 x 8			
#2		19.5 x 6 x 7			
80G1	15.65				
L		44 x 12.5 x 10			
R		46 x 20(̄CCL) x 11			

<sup>1</sup> L x W x H  
<sup>2</sup> L, shape  
<sup>3</sup> Horn, body  
\* Not available  
\*\* Incomplete

TABLE 5-2. MEASUREMENTS OF MALE REPRODUCTIVE ORGANS

Specimen Identification	Body Length (m)	Testes <sup>1</sup> (cm)	Epididymis <sup>1</sup> (cm)
80B3	8.4		
R		24.5 x 7.4 x 4	36 x 2.5 x 2.5
L		*	*
80B5	10.4		
R		18.5 x 4.8 x 7.2	*
L		18.5 x 4.8 x 7.2	*
80WW1	7.8		
R		19 x 6 x 3	29 x 2.5 x 2.5
L		18.5 x 6.5 x 2.5	-

<sup>1</sup> L x W x H

\* Not available

TABLE 5-3. PERIPHERAL PLASMA HORMONE CONCENTRATIONS IN FOUR BOWHEAD WHALES

Hormone	<u>Whale Identification</u>			
	B1 (Female)	B2 (Male)	B7 (Female)	B8 (Male) <sup>1</sup>
Testosterone (ng/ml)	0.07	0.06	0.11	0.09
Estradiol-17 $\beta$ (pg/ml)	34.0	41.0	57.5	50.3
Progesterone (ng/ml)	*	*	*	*
Corticosteroids (ng/ml)	4.1**	7.2	7.3	5.6**
Triiodothyronine (T3) (ng/ml)	1.1	1.7	1.7	1.3
Thyroxine (T4) (ng/ml)	90.0	77.0	107.0	86.0

<sup>1</sup> Ingutuk

\* Non-detectable

\*\* Values are estimates (essentially at the lower limits of detection in the assay).

The portion termed part B is composed of cords of cells which are slightly larger than those of the pars distalis and also form irregular cords or sheets of cells with foamy cytoplasm and indistinct cell outlines (Fig. 5-77). Ventrally there is a narrow band of cells which appears to be an extension of the cortex from part A to part C.

Part C is made up of columns or cords and small clusters of cells which are unlike those of both part A and B. They are smaller than in the other two areas and have a foamy, ill-defined cytoplasm (Fig. 5-78). Occasionally intermingled are acidophils similar to those of the pars distalis (A).

The histological appearance of the line of demarcation between part A and B is apparent in Figures 5-79, 5-80, 5-81.

Adrenal Gland - Macroscopic Findings. The adrenal gland from one whale (80B8) was studied both macroscopically and microscopically. Gross examination revealed it to be composed of an outer, scalloped cortical and an inner medullary region (Fig. 5-82). In the fixed state the adrenal measured 13 x 4.5 x 2 cm and was flattened in appearance with a "hook" at one end (Fig. 5-83). The corticomedullary junction had a scalloped appearance.

Adrenal Gland - Microscopic Findings. Microscopic examination of the bowhead adrenal revealed a thick fibrous capsule containing numerous nerves and vessels. The cortex is divided into distinct pseudolobules by thick bands of collagenous connective tissue projecting at right angles to the capsule (Fig. 5-84). A distinct zona glomerulosa, zona fasciculata, and zona reticularis were present (Fig. 5-85). The zona glomerulosa contains cells arranged in arcs (Figs. 5-86, 5-87) similar to solipeds, carnivores and the pig. The cells of the zona fasciculata and zona reticularis are similar to other mammals. Several clusters of ganglionic cells were present within the medullary region. Cells containing deeply staining basophilic granules were present in the medulla (Fig. 5-87).

Hormone Levels. Plasma concentrations of testosterone, estradiol 17 $\beta$ , progesterone, cortico-steroids, triiodothyronine (T3) and thyroxine (T4) are presented in Table 5-3.

## DISCUSSION

Mammary Glands, Nipples, and Genital Slit. Supernumerary mammary slits have been reported in numerous cetaceans (Arvy, 1973) as well as in the bowhead whale (Durham, 1972) so it is not surprising to find them in one of the two specimens examined in this study.

Previous studies reveal Balaena mysticetus to be similar to cetaceans in general (Durham, 1972) in regard to mammary gland morphology in general and nipples in particular. Grossly the present specimens were similar to previous findings. The specimens were from prepuberal animals which accounts for the lack of mammary glandular tissue, i.e. it is probable that little glandular tissue is present in the prepuberal animal.

The large mass of non-striated muscle bundles between the teat and milk cistern may be of importance to either nipple protrusion or milk ejection during suckling.

The teat cistern lining is remarkable and somewhat different from some of the terrestrial domestic animals since the foldings appear more extensive and the epithelial lining is thicker. The general microscopic configuration is somewhat similar to, but much more complicated than, the goat (Sar and Calhoun, 1966). Unfortunately no previous microscopic descriptions of the organ in cetaceans could be found for comparison. The importance of the bowhead's anatomical configuration in the biology of lactation in this species is unknown.

Clitoris. The clitoris is a rather large, prominent organ which is sufficiently strategically placed to enable it to engage in penile contact and thus to play a role in induced ovulation which is unlikely in baleen whales and likely in toothed whales (Yablokov et al., 1972), or in accelerating the onset of ovulation in cattle.

Vagina. The vagina, as might be expected, was found to be a long organ in spite of the fact that a complete specimen was not available. In dealing with specimens fixed in distorted positions it was not possible to determine whether transverse vaginal folds, as described by Yablokov et al. (1972) for other whales, were present. No convincing evidence of such folds could be found and this supports the description of bowhead vaginas by Durham (1972). Furthermore no evidence was found of a vaginal ligament as reported in baleen whales by Ohsumi (1969) who cites evidence both by himself and others, of their existence in both northern and southern fin, sei, blue, the southern humpback, and North Pacific



right whales. The vaginal band is probably the hymen - between the vulva and vagina proper.

Cervix. The bowhead cervix is remarkable in its size and complexity in that it consists of a series of complex rings separated from each other by "compartments" (Durham, 1972). Durham (1972) described the cervical rings as "funnels", but until seen they cannot be appreciated. The function of this complex structure is probably related to permitting the ascent of sperm with the exclusion of sea water since the rings appear to be a series of valves.

In an earlier study Kenney (1979) failed to recognize the uniqueness of the rings because they had been split open.

The specimens for 1980 were also interesting from the fact that the vaginal type of stratified squamous epithelium extended a considerable length into the cervix. Once the stratified epithelium gave way to the simple columnar with the development of the deep crypts it would appear that the development of a system for storage and slow release of sperm was present.

Durham (1972) described the presence of a cervical "jelly" as being present between the cervical rings. It was not present in the present material. Yablokov et al. (1972) did not find cervical mucous plugs in baleen whales but did so in toothed whales. It seems reasonable that on the basis of Durham's findings the presence or absence of a collection of cervical mucus depends on whether or not the individual has reached puberty and on the stage of the estrous cycle.

Uterus. The uterus is a typical mammalian bicornuate uterus characterized by a relatively long body, somewhat straight horns rather than coiled, and an endometrium characterized by folds rather than caruncles. It thus externally resembles the sow and internally the sow and mare. The folds serve to drastically increase the surface of contact between maternal and fetal tissues.

Oviduct. The bowhead oviduct is remarkably short and non-tortuous unlike terrestrial animals. In addition, the mucosal folds are remarkably broad - unlike the thin ones of most mammals. The third interesting aspect of the bowhead oviduct in the intact specimen was the absence of an infundibulum and ovarian bursa in 80B1. Yablokov et al. (1972) also noticed that the ovaries of baleen whales were not in a "pouch" (bursa). It appeared that in this instance the ampulla opened directly on the mesosalpinx. This finding is in spite of the description of a

large infundibulum by Durham (1972). Does the absence of an infundibulum represent a common anomaly of the bowhead? Only further samples can provide the answer. Since the infundibulum is critical to the pickup of the oocyte at ovulation its absence could contribute to infertility, particularly if the bowhead is nonestrus, as proposed by Yablokov et al. (1972) for baleen whales - or if the lack of infundibulum was bilateral.

Ovary. The size of the ovary appears related to the size and sexual maturity of the individual in the bowhead just as it does in the sperm whale (Best, 1967) although only four were examined as compared to the 454 examined by Best.

The grooves of the ovary are characteristic of baleen whales while in the toothed whales the ovaries are smooth (Yablokov et al., 1972). The significance of the grooves is not known but may be related to increased follicular activity and thus an elevation of the surrounding cortex.

The ovaries are just as impressive by the number of primary follicles as they are by their size. The size of the one corpus luteum examined is also impressive. The trabeculae of the corpus luteum were prominent and develop by an infolding of the ovulated follicle wall producing the scalloped effect. These infoldings not only provide the scaffolding for the developing corpus luteum but also bring vessels to the center of a rapidly developing endocrine gland. At the center where the infoldings, soon to be trabeculae, meet, the fibroblasts form a connective tissue core. This is the nucleus described by Yablokov et al. (1972).

The corpus luteum examined had both pyknotic and vacuolated cells. These are probably signs of involution. It could not be determined by histological observations whether this was a corpus luteum of the estrous cycle or of pregnancy.

The pair of postpuberal ovaries from 80G1 had a large corpus luteum and no noticeable corpora albicantia. There is debate concerning the duration of persistence of corpora albicantia in whales in general (Slijper, 1966). The lack of corpora albicantia in this individual may indicate this is its first breeding season.

Testes. There are two major findings in the examined testicles. First is the lack of identifiable Leydig cells. This finding correlates well with the very low circulating levels of testosterone.

Secondly there is no mediastinum or rete testis due to the fact that the excurrent duct system for sperm begins with collecting tubules which lead

away from the convoluted seminiferous tubules. The collecting tubules originate randomly throughout the parenchyma and pass to the cephalad aspect of the testicle via trabeculae, thus producing no collection of tubules in a mediastinum. We have been unable to find a previous description of this portion of the excurrent duct system. However, this pattern is similar to that in stallions.

Efferent Tubules, Epididymis, and Ductus Deferens. The arrangement of the efferent tubules which conduct sperm from the collecting tubules of the testis to the epididymal duct appear unique in the sense that they are encircled by bundles of connective tissue. They traverse the distance from the tunica albuginea of the testicle to the epididymal duct. They originate from the mesonephric tubules whereas the epididymal duct and ductus deferens originate from the mesonephric duct.

The epididymis of the bowhead prepuberal male whale is remarkable and probably unique among mammals. Grossly it is slightly more than half of the mass of the testicle which is remarkable in itself. Microscopically it appears unique since it is composed of a series of outpouchings from the central tortuous channel. It is the individually wrapped clusters of outpouchings that give the gross appearance of knobiness to the epididymal duct.

The remarkable structure of the epididymis should be examined from post-puberal whales to determine if sperm gain access to the multitude of crypts or glands. They probably do so. The function of these bountiful spaces is probably to serve as storage depots for sperm and they may also aid in the maturation of sperm. In other mammals sperm are sterile when they leave the testicle and achieve fertility as they pass through the epididymis.

The ductus deferens in the specimens examined is also unique in that it has crypts, similar to the tail of the epididymis, in its initial portions and it remains tortuous throughout its length whereas in other mammals it is a non-tortuous organ.

Adrenal: Macroscopically the adrenal gland is similar to that of other mammals having distinct cortical and medullary regions. Microscopically Balaena mysticetus has an adrenal similar to that described in other cetacean species (Simpson and Gardner, 1972). The major variation in the bowhead is the marked amount of connective tissue and the degree of surface cortical lobulation. The degree of pseudolobulation differs among cetacean species and additional bowhead specimens

must be studied in order to properly determine the type of cortical lobulation which is present in this species.

Pituitary. The cetacean pituitary is unique as compared to terrestrial large mammals. The lack of the pars intermedia is common. Furthermore, it is easy to miss the neurohypophysis since it is extrasellar in most instances (Arvy and Pilleri, 1973-4). Neither was found in the present material.

The pars distalis was the most readily identifiable and was comparable to that of large terrestrial mammals. The acidophils were also evident in the two other compartments but to a much smaller degree. To properly determine all the cell types and their function will require considerable study.

Endocrine. The four bowhead whales sampled in the present study represent juvenile individuals all of whom revealed detectable circulating hormone levels of testosterone and estradiol. No difference could be noted between the males and females in the circulating levels of testosterone and estradiol although not enough animals are in the study to test this statistically. It is not possible to make comparisons because testicular steroids have not been reported in large cetaceans. For the ovary, tissue levels of "progestins" (Callow et al., 1935),  $5\alpha$  pregnane- $3\beta$ -al-20-one and progesterone (Prelog and Meister, 1949) have been reported.

The low plasma testosterone level may reflect the prepuberal status of the whales surveyed and the apparent absence histologically of interstitial cells of Leydig in the testes of the bowhead whales examined to date. Likewise, the nondetectable progesterone concentration probably is a reflection of the immaturity of the animals sampled.

The plasma corticosteroid concentrations were surprisingly low (compared to levels in most domestic mammals) in light of the nature of the stress produced by the harvesting procedure. In addition, since no chromatographic separation was performed to separate cortisol from corticosterone, the antibody used in the radioimmunoassay would have measured both hormones in the plasma. The specificity of the antibody for cortisol is 100% while that for corticosterone is approximately 17%. While the presently observed plasma cortisol level in the immature bowhead is about one-tenth that of most domestic species, the relative potency of adrenocorticotrophic hormone (ACTH) pituitary preparation from Balaenoptera musculus and Balaenoptera physalus has been estimated to be about three times

that of a pig's (Hennings, 1950). ACTH of Balaenoptera sp. has been identified and the amino acid content determined (Tamura and Ur, 1970).

The levels of triiodothyronine (T3) and thyroxine (T4) in the plasma were apparently similar in both males and females. No data were available from other cetacean species to compare present values with, so it is impossible to assess seasonal effects and other sources of variation.

#### SUMMARY

The internal and external genitalia of four prepuberal males and three prepuberal females as well as one postpuberal female are described and measured. In addition, blood samples from two male and two female prepuberal individuals were assayed for steroidal and thyroidal hormones.

Intact, complete organs were not available for each individual but a reasonably complete picture of the bowhead, particularly the prepuberal bowhead, can be drawn when these findings are combined with those of Durham (1972), and Kenney (1979).

Two mammary slits were typical - each with a single teat. In one specimen there were two supernumerary slits without teats. The teats had a very thick covering of stratified squamous epithelium while the teat cistern was lined by a large number of longitudinal rugae.

There was a substantial non-striated muscle in the region between the teat and milk cisterns which may play a role in withholding and ejection of milk.

The pigmented genital slit was characterized by an elongate clitoris. The vagina was an elongated organ characterized by longitudinal folds, no evidence of annular folds, and was lined by stratified squamous epithelium.

The cervix was a unique organ with four to seven elongated annular folds separated by empty "compartments". The first part of the cervix was lined by a stratified squamous epithelium similar to that of the vagina except that it was not keratinized. There was a slight, chronic cervicitis in one specimen. The anterior portion of the cervix was characterized by having a typical simple columnar epithelium and bountiful crypts. These crypts extended about 6 cm into the body of the uterus at which point typical endometrial glands commenced. It was hypothesized that the cervical rings serve as valves which serve to enable sperm to ascend while keeping sea water out. It was further hypothesized that the bountiful cervical crypts serve as sperm storage compartments enabling release over a prolonged period of time.

The uterus was bicornuate with a long body and two rather straight (uncoiled) horns. The endometrium was thrown into prominent longitudinal folds and lacked caruncles although it had typical branched tubular glands. The myometrium had a thick, circular inner muscle coat, a middle layer of vessels, and a thinner outer longitudinal muscle coat.

The oviducts were relatively short with little tortuosity and, in the intact specimen examined had no infundibulum. In view of Durham's (1972) description this is probably an anomaly. The longitudinal folds were surprisingly thick and possessed crypts rather than secondary foldings.

The ovaries were large, oval organs in the prepuberal individuals and very elongate in the postpuberal ones. The surface of the ovary was characterized by a network of randomized grooves which were more prominent on one pole than the other. One postpuberal ovary had a very large, pale yellow corpus luteum. The mesovarium was attached to the ovary at a prominent hilus.

Histologically the ovary was covered by a serosa and a tunica albuginea beneath which was a typical mammalian cortex surrounding a very muscular medulla. The cortex contained a bountiful number of primary follicles with a scattering of viable and atretic antral (Graafian) follicles. The primary follicles with their oocytes were in the size range of other mammals. The viable antral follicles had a typical mural granulosa while the theca interna was characterized by the usual theca epithelioid cells. Two types of atresia were noted - cystic and obliterative. The processes were reminiscent of the process in the cow.

The corpus luteum was very large and grossly had a scalloped or convoluted cut-surface. This was due to trabeculae which served to divide the organ into lobules. Histologically the parenchyma contained numerous granulosa lutein cells. In addition to obvious active ones there were some with shrunken or vacuolated cytoplasm. Such changes could be autolytic but are more likely to be associated with involution. No corpora albicantia were evident in the postpuberal ovaries of whale 80G1.

The penis of the bowhead is an elongate, fibroelastic organ with a sigmoid flexure.

The prepuberal testicles were oval organs with a thick tunica albuginea, and no mediastinum evident on cut-surface. Histologically there were numerous seminiferous tubules lined by Sertoli cells and a scattering of spermatogonia. These tubules lead into collecting tubules which entered trabeculae which were directed toward the cephalic end of the testicle. Here they traversed the tunica

albuginea to join with the efferent tubules which were arranged in bundles. These tubules than connected with the epididymal duct.

The epididymis of the bowhead was a remarkable organ because of its very large size macroscopically and because of its very complicated structure microscopically. At this time it appears unique among mammalian epididymides. The complicated microscopic structure may be related to sperm maturation.

The complicated structure of the epididymis carried over into the initial segment of the ductus deferens which then became a single nonglandular duct. Macroscopically the ductus deferens was tortuous in contrast to the nontortuous organ of other mammals.

Macroscopically the adrenal was characterized by a scalloped appearance of the cortex on cut-section. This was due to rather deep penetration of the cortex by trabeculae from the capsule. Histologically the usual three zones of the cortex were present. The microstructure of the zone glomerulosa was similar to that of solipeds in that the cells were more nearly in arcs than glomerular in configuration. The medulla was similar to other mammals.

Macroscopically the pituitary had no pars nervosa. On midsagittal section it was divisible into three zones. The more anterior portion was comparable to the pars distalis with a cortex and medulla. This portion was sharply demarcated by a change in cell type to a middle zone while acidophiles passed from the cortex of the pars distalis on the outside of the middle zone. On the posterior aspect was a third region with yet another cell-type admixed with which were acidophiles similar to those of the pars distalis.

Endocrine. The blood of two prepuberal males and two prepuberal females was assayed for steroidal and thyroidal hormone levels. Testosterone and estradiol, but not progesterone, were detectable. The low levels of testosterone in the males is probably related to the apparent lack of histologically detectable Leydig cells.

Corticosteroid levels were low in view of the mechanism of harvest of whales.

The thyroidal hormone levels were similar in both males and females. No data were available from other cetaceae for comparison.

## REFERENCES

- Arvy, L. and G. Pilleri. 1973-4. On the hypophysis of Platanista indi Blyth, 1859. In: Investigations on Cetacea, G. Pilleri (ed.), Vol. 5. Published by Institute of Brain Anatomy, University of Berne, Berne, Switzerland.
- Best, P. B. 1967. The sperm whale (Physeter cutodon) off the West Coast of South Africa. 1. Ovarian changes and their significance. Published by Division of Sea Fisheries, Beach Road, Sea Point, Capetown, S. Africa.
- Callow, R. K., A. H. Laurie and A. S. Parker. 1935. The corpus luteum of the whale as a source of progesterin. *J. Soc. Chem. Indust.* 54:1025.
- Durham, F. E. 1972. The biology of the bowhead whale. Two-year progress report and working copy for the Arctic Institute of North America.
- Hennings, H. 1950. The whale hypophysis with special reference to its ACTH content. *Acta Endoc.* 5:376-386.
- Kenney, R. M. 1979. Tissues structure/function (RU 280G). In: Investigation of the occurrence and behavior patterns of whales in the vicinity of the Beaufort Sea lease area, J. Kelley and G. Laursen (eds.), pp. 359-393. Final report to the Bureau of Land Management from the Naval Arctic Research Laboratory, Barrow, Alaska.
- Prelog, V. and P. Meister. 1949. Uber die Isolierung von Progesteron aus dem Corpus luteum des Wales. *Helv. Chim. Acta.* 32:2435-2439.
- Rajakoski, E. 1960. The ovarian follicular system in sexually mature heifers with special reference to seasonal, cyclical and left-right variations. *Acta Endoc. Suppl.* 52, pp. 1-68.
- Sar, M. and M. L. Calhoun. 1966. The microscopic anatomy of the integument of the common American goat. *Am. J. Vet. Res.* 27:444.
- Simpson, J. G. and M. R. Gardner. 1972. Comparative microscopic anatomy of selected marine mammals. In: *Mammals of the Sea*, S. R. Ridgway (ed.), pp. 298-418, Charles C. Thomas Company.
- Slijper, E. J. 1966. Functional morphology of the reproductive system in cetacea. In: *Whales, Dolphins and Porpoises*, Kenneth S. Norris (ed.), pp. 277-319, University of California Press.
- Tamura, H. and N. Ur. 1970. Origin of the multiple components of the whale thyroid - stimulating hormone. *Biochem. Biophys. Acta.* 214:566-568.



Yablokov, A. V., V. M. Bel'kovich, and V. I. Borisov. 1972. Kity i del'finy (Whales and dolphins). (In Russ.) Izd-vo. Nauka, Moscow, 472 p. (translated by Joint Publ. Res. Serv., 1974, 528 p. in 2 parts; avail. U.S. Dep. Commer., Natl. Tech. Inf. Serv., Springfield, Va., as JPRS 62150-1 and JPRS 62150-2).

## RESEARCH UNIT 680

### MORPHOLOGICAL STUDIES OF THE VISUAL APPARATUS OF THE BOWHEAD WHALE, BALAENA MYSTICETUS

RICHARD DUBIELZIG, D.V.M.  
GUSTAVO AGIURRE, V.M.D.  
School of Veterinary Medicine  
University of Pennsylvania  
Philadelphia, Pennsylvania 19104

#### INTRODUCTION

Tissue specimens of eyeball, eyelids, and extraocular muscles taken from Eskimo harvested bowhead whales were examined grossly and microscopically. This was performed in the hopes of assessing the importance of vision to the animal and possible complications of contact with oil.

#### OBJECTIVES

To perform morphological studies of the visual apparatus of the bowhead whale, Balaena mysticetus.

#### METHODS

A total of seven eyes from seven different whales were obtained from Eskimo harvested bowhead whales from 1978 to 1980. Four eyes were well enough preserved for accurate measurements and histologic sectioning. Eyes were fixed in 10% neutral buffered formalin. The weight and volume of the eyes were recorded, and measurements were made of the physical dimensions of the ocular structures summarized in Table 6-1. Sections were taken for histologic examination.

#### RESULTS

Gross Observations. The globe was largely spherical but flattened on both the corneal and posterior positions (Fig. 6-1). On sagittal sections the sclera was extremely thick and rigid caudally. The sclera thinned near the limbus but remained rigid, except just around the limbus. Because of the thick caudal sclera, the optically functional portions of the eye were flattened posteriorly (Fig. 6-1).

The cornea was oval shaped in the horizontal plane. There was black pigmentation of the bulbar conjunctiva at the limbus (Fig. 6-2). The cornea was

stretched more or less flat across the anterior segment. The cornea was thick near the limbus and thinned quickly more centrally.

The lens was nearly spherical and very dense and rigid. The pupil was elongated horizontally and slightly bent with the concave side dorsally. The viscosity of the vitreous was very high. The tapetum lucidum was light green to blue and filled the entire fundus except near the ora serrata.

A thick neurovascular plexus surrounded the optic nerve. The nerve is situated to the nasal side of this plexus (Figs. 6-3 and 6-4). Nine arteries from this plexus penetrated the sclera just peripheral to the optic disc to form the posterior choroidal vessels. Four vessels penetrated the thick sclera just anterior to the middle in the anterior-posterior plane. These vessels form the vasculature of the anterior uveal tract.

The eyelids were thick and had no grossly visible eyelashes or glandular structures at the lid margin. The palpebral tissue from nasal to temporal canthus averaged 7.6 cm. On the outer surface the lid was lined by a thick epidermis similar to that found on the rest of the body. At the lid margin the epidermis tapered and became continuous with the conjunctiva. The conjunctival sac extended 3/4 of the way back toward the posterior portion of the eye (Fig. 6-5). This would permit great mobility of the globe within the conjunctival sac. The bulbar conjunctiva was tightly adherant to the sclera. The tendinous attachments of the ocular muscles ran between the sclera and the bulbar conjunctiva. The bulk of the connective tissue of the orbit and eyelids was a firm, rigid, adipose tissue similar to that found subcutaneously throughout the body.

There were only two broad extrinsic ocular muscles. These lie posterior to the globe deep in the orbit. Only a portion of the muscles were submitted from two whales. From each of these muscles there were several tendinous attachments to the equatorial region of the globe. These muscles were quite large, implying an important function in ocular mobility (Figs. 6-6 and 6-7).

Histological Examination. The structure of the cornea was largely similar to that of other mammals. The cornea was thicker at the limbus and rapidly tapered centrally. The thickness peripherally was due to additional deposition of laminated corneal stroma on the inner aspects of the peripheral cornea. Descemet's membrane was very thin.

The filtration angle was a large structure consisting of many trabecular fibers leading to a plexus of dilated veins. The iris had prominent dilated

vessels in the anterior part and well developed smooth muscle posteriorly (Fig. 6-8). The mid-dorsal iris at the papillary margin had the most extensive vascular component. This area may act as an operculum functioning to close the iris to a pinpoint in bright light. The pinpoint pupil would be helpful in adapting for above water vision in two ways, (1) by protecting the predominantly rod retina from bright light, and (2) by adjusting for the natural nearsightedness of the underwater adapted optical system because of the focusing power of a pinpoint aperture.

The ciliary body was almost completely devoid of smooth muscle. There were many clusters of concentrically laminated sensory receptors for the ciliary stroma (Fig. 6-9).

The rigid sclera was composed of very dense strands of collagen. The bands of collagen were tightly interwoven, making the tissue remarkably dense. No mineralization was seen in the sclera. The sclera connective tissue had very few blood vessels.

The neurovascular plexus surrounding the optic nerve was composed of interconnecting arterial vessels which were richly supplied by nerves (Fig. 6-10).

The fibrous tapetum lucidum was found throughout the fundus, except the most peripheral parts. The retina was similar to retinas of other mammals adapted to function in dim light (Fig. 6-11). Ganglion cells and bipolar cells were relatively few. Occasionally, very large ganglion cells were seen. Table 6-2 shows the mean thickness of the retinal layers in the posterior pole, equatorial and peripheral areas.

The eyelids were relatively simple structures. There were no specialized structures at the lid margin. The conjunctival epithelium was similar to that of other species. Mucinous glandular structures were only found on the palpebral side of the conjunctival sac deep down near the fornix. Associated with these glands were laminated sensory nerve endings (Fig. 6-12) similar to those seen in the ciliary body and occasionally in the subepidermal tissue of the lid.

## DISCUSSION

Many of the features of bowhead whale are common to many species of cetaceans. The round, dense lens is an adaptation for underwater vision. The neurovascular plexus around the optic nerve, the thick rigid sclera, the elongated operculated pupil, the nerve endings in the ciliary body, the centrally thin cornea, and the giant ganglion cells of the retina are all features unique to

the cetacean eye (Dawson et al., 1972; Dawson and Perez, 1973; Dra1, 1977; Perez et al., 1974; Vraboc, 1972; Yablokov et al., 1972). The functional significance of these features is not known. Operculate pupils in other species function to reduce the aperture of the pupil in bright light to protect the rod-rich retina from overexposure. An additional function is possible in marine mammals, in that the image on the retina is in focus over a wider range of distances when the pupil aperture is small. This may function to allow for vision above and below water.

The relatively flat cornea may also aid in providing an accommodation mechanism which can be functional both above and below water. A curved cornea functions as part of the refractory system of cornea and lens for vision in air. Underwater, the corneal and aqueous optical density approximates that of water so most or all of the focusing is done by a relatively round and dense lens. If the cornea is flat rather than rounded, then the cornea does not function optically at all so the eye would be similar optically both above and below water. The thick rigid sclera may function to stretch the cornea and thus make it relatively flat.

We would speculate that the cornea would be the structure of the eye most vulnerable to possible effects of exposure to oil. Significant damage to the cornea in other animals that have been studied can result in ulceration, eventual perforation, and blindness.

Sections were made from several areas of retina. It was impossible because of degeneration of tissue to distinguish rods and cones. The relatively thin ganglion cell layer and inner nuclear layer suggest that the receptor cells are primarily rods. Although the retina is generally thicker posterior, there appears to be no area specially adapted for visual acuity. The retina is similar in its makeup to retinas of other species adapted to vision in dim light. The giant ganglion cells seen in bowhead whale retinas had been seen in other cetacean species (Dawson and Perez, 1973; Perez et al., 1972) but the functional significance is not known.

The function of the sensory nerve endings found in the ciliary body, conjunctival sac, and more sparsely in the superficial dermis of the lids is unknown. These resemble pacinian corpuscles and may function in pressure detection. They have been seen in other cetaceans. The lids of the whale are relatively simple structures and appear to function as mechanical and thermal insulation to the orbit.

TABLE 6-1. MEASUREMENTS OF OCULAR STRUCTURES FROM FOUR BOWHEAD WHALES.

	79B2	80B2	80B7	80B8
Volume by water displacement (cc)	150	146	145	155
Weight (gm)	153	147	145	153
Dorsal-ventral (mm)	63	60	60	62
Horizontal (mm)	66	64	63	66
Anterior-posterior (mm)	61	60	60	59
Midcorneal dorsal-ventral (mm)	29	29	32	30
Midcorneal horizontal (mm)	33	34	37	35
Optic nerve diameter (mm)	4x4.5	4.4	4x3.5	4x4

TABLE 6-2. MEAN RETINAL THICKNESS (MICRONS) IN THREE RETINAL LOCI FROM BOWHEAD WHALE 79B2.

Layer	Posterior Pole	Equatorial	Peripheral
Outer segment	24	25	13
Inner segment	13	13	13
Outer nuclear layer	35	35	20
Outer plexiform layer	31	23	8
Inner nuclear layer	23	21	11
Inner plexiform layer	48	39	25
Total thickness of retina	228	206	149

Figure 6-1. Sagittal section of the eye of the bowhead whale. Note the lens (L), thick rigid sclera (S), and vascular plexus (VP).

Figure 6-2. Anterior view of bowhead whale eye showing oval cornea (C) and pigmented bulbar conjunctiva (solid triangles).

Figure 6-3. Lateral view of intact bowhead whale eye showing conical shaped posterior caused by neurovascular plexus (large arrows) around the optic nerve. In this view a portion of the pigmented bulbar conjunctiva (small arrows) is also visible.

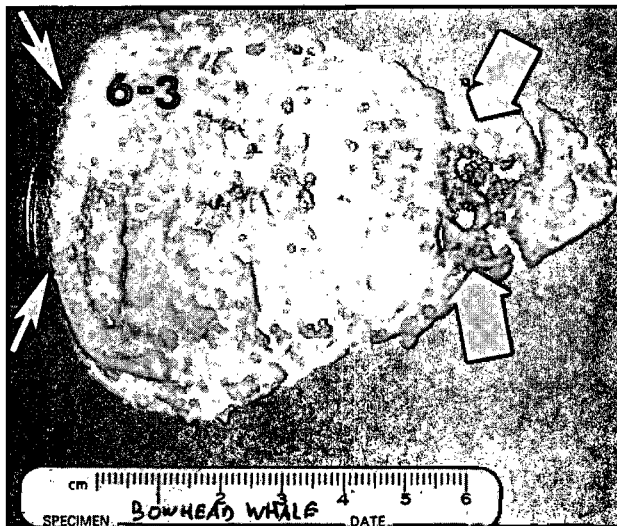
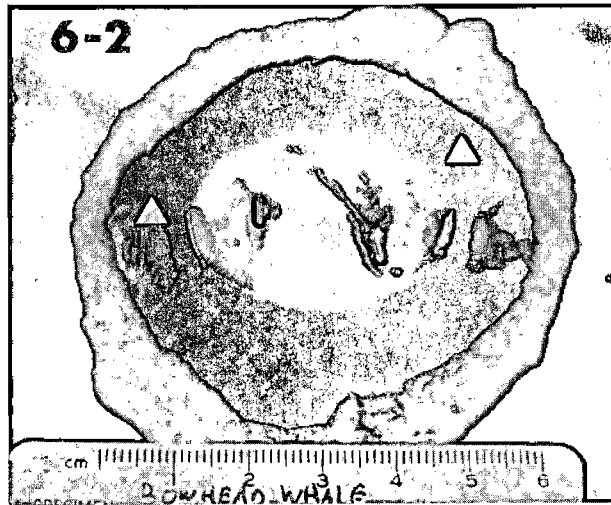
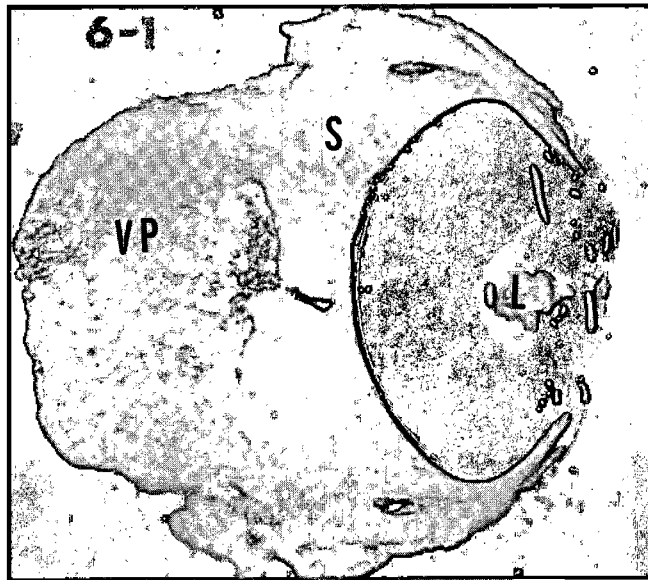




Figure 6-4. Caudal view of bowhead whale eye showing optic nerve (O) surrounded by thick neurovascular plexus (P).

Figure 6-5. Sagittal section of bowhead whale eye with lids (L) and conjunctival sac intact. Notice the deep and exterior conjunctival sac (arrowheads), allowing for free movement of the globe within the sac. Note the thick sclera (S) and the prominent neurovascular plexus (P) behind the eye.

Figure 6-6. Lateral view of eye of bowhead whale (80B7) showing the two large extraocular muscles (M) and their tendinous (T) attachments to the globe. Note also the neurovascular plexus (P) invested in fibrous tissue. A small clamp is holding loose end of one of the muscles.

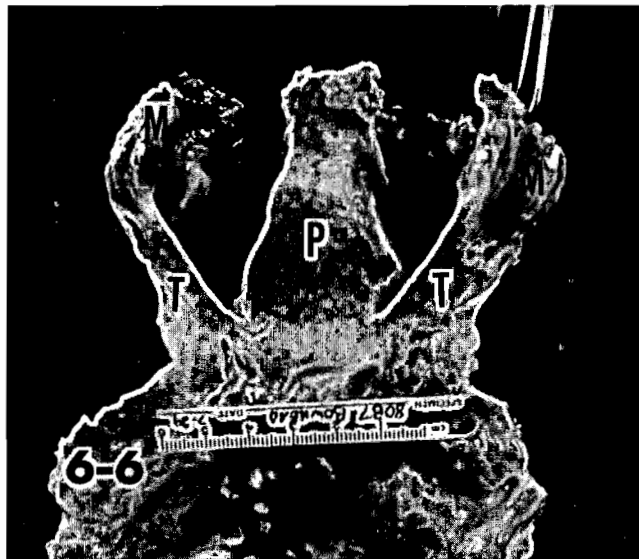
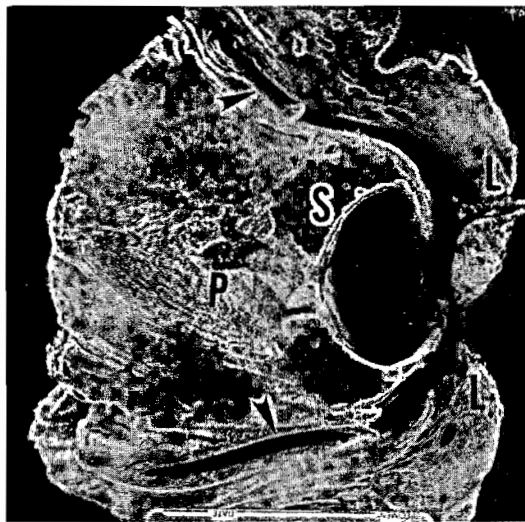
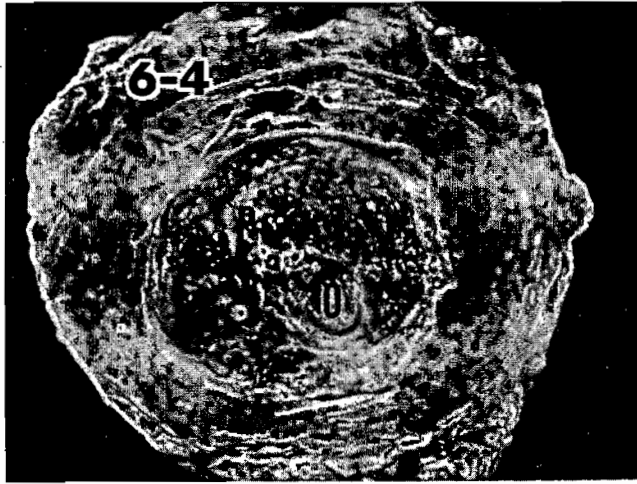


Figure 6-7. Posterior view of same eye as seen in Figure 6-6, showing the multiple tendinous attachments (arrowheads) from each muscle (M). Note also the optic nerve surrounded by the neurovascular plexus (large arrows).

Figure 6-8. Photomicrograph of the iris of a bowhead whale eye showing dilated vasculature (V) anteriorly and dense smooth muscle (M) posteriorly. The smooth muscle is part of the constrictor muscle of the iris. Note also the posterior pigment epithelium (arrows) of the iris. X48.

Figure 6-9. Laminated nerve endings (arrowheads) in the ciliary body of a bowhead whale eye. They resemble pacinian corpuscles and may function in pressure detection. X300.

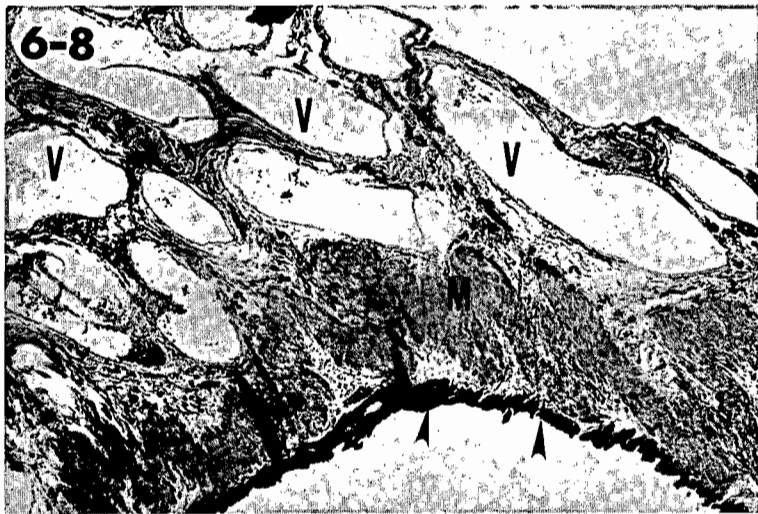
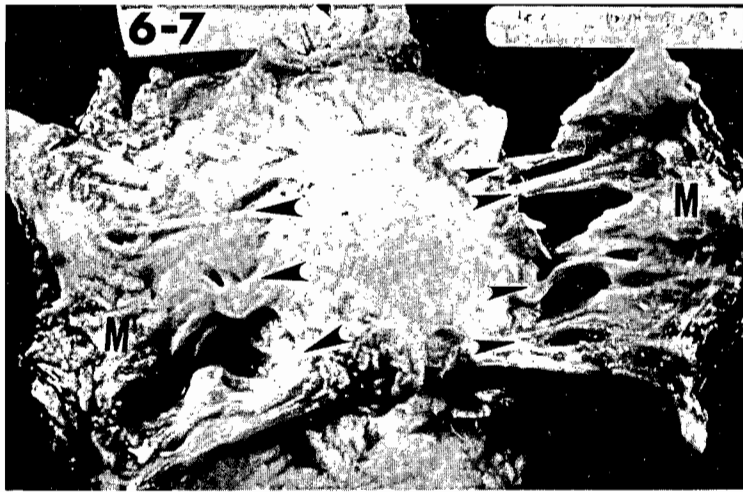
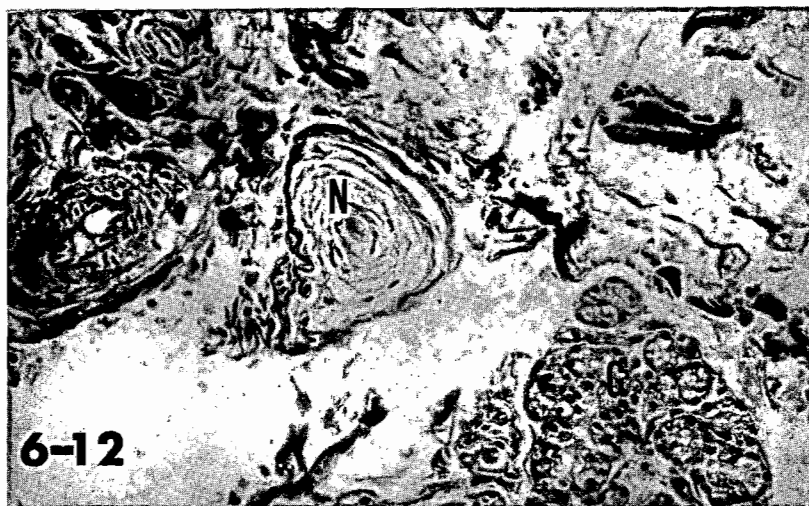
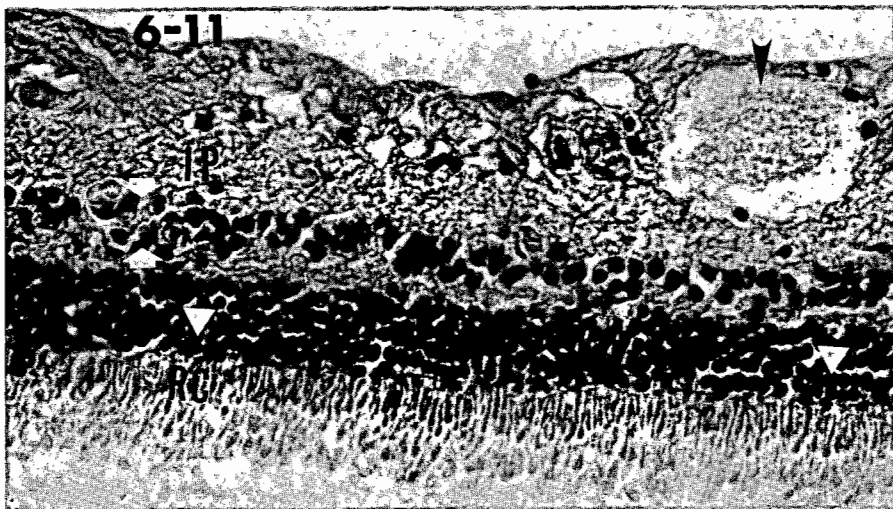


Figure 6-10. Muscular artery (L denotes vessel lumen) and small nerve fiber (arrowheads) from neurovascular plexus. X120.

Figure 6-11. Retina from bowhead whale eye. Note the external nuclear layer (solid white triangles) separating the rods and cones (RC) from the external plexiform layer. Also note the internal nuclear layer (dark layer between white arrows) and the internal plexiform layer (IP). The black arrowhead indicates a giant ganglion cell. X600.

Figure 6-12. Laminated nerve ending (N) in conjunctival sac associated with glandular tissue (G). The glands presumably secrete a lubricating fluid that protects the cornea. X120.



Firsthand observers of bowheads report that the eyes are capable of extensive movement and that the whales are capable of some protrusion of their eyes. The deep conjunctival sac allows for free movement of the globe within the sac. If it were not for the conjunctival sac, the eye would be immobilized by the blubber filling the orbit. The arrangement of the extraocular muscles is especially interesting. The multiple tendinous attachments from the dorsal and ventral muscle suggests that there is probably good control of ocular movement. There is no obvious mechanism by which the whales may protrude the eyes. It is possible, however, that engorgement of the vascular plexus surrounding the optic nerve is capable of causing some protrusion of the globe. If this was the case, the rigid sclera would again be important in resisting changes in the ocular shape.

The morphological studies of the visual apparatus of the bowhead whale suggest that this whale, like other cetaceans, has several modifications which facilitate vision in the underwater environment. Several mechanisms are suggested by which vision above water might also be possible. They probably rely quite heavily on sight in daily functions, but they are probably not capable of great visual acuity. Studies have been made to measure the visual acuity of trained dolphins (Hall et al., 1972). Bowhead whales probably have a visual acuity near that of the dolphins.

#### SUMMARY

Morphological studies were conducted on tissues from Eskimo harvested bowhead whales. Studies of the visual apparatus included gross and histologic observations and measurements. The structure of the globe of the bowhead whale is similar to that of other cetaceans. Speculations were made about the functional significance of the flat cornea, the operculate iris, the laminated nerve endings in the ciliary body, the deep conjunctival sac, the thick rigid sclera, and the vascular plexus surrounding the optic nerve. These whales probably have good vision. The cornea would probably be the area of the eye most vulnerable to injury due to contact with oil.

## REFERENCES

- Dawson, W. W., L. A. Birndorf, and J. M. Perez. 1972. Gross anatomy and optics of the dolphin eye. *Cetology* 10:1-12.
- Dawson, W. W. and J. M. Perez. 1973. Unusual retinal cells in the dolphin eye. *Science* 181:747-749.
- Dral, A. D. G. 1977. On the retinal anatomy of cetacea (mainly Tursiops truncatus). In: *Function Anatomy of Marine Mammals*, R. J. Harrison (ed.), pp. 81-135. Academic Press, New York.
- Hall, N. R., H. F. Hall, M. C. Caldwell, and D. K. Caldwell. 1972. Visual acuity under conditions of near darkness and discrimination learning in the Atlantic bottlenosed dolphin. *Cetology* 12:1-7.
- Perez, J. M., W. W. Dawson, and D. Landau. 1972. Retinal anatomy of the bottle-nosed dolphin. *Cetology* 11:1-11.
- Vraboc, F. 1972. Encapsulated sensory corpuscles in the sclerocorneal boundary tissues of the killer whale (Orcinus orca). *Acta Anat.* 81:23-29.
- Yablokov, A. V. et al. 1972. The eye and other sense organs in whales and dolphins. In: *Whales and Dolphins, Part I*, pp. 291-318. Nauka, Moscow, 1972. (National Technical Information Service Translation.)



## RESEARCH UNIT 780

# THE MICROSCOPIC EXAMINATION OF THE BOWHEAD WHALE, BALAENA MYSTICETUS, AND THE GRAY WHALE, ESCHRICHTIUS ROBUSTUS FOR CHANGES DUE TO TOXIC SUBSTANCES AND INFECTIOUS AGENTS

GEORGE MIGAKI, D.V.M.  
Universities Associated for Research and  
Education in Pathology, Inc.  
9650 Rockville Pike  
Bethesda, Maryland 20014  
and  
Registry of Comparative Pathology  
Armed Forces Institute of Pathology  
Washington, D.C. 20306

### INTRODUCTION

In order to evaluate tissues for evidence of pathology, one must use normal structure as a guide. The normal histological structure of the various tissues of the bowhead whale is being determined through the cooperative efforts of the investigators involved in this effort.

In an endangered animal such as the bowhead whale, the "normal" impact of disease on the population should be investigated. In addition, critical tissues should be monitored throughout the period of offshore oil development for changing instances of disease or influence of toxic substances.

### OBJECTIVES

1. To determine histologically the nature of abnormal tissues in hunter-killed and stranded bowhead and gray whales and to identify the probable cause if possible.
2. To prepare a histological study set of tissues of the bowhead whale through the Registry of Comparative Pathology. Such a study set will represent normal tissues from all available organs and tissue structures that are in satisfactory condition.

## METHODS

All of the tissue specimens came from Eskimo harvested whales by way of RU 180. Only tissues which appeared abnormal to investigators in RU 180 were selected for histologic examination. The selected tissue specimens had been fixed in 10% buffered formalin and each tissue was accompanied by a label which identified the organ and whale number.

On receipt in the laboratory, each tissue specimen was carefully examined for abnormalities and photographed when necessary.

Tissue specimens were cut in blocks, 3-4 mm in thickness, for embedding in paraffin. Tissue sections were cut 8  $\mu$ m in thickness for histopathologic examination. All sections were stained with hematoxylin and eosin (H&E) and when necessary, special stains such as periodic acid-Schiff (PAS), Gomori's methenamine-silver (GMS), Giemsa, or Brown and Brenn (B&B) were also utilized.

Tissue specimens were received from six whales which were identified as 80B1, 80B2, 80B7, 80B8, 80B9 and 80G1 (see RU 180). Specimens from whale 80B1 were accessioned as AFIP 1747957, whale 80B2 as AFIP 1747956, whale 80B7 as AFIP 1747958, whale 80B8 as AFIP 1747954, whale 80B9 as AFIP 1747955, and whale 80G1 as AFIP 1750446.

Normal tissues were selected by investigators in RU 180 for the histological study set.

## RESULTS

Histologic examination was conducted on all of the selected tissue specimens submitted from the 6 whales. The histopathologic findings of the whales are listed in the same order as the RESULTS sections of RU 180.

### Bowhead Whale 80B1

Tag 41: A grayish-white area with irregular margins in the rear of the mouth (Figs 7-1 and 7-2).

Histologic examination of the grayish-white area revealed a complete lack of melanocytes in the basal layer of the epithelium of the oral mucosa (Figs 7-3 and 7-4). The epithelium was otherwise normal. There appeared to be no significant change in the size or shape of the rete ridges of the epithelium, and leukocytic infiltrates were generally lacking in the lamina propria. However, a slight increase in the amount of collagenous fibers was noted in the lamina propria.

Tag 103: Three smooth grayish-white areas in the rear of the mouth. Histologic examination of the grayish-white areas showed the epithelium of the oral mucosa to be essentially normal except that there was a complete absence of melanocytes of the basal layer. The rete ridges of the epithelium were essentially normal and there were no leukocytic infiltrates in the lamina propria. There appeared to be a slight increase in the amount of mature collagenous fibers which were arranged in broad bundles.

Tag 58: Four areas of white skin found on the blowhole (Figs 7-1 and 7-2).

Histologic examination of the white and black portion of the skin showed them to be essentially the same in that the various layers of the epidermis were present. The only difference was that melanocytes were lacking in the basal layer of the epidermis in the white skin. There was no evidence of inflammation in the superficial portion of the dermis and the rete ridges of the epidermis were essentially normal in their size and shape.

#### Bowhead Whale 80B2

Tag 37: A single 2 x 1 x 1 cm raised nodule in the mucosa of the nonglandular part of the stomach. Cut surface showed a cheesy greenish-yellow material.

Histologic examination of the nodule showed it to be a parasitic granulomatous inflammatory process characterized by a large central area of degenerated eosinophils surrounded by a wide zone of macrophages (histiocytes or epithelioid cells), some of which had coalesced forming multinucleated giant cells. Lymphocytes and plasma cells were also noted. The periphery of the nodule was composed of a capsule containing a narrow band of mature collagenous connective tissue fibers. The nodule was located just beneath the epithelium of the gastric mucosa. Such lesions are suggestive of invasion of the stomach wall by a metazoan parasite. Numerous sections of the nodules were cut, but only degenerated fragments of a parasite could be found in the nodule.

Tag 39: A single nodule 1 cm in diameter, in mucosa of the nonglandular part of the stomach.

Histologic examination of the nodule showed that it was located in the submucosa of the gastric wall. The nodule was a granulomatous inflammatory process characterized by a large central area of degenerated eosinophils which was surrounded by a wide zone of epithelioid granulation tissue containing epithelioid cells, multinucleated giant cells, lymphocytes and eosinophils. A thin connective tissue capsule was found on the periphery. Such lesions are suggestive of those caused by a metazoan parasite. Numerous sections were prepared from the nodule but only degenerated fragments of a parasite could be found.

Tag 36: A solitary 2 x 1 cm pinkish-white circumscribed raised mass on the diaphragmatic surface of the liver (Figs 7-5 and 7-6).

Histologic examination of the circumscribed tumor showed it to be a lipoma composed of normal-appearing fat cells (Figs 7-7 and 7-8)). There was no evidence of encapsulation of the lipoma nor was there any evidence of neoplastic cell infiltration of the hepatic tissue. There was some atrophy of the hepatocytes adjacent to the neoplasm, and this was attributed to the compression caused by the expansile growth of the lipoma.

#### Bowhead Whale 80B7

Tag 4: One of several raised nodules, 1 cm in diameter, (Fig 7-9) which were found in the mucosa of the nonglandular portion of the stomach.

Histologic examination of the nodule showed it to be a well encapsulated granulomatous inflammatory process. The center was composed of large amounts of degenerated eosinophils in which cross sections of a nematode were found (Fig 7-10). This parasite was subsequently identified as an anisakine nematode by Dr. R. Heckmann, (RU 1280).

Tag 11: A solitary nodule in the mucosa of the nonglandular portion of the stomach.

Histologic examination of the nodule showed it to be identical to the nodule described in tag 4. Cross sections of a nematode were found in the necrotic center. The nematode was identified as an anisakine nematode.

Tag 25: A solitary raised nodule in the mucosa of the nonglandular portion of the stomach.

Histologic examination of the nodule showed it to be identical to the nodule described for tag 4. Numerous sections of the nodule were cut and examined but only degenerated fragments of a parasite could be demonstrated.

Tag 33: A nodule projecting up 3-4 mm on the mucosa of the nonglandular portion of stomach.

Histologic examination of the nodule showed it to be identical to the nodule described for tag 4. Although this nodule was very suggestive of one caused by a metazoan parasite, no parasite could be found. However, eosinophilic amorphous longitudinal fragments suggestive of degenerated parasites were found in the necrotic center.

Tag 14: A "V shaped" crevice (Figs 7-11 and 7-12) on the skin at the lateral aspect of the upper lip.

Histologic examination of the "V shaped" crevice in the skin showed it to be affected by a necrotic epidermatitis characterized by necrosis and degeneration of the cells in the stratum externum of the epidermis. Numerous colonies of gram-positive septate filamentous micro-organisms, presumed bacteria, were found in damaged tissues and extended downward into the stratum intermedium. In addition, there were small spherical to ovoid unicellular micro-organisms, slightly birefringent, suggestive of diatoms (see RU 1280, RU 1380). The outer layers of the epidermis and dermis were unaffected.

Tag 35: Mushy "fungus-like" tissue on the outer surface of the skin between the snout and blowhole.

Histologic examination of the "fungus-like" lesion on the skin showed a necrotic epidermatitis involving only the superficial layer, that is, the stratum externum of the epidermis. The cells in this layer had undergone extensive degeneration and necrosis in which there were numerous colonies

of gram-positive septate filamentous organisms. These organisms were negative for the PAS and GMS techniques which indicates that they are not fungi. In addition, there were numerous small unicellular ovoid to spherical birfringent forms that were suggestive of diatoms (see RU 1280, RU 1380).

Tag 17: A groove in the skin located anterior-ventral to blowhole. Histologic examination of the groove in the skin showed it to be affected by a necrotic epidermatitis similar to the "V shaped" crevice described for tag 14. The degeneration and necrosis of the cells were confined to the stratum externum; the other layers of the epidermis and dermis remained unaffected. Organisms similar to those described for tag 14 were found invading and surrounding the damaged epithelial cells.

Tag 9: Two large skin lesions on left upper jaw. Histologic examination of the lesions on the skin showed them to be necrotic epidermatitis similar to the lesions described for tag 14. The inflammatory and degenerative changes were confined to the superficial portion of the epidermis; the remainder of the epidermis and the dermis remained unaffected. Microbiological forms similar to those described for tag 14 were found invading and surrounding the damaged epithelial cells.

Tag 14A: Old skin lesion on the tip of the chin (Figs 7-13 and 7-14). Histologic examination of the lesion on the skin showed it to be a chronic active ulcerative necrotic dermatitis characterized by loss or sloughing of the epidermis, and extensive chronic suppurative inflammation extending deep into the dermis and subcutaneous tissue (Figs 7-15 and 7-16). The lesion was surrounded by fibrous tissue. Such lesions are probably the result of some traumatic penetrating object, and the present lesion is indicative of one of long duration.

#### Bowhead Whale 80B8

Tag 2: Two "white dots" in back of mouth.

Histologic examination of the "white dots" in the mouth showed a normal epithelium of the oral mucosa except that there was total absence of melanocytes in the basal layer of the epithelium. The rete ridges appeared to be somewhat wider with more branching than normal. The dermis was essentially normal with no evidence of fibrosis or leukocytic infiltrates.

Tag 4: Skin, lesion from left side of face, lesion part of epidermis starting to peel off (Fig 7-17).

Histologic examination of the lesion in the skin showed it to be a necrotic epidermatitis with an inflammatory process involving only the superficial portion or stratum externum of the epidermis (Fig 7-18). The remainder of the epidermis and dermis were unaffected. Within the degenerated and necrotic epithelial cells of the epidermis, there were numerous gram-positive septate filamentous bacterial forms (Fig 7-19) (see RU 1280, RU 1380). In addition, small ovoid to spherical birefringent unicellular organisms, possibly diatoms, were noted scattered throughout the damaged areas (see RU 1280, RU 1380).

#### Bowhead Whale 80B9

Tag 100: Three erosions of anal mucosa (Figs 7-20 and 7-21).

Histologic examination of the "ulcer" in the anorectal canal showed a discrete area with complete loss of the stratified squamous epithelium. Underneath the desquamated epithelium, there was a severe chronic active inflammatory process characterized by granulation tissue, large accumulations of mononuclear leukocytes (plasma cells, lymphocytes and macrophages), and lesser numbers of polymorphonuclear neutrophils. In addition, in the deeper portions of the inflamed areas, there were numerous lymphoid nodules containing germinal centers (Figs 7-22 and 7-23). Ulcerative lesions of this nature are considered to be of long duration. Special stains designed to demonstrate infectious organisms such as bacteria, fungi and parasites failed to reveal any etiologic agents.

## Bowhead Whale 80G1

The animal had been struck at some time in the past as a healed bomb wound (Figs 7-24 and 7-25) was located (see RU 180).

Histologic examination of the whitish tissue found encapsulating the bomb showed it to be lined by an epidermis which appeared to be essentially normal except for complete absence of melanocytes in the basal layer (Figs 7-26 and 7-27). The rete ridges were irregular in size and shape when compared to normal ones. They were slightly broader in width and showed more branching and varied in their depth of penetration into the dermis. The thickness of the epidermis varied from area to area. There was a considerable amount of fibrosis in the dermis, most of which was characterized by mature collagenous fibers arranged in thick bundles. In some areas the fibrosis was limited to the superficial portions of the dermis, while in other areas it extended downward into the blubber and replaced the adipose tissue. In many areas of the fibrosed dermis, especially the superficial areas, there were numerous collections of mononuclear leukocytes, mostly plasma cells, lymphocytes and histiocytes (Fig 7-28). The leukocytes were located perivascularly.

Polymorphonuclear leukocytes were absent. From these histologic findings it appears that the epidermis had regenerated without the formation of melanocytes. The fibrosis and chronic inflammatory cells in the dermis indicate that the penetration of the skin by the bomb and its subsequent localization had taken place long ago, most likely more than 6 months previously. The normal color of the blubber is whitish-yellow; the whitish firm mass in the blubber represents mature fibrous tissue. The bluish discoloration of tissue beneath the white epidermis of the skin represents leakage and absorption of the material from the bomb.



The second objective of this study was to prepare a study set of tissue sections for histologic examination from available organs that were considered to be satisfactory. In addition to the organs collected from whale 79B1, 79B2 and 79B3 from the previous period of study, organs were collected from whales 80B1, 80B2, 80B7, 80B8, 80B9.

Due to the difficulty involved in obtaining satisfactory tissue specimens from the bowhead whale (see RU 180), it was not possible to prepare and include all of the organs. Specimens such as the spinal cord, some portions of the alimentary and genital tracts and some of the endocrine organs were not included in the study set because they were not made available to us. Provisions have been made so that when such specimens do become available at a later date, they can be added to the set. Included in the study set are the following:

Eyelids	Bronchus
Eyeball	Lung
Bones	Heart
Skeletal muscle	Blood vessels
Skin from various sites	Rete mirabile
Lips	Adrenal
Palate	Testis
Tongue	Epididymis
Stomach	Penis
Intestine	Prepuce
Colon	Kidney
Liver	Bladder
Pancreas	Spleen
Omentum	Thymus
Larynx	Ovary
Lymph nodes	Cervix
Uterus	Brain
Vagina	

- Figure 7-1. Whale 80B1. Top view of tag 41 (A) and tag 58 (B). Tag 41, from the rear of the mouth, shows grayish-white area (arrows) with irregular margins. Tag 58, from the region of the blowhole, shows a discrete area of white skin.
- Figure 7-2. Whale 80B1. Cut surfaces of Fig 7-1, tag 41 (A) and tag 58 (B). Tag 41 shows the distribution of the whitish areas (arrows) in the epithelium (E) of the oral mucosa. Submucosa (S). Tag 58 shows the white epidermis (arrows) located between the black epidermis. Dermis (D).
- Figure 7-3. Whale 80B1. Photomicrograph of tag 41 showing the absence of melanocytes in the basal layer (BL) of the epithelium of the oral mucosa. Note the high upward extension of the dermal papillae (DP) into the epithelium. Dermis (D), blubber (B). H & E, 15X.
- Figure 7-4. Whale 80B1. Tag 41. Higher magnification of Fig 7-3 to illustrate the absence of melanocytes in the basal layer (BL) of the epithelium. H & E, 252X.

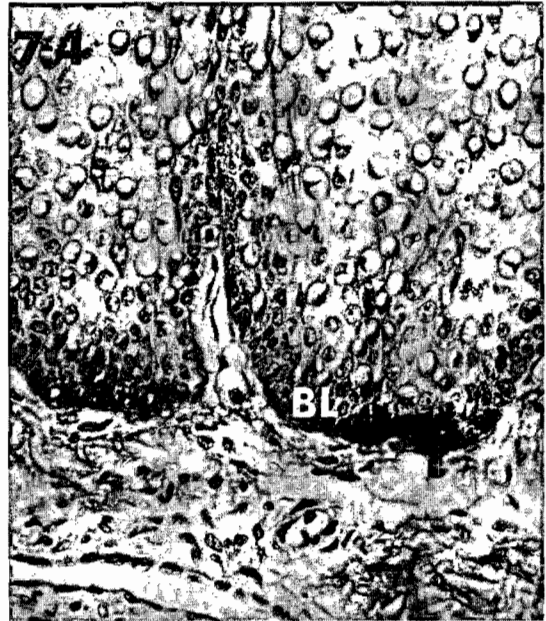
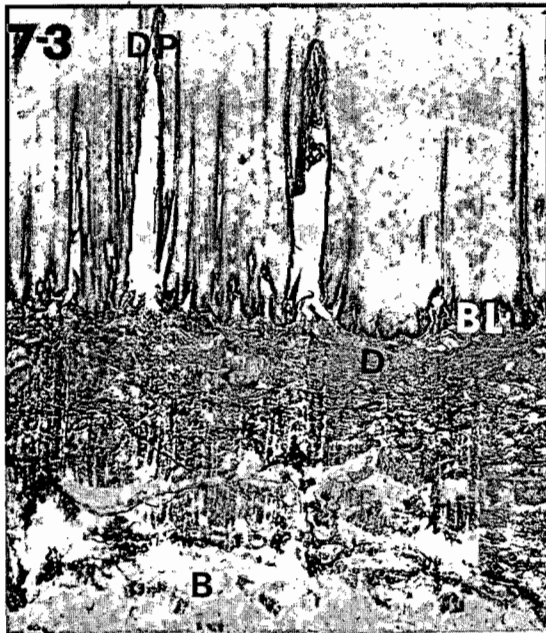
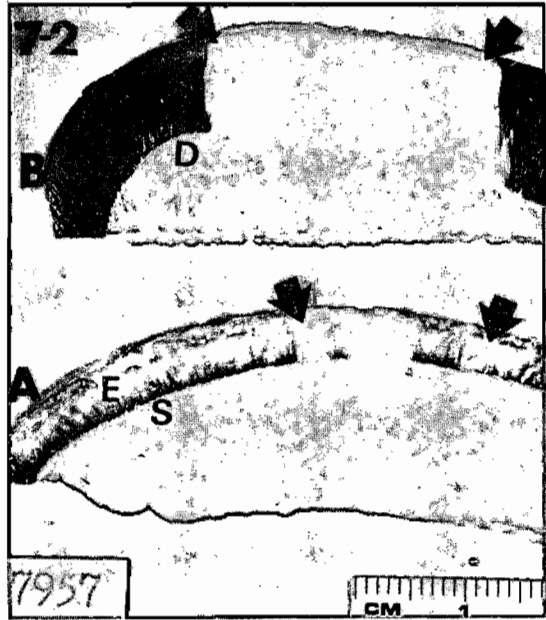
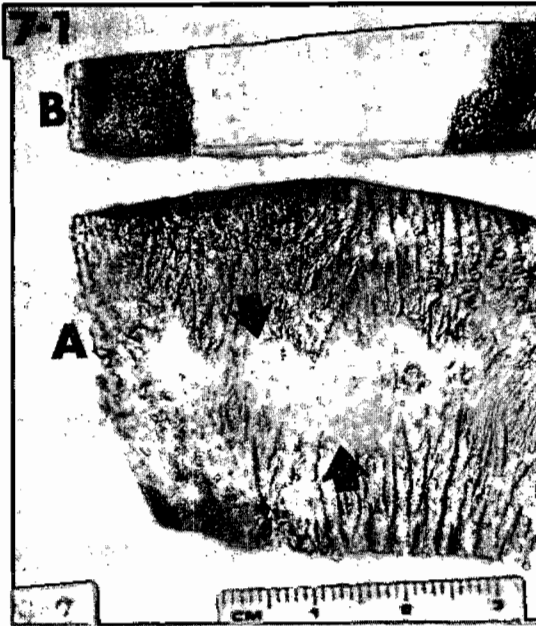
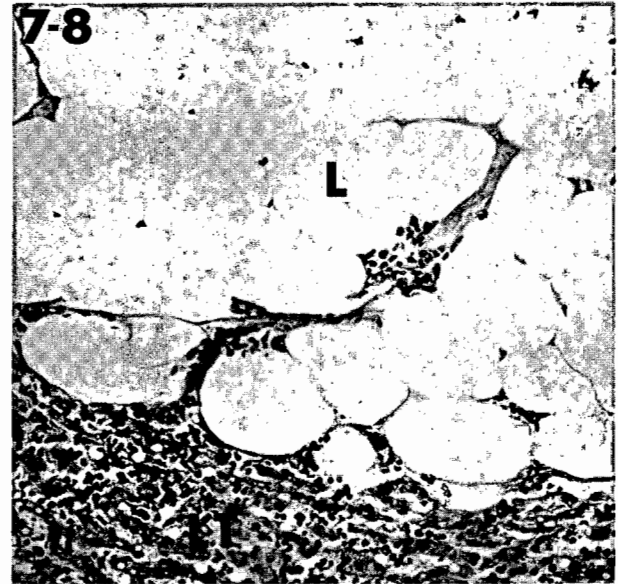
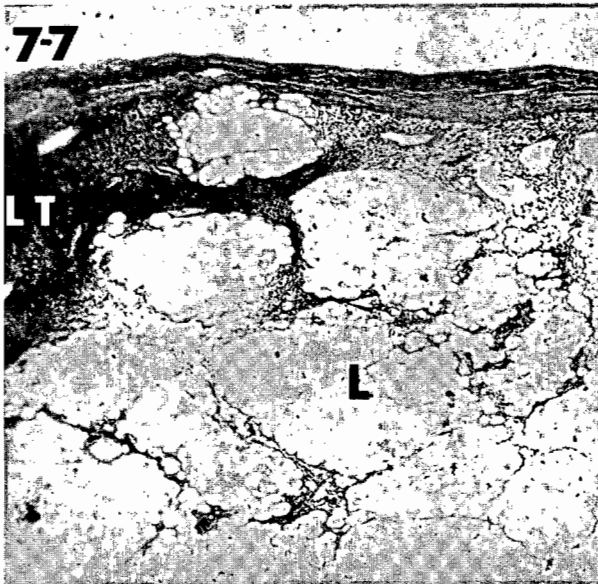
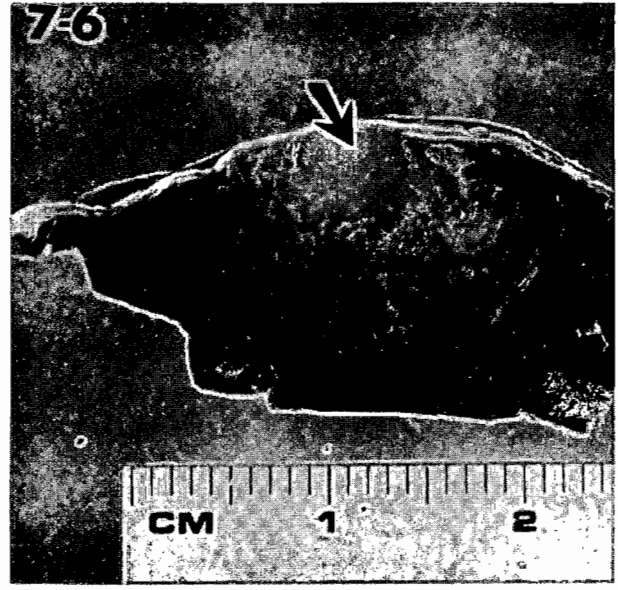
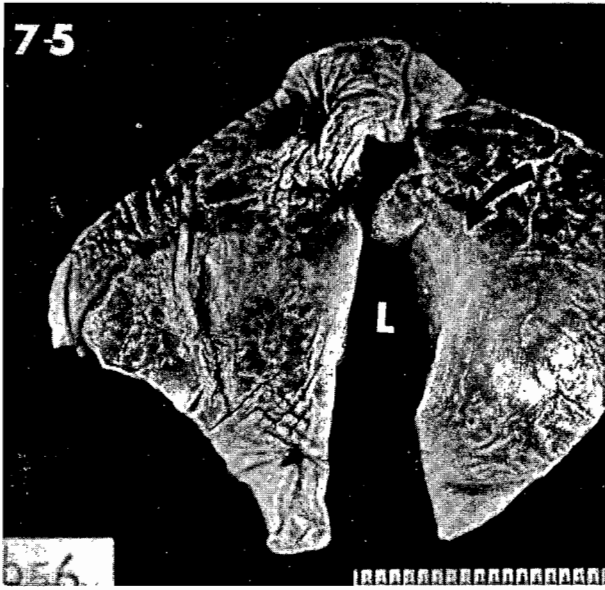


Figure 7-5. Whale 80B2. Tag 36. Dorsal view of the lipoma (arrow) on the diaphragmatic surface of the liver. The lipoma was pinkish-white and raised about 1 mm. Specimens for electron microscopy were removed from the center of the lipoma (L) prior to photographing the neoplasm.

Figure 7-6. Whale 80B2. Tag 36. Cut surface of the lipoma (arrow) in the liver in Fig 7-5. Note the nodular and circumscribed appearance of the lipoma.

Figure 7-7. Whale 80B2. Tag 36. Photomicrograph of the lipoma (L) in the liver. Fat cells are arranged in large masses and separated into lobules by thin connective tissue septa. Liver tissue (LT). H & E, 15X.

Figure 7-8. Whale 80B2. Tag 36. Higher magnification of Fig 7-7 illustrating the morphologic appearance of the fat cells of the lipoma (L). Liver tissue (LT). H & E, 150X.



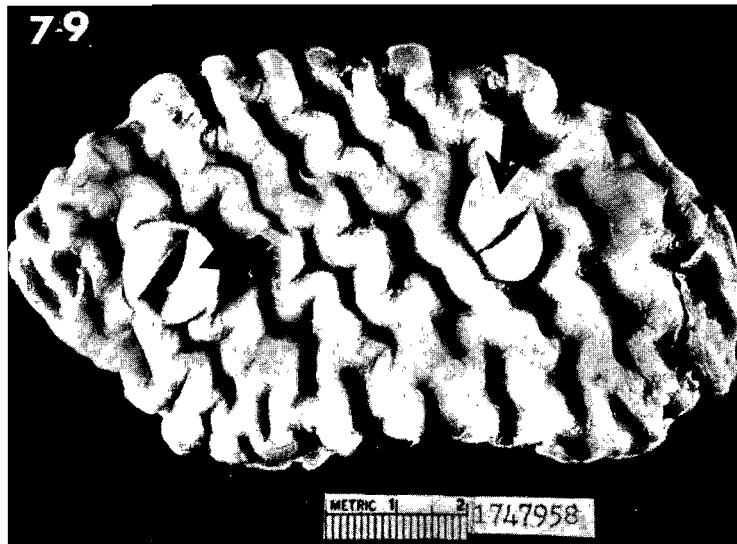


Figure 7-9. Whale 80B7. Tag 4. Two raised nodules (arrows) found on the mucosa of the nonglandular portion of the stomach. Both nodules were incised to obtain material for bacteriologic isolation studies.

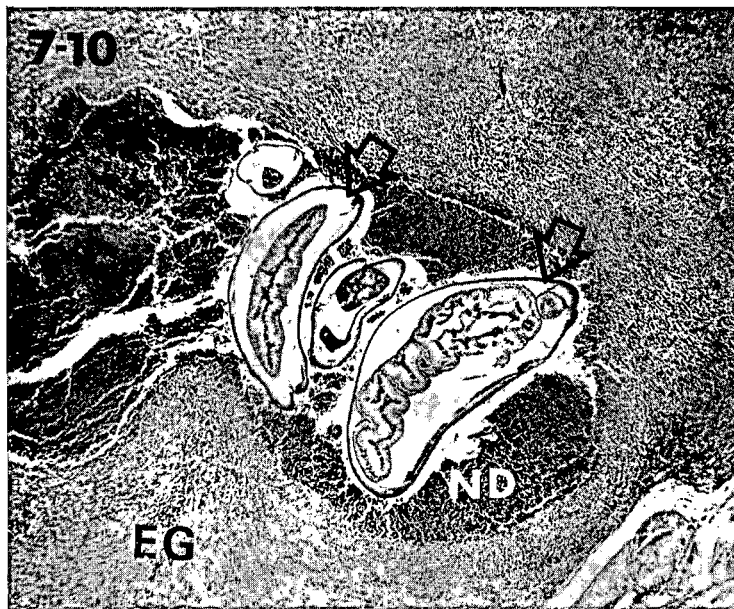


Figure 7-10. Whale 80B7. Tag 4. Photomicrograph of the nodule in the mucosa of the nonglandular portion of the stomach. Note cross section of the parasite (arrows) which was identified as an anisakine nematode by Dr. R. Heckmann (RU 1280). The parasite was found in the necrotic debris (ND) composed of degenerated eosinophils and surrounded by a wide zone of epithelioid granulation tissue (EG). H & E, 25X.

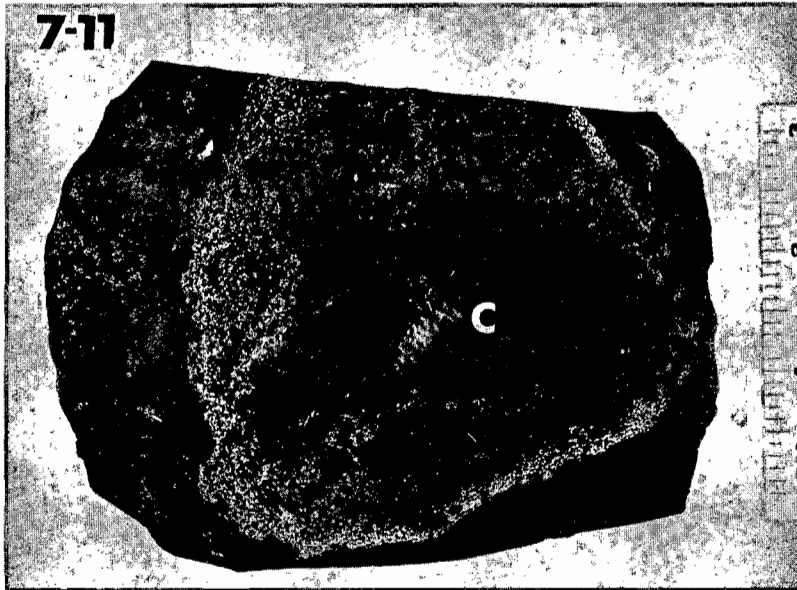


Figure 7-11. Whale 80B7. Tag 14. Top view of a "V-shaped" crevice (C) found on the lateral aspect of the skin on the right side of the upper lip.

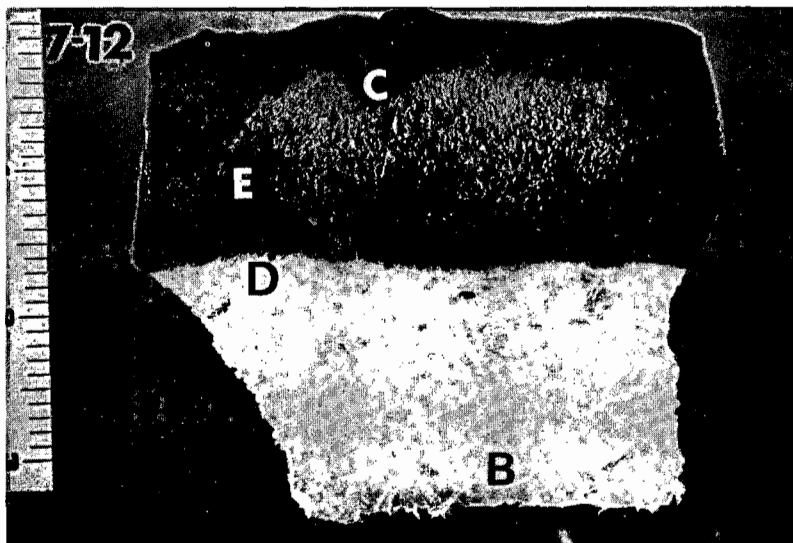


Figure 7-12. Whale 80B7. Tag 14. Cut surface of Fig 7-11 illustrating the extension of the "V-shaped" crevice (C) into the epidermis (E). Dermis (D), blubber (B).

Figure 7-13. Whale 80B7. Tag 14A. Top view of a large deep ulcer (arrows) on the tip of the chin along the ventral midline.

Figure 7-14. Whale 80B7. Tag 14A. Cut surface of specimen of Fig 7-13 to illustrate the deep penetration of the ulcer (U) in the dermis. White epidermis (E) and dermis (D) of the skin of the chin.

Figure 7-15. Whale 80B7. Tag 14A. Photomicrograph of the ulcer (U) and the adjacent epidermis (E) of the chin. There is much fibrosis in the dermis (D) and a considerable amount of leukocytic exudate (LE) on the superficial surface of the ulcer. H & E, 15X.

Figure 7-16. Whale 80B7. Tag 14A. Higher magnification at the edge of the ulcer in Fig 7-15 to illustrate the granulation tissue, leukocytic infiltrates and atrophy of the rete ridge (arrow). H & E, 60X.



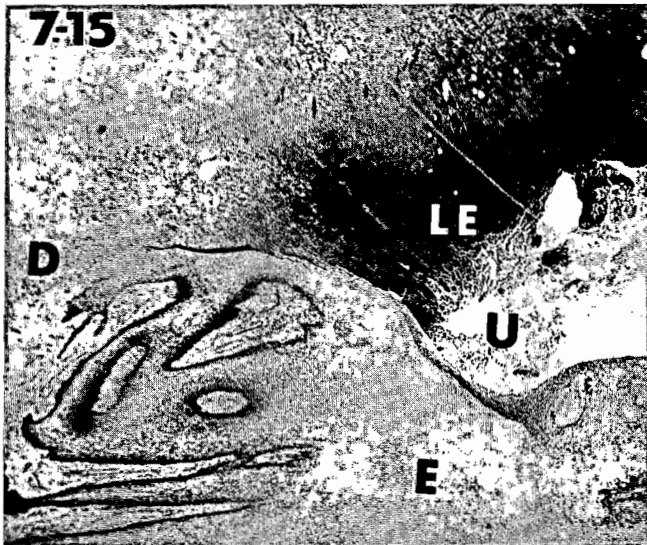
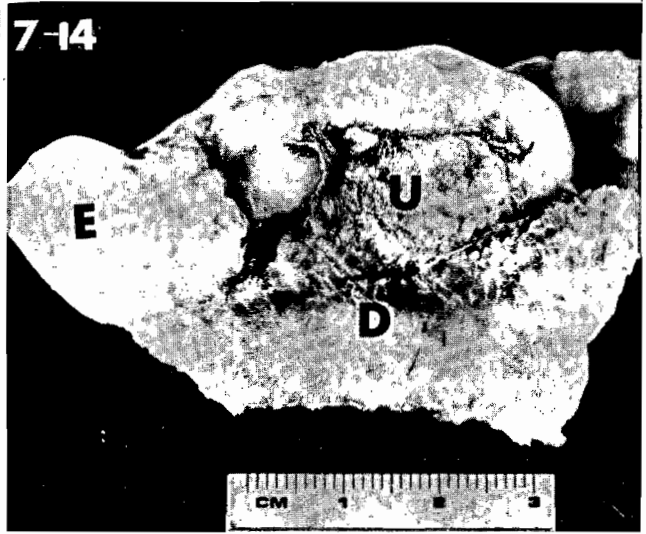


Figure 7-17. Whale 80B8. Tag 4. Top view of the skin of the left side of the face where the outer surface of the lesion is starting to peel off. Note the rough surface (arrows) of the superficial portion of the epidermis.

Figure 7-18. Whale 80B8. Tag 4. Photomicrograph of the rough surface of the superficial portion of the epidermis in Fig 7-17. Note large numbers of colonies of filamentous micro-organisms (arrows) on the surface and extending downward into the epidermis (E). H & E, 157X.

Figure 7-19. Whale 80B8. Tag 4. Higher magnification of Fig 7-18 to illustrate the striated appearance of the filamentous micro-organisms (large arrows). In addition, there are numerous collections of smaller unicellular organisms (thin arrows). H & E, 630X.

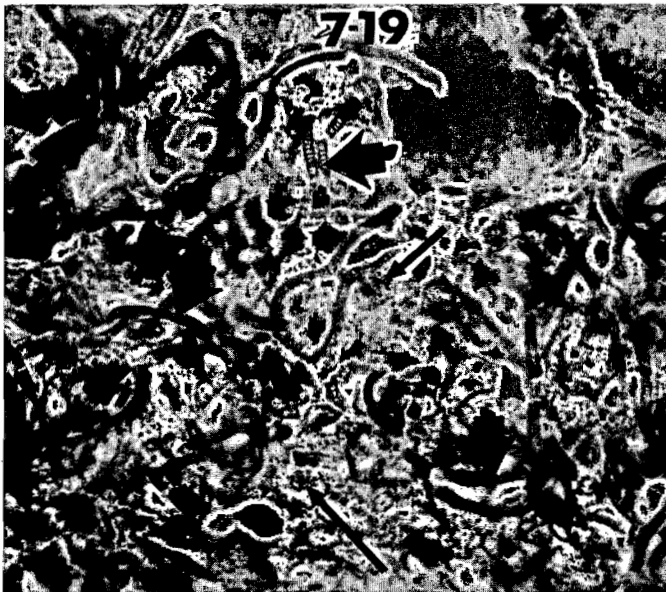
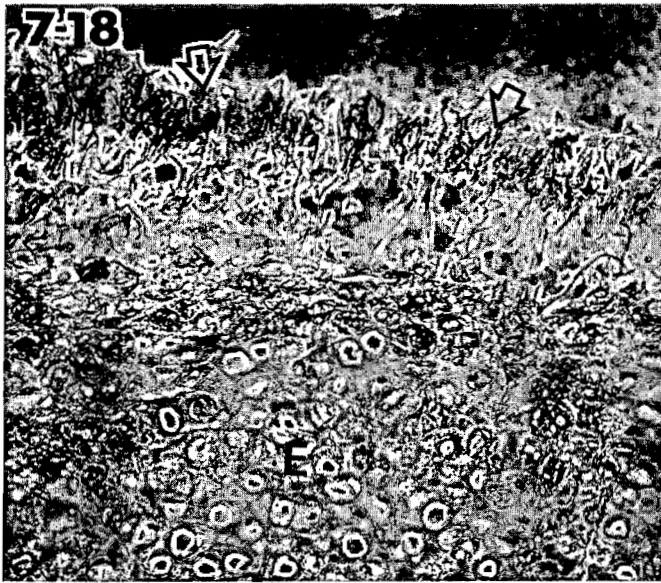
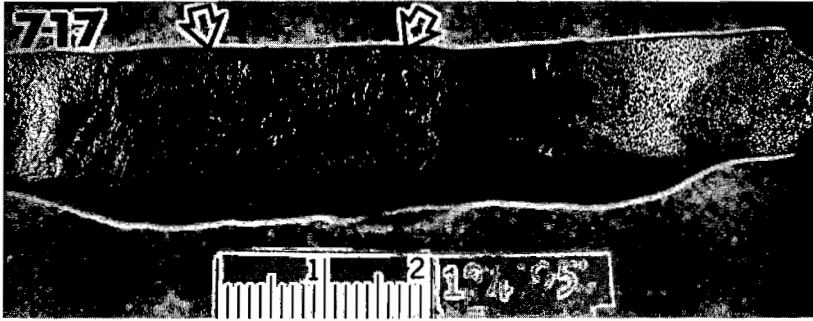
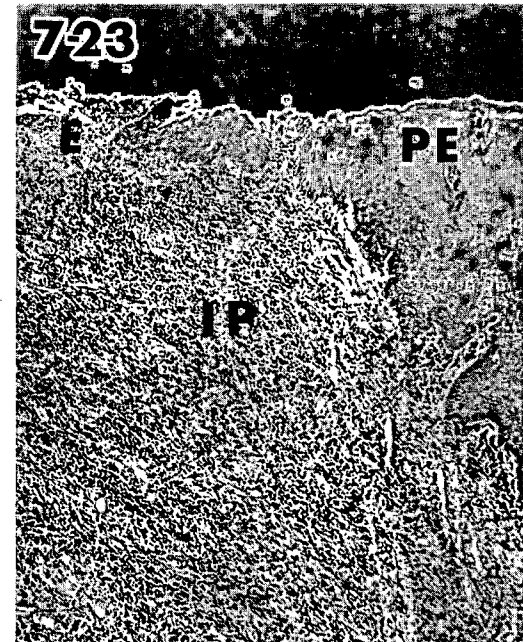
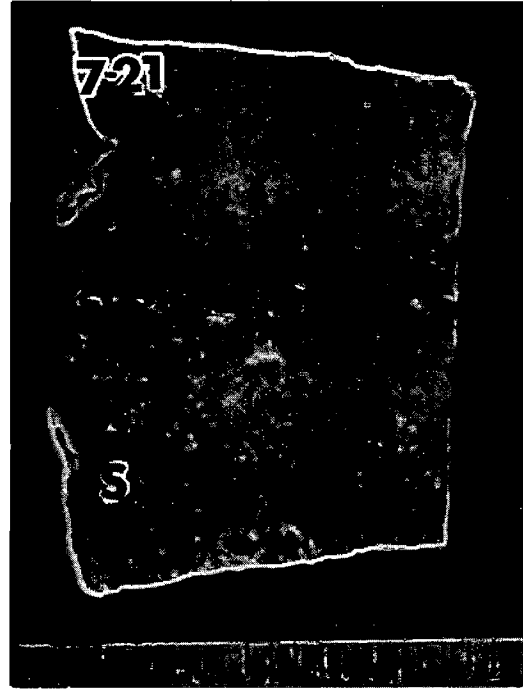
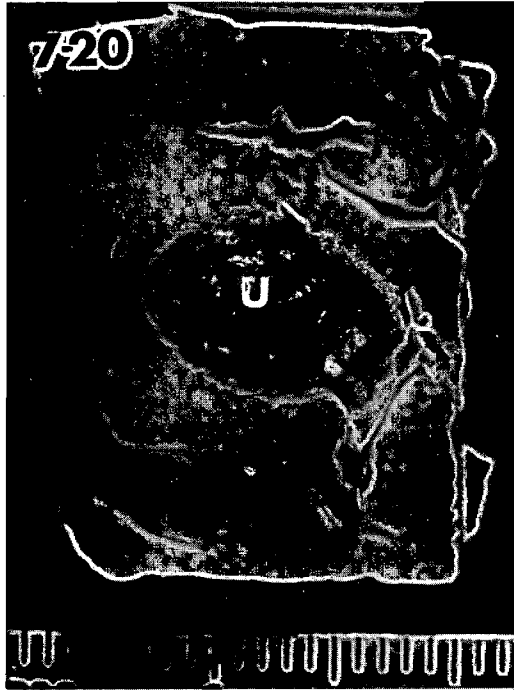


Figure 7-20. Whale 80B9. Tag 100. Top view of a single ulcer (U) found on the anorectal mucosa.

Figure 7-21. Whale 80B9. Tag 100. Cut surface of the ulcer in Fig 7-20 to illustrate the loss of epithelium (arrow) of the anorectal mucosa. Submucosa (S).

Figure 7-22. Whale 80B9. Tag 100. Photomicrograph of the ulcer (arrow) in Fig 7-20 to illustrate the chronic active inflammatory process (IP) beneath the desquamated epithelium. Note lymphoid nodules (LN) with germinal centers. H & E, 15X.

Figure 7-23. Whale 80B9. Tag 100. Higher magnification at the edge of the ulcer in Fig 7-22 to illustrate the desquamated epithelium (E), pre-existing epithelium (PE) and the chronic active inflammatory process (IP) characterized by large numbers of lymphocytes, macrophages and plasma cells. H & E, 60X.



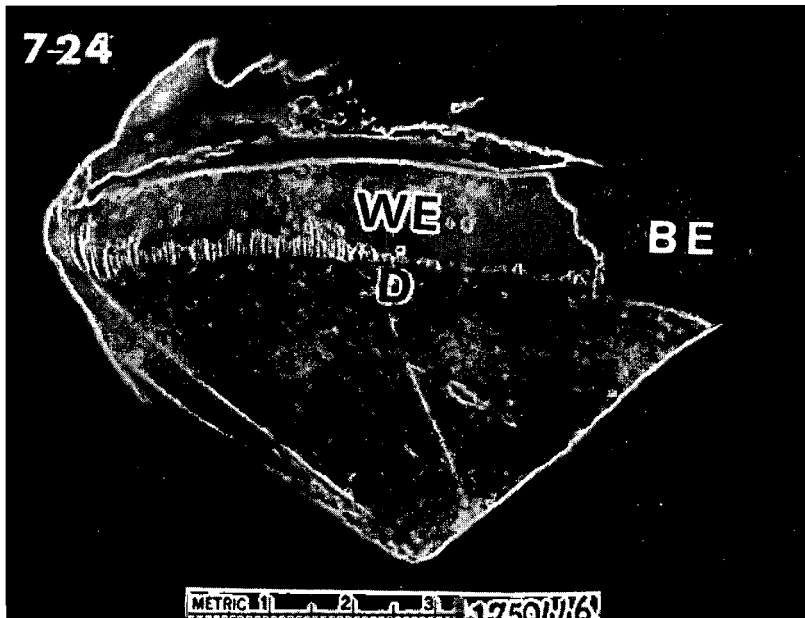


Figure 7-24. Whale 80G1. Skin from the occipital area which was believed to be the entrance of a harpoon. Note the white epidermis (WE) and the normal appearance of the black epidermis (BE). Dermis (D).

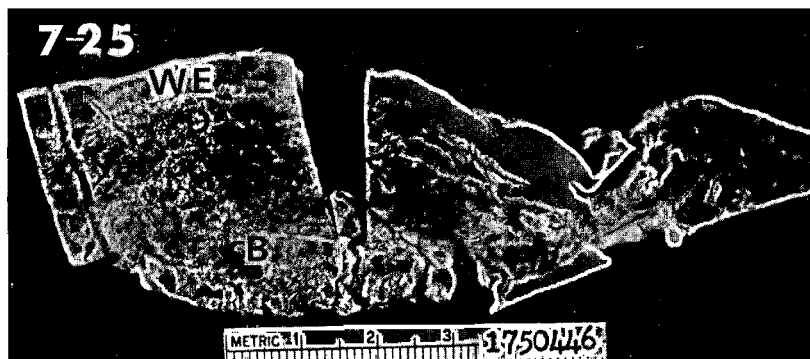


Figure 7-25. Whale 80G1. White epidermis (WE) had encapsulated the bomb fragments. Beneath the white epidermis, the dermis (D) and blubber (B) were both firm and blue. Tissue (arrow) removed for histologic examination.

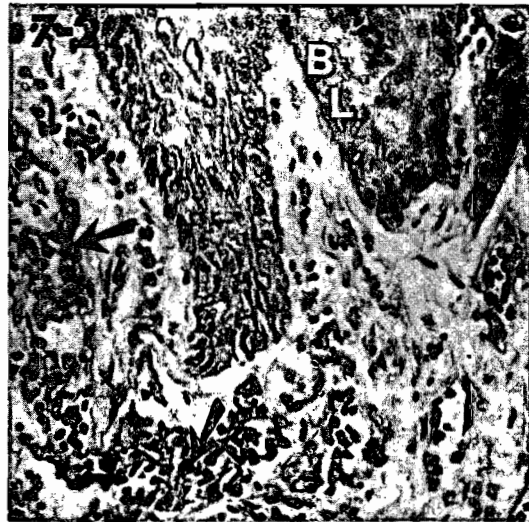
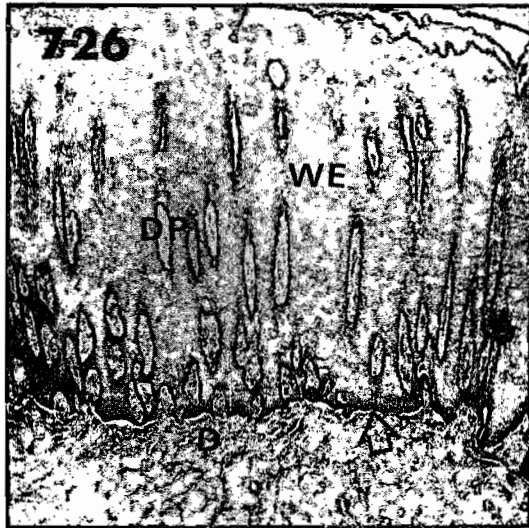


Figure 7-26. Whale 80G1. Photomicrograph of the white skin surrounding the bomb fragments. White epidermis (WE) shows relatively broader rete ridges (arrow) and the dermal papillae (D) appear to be wider than normal. Melanocytes are lacking in the basal layer. There is extensive fibrosis, characterized by large amounts of mature collagenous fibers arranged in broad bundles, in the dermis (D). Small collections of leukocytes are found just beneath the epidermis. H & E, 15X.

Figure 7-27. Whale 80G1. Higher magnification of Fig 7-26 to illustrate the absence of melanocytes in the basal layer (BL) of the epidermis. Note the leukocytic infiltrates (arrows); most are plasma cells, lymphocytes and macrophages. H & E, 252X.

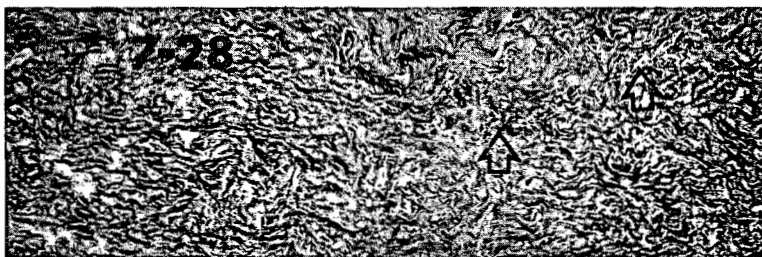


Figure 7-28. Whale 80G1. Photomicrograph of the firm blue area beneath the white skin which had encapsulated the bomb fragments. This is composed of mature collagenous fibers arranged in wide bundles. Small collections of leukocytes (arrows) were found scattered throughout. The blue appearance of this tissue is probably due to fragmentation and absorption of the blue material from the bomb. H & E, 63X.

## DISCUSSION

During this period, selected tissue specimens were received from 6 bowhead whales (80B1, 80B2, 80B7, 80B8, 80B9 and 80G1). Based on the specimens received and studied histologically from these whales, among the most intriguing conditions were the discrete patches of mushy roughened skin as illustrated in Fig 7-17. Although such skin lesions were found only on 2 whales (80B7, 80B8), it is believed that they may be common and a careful examination of the entire skin surface of the whale may be necessary to detect the lesions. There is no anatomic predilection for the lesions, but the head region is one of the common sites. The lesions appeared to be confined to the external layer or the stratum externum (Harrison and Thurley 1974) of the epidermis with little or no degenerative changes occurring in the deeper layers of the epidermis. The dermis and the dermal capillaries were not affected; therefore, the term epidermatitis was used as the diagnosis. Surrounding the degenerated and necrotic epithelial cells were large gram-positive filamentous micro-organisms with a striated appearance. Since they did not stain with GMS and PAS techniques, the organisms were not considered to be fungi but rather bacteria. Identification of the micro-organisms could not be established on tissue sections. Unicellular organisms, which varied in shape from ovoid to spherical and were slightly birefringent, were also found in the damaged areas. Such organisms were suggestive of diatoms (RU 1280, RU 1380). Diatoms have been previously reported on cetaceans (Omura 1950, Nemoto, Brownell and Ishimaru 1977). Further investigation will be necessary to determine the underlying factors that predispose the whales to skin lesions of this nature.

Other common findings were the discrete whitish, somewhat raised, lesions on the oral mucosa at the rear of the mouth. The lesions noted in whales 80B1 and 80B8 were only slightly elevated above the mucosa and were considered to be of long standing and representing the healed stage. Similar oral lesions were found in the caudal area of the mouth in 2 whales (79KK2 and 79KK3) in a previous study period (Migaki 1979). In the latter 2 whales, the lesions were larger, more elevated and were cystic. Due to the anatomical site and the chronic active inflammation, it is believed that a misaligned tip of the baleen plates may have been the cause. The whitish appearance is due to the absence of melanocytes in the basal layer of the epithelium which had



undergone regeneration. Regeneration of the melanocytes in the basal layer will restore the normal black appearance to the oral mucosa. Lesions in the mouth also seen in a previous study period were the numerous flat whitish bumps on the inner surface of the upper lip in 3 whales (79B1, 79B2, 79B3) (Higaki 1979). Histologically, the lesions were composed of dilated dermal papillae containing large numbers of mononuclear leukocytes. The cause was not identified but I suspect that the lesions were due to some low grade irritant. These whitish lesions should not be confused with the small granular tubercles found on the inner surface of the upper and lower lip in the sei and fin whales (Ogawa and Shida 1950), which are composed of well developed dermal papillae with numerous sensory apparatuses and serve as sensitive tactile organs.

Other common skin lesions were the large areas of white skin as illustrated in Fig 7-1. The white skin in this whale (80B1) was found on the blowhole. In whale 80G1, the white skin was found surrounding a bomb. Following penetration of the skin by the bomb, the epidermis had regenerated and formed a "white capsule" around the bomb fragments. Melanocytes were absent in the basal layer of the epidermis and there was extensive fibrosis of the dermis and superficial portion of the blubber. In a previous study, a whale (78KK1) had a white area on the skin in which the fibrous tissue had extended deeply into the blubber (Albert et al 1980). This lesion was considered to be caused by a deep penetrating object such as a harpoon. Healing of the skin wound took place by regeneration of the epidermis without regeneration of the melanocytes, which accounts for the white skin, and fibrosis of the dermis and blubber.

Parasitic nodules due to anisakine larvae were found in the submucosa of the nonglandular portion of the stomach in two whales (80B2, 80B7). The early larval stages of this parasite are found in a variety of fish (Areean 1971, Myers 1975, Smith and Wootten 1978). The parasites were well encapsulated in the submucosa and their presence probably had no significant effect on the general health of the whales.

Several ulcers were found in the anorectal canal of whale 80B9. The ulcers were of long duration as evidenced by the extensive amount of chronic inflammation beneath the desquamated epithelium. Large amounts of mononuclear leukocytes were present throughout as were several lymphoid nodules with germinal centers. The cause of the ulcer remains undetermined.

A small circumscribed lipoma was found on the diaphragmatic surface of the liver in whale 80B2. Lipomas in the liver are considered uncommon; the most common sites for such neoplasms are the pre-existing adipose tissues in the body.

#### SUMMARY

Histologic examination was conducted on tissue specimens submitted from 6 bowhead whales. The selected specimens were considered to be abnormal on gross examination. Such abnormalities included irregularly-shaped large white areas on the skin, elevated and cystic white areas in the posterior part of the mouth, large discrete patches of rough skin, parasitic nodules due to anisakine larvae in the submucosa of the nonglandular portion of the stomach, a small lipoma in the liver, ulcers in the anorectal canal, a deep ulcer in the ventral midline on the tip of the chin and cutaneous encapsulation of bomb fragments.

#### ACKNOWLEDGMENTS

This study was supported in part by Public Health Service Grant no. RR00301-15 from the Division of Research Resources, National Institutes of Health, under the auspices of Universities Associated for Research and Education in Pathology, Inc, Inc.

## REFERENCES

- Albert, T.F., G. Migaki, H.W. Casey and L.M. Philo. 1980. Healed penetrating injury of the bowhead whale, Balaena mysticetus. Mar. Fish. Rev. 42:92-96.
- Arean, V.M. 1971. Anisakiasis. In: Pathology of Protozoal and Helminthic Diseases with Clinical Correlation, R.A. Marcial-Rojas (ed.), pp 846-851. Williams and Wilkins, Baltimore.
- Harrison, R.J. and K.W. Thurley. 1974. Structures of the epidermis in Tursiops, Delphinus, Orcinus and Phocoena. In: Functional Anatomy of Marine Mammals, R.J. Harrison (ed.), pp 45-71. Academic Press, New York.
- Migaki, G. 1979. Tissues (structure/formation) (RU 579a). In: Investigation of the Occurrence and Behavior Patterns of Whales in the Vicinity of the Beaufort Sea Lease Area, J. Kelley and G. Laursen (eds.), pp 213-225. Final Report to the Bureau of Land Management from the Naval Arctic Research Laboratory, Barrow, Alaska.
- Migaki, G. 1979. Tissues (structure/function) (RU 280d). In: Investigation of the Occurrence and Behavior Pattern of Whales in the Vicinity of the Beaufort Sea Lease Area, J. Kelley and G. Laursen (eds.), pp 401-415. Final Report to the Bureau of Land Management from the Naval Arctic Research Laboratory, Barrow, Alaska.
- Myers, B.J. 1975. The nematodes that cause anisakiasis. J. Milk Food Technol. 38:774-782.
- Nemoto, T., R.L. Brownell, Jr., and T. Ishimaru. 1977. Cocconeis diatom on the skin of Franciscana. Sci. Rep. Whales Res. Inst. No. 29:101-105.
- Ogawa, T. and T. Shida. 1950. On the sensory tubercles of lips and of oral cavity in the sei and the fin whale. Sci. Rep. Whales Res. Inst. No. 3:1-16.
- Omura, H. 1950. Diatom infection on blue and fin whales in the Antarctic Whaling Area V (the Ross Sea Area). Sci. Rep. Whales Res. Inst. No. 4:14-26.
- Smith, J.W. and Wootten, R. 1978. Anisakis and anisakiasis. In: Advances in Parasitology, vol 2, W.H.R. Lumsden, R. Muller, J.R. Baker (eds.), pp 93-163. Academic Press, New York.

THE CYTOLOGICAL AND CLINICAL EVALUATION OF BLOOD AND URINE OF THE BOWHEAD WHALE,  
BALAENA MYSTICETUS

WILLIAM MEDWAY, D.V.M., Ph.D.  
School of Veterinary Medicine  
University of Pennsylvania  
3800 Spruce Street  
Philadelphia, Pennsylvania 19104

INTRODUCTION

Blood and urine are the most readily obtainable of the body fluids. The proper cytological and clinical chemical evaluation of each will yield: 1) basic information regarding the composition in the normal animal; 2) information regarding the degree of stress to which the animal is subjected; and, 3) information regarding the animal's state of health.

In an endangered animal such as the bowhead whale whose interaction with its environment may be altered through offshore development, it would seem logical to undertake a detailed study of these body fluids. Such an investigation will obtain "predevelopment" data and provide information on stress and health status as offshore development progresses.

OBJECTIVES

1. To determine the cytological profile of bowhead whale blood.
2. To determine the normal clinical chemical values for bowhead blood and urine.
3. To relate such findings to those normal values of other cetaceans and other better studied mammals.
4. To search for evidence of stress and disease by relating such values to other better studied mammals that have been stressed or diseased.

## METHODS

Whole blood was collected by catchment from Eskimo harvested bowhead whales 80B1, 80B2, 80B7 and 80B8. Heparin was used as the anticoagulant for cytological examination. Some of the blood was allowed to clot and the serum was separated as soon after collection as possible and kept frozen until analyzed. The collection, handling and transmission of the samples to the laboratory was effected by RU 180 of this project. Some whole blood was also fixed with 2% glutaraldehyde for electron microscopic studies.

The sera were analyzed for the common chemical constituents with the GEMINI<sup>a</sup> and GEMSAEC<sup>b</sup> autoanalyzers. The serum proteins were separated by the cellulose acetate procedure using the Gelman<sup>c</sup> apparatus. The constituents Na, K, Cl, total CO<sub>2</sub> and anion gap were determined by the Nova Analyzer<sup>d</sup>. The osmolality was obtained by the freezing point depression (Osmette A)<sup>e</sup>. The blood smears were stained with Wright-Giemsa stain and 100 white blood cells were enumerated.

Urine was obtained by cystocentesis from Eskimo harvested bowhead whale 80B7 and examined both qualitatively and quantitatively by routine procedures. The qualitative tests were done using commercially available dip sticks<sup>f</sup>.

## RESULTS

The results of the differentiation and enumeration of white blood cells are presented in Table 8-1. It should be noted that eosinophils were only found in blood from 80B1 and that there is great variation in other cells when comparing the counts from the four whales.

Table 8-2 shows the results of the electrolyte analyses. These are compared with some results available on blood sera obtained from 79B1 and 79B2. The degree of hemolysis should be noted when comparing results between whales.

In Table 8-3 the results of other blood constituents are presented. Again, the variation of some of the results should be noted. The effect of the harpooning, duration of suffering, etc. should be recalled during interpretation of the results.

- 
- a. Gemini Autoanalyzer. Electro-Nucleonics, Inc., Fairfield, NJ
  - b. Gemaec Autoanalyzer. Electro-Nucleonics, Inc., Fairfield, NJ
  - c. Gelman Sciences. Ann Arbor, MI
  - d. Nova 4 + 4. Nova Biomedical, Newton, MA
  - e. Osmette A. Precision Systems, Inc., Sudbury, MA
  - f. Multistix. Ames Company, Elkhart, IN

TABLE 8-1. WHITE BLOOD CELL DIFFERENTIAL COUNTS OF THE BOWHEAD WHALE

Whale #	Segs %	Lymphs %	Mono %	Eo %	Baso %	Remarks
80B1	76	22	1	1	<1	
80B2	36	64	<1	<1	<1	Leucopenic
80B7	20	79	1	<1	<1	3 nuc rbc
80B8*	47	53	<1	<1	<1	

\* Ingutuk

TABLE 8-2. SOME ELECTROLYTES OF BOWHEAD WHALE SERA

Whale #	Degree of Hemo.	Na meq/l	K meq/l	Cl meq/l	PO <sub>4</sub> mg/dl	Ca mg/dl	Mg mg/dl	Total CO <sub>2</sub> meq/l	Osmol mO/kgH <sub>2</sub> O	Anion Gap meq/l
79B1*	4+	148	---	104	---	---	---	---	---	---
79B2	4+	172	13.7	149	11.6	12.6	---	---	---	---
80B1	1+	170	6.4	122	8	10.3	2.6	27	346	21
80B2	4+	170	8.3	117	8.3	12.4	4.2	11	348	42
80B7	1+	162	8.6	119	10.1	11.6	3.2	29	333	14
80B8*	2+	159	6.1	112	6.7	11.7	2.7	26	324	21

\* Ingutuk

TABLE 8-3. SOME BLOOD CONSTITUENTS OF BOWHEAD WHALE SERA

Whale #	Gluc. mg/dl	Creat. mg/dl	BUN mg/dl	SGOT IU	SAP IU	TP g/dl	Alb. g/dl	Glob. g/dl	A/G	GPT IU	BiI mg/dl
79B1*	232	8.6	60	---	113	7.2	4.2	3.0	1.4	---	---
79B2	93	3.3	49	139	75	2.9	1.2	1.7	0.7	43	0.4
80B1	83	4.8	54	53	313	5.8	3.8	2.0	1.9	12	0.4
80B2	87	5.0	63	121	269	6.1	3.6	2.5	1.4	30	2.0
80B7	188	4.5	66	56	444	6.2	4.0	2.2	1.8	32	0.7
80B8*	148	4.8	66	48	215	6.8	3.9	2.9	1.4	23	0.7

\* Ingutuk

TABLE 8-4. SERUM PROTEIN ELECTROPHORESIS OF THE BOWHEAD WHALE

Whale #	TP g/dl	A1b g/dl	a1pha g/dl	beta g/dl	gamma g/dl	A/G
80B1	5.9	3.8	0.5	0.8	1.0	1.67
80B2	5.6	3.0	0.6	1.4	0.7	1.16
80B7	6.5	4.0	0.8	1.1	0.6	1.64
80B8*	6.9	3.9	0.6	0.9	1.5	1.28

\* Ingutuk

TABLE 8-5. QUALITATIVE EXAMINATION OF URINE SPECIMENS FROM FOUR BOWHEAD WHALES

Whale #	Color	Trans.	pH	Specific Gravity	Protein	Ketones	Glucose	Red. Subs.	Bile	Hemoglobin
78B2	dark amber	clear	5.5	1.032	trace	neg.	neg.	neg.	neg.	neg.
79B1*	dark straw	clear	5	1.032	trace	neg.	trace	trace	neg.	4+
79KK1	pale yellow	very cloudy	5.5	1.028	2+	neg.	neg.	neg.	neg.	4+
80B7	amber	clear	6.0	1.035	1+	neg.	neg.	neg.	neg.	1+

\* Ingutuk



TABLE 8-6. QUANTITATIVE EXAMINATION OF URINE SPECIMENS FROM FOUR BOWHEAD WHALES

Whale #	Na meq/l	K meq/l	Cl meq/l	Urea N mg/dl	Creatinine mg/dl	Osmolality mO/kgH <sub>2</sub> O
7882	183	14.4	n.d.*	3000	400	1440
79B1**	310	11.9	383	900	400	1215
79KK1	220	48	195	560	124	1186
80B7	256	87.3	260	1600	540	1448

\*n.d. not determined

\*\* Ingutuk

TABLE 8-7. MICROSCOPIC EXAMINATION OF URINARY SEDIMENT FROM FOUR BOWHEAD WHALES

Whale #	Red Blood Cells	White Blood Cells	Epithelial Cells	Casts	Miscellaneous
7882	rare	rare	myriads	neg.	Many epithelial cells from entire urinary tract, many unidentified spheroid crystals
79B1 <sup>a</sup>	neg.	neg.	occ.	occ. (C.G.)*	Much amorphous material, few sheets of sloughed epithelial cells
79KK1	0-2/HPF**	1-3/HPF	1-3/HPF	0-1/HPF (C.G.)	Heavy sperm, much amorphous debris
80B7	TNTC***	0-2/HPF	3-5/HPF	neg.	Moderate unidentified crystals. Very light bacteria

<sup>a</sup> Ingutuk

\* C.G. = coarse granular

\*\* HPF - High Power Field

\*\*\* TNTC - too numerous to count

The results of the serum electrophoresis are shown in Table 8-4.

The results of urinalysis on urine from 80B7 are presented in Tables 8-5, 8-6 and 8-7. These are presented for comparative purposes with those obtained on urine from bowhead whales 78B2, 79B1 and 79KK1. The quantitative results represent analyses of discrete samples as opposed to aliquots of a 24-hour specimen.

No white blood cells were found in the specimens prepared for electron microscopy.

#### DISCUSSION

The interpretation of a relative distribution of white blood cells is very difficult to near impossible without total cell counts. With the total cell counts the absolute distribution can be calculated and valid interpretations can be made. The hematological stress response in most species is characterized by a neutrophilia, lymphopenia and eosinopenia (Schalm et al 1975). Only one eosinophil was encountered (80B1) during the course of the enumeration; however, one could find the occasional cell in the other smears, but they were very rare. This may be an indication of a response to stress. Small odontocete whales do elicit a stress response albeit not as marked as in some terrestrial species (Medway et al 1970, Medway and Geraci 1964, Schalm et al 1975). Very few monocytes were identified in any of the smears from the four bowhead whales.

The duration of time between harpooning and actual collection of blood varied between a couple of hours to 14 hours and thus, perhaps not allowing for the development of a good response in some instances. It is not known how quickly the harpooned whales would respond.

The reversal of the neutrophil-lymphocyte ratios seen in three of the whales (80B2, 80B7 and 80B8) cannot be explained unless it is the normal pattern and 80B1 is abnormal. The resolution of this observation will have to await the examination of fresh specimens. Photomicrographs of the various species of white blood cells and red cells have been reported (Medway 1980b). The red blood cells are quite large which agrees with the reports on blood from other cetaceans (Ridgway 1972, Hawkey 1975). One of the whales (80B2) seemed to be leukopenic, based on the number of white cells seen in the smear. The nucleated red blood cells found in the smear from whale 80B7 may be an indication

of anemia or the result of stress (catecholamine release).

Likewise, the electrolytes are difficult to interpret in light of harvesting technique. The degree of hemolysis on a scale from 1-4 indicates that the serum from whale 80B2 was approaching port wine in color. The degree of hemolysis of red cells and the stress of slaughter must have had a profound effect as is evident in the sodium and potassium results. These results are somewhat higher than those reported for the smaller odontocete whales (Medway and Geraci 1965, Ridgway et al 1965, Ridgway et al 1970, Malvin and Rayner 1968, Medway and Muldovan 1966). The values for chloride, phosphate, calcium and magnesium are also higher, however, not to a great degree. The osmolalities strangely enough agree with published results of the smaller odontocete whales (Medway and Geraci 1965, Ridgway et al 1970, Malvin and Rayner 1968, Medway and Muldovan 1966). The anion gaps with the exception of the result for whale 80B2 are reasonably normal. An increase in anion gap in most instances is a result of organic acidosis usually due to increased lactic acid (Gabow et al 1980). This is surely the case in whale 80B2 which perhaps struggled more fiercely than the others during the dying experience.

Total carbon dioxide, again with the exception of whale 80B2, was reasonably normal when compared to the smaller odontocete whales. Unfortunately, there is very little published on any of the large baleen whales with the exception of a special issue of "Marine Fisheries Review" dealing with the California Gray Whale (Special number 1974). However, no comparable blood chemistries are presented.

The results in Table 8-3 are equally fraught with interpretative difficulties. The glucose values are erratic, however, not very markedly; the creatinines are all elevated. These values for creatinine in domestic animals would indicate a fair degree of kidney disease. In this instance the combination of dehydration (decreased blood volume) due to slaughter, resulting in decreased blood flow to the kidneys, undoubtedly affected the blood concentration. Most of the other results in this table are fairly close to those one would expect. The total protein in whale 79B2 is obviously very low and is, no doubt, due to the bleeding as a result of the harpooning (Medway 1980a). Only two animals, 79B2 and 80B2 had elevations of SGOT which would indicate muscle damage. Creatinine phosphokinase, another muscle enzyme, could not be determined due to the hemolysis of the specimens.

The serum protein electrophoretic separations are comparable in many respects to those of the smaller odontocete whales (Medway and Geraci 1965, Ridgway et al 1970, Medway and Muldovan 1966). They are also comparable to those from a California Gray whale (Kenney 1980). The A/G ratios are somewhat different in Tables 8-4 and 8-5 done on the same whale sera because those in the former table were determined by chemical means and by electrophoretic means in the latter.

The results of the urinalyses are perhaps closer to the norm for bowhead whales than any of the other chemical determinations, since the urine was probably in the bladder at the time of harpooning and most likely changed very little in composition. The specific gravity, pH, color, etc. were reasonably normal. The hemoglobin content on a scale from 1-4 based on commercially available dip sticks that do not differentiate between hemoglobin, intact red cells or myoglobin was quite variable, however, was not present in significant amounts to grossly discolor the urine. No attempt was made to determine the presence of myoglobin which may have been present due to exertional myopathy during the agony of death. The urine was free of any of the commonly measured components that indicate kidney pathology. The presence of a 2+ protein in urine from 79KK1 could be indicative of sexual secretions since many spermatozoa were also present.

The results of the quantitative analysis of the urine indicate reasonably normal kidney concentrating ability. With the exception of the potassium in the urine of 80B7, the results are comparable to those of 78B2 which have been reported (Medway 1980).

There were some interesting observations during the examination of the urinary sediment from four bowhead whales. Bowhead whale 78B2 had myriads of epithelial cells probably due to sloughing of the urinary tract mucosa due to post mortem change. Sediment from whale 80B7 was unremarkable. Another interesting finding was the presence of many spermatozoa in the sediment from whale 79KK1. Though the presence of sperm in the urinary sediment of mature males of the domestic species is a common finding, this is the first observation in the bowhead whale. This certainly identified the sexual maturity of the individual (Figs 8-1 and 8-2).

Many crystals were present, they were believed to be primarily triple phosphate and perhaps some urates and oxalates. Their presence is of no clinical significance.



Figure 8-1. Scanning electron photomicrograph of a spermatozoan in the sediment of bowhead whale (79KK1) urine. X12,000

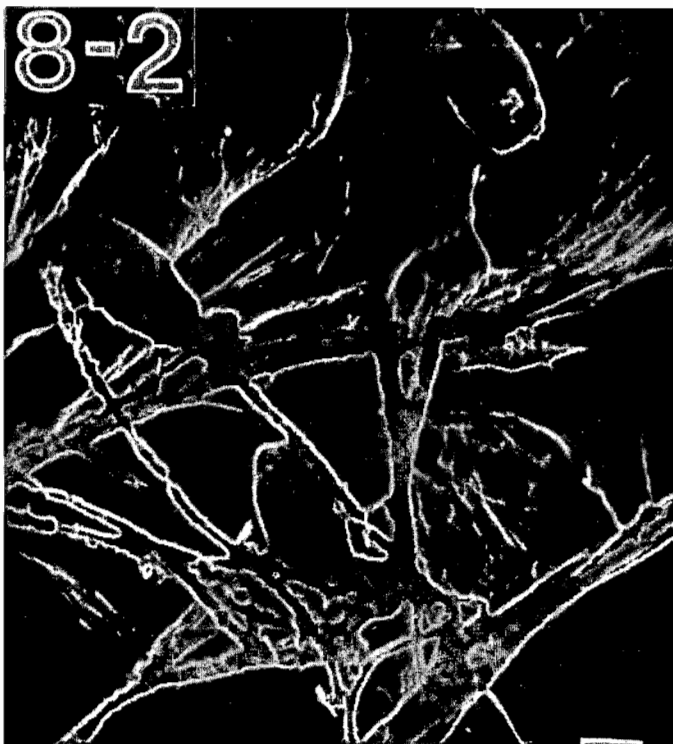


Figure 8-2. Scanning electron photomicrograph of urinary sediment from a bowhead whale (79KK1) showing several spermatozoa. X11,000

## SUMMARY

Blood smears and serum from Eskimo harvested bowhead whales 80B1, 80B2, 80B7 and 80B8 were examined. The inadequacy of the specimens made the results very difficult to interpret.

Urine from bowhead whale 80B7 was also examined and compared to the urine from three other whales from a prior whaling season. Bladder urine is probably the best indicator of the health status of the animal pre-harpooning.

## ACKNOWLEDGMENTS

The author wishes to acknowledge, with thanks, the assistance of Dr. D. F. Cameron, University of Florida Health Center, Gainesville, for the scanning electron micrographs; the personnel in the Clinical Laboratory of the University of Pennsylvania, School of Veterinary Medicine, for their assistance with the various analyses; and Mrs. F. Pappalardo of the Pepper Laboratory, University of Pennsylvania, School of Medicine, for the osmolality determinations.

## REFERENCES

- Gabow, P.A., W. D. Kaehny, P. V. Fennessey et al. 1980. Diagnostic importance of an increased serum anion gap. *N. Eng. J. Med.* 303 (15):854-858.
- Hawkey, D.M. 1975. *Comparative Mammalian Haematology*. William Heinemann Med. Books, Ltd., London, pp 252.
- Kenney, D.W. 1980. Personal communication and unpublished data.
- Malvin, R.L. and M. Rayner. 1968. Renal function and blood chemistry in cetacea. *Am. J. Physiol.* 214(1):187-191.
- Medway, W. and J. R. Geraci. 1964. Hematology of the Bottle-nose dolphin (*Tursiops truncatus*). *Am. J. Physiol.* 207:1367-1370.
- Medway, W. and J. R. Geraci. 1965. Blood chemistry of the Bottle-nose dolphin (*Tursiops truncatus*). *Am. J. Physiol.* 209:169-172.
- Medway, W. and F. Muldovan. 1966. Blood studies on the North Atlantic pilot (Pothead) whale, *Globicephala melaena* (Traill, 1809). *Physiol. Zoo.* 39(2):110-116.
- Medway, W., J. R. Geraci and L. V. Klein. 1970. Hematologic response to administration of a corticosteroid in the Bottlenosed dolphin (*Tursiops truncatus*). *J. Am. Vet. Med. Ass.* 157(5):563-565.
- Medway, W. 1980. Some observations on urine from a bowhead whale. *Mar. Fish. Rev.* 42 (9-10):91-92.

- Medway, W. 1980a. Cytological and clinical-chemical examination of blood and urine of the bowhead whale, Balaena mysticetus. (RU 579c) In: "Investigation of the Occurrence and Behavior Patterns of Whales in the Vicinity of the Beaufort Sea Lease Area." J. Kelley and G. Laursen (eds) pp 265-266. Final Report to the Bureau of Land Management from the Naval Arctic Research Laboratory, Barrow, Alaska.
- Medway, W. 1980b. Cytological and clinical-chemical examination of blood and urine of the bowhead whale, Balaena mysticetus. (RU 280e) In: "Investigation of the Occurrence and Behavior Patterns of Whales in the Vicinity of the Beaufort Sea Lease Area." J. Kelley and G. Laursen (eds) pp 417-434. Final Report to the Bureau of Land Management from the Naval Arctic Research Laboratory, Barrow, Alaska.
- Ridgway, S. H., J. G. Simpson, G. S. Patton and W. G. Gilmartin. 1970. Hematologic findings in certain small cetaceans. J. Am. Vet. Med. Ass. 157(5):566-575.
- Ridgway, S. H. 1972. Mammals of the Sea, Biology and Medicine. Charles C. Thomas, Springfield, IL
- Schalm, O. W., N. C. Jain and E. J. Carroll (eds). 1975. Veterinary Hematology, 3rd Ed., Lea & Febiger, Philadelphia, PA
- Special Number. 1974. The California Gray Whale. Mar. Fish. Rev. 36(4):1-65.

## RESEARCH UNIT 980

### CYTOGENETIC AND MORPHOLOGICAL INVESTIGATION OF VARIABILITY IN THE BOWHEAD WHALE, BALAENA MYSTICETUS

GORDON H. JARRELL, M.S.  
Institute of Arctic Biology  
University of Alaska  
Fairbanks, Alaska 99701

#### INTRODUCTION

This study concerns the genetic relationship of the bowhead and a form of whale known to Inupiat Eskimos as the Ingutuk. Unlike other studies in this report, tissues were not examined to ascertain possible effects of offshore oil and gas development. The genetic and ecological homogeneity of the western arctic bowhead population is an assumption implicit in the design of most present research on bowheads. This assumption is not shared by many people who have a long and intimate knowledge of these whales. The possibility that the Ingutuk represents a distinct population or ecological race has implications for all aspects of bowhead biology.

The people of Barrow and Point Hope, Alaska have long recognized two forms of the bowhead whale. The less common Ingutuk was recognized, but not formally described, by early whalers and naturalists in the Arctic (Bailey and Hendee 1926; Stephanson 1944). Since most of what we know about the Ingutuk has been extracted from the folk-knowledge of various villages, it is not surprising that there are some contradictions and confusions in descriptions of these whales. Several features are consistent in these descriptions, and do in fact distinguish a portion of the bowheads migrating along the Alaskan Arctic Coast (Braham, Durham, Jarrell and Leatherwood 1980). Ingutuks exhibit short baleen, dense bones and great girth in comparison to "normal bowheads." There also seem to be differences in the shape of the flukes and flippers.



## OBJECTIVES

1. To test the hypothesis that chromosomal polymorphism is related to phenotypic polymorphism as represented by two forms of whale.
2. To document and verify the physical features which distinguish the Ingutuk from the regular bowhead.

## METHODS

### Cytogenetic Investigations

Generally the methods employed in this investigation are the usual procedures of mammalian cytogenetics. Small biopsies of skin, lung, or kidney were collected by National Marine Fisheries Service (NMFS) biologists or personnel of RU 180. Only skin was taken from whales sampled more than 24 hours post-mortem since autolysis of other tissues is rapid in these well-insulated animals. This investigation received six bowhead skin samples, four in 1979 and two in 1980, collected by biopsy dart from the Soviet catcher ship Avangard. These samples were collected by Jim Johnson of the NMFS using crossbow and shotgun propelled darts developed by NMFS biologist Mary Nerini. The method and equipment were a refinement of those described by Winn et al (1973).

Tissue samples were handled as aseptically as possible and preserved in vials containing 15 to 20 ml of tissue culture medium. The samples were held at refrigerator temperature (4 to 10°C) and transported to the laboratory in Fairbanks, Alaska as rapidly as possible. Skin samples that had been in storage or transport for as long as three weeks usually showed some viability.

Fibroblast cultures were initiated by allowing the minced sample to attach to the bottom of a 250 ml tissue culture flask. The culture medium used was Mixture 199 (Microbiological Associates) with 15% fetal calf serum, 1% ultrafiltrate of chick embryo, and antibiotics. In most cases cultures were initiated by personnel of the Virology-Rabies Unit, Alaska Dept. of Public Health while I was in the field.

There was considerable difficulty in culturing bowhead cells. Usually it was necessary to disperse the foci of cells growing from bits of the explant, before a confluent monolayer could be attained. Sometimes a flask containing a small number of foci was passed to a smaller (30 ml) flask. Even the best cell lines deteriorated after several passages. When possible a new flask was grown to confluency and dispersed into two flasks. One flask could then be harvested for karyotyping while the second flask was continued and split.

When satisfactory chromosome preparations were obtained from early passages, cell lines were frozen down and stored in liquid nitrogen. In some cases it was possible to provide bowhead cells to RU 1080.

Cells were harvested for karyotyping when the cell monolayer was 50 to 80% confluent. Colcemid at a concentration of 0.06 mcg/ml was added to the culture medium to disrupt the mitotic spindle apparatus and cause an accumulation of cells in metaphase. Usually Colcemid treatment lasted two hours but ranged from one half hour to six hours. This time was often determined by inspecting the treated cells with an inverted microscope for accumulating metaphase cells. Cells were then dispersed with trypsin and versene, resuspended in the culture medium, and pelleted. Hypotonic treatment was with 0.075M potassium chloride for ten to twenty minutes at 37<sup>0</sup> C. Cells were fixed three to five times in one part acetic acid to three parts methanol. Cells suspended in fixative were dropped on to alcohol-cleaned wet microscope slides and air dried.

A variety of differential staining, or "banding", procedures were applied to bowhead chromosomes. Trypsin G-bands were induced by the method of Wang and Fedoroff (1972). C-bands were induced by the BSG technique of Sumner (1972). Active nucleolus organizer regions (NORs) were demonstrated by the Niewczas and Wang (1978) modification of the Ag-I technique of Bloom and Goodpasture (1976).

As reported earlier (Jarrell 1979a), there was difficulty interpreting C-band variability in the smaller chromosomes of the bowhead. An intensive effort to sequentially G-band, photograph, destain, and then C-band bowhead cells has not yet been successful. During this effort the first such sequentially banded preparations from whales were obtained for the belukha, Delphinapterus leucas (Jarrell and Arnason 1981 and Fig 9-1), and the fin whale, Balaenoptera physalus (Fig 9-1). Slides on which several G-banded cells had been photographed were destained by rinsing them for four minutes each, twice in xylene, once in one-to-one xylene and methanol, once in methanol, and once in acetic acid-methanol fixative. The slides were dried and then processed for C-bands by the Sumner (1972) technique but with various reductions in the treatment times. The usual result was that the chromosomes were completely denatured. A continued effort with a consistent supply of excellent bowhead preparations would eventually have produced results. The number of variables encountered in each step of this procedure makes its practicality for intrapopulational studies

questionable. In the absence of a sequential banding procedure, precise identification of C-band heteromorphism in less-distinctive bowhead chromosomes is impossible.

Following staining, slides were scanned for metaphase cells that demonstrated both satisfactory response to the staining procedures and no, or few, overlapping chromosomes. Such cells were photographed with a yellow-green filter through a 100X oil immersion planapochromatic microscope objective. Negatives were printed at a total magnification of 3000X. The photographs of individual chromosomes were then cut out of the prints so that they could be arranged to demonstrate homologous pairing. The chromosomes of the bowhead are arranged in metacentric (m), submetacentric (sm), subtelocentric (st) and telocentric (t) groups (Fig 9-2) on the basis of arm ratios (r) as suggested by Levan, Fredga and Sandberg (1964). The measurements used (Table 9-1) were made on ten cells from a male bowhead (77B9) by Dr. Ulfur Arnason and are not the same as those reported by Jarrell (1979b). On the basis of Dr. Arnason's measurements, two chromosome pairs that had been grouped as metacentrics (m4 and m5 in Jarrell 1979b) are here placed in the submetacentric group.

#### Morphological Investigations

In the course of working for the NMFS as a seasonal field technician at Barrow, I have attempted to document physical features which distinguish the Ingutuk from the regular bowhead. The methods employed have been photography and measurement of baleen and flipper shape. It has been impractical to document fluke shape since the flukes are nearly always removed from the whale before it is hauled out. The data collected in this effort are largely property of the NMFS but their interpretation will be reviewed in the discussion.

#### RESULTS

The same karyotype as described by Jarrell (1979b) characterizes the 21 bowhead whales examined to date. This sample included two whales (79B1 and 80B8) which had the characteristics of Ingutuks and were identified as such by the whaling captains responsible for harvesting these animals.

Differences in the distribution of constitutive heterochromatin (C-bands) were a regular feature of the chromosomes of the bowhead. These heteromorphisms are most pronounced on the ends of the chromosomes (telomeres)

and less pronounced at interstitial and centromeric C-bands. Such heteromorphism, particularly when it occurs in the less distinctive metacentric and submetacentric chromosomes, makes the identification of homologues uncertain. C-band heteromorphism often resulted in landmark features which facilitated the comparison of individual whales in spite of the inability to assign these features to specific chromosomes.

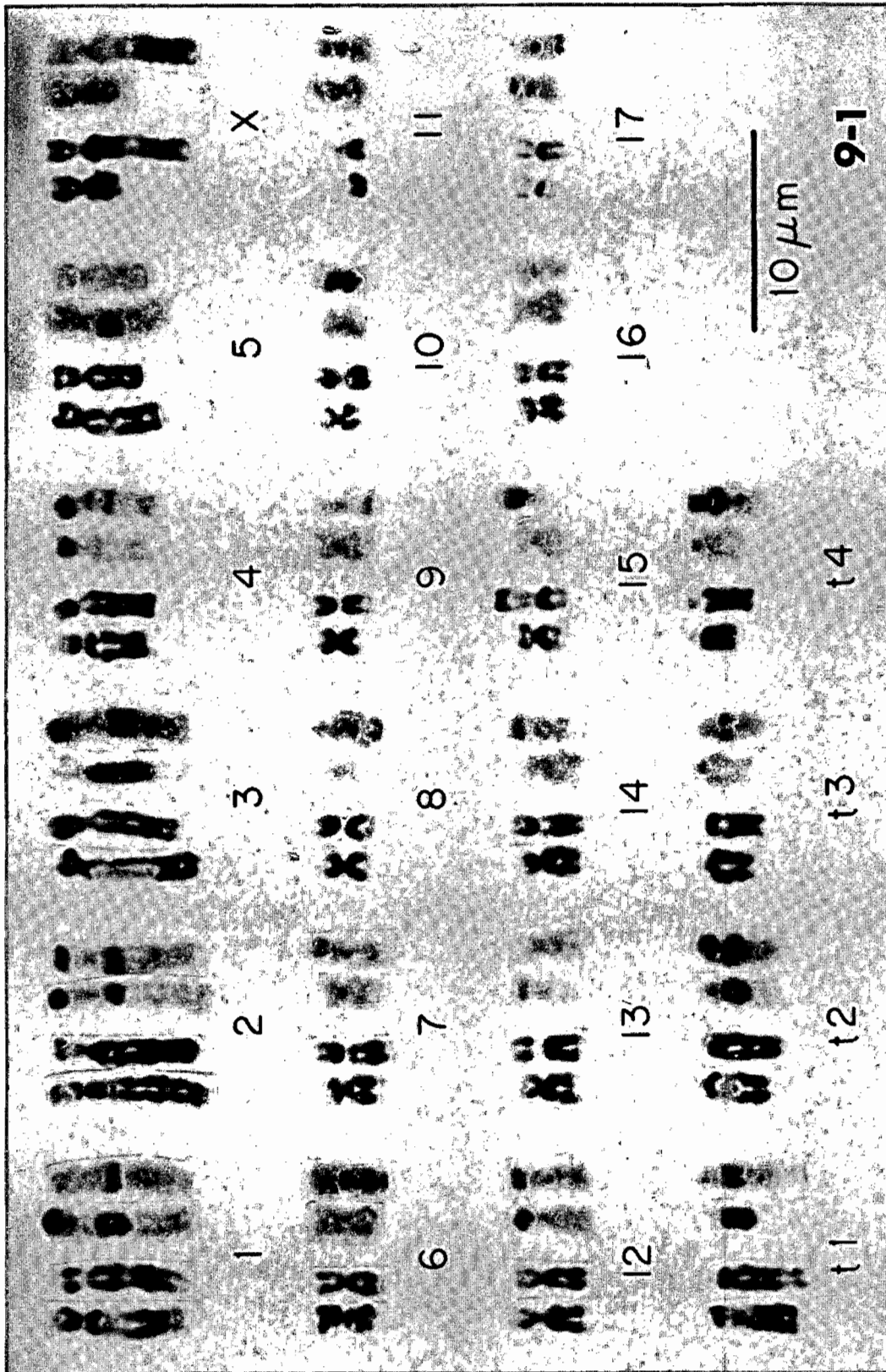
One whale in which the distinctive distribution of heterochromatin caused confusion was an Ingotuk, 79B1 (Jarrell 1979a). This animal had three small metacentric or submetacentric chromosomes bearing large telomeric C-bands (Fig 9-5). Based on the C-bands alone, it seemed likely that two of these might represent a distinctive homologous pair. A highly scorable G-banded cell (Fig 9-4) from this whale clearly reveals that two separate pairs are heteromorphic. The C-banded preparation (Fig 9-5) has been arranged to take this into account. The largest submetacentric of this animal is heterozygous for a telomeric band on the short arm. This identical condition is apparent in several non-Ingotuk whales such as 77B4 (Fig 9-7).

Fig 9-6 shows the C-banded karyotype of another Ingotuk (80B8). This cell does not demonstrate the distinctive features found in Ingotuk 79B1.

Anomalous blocks of heterochromatin were located in the karyotypes of other phenotypically normal non-Ingotuks, for example 80B2 (Fig 9-8).

Bowheads have less C-band positive chromatin than balenopterids (Arnason 1974) or gray whales (Arnason, personal communication). The degree of heteromorphism in this material is consistent with what is apparently the general cetacean condition.

Figure 9-1. A composite karyotype of a belukha, Delphinapterus leucas (left homologues), and a fin whale, Balaenoptera physalus (right homologues). The chromosomes have been sequentially G-banded (left pairs) and C-banded (right pairs). The homology of many pairs is evident. Pairing of the t group chromosomes is tentative. Many of the notable differences in overall shape and G-banding between the chromosomes of these two whales are accounted for by the distribution of C-bands. This is especially evident in pairs 3 and 15. These two species represent an odontocete and mysticete which share the  $2n=44$  basic cetacean karyotype. The  $2n=42$  karyotype of the bowhead was apparently derived from the basic cetacean karyotype by a fusion of chromosome 12 with one of the t group chromosomes to form the largest metacentric (m1) in the bowhead. The whole belukha preparation was presented by Jarrell and Arnason (1981). The Y chromosomes, which are not shown, are minute metacentrics, similar to the Y of the bowhead, in both species (Duffield 1977; Arnason 1974).



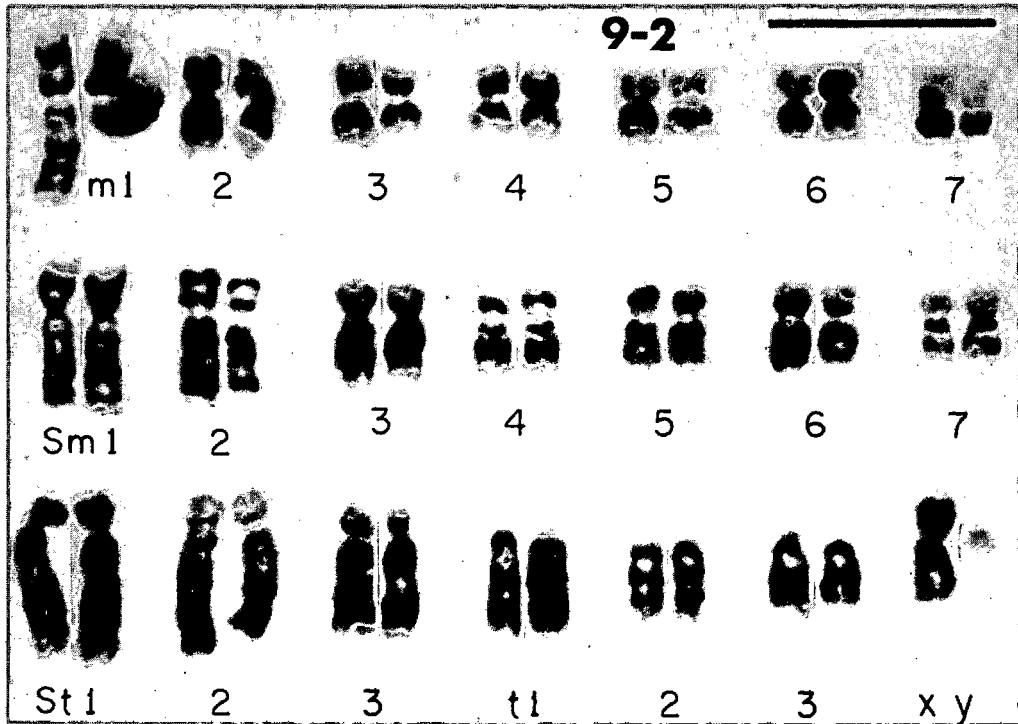


Figure 9-2. G-banded karyotype of a normal bowhead (77B9) demonstrating positive pairing and assignments based on measurements in Table 9-1. Bar = 10 microns



Figure 9-3. C-banded karyotype of 77B9. The identification of chromosomes m3 through m7 and sm3 through sm7 is uncertain. This is a typical bowhead karyotype with no distinctive heteromorphism. Bar = 10 microns

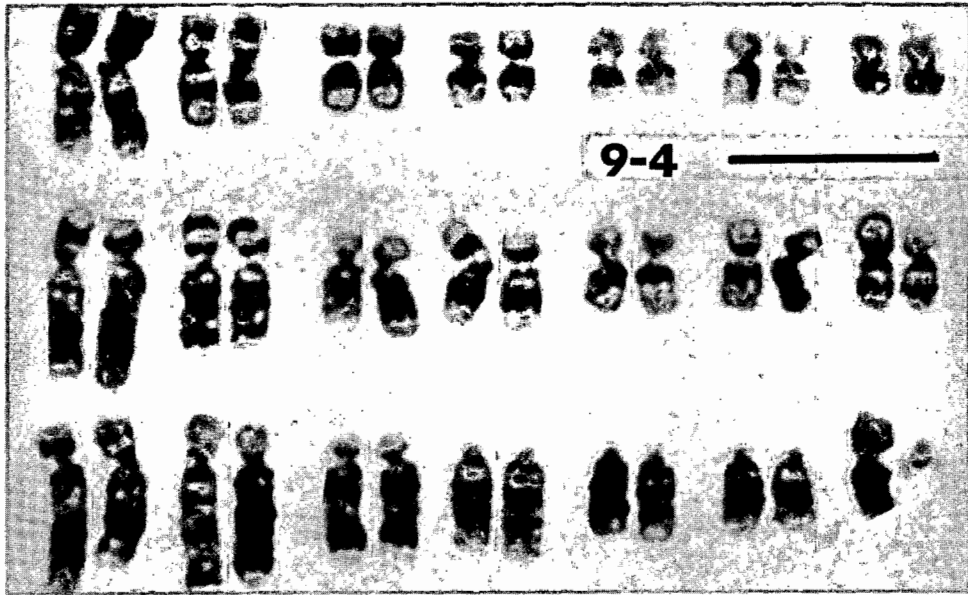


Figure 9-4. G-banded karyotype of an Ingutuk, 79B1. Pairing would be difficult without the complementary C-banded preparation (Fig 9-5) which indicates that several chromosomes have large terminal heteromorphisms. Two of the heteromorphic sites are identifiable on the short arms of sm4 and sm7. Bar = 10 microns

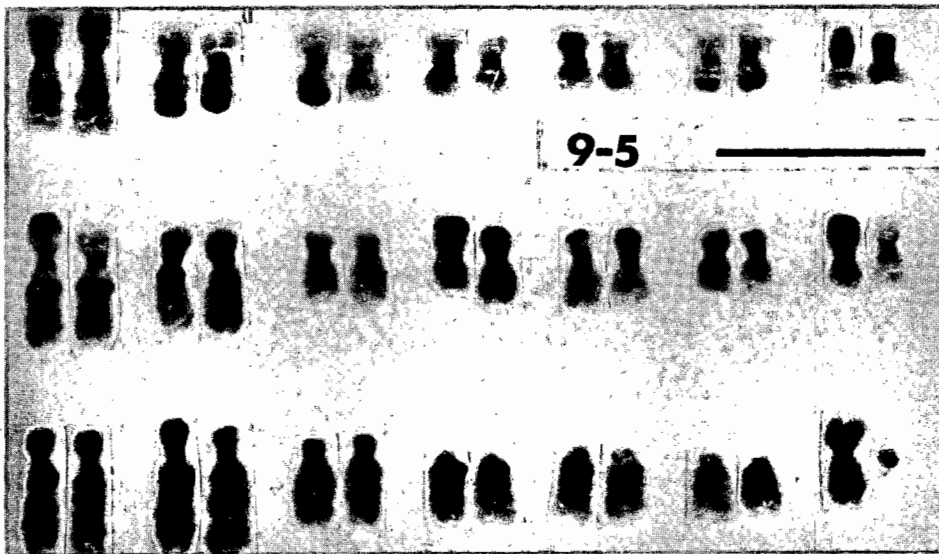


Figure 9-5. C-banded karyotype of 79B1. Two chromosomes with large terminal C-bands are placed in positions indicated by the G-banded preparation (Fig 9-4). Notice the heteromorphic arms on the largest submetacentric (sm1). Bar = 10 microns



Figure 9-6. C-banded preparation of a second Ingutuk, 80B8. Two overlapping pairs account for the darkness of some regions. No telomeric bands comparable to those observed in 79B1 were discernable in this whale. Heteromorphism in the smallest metacentrics (m7) is distinctive. Bar = 10 microns

Figure 9-7. C-banded karyotype of a female normal bowhead, 77B4. This whale exhibits distinctive chromosomal features in common with each of the Ingutuks. The short arms of the largest submetacentrics (sm1) are heteromorphic as in 79B1 (Fig 9-5) and the smallest metacentrics (m7) are heteromorphic as in 80B8 (Fig 9-6). Bar = 10 microns

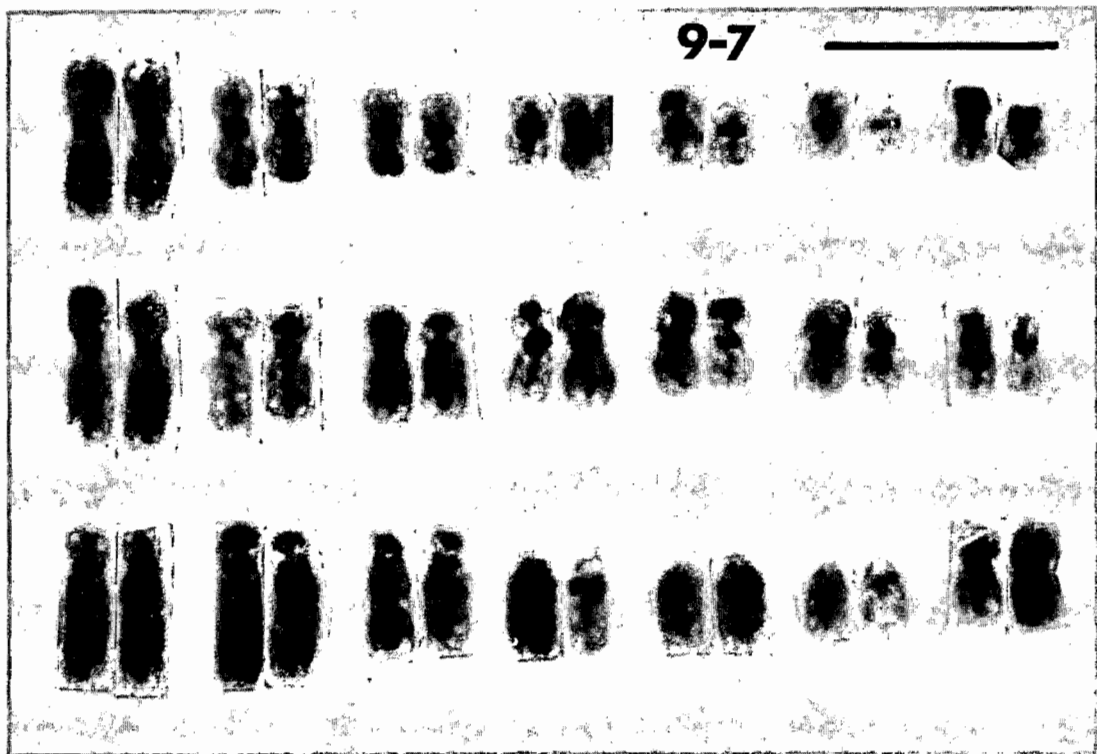


Figure 9-8. C-banded karyotype of 80B2, a normal bowhead. This animal has a distinctive heteromorphism in the sm4 position, similar to Ingutuk 79B1 (Fig 9-4 and 9-5). A unique and striking heteromorphism is present in the sm6 position. Identification of the sites was made from a G-banded preparation which is not shown. Bar = 10 microns

Figure 9-9. Silver stained karyotype of a bowhead (80SH) from Shaktoolik, Alaska showing positive staining on the short arms of the smallest metacentric (m7). This procedure demonstrates the active ribosomal cistrons at the nucleolus organizer region. Because of their common involvement in the nucleolus, the m7 homologues are frequently attached to each other. Bar = 10 microns

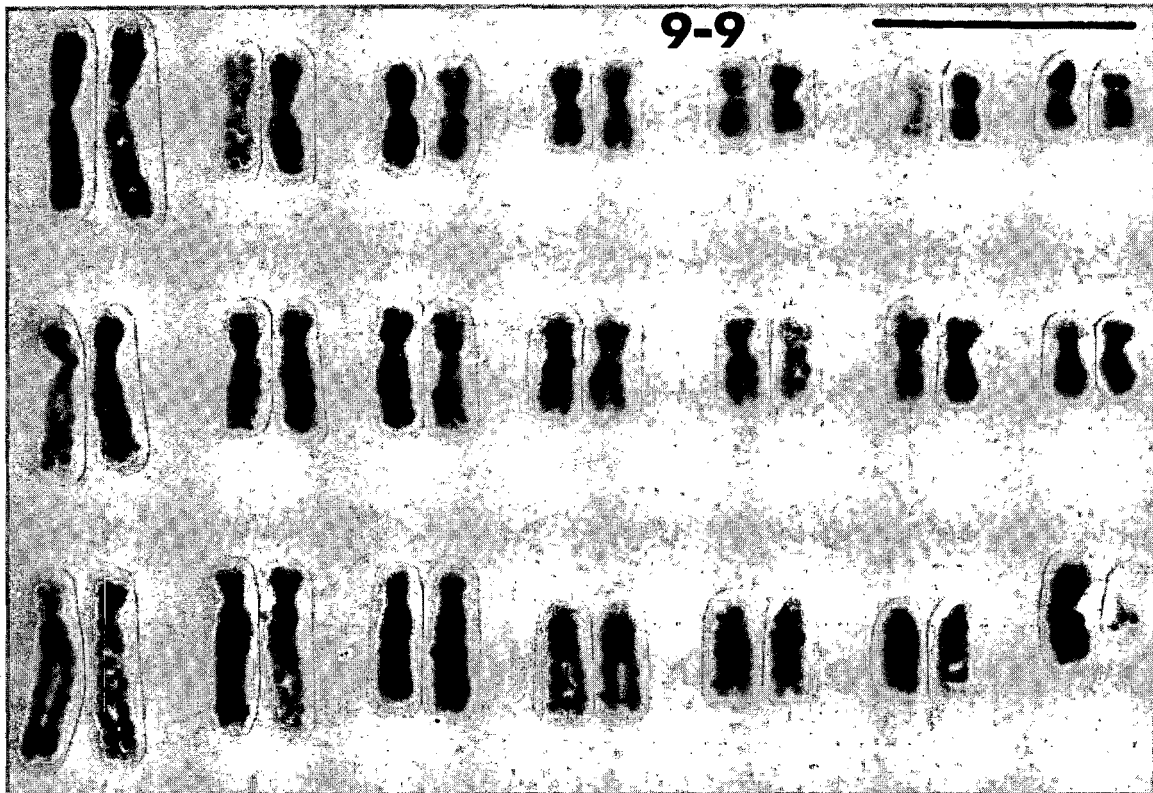
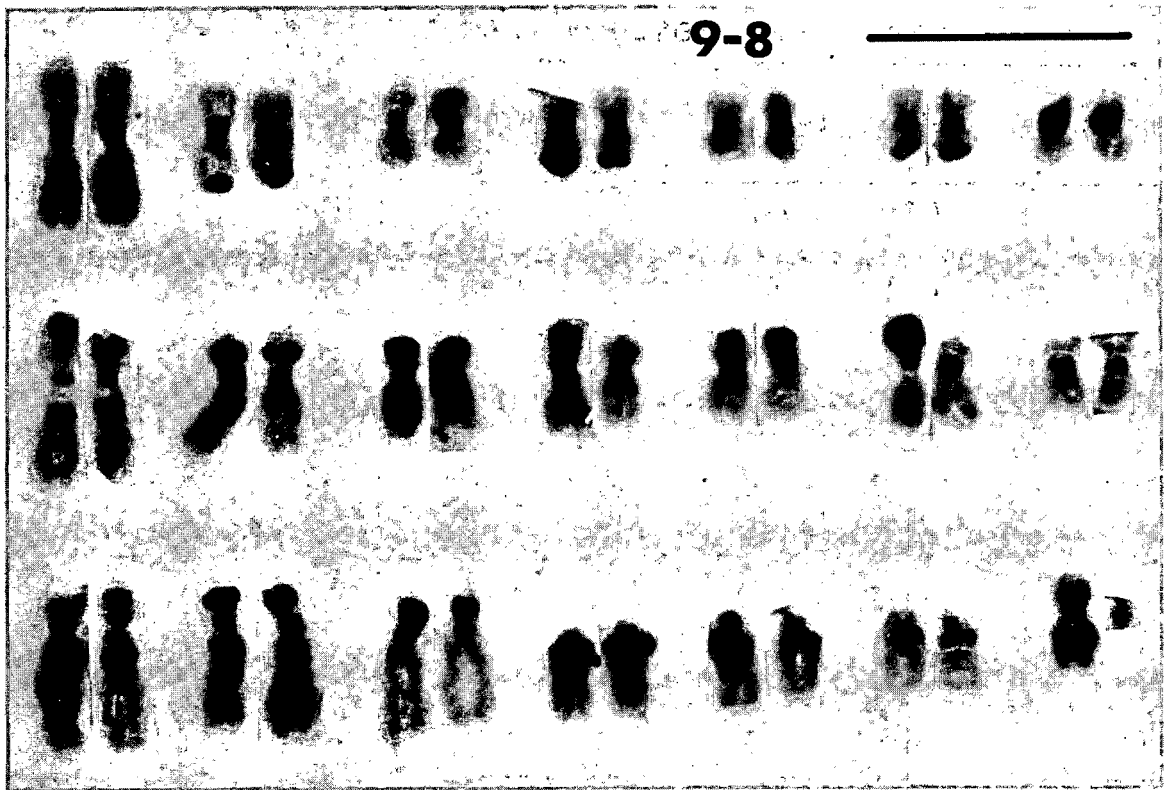


TABLE 9-1. CHROMOSOME MEASUREMENTS OF 10 CELLS FROM BOWHEAD WHALE 77B9

Chromosome	Relative Length*		Arm Ratio (r)	
	Mean	SE	Mean	SE
m1	7.91	0.080	1.40	0.021
m2	4.49	0.084	1.37	0.036
m3	3.38	0.044	1.26	0.032
m4	3.15	0.035	1.35	0.034
m5	2.83	0.039	1.35	0.032
m6	2.60	0.044	1.27	0.035
m7	2.71	0.069	1.22	0.045
sm1	7.30	0.077	2.09	0.035
sm2	5.78	0.068	2.14	0.030
sm3	4.80	0.046	2.04	0.038
sm4	4.44	0.040	2.06	0.044
sm5	4.01	0.032	1.94	0.071
sm6	3.67	0.037	1.86	0.044
sm7	3.42	0.025	1.81	0.043
st1	8.00	0.073	4.16	0.086
st2	7.48	0.086	3.96	0.059
st3	5.95	0.068	4.37	0.092
t1	4.96	0.059	14.98	0.895
t2	4.46	0.055	13.92	1.016
t3	3.74	0.049	13.36	1.232
x	4.92	0.057	1.46	0.046
y	0.97	0.038	1.38	0.049

\*Percent of female haploid length (A + X).

## DISCUSSION

Cytogenetics The hypothesis that C-band polymorphism is related to phenotypic polymorphism as represented by two forms of whale, was falsified by the apparent inconsistency in C-band distribution between two Ingutuks. The unfortunate failure to obtain precise chromosomal assignment of all heteromorphic sites in bowhead and Ingutuk karyotypes leaves room for equivocation. If Ingutuks can be shown to represent genetic morphs, a more precise investigation of C-band polymorphism would be justified. A more workable hypothesis may be that Ingutuks represent an ontogenetic form.

The presence of similar, and clearly identifiable, heteromorphic pairs in Ingutuks and non-Ingutuks strongly suggests a single freely-interbreeding population. This, of course, is further supported by the overall similarity of the karyotypes and by the electrophoretic data reviewed by Braham et al (1980).

Morphology There seem to be no genetic differences between Ingutuks and regular bowheads that can be demonstrated by conventional analysis. Yet there is no question that a suit of features characterize the Ingutuk.

The assertion that Ingutuks have denser bones than regular bowheads is well documented in this report by Drs. Fetter and Everitt of RU 480. They describe the Ingutuk as congenitally osteopetrotic but distinct from animals in which pachyostosis is regarded as an adaptation to the diving habit. They point out that the condition may be self-limiting and reversible, and that the osteochondrotic condition noted in Ingutuks has also been noted in fast-growing large breed dogs. These findings are consistent with the possibility that Ingutuks are fast-growing young bowheads.

The baleen of the Ingutuk has been described as shorter, thinner, lighter in color, and consisting of finer bristles than typical of regular bowheads (Foote 1964). Tomilin (1957) gives a detailed description of baleen growth in the bowhead. In advanced embryos the plates are steel gray, in contrast to generally black in adults. "The 'functional leap' in baleen growth, when the calf begins to consume adult food, usually takes place upon attaining a length of 7-8.5 m in Greenland right whales. This size marks the end of lactation." Such a "functional leap" could well account

for marked differences in baleen length among whales in this size range. Marked differences in baleen length, or other Ingutuk features, are not obvious beyond this approximate size range.

Another feature of Ingutuk baleen is that the "gums" extend further up between the baleen plates (Foote 1964). What is meant by "gums" is the white nonvascular tissue (mammuk) in which the baleen plates are anchored. This non-living tissue is apparently eroded from between the plates as they grow. If a "functional leap" in baleen growth occurred, the amount of mammuk would also increase, perhaps faster than it eroded for a time, thereby accounting for the deeper "gums" of the Ingutuk.

Young fin whales have been described as having a much finer fringe to the baleen than the adults. This feature enables them to exploit small copepods (Calanus finmarchius) in the North Atlantic and Barents Sea (Tomilin 1967 in Gaskin 1876, p 286). A fine baleen fringe may similarly characterize Ingutuks as young bowheads.

Documentation of flipper shape has revealed only that smaller whales have "stubbier" flippers, that is relatively broader at the insertion or base. The flipper shapes of individual whales seem quite variable and the flipper of a recent Ingutuk, 80B8, was not distinctive.

The fluke shape of Ingutuks was described by Foote (1964) as having the tips trailing back in contrast to the straighter trailing edge of regular bowhead flukes. I have noticed this feature in two Ingutuks, 79B1 and 79B3. Recently Durham presented a photograph (Fig 6-C in Durham 1980) of the flukes of a neonatal bowhead. In this photograph the trailing tips of the flukes are obvious suggesting this feature might be retained in Ingutuks from the neonatal period.

A double layer of fat has been described as a feature of Ingutuks (Foote 1964; Jarrell 1979a) but also characterizes normal bowheads. The blubber is the hypodermis. It contains much connective tissue and may be mostly insulative and structural in function. Under the blubber, on much of the body, is a loose layer of adipose tissue. This may be several cm thick on an Ingutuk but it is certainly evident on normal bowheads, especially in the fall. This suggests that sub-hypodermal fat is an energy storage organ, which is not to imply that the hypodermal blubber may not also serve in this capacity.

The possibility that Ingutuks are young bowheads is not a new suggestion. Stephanson (1944) reported that some Eskimos thought Ingutuks

were one or two year old bowheads while others thought that they were a separate species. Recently Mitchell (1977) concluded that Ingutuks are young bowheads. The fact that so few mature whales are taken in the Eskimo harvest makes it difficult to resolve whether or not large Ingutuks occur. It is clear that the Ingutuks harvested in the last couple years were less than full grown as evidenced by epiphyseal closure.

Two possibilities can be definitively rejected: 1) Ingutuks are not strictly young females. Foote's (1964) Ingutuk was a male, as were 78B3, 79B1, 79B3 and 80B8; 2) Ingutuks are not black right whales, Balaena (Eubalaena) glacialis (Braham et al 1980). Foote (1964) was a proponent of this hypothesis. He was not aware that black right whales have their characteristic callosities from birth. Black right whales have 228 to 259 baleen plates (Omura 1958). Ingutuks have over three hundred, as is characteristic of bowheads.

I would suggest that Ingutuks are approximately one year old animals, recently separated from their mothers. They still carry large stores of energy in the form of sub-hypodermal fat and large stores of calcium in their unremodeled bones. Baleen growth is occurring rapidly in the dietary transition from milk to prey.

#### SUMMARY

Cytogenetic evaluation of Ingutuk and normal bowhead whales by G- and C-banding of chromosomes revealed no consistent differences between these forms. Technical limitations precluded definitive falsification of the hypothesis that C-band heteromorphism is correlated with phenotypic polymorphism. The distribution of some clearly identified heteromorphic chromosome pairs in both forms of whale suggests a single freely-interbreeding population. Morphological features of the Ingutuk were reviewed and it was argued that Ingutuks are yearling bowheads.



## REFERENCES

- Arnason, U. 1974. Comparative chromosome studies in Cetacea. *Hereditas* 77:1-36.
- Bailey, A.M. and R.W. Hendee. 1926. Notes on the mammals of northwestern Alaska. *J. Mamm.* 7:9-28.
- Bloom, S.E. and C. Goodpasture. 1976. An improved technique for silver staining of nucleolar organizer regions in human chromosomes. *Hum. Genet.* 34:199-206.
- Braham, H.W., F.E. Durham, G.H. Jarrell and S. Leatherwood. Ingotuk: A morphological variant of the bowhead whale, *Balaena mysticetus*. *Mar. Fish. Rev.* 42:70-73.
- Duffield, D.A. 1977. Phylokaryotypic evaluation of the Cetacea. Phd. thesis, Univ. of California, Los Angeles. 171 pp.
- Durham, F.E. 1980. External morphology of bowhead fetuses and calves. *Mar. Fish. Rev.* 42:74-80.
- Foote, D.C. 1964. Observations on the bowhead whale at Pt. Hope, Alaska. McGill Univ., Montreal. Report for U.S. Atomic Energy Comm. 76 pp.
- Gaskin, D.E. 1976. The evolution, zoogeography and ecology of Cetacea. *Oceanogr. Mar. Biol. Ann. Rev.* 14:246-346.
- Jarrell, G.H. 1979a Tissues (structure/function) (RU 579d). In: Investigation of the occurrence and behavior patterns of whales in the vicinity of the Beaufort Sea lease area, J. Kelley and G. Laursen (eds.), pp 267-287. Final report to the Bureau of Land Management from the Naval Arctic Research Laboratory, Barrow, Alaska.
- Jarrell, G.H. 1979b. Karyotype of the bowhead whale (*Balaena mysticetus*). *J. Mamm.* 60:607-610.
- Jarrell, G.H. and U. Arnason. 1981. Banded karyotypes of a belukha whale, *Delphinapterus leucas*. *Hereditas* 95 (In press).
- Levan, A., K. Fredga and A.A. Sandberg. 1964. Nomenclature for centromeric position on chromosomes. *Hereditas* 52:201-220.
- Mitchell, E. 1977. Initial population size of bowhead whale (*Balaena mysticetus*) stocks: cumulative catch estimates. *Int. Whaling Comm.* SC/29/Doc. 33 147 pp.
- Niewczas, V. and H.S. Wang. 1978. A simple pretreatment for improving Ag-NOR staining. *Mamm. Chrom. Newl.* 19:137-139.
- Omura, H. 1958. North Pacific right whale. *Sci. Rept. Whales Res. Inst.* 13:1-52.

- Stephanson, V. 1944. Arctic Manual. Macmillan Co., New York 556 pp.
- Sumner, A.T. 1972. A simple technique for demonstrating centromeric heterochromatin. Exp. Cell. Res. 75:304-306.
- Tomilin, A.G. 1957. Mammals of the USSR and adjacent countries. Vol. IX Cetacea. (Izdatel Istvo Akademi Nauk SSSR, Moskva.) Isreal Program for Scientific Translations TT 65-50086, 1967. 717 pp.
- Winn, H.E., W. L. Bischoff and A.G. Taruski. 1973. Cytological sexing of cetacea. Mar. Biol. 23:343-346.
- Wang, H.C. and S. Fedoroff. 1972. Banding in human chromosomes treated with trypsin. Nature New Biol. 235:52-53.

INVESTIGATIONS OF THE SERUM ANTIBODIES AND VIRUSES  
OF THE BOWHEAD WHALE, BALAENA MYSTICETUS

ALVIN W. SMITH, D.V.M., M.S., Ph.D.  
School of Veterinary Medicine  
Oregon State University  
Corvallis, Oregon 97331

DOUGLAS E. SKILLING, B.S.  
San Diego Zoological Society  
Research Department  
P.O. Box 550  
San Diego, California 92112

KURT BENIRSCHKE, M.D., Ph.D.  
San Diego Zoological Society  
Research Department  
P.O. Box 550  
San Diego, California 92112

INTRODUCTION

Any animal examined in enough detail will be found to either harbor or have suffered the effects of infectious disease agents. It is well established that these naturally occurring diseases do manifest themselves as omnipresent and potent regulators of animal populations. It is equally well known that stress compromises body defenses against invasion by disease agents. Whether the sources of stress be an altered or reduced food supply or some form of harrassment, the physiologic effects of stress will remain generally the same and will be manifest in part as reduced resistance to disease.

The endangered bowhead whale population is reported to have remained at its current reduced level of about 2,300 for approximately 70 years with no tendency toward returning to its precommercial exploitation level estimated

at 20,000 to 40,000 (Evans and Cuccarese 1980). The only documented causes of death have been the Eskimo subsistence harvest and rare reports of whales trapped in the ice (Evans and Cuccarese 1980, Braham et al 1979). In the latter instance such occurrences could be precipitated by altered reaction to behavioral cues, reduced energy reserves or other manifestations of a compromise in general health. Certainly infectious diseases can cause all of these changes and in addition can contribute to natural mortality and reproductive failure. This and previous reports (Smith 1979, Johnson and Shum 1979) are the first attempts to evaluate the effects of infectious diseases on this endangered species. Although studies involving the proper collection, transportation and storage of highly perishable pathogenic microbes are extremely difficult in arctic areas, such studies are an essential part of assessing effects that could be induced by habitat disturbance. Such stresses can be expected to exacerbate the effects of the naturally occurring diseases including mortality among bowhead whale or any other populations.

#### OBJECTIVES

1. To examine serum taken from harvested whales for evidence of antibody response to major animal pathogens and known marine mammal pathogens.
2. To attempt to isolate and thereby characterize viruses which the whale may harbor.

#### METHODS

All samples came from Eskimo harvested bowhead whales through the activities of RU 180 and were of three general categories as follows: Whole serum for specific antibody studies, frozen tissue and swab samples for virus isolation and fresh tissues for growing cell cultures.

##### Serum Antibody Studies

Serums were received from four whales, 80B1, 80B2, 80B7, and 80B8. Each was examined for agglutinating antibodies to Leptospira interrogans serovars, ballum, canicola, ictero hemorrhagica, batavia, grippotyphosa, pyogens, autumnalis, wolffi, and pomona using the slide agglutination test (Alexander 1970). In this test bowhead whale serums were mixed with high concentrations of formalin fixed leptospire. Positive serums contain antibodies which cause the leptospire to bind together in clumps and these clumps can be recognized under a microscope.

In addition, each was tested for serum neutralizing antibodies to the 11 published serotypes of marine calicivirus (Smith et al 1981), one untyped walrus calicivirus (Ritter 1978), and 12 of the 13 known exotic caliciviruses (Dardiri 1981). The microtiter neutralization technique as modified was used for these tests (Monto and Bryan 1974, Smith et al 1976). In this test a virus of known type and concentration was mixed with whale serum diluted 1:10 and then incubated for an hour and then mixed with Vero cells. In positive serums antibody binds the virus rendering it incapable of destroying the Vero cells. Positive serums were diluted to the endpoint of activity to determine antibody titers.

Serums were tested for antibodies to influenza A virus using the Advanced Laboratory Techniques for Influenza Diagnosis published by the U.S. Department of Health and Welfare, Center for Disease Control, Atlanta, Georgia. This test is based on the knowledge that the influenza virus has surface hemagglutinins which agglutinate chicken red blood cells. Any specific antibodies in bowhead whale or other serums to be tested will bind to the viral hemagglutinins blocking the agglutination reaction (Easterday 1981). Alternatively, an immuno diffusion procedure was also used to test for type A influenza antibodies (Dardiri 1981).

#### Viral Isolation Studies

Attempts to isolate virus were designed using specialized tissue culture techniques to detect both cell associated and released virus. Cell lines used were African Green Monkey Kidney (Vero), a very broad spectrum cell type known to be especially sensitive for caliciviruses, Madin Darby Bovine Kidney (MDBK), another broad spectrum continuous cell line known to be sensitive for influenza virus and Skilling Smith Balaena Testis (SSBT) derived from bowhead 80B3 and possibly better suited for isolating whale specific viruses.

Dacron swab samples and snips of selected tissues from whales 80B1, 80B2, 80B7, and 80B8 were placed in one dram vials with tissue culture media and immediately frozen. These 48 samples were processed for isolating released virus by grinding with sterile sand in a mortar and pestle and then clarifying by low speed centrifugation (2500 rpm for 15 min.). The supernatant was filtered using milipore filters with a 0.45  $\mu$  pore diameter and then 0.2 ml of this was absorbed to the respective cell cultures in roller tubes. Each tube was fed and incubated at 37<sup>0</sup>C and read daily for cytopathology and each

culture was passaged for at least three passes as each monolayer began to deteriorate.

An additional 18 samples from whales 80B1, 80B2, 80B3, 80B5, 80B7 and 80B8 were processed to grow tissue cultures and to isolate cell associated viruses. These were received chilled (not frozen) as 1 to 5 gm samples of chopped tissue placed in 125 ml tissue culture flasks containing tissue culture media. These tissues were minced and rinsed several times, then each was bedded into two or more plastic flasks and overlaid onto the Vero cell or MDBK cell monolayers. In this latter instance, the tubes were held stationary for some time and not always placed on a roller drum. They were incubated at 37°C, observed daily for cytopathology and passaged directly as necessary for at least three passes without freezing.

Growing Bowhead Cell Cultures. The minced tissues bedded in plastic flasks as described above, were incubated at 37°C and observed for cell replication. Those tissues which grew to confluent monolayers were trypsinized, washed and passaged to new flasks. Eventually all were preserved in liquid nitrogen. 80B3 testis was labeled cell line SSBT and used for virus isolation attempts as described above.

## RESULTS

Serum Antibody Studies There were no agglutinating antibodies detected for any of the Leptospira interrogans serovars tested.

There was virus neutralizing activity, presumably antibody, against 3 of the 12 marine caliciviruses tested and against 2 of the 12 exotic caliciviruses tested (Table 10-1 and 10-2). The origin and different animal species from which these 24 viruses have been isolated is listed (Table 10-3) and shows that all three marine calicivirus types causing antigenic stimulus to the bowhead has previously been isolated from Northern fur seals (Callorhinus ursinus) in the Bering Sea. Two additional Bering Sea isolates, one from fur seals in 1972 (SMSV-1) and one from walruses did not cause detectable serum neutralizing activity in the four whales' serums. The findings of VESVJ<sub>56</sub> and VESVK<sub>56</sub> antibodies is remarkable in that these two agents have only been isolated once and that was from infected domestic swine sampled in New Jersey in 1956.

There were no detectable antibodies to the influenza viruses tested (Table 10-4).

TABLE 10-1. MARINE CALICIVIRUS ANTIBODIES IN BOWHEAD WHALES

Virus	Serum Tested <sup>1</sup>			
	80B1	80B2	80B7	80B8
SMSV-1 <sup>2</sup>	-	-	-	-
SMSV-2	-	-	-	-
SMSV-4	-	-	-	-
SMSV-5	1:20	1:20	1:10	-
SMSV-6	-	-	-	-
SMSV-7	-	-	-	-
SMSV-8	-	1:10	-	1:20
SMSV-9	-	-	-	-
SMSV-10	1:40	-	1:40	-
SMSV-11	-	-	-	-
SMSV-12	-	-	-	-
Walrus	-	-	-	-

1. Values given are for terminal antibody titers. All others tested negative at a serum dilution of 1:10.
2. SMSV stands for San Miguel Sea Lion virus and the subsequent number is the serotype determined by cross neutralization tests where 20 antibody units are tested against 100 tissue culture infective doses of virus. If neutralization does not occur, the serotypes differ.

TABLE 10-2. EXOTIC CALICIVIRUS ANTIBODIES IN BOWHEAD WHALES

Virus	Serum Tested <sup>1</sup>			
	80B1	80B2	80B7	80B8
VESV-A <sub>48</sub> <sup>2</sup>	-	-	-	-
VESV-B <sub>51</sub>	-	-	-	-
VESV-C <sub>52</sub>	-	-	-	-
VESV-D <sub>53</sub>	-	-	-	-
VESV-E <sub>54</sub>	-	-	-	-
VESV-F <sub>55</sub>	-	-	-	-
VESV-G <sub>55</sub>	-	-	-	-
VESV-H <sub>54</sub>	-	-	-	-
VESV-I <sub>55</sub>	-	-	-	-
VESV-J <sub>56</sub>	-	1:71	-	-
VESV-K <sub>56</sub>	1:22	1:110	-	-
VESV-1934B <sup>3</sup>	-	-	-	-

1. Values given are for terminal antibody titers. All negatives were at an initial serum dilution of 1:11.
2. VESV stands for Vesicular Exanthema of Swine Virus. The A was the first in an alphabeticized series of isolates and the subscript 48 was the year of isolation.
3. The virus was isolated from swine in California in 1934.



TABLE 10-3. ORIGINS AND DISTRIBUTION OF 14 CALICIVIRUS SEROTYPES USED TO TEST FOR ANTIBODIES IN BOWHEAD WHALES

Virus	Species and Place of Isolation	Species, number of animals tested and geographic location of animals carrying specific antibodies
SMSV-1	1. California sea lion (1972) San Miguel Island, Calif. 2. Northern fur seal (1972) Pribilof Islands, Alaska	1. California sea lions (22/80) <sup>1</sup> Southern and Central Calif. coast 2. Northern fur seal (2/855) Southern Calif. and Bering Sea 3. Fin whale (1/21) California 4. Feral swine (1/49) Southern California
SMSV-2	1. California sea lion (1972) San Miguel Island, Calif.	1. California sea lion (32/80) Southern and Central Calif. coast 2. Northern fur seals (115/855) Southern Calif. and Bering Sea 3. Gray whales (5/16) California 4. Feral swine (10/49) Southern California 5. Feral donkeys (2/13) Southern California
SMSV-4	1. California sea lions (1973) San Miguel Island, Calif. 2. Domestic swine (1976) Sonoma County, Calif.	1. California sea lions (4/80) Southern California 2. Domestic swine Sonoma County, Calif.
SMSV-5	1. Northern fur seal (1973) Pribilof Islands, Alaska	1. Northern fur seal (246/855) Bering Sea and Southern Calif. 2. Calif. sea lions (34/80) Southern Calif. coast 3. Gray whales (9/16) California 4. Sperm whale (2/10) North Pacific

TABLE 10-3 (continued)

		5. Fin whale (2/21) North Pacific
		6. Sei whale (5/7) North Pacific
		7. Feral swine (2/49)
		8. Bowhead whale (3/4) <sup>2</sup> Barrow, Alaska
SMSV-6	1. Calif. sea lion (1975) San Miguel Island, Calif.	1. California sea lion (33/115) Southern and Central Calif. coast
	2. Opaleye perch (1977) San Nicholas Island, Calif.	2. Northern fur seal (7/83) Southern California
		3. Gray whales, elephant seals and Bowhead whales (0/4)
SMSV-7	1. Opaleye perch (1976) San Nicholas Island, Calif.	1. Only Bowhead whales tested. (0/4)
	2. Northern elephant seals (1976) San Miguel Island, Calif.	
	3. Sea lion liver fluke <u>Zalophatrema</u> San Diego, Calif.	
SMSV-8	1. Northern fur seal (1975) Pribilof Islands, Alaska	1. Bowhead whales (2/4) Barrow, Alaska
		2. No other species tested for antibodies
SMSV-9	1. California sea lion (1975)	1. Only Bowhead whales tested (0/4)
SMSV-10	1. Northern fur seal (1977) Pribilof Islands, Alaska	1. Bowhead whale (2/4) Barrow, Alaska
		2. No other species tested.
SMSV-11	1. Northern fur seal (1977)	1. Only Bowhead whales tested. (0/4)
SMSV-12	1. California sea lion (1977) San Miguel Island, Calif.	1. Only Bowhead shales tested. (0/4)
	2. Northern fur seal (1977) San Miguel Island, Calif.	

TABLE 10-3 (continued)

Walrus virus	1. Walrus (1978)	1. Only Bowhead whales tested (0/4)
VESV-J <sub>56</sub>	1. Domestic swine (1956) Sicaucus, New Jersey	1. California sea lions (45/80) Southern and Central Calif. coast 2. Gray whales (2/16) California coast 3. Bowhead whales (2/4) Barrow, Alaska 4. Other whale species not tested.
VESV-K <sub>56</sub>	1. Domestic swine (1956) Sicaucus, New Jersey	1. California sea lions (34/80) Southern and Central Calif. coast 2. Feral swine (4/49) Southern California coast 3. Bowhead whales (2/4) Barrow, Alaska 4. No other whales tested except 16 Gray whales which tested negative.

1. Numbers in parentheses are the number positive out of the total tested.
2. All Bowhead data pertain to the present study.

TABLE 10-4. INFLUENZA ANTIBODY TESTS IN BOWHEAD WHALES<sup>1</sup>

Viruses	Bowhead Whale Serums			
	80B1	80B2	80B3	80B4
"A" Influenza Viruses				
Human Types				
H0	-	-	-	-
H1	-	-	-	-
H2	-	-	-	-
H3	-	-	-	-
Avian Types <sup>2</sup>				
Hav1 (H7)	-	-	-	-
Hav2 (H10)	-	-	-	-
Hav3 (H11)	-	-	-	-
Hav4 (H4)	-	-	-	-
Hav5 (H5)	-	-	-	-
Hav6 (H6)	-	-	-	-
Hav7 (H3)	-	-	-	-
Hav8 (H8)	-	-	-	-
Hav9 (H9)	-	-	-	-
Hav10 (H12)	-	-	-	-
Hav11 (H13)	-	-	-	-
Swine Types				
HSW1 (H1)	-	-	-	-
Equine Types				
Heq1 (H7)	-	-	-	-
Heq2 (H3)	-	-	-	-
"B" Influenza Virus Types				
B/Lee	-	-	-	-
B/Victoria	-	-	-	-
B/Hong Kong	-	-	-	-
New Castle Disease Virus				
LaSota	-	-	-	-

TABLE 10-4 (continued)

---

1. All tests were negative although there is an unconfirmed report of the Russians isolating influenza virus from a great whale and some captive dolphins are known to have influenza antibody titers.
2. These virus isolates were not only from terrestrial birds such as turkeys, chickens and quail, but also from water fowl including ducks, terns, a shearwater and a gull. Type Hav1 was first isolated from turkeys in Oregon in 1971. The Neuraminidase antigen of that isolate was Hav2 whereas a second Hav1 type tested was recently isolated from seals dying of pneumonia on the Massachusetts coast. However, this virus had a different neuraminidase antigen designated Neq1.

TABLE 10-5. BOWHEAD WHALE SAMPLES PROCESSED FOR VIRUS ISOLATION

80B1	80B2	80B7	80B8
<u>Frozen Swab Samples</u>			
Bronchus	Bronchus	Stomach abscess	Blowhole
Colon		Uterus	Conjunctiva
Blowhole		Large bowel	Prepuce
		Proximal colon	Large bowel
		Blowhole	Rectum
		Conjunctiva	
<u>Frozen Tissue Samples</u>			
Lung	Lung	Lung	Liver
Liver	Lymph node	Thymus	Kidney
Spinal cord	(bronchial)	Liver	Spleen
Brain	Thymus or fat <sup>1</sup>	Kidney	Large bowel
Colon	Liver	Spleen	Testis
Kidney	Spleen	Large bowel	Spinal cord
Spleen	Kidney	Colon	Brain
	Colon-mucosa		Thymus
	Spinal cord		Lung
<u>Chilled Tissues for Cell Culture<sup>2</sup></u>			
Skin	Skin	Skin	Skin
Kidney	Kidney	Kidney	Kidney
Lung	Lung	Lung	Lung
		Ovary	Testis
		Liver	

1. Exact nature of this tissue not determined at time of sample collection.
2. In addition, testis was submitted for 80B3 and 80B5.

TABLE 10-6. NEUTRALIZING ANTIBODY SCREENING OF BOWHEAD WHALE ADENOVIRUSES

Serums Tested	Virus Type	
	80B1-C	80B7-C
80B1 (Bowhead whale)	-	-
80B2 " "	-	-
80B7 " "	-	-
80B8 " "	-	-
Antiserum/Strain Bovine-1 10	-	-
Antiserum/Strain Bovine-2 19	-	-
Antiserum/Strain Bovine-3 WBR1	-	-
Antiserum/Strain Bovine-4 PHD-62	-	-
Antiserum/Strain Bovine-5 BA-65	-	-
Antiserum/Strain Bovine-6 67331	-	-
Antiserum/Strain Bovine-7 Fukori	-	-
Antiserum/Strain Bovine-8 Misk	-	-
Antiserum Persian gazelle-1	-	-
Antiserum Persian gazelle-2	-	-

Figure 10-1. Transmission electron photomicrograph of Vero cells infected with 80B7 colon adenovirus. The virus particles measure 72 nm in diameter and are shown at 112,000X. Some aggregates are still within the nucleus (arrows a) whereas other single virions have passed into the cytoplasm (arrow b). The inset is a negatively stained preparation from the infected Vero cells showing a typical 72 nm size particle with capsomers and the morphology of an adenovirus except that the filaments are not visible.



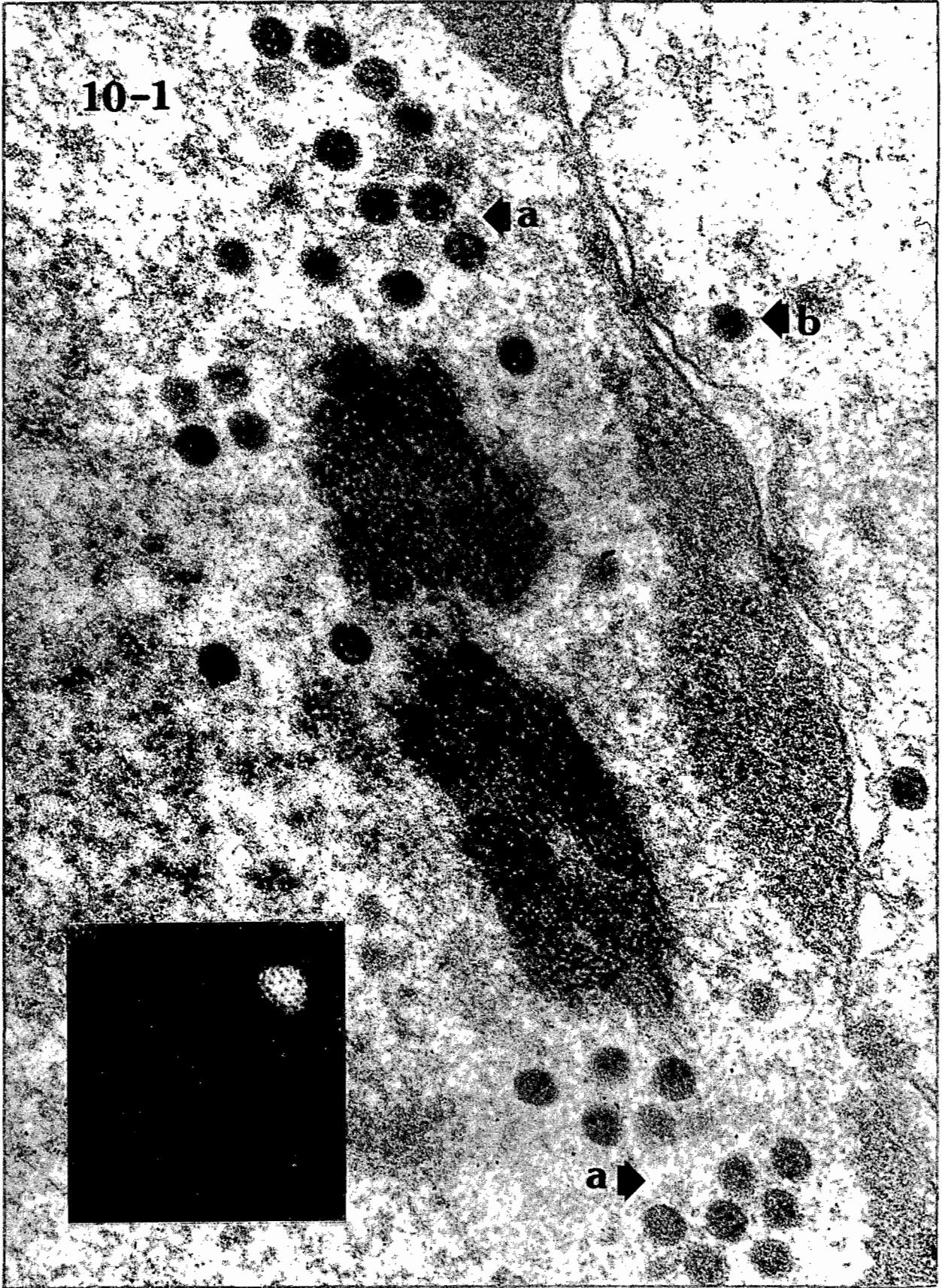


TABLE 10-7. BOWHEAD WHALE CELL CULTURES

Tissue Submitted	Cell Type	Passage Number	Frozen in Liquid Nitrogen
80B1			
Skin		1	0
Kidney	epithelial mixed	3	1 ampule pass 3
Lung		1	0
80B2			
Skin		1	0
Kidney		1	0
Lung		1	0
80B3			
Testis	fibroblast mixed	passage 8	3 ampules pass 3
80B5			
Testis		1	0
80B7			
Skin		1	0
Left kidney		1	0
Ovary		1	0
Liver		1	0
80B8			
Skin		1	0
Kidney	epithelial mixed	pass 2	1 ampule pass 2
Lung		1	0
Testis		1	0

### Virus Isolation Studies

Two samples yielded virus isolates in MDBK cells (Table 10-5). These were shown by physicochemical tests and by morphology to be adenoviruses (Fig 10-1). All four whale serums were tested for presence of neutralizing antibody to these agents and all were negative (Table 10-6). In addition, both isolates, adenovirus 80B1-C (C for colon) and adenovirus 80B7-C did not react with antiserum to eight bovine adenoviruses and two adenoviruses isolated from Persian gazelles (Table 10-6). Whether the two bowhead whale viruses are of identical serotypes has not yet been determined and tests to compare them with sei whale adenovirus isolate has not yet been completed (Smith and Skilling 1979). None of the tissues tested were shown to contain cell associated viruses, using the overlay techniques described.

### Growing Bowhead Cell Cultures

Tissues received from three of six whales were viable and primary cell lines were grown from kidney and testis then stored frozen (Table 10-7). In general, the cell lines grow quite slowly, taking 45 days to reach confluence when split 1 to 2 and, as has been the case with all the marine mammal cell lines we have started except for one (SSZS) (Smith 1979), the bowhead cells lose vitality and die after 6-9 passages.

## DISCUSSION

The absence of *Leptospire* antibodies in the four bowhead whale serums examined compares to a similar negative finding in the serums of 64 great whales previously examined (Smith and Skilling 1977). This finding is somewhat surprising in that Northern fur seals in the Bering Sea are routinely infected with *Leptospires* and these infections presumably occur at sea (Smith et al 1977). Stellar sea lions are known to carry *Leptospira* antibodies (Smith and Skilling 1977) and this pathogen has been isolated from Harbor seals sampled along the Alaskan coast (Ritter 1978). This absence of antibodies does not confirm that bowhead whales are free of *Leptospirosis* or that they never contact the pathogenic *Leptospires* since certain species, for example rats, may acquire lifelong infections without developing detectable antibodies. Should it be demonstrated that bowhead whales can become infected with *Leptospires*, then the public health impact of this should be considered for personnel who handle whale tissues or body fluids. Additionally, the disease, if it does occur among bowhead whales, would be expected to adversely affect the bowhead population much as it does other mammals.

The finding in bowhead whales of antibodies to three caliciviruses (San Miguel seal lion viruses types SMSV-5, SMSV-8 and SMSV-10) previously isolated from fur seals in the Bering Sea suggests that there may be a Bering Sea cycle for these agents. Attempts have been made to show that Northern fur seal could acquire calicivirus infections from fish reservoirs in Southern California and transport these to the Bering Sea (Smith et al 1980).

An SMSV-5 epizootic swept through the Northern fur seal herd on the Pribilof Islands in 1973 and apparently caused increased mortality at sea among that year's pup crop. This same agent, SMSV-5, appears to have infected a whole variety of whales and other species as far south as Southern California suggesting that geographic or other barriers to disease among ocean populations are poorly defined. The suggestion that specific diseases having reservoirs in Southern California waters and infecting land mammals could also infect an endangered species of whale whose year-round habitat is that of ice dominated waters is a new concept herein supported by the detection of specific San Miguel sea lion virus antibodies in these whale's serum.

Although vesicular exanthema of swine viruses J<sub>56</sub> and K<sub>56</sub> were only isolated once and that was some 25 years ago on a New Jersey swine ranch, there is ample serologic evidence (Table 10-3) to show that both these viruses have remained antigenically unaltered and very active along the Southern California coast. As was the case with SMSV-5 and presumable SMSV-8 and SMSV-10, VESV-J and VESV-K have had an effective vehicle for their spread to bowhead whales inhabiting the Bering, Chukchi and Beaufort seas. Additional evidence that bowhead whales can be infected by a marine calicivirus was demonstrated by experimentally infecting and growing SMSV-2 in bowhead whale cell lines (Smith 1979). This, combined with the solid demonstration of strong antigenic stimulation by specific caliciviruses, provides good evidence suggesting that the bowhead is an established host for this virus group.

In species where their effect has been studied, caliciviruses cause blisters and ulcers of the skin, lips, mouth and tongue, aborted and weakened newborn, agalactia, pneumonia, enteritis, myocarditis, and encephalitis. Presumably some or all of these disease traits would be expressed among calicivirus infected bowhead whales during some portion of their life cycle. It would be hard to imagine that caliciviruses do not adversely impact and alter the state of general health of bowhead whales and it is probable that

such disease effects would be amplified if the host species is placed under additional stress.

It was somewhat surprising to the scientists conducting these studies that bowhead whales did not have detectable antibodies to influenza viruses, especially when it is known that waterfowl and pelagic birds sampled at Point Barrow are at times shedding influenza virus. We are not suggesting that all bird influenza viruses should be thought to be transmissible to bowhead whales, although these viruses are known to be actively evolving between host species and predominantly avian virus types have been repeatedly shown to naturally infect mammals. Essentially all mammalian species studied in depth have been found to carry influenza virus antibodies. Because influenza disease cycles can be demonstrated in pelagic arctic birds, this would suggest that cycles for these same or similar influenza viruses might have developed in bowhead whales (Easterday 1976). Based on our limited sample, this is apparently not the case, and one possible explanation for this could be as follows: the bowhead's habitat is wind scoured and does not lend itself to the buildup of high concentrations of organic particulates (droplets containing virus) per volume of air as could occur in high density bird rookeries, burrows, nests and buildings. Since influenza virus is generally transmitted by the respiratory tract, it may be that concentrations of airborne virus do not reach infective levels for bowhead whales.

The isolation of two viruses from the four whales sampled was unexpected. Since 1965, there have been many well planned research efforts to isolate viruses from cetaceans, however, almost all have failed and the viruses reported here are only the third and fourth known virus isolates from great whales. The first, presumably an enterovirus, was isolated in 1968 from the rectum of a gray whale (Watkins 1969). The second was isolated from the rectum of a sei whale sampled in Antarctic waters by Murray Dailey 1977 (Smith and Skilling 1979). In addition, there are unconfirmed reports of a herpesvirus isolate from a sperm whale and an influenza virus isolated by Russian investigators from an unknown whale species.

Adenoviruses in general are known to cause respiratory infections, enteritis, hepatitis, conjunctivities and tumors. Presumably the bowhead whale adenoviruses could have similar effects on individual animals within the species.

There were no detectable antibodies in the bowhead whales against these two viruses and although this was somewhat unexpected, it is not altogether unusual for a host to shed virus and not show antibodies. This can occur in persistent infections as well as during the very early stages of typical infections. Other explanations would be that these viruses were not replicating in the whale but were simply passing through the digestive tract, or that the samples became contaminated with human or other species of adenoviruses. Although unlikely, these latter possibilities must be considered.

These investigations of infectious diseases of bowhead whales have identified specific viral agents that are known to impact other marine and terrestrial mammal populations and have demonstrated the presence of their antigenic footprints in the bowhead. A salutary management option available for the bowhead whale could be to develop control measures against selected naturally occurring diseases. It would seem that such things as upwind aerosol vaccines or vaccine darts would be feasible and may be useful as a means of disease control. Control of disease may ultimately be an attractive way of increasing bowhead whale numbers should the bowhead whale populations become further reduced through other events.

#### SUMMARY

Tissues, swab samples and serums from four Eskimo harvested bowhead whales were examined for specific antibodies and processed to grow cell cultures and isolate bowhead whale viruses. All serums were negative for antibodies to nine serovars of Leptospira interrogans and to 22 different hemagglutinating types of influenza virus. Out of 12 marine calicivirus serotypes tested (San Miguel sea lion virus, SMSV, 1, 2, 4-12 and walrus), three of the four whales were positive for SMSV-5 and two were positive for SMSV-8 and two were positive for SMSV-10. All three of three virus types had been previously isolated from marine mammals in the Bering Sea. Twelve serotypes of exotic calicivirus (vesicular exanthema of swine virus, VESV, types A-K 1934B) were tested against the four whale serums and two were positive for VESV-J antibodies, and two were positive for VESV-K antibodies. Two viruses were isolated from colon samples and these were determined to be adenoviruses of unknown type. There was no evidence to prove or disprove their infectivity for bowhead whales. Three different primary bowhead whale cell lines were grown and ampules of these stock cells were preserved in liquid nitrogen.

## ACKNOWLEDGEMENTS

Electron microscopy was accomplished by Maryanne Bache-Wimmer of the San Diego Zoo working in cooperation with Dr. Sheldon Diamond and using the Zeiss 10 scope belonging to the Clinical Investigation Section of the Naval Regional Medical Center, Balboa, San Diego, California. Dr. Jerry Callis arranged for serums to be examined for exotic animal disease antibodies at the Plum Island Animal Disease Center and Dr. Bernard Easterday arranged for influenza antibody tests at the School of Veterinary Medicine, Madison, Wisconsin.

## REFERENCES

- Alexander, A.O. 1970. *Leptospira*. In: Manual of Clinical Microbiology, J.E. Blair, E.H. Lennette and J.P. Truant (eds.) Am. Soc. of Microbiol. pp. 244-250.
- Braham, H.W., B.D. Krogman and G. Carroll. 1979. Population biology of the bowhead whale (*Balaena mysticetus*). II: Migration, distribution and abundance in the Bering Chukchi, and Beaufort Seas with notes on the distribution and life history of white whales (*Delphinapterus leucas*). Draft. U.S. National Marine Fisheries Service, Seattle, WA. RU69, Final Report. 117 pp.
- Dardiri, A. 1981. Unpublished data. Dr. Dardiri tested four bowhead whale serums for exotic vesicular exanthema of swine virus antibodies and influenza antibodies using the biological containment facilities at the Plum Island Animal Disease Center, Greenport, Long Island, New York.
- Easterday, B.C. 1976. Personal communication.
- Easterday, B.C. 1981. Unpublished data. Dr. Easterday screened four bowhead whale serums against a battery of influenza antigens at the School of Veterinary Medicine, University of Wisconsin, Madison, Wisconsin.
- Evans, C.D. and S.V. Cuccarese. 1980. The Bowhead Whale: Biological Basis for Management. A report to the Alaskan Eskimo Whaling Commission from the Arctic Environmental Information and Data Center, Anchorage, Alaska.
- Johnson, D.G. and A. Shum. 1979. Tissues, structure/function (RU280i). In: Investigation of the Occurrence and Behavior patterns of Whales in the Vicinity of the Beaufort Seas Lease Area, J. Kelley and G. Laursen (eds.) pp. 459-465. Final Report to the Bureau of Land Management from the Naval Arctic Research Laboratory, Barrow, Alaska.

- Monto, A.S. and E.R. Bryan. 1974. Microneutralization test for detection of rhinovirus antibodies. Proc. Soc. Exp. Biol. Med. 145:690-694.
- Ritter, D. 1978. Unpublished data. Dr. Carlton Ray had collected fecal samples from walruses and given these to Dr. Ritter, Univ. of Alaska for virus isolation. Dr. Ritter isolated three viruses and forwarded these to Dr. Al Smith at the Naval Ocean Systems Center and Mr. Douglas Skilling at the San Diego Zoo for identification. They were identified as calicivirus, all the same serotype but different than the other 11 known serotypes of marine calicivirus.
- Ritter, D. 1978. Personal communication.
- Smith, A. W. 1979. Tissues structure/function (RU-280h). In: Investigation of the Occurrence and Behavior Patterns of Whales in the Vicinity of the Beaufort Sea Lease Area, J. Kelley and G. Laursen (eds.), pp. 445-458. Final Report to the Bureau of Land Management from the Naval Arctic Research Laboratory, Barrow, Alaska.
- Smith, A.W., T.G. Akers, C.M. Prato and Bray. 1976. Prevalence and distribution of four serotypes of SMSV serum neutralizing antibodies in wild animal populations. J. Wildlife Dis. 12:326-344.
- Smith, A.W, R.J. Brown, D.E. Skilling, H.L. Bray and M.C. Keyes. 1977. Naturally-occurring Leptospirosis in Northern fur seals. J. Wildlife Dis. 13:144-148.
- Smith, A.W. and D.E. Skilling. 1977. Unpublished data.
- Smith, A.W. and D.E. Skilling. 1979. Viruses and virus diseases of marine mammals. Am. J. Vet. Res. 175(9):918-920.
- Smith, A.W, D.E. Skilling and A.B. Latham. 1981. Isolation and identification of five new serotypes of calicivirus from marine mammals. Am. J. Vet. Res. 42(4):690-691.
- Smith, A.W., D.E. Skilling and R.J. Brown. 1980. Preliminary investigation of a possible lung worm (Parafilaroides decorus), fish (Girella nigricans) and marine mammal (Callorhinus ursinus) cycle for San Miguel sea lion virus type 5. Am. J. Vet. Res. 41(11):1845-1849.
- Watkins, H.M.S., G.R.L. Worthington, A.B. Latham and A. Leibovitz. 1969. Isolation of enterovirus from the California gray whale (Eschrichtius gibbosus). Am. Soc. of Microbiol. Bacteriological Proceedings, Abstracts, 69th Annual Meeting, p. 180.



RESEARCH UNIT 1180

BACTERIOLOGICAL STUDY OF THE BOWHEAD WHALE, BALAENA MYSTICETUS

D. GORDON JOHNSTON, M.D., F.C.A.P.  
Marine Biomedical Research Laboratory  
St. John's Hospital  
Oxnard, California 93030  
Clinical Professor of Medicine  
UCLA School of Medicine  
Los Angeles, California 90024

and

ARCHIE C. SHUM, Ph. D.  
Marine Biomedical Research Laboratory  
St. John's Hospital  
Oxnard, California 93030

INTRODUCTION

Assessment of the species of bacteria in bowhead whales and their environment is an essential element of a comprehensive study of the whale. The following data describe samples of the microflora of the whales, and possibly, their environment.

## OBJECTIVES

1. To isolate and identify bacteria from specimens collected from the Eskimo harvested bowhead whales, Balaena mysticetus.
2. To draw conclusions as to the significance of the presence of these bacteria.

## METHODS

Collection of Specimens                      Specimens were collected from Eskimo harvested bowhead whales during the fall of 1979 and the spring of 1980 whaling seasons. A total of nine whales were sampled, five in 1979 and four in 1980. Sterile cotton swabs were used for sampling various sites of the body (Table 11-1). After sampling, the swabs were placed in the following transport devices: Amies transport medium containing activated charcoal (Clinical Standard Laboratories, Carson, California), anaerobic culturette (Marion Scientific Corporation, Kansas City, Missouri), and the thioglycollate broth supplemented with vitamin K<sub>1</sub>, hemin, and CaCO<sub>3</sub>. The specimens were in refrigeration temperature until mailed, special delivery, to the Marine Biomedical Laboratory, St. John's Hospital, Oxnard, California.

Culture                      Upon receiving the specimens at the laboratory, the specimens were inoculated into blood agar plates (BAP), containing 6.6% sheep's red blood cells, chocolate agar plates (CAP), McConkey agar plates (MAC), brucella blood agar plates supplemented with manadione (BMB), kanamycin-vancomycin-laked blood agar plates supplemented with manadione (KV) and thioglycollate broth supplemented with hemin, vitamin K<sub>1</sub> and CaCO<sub>3</sub> (THIO). The BAPs and MACs were incubated inside a candle jar (3-5% CO<sub>2</sub>) at 22°C and 37°C. The BMBs, KVs and THIOs were incubated anaerobically in a GasPak jar (BBL, Division of BioQuest, Cockeysville, Maryland) at 37°C. No quantitative determination of bacterial isolates were attempted. Procedures for isolation and identification of clinical bacterial isolates were followed (Finegold, Martin and Scott 1978, Lennette, Spaulding and Truant 1974, MacFaddin 1976, Washington 1974).

Isolation and Identification                      All dissimilar colonies from all plates were selected from all primary cultures. All bacterial isolates selected from the primary cultures were reisolated from single colony to BAP, MAC, CAP or BMB to obtain pure cultures.

Media used for identification of selected isolates were: triple sugar iron (TSI) agar slant, lysine iron agar (LIA) slant, Christensen's urea agar

slant, Simmon's citrate agar slant, tryptone broth, gluconate broth, methyl red-Voges Proskauer broth, OF-medium with glucose, maltose and other carbohydrates, nitrate broth, acetamide broth, cystine tryptic agar deeps for carbohydrate fermentation determination, motility deep, gelatin deep, egg yolk agar for lipase and lecithinase production, litmus milk, iron milk, 6.5% NaCl broth and the API 20E system (Analytab Productions, Division of Ayerst Laboratories, 200 Express Street, Plainview, New York 11803). Other tests employed were H<sub>2</sub>S production, fluorescence, cytochrome oxidase activities, production of coagulase, production of catalase, and hemolysis of sheep's red blood cells. Characterization of anaerobic bacteria was done by either the API 20A system for identification of anaerobes or the method outlined in the Virginia Polytechnic Institute (VPI) Anaerobic Laboratory Manual (Holdeman, Cato and Moore, 1977).

#### Electron microscopy

Transmission electron microscopy was performed.

Bacteria tested were either grown in brain heart infusion broth (BHI) or on BAP. The broth cultures were either grown at a stationary position at room temperature or on a reciprocating platform shaker (New Brunswick Scientific, model R-2, Edison, New Jersey) at 250 rpm at 37°C. After the bacterial cultures reached their mid-log growth phase which has a turbidity of McFarland nephelometer barium sulfate standard No. 2, glutaraldehyde in 0.1M sodium cacodylate buffer, pH 7.3, was added to the broth mixtures to a final concentration of 2% (v/v). The bacterial cultures were left standing at 4°C overnight. The contents were then centrifuged at 500 x g for 10 minutes. The supernates were decanted and the sediments were washed three times with the same buffer without glutaraldehyde. The resulting pellets were then postfixed with 1% osmium tetroxide in 0.2M sodium cacodylate buffer, pH 7.2, for one hour at room temperature. After washing the postfixed materials in 0.2M sodium cacodylate buffer, pH 7.2, three times, the resulting sediments were stained en bloc in 2% aqueous uranyl acetate (w/v) for 20 minutes. The contents were once again centrifuged and the supernates decanted. The pellets were then suspended in melted 2% purified agar (Difco). After the agar was solidified, it was cut into small slices (2 x 4 mm) and dehydrated. Dehydration was carried out in graded ethyl alcohols: 50%, 70%, 95% for 5 minutes each, then thrice in 100% ethyl alcohol for 5 minutes each. The dehydrated specimens were then processed through propylene oxide three times at 10 minutes each. Infiltration of the specimens was done in a 50-50 mixture of Epon 812 and propylene oxide in a vacuum of 10<sup>-3</sup> mm Hg, followed by infiltration of 100% Epon 812 in a vacuum of 10<sup>-3</sup> mm Hg. The specimens were then embedded in Epon 812

at 77°C for 18 hours. The thin sections were cut on glass knives on a Sorvall Porter-Blum (model MT-1) ultra-microtome (Ivan Sorvall Inc., Newtown, Connecticut). Sections were stained in 2% aqueous uranyl acetate for 30 minutes, washed in deionized water, and stained again with Reynold's lead citrate solution for 4 minutes. After washing in deionized water, the sections were examined in a Hitachi HS-9 electron microscope (Hitachi, Ltd., Tokyo, Japan) operating at 75 KV.

Bacterial cultures were also prepared for negative staining. The broth cultures were harvested by centrifugation at 500 rpm for 10 minutes and washed once in deionized water. The sediments were then suspended in deionized water to a turbidity of McFarland standard No. 1. For plate cultures, a cotton swab was used to pick up bacteria from the plate and resuspended in a tube of sterile deionized water to a turbidity of McFarland standard no. 1. The bacterial suspensions were placed on copper grids (200 mesh) which were coated with Formvar film and a layer of carbon. The carbon was evaporated onto the Formvar filmed grids with a Hitachi carbon evaporator (type HUS-4). After the drop of bacterial suspension was let stand for one minute on the copper grid, excess water was drained by touching the edge of the grid to a filter paper (Whatman, No. 1). A drop of 1% aqueous phosphotungstic acid was put onto the grid and immediately drained of any excess phosphotungstic acid with filter paper. The resulting negatively stained bacteria were examined with the Hitachi electron microscope at 75 KV.

Lyophilization            Samples of all bacteria isolated were lyophilized for preservation and later study. Each bacterium was grown on BAP. A heavy suspension of bacterial cells was made in 1 ml of sterile skim milk in a sterile 10 ml freeze-drying serum vial. After quick freezing of the cell suspensions in a dry ice-acetone bath, the frozen samples were put into the adapter of an automatic lyophilizer (Vitrisc model 10-101, The Welsh Scientific Co., 7300 N. Linder Ave., Skokie, Illinois 60076). The lyophilized cultures were stored at room temperature or 4°C. To reconstitute the lyophilized culture, 1 ml of sterile deionized water was used. Viability was determined by subculturing on appropriate media.

TABLE 11-1.

LOCATIONS SAMPLED AND ISOLATES OF  
BACTERIOLOGICAL STUDIES OF BALAENA MYSTICETUS

Year	No. Whales Examined	Total No. Specimens	Specimen Site	No. Isolates
1979	5	12	Mouth	6
			Mouth nodule	3
			Lung	4
			Blubber *	1
			Small Bronchus	0
			Small Intestine	2
			Trachea	9
			Urine	3
			Uterus	2
			1980	4
Lung	1			
Stomach abscess	1			

\* This sample was taken from a stranded whale (79B4).

## RESULTS

Bacteria isolated and identified from various sites of five bowhead whales examined in 1979 are listed in Table 11-2. Those from four of the bowhead whales harvested in 1980 are listed in Table 11-3. Some of the bacterial isolates were identified to genus and species. However, other isolates are yet to be identified owing to characteristics that fail to match those of the common clinical bacterial species. No fungus was isolated. No attempt was made for isolation of mycobacteria or pleuropneumonia-like organisms (PPL0) in this study. There were a total of sixteen different bacterial species isolated from four of the five bowhead whales examined in 1979 with none recovered from whale 79KK4. However, the only specimen analyzed from 79KK4 was taken from a small bronchus. Ten different bacterial species were isolated from four bowhead whales examined in 1980 (Table 11-3). Most of the isolates in the 1979-80 study period were aerobic or facultative gram negative bacilli including: Acinetobacter calcoaceticus v. lowfii, Alcaligenes species, Bordetella bronchisepticum, Citrobacter species, Enterobacter agglomerans, Escherichia coli, Pleisomonas shigelloides, Pseudomonas fluorescens, Pseudomonas species and Vibrio parahaemolyticus. Other aerobic or facultative bacteria identified were Branhamella catarrhalis, Micrococcus species, Staphylococcus aureus, and Staphylococcus epidermidis. The alpha-hemolytic streptococcus and the beta-hemolytic streptococcus are not fully characterized. Among the anaerobes, Clostridium sordellii and Clostridium species were predominant anaerobic organisms recovered. An anaerobic gram positive bacillus and an anaerobic gram positive coccus are yet to be identified. Other bacteria not yet classified are: pleomorphic aerobic gram positive bacillus, aerobic gram negative diplococcus, aerobic gram positive diplococcus and aerobic gram negative non-fermentative bacillus.

Of all the specimens analyzed, seventeen were from the respiratory tract (six from the upper and eleven from the lower respiratory tracts). Bacteria isolated from the upper respiratory tract specimens are presented in Table 11-4. Those from the lower respiratory tract specimens are presented in Table 11-5. Since sampling of the upper respiratory tract of the 1980 bowhead whales was not done, all bacterial isolates from those whales were from the lower respiratory tract. Four bacterial species isolated from the lung specimen of whale 79KK2 (Table 11-2, aerobic non-fermentative gram negative bacillus, anaerobic gram positive coccus, Citrobacter species, and Pseudomonas species), were also isolated from the upper respiratory tract specimens of the same whale. Such a finding suggests that aspiration of the upper respiratory tract flora to the lung might occur at the time

of harvesting or that some movement of microbes occurred after the whale's death.

One bacterial isolate, pleomorphic aerobic gram positive bacillus, was recovered from eight different specimens from four whales (79KK1, 79KK2, 80B1 and 80B8). This organism seems to be the only common bacterium among the examined bowhead whales since most bacterial isolates from the 1979 bowhead whales differ from those of the 1980 bowhead whales.

Light and electron microscopic studies were undertaken for some of the not yet identified bacterial isolates. These may be two different aerobic gram positive bacilli showing different forms of pleomorphism. Figure 11-1 shows the gram staining morphology of the first pleomorphic bacillus isolated from whale 80B1. This bacterium is normally rod shaped but it has a tendency of swelling subterminally or terminally. The negative staining electron photomicrographs presented in Figures 11-2 and 11-3 demonstrate these phenomena. Figure 11-4 reveals the branching characteristics of the second pleomorphic bacillus (gram stain), isolated from whale 80B1. This organism was also isolated from whales 79KK1, 79KK2, and 80B8. In addition to its branching characteristics, this bacterium also swells along its rod shaped body as seen in Figure 11-5. However, this bacterium tends to branch rather than swell (Figure 11-6). In addition to the differences in cellular morphology, these two pleomorphic gram positive bacilli also differ in their colonial morphology when they are grown on BAP. However, further studies are needed to differentiate them in order to conclude that they are actually different species.

Figure 11-7 is an electron photomicrograph of a thin section of dividing cells of an aerobic gram positive diplococcus isolated from whale 80B7. The same bacterium was also isolated from whale 79KK2.

The Hoffman modulation differential interference contrast photomicrograph of an aerobic gram positive coccus isolated from whale 80B7 is seen in Figure 11-8. This organism forms a cube of eight round cells. Figures 11-9 and 11-10 are electron photomicrographs of thin sections of this organism which is tentatively identified as Micrococcus species.

TABLE 11-2.

## BACTERIAL ISOLATES FROM BOWHEAD WHALES (1979)

Whale No.	Specimen	Bacteria
79KK1	Mouth (tongue swab)	Aerobic gram + bacillus, pleomorphic Aerobic gram - diplococcus <u>Alcaligenes</u> species <u>Clostridium</u> species <u>Pseudomonas flourescens</u> <u>Pseudomonas</u> species
	Trachea	Aerobic non-fermentative gram - bacillus beta-hemolytic streptococcus <u>Branhamella catarrhalis</u> <u>Clostridium sordellii</u>
	Urine	alpha-hemolytic streptococcus Aerobic gram + bacillus, pleomorphic <u>Pseudomonas</u> species
79KK2	Lung	Aerobic non-fermentative gram - bacillus Anaerobic gram + coccus <u>Citrobacter</u> species <u>Pseudomonas</u> species
	Mouth	<u>Pseudomonas</u> species
	Mouth Nodule	Aerobic gram + bacillus, pleomorphic Aerobic non-fermentative gram - Bacillus <u>Alcaligenes</u> species
	Trachea	Aerobic gram - diplococcus Aerobic non-fermentative gram - bacillus Anaerobic gram + bacillus Anaerobic gram + coccus <u>Citrobacter</u> species <u>Vibrio parahaemolyticus</u>
	Uterus	Aerobic gram + bacillus, pleomorphic Aerobic gram + diplococcus
79KK3	Small Intestine	Aerobic non-fermentative gram - bacillus Anaerobic gram + coccus
	Small Bronchus	no isolate
79KK4	Small Bronchus	no isolate
79B4	Blubber (from stranded whale)	<u>Escherichia coli</u>



TABLE 11-3.

## BACTERIAL ISOLATES FROM BOWHEAD WHALES (1980)

Whale No.	Specimen	Bacteria
80B1	Bronchus	Aerobic gram + bacillus, pleomorphic
	Lung	Aerobic gram + bacillus, pleomorphic
80B2	Stomach Abscess	<u>Staphylococcus epidermidis</u>
	Bronchus	<u>Staphylococcus epidermidis</u>
80B7	Bronchus #1	<u>Acinetobacter calcoaceticus v. lowfii</u>
		<u>alpha-hemolytic streptococcus</u>
		<u>Enterobacter agglomerans</u>
	Bronchus #2	Aerobic gram + diplococcus
		<u>Enterobacter agglomerans</u>
	<u>Micrococcus species</u>	
	<u>Pleisomonas shigelloides</u>	
	<u>Staphylococcus aureus</u>	
80B8	Stomach Abscess	no isolate
	Bronchus-B	Aerobic gram + bacillus, pleomorphic <u>Bordetella bronchisepticum</u>
	Bronchus #1	Aerobic gram + bacillus, pleomorphic
	Bronchus #2	no isolate

TABLE 11-4.

## BACTERIA ISOLATED FROM UPPER RESPIRATORY TRACT\*

---

1979	Aerobic gram + bacillus, pleomorphic Aerobic gram + diplococcus Aerobic gram - diplococcus Aerobic non-fermentative gram - bacillus <u>Alcaligenes</u> species beta-hemolytic streptococcus <u>Branhamella catarrhalis</u> <u>Citrobacter</u> species <u>Clostridium sordellii</u> <u>Clostridium</u> species <u>Pseudomonas fluorescens</u> <u>Pseudomonas</u> species <u>Vibrio parahaemolyticus</u>
------	--

---

\* blow hole, pharynx, hypopharynx, larynx

TABLE 11-5.

## BACTERIA ISOLATED FROM THE LOWER RESPIRATORY TRACT\*

---

1979	Aerobic non-fermentative gram - bacillus Anaerobic gram + coccus <u>Citrobacter</u> species <u>Pseudomonas</u> species
1980	Aerobic gram + bacillus, pleomorphic Aerobic gram + diplococcus <u>Acinetobacter calcoaceticus v. lowfii</u> alpha-hemolytic streptococcus <u>Bordetella bronchisepticum</u> <u>Enterobacter agglomerans</u> <u>Micrococcus</u> species <u>Pleisomonas shigelloides</u> <u>Staphylococcus aureus</u> <u>Staphylococcus epidermidis</u>

---

\* trachea, bronchi, pulmonary parenchyma

TABLE 11-6. COMPARISON OF BACTERIA ISOLATED FROM ARCTIC PORPOISES AND BOWHEAD WHALES

Bacteria	Arctic Porpoises *	Bowhead Whale
<u>Micrococcus</u> species		X
<u>Staphylococcus aureus</u>		X
<u>Staphylococcus epidermidis</u>	X	X
<u>Streptococcus</u> , alpha	X	X
beta		X
gamma	X	
<u>Streptococcus fecalis</u>	X	
Aerobic gram + pleomorphic bacillus	X	X
<u>Branhamella catarrhalis</u>		X
<u>Neisseria</u> species	X	X
<u>Achromobacter</u> species	X	
<u>Acinetobacter calcoaceticus</u>	X	X
<u>Alcaligenes</u> species	X	X
<u>Bordetella bronchisepticum</u>		X
<u>Citrobacter</u> species	X	X
<u>Enterobacter</u> species	X	X
<u>Escherichia coli</u>		X
<u>Pleisomonas shigelloides</u>		X
<u>Proteus</u> species	X	
<u>Pseudomonas aeruginosa</u>	X	
<u>Pseudomonas fluorescens</u>	X	X
<u>Pseudomonas</u> species	X	X
<u>Serratia</u> species	X	
<u>Vibrio parahaemolyticus</u>		X

\* Tursiops truncatus, Delphinus delphid, Stenella coeruleoalba, Stenella plagiodon.

Figure 11-1. Photomicrograph of gram stain of a pleomorphic gram positive bacillus isolated from bowhead whale 80B1. The rod shaped bacterium swells subterminally or terminally. X 5,000.

Figure 11-2. Electron photomicrograph of a pleomorphic gram positive bacillus (negative stain with phosphotungstic acid) isolated from bowhead whale 80B1 showing subterminal swelling. X 24,000.

Figure 11-3. Electron photomicrograph of a pleomorphic gram positive bacillus (negative stain with phosphotungstic acid) isolated from bowhead whale 80B1 showing terminal swelling. X 24,000. The bacteria seen in Figures 11-1 through 11-3 are the same isolate.

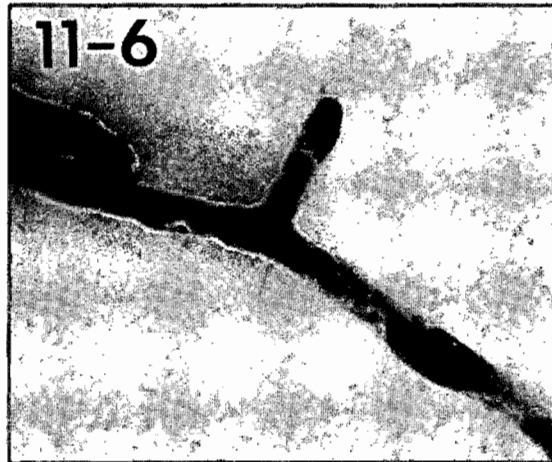
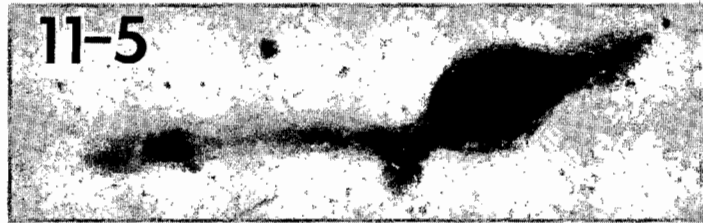
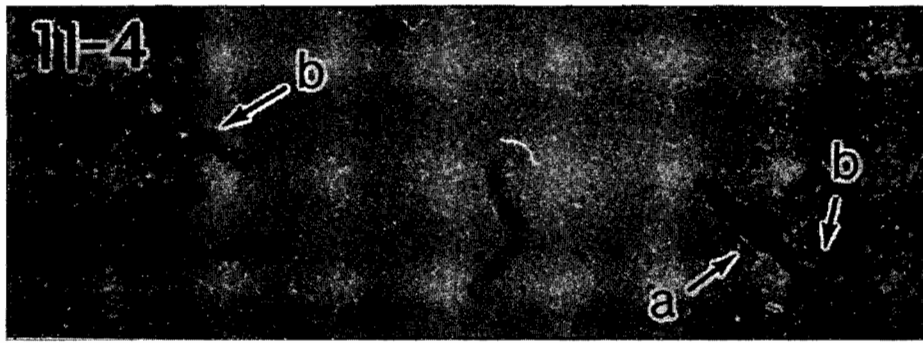


Figure 11-4. Photomicrograph of gram stain of pleomorphic gram positive bacillus isolated from bowhead whale 80B1. This rod shaped bacterium demonstrates pleomorphism by (a) swelling and (b) branching. It was also isolated from whales 79KK1, 79KK2 and 80B8. X 5,000.

Figure 11-5. Electron photomicrograph of a pleomorphic gram positive bacillus (negative stain with phosphotungstic acid) isolated from bowhead whale 80B1 showing its swelling characteristic. X 14,000. It was also isolated from whales 79KK1, 79KK2 and 80B8.

Figure 11-6. Electron photomicrograph of a pleomorphic gram positive bacillus (negative stain with phosphotungstic acid) isolated from bowhead whale 80B1 showing its branching characteristic. X 12,000. It was also isolated from whales 79KK1, 79KK2 and 80B8. The bacteria seen in Figures 11-4 through 11-6 are the same isolate.

Figure 11-7. Electron photomicrograph of an aerobic gram positive diplococcus from bowhead whale 80B7 showing dividing cells. X 54,000. This bacterium was also isolated from whale 79KK2. cw = cell wall.

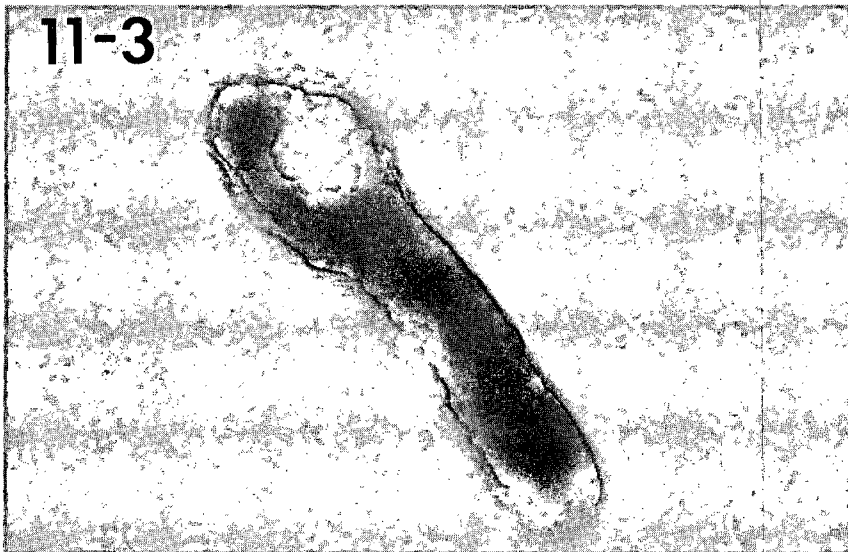
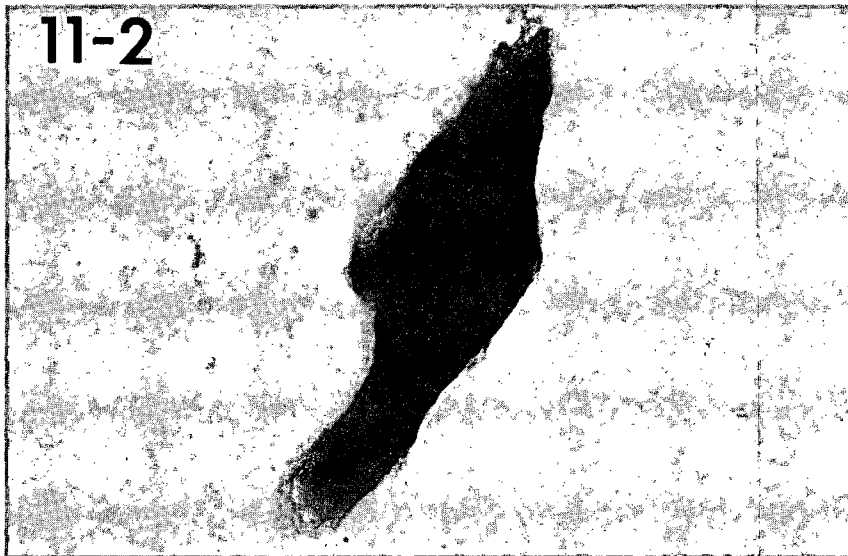
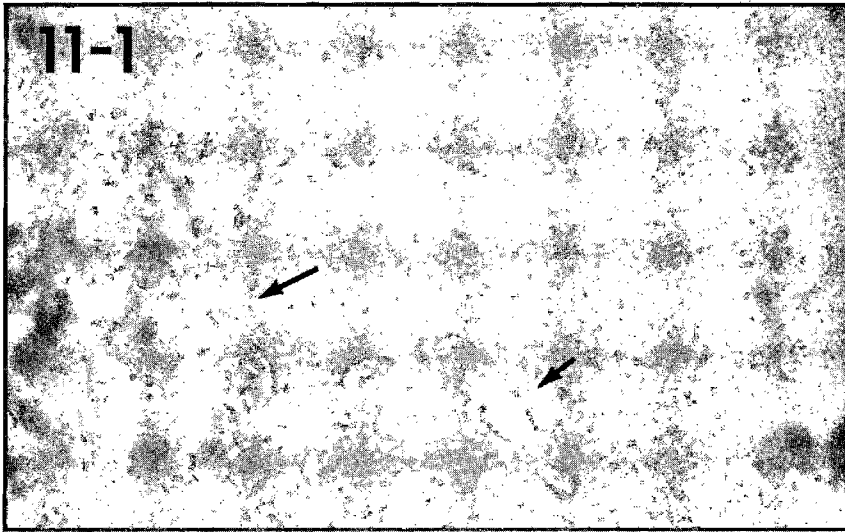
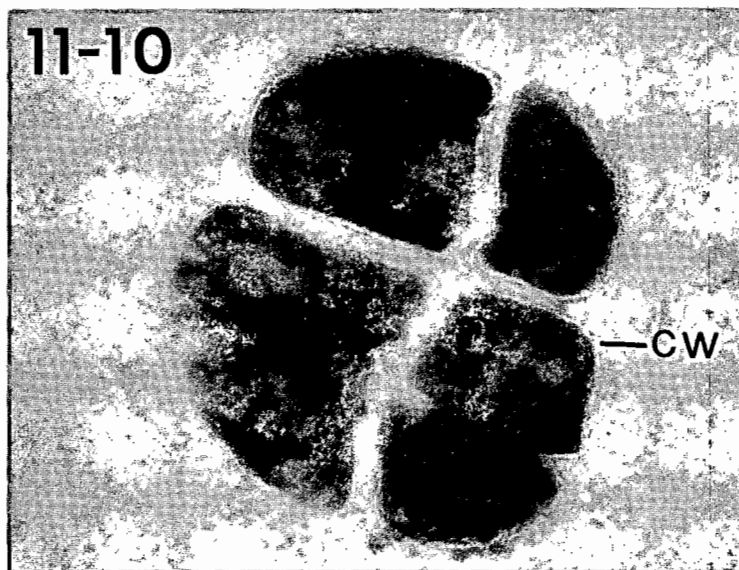
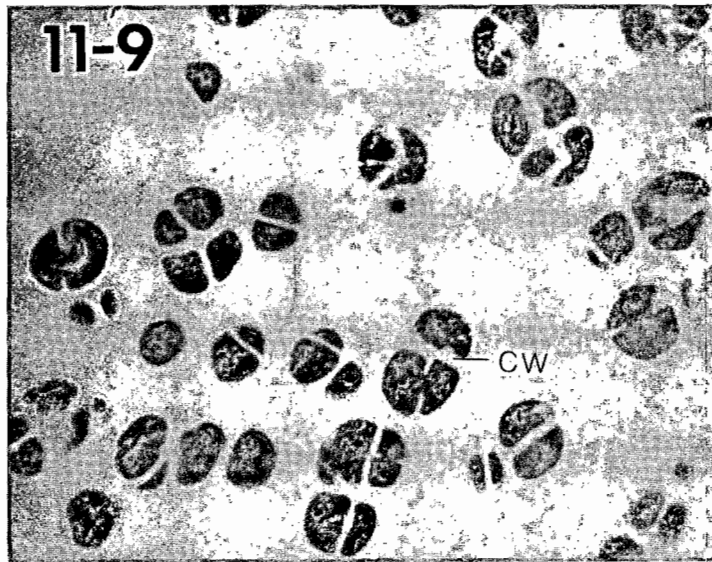
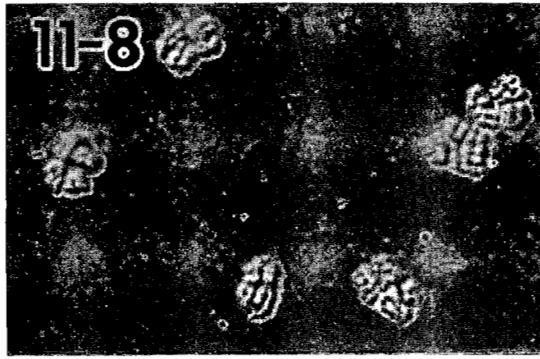


Figure 11-8. Hoffman modulation differential interference contrast photomicrograph of Micrococcus species isolated from bowhead whale 80B7. This bacterium has a morphology of a cube of eight round cells. X 960.

Figure 11-9. Transmission electron photomicrograph of Micrococcus species isolated from bowhead whale 80B7 showing the arrangement of the cells and their cell walls (cw). X 13,000.

Figure 11-10. Transmission electron photomicrograph of Micrococcus species isolated from bowhead whale 80B7 showing the arrangement of cells and their cell walls (cw). X 63,000. The bacteria seen in Figures 11-8 through 11-10 are the same isolate.





## DISCUSSION

A total of twenty-two specimens were submitted from nine bowhead whales, of which four specimens contained no organisms. The remaining eighteen specimens each contained one or more bacterial isolates. Enteric bacteria were not detected in large numbers, however, only one specimen from the intestinal tract was analyzed. Most of the specimens were from the respiratory tract. This presents difficulties in evaluating the normal flora of the bowhead whale. This problem is compounded by the time required for killing and beaching the whales before samples could be taken; sometimes it was only a matter of hours, however, days could be involved in the process. The possible contamination from sea water alone cannot yet be evaluated since appropriate sea water samples have not yet been collected. Refrigeration of the specimens appears to have been helpful in recovering non-fermentative gram negative aerobic bacteria. Anaerobes were not isolated from the 1980 whale samples despite added precaution and attempt to preserve and transport specimens favoring anaerobic bacteria recovery. Specific precautions for sampling anaerobes were not included in this study, but should be included in future observations despite the technical and logistical problems attending anaerobic culture techniques. A few facultative organisms were recovered. Among anaerobes isolated from the 1979 whale samples, Clostridium, a spore former, survived refrigeration and transportation, whereas non-spore forming anaerobes were not identified.

Among the isolates Vibrio parahaemolyticus, Citrobacter species, Escherichia coli, Branhamella catarrhalis, Acinetobacter calcoaceticus v. lowfii, Enterobacter agglomerans, Bordetella bronchisepticum, Pleisomonas shigelloides, and Staphylococcus aureus are pathogenic or potentially pathogenic to man. Vibrio parahaemolyticus and Pleisomonas shigelloides have also been associated with shell fish food poisoning, causing diarrhea in man and Vibrio parahaemolyticus does survive well in the marine environment. All of the above mentioned bacteria can cause both upper and lower respiratory tract infections as well as being normal flora to the upper respiratory tract.

Several bacteria have not yet been identified and a few may represent new species. Work will continue on the identification of these bacteria.

Bacteria isolated in 1968 from arctic porpoises (Johnston and Fung 1971) are compared to isolates from bowhead whales in this study (Table 11-6).

There are common bacteria isolated from both the arctic porpoises and the bowhead whales. There is a striking similarity in the E. coli, though a normal

part of the flora in most warm blooded animals, has not been isolated from arctic porpoises and only isolated once from the bowhead whale. This single isolate of E. coli was from a stranded bowhead whale (79B4) in which the sample was taken from deep within decomposing blubber.

We cannot be certain as to the exact origin of the bacteria isolated during these two years of observation. They may be indigenous within the whale population or they may be some representatives of sea environment and some may represent origin from sites of land and water pollution along the inhabited coastal regions. The answer to this could be obtained by studies of environmental samples from these areas.

## SUMMARY

Twenty two specimens from nine bowhead whales were received for microbiological studies during the fall of 1979 and the spring of 1980. Bacteria were isolated from eighteen specimens. Four specimens contained no organisms. There were sixteen different bacterial species isolated from the 1979 whales and ten different bacterial species isolated from the 1980 whales. Most of the isolates were aerobic or facultative gram negative bacilli including: Acinetobacter calcoaceticus v. lowfii, Alcaligenes species, Bordetella bronchisepticum, Citrobacter species, Enterobacter agglomerans, Escherichia coli, Pleisomonas shigelloides, Pseudomonas fluorescens, Pseudomonas species, Vibrio parahaemolyticus, and a yet to be identified aerobic non-fermentative bacillus. Other aerobic or facultative bacteria are: alpha-hemolytic streptococcus, beta-hemolytic streptococcus, Branhamella catarrhalis, Micrococcus species, Staphylococcus aureus, Staphylococcus epidermidis, aerobic gram positive diplococcus, aerobic gram negative diplococcus and pleomorphic aerobic gram positive bacillus. Light and electron microscopic studies were done on some of the unidentified bacterial isolates.

## ACKNOWLEDGEMENTS

It is a pleasure to acknowledge the assistance provided by Harlan Schwartz for the electron microscopy preparation of bacterial isolates and Sharon Heck, for assistance in preparation of this report.

## REFERENCES

- Finegold, S. M., W. J. Martin, and E. G. Scott. 1978. Bailey and Scott's Diagnostic Microbiology. The C. V. Mosby Co., Saint Louis Missouri.
- Holdeman, L. V., E. P. Cato, and W. E. C. Moore. 1977. Anaerobe Laboratory Manual. 4th ed. Anaerobe Laboratory, Virginia Polytechnic Institute and State University, Blacksburg, Virginia 24061.
- Johnston, D. G., and J. Fung. 1971. Bacteria of Marine Mammals, marine environment and man. In: Colloque International Sur l'Exploration des Oceans. Bordeaux, France, March 9-12.
- Lennette, E. H., E. H. Spaulding, and J. P. Truant. 1974. Manual of Clinical Microbiology, 2nd ed. American Society for Microbiology. Washington, D. C.
- MacFaddin, J. F. 1976. Biochemical Tests for Identification of Medical Bacteria. The Williams and Wilkins Co., Baltimore, Maryland.
- Washington, J. A., II. 1974. Laboratory Procedures in Clinical Microbiology. Little, Brown and Co., Boston, Mass.

## RESEARCH UNIT 1280

### PARASITOLOGICAL STUDY OF THE BOWHEAD WHALE, BALAENA MYSTICETUS

RICHARD A. HECKMANN, Ph.D.  
Department of Zoology  
Brigham Young University  
Provo, Utah 84602

#### INTRODUCTION

Cetaceans throughout the world are known to be infested and infected with parasites (Dailey and Brownell, 1972). This does not necessarily mean that the hosts are seriously affected or damaged. But if stress and/or nutritional imbalances occur in addition to the parasite load then the animal may become weak and possibly die. Recent publications (Stroud and Roffe, 1979; Dailey and Walker, 1978; Marten et al., 1970; Ridgway and Dailey, 1972) indicated that helminths were a possible factor in cetacean strandings.

Activities associated with offshore oil and gas development may increase the stress to bowhead whales and thereby allow for an increase in parasite burden. It therefore seems reasonable to attempt to determine the types of parasites harbored by bowhead whales.

The primary goal of this study is to examine bowhead whale tissue and organ systems for parasites.

#### OBJECTIVES

1. To examine cetacean tissue and organ systems supplied by RU 180 for the presence of parasites.
2. To correlate the results of the above examination (1) with published data on other whale species relative to parasite life cycles.
3. Establish a list of parasites which may be specific for bowhead whales in the Arctic Ocean.
4. To determine, to the extent possible from supplied material, the parasite burden of sampled whales.

#### METHODS

Samples of harvested bowhead whale tissues and colon contents were collected by RU 180, fixed in 10% formalin and shipped to the parasitology

laboratory at Brigham Young University. Smears of blood from whales were air dried and sent with the above samples. The samples were processed as indicated below.

Intestine, Liver, Diaphragm. After recording the code for the sample each specimen was weighed, measured and finally dissected to examine for parasites. Intestinal segments were cut lengthwise and the lumen was examined for macroscopic parasites. Samples of lumen contents were placed on glass slides and examined with a light microscope. Slides of lumen contents from the intestine were also fixed and stained with iron haematoxylin, trichrome or Giemsa-Wrights stains. After staining each slide was examined for parasites. Sections of liver and diaphragm were placed in separate jars containing a standard digestive enzyme solution (pepsin and hydrochloric acid in water) for 24 to 48 hours at 37°C. This procedure digests host tissue but not nematode larvae or adults. The material was then centrifuged and examined by light microscopy.

Colon Contents. Formalin fixed colon contents were examined by the same procedure as outlined for lumen contents from the intestine. The same stains were used for preparation of permanent slides.

Blood Smears. Standard methods were followed in the examination of blood smears for parasites. A combination Giemsa-Wrights stain was used for maximum staining of any intracellular or extracellular parasites present. Each stained slide was examined for at least 10 minutes at 400X and 1000X magnification.

Trematodes were processed by two methods. Specimens were fixed in both an alcohol-formalin-acetic acid solution (AFA) and gluteraldehyde. Those fixed in AFA were stained with semichons carmine and mounted on glass slides. Gluteraldehyde fixative in an acrolein buffer was used for those specimens to be examined by scanning electron microscopy (SEM). For SEM each fluke was critically point dried, mounted on a specimen holder, coated with gold for three minutes with a CS mini coater sputter and then viewed with an AMRAY 1000A scanning electron microscope operating at 20 Kv. The whale louse, Cyamus ceti, was also examined with SEM.

A paraffin-embedded block of tissue containing a larval nematode was provided by another RU. This block was processed for histology and sections were

stained with haemotoxylin and eosin, trichrome and periodic acid-Schiff. One other nematode found free in the stomach of a bowhead was provided by RU 1480.

Skin samples representing normal and eroded areas were provided by RU 780, RU 1080 and RU 1380 for parasite examination. These samples were prepared for SEM and light microscopy as explained above for flukes and nematodes.

Results of the parasite examination were summarized and compared with the existing list for the bowhead whale, gray whale and blue whale.

## RESULTS

Table 12-1 lists the specimens obtained with data on whale number, type and amount of tissue. Parasites found in the respective tissues are listed in Table 12-2.

In addition to the specimens listed in the tables, samples of skin (diatom infested) from RUs 780, 1080 and 1380, a sample of forestomach from RU 780 embedded in a paraffin block for sectioning (larval nematode) and one nematode from RU 1480 were received.

Protozoa. Two species of protozoa (one amoeboid and one flagellated) were found in the formalin fixed colon contents of 80B7. The amoeboid form appears to be a new species while the flagellated form does not. Both represent the first known protozoa described from the bowhead whale.

A. Amoeboid protozoan. An amoeba (Figs 12-1, 12-2) from the colon contents of 80B7 had the following characteristics based on examination of 100 protozoa in stained preparations: trophozoite and cyst stages, cysts containing one to four nuclei, cysts oval in shape ranging from 15-18  $\mu$ m in diameter, nuclei spheroidal to ovoidal, nuclei randomly distributed for multinucleate forms and centrally located in uninucleate forms, nuclei which occupy approximately 10% of the cell volume, pseudopodia vacuoles varying in number, both food and water vacuoles present, chromatoid-like bodies in cytoplasm and peripheral nonchromatic granules common in the intestinal contents of 80B7. Based on these observations the author considers this amoeba to be a species of Entamoeba Casagrandi and Barbagallo, 1895 due to similar characteristics (Kudo 1966). Thus, the classification for this amoeba would be:

Phylum: Sarcomastigophora (Levine et al 1980)

Subphylum: Sarcodina

Class: Lobosea

Order: Amoebida

Family: Endamoebidae

Genus: Entamoeba sp.

Further literature search and examinations of the protozoan will hopefully permit a species determination. The genus Entamoeba is common in many vertebrate species (Olsen 1974) and several species are parasitic, damaging the intestinal lining (Faust 1975).

B. Flagellated protozoan. From the same formalin fixed colon contents (80B7) containing an amoeboid protozoan a total of three flagellates were observed in the material examined. Insufficient specimens were available for species determination. The single celled organism (Fig 12-3) appeared to be much like a species of Chilomastix (Faust 1975) or the "pear" formed Hexamita (Olsen 1974).

Diatoms. Four genera of diatoms were observed on the skin specimens (Figs 12-4 through 12-8).

Phylum: Chrysophyta (plants)

Genera: Cocconeis sp.

Stauroneis sp.

Navicula sp.

Gomphonema sp.

Diatoms are plants belonging to the phylum Chrysophyta characterized by silicon cell walls (Fuller 1960). They are found in both fresh- and saltwater and are composed of single cells. There are a large number of diatom species. We observed diatoms on the normal skin surface, in erosions of the skin and several layers below the surface of the skin (Figs 12-8 through 12-11). The forms observed on the skin surface could be considered parasitic (Omura 1950, Nemoto 1956, Nemoto et al 1977).

Helminths. Three species were identified. One was a digenetic trematode (fluke) and two were nematodes (roundworms).



## A. Flukes

Phylum: Platyhelminthes

Class: Trematoda (Digenea)

Family: Notocotylidae

Genus, species: Ogmogaster plicatus

Species of the genus Ogmogaster have been reported from both pinnipeds and cetaceans. In the present study twenty-four specimens were collected from intestinal segments of three bowhead whales. Reported in the Antarctic and Northern Pacific Ocean, these flukes apparently cause no damage to the host (Dailey and Brownell 1972). The anatomy of O. plicatus was studied and appears to be similar to the antarctic form (Rausch and Fay 1966). The fluke has been reported recently from the bowhead whale (Shults 1979), and has been compared with O. antarcticus, O. trilineatus and O. pentalineatus (Rausch and Rice 1970). One of the many characteristics for the species of Ogmogaster is the number of parallel, longitudinal ridges on the ventral surface. Ogmogaster plicatus is characterized by 19 to 28 ridges with an average of 23 (Rausch and Fay 1966). Figures 12-12 and 12-13 represent the dorsal and ventral surfaces of O. plicatus collected during this study. The life cycle for this species is unknown.

## B. Anisakid-type larvae

Phylum: Nematoda (the Aschelminthes; Barnes 1980)

Order: Ascaridata

Family: Anisakidae

A block of paraffin-mounted bowhead forestomach was provided for examination by RU 780. It contained larval nematodes which had an anisakid appearance (Schmidt and Roberts 1981) (Fig 12-14). No adult stages of this roundworm were found in the samples received. A description of the life cycle of Anisakis is found in parasitology texts (Faust, 1975; Schmidt, 1977) and in recent publications (Smith 1971, Wootten and Waddell 1977, Smith and Wootten 1978, Wootten 1978). Adult stages of this nematode are characteristically found in marine mammal stomachs. The worm examined in this instance was found in the submucosa of the forestomach and was in the migratory larval phase of its life cycle. Larval characteristics for species of Anisakis include: esophagus has a ventriculus that ends obliquely at its junction with the intestine (Hadidjaja et al 1978), no ventricular appendage nor intestinal caecum, tail is blunt and terminates in a distinct mucron (Oshima 1972, Shiraki 1974, Smith and

Wootten 1978), prominent boring tooth (mucron) present (Smith and Wootten 1978). For the life cycle of Anisakis sp., euphausiids (crustaceans) are probably the most important intermediate host (Smith 1971, Smith and Wootten 1978). Euphausiids are a source of food for the bowhead whale (Lowry and Burns 1979). After examination of serial sections of the larval nematode, the following characteristics were noted; no bursa or prominent teeth, blunt tail with mucron remains present, trilobed lips, dentigerous ridge anterior end, no terminal enlargement for the esophagus, no alae, and overlapping annulations on the surface. The nematode is apparently a species of Anisakis. Due to the lack of adult worms which are required for a definitive taxonomic assignment (Smith and Wootten 1978) and the taxonomic confusion of the Family Anisakidae, the larval nematode will be referred to as "anisakid type" (Schmidt and Roberts 1981) as preferred by most parasitologists. Yokogawa and Yoshimura (1967) reported larval anisakiasis in the gastrointestinal tract of Japanese people. Recently cases of anisakiasis have been reported in the United States and last year larval stages of this roundworm obtained from salmon harvested at Barrow, Alaska were sent to this laboratory.

C. Anisakid roundworm (one specimen)

Phylum: Nematoda

Order: Ascaridata

One worm which was found free in the stomach was sent to this laboratory from RU 1480. This roundworm is probably Anisakis or Contracaecum. The condition of the preserved nematode was not adequate for study, preventing assignment of a definitive name. Members of the genera Contracaecum and Anisakis are considered among the most common parasites in the stomachs of pinnipeds (Dailey and Brownell 1972).

Whale Lice. One species of "louse", a modified amphipod, was observed (Fig 12-15).

Phylum: Arthropoda

Class: Crustacea

Order: Amphipoda

Genus, species: Cyamus ceti

The cyamids have a vestigial abdomen with large legs but, unlike most amphipods, the body is broad and depressed. The cyamids of whales have a high

degree of host specificity; however, the same species that occurs on the bowhead whale is found on gray whales. The species Cyamus ceti was one of the most common parasites observed during this and a previous study. Possible damage to the host integument where the parasite attaches has been described (Heckmann 1979).

Figure 12-15 illustrates the ventral surface of a whale louse. Note the enlarged appendages with numerous hooks. The mouthparts and appendages are highly modified for the ectoparasitic mode of life. The cyamids have a direct life history with the young being released from the brood-pouch of the female. Amphipods have no free-swimming stage. Subsequent moultings produce sexually mature adults. Cyamids can be one host parasites.

#### Comments on Other Parasites Reported for the Bowhead Whale.

NEMATODE. Crassicauda crassicauda is a nematode parasitizing the urogenital system and sometimes other parts of the body. Although the life cycle of C. crassicauda has not been determined, members of the order to which this genus belongs parasitize the body cavity, blood sinuses, air bladder or tissues of aquatic vertebrates. Copepods are considered to be intermediate hosts. For cetaceans the nematode Crassicauda crassicauda has been reported from Tursiops truncatus (bottlenosed dolphin), Balaenoptera musculus (blue whale), Megaptera novaeangliae (humpback whale), Balaena mysticetus (bowhead whale), Ziphius cavirostris (Cuvier's beaked whale), Balaenoptera acutorostrata (minke whale), Balaenoptera borealis (sei whale), and Balaenoptera physalus (fin whale) (Dailey and Brownell 1972).

TREMATODE. Lecithodesmus goliath is a trematode parasitizing the bile ducts of Cetacea. The eggs of this fluke are large and triangular in cross-section. Molluscs are intermediate hosts. Metacercariae could be ingested with the molluscan intermediate host (Dailey and Brownell 1972). Small clams (bivalves) have been reported from the colon of a bowhead whale (Lowry and Burns 1979).

ACANTHOCEPHALA. Bolbosoma balaenae is an acanthocephalan that is found in the intestine of marine mammals (Dailey and Brownell 1972).

The parasites observed during this study and all those reported for the bowhead whale are listed in Table 12-3. The parasites reported for the bowhead whale as well as those reported for the gray whale and blue whale are listed in Table 12-4.

TABLE 12-1. BOWHEAD WHALE SPECIMENS EXAMINED FOR PARASITES

Whale Number	Type of Specimen	Specimen Length (cm)	Specimen Weight (Kg)
80B1	Blood smears (4 slides)	-	-
	Intestine segments		
	A	83	7.3
	B	107	8.6
	C	99	3.15
80B2	D	134	2.25
	Blood smears (2 slides)	-	-
	Intestine segments		
	A	87	6.75
	B	59	3.15
80B7	Liver sample	-	2.7
	Blood smears (2 slides)	-	-
	Intestine segments		
	A	78	1.21
	B	75	2.41
	C	44.5	4.70
	Liver sample	-	2.3
80B8	Diaphragm sample	-	0.7
	Blood smears (2 slides)	-	-
	Intestine segment	96	4.5
	Diaphragm sample	-	0.6
	80B9	Louse on baleen	-
Liver sample		-	1.35
Colon segment		95	9.9

TABLE 12-2. BOWHEAD WHALE TISSUES EXAMINED AND PARASITES OBSERVED

Whale Number	Tissue Examined	Special Procedures	Parasites Observed
80B1	Blood smears	Giemsa-Wright stain	None
	Intestine segments		
	A		None
	B		None
	C		None
80B2	Blood smears	Giemsa-Wright stain	None
	Intestine segments		
	A		4 trematodes
	B		2 trematodes
	Liver sample		None
*Liver sample	**Digestive fluid	None	
80B7	Blood smears	Giemsa-Wright stain	None
	Intestine segments		
	A		None
	B		None
	C		8 trematodes
	Liver sample		None
	*Liver sample	**Digestive fluid	None
Diaphragm sample		None	
*Diaphragm sample	**Digestive fluid	None	
Colon contents	Fixed in formalin stained with three stains	2 protozoan species Amoeboid form Flagellate form	
80B8	Blood smears	Giemsa-Wright stain	None
	Intestine segment		10 trematodes
	Diaphragm sample		None
	*Diaphragm sample	**Digestive fluid	None

TABLE 12-2. CONTINUED

Whale Number	Tissue Examined	Special Procedures	Parasites Observed
80B9	Baleen piece		"Louse" attached ( <u>Cyamus</u> sp.)
	Liver sample		None
	*Liver sample	**Digestive fluid	None
	Colon		None

\* Small pieces were removed from the samples of liver and diaphragm and placed into beakers containing digestive fluid.

\*\*Digestive fluid: An aqueous solution of pepsin and hydrochloric acid used to digest host tissue and leave nematodes intact.

TABLE 12-3. CONSOLIDATED LISTING OF PARASITES FOR THE BOWHEAD WHALE

Parasite	Location in Host
Protozoa	
*Amoeba form	Colon, small intestine
*Flagellate form	Colon, small intestine
Diatoms (Plant)	
* <u>Cocconeis</u>	Skin, normal and eroded areas
* <u>Stauroneis</u>	Skin, normal and eroded areas
* <u>Navicula</u>	Skin, normal and eroded areas
* <u>Gomphonema</u>	Skin, normal and eroded areas
Acanthocephala	
* <u>Boalbosoma balaenae</u>	Intestine
Cestoda	
** <u>Phyllobothrium delphini</u>	Tissue (blubber)
Trematoda	
* <u>Ogmogaster plicatus</u>	Intestine
** <u>Lecithodesmus goliath</u>	Bile ducts
Nematodes	
*Anisakis type larvae	Forestomach submucosa, encysted
*Anisakid: <u>Contracaecum</u> or <u>Anisakis</u>	Stomach
** <u>Crassicauda crassicauda</u>	Intestine
Amphipoda (Whale Lice)	
* <u>Cyamus ceti</u>	Attached to baleen

\* Parasites observed during this study.

\*\*Parasites not observed during this study, but reported for the bowhead whale (Dailey and Brownell 1972).

TABLE 12-4. COMPARISON OF PARASITES OBSERVED IN THREE SPECIES OF BALEEN WHALES

Host	Protozoa			Acanthocephala					Cestoda				Trematoda				Nematoda					Amphipoda	
	E	F	D	B <sub>1</sub>	B <sub>2</sub>	B <sub>3</sub>	B <sub>4</sub>	C	P <sub>1</sub>	P <sub>2</sub>	P <sub>3</sub>	T	O <sub>1</sub>	O <sub>2</sub>	O <sub>3</sub>	L	A	A <sub>1</sub>	C <sub>1</sub>	C <sub>2</sub>	P	C	
Gray Whale*	0	0	0	0	0	0	0	X	0	X	X	0	0	X	X	0	0	0	0	0	0	0	0
Blue Whale*	0	0	0	X	X	X	X	0	0	X	0	X	X	X	0	0	X	0	X	0	X	X	X
Bowhead Whale**	X	X	X	X	0	0	0	0	X	0	0	0	X	X	0	X	0	X	X	X	0	0	X

0 = Not observed; X = Observed in host

Codes for Parasites

Protozoa

- E = Amoeboid form
- F = Flagellate
- D = Diatoms: 4 species

Acanthocephala

- B<sub>1</sub> = Bolbosoma balaenae
- B<sub>2</sub> = Bolbosoma brevicolle
- B<sub>3</sub> = Bolbosoma hamiltoni
- B<sub>4</sub> = Bolbosoma turbinella
- C = Corynosoma sp.

Cestoda

- P<sub>1</sub> = Phyllobothrium delphini
- P<sub>2</sub> = Priapocephalus sp.
- P<sub>3</sub> = Pseudophyllidae sp.
- T = Tetrabothis affinis

Trematoda

- O<sub>1</sub> = Ogmogaster plicatus
- O<sub>2</sub> = Ogmogaster antarcticus
- O<sub>3</sub> = Ogmogaster pentalineatus
- L = Lecithodesmus goliath

Nematoda

- A = Anisakis
- A<sub>1</sub> = Anisakis type larvae
- C<sub>1</sub> = Crassicauda crassicauda
- C<sub>2</sub> = Contracaecum sp.
- P = Porrocaecum decipiens

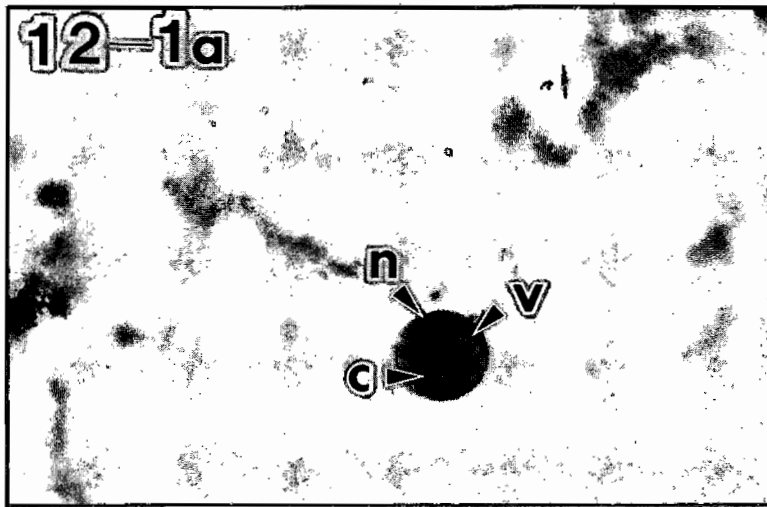
Amphipoda

- C = Cyamus ceti

\* Dailey and Brownell 1972

\*\*This study and Dailey and Brownell 1972





12-1b

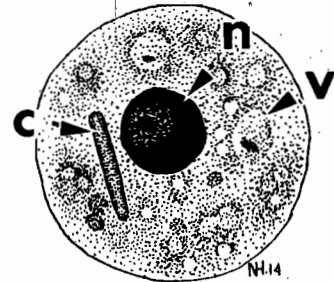
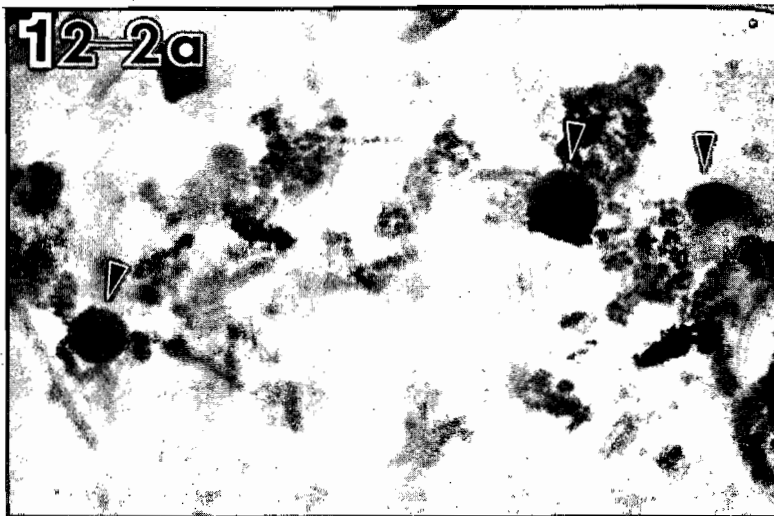


Figure 12-1. An amoeboid parasite (*Entamoeba* sp.) from the colon contents of a bowhead whale (80B7). There is a single endosome within the nucleus. A single nucleated (n) form with vacuoles (v) and chromatoid body (c). 1000X (12-1a). A line drawing (12-1b) represents key characteristics of the protozoan.



12-2b

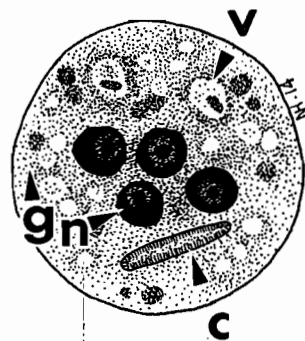


Figure 12-2. Three protozoa (12-2a) representing the many seen in the colon contents of bowhead whale 80B7. 1000X. A line drawing (12-2b) representing the 4 nucleated (n) phase of the *Entamoeba* sp. cyst with vacuoles (v), chromatoid body (c) and granules (g).

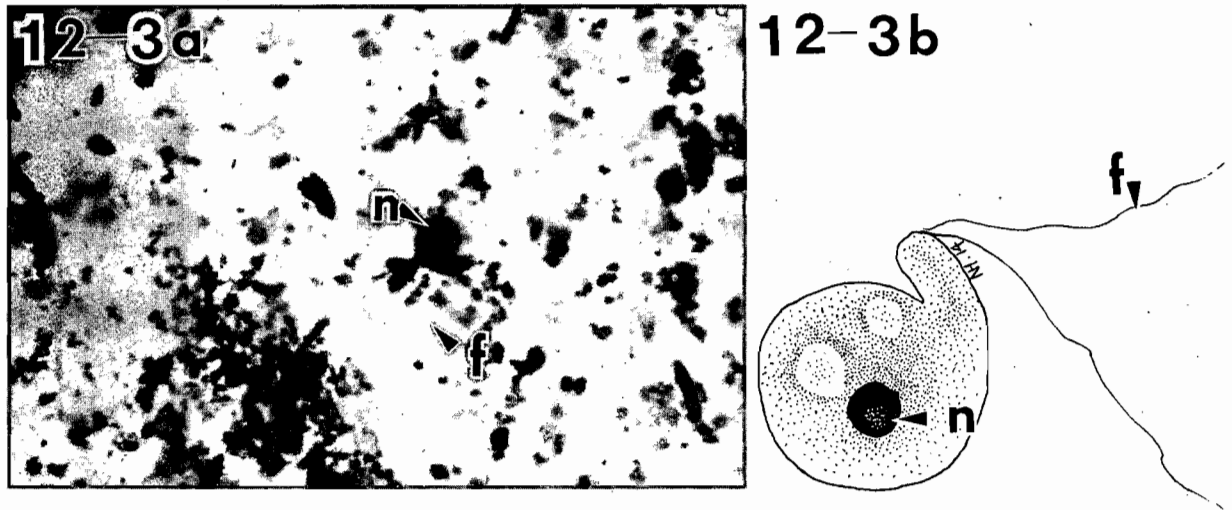


Figure 12-3. A flagellated protozoan (12-3a) with locomotor organelle (f) extending out. Characterized by a single nucleus (n) and a shape similar to *Chilomastix* sp. 1000 X. A line drawing (12-3b) better represents the detail.

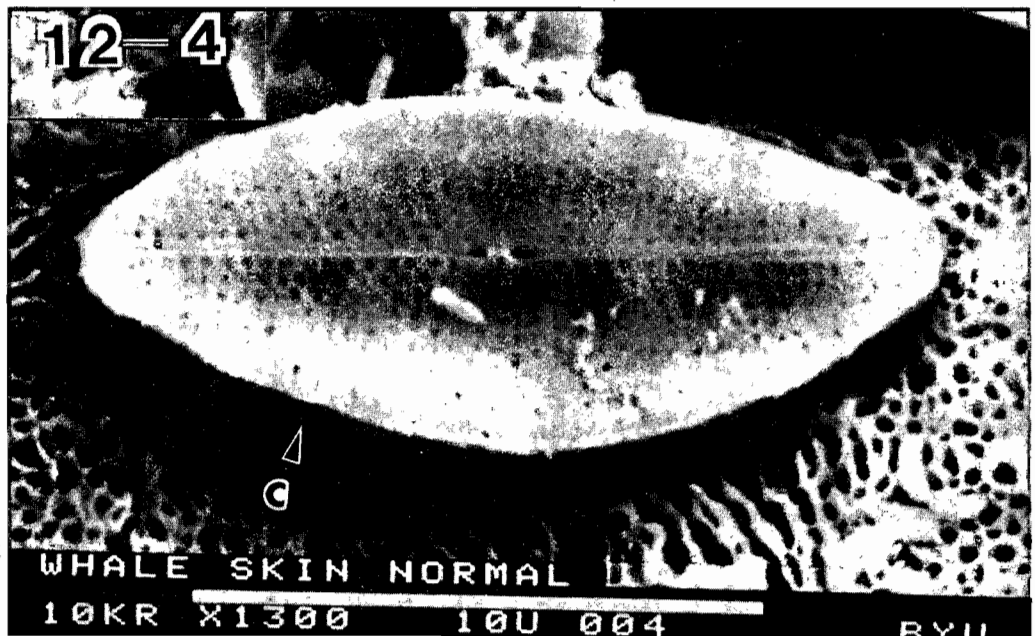


Figure 12-4. A SEM (scanning electron microscopy) photomicrograph of a diatom (c) *Cocconeis* sp. on the surface of bowhead whale skin. Note the captions at the bottom of the figure: Source of specimen (whale skin normal), high voltage used (10 KR), magnification (X1300), micron bar 10U, number of photograph (004) and location of laboratory (BYU). These captions will appear on all SEM photomicrographs.



Figure 12-5. An SEM photomicrograph of a diatom (n) *Navicula* sp. X1300.

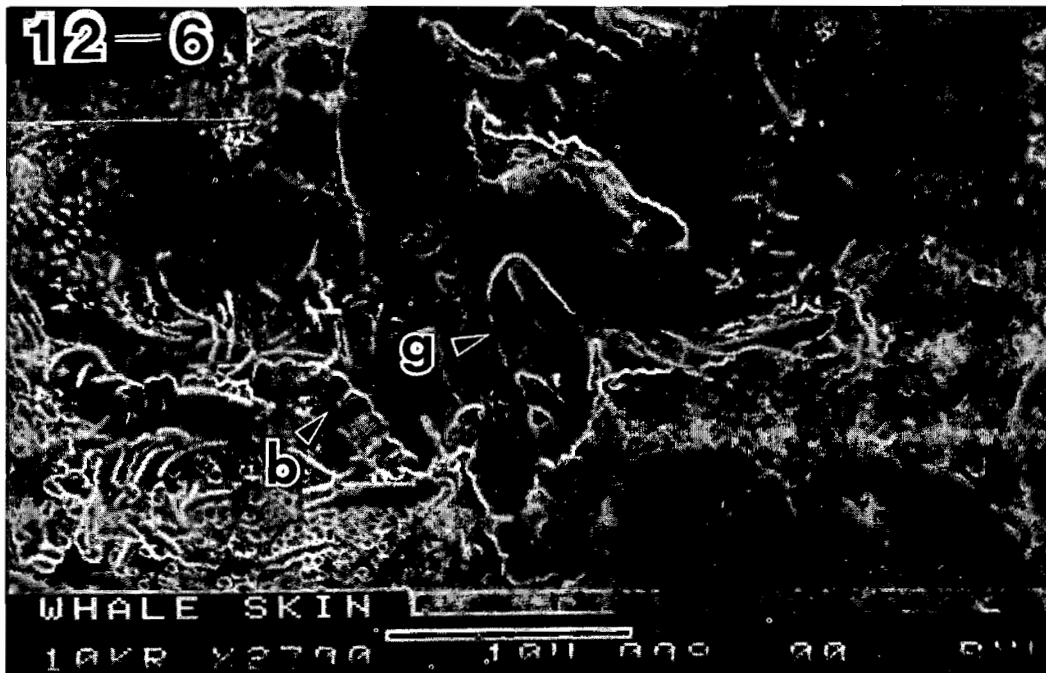


Figure 12-6. An SEM photomicrograph of a diatom (g) *Gomphonema* sp. X2300, in an eroded area of whale skin. Note the chains of bacteria (b) in the same area.

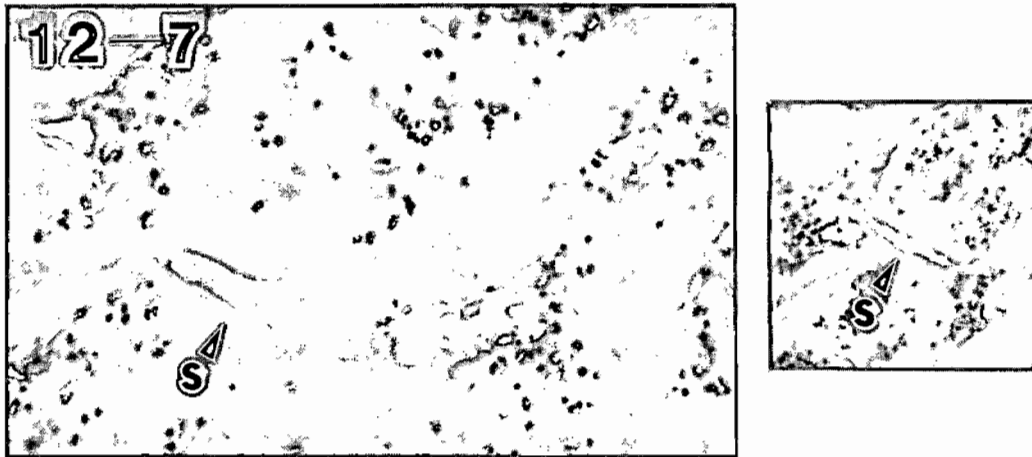


Figure 12-7. A diatom (s) *Stauroneis* sp. at two magnifications (1000X and 400X), in a section of bowhead whale skin.

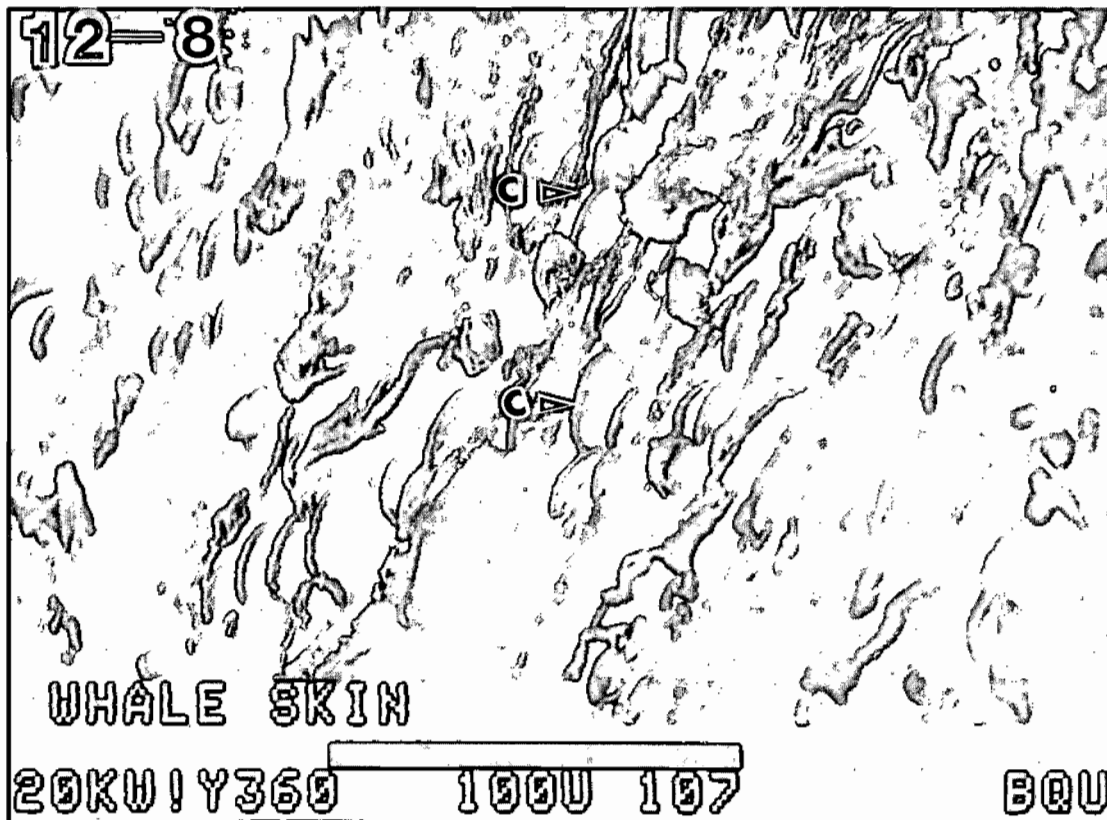


Figure 12-8. An SEM photomicrograph of pockets of diatoms (C = *Cocconeis* sp., arrowheads) found 0.5 to 1.5 cm below the surface of whale skin. This is a sectioned piece of skin that has been prepared for SEM. 360X.

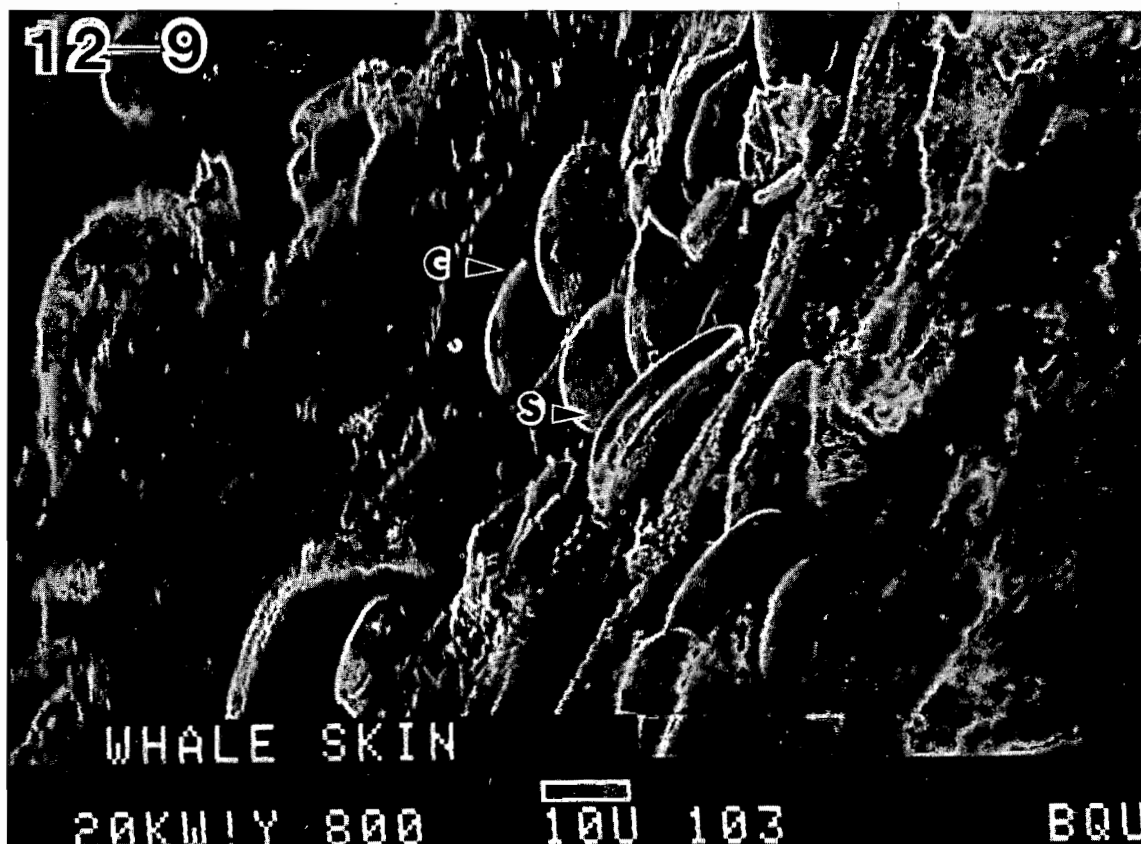


Figure 12-9. A higher magnification of Figure 12-8 showing diatoms (c) Cocconeis sp. in whale skin with silicious walls (s) visible. 800X.

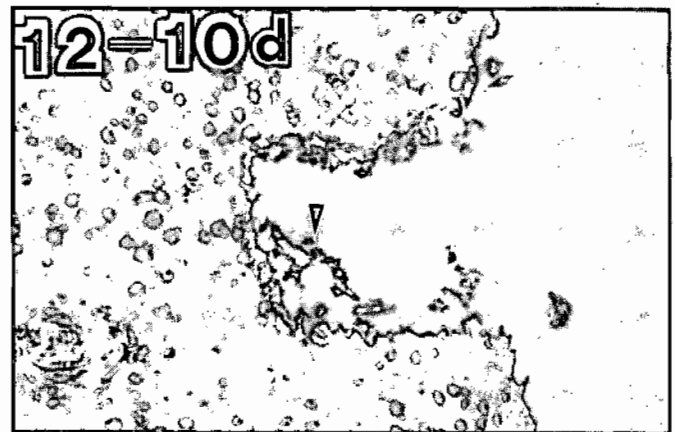
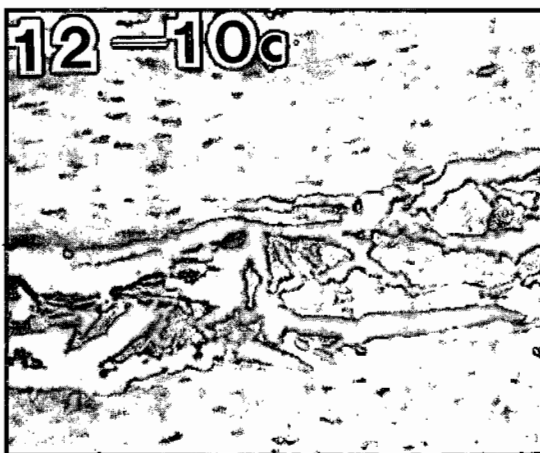
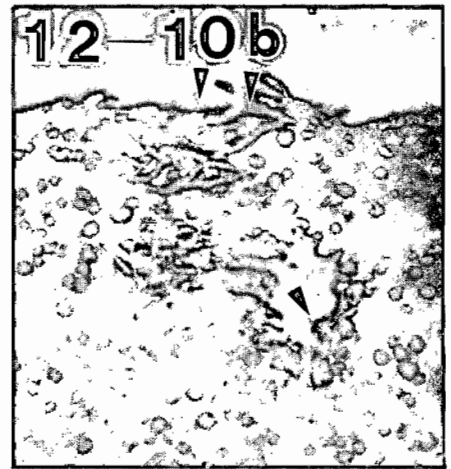
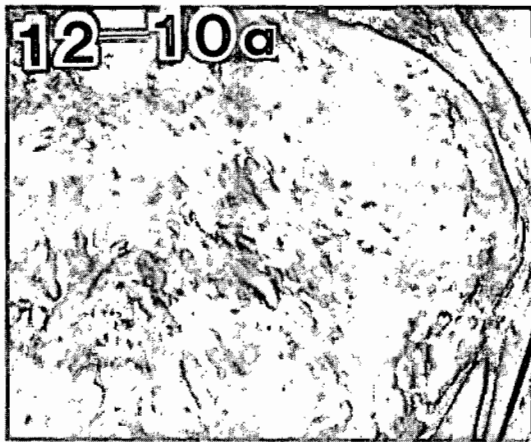


Figure 12-10. A series of four photomicrographs of sectioned skin showing areas where no diatoms were found (a) (400X), small breaks (b) in the epidermis (400X) showing diatoms (arrowheads), wider breaks (c) (400X) and open eroded areas (400X) with diatoms (d).

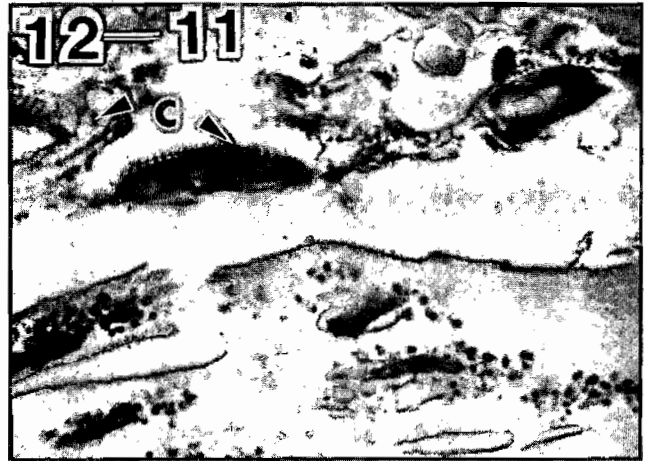
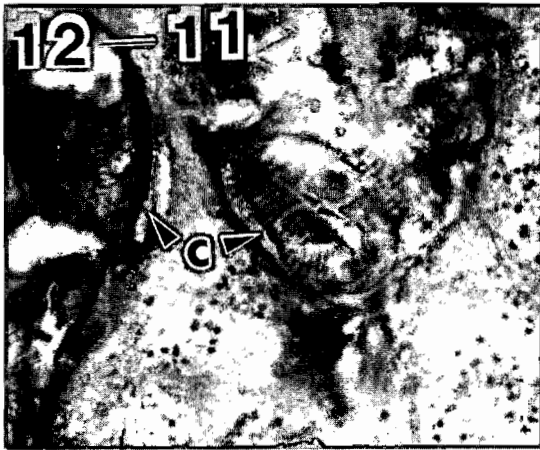


Figure 12-11. Two figures at 1000X showing a diatom (c) Cocconeis sp. in sections of bowhead whale skin. These represent higher magnifications of Figures 12-10b and 12-10d.



Figure 12-12. An SEM photomicrograph of the dorsal surface of Ogmogaster plicatus, 180X. Note folds (f) in the surface of the fluke. At higher magnifications, 1200X, pits were visible which are for sensory functions.

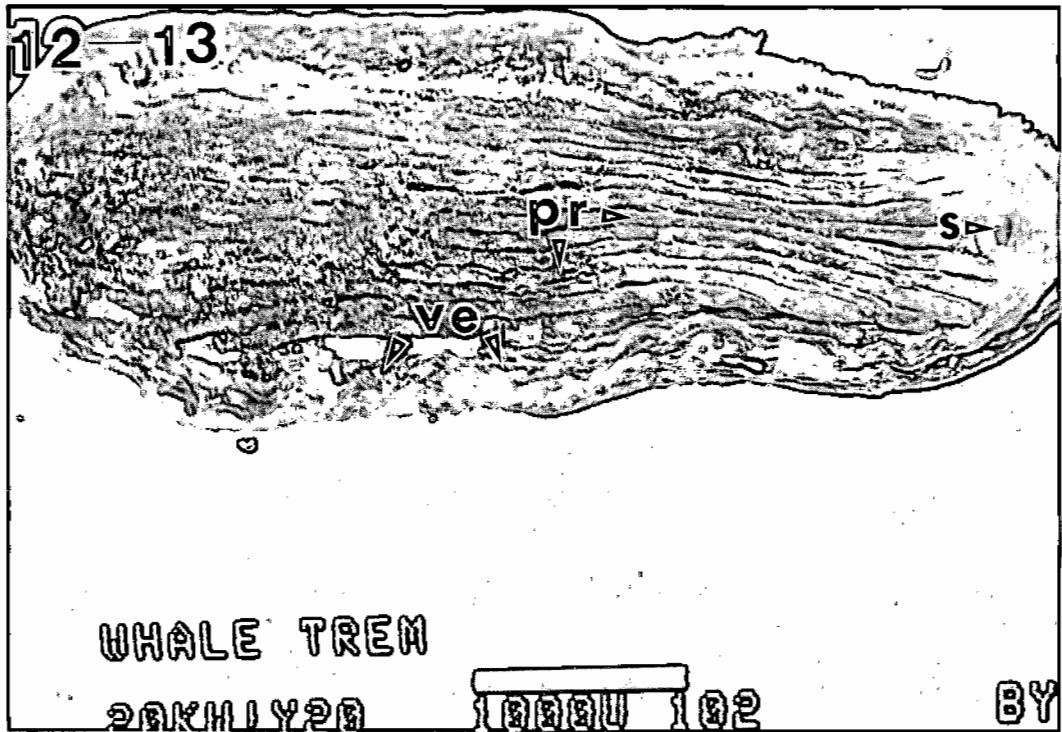


Figure 12-13. An SEM photomicrograph of *Ogmogaster plicatus*, ventral surface 20X. Note the sucker (s) and variegated edge (ve) of the fluke. The variegated edge and parallel, longitudinal ridges (pr) which range from 19 to 28 in number for *O. plicatus* are key characteristics for this species.



Figure 12-14. The larval anisakid type roundworm found encysted (c) in the submucosa (sm) of the bowhead whale forestomach. Note the inflammatory (i) response around the worm. 100X.



12-15

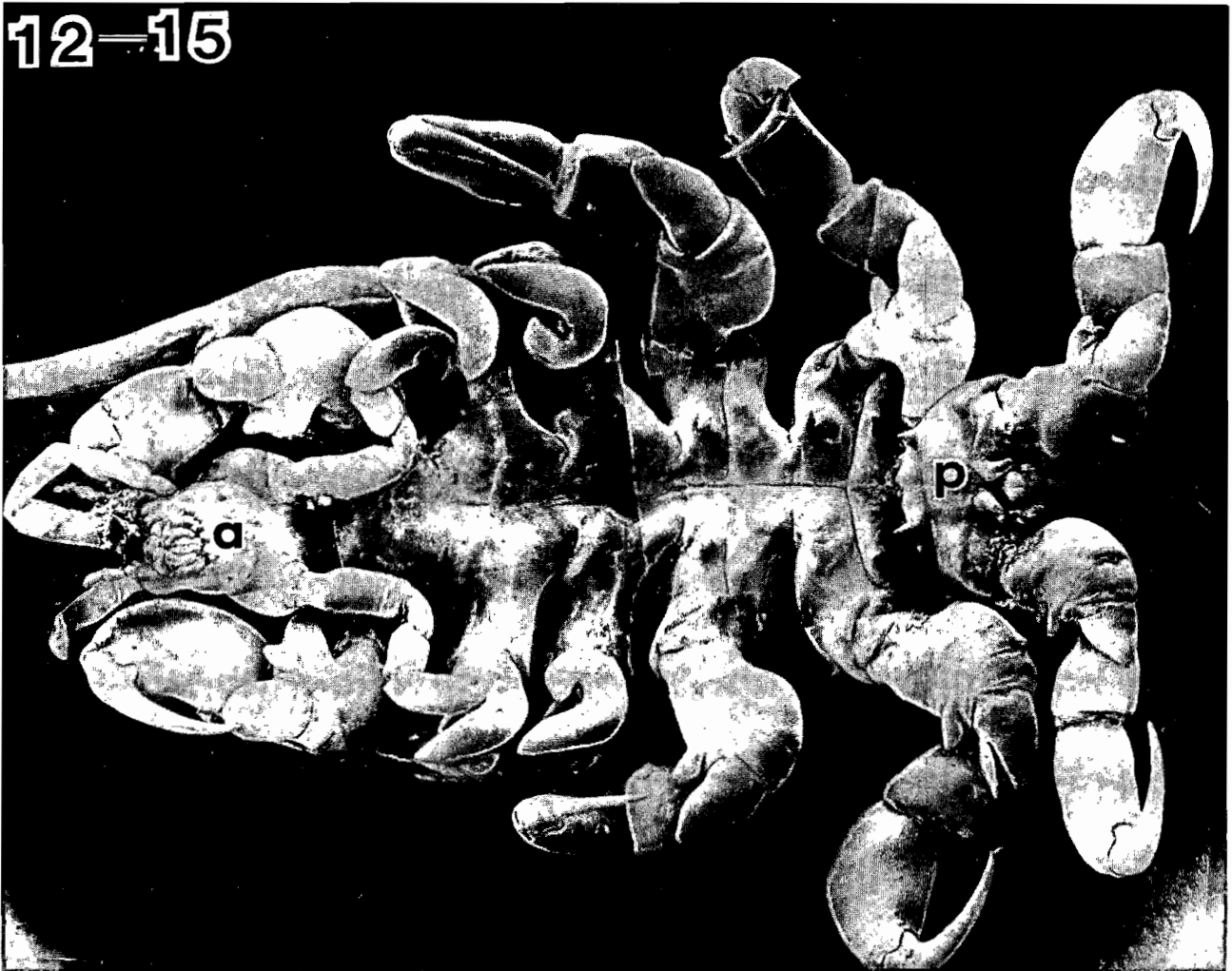


Figure 12-15. An SEM photomicrograph of the ventral surface of the male whale louse, *Cyamus ceti*, showing the highly modified nature of amphipod for parasitism. The anterior (a) and posterior (p) ends are labeled. Approximately 8X.

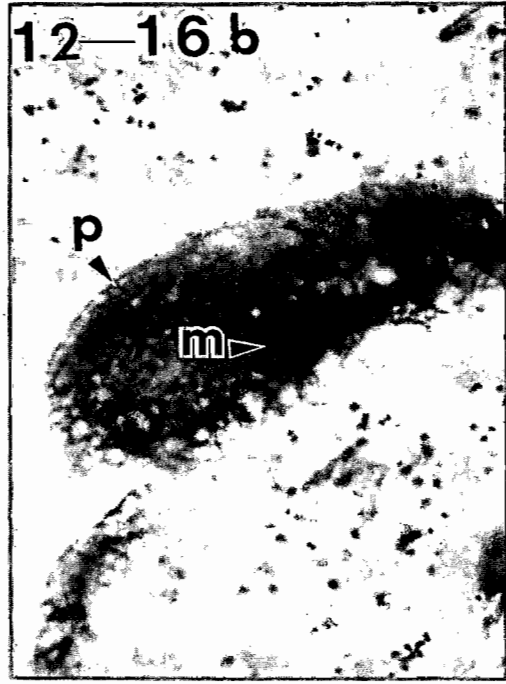


Figure 12-16. Protozoa (p) are also attached along the exposed surface of the skin erosions and breaks (e). These protozoa are probably ciliates due to size and a large macronucleus (m). 400X and 1000X.



Figure 12-17. Bacteria (b) are also present in the eroded areas of bowhead whale skin. The filamentous bacterium is common in these areas which also contain diatoms (d) and protozoa 400X and 1000X.

## DISCUSSION

During the past 2 1/2 years samples of bowhead whale tissue have been examined for parasites. From a limited number of bowhead whales two protozoans, four genera of diatoms and a nematode have been added to the existing list of parasites (Table 12-3). With additional samples the list would most likely be expanded, especially the protozoan forms. Data from this study confirmed the presence of both Cyamus ceti (whale louse) and Ogmogaster as previously described for the bowhead (Shults 1979). The samples of blood from four whales were negative for parasites.

In accordance with currently known dietary habits, the bowhead whale is not subject to many of the internal parasites found in marine mammals that feed on fish, large crustaceans and molluscs. Fish, large crustaceans and molluscs are common intermediate hosts for helminths of marine mammals.

The basis for placing one of the protozoans (found in the colon contents of 80B7) in the family Endamoebidae is their small size and location, and the presence of one to four nuclei per cyst and numerous food vacuoles in the cytoplasm. Members of the Endamoebidae are typically parasites or commensals of the digestive systems of arthropods and vertebrates (Schmidt and Roberts 1981). Species of Entamoeba are common endocommensals and parasites of the digestive system of vertebrate and invertebrate hosts. Examination of additional material from the bowhead colon will allow a more definite classification of the flagellated protozoan to be made. Only three examples of the flagellate were observed after screening the material during 1980. The present study is the first record of a protozoan parasite for the bowhead whale.

Diatoms are common organisms attached to the skin of whales (Nemoto 1956). Diatoms were found on the skin of bowhead whales harvested in 1979 and 1980. Diatoms, common inhabitants of both freshwater and ocean water, are single-celled plants with silicon walls. Four genera were identified in the present study and a series of slides were prepared to show the depth to which the diatoms penetrate into the host skin. Diatoms were more numerous (5 to 10 times) in the eroded areas of the host's skin. Bacteria and protozoa were also found in these erosions. Japanese workers consider diatoms to be parasitic on whale skin (Omura 1950, Nemoto et al 1977). Once an opening is established in the outer surface of the skin, diatoms, bacteria and protozoa (Figs 12-16 and 12-17) may opportunistically invade this niche. Excessive numbers of such opportunists may

further damage the skin. The cyamid found on bowhead skin, Cyamus ceti, could create a lesion sufficient to allow entry of diatoms.

The nematode Anisakis is common in marine mammals (Dailey and Brownell 1972). Larval anisakids have been reported in the digestive tract of humans (anisakiasis), and in Europe and Japan there are records incriminating this helminth as a possible cause of host death (Faust 1975, Schmidt and Roberts 1977). A limited number of cases of anisakiasis have been reported in North America (Myers 1979).

No adult tapeworms have been reported for the bowhead whale. However, a cestode larva, Phyllobothrium delphini (plerocercoid), has been found in the blubber of cetaceans, including that of bowhead (Daily and Brownell 1972). This plerocercoid was not found in the bowhead samples examined in this study.

With the results of the present study, the current list of parasites for the bowhead whale includes two protozoa, four diatoms, two trematodes, one cestode, one acanthocephalan, two nematodes and one amphipod (louse).

Two problems exist in completing the objectives of the study. First, material sent from harvested whales was limited due to difficult field conditions and Eskimo use of harvested products. Second, no brain tissue or middle and inner ears (otic vesicles) were available for study. The ideal situation for examining tissue for parasites is to be "on site" when an animal is butchered. The importance of tissue from the brain and ear relates to the implication of two helminths in whale strandings (Ridgway and Dailey 1972, Stroud and Dailey 1978). The brains of stranded animals have frequently revealed lesions induced by trematode (Nasitrema) eggs, and a species of Stenurus, a nematode, has been found in the ears of cetaceans which have stranded.

#### SUMMARY

Blood, tissue and colon content samples from five bowhead whales were examined for ecto- and endoparasites. Two protozoans, four genera of diatoms, one species of fluke, two species of roundworms and one species of "louse" were found in samples. There were no blood parasites. The diatoms and whale "lice" (Cyamus), with accompanying protozoa and bacteria, can be damaging to the skin of the bowhead whale. A sequence of figures are presented which show possible skin damage due to diatoms. The larval nematode, anisakid type, found in the submucosa of the forestomach of one whale generated a prominent inflammatory host response. Protozoa found in the colon contents include a flagellate and

a sarcodinan. The sarcodinan, which was common in the colon of whale 80B7, belongs to the genus Entamoeba and is probably a new species. Ogmogaster plicatus, a trematode, was confirmed as part of the helminth fauna of the bowhead whale. The data from this study are compared with previous lists of parasites for the bowhead whale and two other species of baleen whales. From the results presented, the previous list of parasites for the bowhead whale has been expanded to include eight additional names.

#### ACKNOWLEDGEMENTS

Dr. Robert Warnock and Dr. Lauritz Jensen were research associates on this project. Dr. Sam Rushforth, Department of Botany, Brigham Young University, confirmed the identification of the diatoms. Mr. James Allen supervised the electron microscope equipment used for this study. Most sincere thanks to my laboratory supervisor, Bruce Coleman, for his help on this project.

## REFERENCES

Included in this list are references cited in the report and others pertinent to the study.

- Arvy, L. 1978. (Fac. Med. CNRS 45 Rue des St. Peres 75006, Paris, France.)  
The skin, the keratinous appendages and their parasites in Cetacea. *Vie Milieu Sec. A. Biol. Mar.* 27(2):137-190.
- Barnes, R. A. 1980. *Invertebrate Zoology*, Saunders College, Philadelphia, pp. 263-312.
- Baylis, H. A. 1932. A list of worms parasitic in Cetacea. *Discovery Rep.*, 6:393-418.
- Beverly-Burton, M. 1978. Helminthes of the alimentary tract from a stranded herd of the Atlantic white-sided dolphin, Lagenorhynchus acutus. *J. Fish. Res. Board Canada* 35:1356-1359.
- Breland, K. and M. Breland. 1968. *Animal Behavior*, Macmillan, New York, p. 82-83.
- Dailey, M. D. and R. L. Brownell. 1972. A Checklist of Marine Mammal Parasites. In: *Mammals of the Sea, Biology and Medicine*. S. Ridgway (ed.), pp. 528-589. Charles C. Thomas Co.
- Dailey, M. D. and W. F. Perrin. 1973. Helminth parasites of porpoises of the genus Stenella in the Eastern Tropical Pacific, with descriptions of two new species: Mastigonema stenellae gen. et sp. n. (Nematoda: Spiruroidea) and Zalophotrema pacificum sp. n. (Trematoda: Digenea). *Fish. Bull.* 71: 455-471.
- Dailey, M. and R. Stroud. 1978. Parasites and associated pathology observed in cetaceans stranded along the Oregon coast. *J. Wildlife Dis.* 14(4):503-512.
- Dailey, M. D. and W. A. Walker. 1978. Parasitism as a factor (?) in single strandings of southern California cetaceans. *J. Parasitol.* 64:593-596.
- Dudok Van Heel, W. H. 1966. Navigation in Cetacea. In: *Whales, Dolphins and Porpoises*. University of California Press, Berkeley, p. 597-606.
- Durham, F. E. 1972. History of Bowhead whaling and Greenland or Bowhead whale. In: *Baleen Whales: In Eastern North Pacific and Arctic Waters*. Alice Seed (ed.). Pacific Search Press.
- Faust, E. C., P. C. Beaver and R. C. Jung. 1975. *Animal Agents and Vectors of Human Disease*. Lea and Febiger.

- Fraker, M. A., D. E. Sergeant and W. Hoek. 1978. Bowhead and White Whales in the Southern Beaufort Sea. Beaufort Sea Project. Dept. of Fisheries and the Environment. Sidney, B.C. Canada.
- Fuller, H. J. and O. Tippe. 1960. College Botany. Holt, Rinehart and Winston, Co.
- Geraci, J. R., M. D. Dailey and D. J. St. Aubin. 1978. Parasite mastitis in the Atlantic white-sided dolphin, Lagenorhynchus acutus, as a possible factor in herd productivity. J. Fish. Res. Bd. Can. 35:1350-1355.
- Hadidjaja, P., D. I. Herry, H. Mahfudin-Burhanuddin and M. Hutomo. 1978. Larvae of anisakidae in marine fish of coastal waters near Jakarta, Indonesia. J. Trop. Med. and Hygiene. 27:51-54.
- Heckmann, R. A., R. Warnock and L. Jensen. 1979. (Parasites) (RU-979) In: Investigation of the Occurrence and Behavior Patterns of Whales in the Vicinity of the Beaufort Sea Lease Area. J. Kelley and G. Laursen (eds.), pp. 517-538. Final Report to the Bureau of Land Management from the Naval Arctic Research Laboratory, Barrow, Alaska.
- Kenyon, A. J. and B. J. Kenyon. 1977. Prevalence of Pharurus pallosii in the beluga whale (Delphinapterus leucas) of Churchill River Basin. Manitoba J. Wildlife Dis. 13(4):388-340.
- Kudo, R. R. 1966. Protozoology. Charles C. Thomas, Springfield, Illinois. pp. 518-564.
- Leung, Y. 1967. An illustrated key to the species of whale-lice (Amphipoda, Cyamidae), ectoparasites of Cetacea, with a guide to the literature. Crustaceana 12:279-291 .
- Levine, N. D., J. O. Corliss, F. E. G. Cox, G. Deroux, J. Grain, B. M. Honingberg, G. F. Leedale, A. R. Loeblich, III, J. Lom, D. Lynn, E. G. Merinfeld, F. C. Page, G. Poljansky, V. Sprague, J. Vavra, and F. G. Wallace. 1980. A newly revised classification of protozoa. J. Protozoology 27:37-58.
- Lowry, L. R. and J. Burns. 1979. (Tissues, Structure and Function) (RU 280g) In: Investigation of the Occurrence and Behavior Patterns of Whales in the Vicinity of the Beaufort Sea Lease Area. J. Kelley and G. Laursen (eds.), pp. 437-447. Final Report to the Bureau of Land Management from the Naval Arctic Research Laboratory, Barrow, Alaska.
- Margolis, L. and M. D. Dailey. 1972. Revised annotated list of parasites from sea mammals caught off the West coast of North America. National Oceanic and Atmospheric Administration Technical Report NMFS SRF-647.

- Margolis, H. S., J. P. Middaugh and R. D. Burgess. 1979. Arctic trichinosis: Two Alaskan outbreaks from walrus meat. *J. Inf. Dis.* 139:102-105.
- Martin, W. E., C. K. Haun, H. S. Barrow, and H. Cravioto. 1970. Nematode damage to brain of striped dolphin, Lagenorhynchus obliquidens. *Trans. Am. Microsc. Soc.* 89:200-205.
- Meyers, B. J. 1979. Anisakine nematodes in fresh commercial fish from waters along the Washington, Oregon and California coasts. *J. Food Protection* 42:380-384.
- Neiland, K. 1962. Alaskan species of acanthocephalan genus Corynosoma Luche, 1904. *J. Parasitol.* 48(1):69-76.
- Nemoto, T. 1956. On the diatoms of the skin film of whales in the Northern Pacific. *Sci. Rep. Whales Res. Inst.* 11:99-132.
- Nemoto, T., R. L. Brownell, Jr. and T. Ishimaru. 1977. Cocconeis diatoms on the skin of Franciscana. *Sci. Rep. Whales Res. Inst.* 29:101-105.
- Olsen, O. W. 1974. *Animal Parasites, Their Life Cycles and Ecology*. University Park Press.
- Omura, H. 1950. Diatom infection on blue and fin whales in the antarctic whaling area V (the Ross Sea area). *Sci. Rep. Whales Res. Inst.* 4:14-26.
- Oshima, T. 1972. Anisakis and anisakiasis in Japan and adjacent areas. *In: Progress of Medical Parasitology in Japan*. K. Morishita, Y. Komuja and H. Matsubayashi, eds., Vol. IV, pp. 301-393. Meguro Parasitological Museum, Tokyo.
- Rausch, R. L., and F. H. Fay. 1966. Studies on the helminth fauna of Alaska. XLIV. Revision of Ogmogaster Jagerskiold, 1891, with a description of O. pentalineatus sp. n. (Trematoda: Notocotylidae). *J. Parasitol.* 52: 26-38.
- Rausch, R. L., and D. W. Rice. 1970. Ogmogaster trilineatus sp. n. (Trematoda: Notocotylidae). *Proc. Helm. Soc. Wash.* 37:196-200.
- Ridgway, S. H. 1972. Homeostasis in the Aquatic Environment. *In: Mammals of the Sea, Biology and Medicine*. S. Ridgway (ed.) pp. 590-747. Charles C. Thomas Co.
- Ridgway, S. H., and M. D. Dailey. 1972. Cerebral and cerebellar involvement of trematode parasites in dolphins and their possible role in stranding. *J. Wildl. Dis.* 8:33-43.
- Schmidt, G. D. and L. S. Roberts. 1977. *Foundations of Parasitology*. C. V. Mosby Co.



- Schmidt, G. D. and L. S. Roberts. 1981. "Foundations of Parasitology". C. V. Mosby Co., St. Louis. p. 492.
- Schroeder, R. J., C. A. Delli Quadri, R. W. McIntyre, and W. A. Walker. 1973. Marine mammal disease surveillance program in Los Angeles County. J. Am. Vet. Med. Assoc. 163:580-581.
- Shiraki, T. 1974. Larval nematodes of the family anisakidae (Nematoda) in the northern Sea of Japan - as a causative agent of eosinophilic phlegmone or granuloma in the gastro-intestinal tract. Acta Medica et Biologica 22: 57-98.
- Shults, L. M. 1978. Pricetrema phocae and Pricetrema eurnetopii sp. n. (Trematode Heterophnyidae) from Pinniped in the North Pacific. Can. J. Zool. 56(3):382-385.
- Shults, L. M. 1979. Ogmogaster antarcticus Johnston, 1931 (Trematoda: Notocotylidae) from the bowhead whale, Balaena mysticetus L., at Barrow, Alaska. Can. J. Zool. 57:1347-1348.
- Smith, J. W. 1971. Thysanoessa inermis and T. longicaudata (Euphausiidae) as first intermediate hosts of Anisakis sp. (Nematoda: Ascaridata) in the North Sea, to the North of Scotland and at Faroe. Nature 234:478.
- Smith, J. W. and R. Wootten. 1978. Anisakis and Anisakiasis. In: Advances in Parasitology (16). W. H. R. Lumsden, R. Muller and J. R. Baker, eds., pp. 93-163.
- Stock, J. H. 1977. Whale-lice (Amphipoda, Cyamidae) on Lagenorhynchus albirostris in Dutch waters. Crustaceana (Leiden) 32(2):206.
- Stroud, R. K. and M. D. Dailey. 1978. Parasites and associated pathology in pinnipeds stranded along the Oregon coast. J. Wildlife Dis. 14:292-298.
- Stroud, R. K. and T. J. Roffe. 1979. Causes of death in marine mammals stranded along the Oregon Coast. J. Wildlife Dis. 15:91-97.
- Wootten, R. 1978. The occurrence of larval anisakid nematodes in small gadoids from Scottish waters. J. Mar. Biol. Ass. U.K. 58:347-356.
- Wootten, R. and I. F. Waddell. 1977. The occurrence of larval nematodes in the musculature of cod and whiting from Scottish waters. J. du Conseil. Int. Explor. Mer. 37:266-273.
- Yamaguti, S. 1958. Systema helminthum. Vol. I. The digenetic trematodes of vertebrates, Part 1 and 2. Interscience Publishers, Inc., New York, NY. 1575 pp.
- Yamaguti, S. 1958. Systema helminthum. Vol. II. The cestodes of vertebrates. Interscience Publishers, Inc., New York, NY. 860 pp.

- Yamaguti, S. 1961. Systema helminthum. Vol. III. The nematodes of vertebrates, Parts 1 and 2. Interscience Publishers, Inc., New York, NY. 679 and 1261 pp.
- Yamaguti, S. 1963(a). Systema helminthum. Vol. IV. Monogénea and Aspidocotylea. Interscience Publishers, Inc., New York, NY. 699 pp.
- Yamaguti, S. 1963(b). Systema helminthum. Vol. V. Acanthocephala. Interscience Publishers, Inc., New York, NY. 423 pp.
- Yokogawa, M. and H. Yoshimura. 1967. Clinicopathological studies on larval anasakiasis in Japan. *Amer. J. Trop. Med. Hyg.* 16:723-728.

## RESEARCH UNIT 1380

### DETERMINATION OF THE GROSS AND MICROSCOPIC STRUCTURE OF THE LUNG, KIDNEY, BRAIN AND SKIN OF THE BOWHEAD WHALE, BALAENA MYSTICETUS

JERROLD T. HALDIMAN, B.A., M.S., Ph.D.

YAHYA Z. ABDELBAKI, B.S., B.V.S., M.R.V.C.S., M.S., Ph.D.

FAHRI K. AL-BAGDADI, B.V.M.S., M.S., M.S., Ph.D.

DENNIS W. DUFFIELD, B.S., D.V.M., Ph.D.

WILLIAM G. HENK, B.S., M.Ed., Ph.D.

ROBERT W. HENRY, D.V.M., M.S., Ph.D.

Department of Veterinary Anatomy and Fine Structure

School of Veterinary Medicine

Louisiana State University

Baton Rouge, Louisiana 70803

## INTRODUCTION

The determination of the normal configurations, visible morphology, and microscopic structure of any animal tissue, organ, or organ system is fundamental to the ultimate understanding of their functions and possible reactions to a normal or changed environment. Anatomical study, therefore, is the first step in establishing the normal ranges present in a naturally occurring population to serve as the data base for use in comparisons with other species. This Research Unit dealt specifically with the lungs (including other organs of the respiratory system), the kidneys (including urinary bladder), the brain, and the skin (including vibrissae, baleen, and hard palate). The literature is very sparse concerning the anatomy of the bowhead whale. It consists primarily of a single gross anatomical description of the skeleton and larynx (Eschricht and Reinhardt 1866) and scattered comments in Slijper (1979) and Ridgway (1972). Histological studies on the bowhead are represented primarily by the beginning studies presented by Migaki (1979), Kenney and Everitt (1979), and Fetter and Everitt (1979).

## OBJECTIVES

1. To determine the normal gross, subgross, and microscopic structure of the lungs, kidneys, brain, and skin of the bowhead whale.
2. To compare determined structure with that of other cetaceans and better studied animals.
3. To assess function in light of the determined structure.

## METHODS

Intact organs, slices, and various sized chunks of organs collected from Eskimo-harvested bowhead whales were supplied already fixed in 10% buffered formalin by the personnel of RU 180 as previously described. All specimens were photographed upon arrival and logged in with verification of identifying tags followed by storage in fresh solutions of 10% buffered formalin.

Two mm slices of selected tissues for electron microscopy were received in 5% sucrose in 0.1 M sodium cacodylate buffer at pH 7.4 from the personnel of RU 180 after prior fixation for 6 hours in 2% formaldehyde and 1.25% glutaraldehyde in 0.1 M sodium cacodylate buffer. The samples were treated in the following manner: (1) washed in 0.1 M sodium cacodylate with 5% (w/v) sucrose added at pH 7.2 (BUF-A) for 10 min; (2) postfixed in 1% (w/v) osmium tetroxide in 0.1 M sodium cacodylate for 2 hours; (3) washed in BUF-A for 10 min; (4) treated with 1% (w/v) tannic acid in 0.1 M sodium cacodylate at pH 7.2 (TA) (Simionescu and Simionescu 1976) for 1 hour; (5) washed in BUF-A for 10 min; (6) dehydrated through an ethanol-propylene oxide series; (7) embedded in Epon-812; (8) sectioned (60-90 nm) on an LKB-IV or Sorvall MT-28 ultramicrotome; (9) stained with uranyl acetate (Watson 1958) and lead citrate (Reynolds 1963); and (10) viewed in a Zeiss EM-10 or EM-109 transmission electron microscope (TEM). Samples of formalin fixed tissues were also taken from selected larger specimens and processed for TEM as above with step 5 omitted.

Samples for scanning electron microscopy (SEM) were also removed from selected larger specimens fixed in formalin and processed as follows: (1) dehydrated through an ethanol (ETOH) series (50-100%); (2) critical point dried (CPD) from 100% ETOH in CO<sub>2</sub>; (3) mounted; (4) coated with 300-500 nm of gold-palladium in a Hummer V sputter coater; and (5) viewed in a Cambridge S-150 SEM at 20 kv.

Additional small samples of selected regions from the formalin fixed large samples were prepared for routine visible light microscopy (LM) in

the following manner: (1) dehydrated in a graded series of isopropyl alcohols and infiltrated with Paraplast II in a Trimatic tissue processor; (2) embedded in fresh Paraplast II; (3) sectioned at 4-6  $\mu\text{m}$  with an American Optical 820 Spencer microtome; (4) mounted on glass slides; and (5) prepared for study by coverslipping after staining of individual slides in a series with hematoxylin and eosin (H and E) for general morphology, Verhoeff's elastin stain (Ver) for elastic fibers, periodic acid-Schiff reagent (PAS) for the basal lamina and mucopolysaccharides, Masson's trichrome (Mass) or Milligan's trichrome (Mill) for differentiation of tissue elements (especially collagen fibers), or Bodian's nerve fiber stain (Bod).

In addition, a limited number of samples were also prepared for LM by: (1) dehydration and embedding in Epon-812 as described above; (2) sectioned at 1-2  $\mu\text{m}$  (semithin sections) on an LKB-IV or Sorvall JB-4 microtome; and (3) coverslipped after staining with a mixture of 1% (w/v) methylene blue and 1% (w/v) azure II in distilled water.

Gross measurements were made with a metal meter stick or vernier caliper as appropriate. Measurements accomplished by microscope were made with calibrated ocular micrometers. Appropriate photographs were taken and drawings were made at several stages of dissection.

The types of samples, variations of the above general procedures, and other specialized techniques applicable to only some of the tissues received were:

## I. Lung

Fourteen samples of lung and bronchial tissue from five bowhead whales (79B1, 80B1, 80B2, 80B7, 80B8), a slice of the blowhole (80B2), the cranial portion of the larynx from 79B1, the caudal portion of the larynx with complete trachea and bronchial bifurcation from 80B1, and entire lungs from 79B1, 80B1, 80B2, 80B7 and 80B8 were received in 10% buffered formalin from RU 180.

The entire lung of 80B1 was injected with vinyl acetate (red-arteries, blue-veins, yellow-bronchi and bronchioles) followed by 25% KOH digestion. Two other entire lungs (80B2 and 80B8) were dissected grossly to expose the bronchial trees as far as possible. The blowhole from 79KK1 was cut into approximately 4 cm transverse slabs to expose internal structure. The partial larynxes from 79B1 and 80B1 were also cut into approximately 4 cm

sections after partial dissection. After complete dissection, the cartilaginous portions were reconstructed to establish sizes and configurations of the laryngeal cartilages. The trachea and primary bronchial bifurcation of 80B1 were dissected free of adjoining material. Small samples for LM and SEM were removed from large specimens for study when no small samples of that organ had been provided otherwise. Four 2 mm slices of lung tissue for electron microscopy from 80B2 and 80B8 were also received and processed as described in general methods.

## II. Kidney

Nine samples of kidney from six bowhead whales (79B1, 79B2, 80B1, 80B2, 80B7 and 80B8) and two samples of urinary bladder (79B1, 80B7) were received from RU 180.

Gross dissections were conducted to identify the extent of the peritoneal covering, the arrangements of the renicules, the vascular patterns, and the arrangement of ureteral branches. Colored neoprene latex (red-arteries, blue-veins, yellow-ureters) was injected into the arteries, veins, ureteral branches of several kidney pieces. The sample from 79B1 was then macerated in 10% KOH to reveal the calyx casts and stored in 10% buffered formalin for study and photography. The veins of sample 80B1, Tag 105 were injected with radiopaque Microfil\* for determination of venous patterns visually and by radiography.

Microdissections were performed utilizing a Zeiss OM-1 surgical microscope. Several typical renicules were sectioned in 1 mm slices for determination of corticomedullary ratios and sporta perimedullaris configuration. Routine histological sections (LM) and TEM sections were prepared and stained as listed previously. Milligan's trichrome stain was also utilized to differentiate collagen fibers and smooth muscle cells. Five 2 mm slices of kidney tissue for electron microscopy from 80B1 and 80B8 were also received.

## III. Brain

The brain of 80B1 described as "damaged in removal" was received from RU 180. The forebrain was separated from the brain stem through the mid-

---

\* MV-122 yellow Microfil silicone rubber injection compound, Canton Bio-Medical Products, Inc. P. O. Box 2017, Boulder, CO 80302

brain with accompanying severe distortions, and was itself separated roughly into two halves with each missing its temporal lobe. Much later six brains (79B1, 79KK2, 79KK3, 79KK4, 80B2, and 80B8) were received from Dr. Sam Ridgway of the Naval Ocean Systems Center (NOSC) in San Diego, California. These had been more complete than 80B1, but before they were sent to our laboratory the cerebellum had been removed, the brain stem was cut in various ways, and the forebrain had been sectioned either transversely or horizontally. All of the brains were extremely fragile and with any manipulation, tended to disintegrate.

Sketches and photographs which required a minimum of manipulation were made of 80B1. The sectioned brains were carefully reviewed in the hope of gaining impressions of the anatomy of the bowhead brain not obtained from 80B1. Those forebrain slices which arrived arranged in order and wrapped in cheesecloth were reapproximated to the maximum extent possible. The slices were serially removed to observe internal structures then reapproximated and rewrapped. A reasonably intact forebrain was photographed as reconstructed, and then sections from it were removed and photographed. Selected pieces from other brains which demonstrated particular features were sketched or photographed, and notes were taken on each brain for future references. Two photographs of intact bowhead brains were received much later from NOSC and are included in this section of the report.

#### IV. Skin

Eighty-seven small to medium sized samples of skin, baleen, and hard palate from 79B1, 79B2, 79B3, 80B1, 80B2, 80B7, and 80B8 were received in 10% buffered formalin from RU 180 as previously described. Small pieces through the entire epidermis and into the dermis were cut out for tissue processing and sectioning (previously described) in longitudinal (vertical cut parallel to body axis) and transverse (vertical cut perpendicular to body axis) planes. Additional small pieces were trimmed to mark the rostral orientation and cut horizontally (parallel to the outer epidermal surface) for frontal sections at from 3-5 recorded levels. The routine stains listed previously were performed on representative slides. In addition an Ayoub-Shklar stain (Luna 1968) to specifically differentiate nonkeratinized cells with prekeratin granules from keratinized cells was utilized on representative slides. Gram stain was utilized for bacteria on the skin and in lesions. In addition, frontal serial sections were prepared from 5 pieces of skin, vibrissae, and

baleen hairs. Vertical serial sections were also prepared from 3 vibrissae and 3 pieces of baleen. Eight 2 mm slices of skin from 80B1, 80B7, and 80B8 were also received and processed as described in electron microscopy methods.

Determination of the number of dermal papillae per square millimeter was accomplished with a calibrated ocular reticule and a Zeiss MOP-3 digital image analyzer. Epidermal thickness and other gross measurements were performed with vernier calipers from the formalin fixed samples supplied by RU 180. Measurement of dermal papilla size and other measurements from histological slides utilized a calibrated ocular micrometer.

A 20 gallon aquarium was filled with artificial sea water (Instant Ocean\*) adjusted to 1.020 specific gravity and Prudhoe Bay crude oil\*\* was poured into the aquarium to form an oil slick over approximately 3/4 of the water surface. The tank and contents were cooled overnight and then maintained in a cold room kept at 3°C.

Small pieces of skin from the blowhole with vibrissa (79KK1) and chin with 3 vibrissae (79B2) were fitted with a wire harness to maintain the epidermis in a dorsal position and suspended in the aquarium at the oil free end. After overnight cooling to assure that water, oil, and skin pieces were the same temperature, the skin samples were individually lifted through the oil slick and returned to the water through the oil slick 3 times with moderate agitation in an attempt to simulate the breathing movements of bowhead whales. The samples were then photographed in another container of 3°C artificial sea water. Three additional samples without vibrissae from 80B1, Tag 54 chin, 80B7, Tag 12 upper lip with sensory papillae, and 80B1, Tag 53 outer lower lip were photographed after harnessing and cooling to 3°C and then dipped as above and rephotographed. Three additional samples of skin without vibrissae but with visible lesions from 80B7, Tag 22 outer upper lip, 80B8, Tag 30 lower jaw midline, and 80B8, Tag 3A outer upper lip were also tested as above except the epidermis was kept in a ventral position as if on the animal.

---

\* Instant Ocean manufactured by Aquarium Systems, Mentor, OH

\*\* A one gallon container of Prudhoe Bay raw crude oil was kindly supplied by the Research and Development Department of Arco Oil and Gas Co., Dallas TX and is gratefully acknowledged.



## RESULTS

The results of the gross, subgross, and microscopic studies of the Lung/Skin Research Unit were as varied as the methods utilized and the diversity of tissues and organs available for collection by RU 180. The number and type of samples made available has had a direct effect on results. The extreme weather and other collection conditions imposed on RU 180 personnel prevented some samples from being as well or as quickly preserved as is usually required for most types of anatomical study. Organ and medium sized sample quality overall was good to excellent with only a small proportion exhibiting some internal deterioration. Samples for electron microscopy, however, were not as well preserved: their condition ranged from adequate to poor apparently owing to autolysis and temperature constraints. Results are presented from all samples studied since they represent in some cases the first and in other cases the best samples of bowhead whale tissues and organs available for anatomical analysis to date. Standard anatomical terminology based on that prescribed in the *Nomina Anatomica Veterinaria* (Schaller et al 1973) is used.

### I. Lung

The respiratory system was studied from the external nares (blowholes) to the alveoli within the lung where actual gaseous exchange occurs (with the exception of the nasal passages which were not available). The total amount of pulmonary tissue viewed grossly was lower in proportion to the conducting airways than we expected from 10.32 m (average) animals.

The external nares, commonly referred to as the blowholes, have a cutaneous covering. They are situated on the dorsum of the skull in a recessed area in the maxillae. The external nares of 79KK1 were symmetrical, 20 cm in length and separated 3 cm rostrally. They curved caudolaterally in a semicircular fashion and were separated 18 cm at their caudal extent (Fig 13-1). Eight tactile hairs, 9-12 mm long and arranged in a V-shaped configuration were located between the caudal extremities of the right and left nares (Fig 13-2). The nares led into paired right and left vestibuli and on into right and left nasal cavities which were divided by paired cartilages surrounded by dense vascular connective tissue (Fig 13-3). Rostrally the cartilages were 15 cm below the dorsal surface (Fig 13-4A) and then inclined caudally to lie only 2 cm below the dorsum in the midportion of the external

nares (Fig 13-4E). The cartilages then declined caudally to lie 6 cm below the dorsal surface (Fig 13-4F). The cartilages were surrounded by vascular tissue, became pleated caudally and curved laterally to partially surround the meati (Fig 13-4G).

The vestibular epithelium was 2 mm thick overlying a very tendinous lamina propria that was 10 mm thick. The stratified squamous epithelium was keratinized with a 15  $\mu$ m thick stratum corneum (Figs 13-5, 13-6). Connective tissue papillae averaging 800  $\mu$ m long interdigitated with the epithelium. The stratum basale and stratum spinosum appeared typical with the outer layers of the spinosum becoming flattened gradually toward the stratum corneum. No sensory nerve endings were noted in the lamina propria of this region.

Between the nasal septa, the tissue was histologically dense irregular connective tissue sheets (Fig 13-7) interlaced with some adipose tissue and longitudinally arranged tendinous tissue. The region was heavily vascularized.

The rostral and lateral walls of the vestibuli and the nasal cavities contained an anatomical sphincter which appeared to passively push the vestibular walls medially to close the nares. This narial sphincter was made of specialized blubber laced with radially oriented 2-4 mm diameter skeletal muscle bundles (Figs 13-4, 13-8, 13-9). The orientation of the muscle fibers appeared to be directed to the medial surfaces of the recessed areas in the maxillae.

The depths of the cartilages (Fig 13-10) led to an osseous midline septum thus completing the division into totally separate right and left nearly vertical nasal cavities. The internal nares lead into the vertically elongated nasopharynx which lies dorsal to the soft palate, but was not available for study. The nasopharynx communicated with the laryngopharynx via a circular opening in the soft palate (79B1) which was surrounded by skeletal muscle commonly referred to as the palatopharyngeal sphincter (Fig 13-10).

The larynx (79B1 and 80B1) was composed of the four classical cartilages which differed in arrangement and structure from those of terrestrial mammals (Figs 13-11, 13-12, 13-13). The rostral extension was typically cetacean, but blunter. The rostral free end of the epiglottic cartilage did not extend beyond the arytenoid cartilages. The epiglottic cartilage had a longitudinal median pyramidal eminence which fit between the rounded ventral surfaces of the arytenoid cartilages (Fig 13-10). The caudal end of the epiglottic

tic cartilage was assumed to be continuous with the cranioventral aspect of the thyroid cartilages (Fig 13-11).

The rostral most portions of the arytenoid cartilages displayed corniculate processes which lay rostral to the cricoid cartilages (Figs 13-11, 13-14). The arytenoid cartilages extended the entire length of the larynx and laid ventral to the cricoid cartilage, but dorsal to the thyroid cartilages. Their caudal tips were connected by dense connective tissue and were not fused (Figs 13-12B, 13-13B).

The cricoid cartilage was a flattened plate rostrally which became trough shaped caudally (Figs 13-12B, 13-13B, 13-15A, 13-16A) and was partially fused to the first tracheal ring. The thyroid cartilages were paired and formed a shallow wedge as they fused in the midline (Figs 13-15A, 13-1A). Caudal cornua extended caudad beyond the larynx proper, lay next to and attached to the laryngeal sac muscle via dense connective tissue near the second tracheal ring (Fig 13-17). The cranial cornua inclined craniodorsally and then curved caudally to lay along the dorsolateral aspect of the cricoid cartilages (Fig 13-12). The cricothyroid muscle was well developed arising from the dorsum of the thyroid cartilage near the midline (Fig 13-16B).

Measurements of the caudal portion of the larynx of 80B1 were: cricoid cartilage was 24 cm long, 19 cm wide and 13 cm deep; thyroid cartilage was 30 cm long by 17 cm wide; the cranial cornua of the thyroid cartilage were 22 cm long; and the arytenoid cartilages of 79B1 measured 14 cm and 13 cm respectively in length. The corniculate process was 5 cm long.

The dorsal (inner) epiglottic epithelium (Fig 13-18) was 875  $\mu\text{m}$  thick, keratinized, stratified squamous with a 50  $\mu\text{m}$  thick stratum corneum. Sensory papillae up to 700  $\mu\text{m}$  long occurred from 0.25-0.4 mm apart with smaller nonsensory papillae in between (Fig 13-19). The lamina propria was 5500  $\mu\text{m}$  thick and consisted of dense irregular connective tissue overlying hyaline cartilage. The ventral (outer) epiglottic surface was 550-1000  $\mu\text{m}$  thick keratinized stratified squamous epithelium with a 40  $\mu\text{m}$  stratum corneum and 350-800  $\mu\text{m}$  long sensory papillae (Fig 13-20A). The 875  $\mu\text{m}$  thick lamina propria contained numerous blood vessels, nerves, Herbsti-like encapsulated sensory nerve endings and dense irregular connective tissue. The submucosa contained compound tubuloalveolar mucoserous glands with serous demilunes (Fig 13-20B). The gland excretory ducts were 450  $\mu\text{m}$  in diameter with stratified cuboidal to stratified columnar epithelium up to 110  $\mu\text{m}$  thick. The median ridge of the epiglottic epithelium was 925  $\mu\text{m}$  thick stratified squamous with a 62.5  $\mu\text{m}$

stratum corneum. No sensory nerve endings were seen, although small nerve tracts were present. The papillae of the lamina propria were 750  $\mu$ m high.

The inner surface of the arytenoid cartilages (Fig 13-21) was 750  $\mu$ m thick keratinized stratified squamous epithelium with a 50  $\mu$ m stratum corneum. Sensory papillae up to 625  $\mu$ m long occurred from 0.4-0.6 mm apart with smaller nonsensory papillae in between (Fig 13-22). The lamina propria was dense irregular connective tissue 1875  $\mu$ m thick and overlaying vascularized hyaline cartilage. The lamina propria of the outer epithelium of the arytenoid consisted of a superficial layer of dense irregular connective tissue 150  $\mu$ m thick and a deeper layer 5.75 mm thick of adipose connective tissue over the hyaline cartilage.

Near the caudal end of the arytenoid cartilages, the covering was 250  $\mu$ m thick stratified squamous epithelium with a 12.5  $\mu$ m thick stratum corneum that was parakeratotic. Some areas, however, appeared to change to a thick pseudostratified columnar type. The connective tissue papillae were up to 150  $\mu$ m high. The lamina propria was heavily infiltrated with plasma cells and the deeper parts of the lamina had elastic fibers. The caudalmost aspects of the arytenoid cartilages were covered with 20  $\mu$ m ciliated pseudostratified columnar epithelium whose surface cells produced mucus. The lamina propria contained dense irregular connective tissue with simple tubuloalveolar mucous glands and a 750  $\mu$ m thick elastic lamina with longitudinally oriented fibers in lieu of a muscularis mucosae.

Rostrally, the laryngeal cavity lies between the arytenoid and epiglottic cartilages. Caudally it divided into a ventral portion which had a caudal diverticulum (the laryngeal sac), and a dorsal portion which led into the trachea. The ventral portion lays between the arytenoid and thyroid cartilages. The laryngeal sac was a mucous membrane lined diverticulum from the caudalmost area of the ventral laryngeal cavity. It was surrounded by circularly arranged skeletal muscle (Fig 13-23) which formed the floor of the tracheal airway between the open tips of the C-shaped cartilages (Fig 13-23B). The laryngeal sac was 10 cm long and from 3.5 to 5.5 cm wide. It had stratified squamous epithelium which was 500  $\mu$ m thick with connective tissue papillae up to 350  $\mu$ m high. The parakeratotic stratum corneum was 25  $\mu$ m thick. Sensory nerve tracts were seen in the lamina propria, but no sensory nerve endings were noted. The lamina propria was deep with small skeletal muscle bundles, adipose cells (Fig 13-24), and nerve tracts throughout. The dorsal portion of the laryngeal cavity was inclined dorsocaudally between the aryten-

oid cartilages passing over their caudal aspects and ventral to the cricoid cartilage to communicate directly with the tracheal airway.

The trachea (80B1) was composed of ten white tracheal cartilages which were C-shaped with distinct yellow elastic connective tissue surrounding them. The ventral aspect of the trachea contained the open portion of the C-shaped cartilages. The space between their free ends was closed by the circularly arranged laryngeal sac muscle which surrounded the sac (Fig 13-23). The first tracheal cartilage was partially fused with the caudal aspect of the cricoid cartilage. The caudal four tracheal cartilages were closed by a cartilaginous plate, dense connective tissue and muscle (Fig 13-25). The tracheal cartilages were not symmetrical but often overlapped the preceding tracheal cartilage. The trachea was dorsoventrally flattened with inside vertical height of 7-9 cm and horizontal width of 16-16.5 cm. The tracheal length was 19 cm. The laryngeal sac muscle mass was V-shaped and served as part of the ventral tracheal floor. It extended throughout the tracheal length tapering to a fine point near the tracheal bifurcation. Cranially it encompassed the laryngeal sac and caudally held the tracheal plate. The tracheal plate was hyaline cartilage 6 cm long X 2-5 cm wide and up to 1 cm thick (Fig 13-25). It served, along with the laryngeal sac muscle, as the tracheal floor. The dorsal surface of the trachea was slightly concave and was overlain by the esophagus.

The epithelium changed abruptly on the dorsal wall of the laryngo-tracheal junction from 100  $\mu$ m nonkeratinized stratified squamous with 1-2 mm diameter lymphatic nodules in the lamina propria (Fig 13-26) to 50  $\mu$ m ciliated pseudostratified columnar with diffuse lymphatic tissue underneath (Fig 13-27). The propria consisted of dense irregular elastic connective tissue and adipose cells. Midway in the tracheal length the ciliated pseudostratified columnar epithelium was 32.5  $\mu$ m thick. The dense irregular connective tissue of the lamina propria contained a 400  $\mu$ m layer of mucous glands and an elastic lamina 150  $\mu$ m thick. The vascularized hyaline tracheal cartilages were 8 mm thick (Fig 13-28).

The tracheal bifurcation (80B1) was 19 cm caudal to the cricoid cartilage (Fig 13-29A). The right primary bronchus (80B1) came off at a 130° angle while the left one arose at a 120° angle. The primary bronchi were yellow except for the cartilage and 13 cm long. At their bifurcation they were dorsoventrally compressed with inner dimensions of 11 x 7 cm for the left and 13 x 7 cm for the right (Fig 13-29C). Primary bronchi measurements for 80B2

were 11 x 6.5 cm and 12 x 7 cm for 80B7. The bronchi contained complete rings of hyaline cartilage which branched and anastomosed. The histological specimens were taken from gross specimens and not all areas sampled had cilia. This may have been due to poor preservation. The epithelium was pseudostratified columnar (Fig 13-30, 13-31, 13-32) 45  $\mu$ m in height. The lamina propria contained simple branched alveolar mucous glands interdigitated into 1.9 mm thick elastic laminae which had predominately longitudinally oriented fibers. No nerve fibers were noted. Complete 9.8 mm thick hyaline cartilage rings were permeated with connective tissue channels containing blood vessels. The tunica adventitia was typical dense irregular connective tissue with no smooth muscle.

The surface epithelium of the 80B8 main bronchus was composed of both ciliated and nonciliated cells (Fig 13-33). The nonciliated cells bulged from the surface and possessed numerous microvilli (Fig 13-34). The ciliated cells also possessed microvilli positioned among the cilia but these were more slender than the microvilli of nonciliated cells (Fig 13-35). Observation of the main bronchus of 80B1 revealed a poorly preserved surface covered with debris. Ciliated cells were visible in distinct rows but cells containing microvilli were not observed (Fig 13-36). Poor preservation renders these observations suspect.

Tissue from the main bronchus of 80B8 was examined with a transmission electron microscope and contained nonciliated mucus producing cells with microvilli on their surfaces (Fig 13-37). The columnar cells of this epithelium were of two types based on staining characteristics and morphology. One cell type possessed a highly vesicular cytoplasm which stained heavily. The other type stained less densely and contained fewer vesicles. Both types contained numerous secretory vesicles (Figs 13-37, 13-38). Since preservation was not optimal, these morphological and staining differences could simply have been due to poor preservation with vesiculation due to post mortem disintegration. Near the base of these columnar epithelial cells was one or more strata of basal cells. The basal portions of the columnar cells consisted of a complex of numerous fine fingerlike processes which wound among the processes of basal cells to ultimately rest on the basal lamina which separated the epithelium from the underlying connective tissue (Figs 13-37, 13-38). The dense staining cells were particularly useful in following these processes (Figs 13-37, 13-38).

The basal cells were shorter than the columnar cells with numerous surface processes which interdigitated with processes of adjacent basal cells and with those of columnar cells (Figs 13-37, 13-38, 13-39). Desmosomes were seen along many of these processes (Figs 13-39, 13-40). Whether these desmosomes joined only basal cell processes or also joined columnar cells processes could not be determined. Hemidesmosomes joined basal cells to the basal lamina (Fig 13-40). The basal lamina measured approximately 100 nm in thickness. Beneath the basal lamina, fibroblasts and numerous fine collagen fibers were seen (Figs 13-33, 13-34) as well as a large number of plasma cells identified by a distinctive pattern of heterochromatin distribution and the expanded cisternae of rough endoplasmic reticulum (Figs 13-41, 13-42).

Mucous glands were found deep in the connective tissue (Figs 13-43, 13-44). Their secretory cells rested on a basal lamina and secretory granules were accumulated in the apical regions. The apical region of these cells contained numerous microvilli and the cytoplasm was rich with endoplasmic reticulum (Figs 13-43, 13-44). Junctions were seen on the lateral surfaces of adjoining cells and canaliculi appeared to be present between some cells (Fig 13-44).

The principal bronchi (80B1, 80B2, 80B7 and 80B8) divided into cranial and caudal lobar bronchi (Fig 13-45) 13 cm caudal to the tracheal bifurcation. The cranial lobar bronchus (80B1) of the left lung arose at a less obtuse angle ( $145^\circ$ ) than did the cranial lobar bronchus of the right lung ( $160^\circ$ ). The cartilaginous rings were white in color and complete, but branched and anastomosed. Bronchial lymph nodes (80B7) were present. The epithelium was ciliated pseudostratified columnar. The pulmonary artery coursed dorsolaterally between the bifurcation of the principal bronchi (Figs 13-46, 13-47) the arterial branches followed the branching of the bronchial tree along its dorsolateral aspects. The major pulmonary vein lay just caudo-medial to the artery. Its branches did not follow the bronchi deeply, however, but lay just beneath the pleura on the ventromedial surface of the lung (Fig 13-46). The lobar bronchi branched dichotomously into smaller dissectable segmental branches ranging from 1-5 cm in external diameter. Relatively large segmental bronchi were routinely found lying near the lung surface (Fig 13-45).

Mid sized (19 x 31 mm) segmental bronchi (80B1) of the ordinary bowhead (Fig 13-48) had 68  $\mu$ m thick ciliated pseudostratified columnar epithelium with mucus producing pockets. The loose connective tissue lamina propria

had abundant longitudinally oriented, 150  $\mu\text{m}$  thick laminae of elastic fibers and abundant plasma cells, but no mucous glands. Cartilage rings were 3.8 mm thick. The Ingutuk variant (80B8) had the same type of epithelium (Figs 13-49, 13-50), but it was only 30  $\mu\text{m}$  thick. The loose connective tissue lamina propria had 98  $\mu\text{m}$  thick elastic laminae and cartilage rings which were 3.6 mm thick.

Smaller segmental bronchi (15 mm) of the ordinary bowhead (80B7) had ciliated pseudostratified columnar epithelium 96  $\mu\text{m}$  thick (Fig 13-51). The lamina propria was of loose connective tissue with 75  $\mu\text{m}$  thick elastic laminae and mucous glands. The cartilage rings were 2.47 mm thick surrounded by dense irregular connective tissue. The Ingutuk variant (80B8) was similar with 41.8  $\mu\text{m}$  epithelium (Fig 13-52) and elastic lamina 450  $\mu\text{m}$  thick in the loose connective tissue lamina propria which also contained mucous glands. The cartilaginous rings measured 1.5 mm thick and were surrounded by dense irregular connective tissue.

A 1 cm bronchus from 80B8 was examined with the scanning electron microscope. The surface epithelium resting on the connective tissue which overlay cartilage bands was composed of both ciliated and nonciliated cells which were similar to those seen in the main bronchus (Figs 13-53, 13-54, 13-55). The number of ciliated cells was greatly increased with some areas completely covered by cilia (Fig 13-54).

Smaller segmental bronchi (1.5-3 mm) from 80B1 and 80B8 had 30  $\mu\text{m}$  thick ciliated pseudostratified columnar epithelium. The loose connective tissue lamina propria had mucous glands. The cartilage rings were 0.75 mm thick (Figs 13-56, 13-57). Two mm bronchi from 80B8 and 80B1 were examined with SEM. In both cases the epithelium rested on connective tissue which overlays cartilage bands (Fig 13-58). The epithelium was largely covered by a mucous coating in which debris was embedded (Figs 13-59, 13-62). Beneath the mucus, the cell surfaces appeared to be uniformly ciliated (Figs 13-60, 13-61, 13-63, 13-64). Cilia could be seen to be the surface modifications of columnar epithelial cells (Figs 13-62, 13-63).

Bronchioles 1.5 to 0.3 mm in diameter (80B1 and 80B8) had 30  $\mu\text{m}$  high ciliated pseudostratified columnar epithelium. The presence of a circularly arranged muscularis mucosae (smooth muscle) caused the tunica muscularis to be thrown into folds (Figs 13-65, 13-66). Myoelastic sphincters were not present. No mucous glands occurred in the lamina propria and the cartilage became plaques instead of rings.



Respiratory bronchioles 0.68 to 0.36 mm in diameter (79B1 and 80B2) had respiratory (simple squamous) epithelium closely covering a capillary network (Figs 13-67, 13-68). The lamina propria was loose connective tissue in the larger respiratory bronchioles, but became dense irregular connective tissue in the smaller ones. No glands were present. A muscularis mucosae of smooth muscle with elastic fibers occurred in bronchioles of 0.5-0.68 mm diameter. In smaller respiratory bronchioles the muscularis mucosae position was occupied only by elastic fibers. Individual alveoli and alveolar ducts penetrated the mucosa between the cartilaginous plaques with their orifices surrounded by exclusively elastic fiber sphincters.

Examination of respiratory bronchioles with a transmission electron microscope revealed a surface epithelium composed of type I and type II pneumocytes resting on a basal lamina (Figs 13-69, 13-70). Thin cytoplasmic processes of type I pneumocytes extended over capillaries and in places shared a common basal lamina with the capillary endothelial cells (Fig 13-69). Type II pneumocytes were found between capillaries and were identified by their numerous microvilli and the presence of multilamellar bodies in their cytoplasm (Fig 13-69, 13-70). Occasionally, type II pneumocytes extended over capillaries greatly increasing the blood-air barrier (Fig 13-70). The lateral surfaces of adjacent pneumocytes showed complex interdigitations and cell junctions including desmosomes (Fig 13-70). Beneath the basal lamina, the connective tissue was composed of collagen fibers among which numerous fibroblasts and their processes could be seen (Figs 13-69, 13-70). Beneath this fibrous layer, typical hyaline cartilage could be seen (Fig 13-71) in which chondrocytes of varying structure were evident (Figs 13-71, 13-72). See Tables 13-1 and 13-2 for a comparison of bronchial and bronchiolar structures.

Alveolar ducts measured 0.46-0.6 mm (80B2) with the tunica mucosa (Fig 13-73) lined exclusively with respiratory epithelium (simple squamous covering capillaries) and alveolar sacs protruding peripherally. Cartilage plaques and mucous glands were absent. An undetermined number of alveoli were connected to the alveolar sacs. Orifices to alveolar sacs and to individual alveoli were surrounded by exclusively elastic fiber sphincters (Figs 13-74, 13-75). Frequently with light microscopy, the sphincter areas appeared not to have an epithelial covering. Semi-thin sections cut from Epon embedded material (Figs 13-76, 13-77) showed clearly that type I pneumocytes of the respiratory epithelium always covered such areas as well as the capillaries. Ultrastructurally the epithelium covering the elastic sphincters (80B8) was

TABLE 13-1. COMPARISON OF THE MICROSCOPIC STRUCTURE OF AIRWAYS IN  
ORDINARY BOWHEAD WHALE LUNGS

Structure	Inside Diameter (mm)	Epithelial Height ( $\mu$ m)	Elastic Lamina Thickness (mm)	Gland Occurrence	Cartilage Thickness (mm)	Smooth Muscle Occurrence
Lobar Bronchus	19 X 31	69*	0.15	+	3.8	-
Segmental Bronchus	16	96*	0.75	+	2.47	-
Segmental Bronchus	6	34.2*	n.o.	-	n.o.	-
Segmental Bronchus	1.37	34.2*	n.o.	-	0.13	-
Bronchiole	0.75	30.0*	-	-	n.o.	+
Respiratory Bronchiole	0.64	Resp**	-	-	n.o.	+
Respiratory Bronchiole	0.48	Resp	-	-	0.01	+
Respiratory Bronchiole	0.45	Resp	-	-	-	-

\* Ciliated pseudostratified columnar epithelium

\*\* Respiratory epithelium

n.o. Not observed

TABLE 13-2. COMPARISON OF THE MICROSCOPIC STRUCTURE OF AIRWAYS IN  
INGUTUK VARIANTS

Structure	Inside Diameter (mm)	Epithelial Height (μm)	Elastic Lamina Thickness (mm)	Gland Occurrence	Cartilage Thickness (mm)	Smooth Muscle Occurrence
Primary Bronchus	38 X 95	45.0*	1.9	+	9.8	-
Segmental Bronchus	19.8 X 33.2	30.0*	0.98	+	3.6	-
Segmental Bronchus	8.2 X 14.8	41.8*	0.45	+	1.5	-
Segmental Bronchus	3.7	38.0*	1.06	n.o.	3.42	-
Segmental Bronchus	3.4	30.0*	0.7	+	0.6	-
Segmental Bronchus	3.3	30.0*	n.m.	n.o.	0.75	-
Segmental Bronchus	2.89	22.8*	n.m.	n.o.	1.36	-
Segmental Bronchus	2.24	30.0*	n.m.	+	0.56	-
Bronchiole	0.59	30.0*	-	-	-	-
Bronchiole	0.36	30.0*	-	-	-	+
Bronchiole	0.3	30.0*	-	-	-	+
Respiratory Bronchiole	0.24	Resp**	-	-	-	-

\* Ciliated pseudostratified columnar epithelium

\*\* Respiratory epithelium

n.m. Not measured

n.o. Not observed

similar to that of the respiratory bronchioles (Fig 13-78). A number of fibroblast like cells were seen beneath the epithelium while below them were numerous elastic fibers (Fig 13-78) composed of amorphous substance and microfibrils (Fig 13-79). Among these elastic fibers were delicate collagen fibers and fibroblasts (Figs 13-79, 13-80). The fibroblasts possessed many fine processes which extended outward in all directions and were visible in virtually any section through the sphincter (Figs 13-79, 13-80, 13-81). Similar structures with somewhat poorer preservation were seen in 80B2 (Fig 13-81).

Each alveolus was also lined with respiratory epithelium covering individual capillary beds of the cetacean type. The interalveolar septa (Fig 13-82) were composed of loose connective tissue with a capillary bed as well as covering respiratory epithelium on each side. TEM photomicrographs clearly demonstrated the same arrangement (Fig 13-87). A very dense staining material was observable just outside the plasma membranes of respiratory epithelial cells. Within the lumen of all cavities lined by respiratory epithelium, multilamellar bodies could be seen in various stages of disintegration (Figs 13-78, 13-88). They appeared to be composed of membranous material arranged in concentric swirls (Fig 13-83) and may have contained tubular myelin (Fig 13-84). Scanning electron photomicrographs revealed an alveolar wall consisting of two capillary networks separated by an alveolar septum (Fig 13-85). Red blood cells could be seen within the capillaries (Fig 13-86). With TEM, typical type I and type II pneumocytes became evident making up the respiratory epithelium. The septal thickness, while quite variable, appeared to be about 6  $\mu\text{m}$  from basal lamina to basal lamina in the relatively expanded condition. The septum appeared to consist of loose connective tissue in which relatively few collagen fibrils occurred. Fibroblasts were evident within this matrix (Fig 13-87). Monocyte-like cells were occasionally seen in the capillaries beneath the respiratory epithelium (Figs 13-88, 13-89). In addition to the usual complement of organelles and multilamellar bodies, one type II pneumocyte displayed an inclusion resembling a thumb print (Fig 13-89) which is still unidentified.

The pleura was thick, fibrous and had abundant elastic fibers (Figs 13-91, 13-92). No lobulation was evident either in the pleura or in the parenchyma of the lung to divide it into cranial and caudal lobes. The gross measurements of the preserved lungs are listed in Table 13-3. The lungs were roughly rectangular with nearly uniform thickness. The hilus area was large measuring 26-29 cm mediolaterally and 30-47 cm craniocaudally (Figs 13-93, 13-94).

TABLE 13-3. GROSS MEASUREMENTS OF INDIVIDUAL LUNGS OF BOWHEADS AND INGUTUK VARIANTS

Whale Number	Whale Length (m)	Lung Thickness (cm)	Lung Length			Lung Width			Lung
			Dorsal (cm)	Middle (cm)	Ventral (cm)	Cranial (cm)	Middle (cm)	Caudal (cm)	
80B8*	8.7	12	71	72	72	41	38	30	Right
79B1*	8.7	11	90	87	85	37	44	44	Right
Average		11.5	80.5	79.5	78.5	39	41	37	
80B1	10.9	12	72	71	73	38	42	46	Left
80B2	10.8	13	79	77	76	52	50	48	Right
80B7	10.0	13	75	77	80	37	42	45	Left
Average		12.6	75.3	75	76.3	42.3	44.6	46.3	

\* Ingutuk

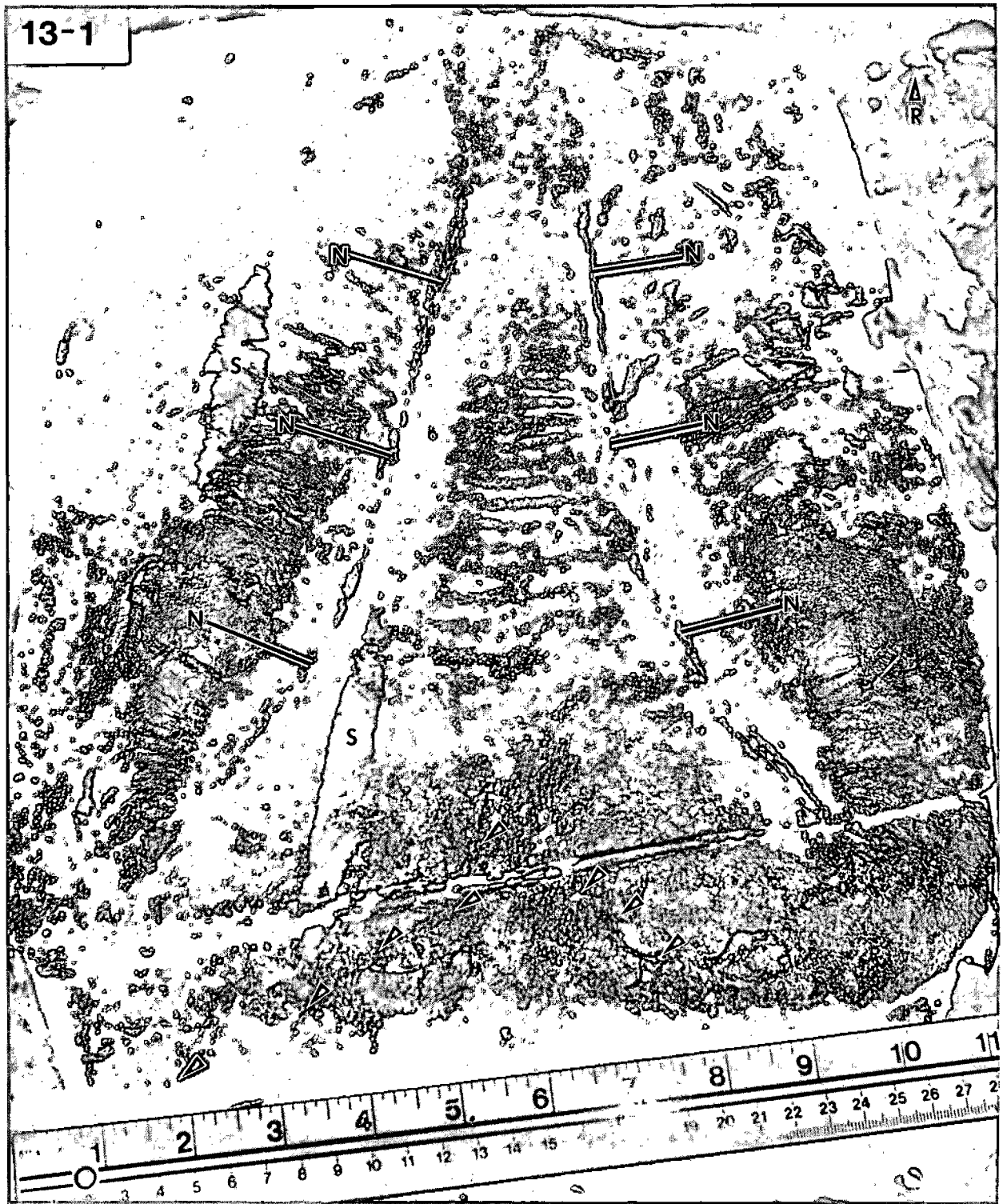


Figure 13-1. Photograph of the external nares (blowholes), dorsal view, 79KK1. The paired external nares (N) lie close together rostrally and curve caudolaterally to lie 18 cm apart. Tactile hairs (arrowheads) lie just caudal to the nares. Rostral (R). Apparent scars (S) are also visible.



Figure 13-2. Photograph, dorsal view of tactile hairs, 79KK1. Eight tactile hairs (arrowheads) are visible just caudomedial to the external nares. Rostral (R). X0.9

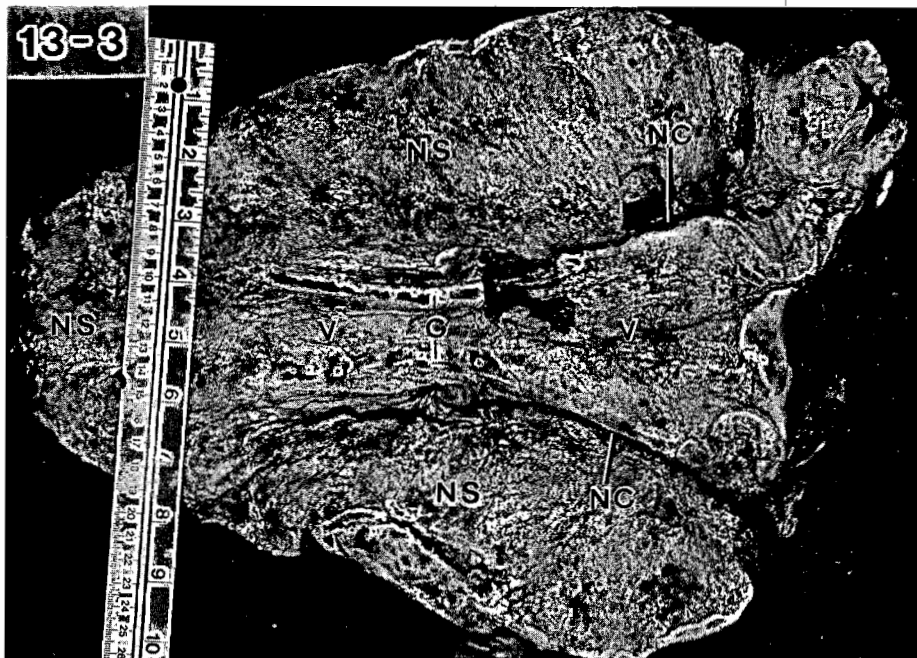


Figure 13-3. Photograph, ventral view of the paired nasal cartilages, 79KK1. Right and left vestibuli and nasal cavities (NC) are separated by the paired nasal cartilages (C). The nasal sphincter (NS) lies lateral and rostral to each cavity. Note the dense vascular connective tissue (V) between the nasal cartilages.

Figure 13-4. Photographs of serial transverse sections through the external nares, vestibule and nasal cavity, 79KK1. X0.22

- A. The rostralmost serial section of the series. Note the cutaneous (E) covering. The paired nasal cartilages (C) are just becoming evident in the ventral aspect of the section. Note the narial sphincter (NS) of specialized blubber with cut bundles of skeletal muscle (arrows). Only the rostradorsal portions of the vestibule (V) are evident.
- B. The second serial section moving caudally. Note the increased depth of the vestibule and nasal cavity (CV). The narial sphincter (NS) tissue is seen with its muscle fibers. The nasal cartilages (C) are increased in height.
- C. and D. The third (C) and fourth (D) serial sections moving caudally. The nasal cartilages (C) are increased in height as the vestibule and nasal cavities (CV) extend through the entire depth of the sections. Narial sphincter (NS).
- E. The fifth section. Note the cartilages (C) are now inclined near the epidermis and are pleated. The narial sphincter (NS) is more circular in appearance.
- F. The sixth section. The nasal cartilages (C) are more pleated, curve laterally and decline in height.
- G. The caudalmost aspect of the external nares which we examined. Note the extensive pleating (C) of the nasal cartilages which nearly surround the nasal cavities (arrowheads) emerging ventrally.



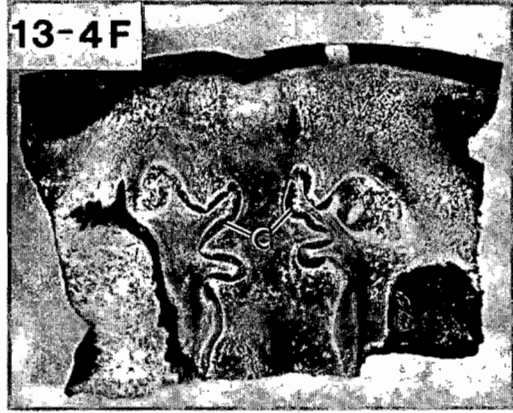
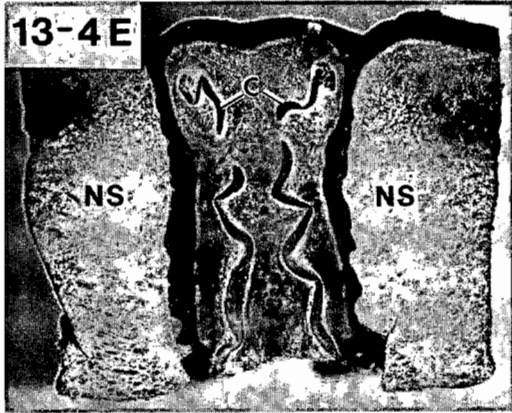
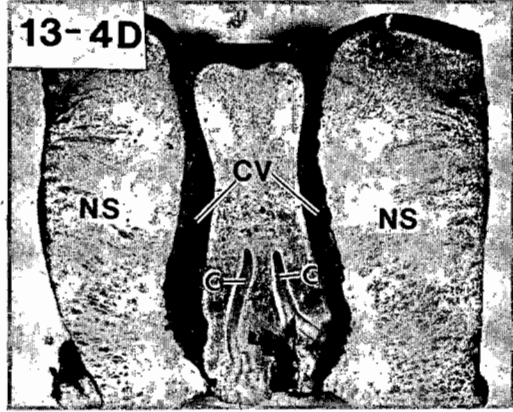
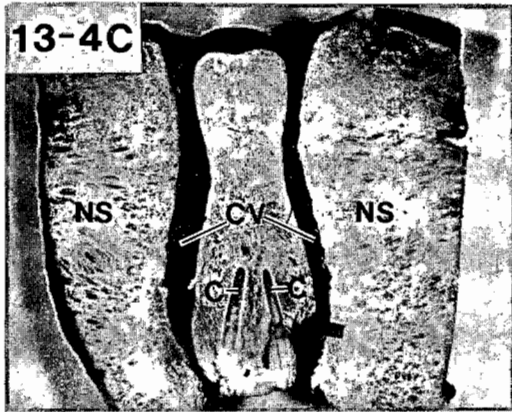
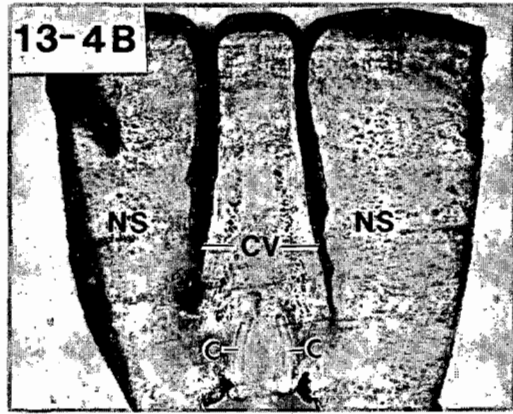
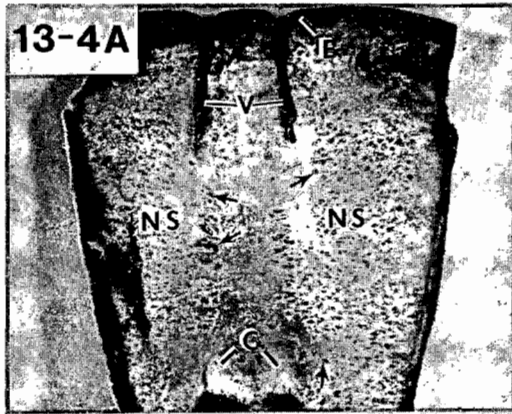


Figure 13-5. Photomicrograph of the nasal mucosa of 79KK1 at 20 cm into the vestibule from the body surface. The mucosal epithelium (E) is keratinized stratified squamous covering dense irregular connective tissue of the lamina propria (LP). Vascularized connective tissue papillae (P) interdigitate with the epithelium. L.S.\*, H and E, X50

Figure 13-6. Higher magnification photomicrograph of the stratum corneum of Fig 13-5. The surface cell layers (stratum corneum) are of the typical flattened keratinized squamous type, the same as occurs in any moist keratinized stratified squamous epithelium in terrestrial mammals. Cell junctions (arrows) are barely discernible and the pyknotic nuclei (Nu) have not disappeared completely in the lower layers. X.S.\*, H and E, X320

Figure 13-7. Photomicrograph of the interseptal tissue of 79KK1 taken 18 cm below the body surface. Dense irregular connective tissue (DCT) contains aggregations of adipose cells (AC) in a lower proportion than seen in blubber (see Fig 13-9A). Several fascicles of tendinous connective tissue (T), arteries (A), veins (V) and nerve tracts (N) are also present. X.S., H and E. X130

\*L.S. = longitudinal section, X.S. = transverse section

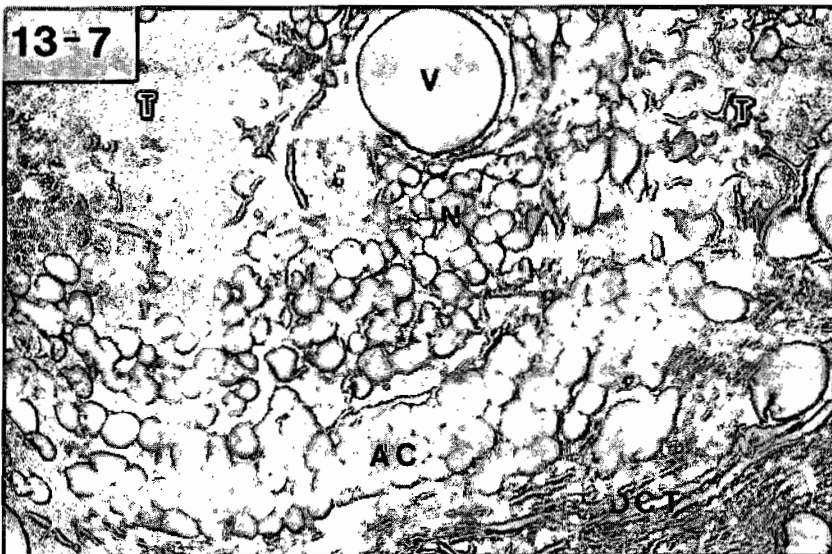
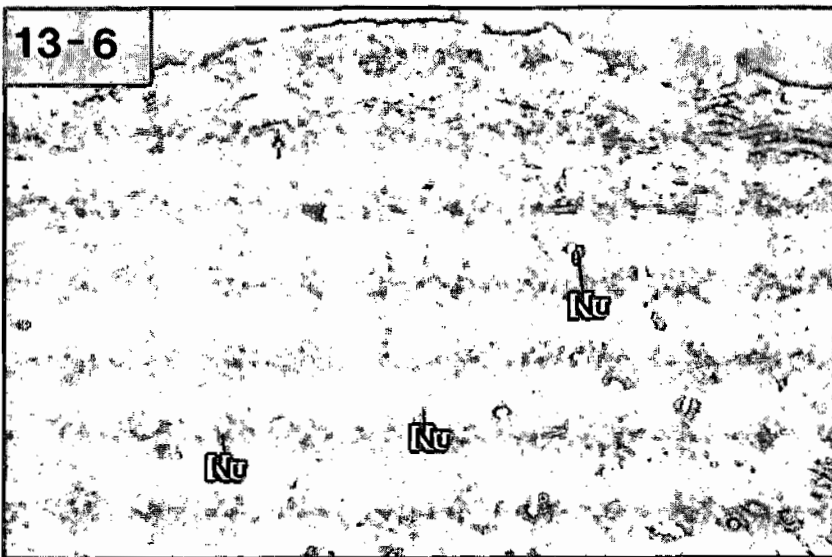
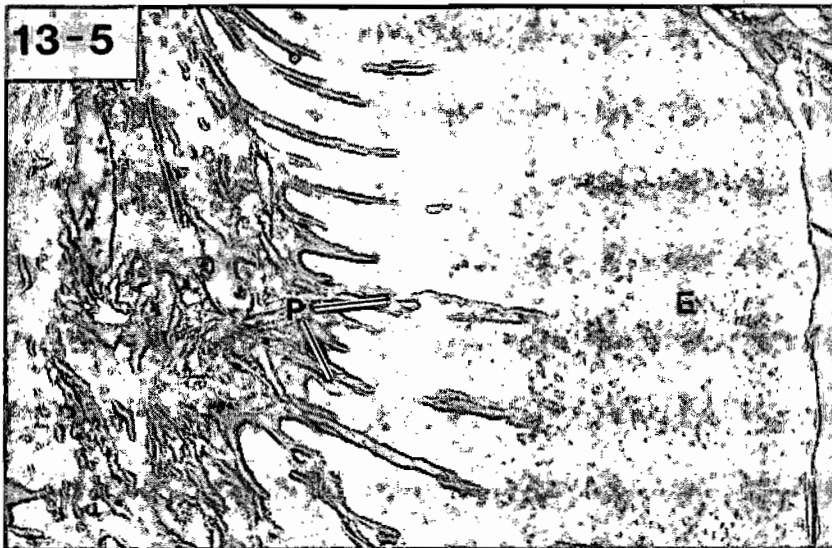


Figure 13-8. Photograph of a lateral view of the narial sphincter, 79KK1. Note the circular arrangement of the mass of blubber (B) extending nearly to the epidermis (E). The skeletal muscle fibers (arrows) have been cut from their attachment to the maxillae. Rostral (R).

Figure 13-9. Photomicrographs of the narial sphincter, 79KK1.

- A. Low magnification of a transverse section of the narial sphincter at 6.5 cm below the body surface and 9.5 cm lateral to the vestibule. The sphincter is specialized blubber with abundant adipose connective tissue (AC) laced with dense irregular connective tissue (DCT). Numerous 2-4 mm diameter fascicles of skeletal muscle (SK) permeate the entire mass apparently pulling the lateral wall of the vestibule laterad when contracted to open the nostril. L.S., H and E, X21
- B. Higher magnification of one skeletal muscle fascicle from Fig 13-9A. Individual skeletal muscle fibers (SKF) are of the light muscle type with myofibrils and peripherally located nuclei (Nu). L.S., H and E, X130
- C. High magnification of a longitudinal section through a muscle bundle of the narial sphincter of 79KK1. The striations (arrows) verify that the fibers are skeletal in type. L.S., H and E, X260

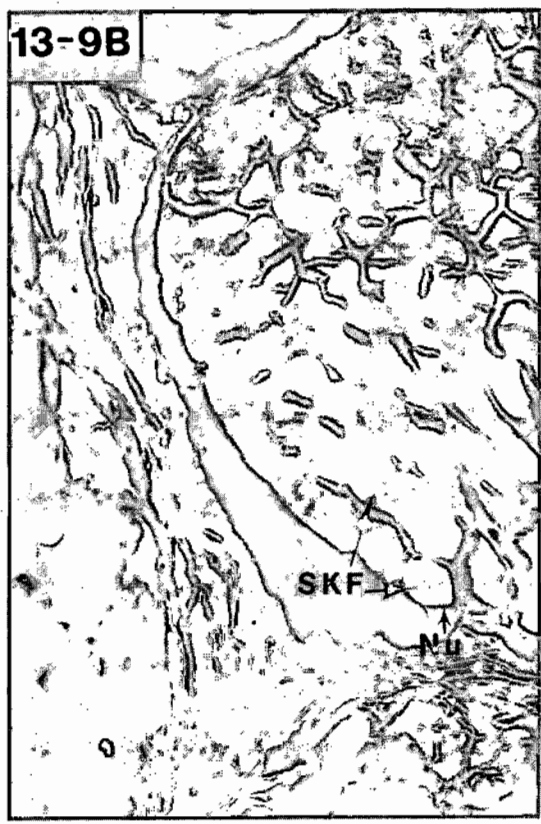
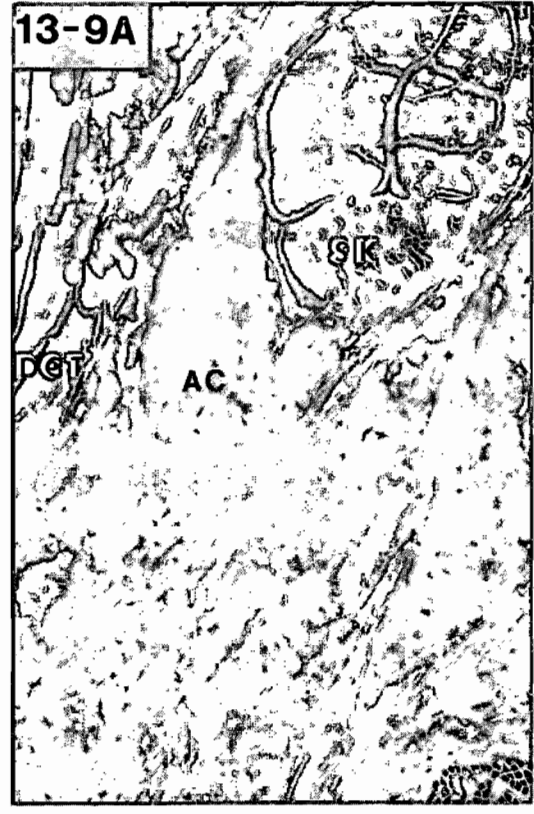


Figure 13-10. Photographs of the rostral end of the larynx, caudal portion of the palatopharyngeal sphincter and the pharyngeal wall, 79B1.

- A. Partial view of the pharynx and rostral larynx. The epiglottic cartilage (E) with its median pyramidal eminence (M) is seen fitting tightly up between the arytenoid cartilages (A) effecting a sealing anatomical closure. The cut palatopharyngeal sphincter (S) partially obscures the pharyngeal opening (arrowhead) of the esophagus. The short aryepiglottic fold (Ae) attaches the arytenoid cartilage to the epiglottic cartilage. X0.85
  
- B. Drawing of the rostral larynx. The median pyramidal eminence (M) of the epiglottic cartilage (E) serves as a sealing device when the whale swallows. The muscular palatopharyngeal sphincter (S) in the caudal soft palate lies rostradorsal to the esophageal opening (arrowhead). Aryepiglottic fold (Ae), corniculate processes (C) of the arytenoid cartilages, caudal pharyngeal wall (W).
  
- C. Oblique view of the rostral larynx. The corniculate processes (C) of the arytenoid cartilages (A) curve dorsally forming the dorsolateral rim of the laryngeal opening. Soft palate (P), epiglottic cartilage (E). Note raised areas on pharyngeal surface ventral to the epiglottic cartilage which are openings of glands (G). X0.9

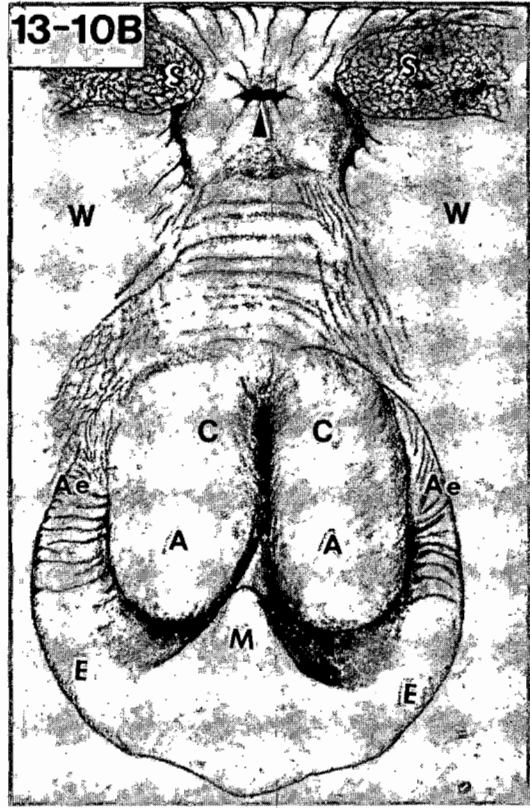


Figure 13-11. Composite drawing of the laryngeal cartilages using parts from 80B1 and 79B1. The lightly stippled area(S) represents parts which we did not have. The arytenoid cartilages (A) extend the complete length of the larynx. Corniculate process (Cp) of the arytenoid cartilage, epiglottic cartilage (E), cricoid cartilage (C), thyroid cartilage (T), caudal cornu (CC) and cranial cornu (Cr) of the thyroid cartilage. Rostral (R).



13-11

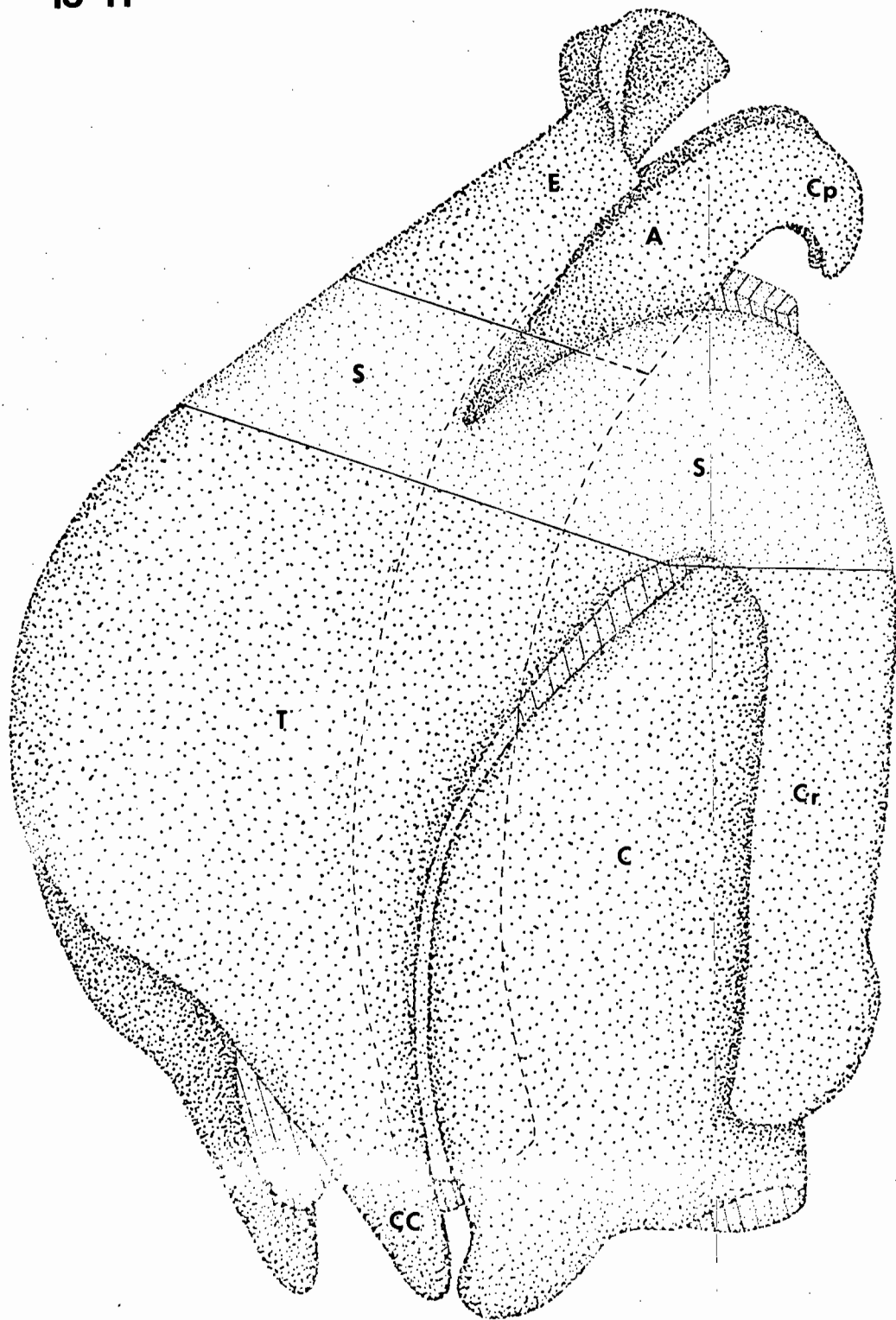
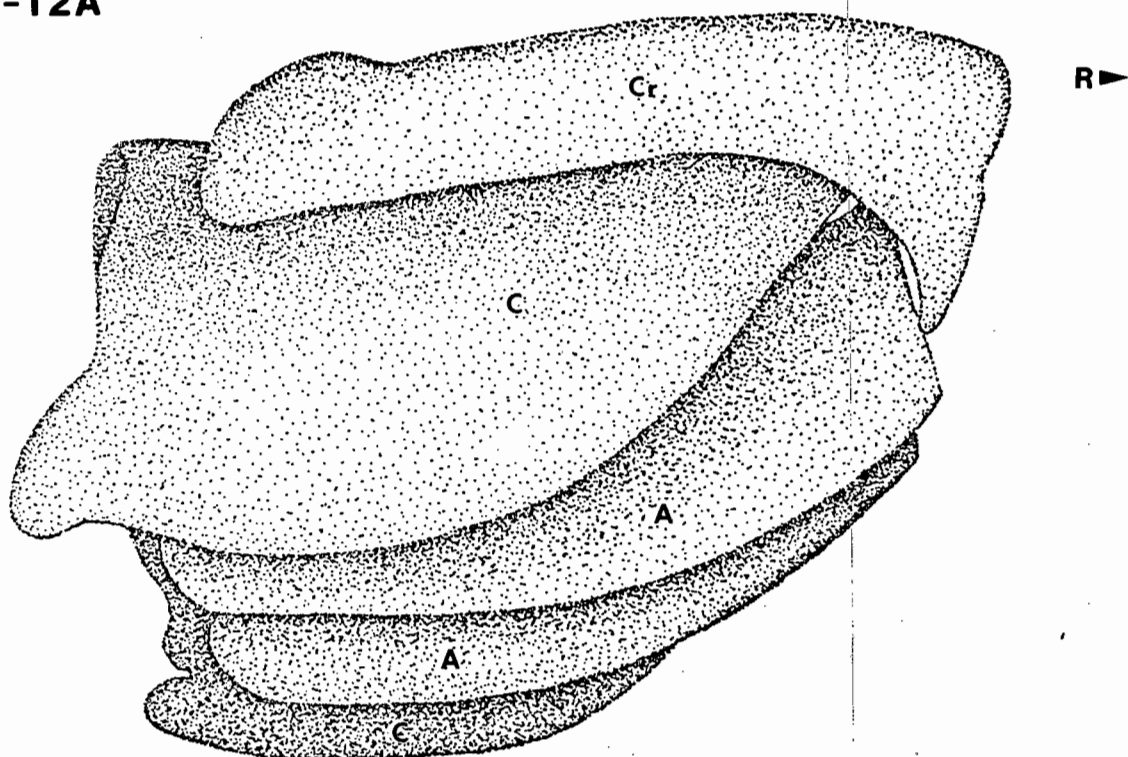


Figure 13-12. Composite drawings of the arytenoid, cricoid and thyroid cartilages of 80B1.

- A. Ventrolateral view showing the position of the arytenoid cartilages (A) in relationship to the cricoids (C) and the cranial cornu (Cr) of the thyroid cartilage. Rostral (R).
- B. Cranioventral view showing the cricoid (C) cartilage is trough-shaped and not signet ring shaped. The rostral portion of the cricoid cartilage is a flattened plate. The thyroid cartilage (T) serves as a ventral floor of the larynx. Cranial cornu (Cr), of the thyroid cartilage arytenoid cartilage (A).

13-12A



13-12B

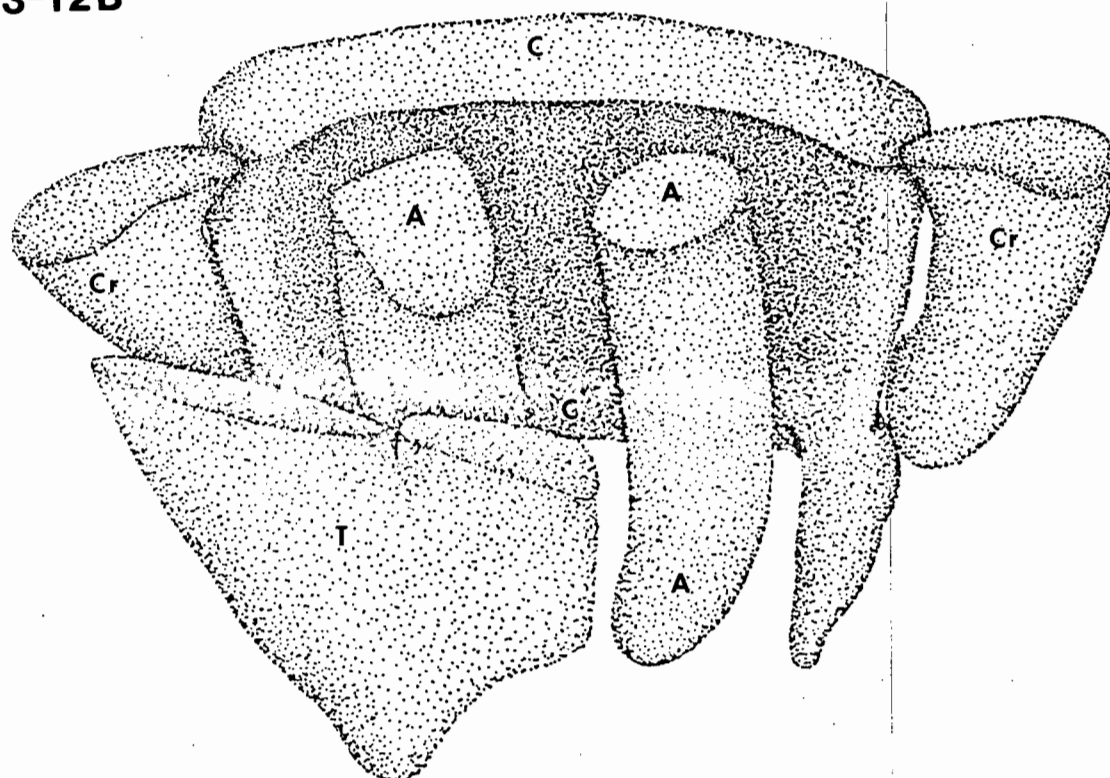
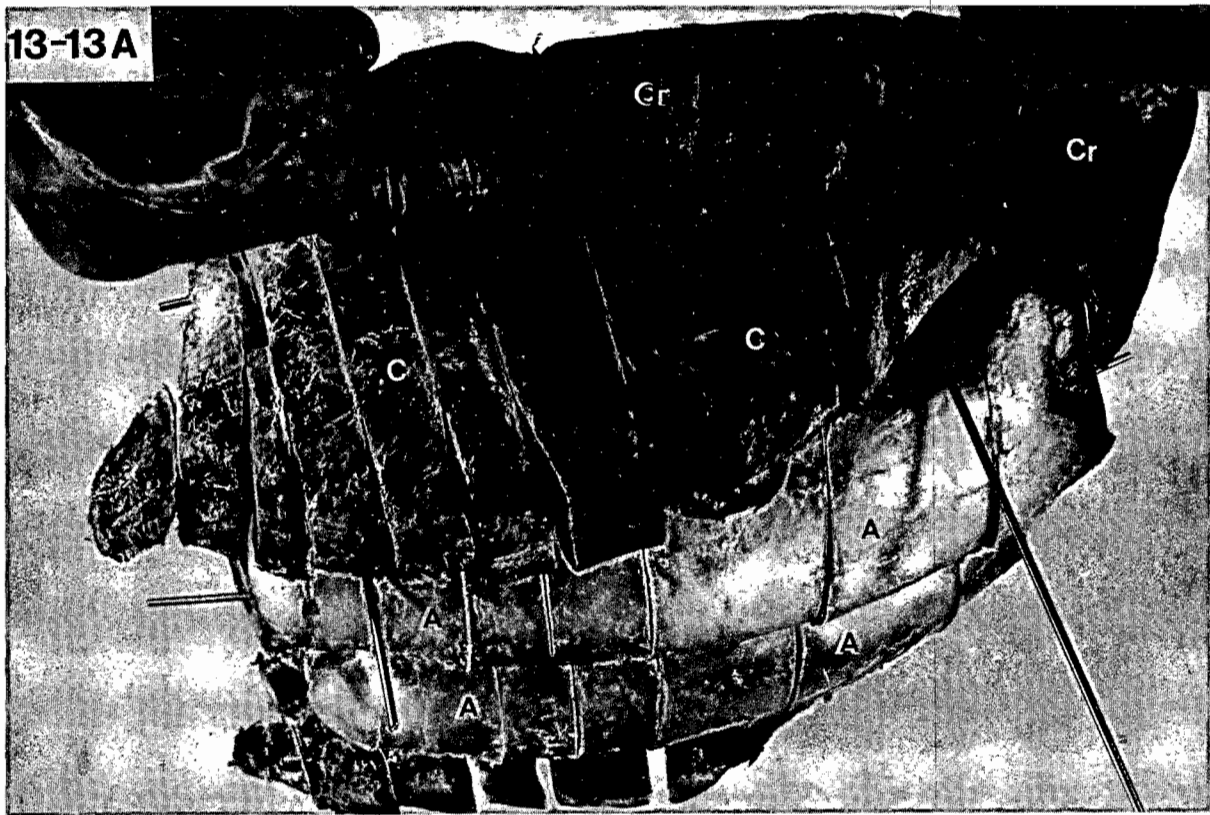


Figure 13-13. Photographs of the reconstruction of the serially sectioned cricoid, arytenoid and the thyroid cartilages.

- A. Right ventral, lateral view showing the relationship of the cricoid (C), arytenoid (A) and cranial cornu (Cr) of the thyroid cartilage. X0.5
  
- B. Cranioventral view. Note the arytenoid cartilages (A) are not fused caudally (N). The thyroid cartilage (T) forms the floor of the larynx. C - cricoid; Cr - cranial cornua of the thyroid cartilage. X0.5

13-13A



13-13B



Figure 13-14. Photographs of the corniculate process of the right arytenoid cartilage, 79B1.

- A. Lateral view. The corniculate process (Cp) curves dorso-medially as the rostradorsal end of the right arytenoid cartilage (A). R - rostral X1
- B. Drawing of the corniculate process (Cp) of the right arytenoid cartilage (A).
- C. Dorsal view. The corniculate process (Cp) of the arytenoid cartilage extends rostral to the cricoid cartilage (C). Caudal extensions of cranial cornua of the thyroid cartilage (Cr). X0.35

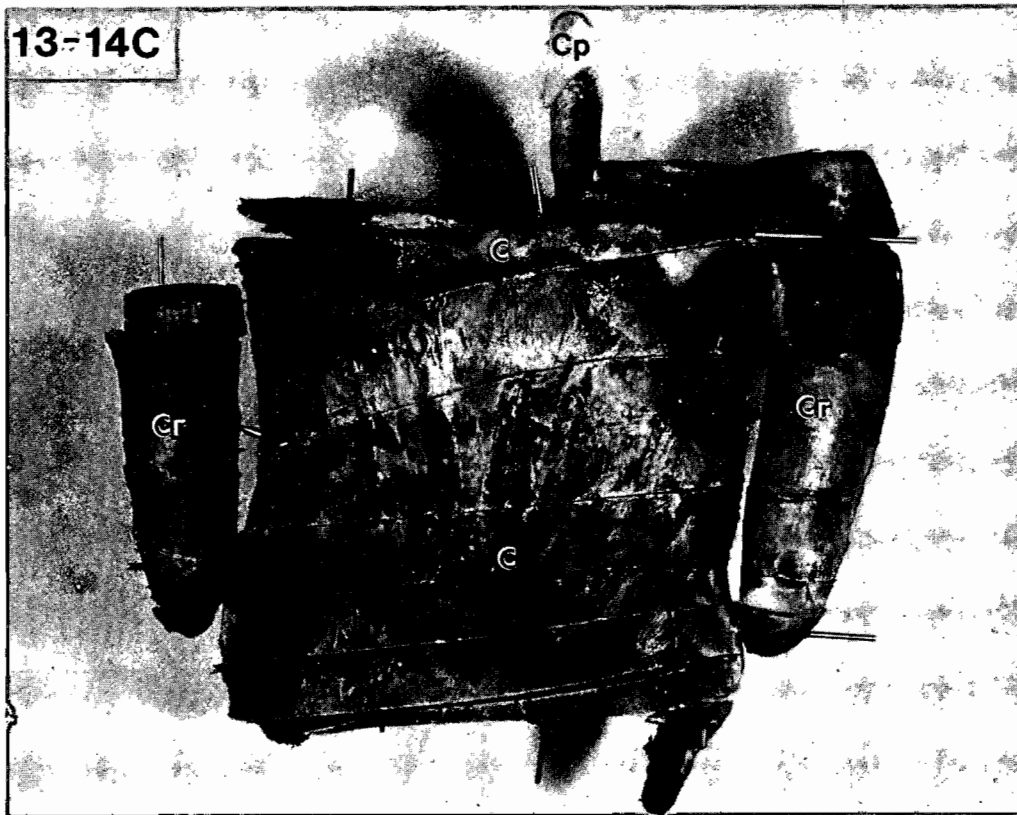
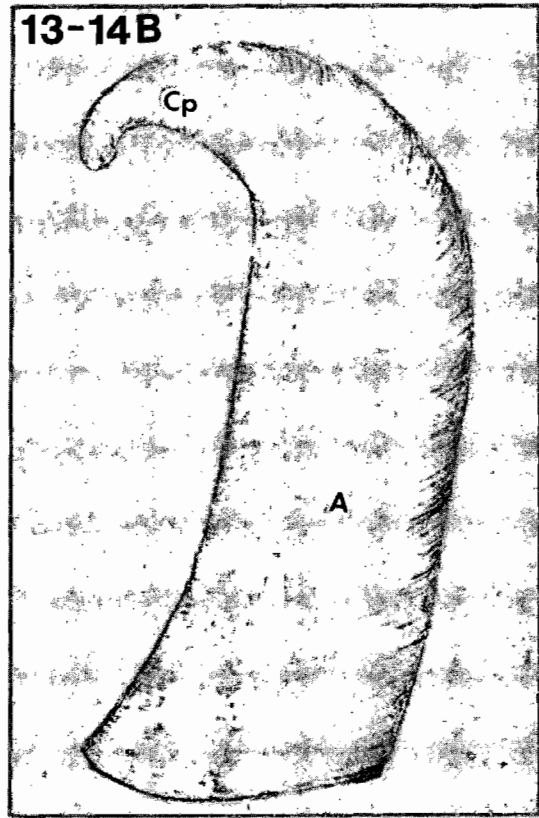
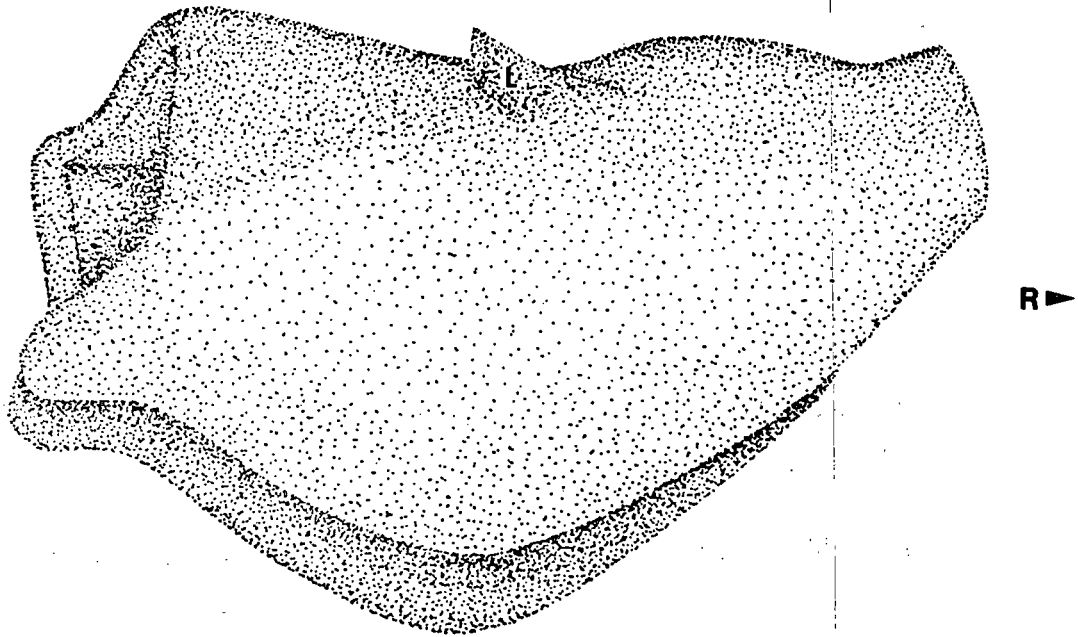


Figure 13-15. Drawings of reconstructions of serially sectioned cricoid and thyroid cartilages, 80B1.

- A. Right lateral view. The cricoid cartilage is trough shaped with the ventral aspect open. Note the ligament (L) for the attachment of the caudal end of the right cranial cornua of the thyroid cartilage. Rostral (R)
  
- B. Left lateral view. Thyroid cartilages form a shallow wedge as the right (R) and left (L) cartilages fuse on the midline (arrowheads). Prominent caudal cornua (Cc) attach to the connective tissue covering the laryngeal sac muscle. Rostral (R)



13-15A



13-15B

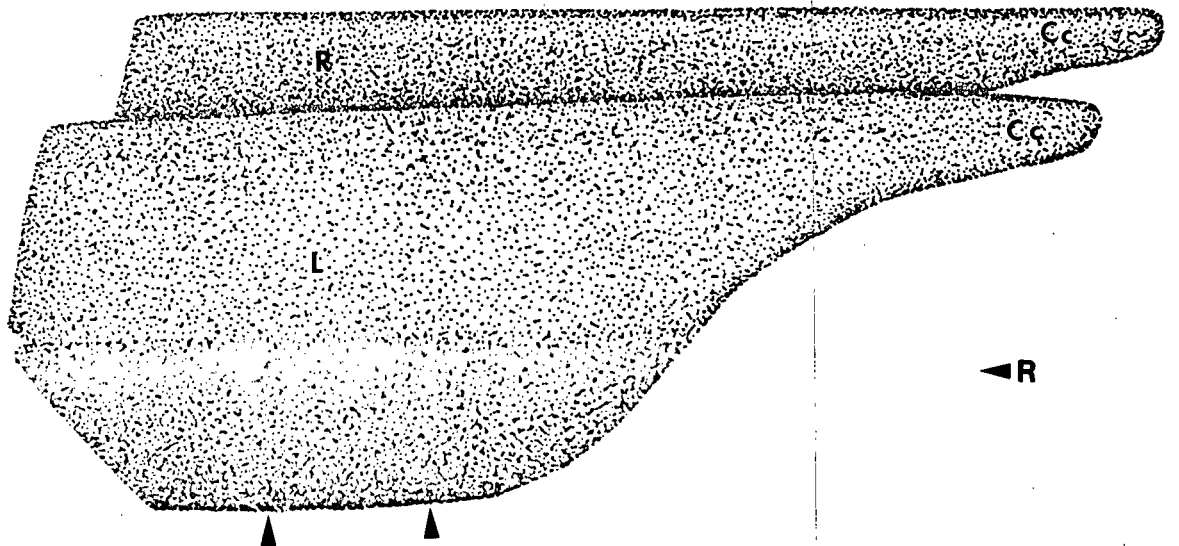
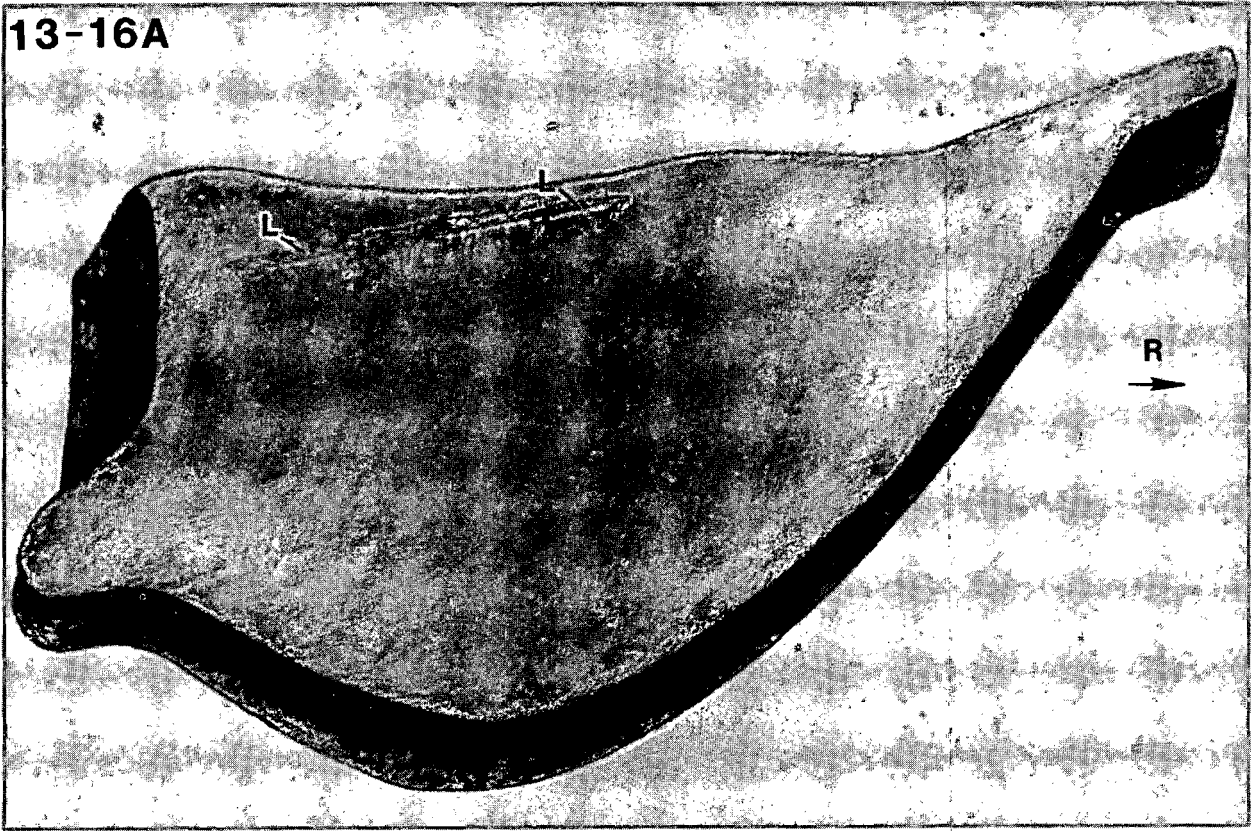


Figure 13-16. Photographs of a drawing of the cricoid and of the thyroid cartilages.

- A. The conception of the entire cricoid cartilage (79B1). Note it begins rostrally (R) as a flattened plate and becomes trough shaped caudally. Note the cut ligament (L) which serves for attachment of the caudal ends of the cranial cornu of the thyroid cartilage.
  
- B. Thyroid cartilages, dorsal view 80B1. Note the caudal cornua (Cc) and the transected skeletal muscle (S) (cricothyroid muscle) on each side of the midline (arrowheads). The left caudal cornu is incomplete. X0.14
  
- C. Thyroid cartilages, ventral view (80B1). Caudal cornua (Cc), ventral midline (arrowheads). X0.16.

13-16A



13-16B



13-16C

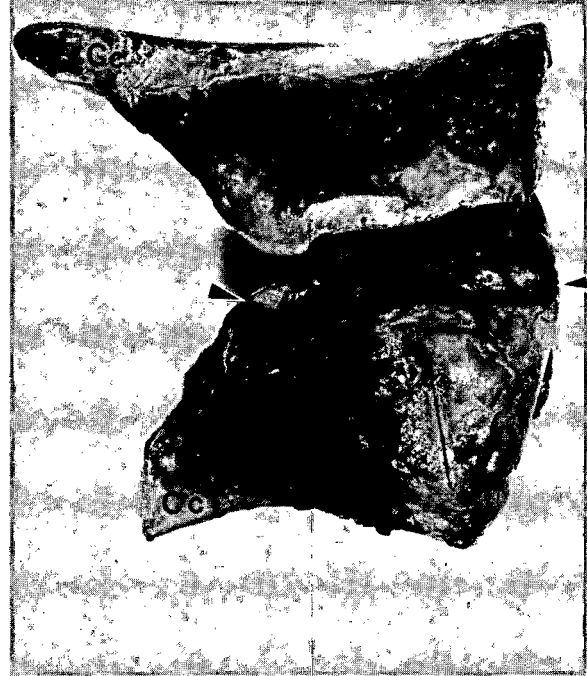


Figure 13-17. Photograph showing that the caudal cornua of the thyroid cartilages attach (arrowheads) via tough connective tissue sheets to the laryngeal sac muscle (M) at the level of the second tracheal ring, 80B1. The arytenoid cartilages (A) are connected caudally by dense connective tissue (Ct). Primary Bronchi (P). X0.4

13-17



Figure 13-18. Photomicrograph of the mucosal layer of the rostral extension of the epiglottis, 79B1. The epithelium (E) is pigmented, keratinized, stratified squamous with vascularized connective tissue papillae (P) and periodic sensory papillae (SP). The lamina propria (LP) is typical dense irregular connective tissue with elastic fibers, blood vessels, nerve tracts, and adipose cells. L.S., H and E, X50

Figure 13-19. Higher magnification photomicrograph of the sensory papilla of Fig 13-18. The normal layers of the keratinized stratified squamous epithelium show well as stratum basale (B), stratum spinosum (S), and the keratinized stratum corneum (C). The sensory papilla is composed of one or more convoluted and elongated Herbsti-like encapsulated nerve end organs (arrows) surrounded by dense irregular connective tissue. L.S., H and E, X130

Figure 13-20. Photomicrograph of the ventral (outer) mucosa of the epiglottis, 79B1.

- A. The deep propria submucosa (PS) contains mucoserous glands (arrowheads). A large excretory duct (D) is seen near the epidermis (E). X.S., Masson's stain, X50
- B. Serous demilunes (arrowheads) are seen on the periphery of mucous acini (A) in the glands from Figure 13-20A. X.S. Masson's stain, X320

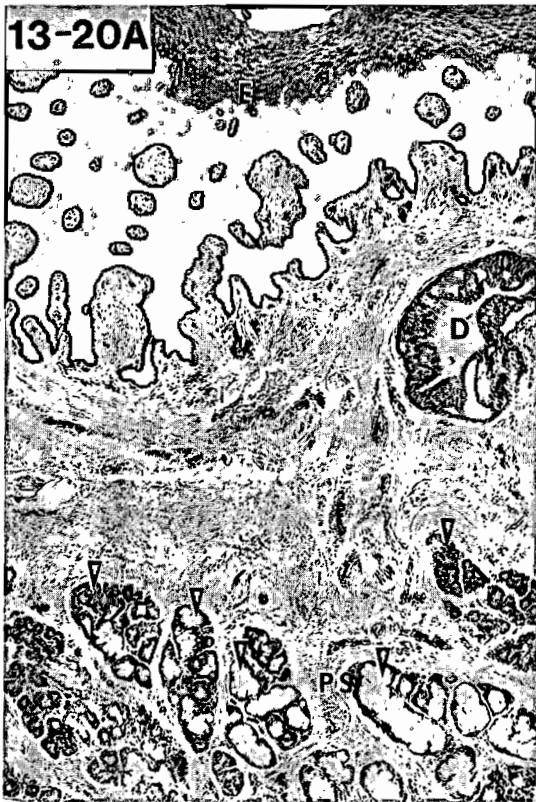
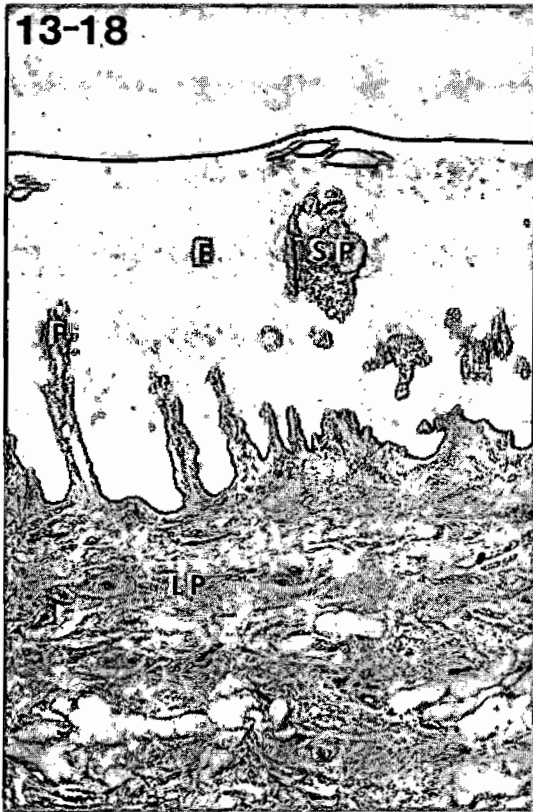


Figure 13-21. Photomicrograph of the mucosal layer and hyaline cartilage of the mediorostral surface of the left arytenoid of 79B1. The mucosa is typical dense irregular connective tissue (CT) with elastic fibers, blood vessels, and nerve tracts covered by a pigmented, keratinized, stratified squamous epithelium (E) as on the epiglottis (Fig 13-18). Enlarged sensory papillae (SP) are interspersed with connective tissue papillae (P). The arytenoid cartilage (HC) is of the hyaline type with vascular channels (VC) filled with blood vessels and loose connective tissue. L.S., H and E, X21

Figure 13-22. Higher magnification photomicrograph of the sensory papilla (SP) in Fig 13-21. The elongated and convoluted nature of the Herbsti-like sensory, encapsulated, nerve end organ (arrow) shows well. The layers of the epithelium can be seen: stratum corneum (C), stratum spinosum (S) and stratum basale (B).



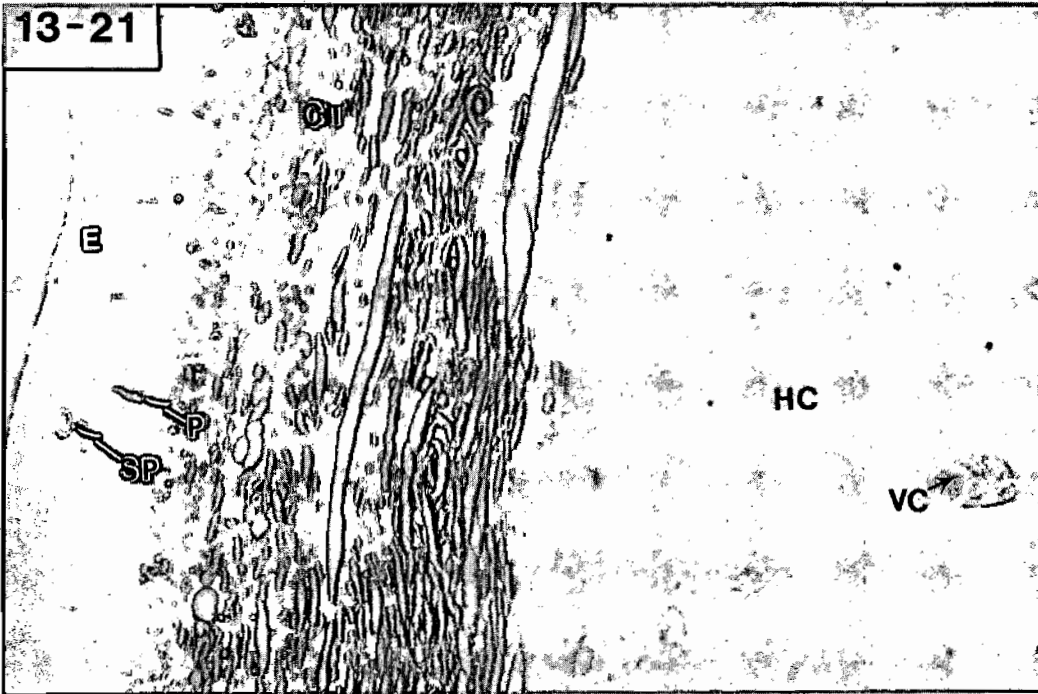
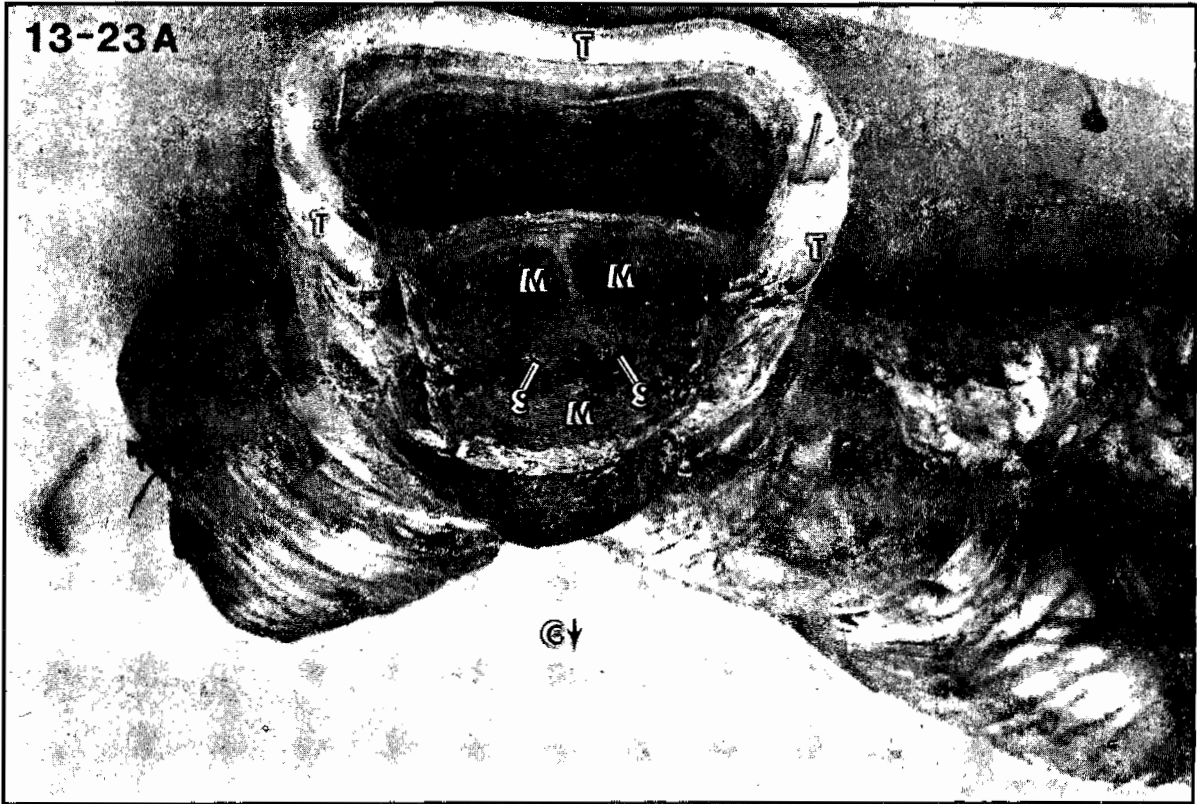


Figure 13-23. Photographs of the trachea and laryngeal sac, 80B1.

- A. Cranial view. This reconstruction of serial sections shows the laryngeal sac (S) to be a caudal diverticulum of the caudal portion of the laryngeal cavity. It has a heavy muscular wall (M) which serves to close the ventral open portions of the "C" shaped tracheal cartilages (T). Caudal (C). X0.04
  
- B. This section is through the midportion of the laryngeal sac (S) which is surrounded by the laryngeal sac muscle (M). The "C" shaped tracheal cartilages (T) are seen. X0.5

13-23A



13-23B

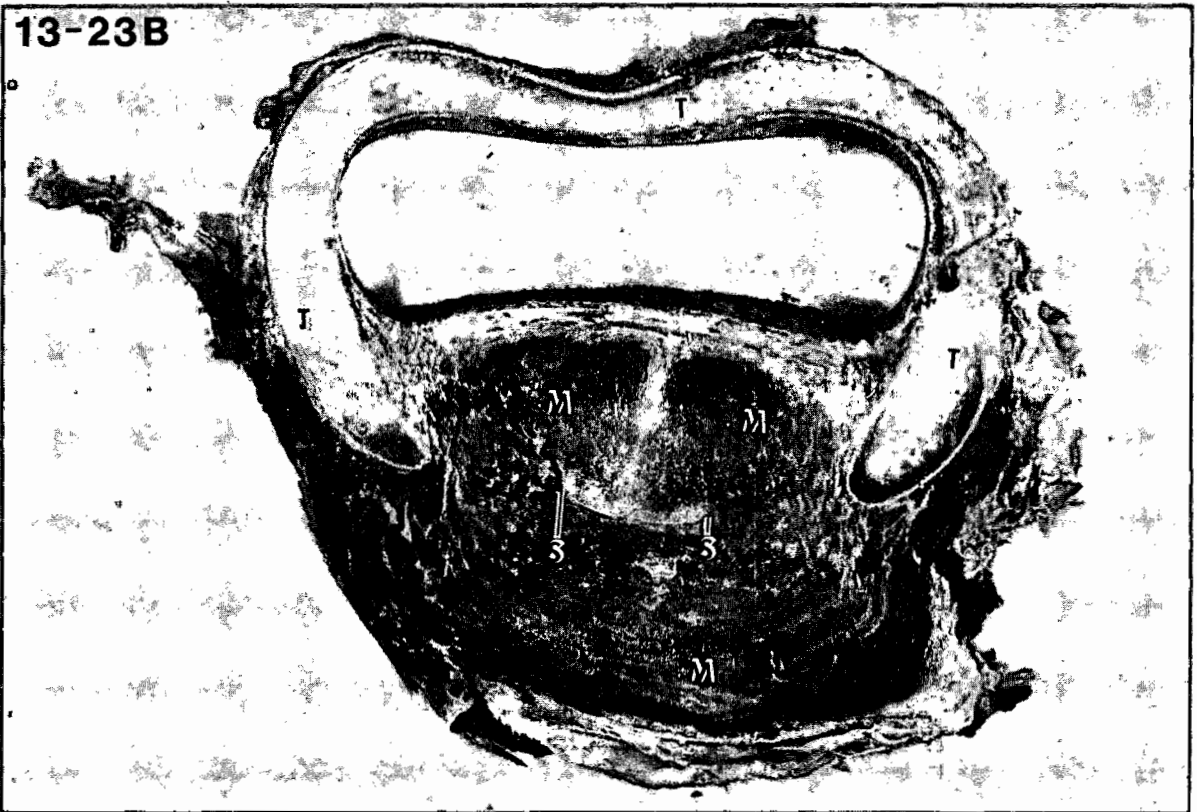
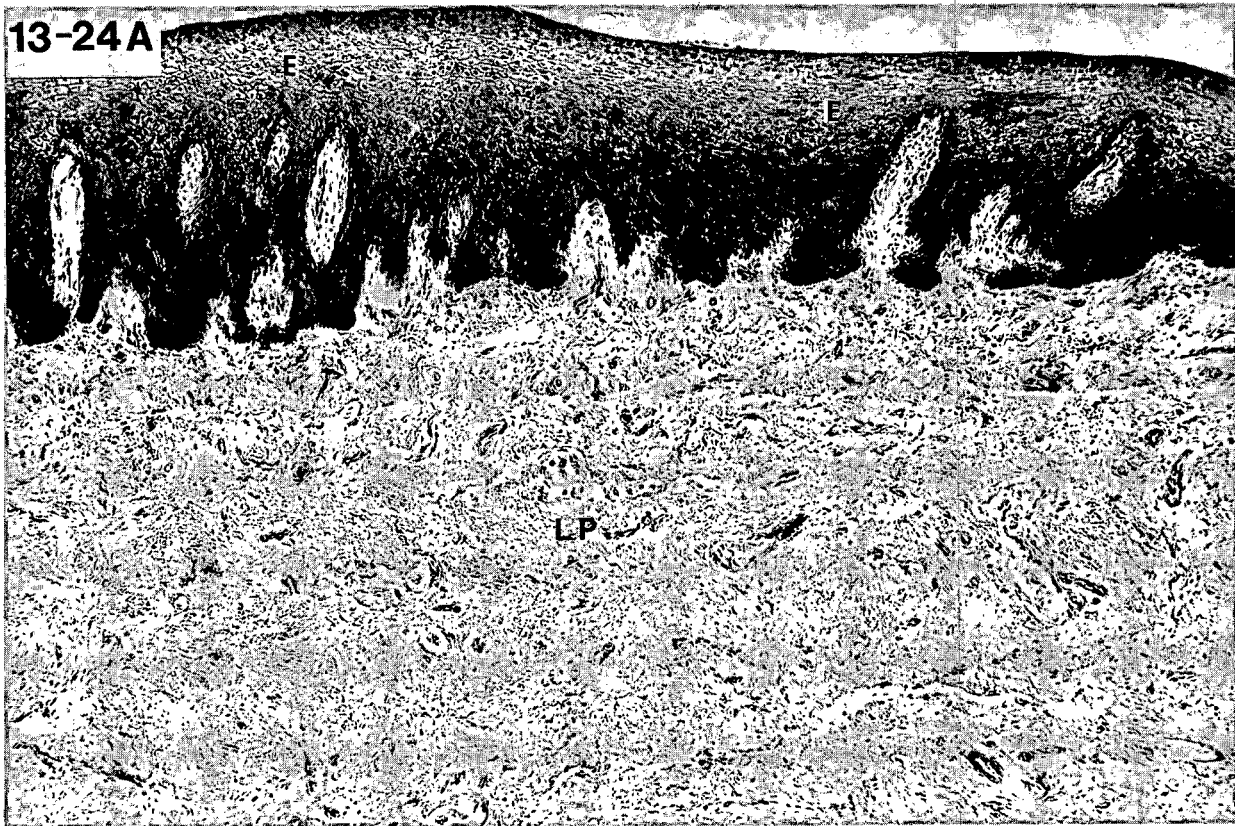


Figure 13-24. Photomicrographs of the laryngeal sac microanatomy, 80B1.

- A. The laryngeal sac is a mucous membrane lined diverticulum. The epithelium (E) is stratified squamous. The lamina propria (LP) is dense irregular connective tissue with increased amounts of elastic fibers which overlays the laryngeal sac muscle. (not shown) X.S, Masson's stain. X50
  
- B. The wall of the sac has skeletal muscle bundles (arrows). Adipose cells (A). X.S., Masson's stain. X530

13-24A



13-24B

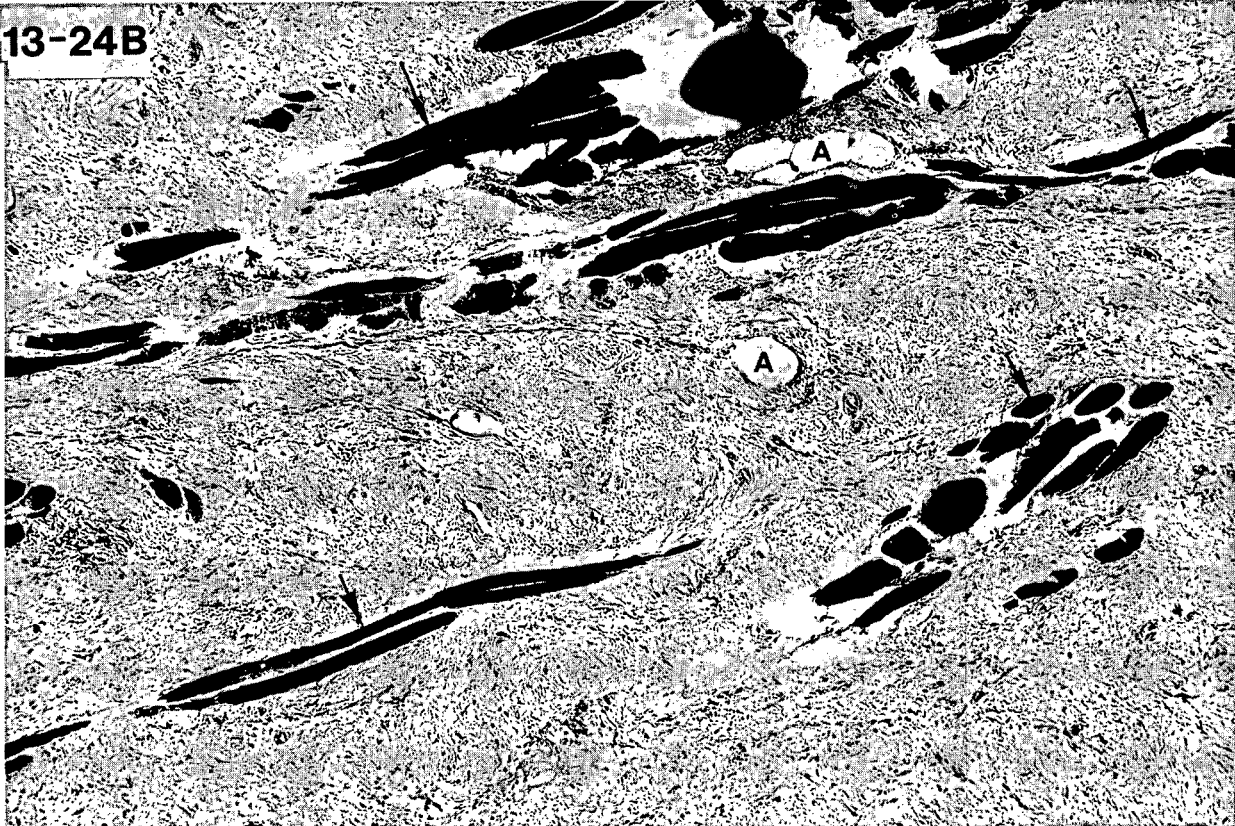
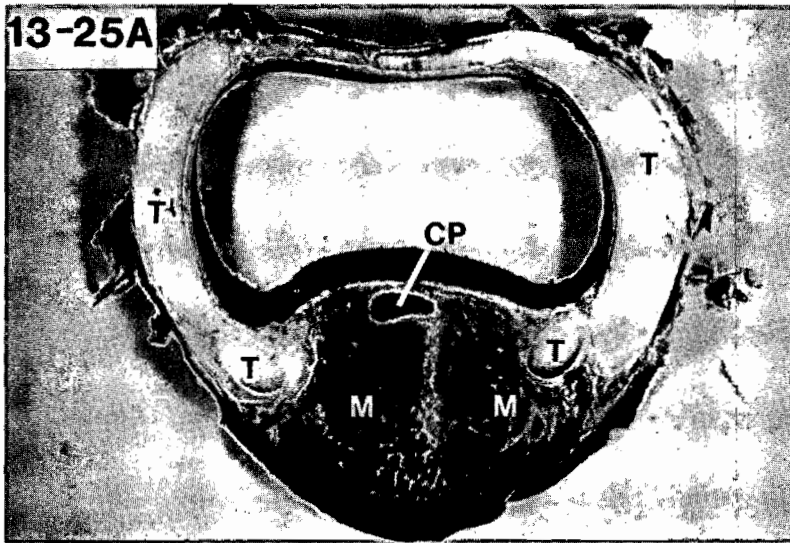


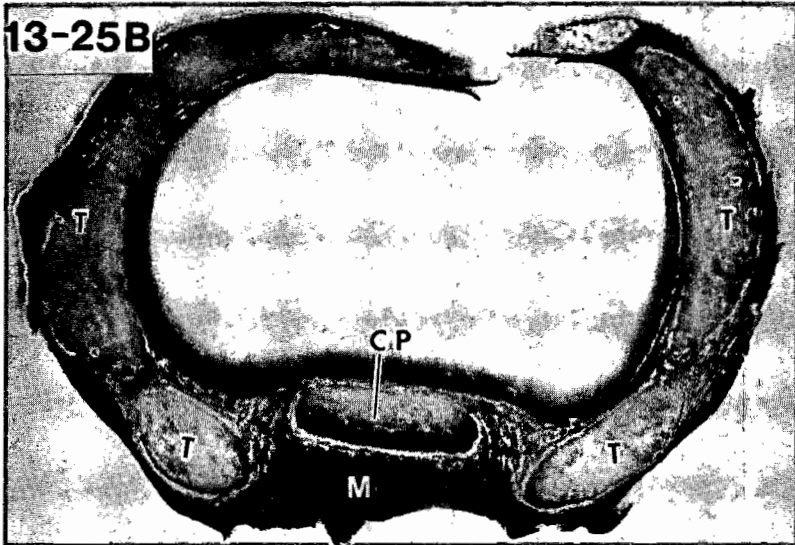
Figure 13-25. Photographs showing the caudal one-third of the ventral trachea is closed by a cartilaginous plate, dense connective tissue and muscle, 80B1.

- A. The rostralmost tip of the cartilaginous plate (CP) is surrounded by laryngeal sac muscle (M). Tracheal cartilages (T). X0.35
  
- B. The middle portion of cartilaginous plate (CP) surrounded by laryngeal sac muscle (M). Tracheal cartilages (T). X0.4
  
- C. The caudal portion of cartilaginous plate (CP). Laryngeal sac muscle (M), overlapping tracheal cartilages (T), lumen of right principal bronchus (P). X0.4

13-25A



13-25B



13-25C

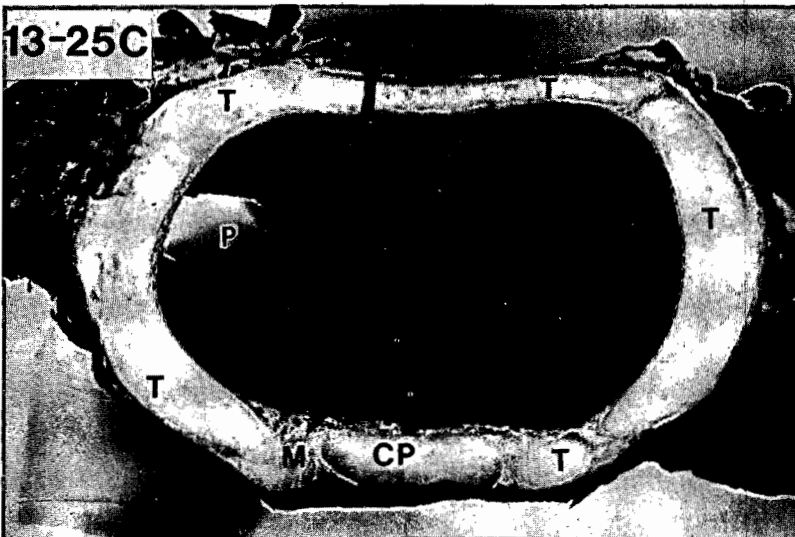


Figure 13-26. Photomicrographs of a longitudinal section of the larynx near the laryngotracheal junction, 80B1.

- A. The laryngeal epithelium (E) is nonkeratinized stratified squamous changing to ciliated pseudostratified columnar epithelium of the laryngotracheal junction. The lamina propria (LP) has lymphatic nodules (N) just deep to the epithelium which is underlain by a dense irregular connective tissue. The connective tissue has abundant elastic and collagen fibers and some adipose cells (A). L.S., H and E, X50
  
- B. Higher magnification of the lymph nodule (N) in Figure 13-26A. Labels as above. L.S., H and E, X130

Figure 13-27. Photomicrographs of a longitudinal section of the trachea at the laryngotracheal junction, 80B1.

- A. The tracheal epithelium at the laryngotracheal junction is primarily ciliated pseudostratified columnar epithelium (E), however, it is a transitional area from the stratified squamous epithelium of the larynx. The lymphatic (L) infiltration of the lamina propria (LP) is diffuse with only occasional nodular formation. The connective tissue is highly elastic. L.S., H and E, X50
  
- B. This is a higher magnification of Fig 13-27A illustrating the more diffuse nature of the lymphatic tissue (L) underlying the epithelium (E). LP - lamina propria. L.S., H and E, X130



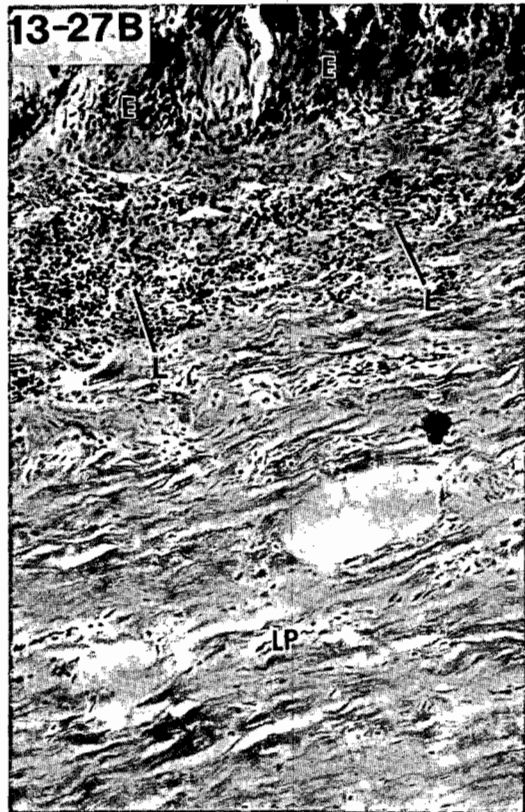
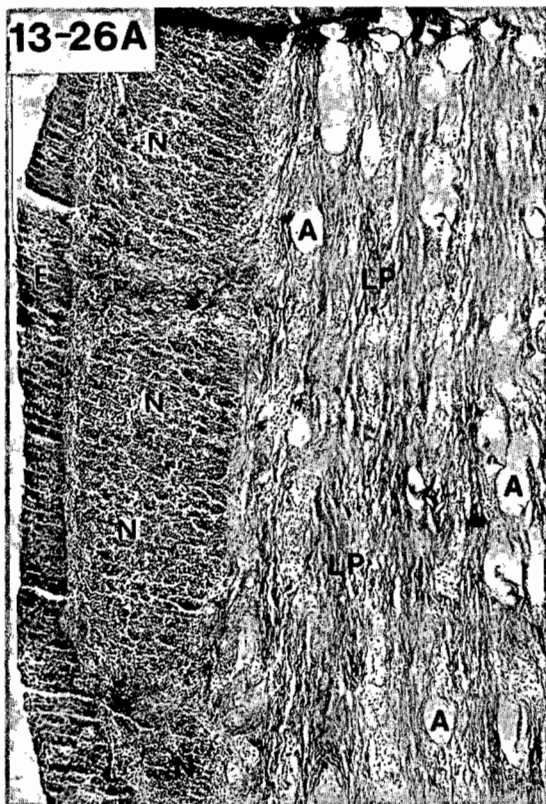


Figure 13-28. Photomicrographs of a longitudinal section of the mid-trachea, 80B1.

- A. The tracheal epithelium (E) at this level is ciliated pseudostratified columnar. The lamina propria has dense irregular elastic fibers (EF) and contains a 400  $\mu$ m layer of mucous glands (G). L.S., H and E. X50.
  
- B. Higher magnification of Fig 13-28A. Bundles of elastic fibers (EF) course through the mucous glands (G) which are just below the ciliated pseudostratified columnar epithelium (E). L.S., H and E. X130.
  
- C. Section through the junction of two tracheal cartilages (TC). Note the high percentage of elastic fibers (EF). L.S., Verhoeff stain. X50

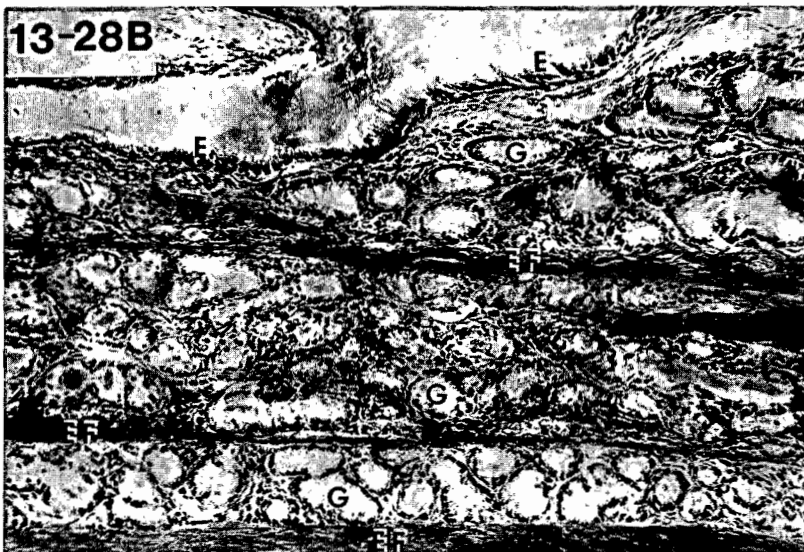
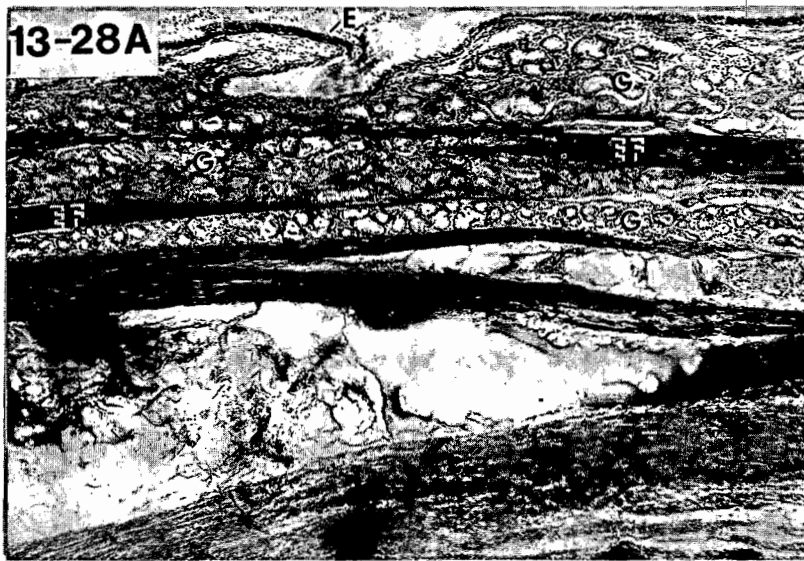


Figure 13-29. Photographs of the tracheal bifurcation, 80B1.

- A. A cranial view showing the lumina (L) of the principal bronchi (B). Trachea (T). X0.4
- B. A dorsal view of the slight depression (D) formed by the esophagus as it lies on the dorsal surface of the trachea. The tracheal cartilages (R) are open ventrally. Bronchi (B). X0.25
- C. A ventral view as the trachea (T) bifurcates 19 cm caudal to the cricoid cartilage. The principal bronchi (B) which result from the tracheal division have complete cartilaginous rings (R) which branch and anastomose. Laryngeal sac muscle (M). X0.75
- D. A ventral view demonstrating the ventrally open tracheal cartilages (C) but the complete principal bronchial rings (R). The open cartilages are closed by the laryngeal sac muscle (M) except where it has been removed. X0.25

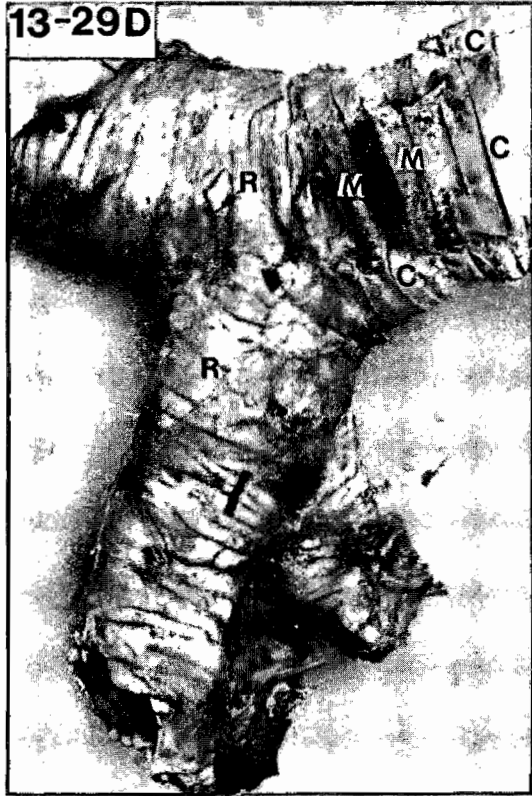
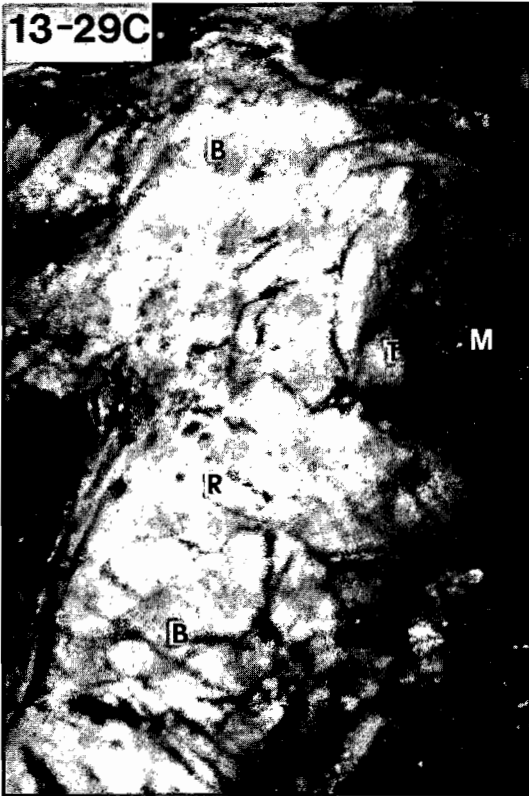
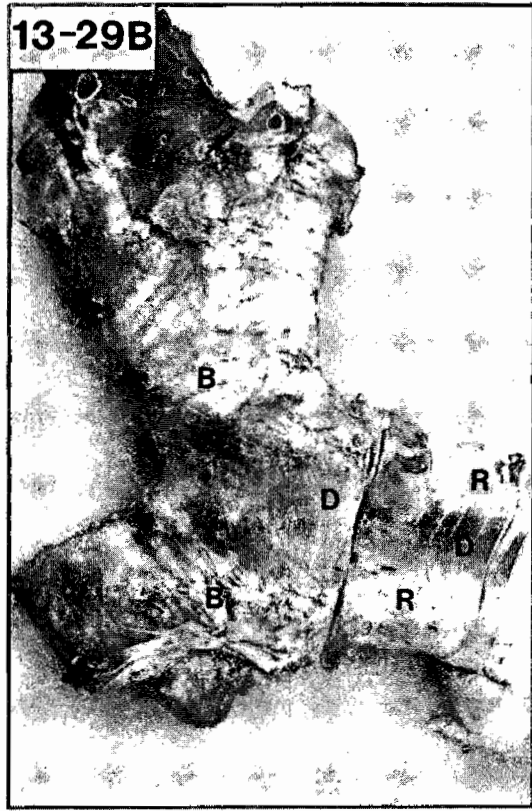


Figure 13-30. Photomicrograph of the mucosal lining of a primary bronchus of 38 x 95 mm size from 80B8 Tag 3. Ciliated pseudostratified columnar epithelium (Ep) lines the bronchus covering a dense irregular connective tissue lamina propria with mucosal mucous glands (G). Thick laminae of longitudinally oriented dense elastic fibers (E) are located between the lamina propria and the dense irregular connective tissue surrounded hyaline cartilage ring (not in picture). X.S., H and E, X130

Figure 13-31. Higher magnification photomicrograph of the mucosa in Fig 13-30. The mucus producing cells (arrows) of the pseudostratified columnar epithelium (Ep) and mucosal mucous glands (G) are well illustrated. The elastic lamina (E) is also illustrated. X.S., H and E, X320

Figure 13-32. Photomicrograph of a semi-thin section of the mucosa of the primary bronchus of 80B8 Tag 3. The mucous nature of the tall cells (M) is more visible. Tall surface cells reach the basement membrane (arrow). TEM (see Fig 13-33) provides the verification. The vascularity (V) of the dense irregular connective tissue (D) of the lamina propria is also visible. Epon, X.S., Toluidine blue stain, X160

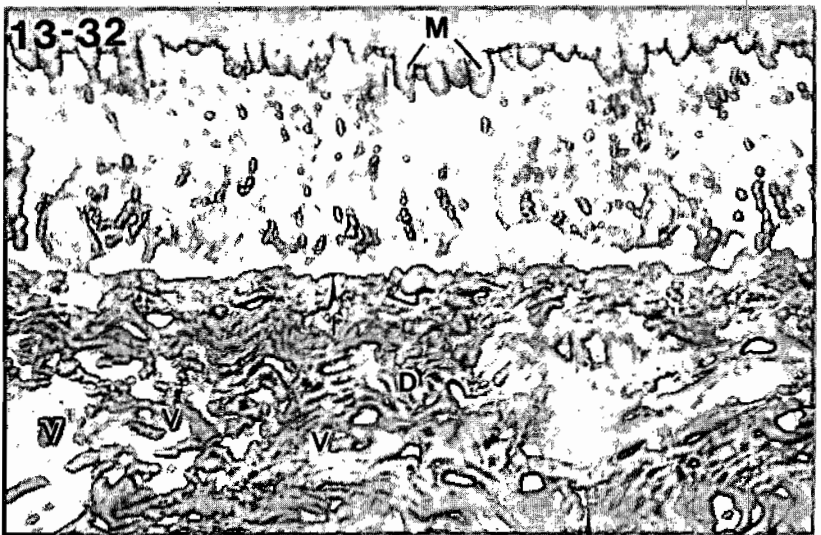
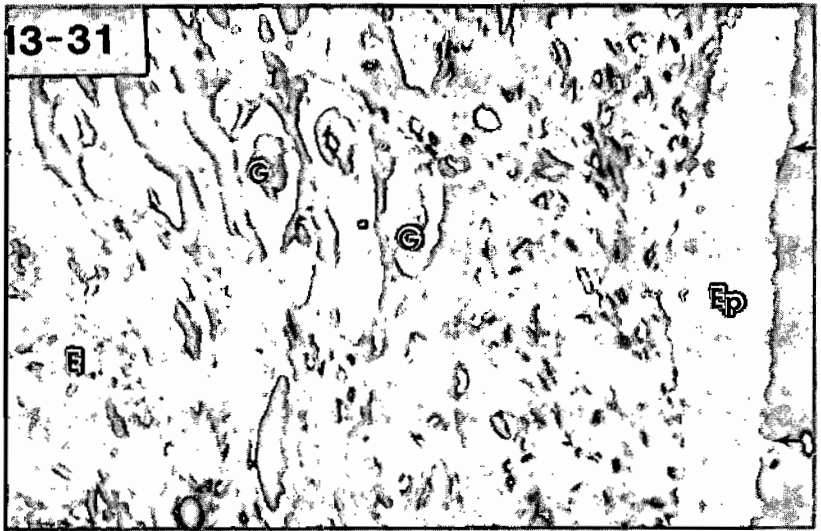
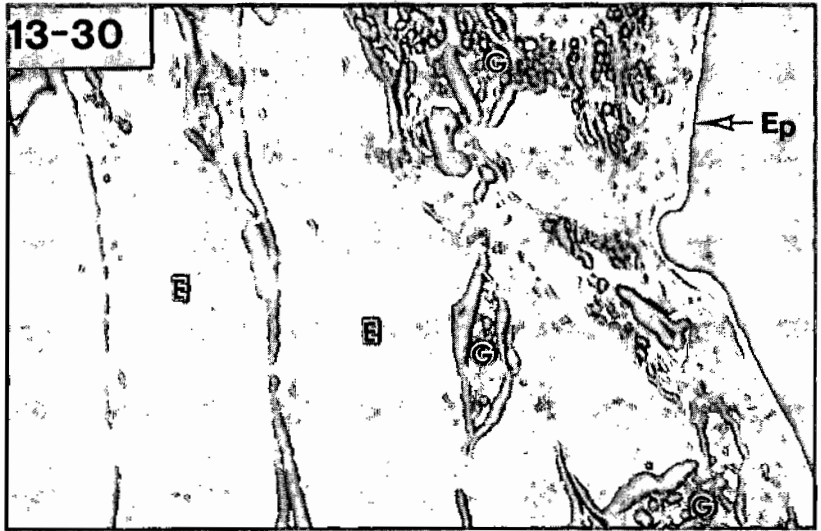


Figure 13-33. Scanning electron photomicrograph of a representative area of the surface of the primary bronchus of whale 80B8. Numerous ciliated cells (C) and nonciliated cells containing microvilli (NC) may be seen. The number of ciliated and nonciliated cells appear to be about equal. X3,800

Figure 13-34. Higher magnification scanning electron photomicrograph of a region similar to that seen in Fig 13-33. Nonciliated cells may be seen bulging from the surface with numerous microvilli (MV). X7,500



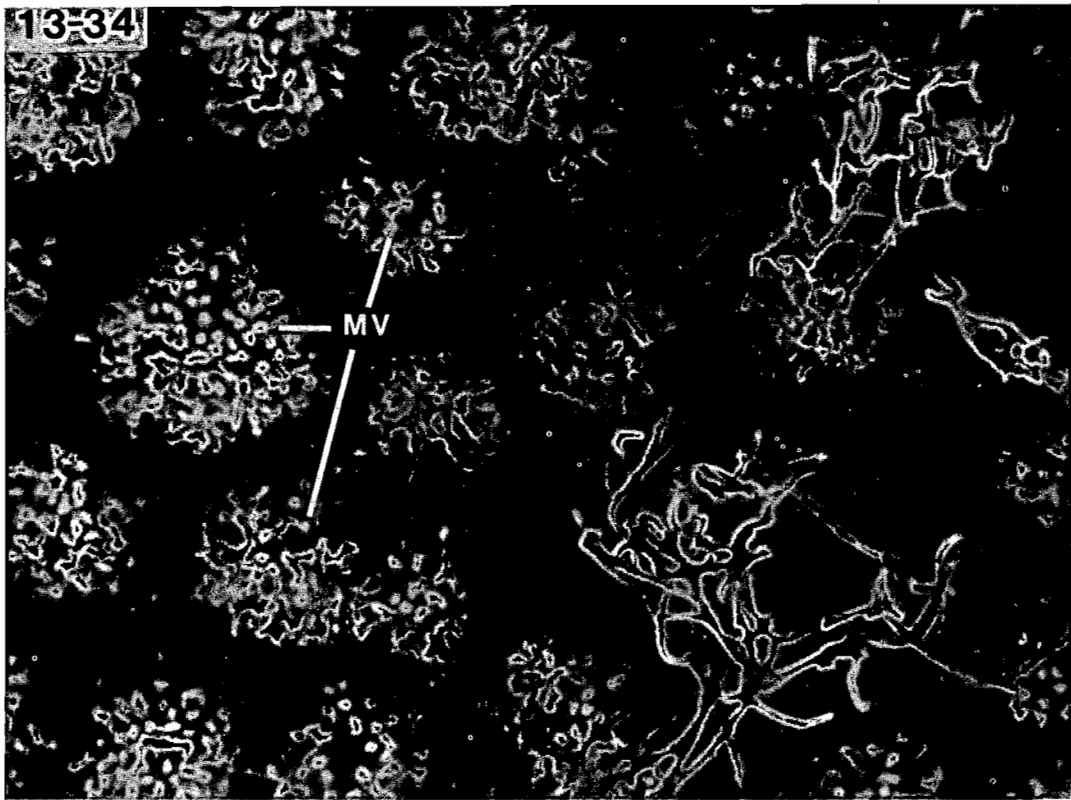
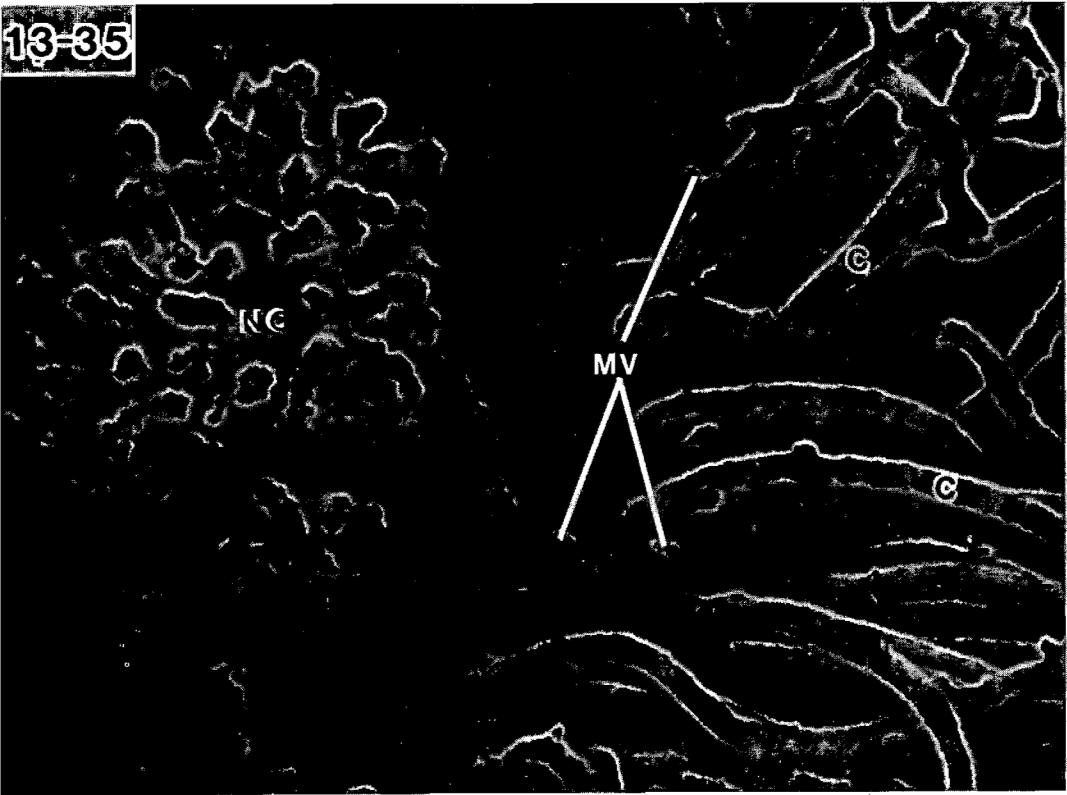


Figure 13-35. Higher magnification scanning electron photomicrograph of a region similar to that seen in Fig 13-33. The ciliated cells are seen to have microvilli (MV) interspersed among the cilia (C). The microvilli of ciliated cells are more slender than those seen on the surface of nonciliated cells (NC). X22,400.

Figure 13-36. Scanning electron photomicrograph of a representative area of the surface of the primary bronchus of whale 80B1. Rows of ciliated cells (C) are seen to alternate with nonciliated regions. The nonciliated region shows no evidence of cells possessing only microvilli on their surfaces. Debris (D) may be seen in the nonciliated regions. The lack of cells possessing only microvilli and the presence of debris may indicate poor tissue preservation. X5,300

13-35



13-36

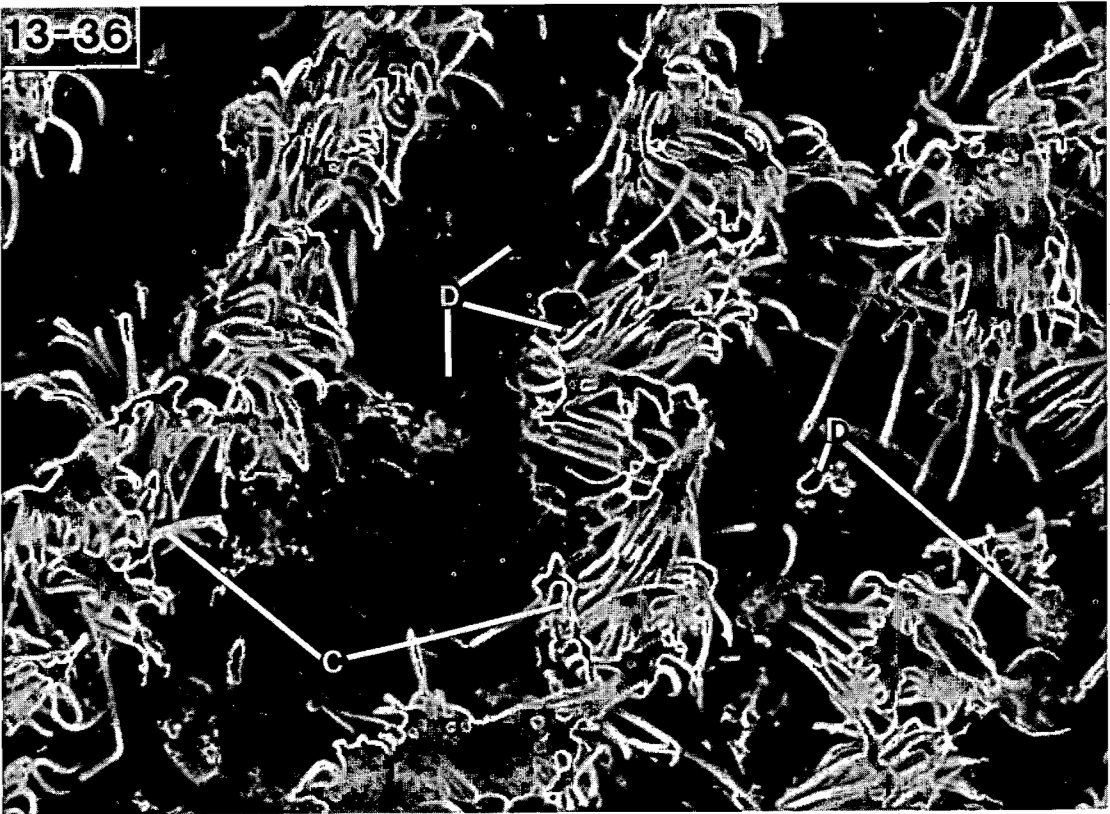


Figure 13-37. Transmission electron photomicrographic montage illustrating a portion of the primary bronchus of whale 80B8. In this region only mucus producing cells are seen at the luminal surface. Microvilli (MV) protrude from their surfaces. Cells with two different staining characteristics (light and dark) may be seen. Both cell types contain mucus granules (MG). The lateral surfaces of these columnar cells show complex interdigitations and near the base possess extremely delicate and tortuous cytoplasmic projections. Intermediate cells (IM) and basal cells (BC) are also evident in this micrograph. A thin basal lamina (BL) may be seen beneath the basal cells and below it collagen of the underlying connective tissue. The extension of columnar mucous cell processes to the basal lamina may best be seen by following the fine processes of a densely stained cell (arrow). X4,100

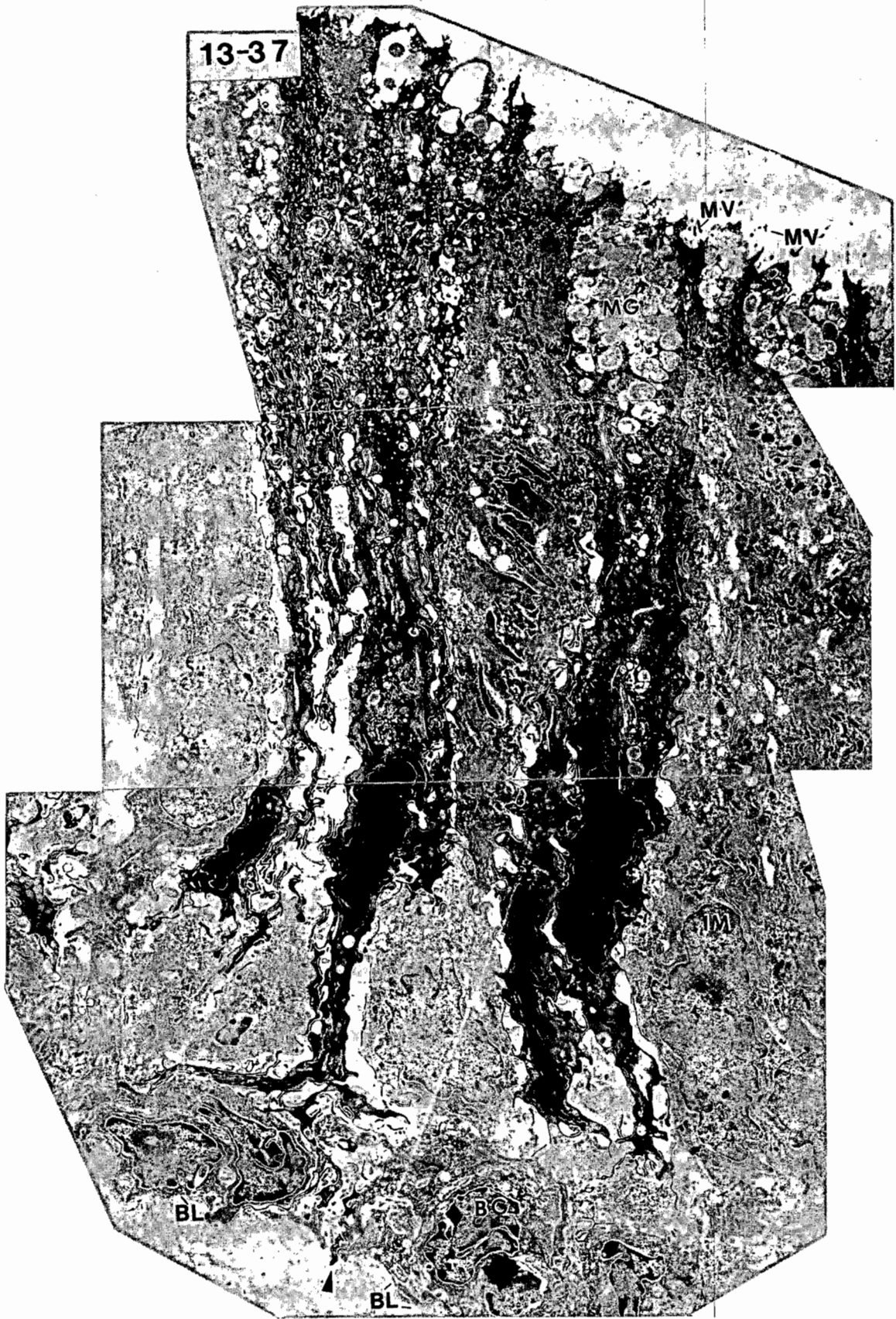
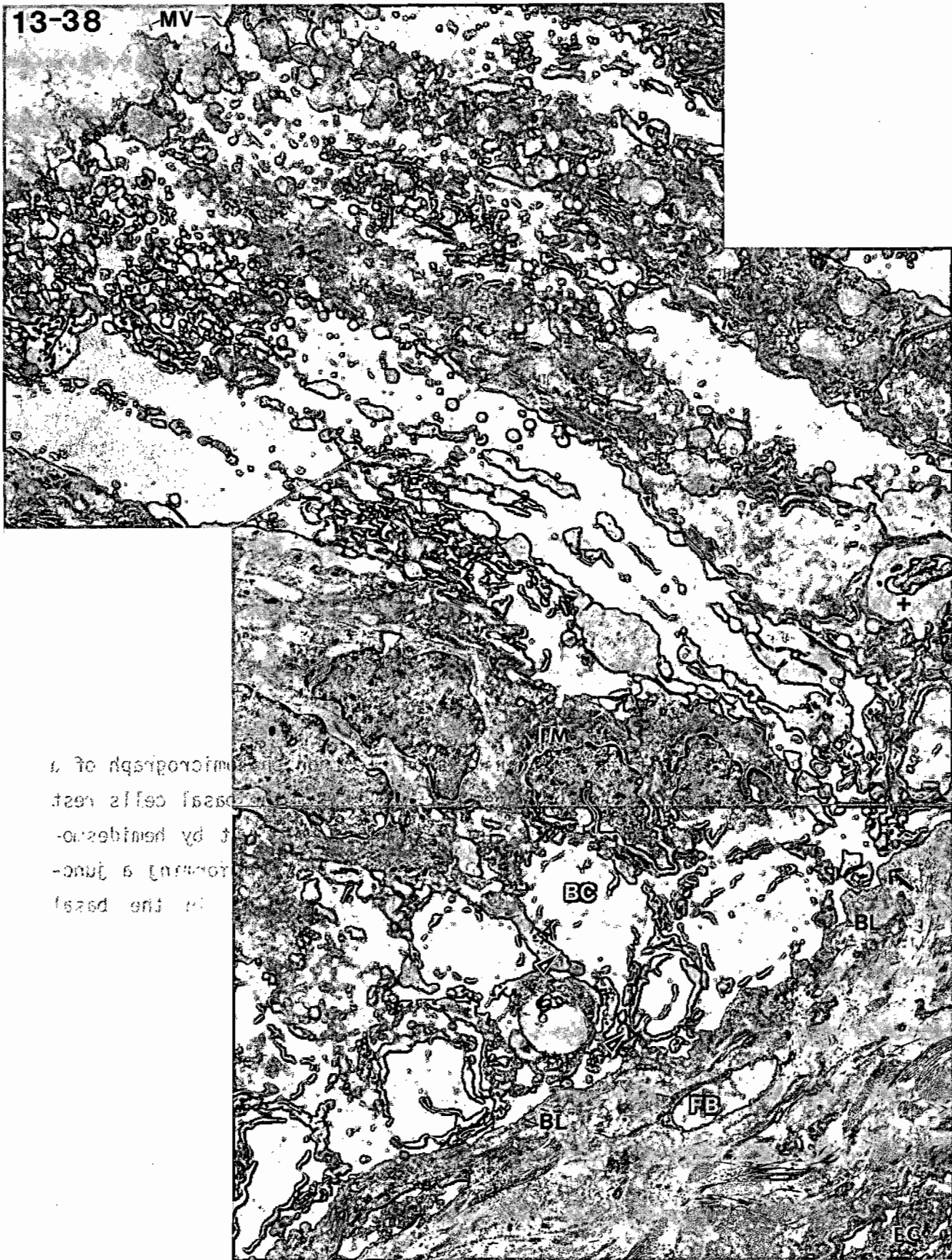


Figure 13-38. Transmission electron photomicrographic montage illustrating a portion of a primary bronchus of whale 80B8. Microvilli (MV) may be seen protruding from the luminal surface of the columnar mucous cells whose basic morphology is similar to that described in Fig 13-37. The basal portion of a densely staining cell may be clearly seen to contact the basal lamina (BL) at the arrow. Intermediate (IM) and basal (BC) cells may be seen. Certain regions appear to contain two layers of basal cells (arrowheads). A mononuclear cell, (+) possibly a lymphocyte, may be seen infiltrating the epithelium. Beneath the basal lamina (BL) collagen and fibroblast nuclei (FB) are evident. An endothelial cell (EC) may be seen lining a small vessel in the connective tissue. X4,100

13-38

MV



Micrograph of basal cells resting on basement membrane by hemidesmosomes forming a junctional complex at the basal end of

Figure 13-39. Transmission electron photomicrograph of the basal region of the lining epithelium from the primary bronchus of whale 80B8. Complex interdigitations of the cytoplasmic processes of cells in the basal region may be seen. Desmosomes (D) forming junctions between adjacent processes are evident. The nuclei (N) of basal cells are also evident exhibiting deep invaginations and occasional nucleoli (NI). X14,600

Figure 13-40. Higher magnification transmission electron photomicrograph of a region similar to that seen in Fig 13-39. The basal cells rest on the basal lamina (BL) and are anchored to it by hemidesmosomes (HD). A desmosome (D) can also be seen forming a junction between cytoplasmic extensions of cells in the basal region. X30,000



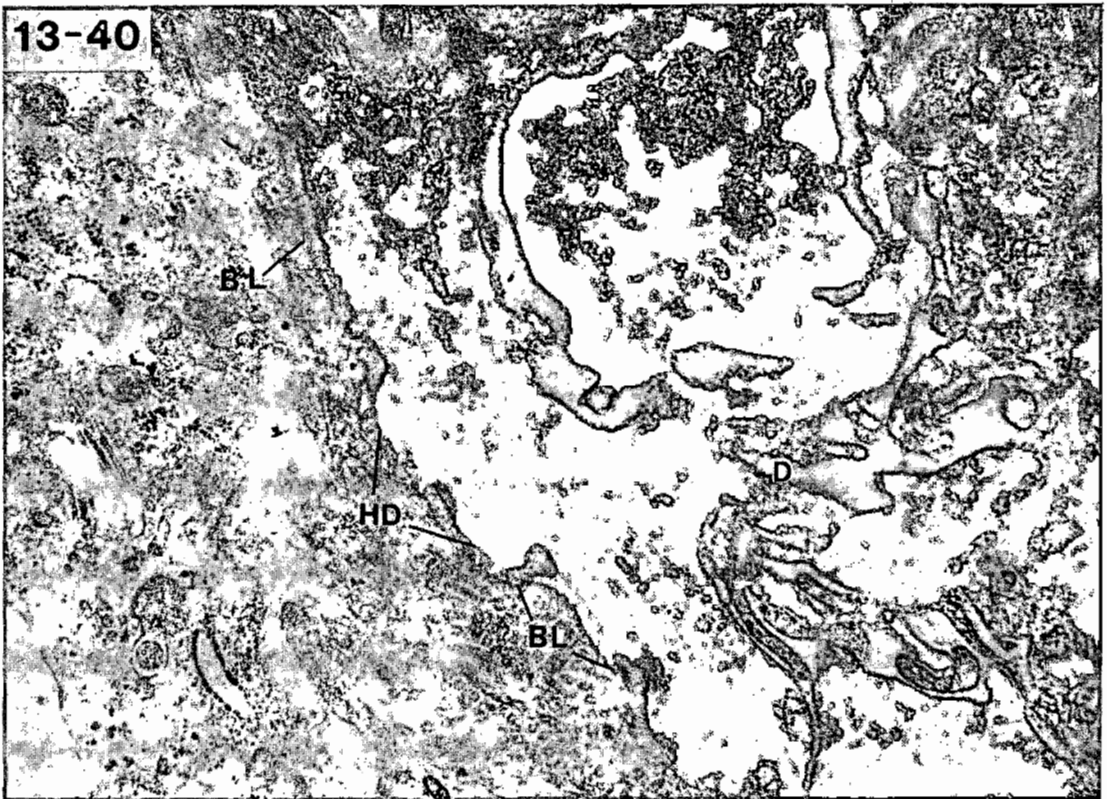
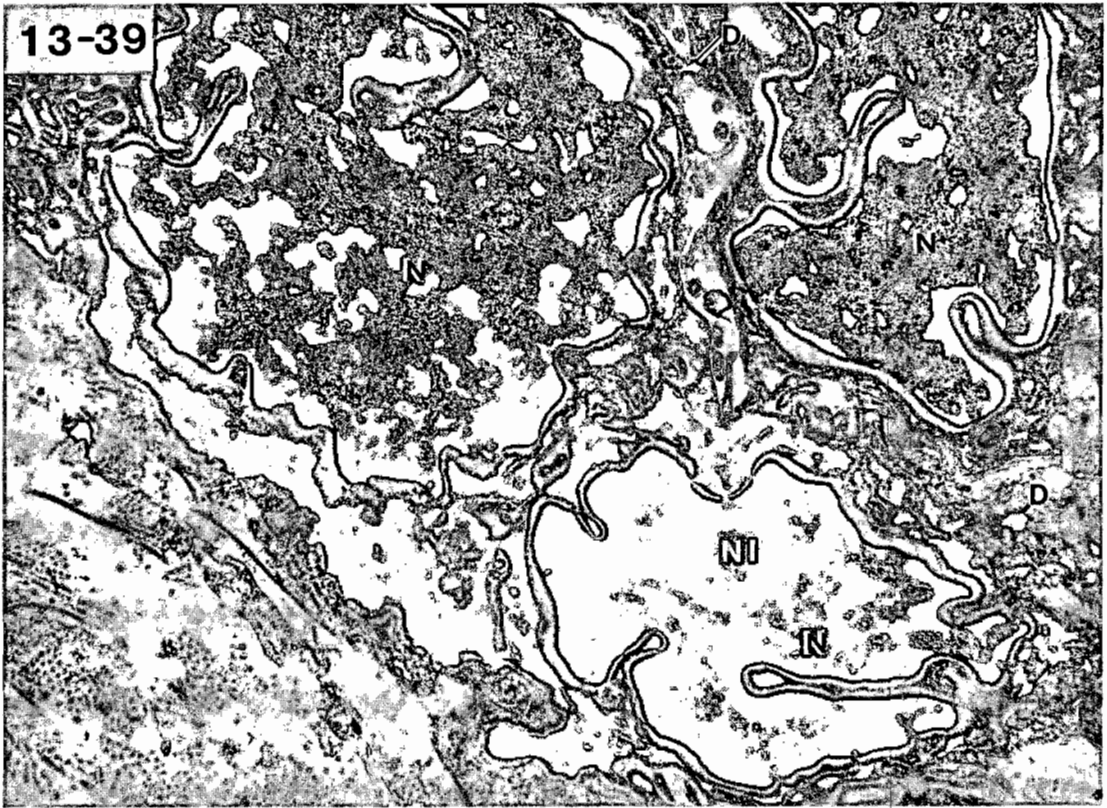


Figure 13-41. Transmission electron photomicrograph of a plasma cell in loose connective tissue beneath the epithelium of a primary bronchus of whale 80B8. This cell displays typical plasma cell morphology with highly expanded cisternae of rough endoplasmic reticulum evident (arrows). X14,500

Figure 13-42. Transmission electron photomicrograph of a plasma cell similar to that shown in Fig 13-41 but displaying the characteristic cartwheel distribution of heterochromatin within the nucleus. A number of electron dense inclusions (I) are evident in a region of cytoplasm devoid of rough endoplasmic reticulum. X10,300

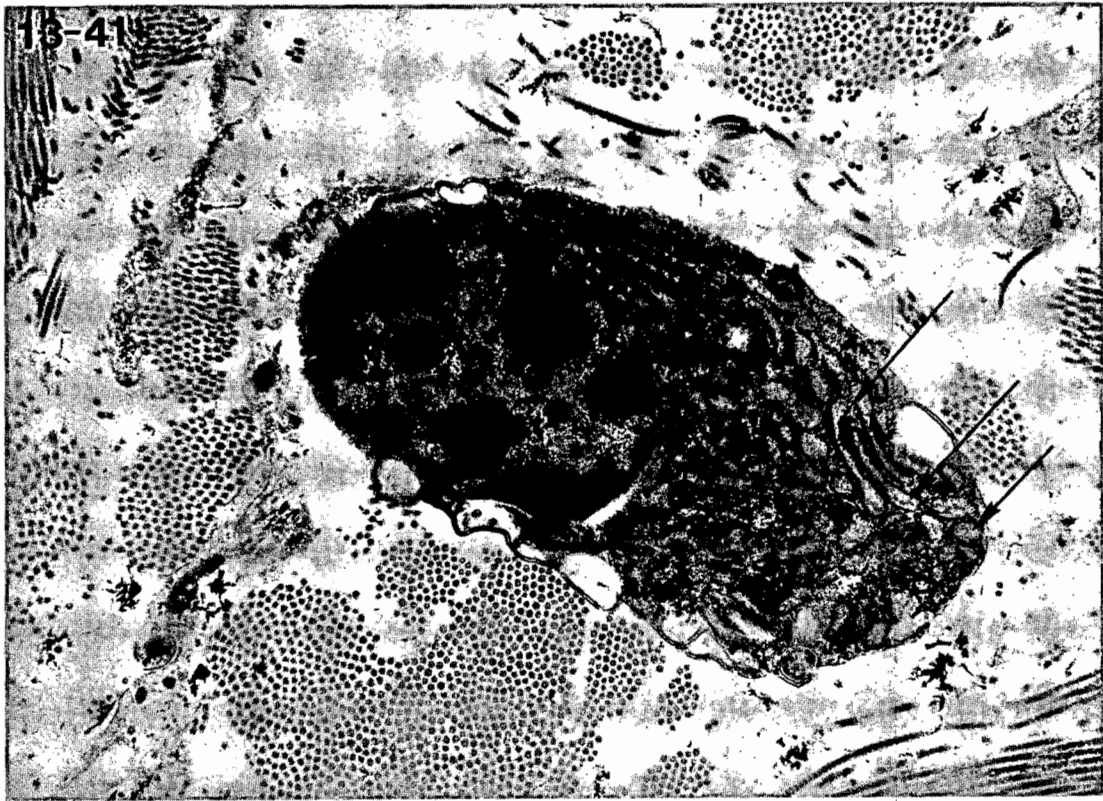
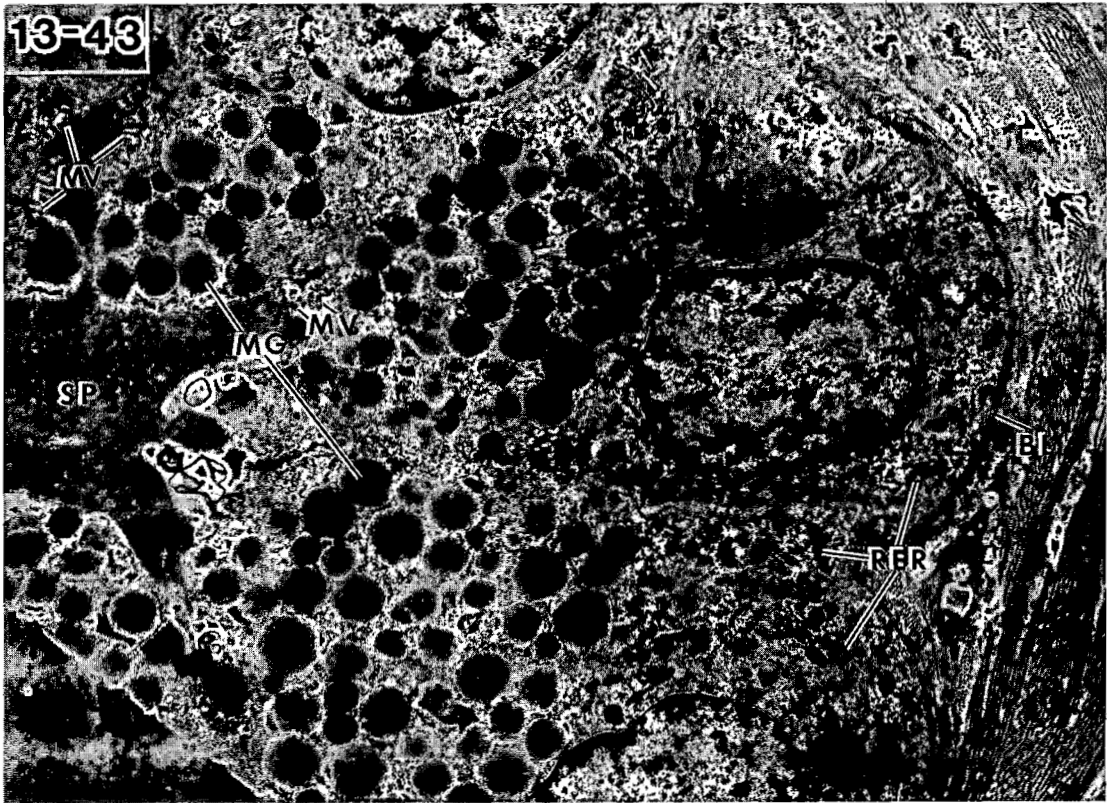


Figure 13-43. Transmission electron photomicrograph of cells of a submucosal mucous gland in the primary bronchus of whale 80B8. The apical surface of these cells display microvilli (MV) which extend into the lumen filled with secretory product (SP). Numerous mucous granules (MG) may be seen near the cell apex. Rough endoplasmic reticulum (RER) is evident in the cytoplasm. The cells rest on a basal lamina (BL) which separates them from the underlying connective tissue. X7,100

Figure 13-44. Transmission electron photomicrograph of cells similar to those shown in Fig 13-43. Apical microvilli (MV) are visible as are many junctional regions (J) between adjoining cells. An inter-cellular canaliculus (IC) may also be seen. X9,800

13-43



13-44

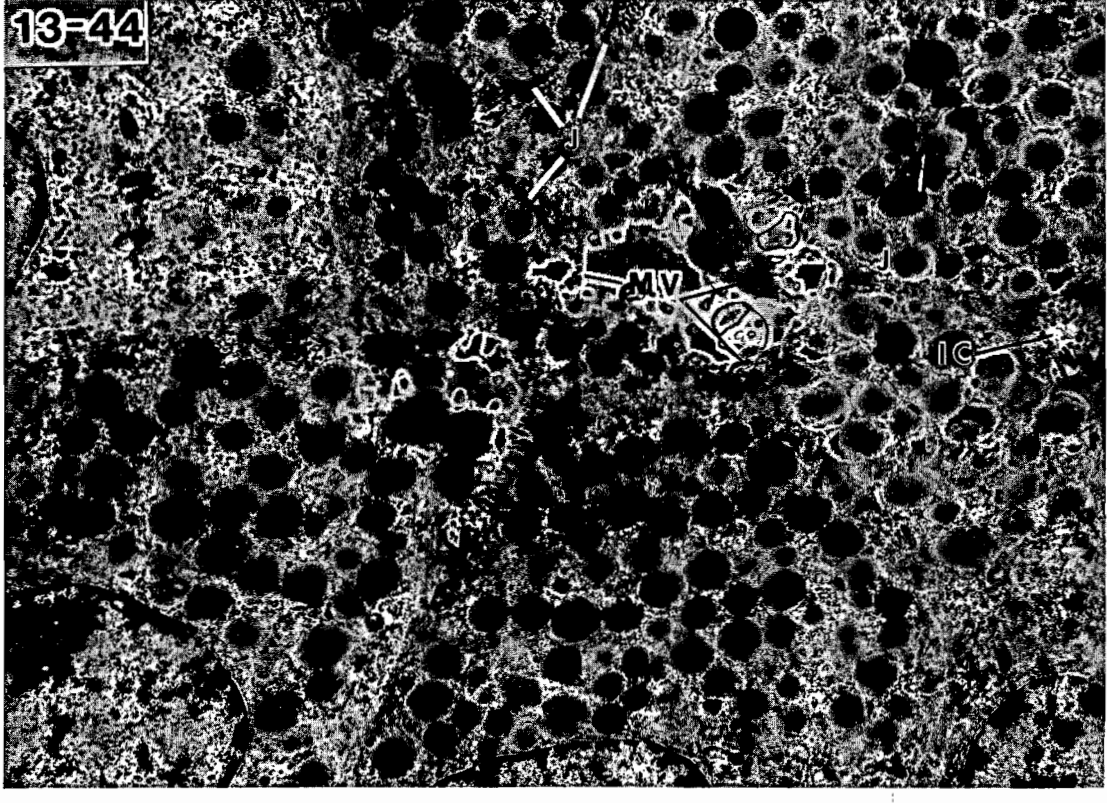


Figure 13-45. Photographs of the principal bronchial bifurcation into lobar bronchi.

- A. Dorsal view (80B1). The principal bronchi (P) bifurcate into cranial (Cr) and caudal (C) lobar bronchi 13 cm caudolateral to the tracheal bifurcation (T). The left cranial lobar (LCr) bronchus leaves at a less obtuse angle ( $145^{\circ}$ ) than does the right cranial lobar bronchus ( $160^{\circ}$ ). X0.23
  
- B. Ventral (medial) view (80B1). This vinyl acetate cast of the bronchial tree shows the lobar bronchi (L) of the left lung. The dichotomous branching of the principal bronchi into segmental bronchi (S) is seen. X0.16
  
- C. Ventral (medial) view (80B7). The principal bronchus (P) divides into cranial (Cr) and caudal (C) lobar bronchi in this left lung. The left pulmonary artery (A) and vein (V) are seen just caudal to the bifurcation. X0.13

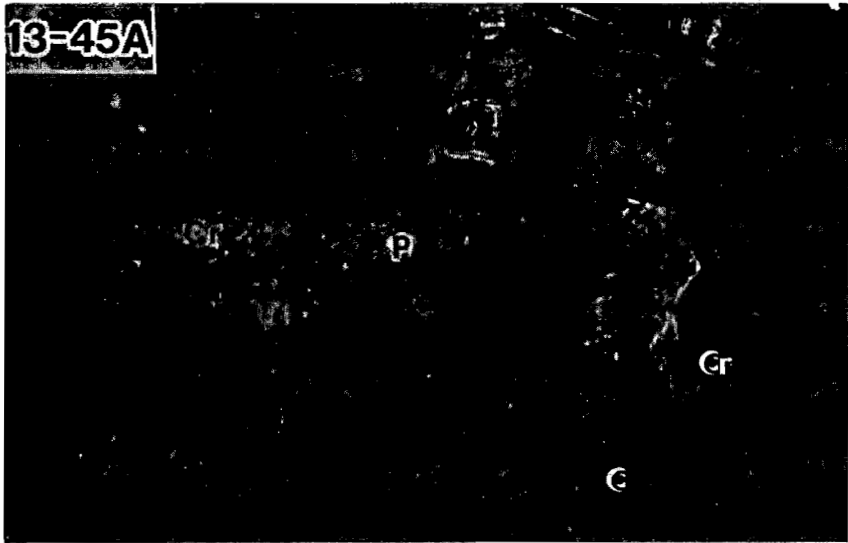


Figure 13-46. Photographs of the principal bronchus bifurcation, pulmonary artery and vein.

- A. The pulmonary artery (A) and vein (V) (80B7) are found just caudal to the bifurcation of the principal bronchus (P). The branching of the pulmonary artery is deep and follows the bronchial tree (Fig B). The venous branching (arrowheads) is superficial lying just below the pleura. Bronchial lymph nodes (N) are seen among the veins on the ventral (medial) surface of the left lung. X0.2
  
- B. The pulmonary artery (A) (80B1) and its branches can be seen lying next to and following the bronchial tree in this vinyl acetate cast. The arteries lie on the dorsal aspect of this cast of the left bronchial tree. X0.25



13-46A



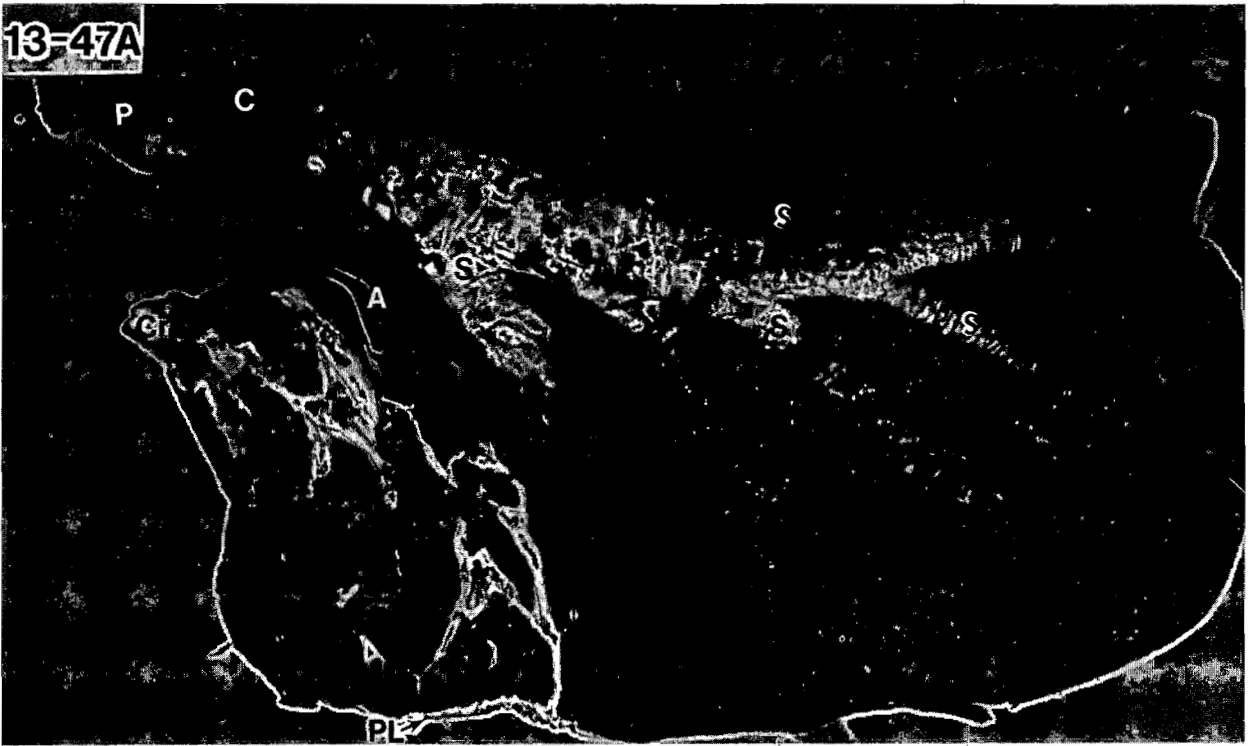
13-46B



Figure 13-47. Photographs of the principal bronchus bifurcation, pulmonary artery and vein.

- A. The right pulmonary artery (A) (80B2) is seen lying caudal to the bifurcation of the principal bronchus (P). The cranial lobar bronchus (Cr) is torn away from the bifurcation. Note the dichotomous branching of the caudal lobar bronchus (C) into numerous segmental bronchi (S) which course near the surface beneath the pleura (PL). Ventral (medial) view. X0.18
  
- B. The pulmonary artery (A) (80B8) is seen lying just caudal to the bifurcation of the principal bronchus (P). Right cranial (Cr) and caudal (C) lobar bronchi can be seen as well as segmental bronchi (S) on this dissected lung. The thick pleura (PL) can be seen, but there is no evidence of the parenchyma being divided into lobes. Ventral (medial) view. X0.21

13-47A



13-47B

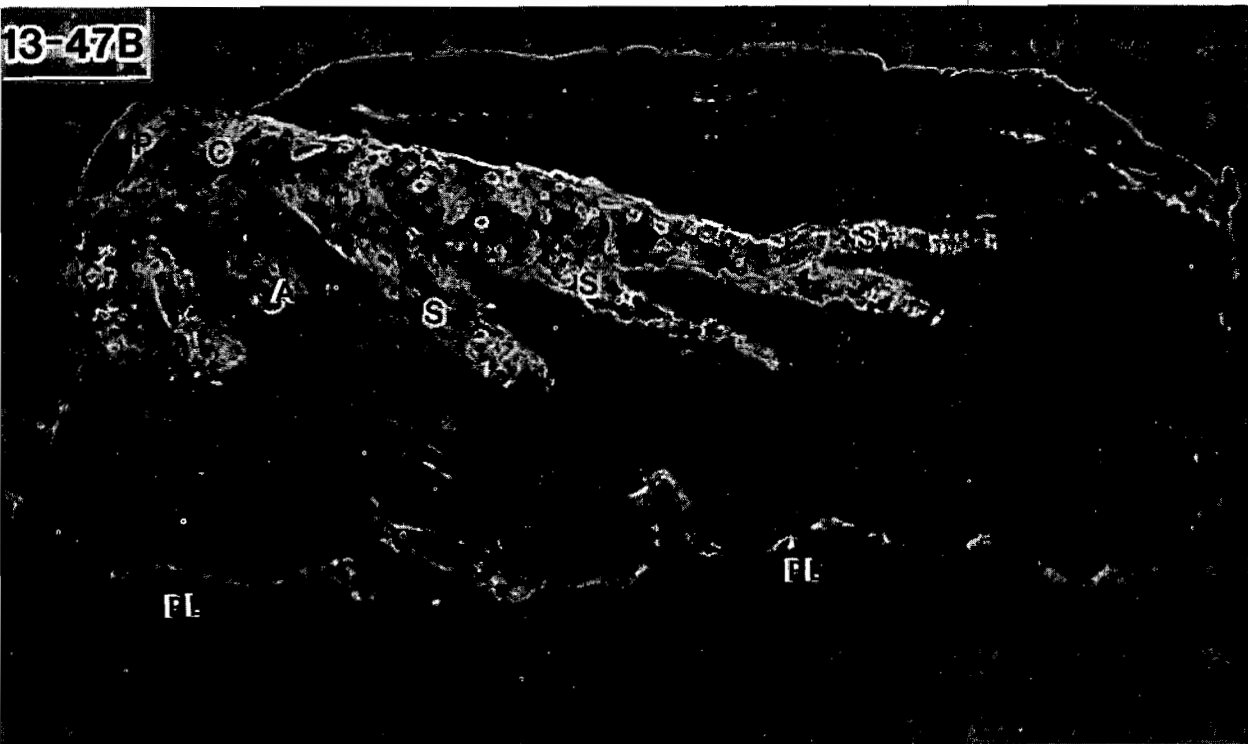


Figure 13-48. Photomicrograph of the mucosal lining of the 19 x 31 mm bronchus from 80B1 taken near the center of the cartilagenous ring. The lamina propria (LP) consists of vascularized dense irregular connective tissue without mucous glands and is covered with a ciliated pseudostratified columnar epithelium (EP). Instead of a muscularis mucosae, longitudinally oriented laminae of dense elastic fibers (F) only are present. The hyaline cartilage ring (HC) is covered by a dense irregular connective tissue perichondrium. X.S., H and E, X50

Figure 13-49. Photomicrograph of a similar sized bronchus (19 x 33 mm) from 80B8 taken near the junction between cartilage rings. The mucosa has mucous glands (G) in addition to the layers visible in Fig 13-48 which interdigitate with the longitudinal elastic laminae (E). X.S., H and E, X50

Figure 13-50. Higher magnification photomicrograph of the mucosa in Fig. 13-49. Cilia (arrow) are visible as well as the pseudostratified columnar nature of the epithelium (Ep) and the mucous glands (G). X.S., H and E, X120

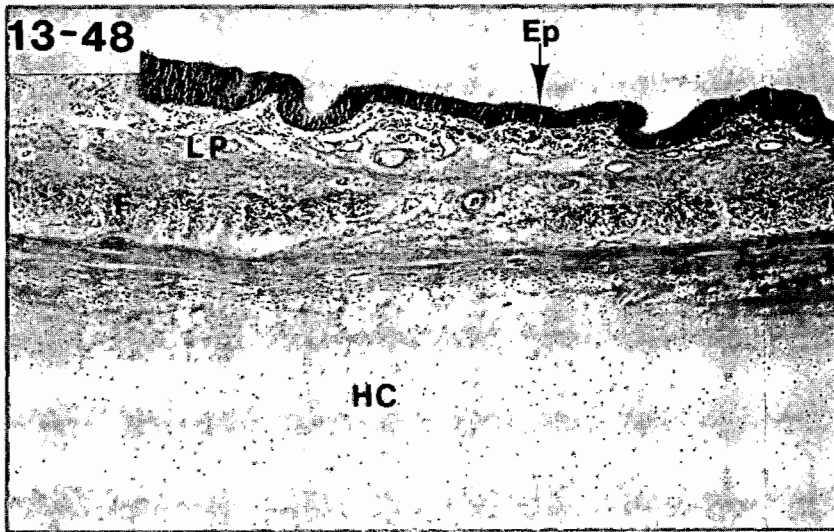


Figure 13-51. Photomicrograph of the mucosa and cartilage of a 16 mm bronchus from 80B7. The basic structure is the same as in large bronchi (Figs 13-48, 13-49). Mucus and debris (D) are present on the epithelial surface. The longitudinal elastic lamina (E) is thinner representing the only significant changes other than size. X.S., H and E, X130

Figure 13-52. Photomicrograph of a semi-thin section of the mucosa of a 10 mm bronchus of 80B8. The epithelium is ciliated pseudostratified columnar (Ep). The tall columnar cells (arrow) penetrate between the basal cell layer (arrowhead) to the basement membrane. Epon, X.S., Toluidine blue stain, X160

Figure 13-53. Scanning electron photomicrograph of a portion of a 10 mm bronchus from whale 80B8. Both the ciliated surface epithelium (SE) and the underlying cartilage (C) and associated connective tissue may be seen. X47

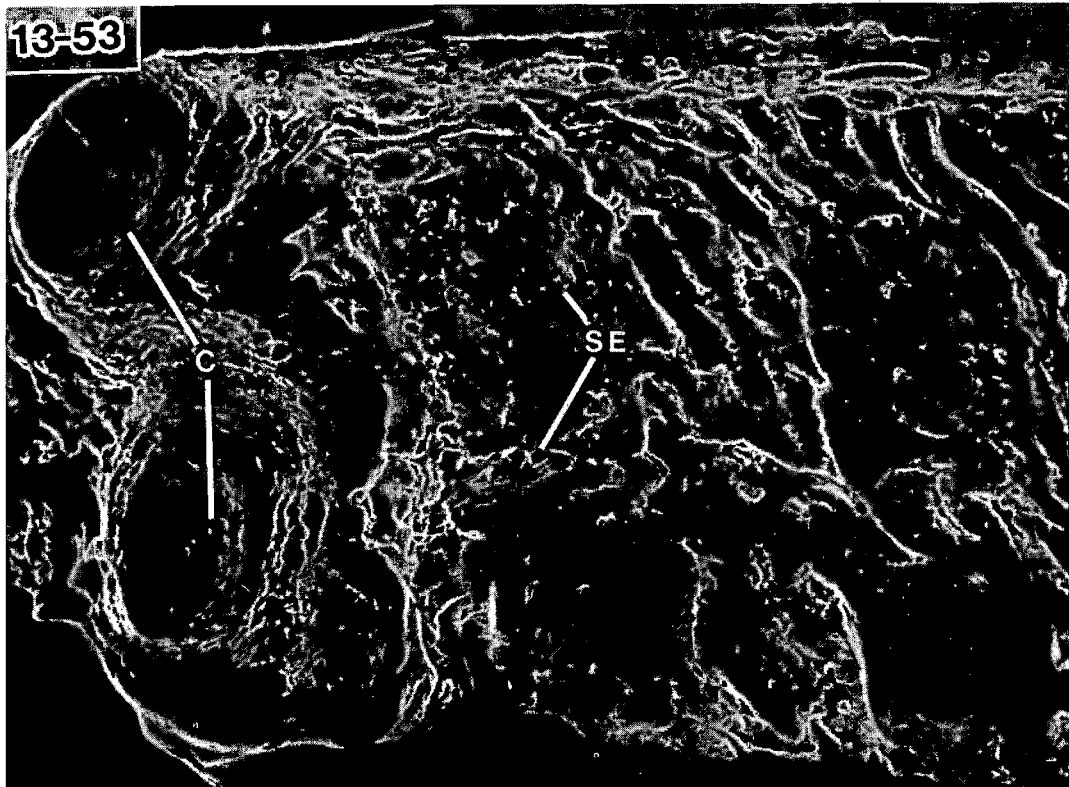
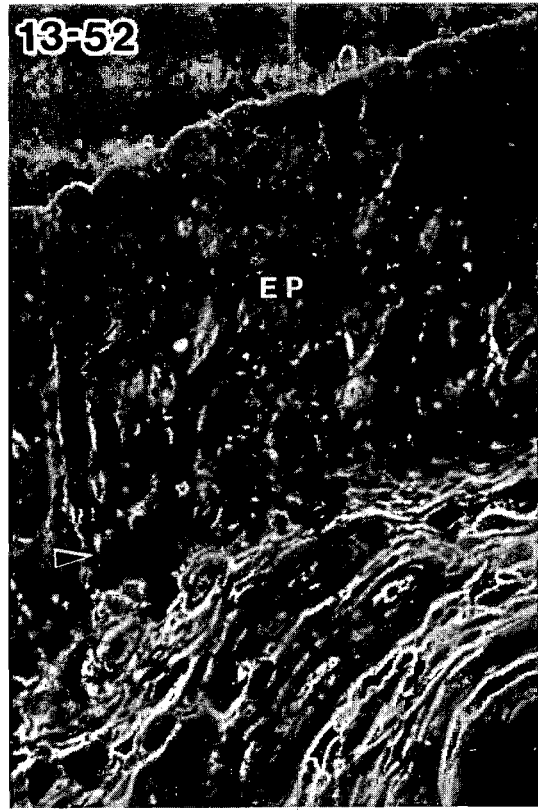
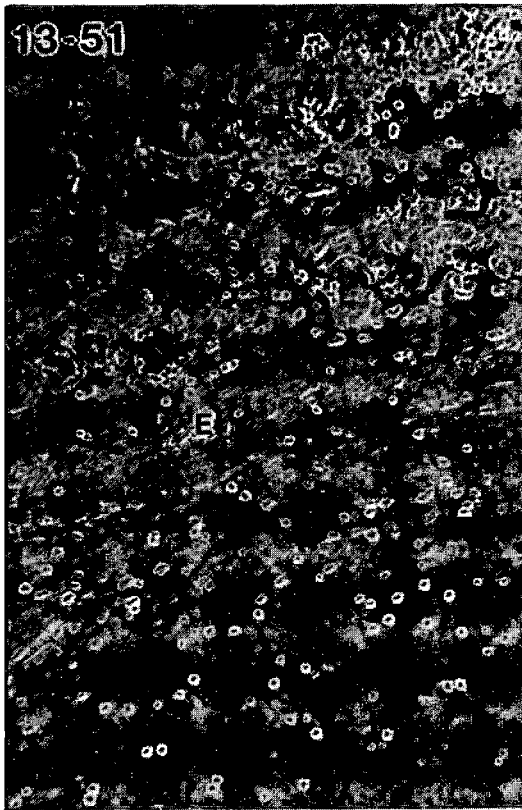
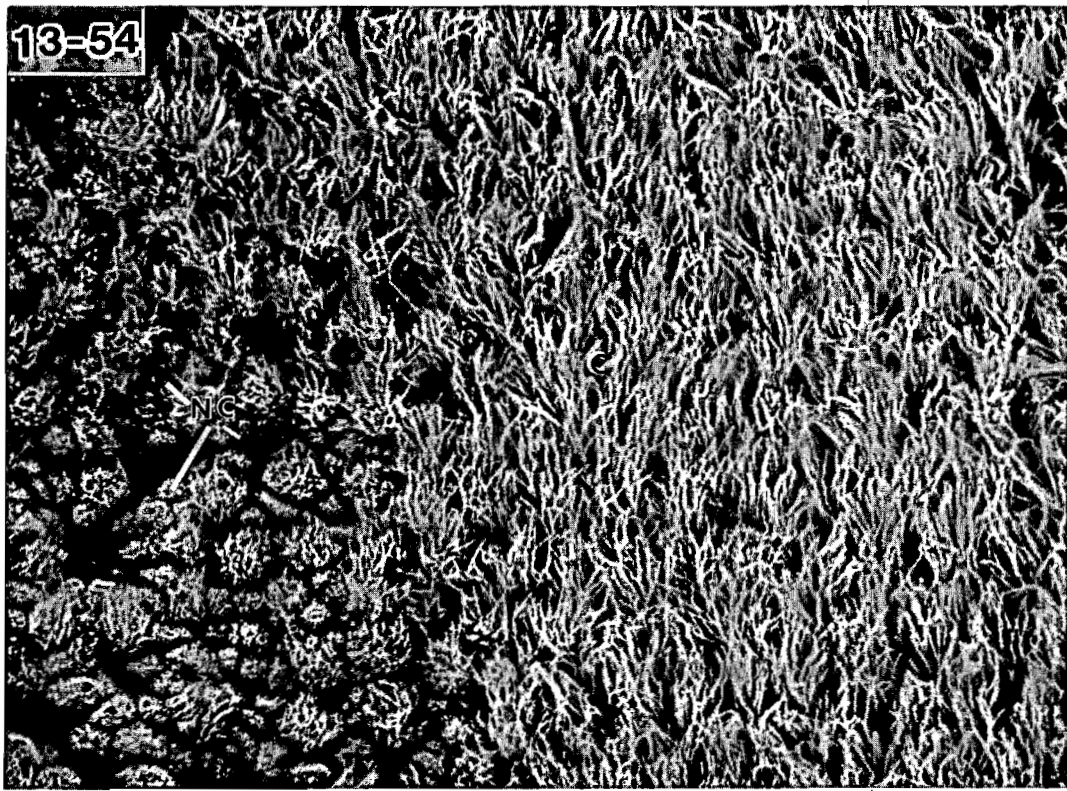


Figure 13-54. Higher magnification scanning electron photomicrograph of a portion of the bronchus shown in Fig 13-53. Both ciliated and nonciliated epithelial cells are seen. The number of ciliated cells (C) appears to be much greater than nonciliated cells (NC). X1,300

Figure 13-55. Higher magnification scanning electron photomicrograph of a portion of the bronchus shown in Figure 13-53. Individual ciliated and nonciliated cells may be seen. Nonciliated cells possess numbers of microvilli (MV). Ciliated cells also appear to possess thin microvilli (arrows). X7,500



13-54



13-55

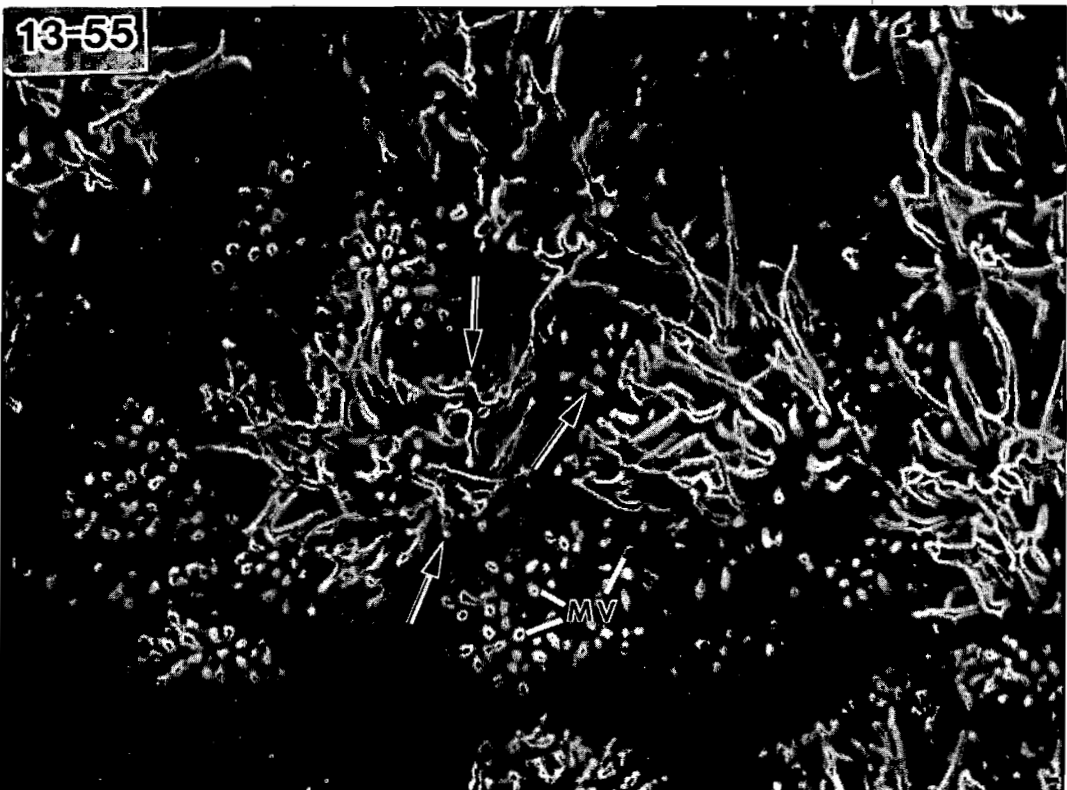


Figure 13-56. Photomicrograph of a small bronchus (3.7 mm) from 80B8. The entire bronchial wall is visible surrounded by pulmonary tissue (P). Mucous glands (G) are still present tending to be less abundant at the level of the cartilaginous rings (R). The elastic lamina is no longer present. A nerve trunk (N) runs just outside the rings. L.S., H and E, X50

Figure 13-57. Photomicrograph of a slightly smaller bronchus (3.2 mm) from 80B8. The bronchial wall is even thinner with the mucous glands (G) occurring only between the cartilage rings (R). The surrounding pulmonary tissue (P) intrudes (arrow) between rings. L.S., H and E. X50.

Figure 13-58. Scanning electron photomicrograph of an excised portion of a 2 mm bronchus from whale 80B8. The ciliated epithelium (CE) is evident as is the hyaline cartilage (HC) which underlies it. Exposed lung parenchyma (P) can be seen beneath the bronchus. X40

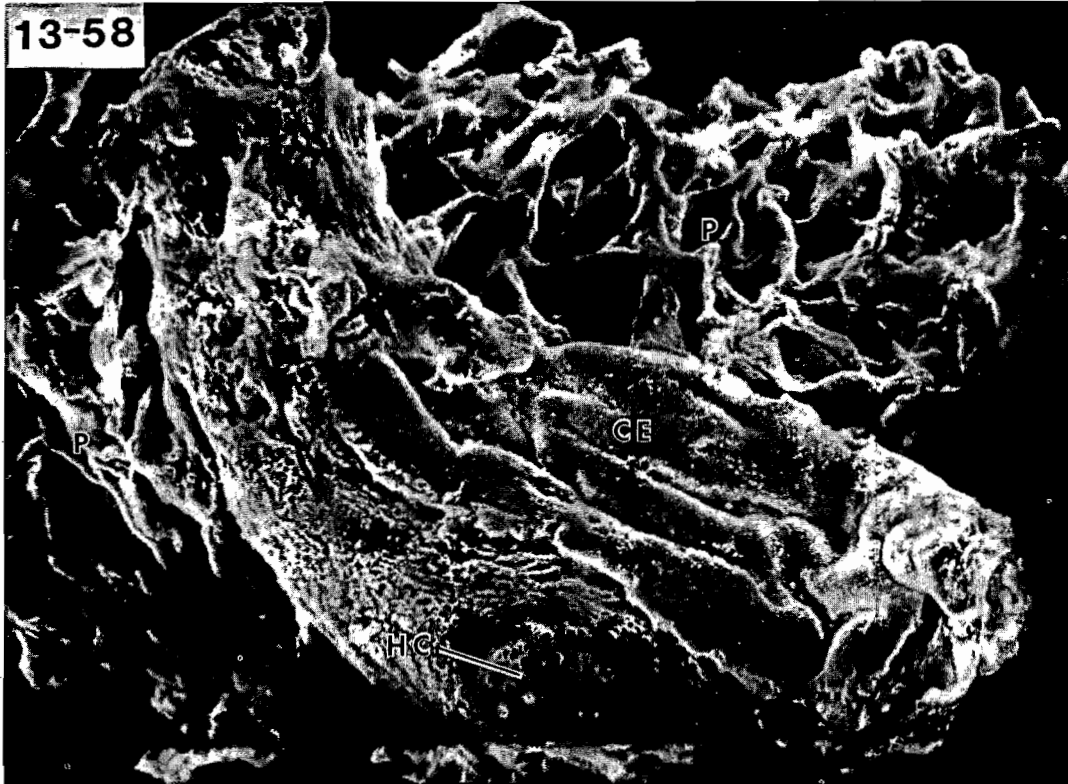
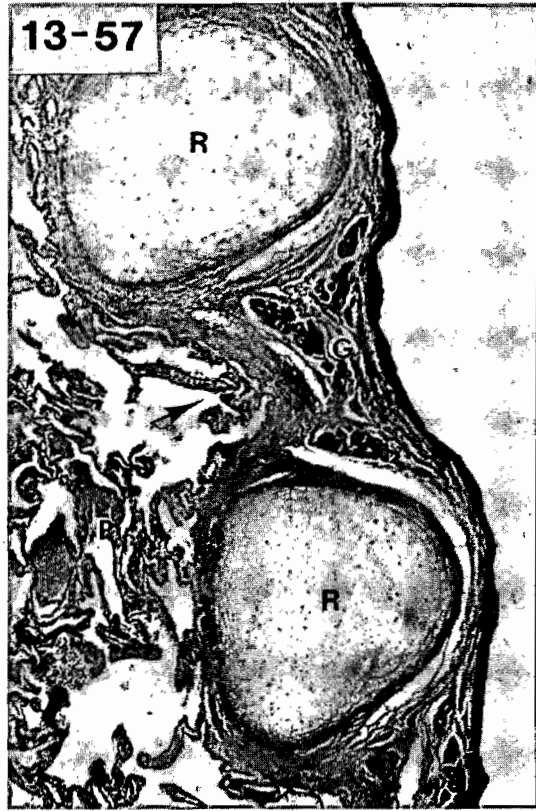
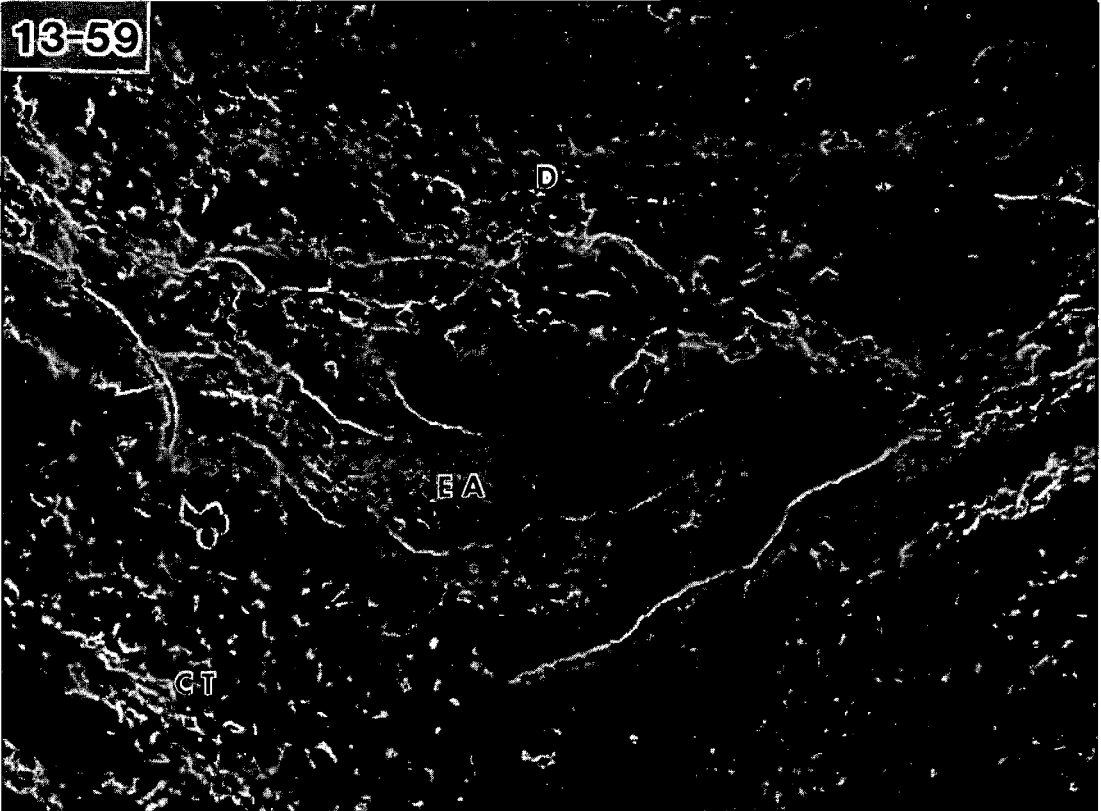


Figure 13-59. Higher magnification scanning electron photomicrograph of the surface and cut edge of the bronchus shown in Fig 13-58. Debris (D) can be seen covering the surface except in an exposed area (EA) where the debris is lifted from the surface revealing the ciliated surface below. Connective tissue (CT) can be seen beneath the epithelium. X250

Figure 13-60. Higher magnification scanning electron photomicrograph of the surface of the bronchus shown in Fig 13-58. The uniformly ciliated epithelium is thrown into folds. Red blood cell (R). X640

13-59



13-60

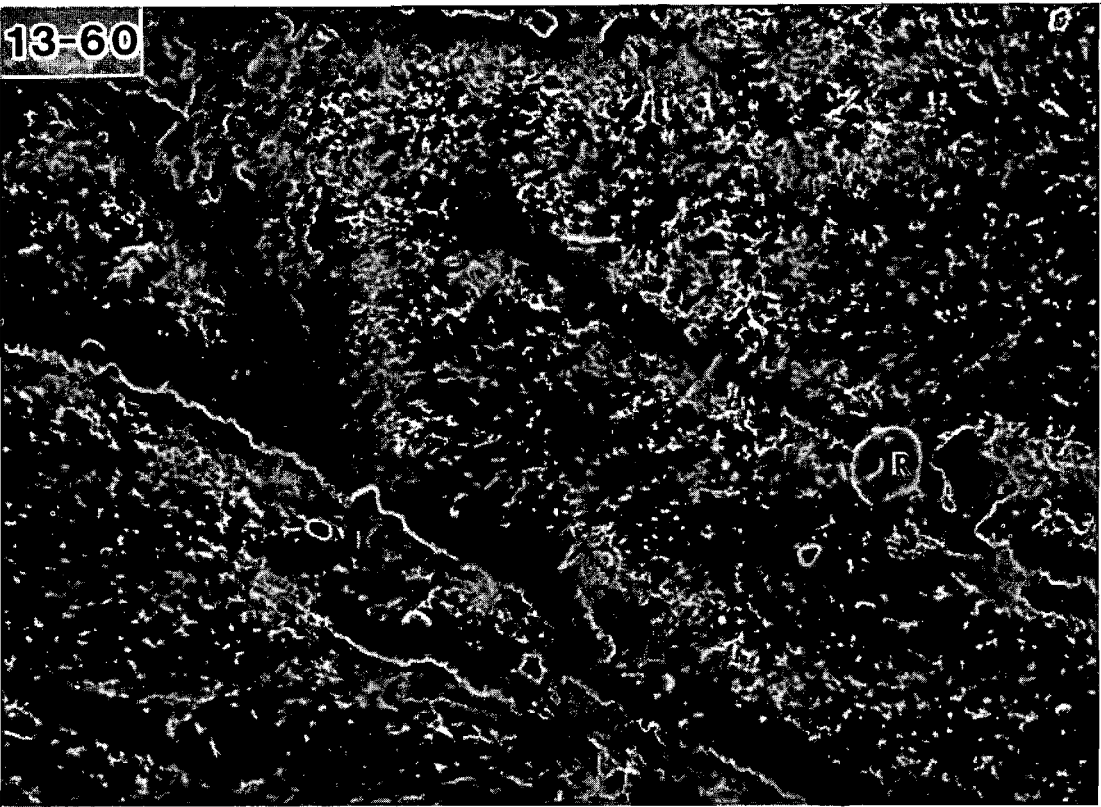
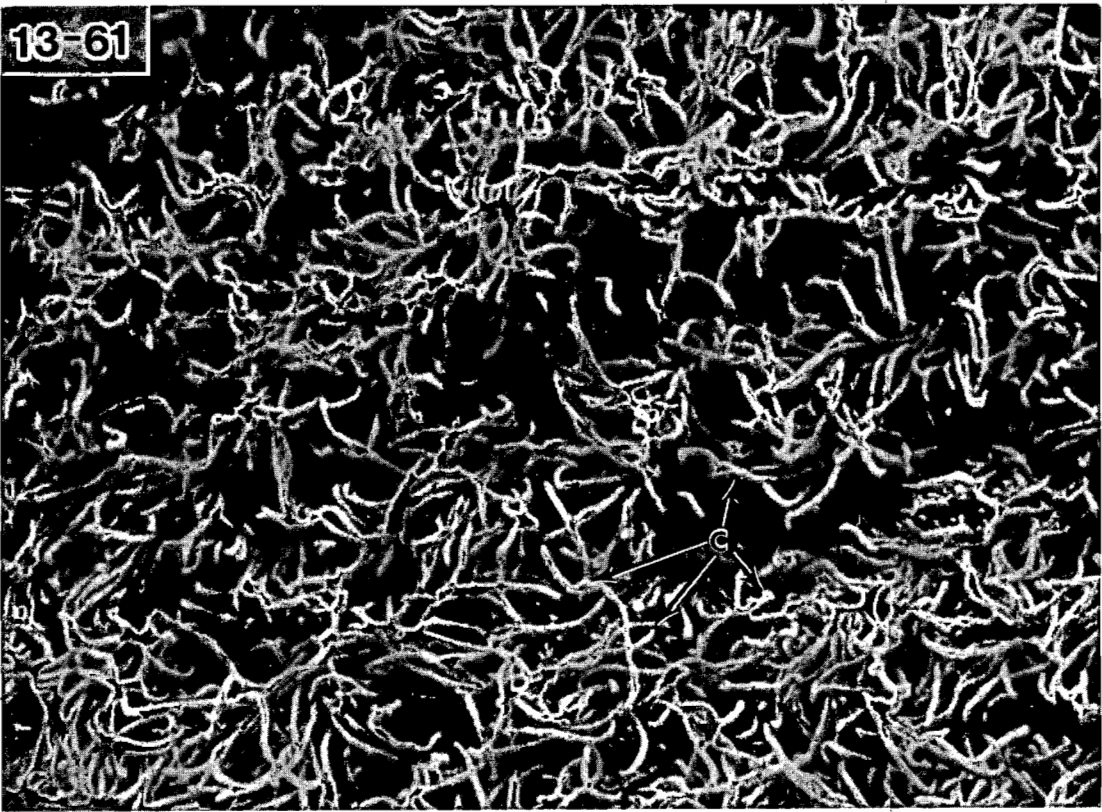


Figure 13-61. Higher magnification scanning electron photomicrograph of the surface of the bronchus shown in Fig 13-58. Cilia (C) are clearly evident but the borders of ciliated cells are difficult to see due to the large number of cilia and their uniform distribution. X4,200

Figure 13-62. Scanning electron photomicrograph of a portion of a 2 mm bronchus taken from whale 80B1. Debris (D) covers a portion of the surface. A portion of the surface is relatively free (F) of debris. The columnar nature of the epithelium is evident (arrows) as is the connective tissue (CT) beneath the epithelium. X270

13-61



13-62

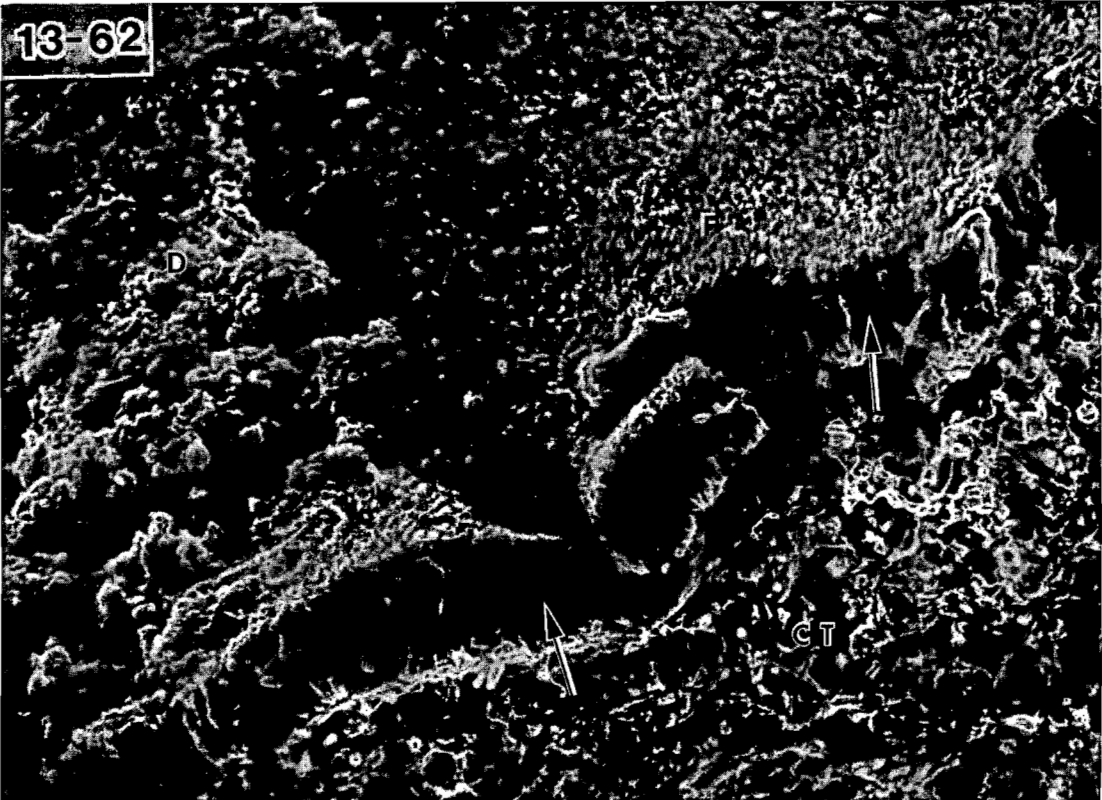
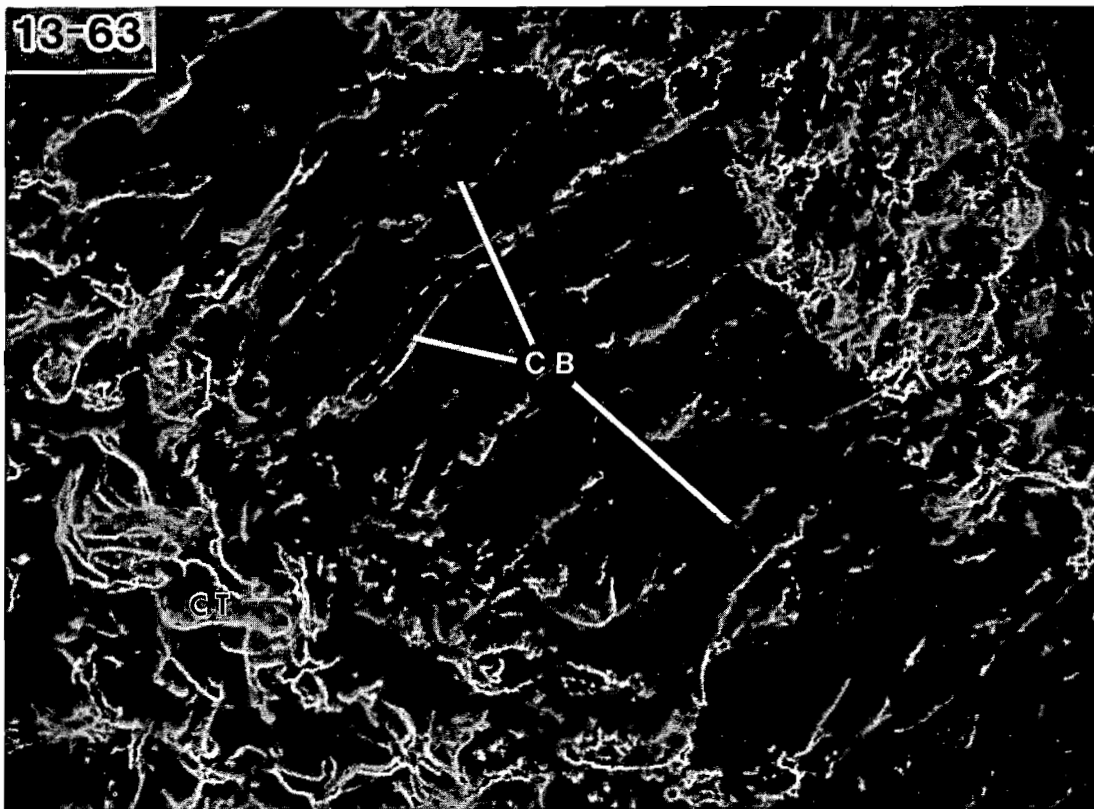


Figure 13-63. Higher magnification scanning electron photomicrograph of a portion of the bronchus shown in Fig 13-62. The columnar cell bodies (CB) of the ciliated epithelial cells can be seen in this area where the epithelium has been broken perpendicular to the surface of the bronchus. Fibers of the underlying connective tissue (CT) are also evident. X890

Figure 13-64. Higher magnification scanning electron photomicrograph of the surface of the bronchus shown in Fig 13-62. The uniform character of the ciliated epithelium is evident. X2,400



13-63



13-64

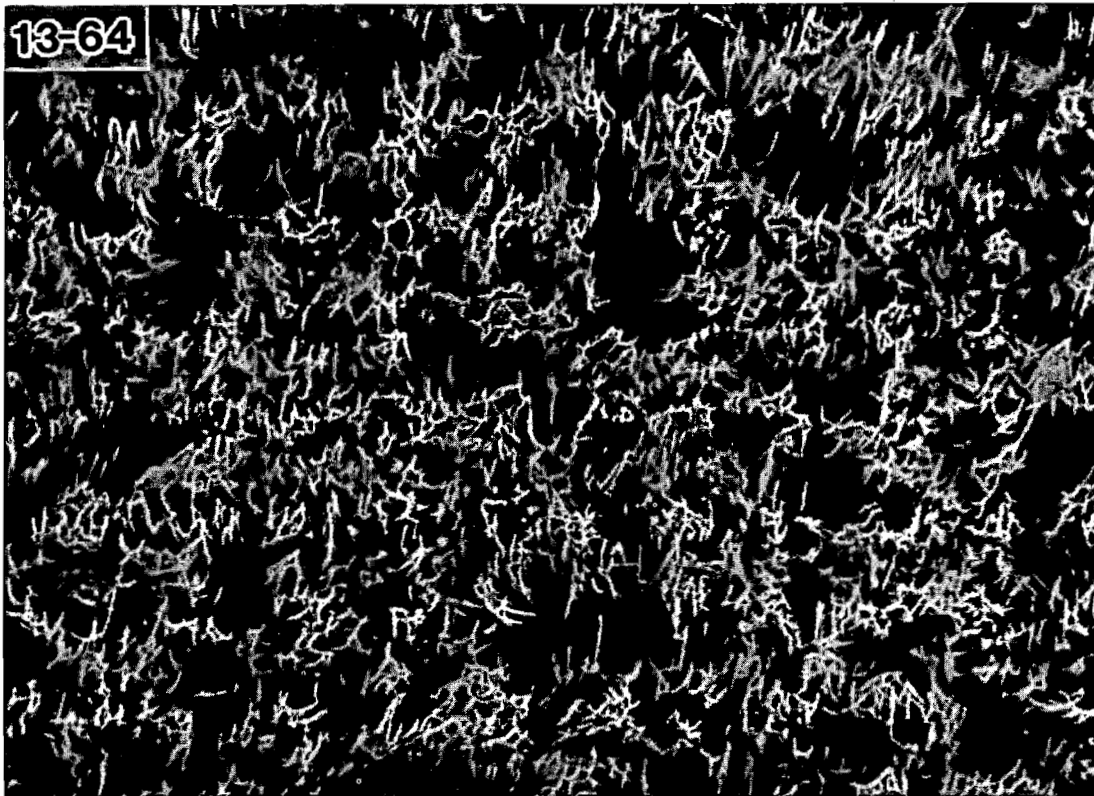


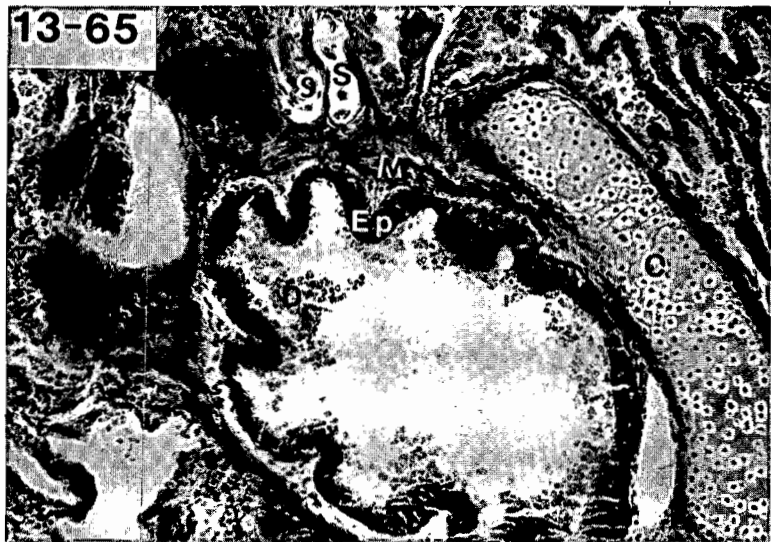
Figure 13-65. Photomicrograph of a bronchiole (1.9 mm) from 80B8 illustrates the typical mammalian characteristic of a folded lining with ciliated pseudostratified columnar epithelium (Ep) owing to the contraction of the circular smooth muscle (M) layer present within the mucosa for the first time. The cetacean modification of cartilage plaques (C) within the bronchiolar wall is well demonstrated. Note the Herbsti-like elongated and convoluted sensory end organ (S) within the bronchiolar wall. D - debris. X.S., Verhoeff stain, X130

Figure 13-66. Photomicrographs of a nerve tract and Herbsti-like encapsulated sensory nerve ending in a bronchiole of 80B8. Serial sections permit one to follow the connection of the nerve end organ to its afferent nerve tract. Follow illustration top to bottom (A-C) for nerve tract to end organ. The sensory nerve impulse actually originates and proceeds from illustration C to A. Sections cut at 5  $\mu$ m. X130

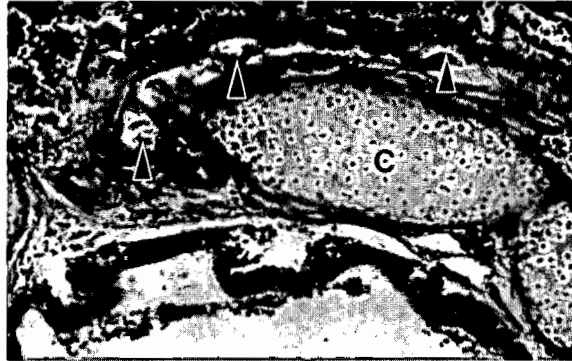
A. The nerve tract (arrowheads) connects to a larger tract adjacent to a small bronchus (out of the picture to right). Cartilage (C). Section is 20 sections above B. Masson's stain.

B. The Herbsti-like end organ (arrowheads) expands and becomes convoluted within the bronchiolar wall between cartilage plaques (C). Section is 18 sections above C. Masson's stain.

C. The Herbsti-like end organ (arrowhead) continues down the bronchiolar wall. H and E stain.



**13-66A**



**13-66B**



**13-66C**



Figure 13-67. Photomicrographs of terminal bronchioles.

- A. Terminal bronchiole (500  $\mu\text{m}$ ) of 80B1. The lamina propria (LP) is loose connective tissue with circularly arranged smooth muscle (M). The ciliated pseudostratified columnar epithelium (Ep) begins to change from very low cuboidal to simple squamous (arrows) which is not respiratory in the furrows caused by muscle contraction. The debris (D) is hemorrhage from collection. X.S., H and E, X130
- B. Terminal bronchiole (about 350  $\mu\text{m}$ ) of 80B8. Apparently just before transforming into a respiratory bronchiole, the terminal bronchiole connects (arrows) through the bronchiolar wall to a few alveoli for a short distance. Smooth muscle (M) and the lack of mucous glands is typical. X.S., H and E, X130

Figure 13-68. Photomicrograph of a terminal bronchiole (320  $\mu\text{m}$ ) leading into respiratory bronchiole from 80B1. Debris (D) in airway is hemorrhage from collection process. The terminal bronchiole (TB) has ciliated pseudostratified columnar epithelium (Ep), distinct cartilage plaque (C), and circular smooth muscle (M) as other bronchioles (see Fig 13-67). The transition to respiratory bronchiole (RB) involves a change in epithelium (arrows) to simple squamous covering capillaries closely (respiratory epithelium) and reduction in size of cartilage plaques. Longitudinal elastic fibers (E). Individual alveoli connecting to the respiratory bronchiole were missed in this section. L.S., Verhoeff stain, X50

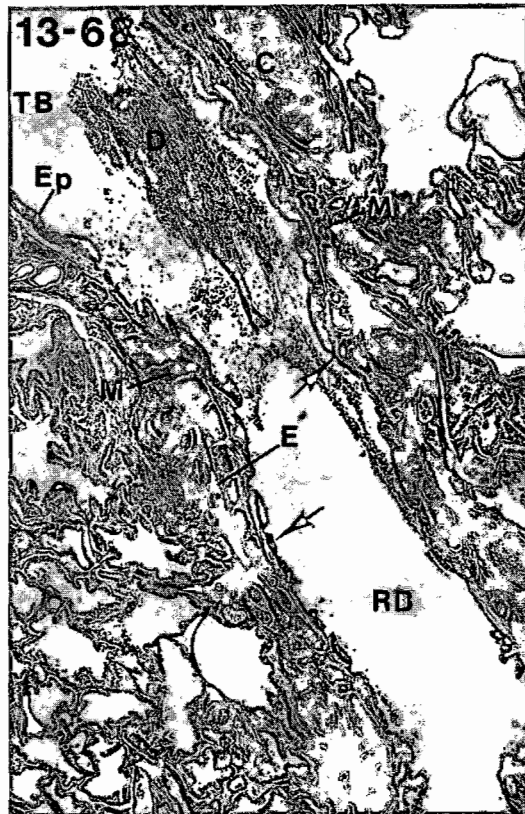
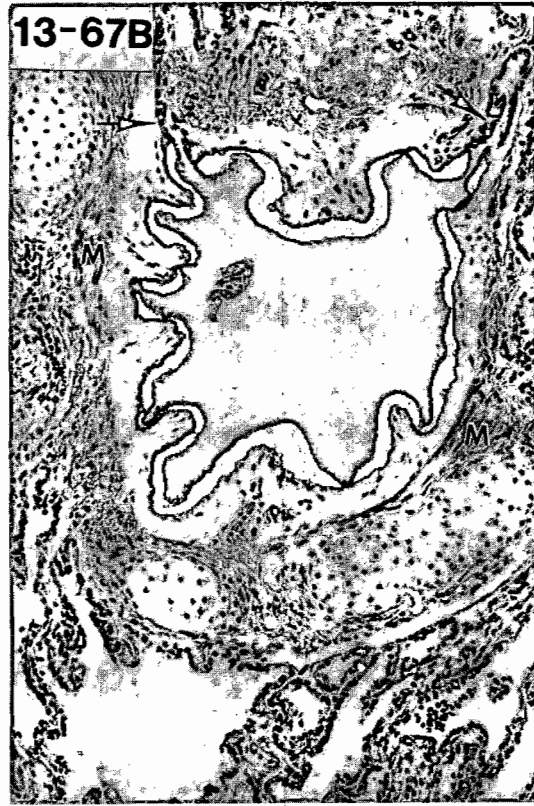
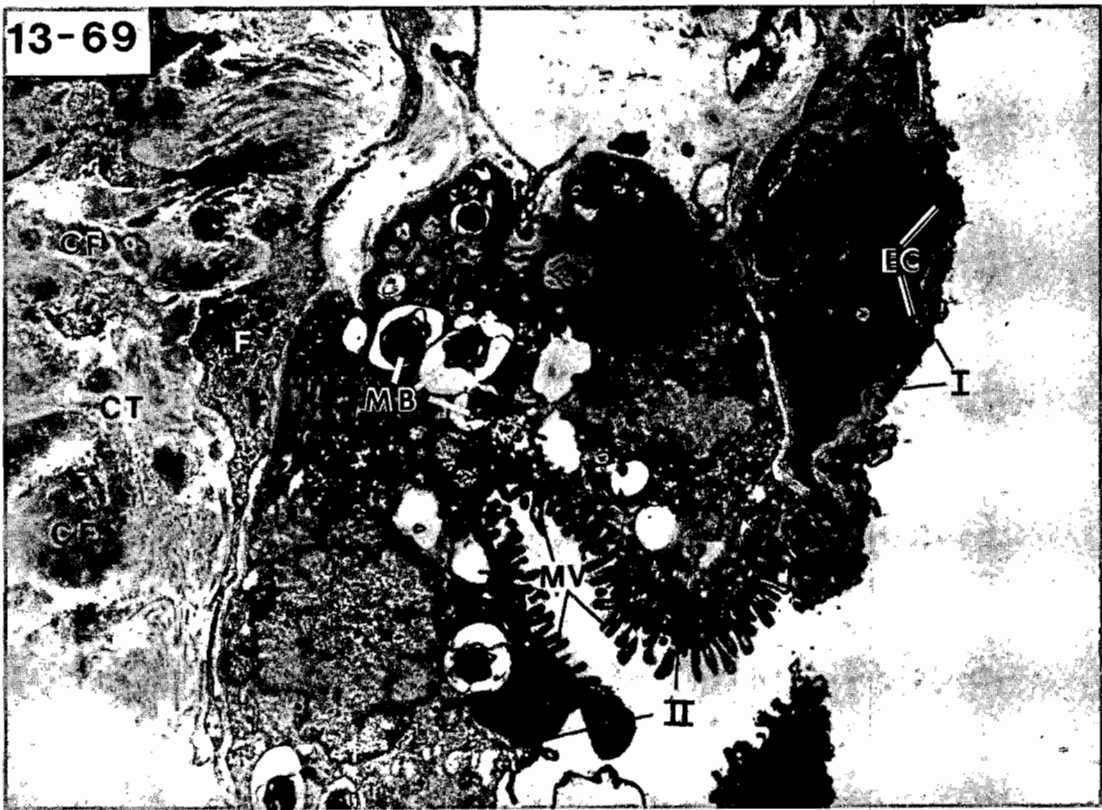


Figure 13-69. Transmission electron photomicrograph of a portion of a respiratory bronchus from whale 80B8. A thin cytoplasmic process of a type I pneumocyte may be seen extending over a capillary (I). A shared basal lamina separates the type I cell from the endothelial cell (EC) lining the capillary. A type II pneumocyte (II) with surface microvilli (MV) and multilamellar bodies (MB) is also evident. Dense irregular connective tissue (CT) with processes from fibroblasts (F) is seen beneath the epithelium. Collagen fibers (CF) are also visible. X7,000

Figure 13-70. Transmission electron photomicrograph of a bronchus similar to that shown in Fig 13-69. A type II pneumocyte (II) covers the capillary (C) seen here. Junctional regions may be seen between adjacent pneumocytes (arrows). Complex lateral extensions are seen between two type II pneumocytes (arrowhead). Collagen (CF) and fibroblasts (F) may also be seen beneath the epithelium. X8,800

13-69



13-70



Figure 13-71. Transmission electron photomicrograph of hyaline cartilage from a respiratory bronchiole taken from whale 80B8. The densely packed collagen (CF) is evident as are several chondrocytes (CH). X5,700

Figure 13-72. Transmission electron photomicrograph of a chondrocyte from a region of hyaline cartilage in a respiratory bronchiole from whale 80B8. The nucleus (N), lipid inclusions (L), mitochondria (M), as well as other cytoplasmic structures may be seen. Many thin cytoplasmic extensions (CX) may be seen radiating from the cell body. X10,700



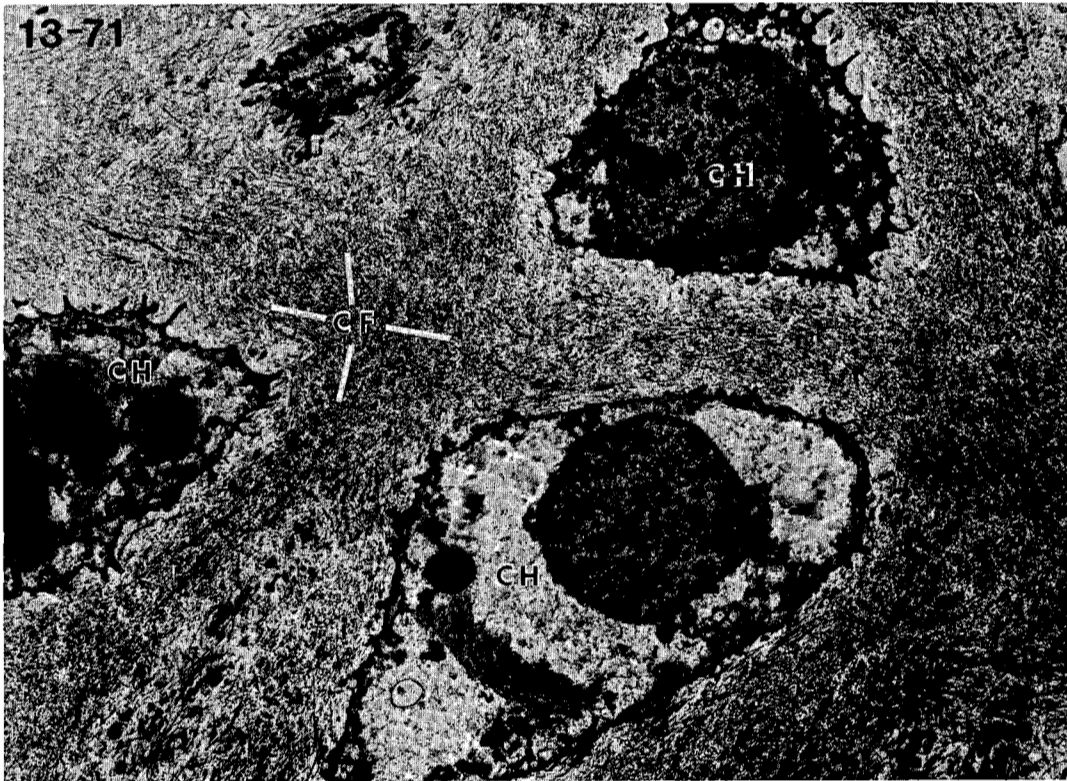


Figure 13-73. Photomicrographic montage of a terminal bronchiole, respiratory bronchioles, alveolar duct, alveolar sacs, and alveoli of 80B8. The entire final pathway from the termination of the airway (terminal bronchiole-TB) to the ultimate sites of gaseous exchange (alveoli) show well in this composite. Gaseous exchange occurs from the first alveoli arising directly from the terminal bronchioles (none visible, see Fig 13-67B), the small alveolar sacs (SAS) and alveoli (A2) arising from the respiratory bronchioles, as well as the respiratory epithelium (arrows) lining the respiratory bronchioles (RB), the alveolar ducts (AD), the large alveolar sacs (LAS), and the terminal alveoli (TA). Cartilage plaques (C) extend throughout the respiratory bronchioles. The walls of alveolar ducts are highly fenestrated by the orifices of almost continuous eruptions of alveoli and small and large alveolar sacs. About all that remains are widely spaced pillars and plaques of loose connective tissue containing spirally and circularly arranged concentrations of elastic fibers (E). X.S., H and E, X50

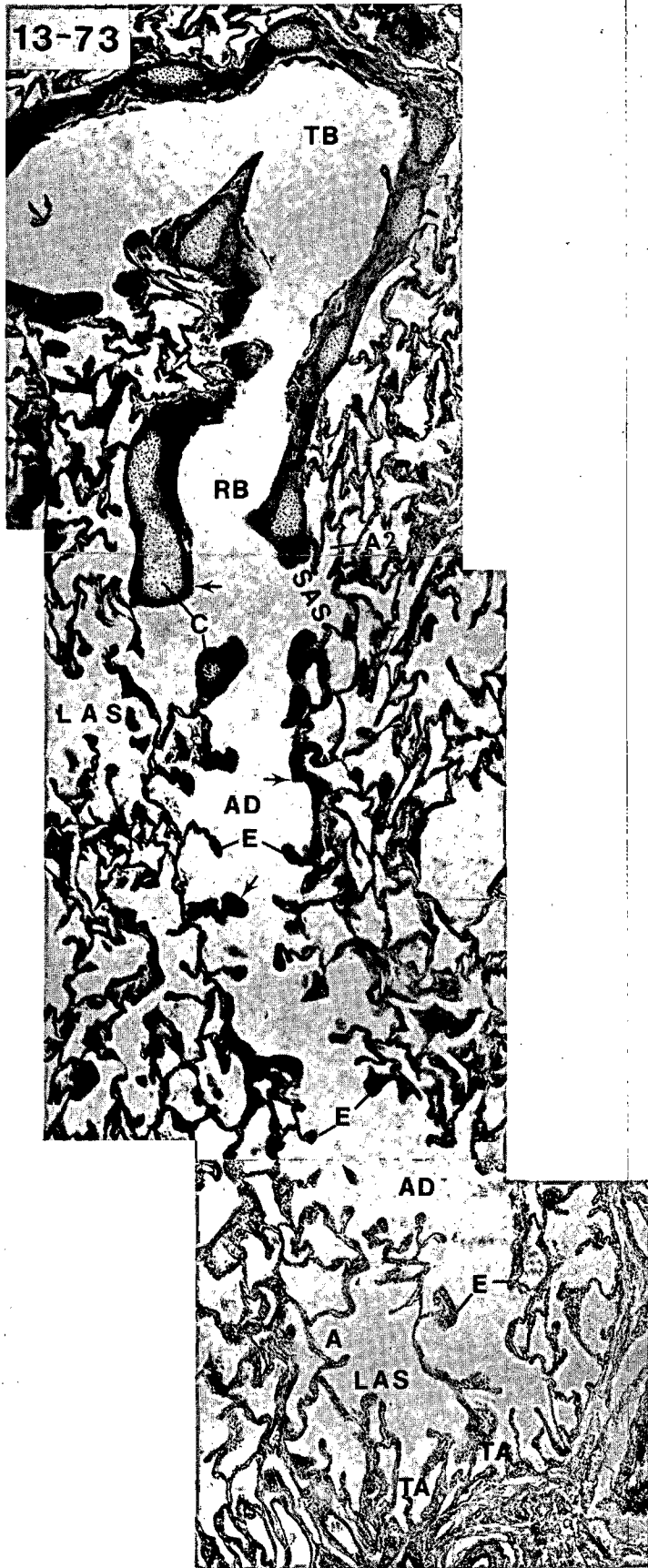


Figure 13-74. Photomicrograph of an alveolar duct and alveolar sac from 80B2. The wall of the alveolar duct (AD) is penetrated by the orifices of individual alveoli (A) and is composed of spirally arranged elastic fibers (arrows) that encircle the duct and, particularly, the orifices forming sphincters. The surface is covered by respiratory epithelium. Alveolar sacs (AS) are likewise constructed with the elastic fibers confined mostly in the sphincters leading to their alveoli (A2). Small pulmonary arteries (PA) are encased in minimal amounts of dense irregular connective tissue and give rise abruptly to thin walled arterioles (Ar). Thin walled veins (V) are also located in the connective tissue. X.S., Verhoeff stain, X50

Figure 13-75. Higher magnification photomicrograph of an alveolar duct wall from 80B2. The alveolar duct wall (W) consists predominantly of dense elastic tissue (E) composed of fibroblasts, elastic fibers, and occasional arterioles (Ar). The surface is covered by a respiratory epithelium (simple squamous cells closely covering capillaries). The arrows indicate the epithelium and erythrocytes in the capillaries. Debris (D) is primarily blood cells from collection and some mucus. L.S., H and E, X130

Figure 13-76. Photomicrograph of a semi-thin section of the alveolar duct wall from 80B8. The mucosa is lined with respiratory (simple squamous) epithelium covering erythrocytes (RBC) in capillaries. The wall contains numerous spirally arranged elastic fibers (arrows). The only cells present within the wall are fibroblasts (F). No smooth muscle cells occur. The inter-alveolar septa (S) are generally devoid of elastic fibers. Epon, L.S., Toluidine blue stain, X160

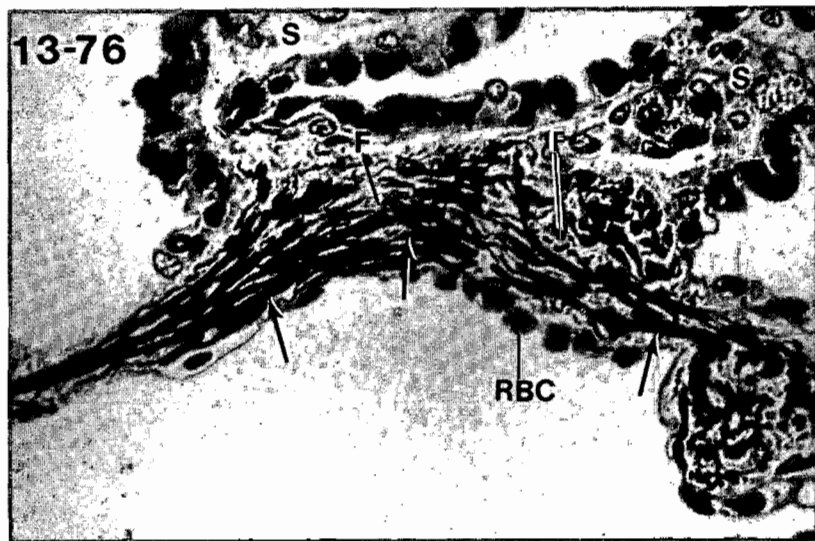
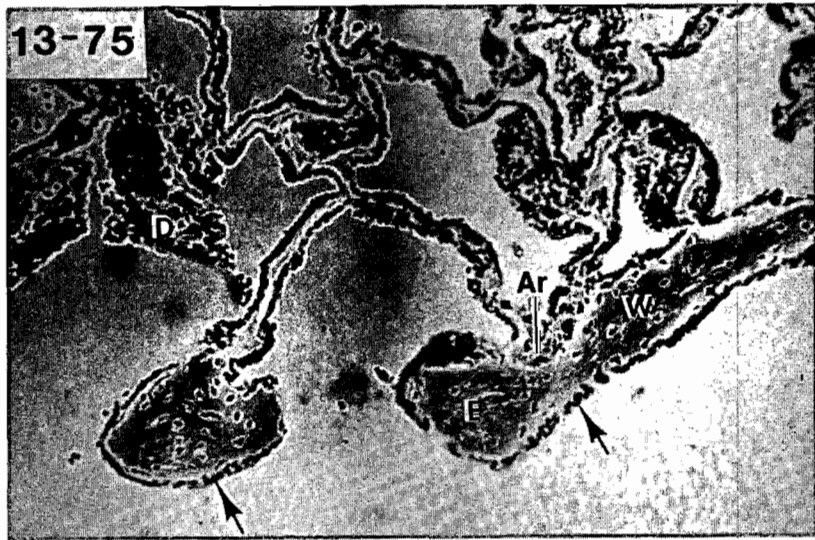


Figure 13-77. Photomicrograph of a semi-thin section of an alveolar sac orifice from 80B8. The margins of the alveolar sacs (AS) contain fibroblasts (nucleus - arrow) and elastic fibers (black) without smooth muscle cells. An apparent macrophage (M) was caught within the lumen. Epon, X.S., Toluidine blue stain X160

Figure 13-78. Transmission electron photomicrograph of the epithelium over an elastic sphincter from the lung of whale 80B8. Both type I (I) and type II (II) pneumocytes are seen. The nucleus of a type I pneumocyte (N) is also seen in this micrograph. Fibroblasts (F) in the connective tissue beneath the basal lamina may be seen. Elastic fibers (EF) are the prominent feature of this subepithelial connective tissue. X4,700

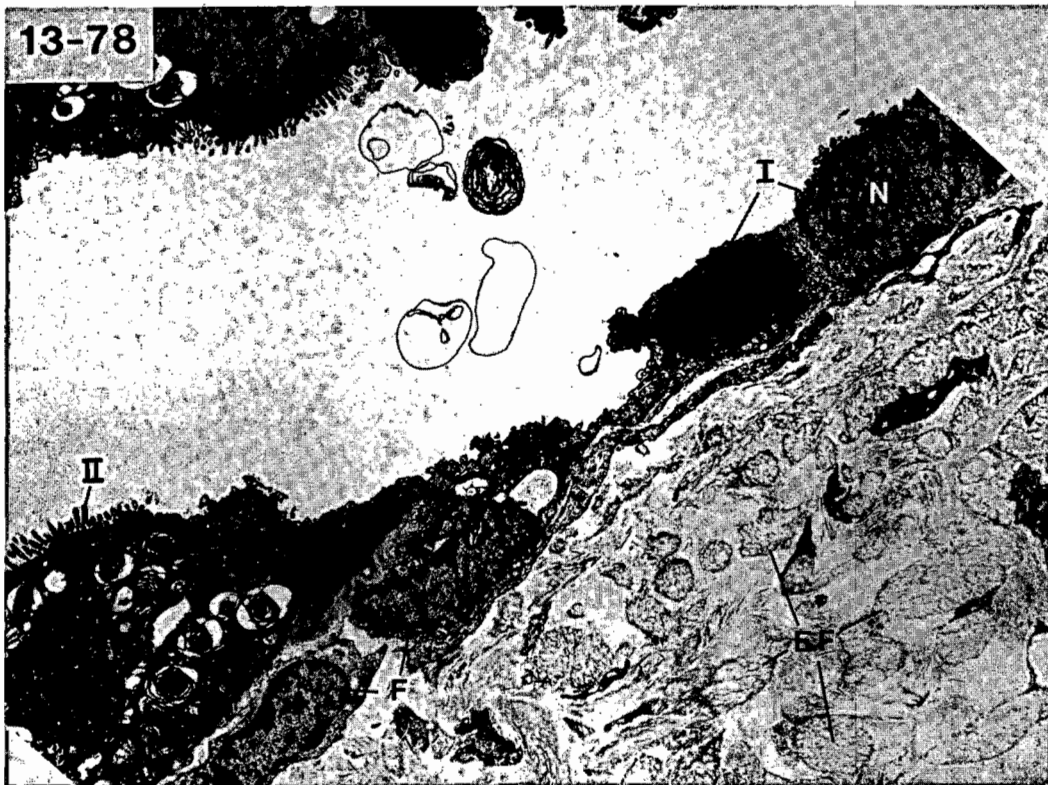
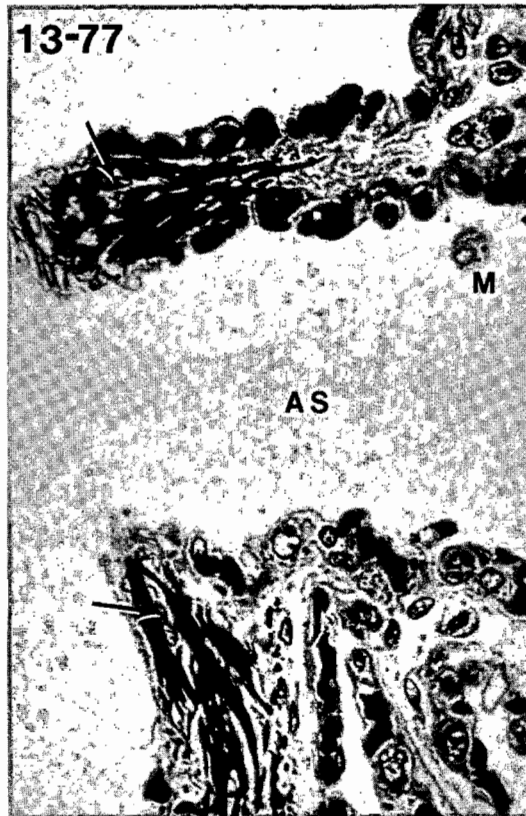
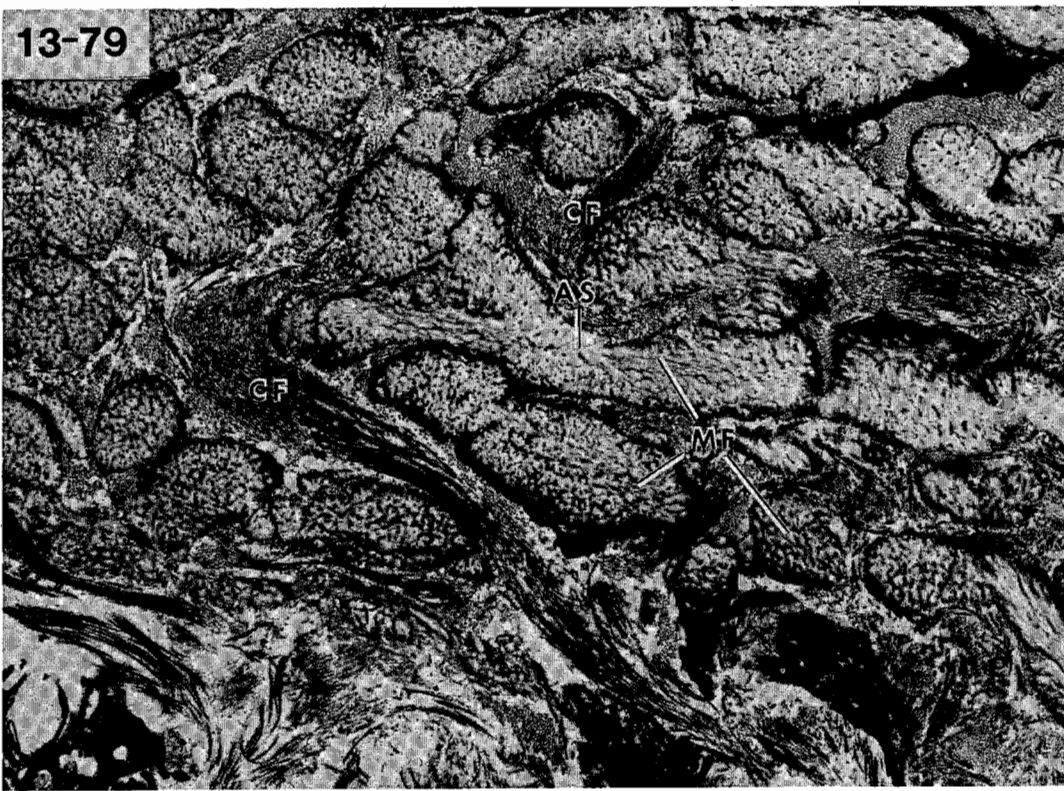


Figure 13-79. Higher magnification transmission electron photomicrograph of a region of the connective tissue shown in Fig 13-78. Elastic fibers are evident. The elastic fibers are composed of microfibrils (MF) and amorphous substance (AS). Mixed among the elastic fibers are delicate collagen fibers (CF). X8,900

Figure 13-80. Transmission electron photomicrograph through a more cellular region of an elastic sphincter from whale 80B8. Both collagen (CF) and elastic fibers (EF) are evident. Fibroblast-like cells are seen. These cells display narrow, irregular, cell processes (P) extending away from the cell body. A pair of centrioles (CL) are evident in one fibroblast. No evidence of smooth muscle is seen. X8,900



13-79



13-80



Figure 13-81. Transmission electron photomicrograph of a portion of an elastic sphincter from the lung of whale 80B2. The preservation is not as good as shown for whale 80B8 in Figs 13-78 and 13-79. Many open spaces are seen in the fibroblasts (F). Many cells are seen in the micrographs but no smooth muscle is evident. X5,600

Figure 13-82. Photomicrograph of a semi-thin section of an interalveolar septum from 80B8. The septum between adjacent alveoli is typically cetacean consisting of loose connective tissue with fine collagen fibers (C) and fibroblasts (F). Each alveolar lumen is not only lined with its own simple squamous epithelium, but each has its own capillary network filled here with erythrocytes (RBC). The entrance to each alveolus is controlled by an elastic sphincter (arrow). Epon, X.S., Toluidine blue stain, X160

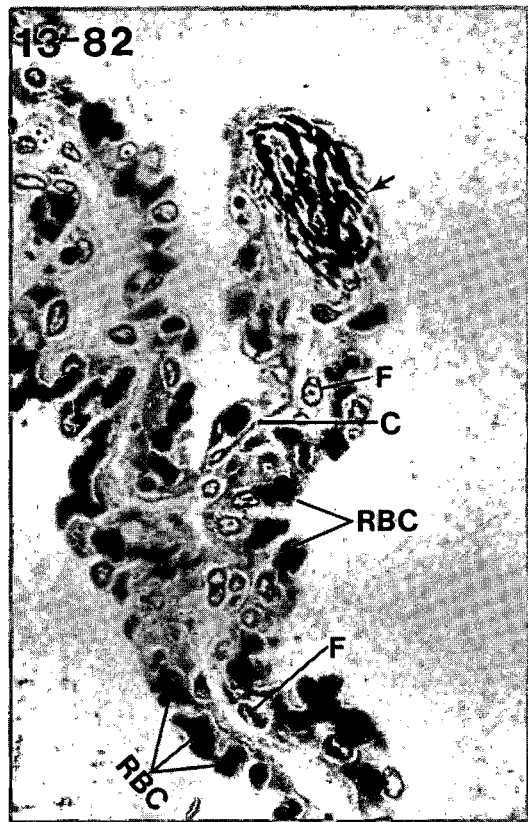


Figure 13-83. Transmission electron photomicrograph of a multilamellar body extruded by a type II pneumocyte into the lumen of an airway lined by respiratory epithelium from whale 80B8. Concentric rings of membranous material may be seen. This probably represents material destined to form the surfactant coating over the respiratory epithelium. X27,500

Figure 13-84. Transmission electron photomicrograph of a multilamellar body similar to that shown in Fig 13-83. Tubular myelin (TM) often seen in mammalian lungs is evident. X16,500

13-83

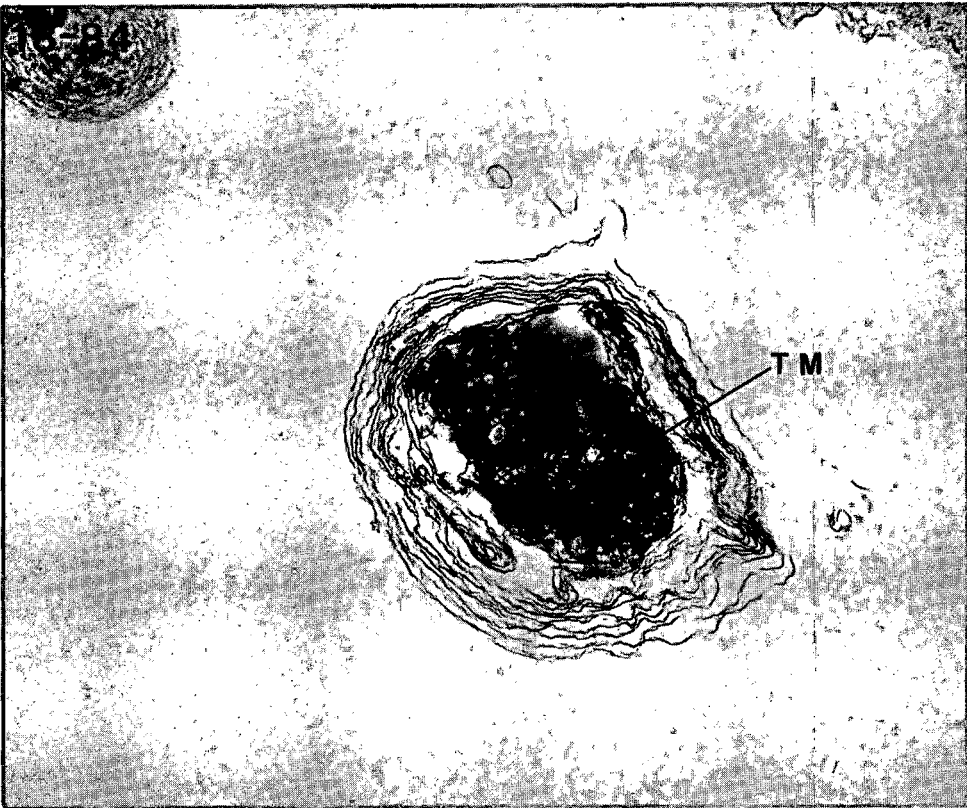
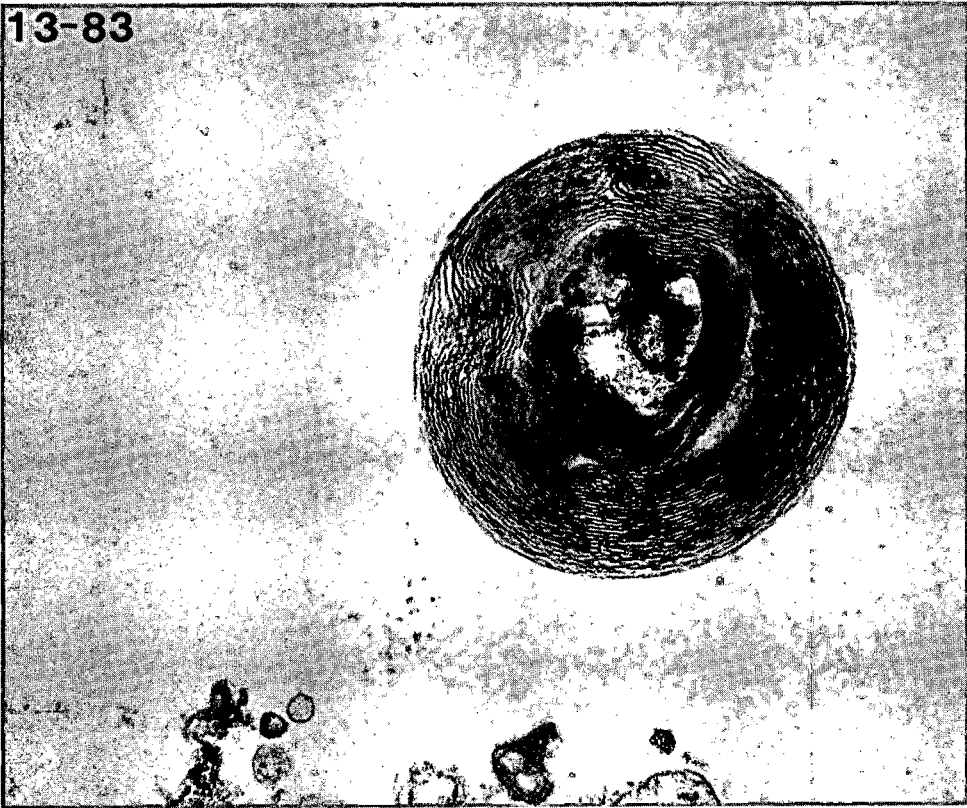


Figure 13-85. Scanning electron photomicrograph of alveoli from the lung of whale 80B1. The alveolar septum (S) and alveolar epithelium (AE) are evident. X1,400

Figure 13-86. Higher magnification scanning electron photomicrograph of a region of an alveolus shown in Fig 13-85. Red blood cells (RBC) are evident within the capillaries while collagen fibers (CF) are seen in the connective tissue. X6,700

13-85



13-86

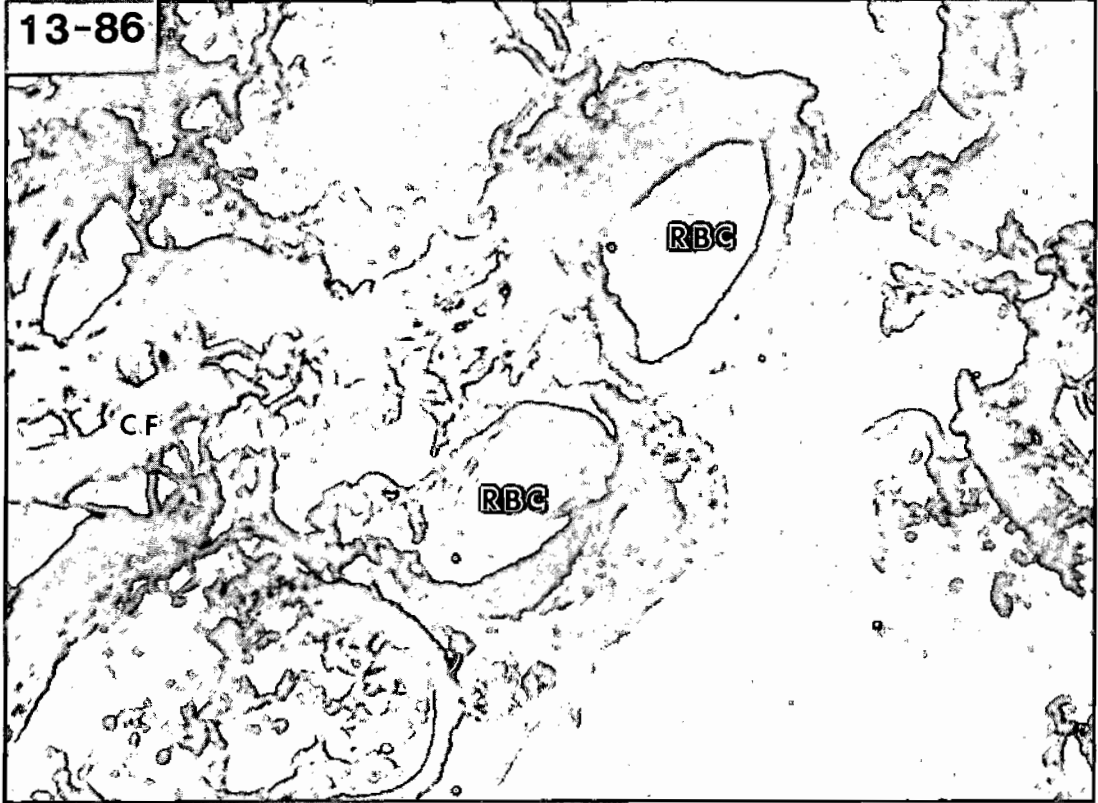
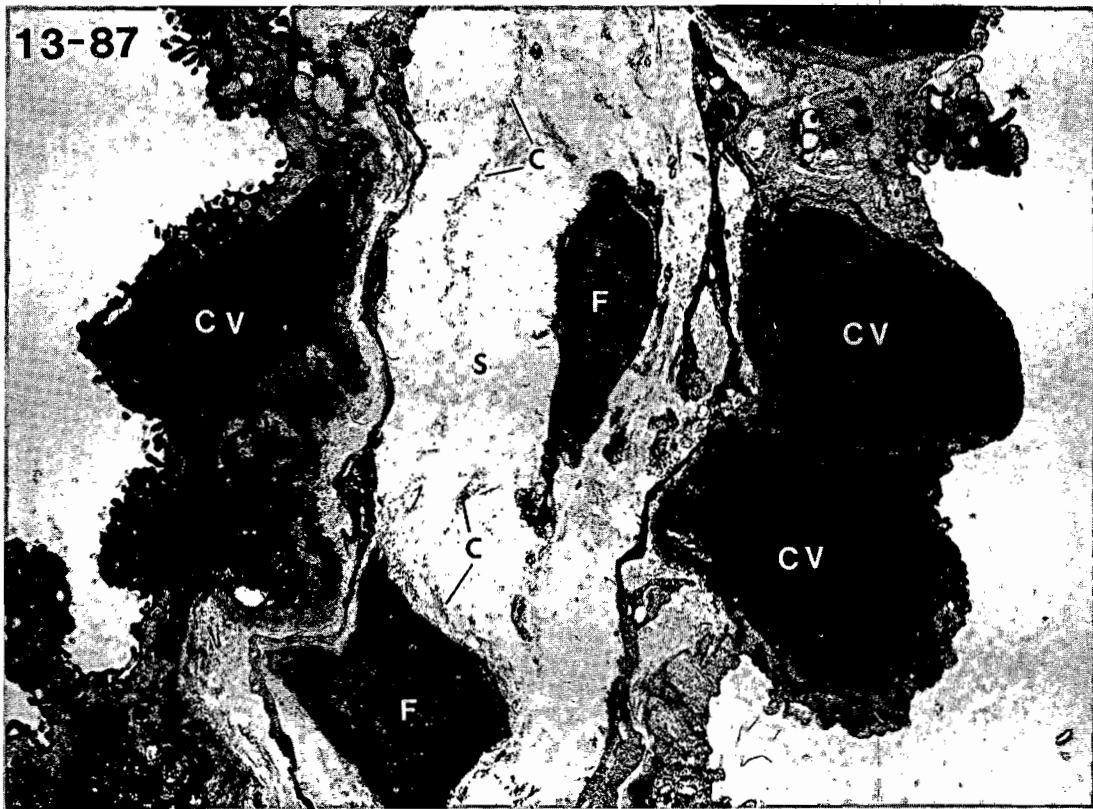


Figure 13-87. Transmission electron photomicrograph of a portion of an alveolar wall from the lung of whale 80B8. Capillaries (CV) line both sides of the alveolar septum (S) and are covered with respiratory epithelium similar to that seen elsewhere. Fibroblasts (F) and collagen (C) are evident within the septum. X7,200

Figure 13-88. Transmission electron photomicrograph of a portion of the respiratory epithelium from the lung of whale 80B8. Two mononuclear cells (MNA and MNB) are evident. These probably represent phagocytic cells (possibly a monocyte) in the capillary (MNA) and a connective tissue macrophage (MNB). Free multilamellar bodies (ML) are also seen. X9,000



13-87



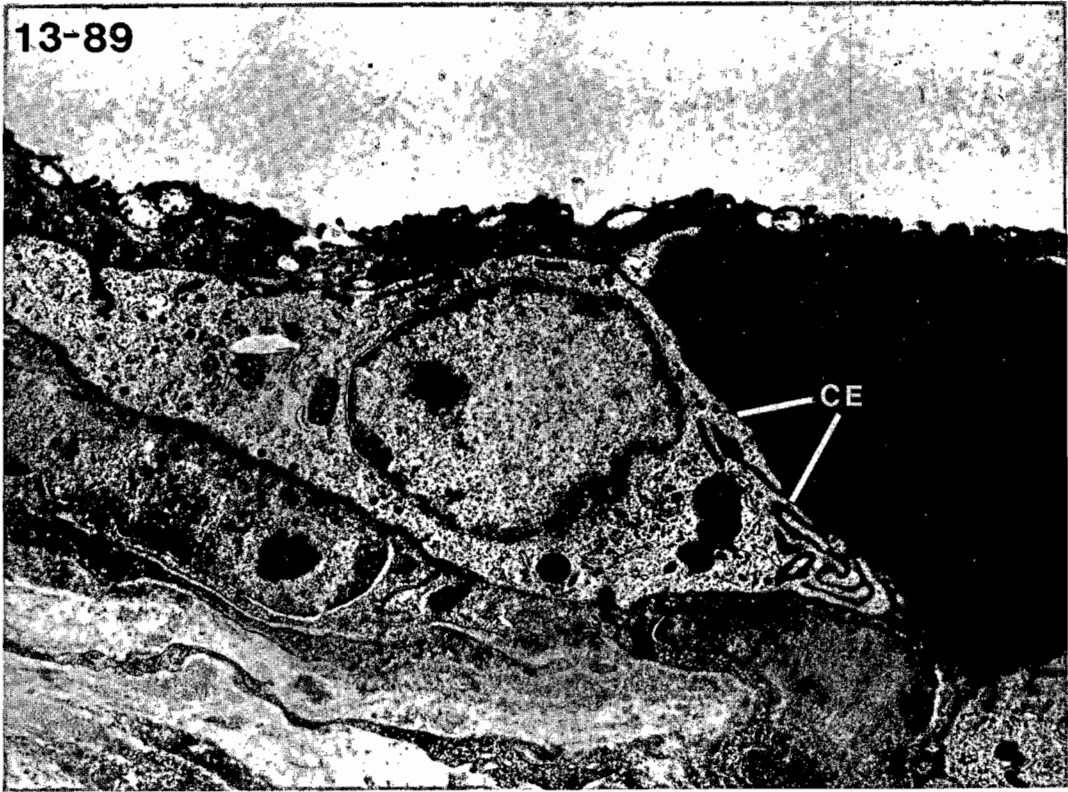
13-88



Figure 13-89. Higher magnification transmission electron photomicrograph of a mononuclear cell similar to that shown in Fig 13-88. Complex cytoplasmic extensions (CE) are seen as are numerous organelles within the cytoplasm. This is probably a monocytic cell. X10,400

Figure 13-90. Transmission electron photomicrograph of a type II pneumocyte from the lung of whale 80B8. Along with the usual intracellular organelles, an inclusion showing a fingerprint-like structure is seen (FP). X15,300

13-89



13-90



Figure 13-91. Photomicrograph, lung with pleura, 80B1. The 1.2-2.4 mm thick elasticized pleura is predominantly dense irregular connective tissue (Ct) throughout with the outermost region highly elasticized (E). Various sized arteries (A) and veins (V) occur randomly. The only "septa" (S) within the lung tissue are typical as illustrated and seem to be confined to the coursing of the pulmonary vessels. Large continuations of pulmonary tissue (P) are the rule. Note the numerous alveolar sacs (AS) surrounded by their connecting alveoli. X.S, Verhoeff stain, X50

Figure 13-92. Higher magnification photomicrograph of the pleural wall in Fig 13-91. The outer surface is covered with typical mesothelium (arrow) and a thin region of dense irregular connective tissue followed by a variably thick concentration of elastic fibers (black wavy lines) and then dense irregular connective tissue continues inwardly with the more usual quantity of elastic fibers. Large thin walled arteries (A) and veins (V) course randomly. X.S., Verhoeff stain, X160

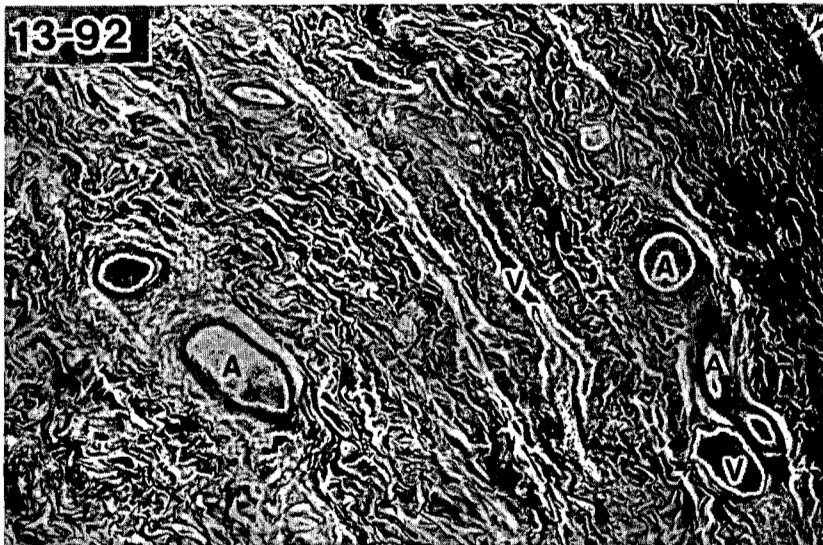
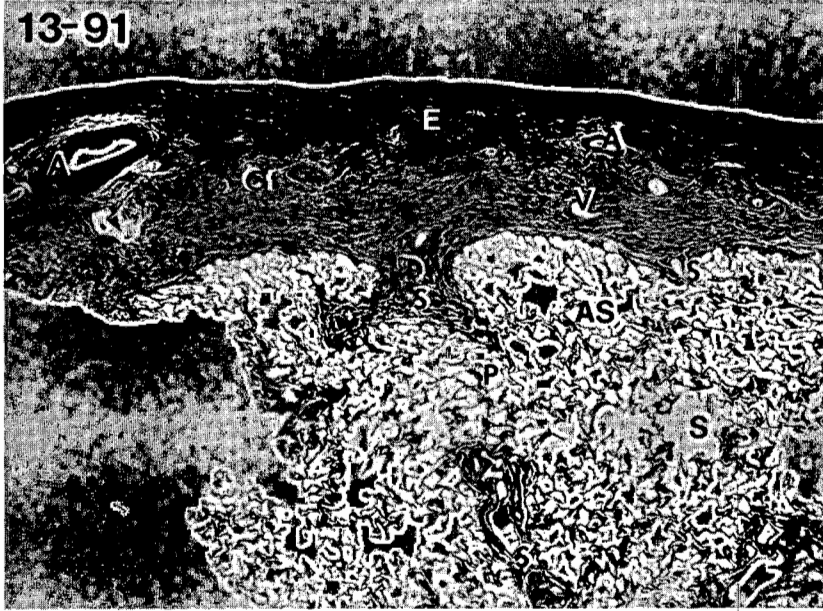
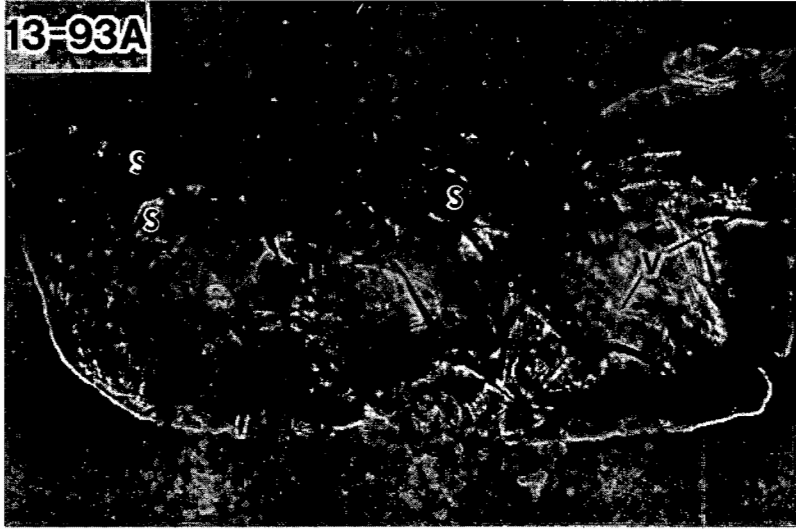


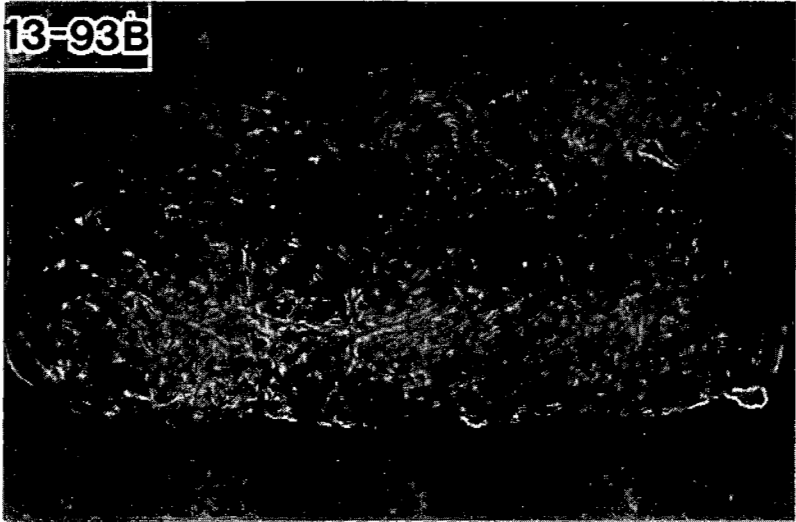
Figure 13-93. Photographs of the lungs of 79B1 and 80B2.

- A. Ventral (medial) view of 79B1, a right lung of an Ingutuk. The lobar bronchi are removed and segmental bronchi (S) are seen in the hilar region. The superficial location of the veins (V) just below the pleura should be noted. X0.11
  
- B. The dorsal (lateral) surface of 79B1 demonstrates creases in the thick pleura (arrows) which are fixation related and not signs of lobation. X0.12
  
- C. The dorsal (lateral) surface of 80B2. External creases in the pleura (arrows) are fixation artifact and not lobar septa. The principal bronchus (C). The opening (O) where the cranial lobar bronchus is torn away can be seen. Medial view is in Fig 13-47A. X0.13

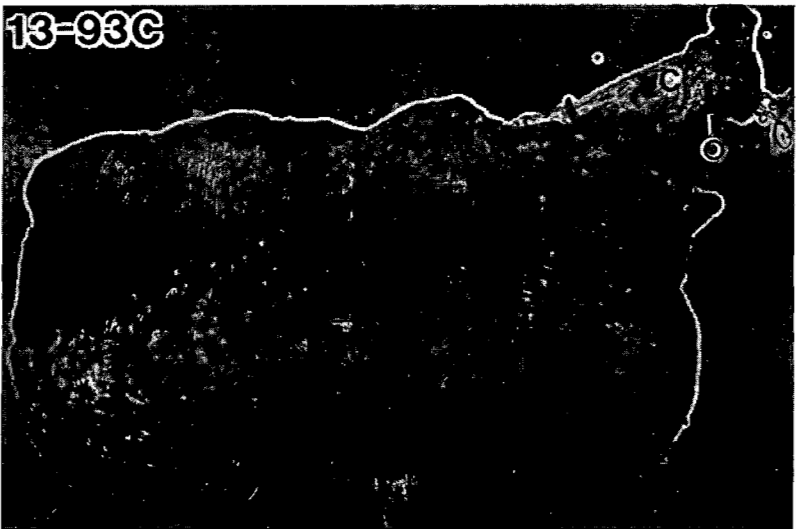
13-93A



13-93B



13-93C



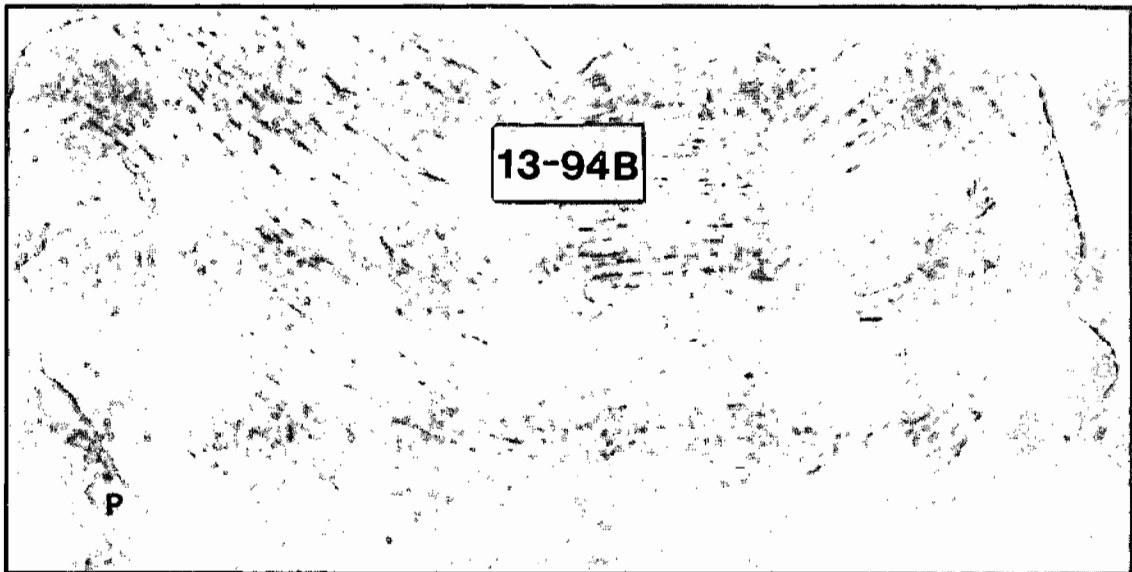
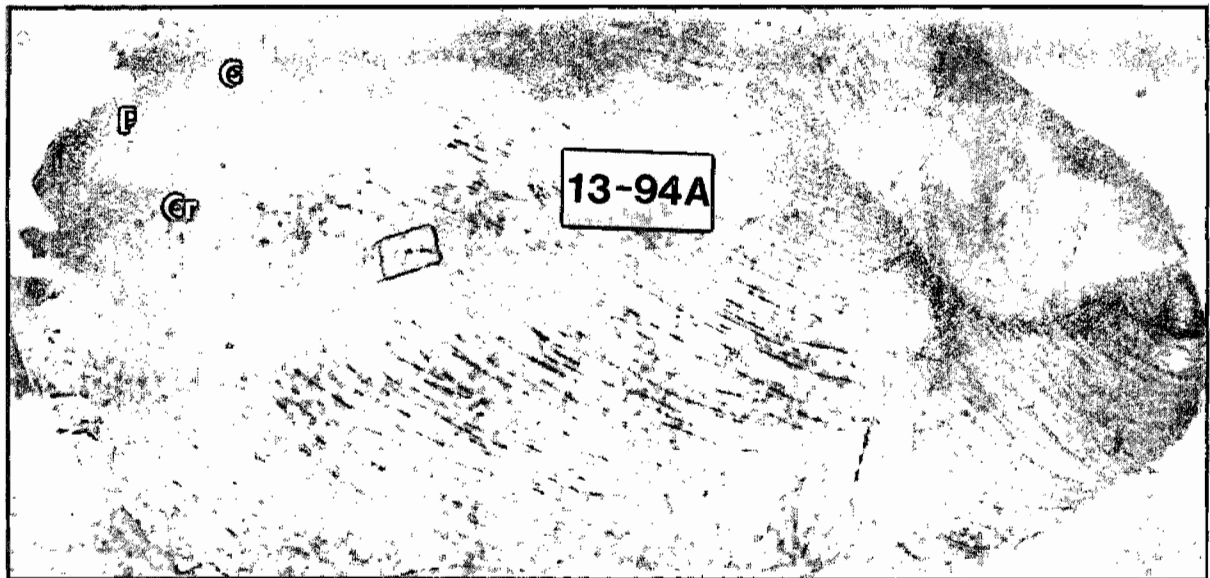


Figure 13-94. Photographs of the lung of 80B7 and 80B8.

- A. The dorsal (lateral) surface of 80B7. The principal bronchus (P) can be seen dividing into cranial (Cr) and caudal (C) lobar bronchi. The thick pleura covering is wrinkled due to its high elastic content and fixation. The large crease (arrows) is fixation and shipping artifact. The medial view can be seen in Fig 13-46A. X0.18
- B. The dorsal (lateral) surface of 80B8. Note the thick wrinkling of the pleura is cut away near the principal bronchus (P) showing the underlying parenchyma. The large groove (arrow) is from shipping. X0.21



## II. Kidney

Owing to the fact that all the specimens received were small chunks of kidney tissue and not the whole organ, it was not possible to determine the general morphology of the kidney of the bowhead whale. Thus, no description is given of the peritoneal investment of the organ, the existence and location of the hilus and renal sinus, overall measurements, or the pattern of entrance or emergence of arteries, veins and ureters. All samples received had one or two surfaces invested with a layer of fascia that contained yellowish colored adipose tissue. When this fascia was pulled away from the kidney tissue, a thin layer remained adherent to the surface (Fig 13-95). This surface fascia did not contain any large blood vessels.

None of the samples demonstrated any of the main renal arteries, veins or ureters. Only smaller branches were represented in the specimens received. Maximum diameters of branches of the renal artery were 5 mm, renal veins 15 mm, and ureteral branches 8 mm. These structures were completely invested by loose fascia that also joined the many kidney lobules together.

In one specimen (80B7) the sample was taken from the margin of the left kidney. The artery, vein and ureteral branch, with their fascia covering, were located in an indentation on the surface of the specimen. The indentation looked like the renal sinus (Figs 13-96, 13-97), however, the small diameter of the vessels indicated that it might be the tip of the sinus. This also implied that the main renal artery branched as it approached the sinus, while the main renal vein and ureter were formed from smaller branches in the sinus. From this we may speculate that the kidney of the bowhead whale has an elongate hilus that extends the whole length of its medial surface.

The kidney of the bowhead whale is highly lobated. It is divided into small lobes or renicules. They were found to exist individually or in clusters of three to five (Figs 13-98, 13-99, 13-100, 13-101). Individual renicules had a complete fascial investment while those in a cluster shared a common investment of fascia with incomplete partitions between renicules (Fig 13-99).

Dissection of the fascia of various clusters exposed the branches of the ureter, renal artery, and renal vein which were completely embedded in it (Figs 13-101, 13-102). A striking feature of the kidney of this whale was the elaborate network of very thin walled veins that surrounded the arterial and ureteral branches (Figs 13-102, 13-103, 13-105). These veins had large lumina, being as much as 8 mm in diameter as compared to 2 mm for arteries and

3 mm for ureters. The veins filled most of the space between renicules and clusters of renicules (Figs 13-103, 13-104, 13-105). When opened there were no discernible valves, but tributaries opened into larger veins on raised folds of the tunica intima (Fig 13-106).

#### Renicules

Each renicule was made of a conical shaped unit. The base of the cone was superficial and the tip of the cone was directed towards the center of the kidney. The cortical parts of the renicules were the only visible structures on the surface (Fig 13-98). The medullary parts were not visible because they were surrounded by large thin walled veins and fascia (Fig 13-101). The outline of the base of the cone was polyhedral and the sides of the renicule were flattened owing to their crowding by neighboring renicules. Blood vessels entered and left the renicules at the corticomedullary junction (Figs 13-107, 13-108). The ureteral branch or infundibulum left the calyx at the tip of the renicule (Fig 13-109). The renicular cortex was narrower than the medulla. It capped the medulla and extended about half of the width on the sides. The cortex was covered by a very thin transparent capsule (Fig 13-110). Subcapsular veins were easily demonstrated as a network of thin walled vessels filled with brown coagulated blood. When branches of the renal veins were injected with colored latex or Microfil, some of the subcapsular veins became filled with the injection mass (Figs 13-111, 13-112, 13-113). The largest diameter of a renicule was at its base, ranging from 7.8-14.1 mm. The smallest diameter was represented by a line extending from the base to the apex of the renicule which ranged from 7-10.1 mm (Figs 13-114, 13-115).

Microdissection of renicules revealed that two or more units in a cluster could have fused cortices but retained separate renal papillae (Fig 13-116). Each renal papilla was intimately surrounded by a calyx. A latex rubber cast of calyces clearly demonstrated the chalice shape of these structures (Fig 13-117). More than one calyx could join to empty in one infundibulum (Fig 13-118). The majority, however, emptied independently. On vertical sections of renicules, the cortex, medulla and intermedullary regions were clearly demonstrated. The cortex of the formalin fixed renicule was dark brown in color and represented the outer one-fifth to one-third of the thickness of the renicule. The medulla was dark toward the cortex but was much lighter distally and occupied the remainder of the parenchymal thickness of the renicule (Figs 13-109, 13-110, 13-114, 13-115).

The corticomedullary junction (sporta perimedullaris) was represented by a very thin, white connective tissue band between cortex and medulla which contained arteries and veins (Figs 13-109, 13-110, 13-114, 13-118). The cortex measured 2-3 mm in thickness while the medulla occupied the other two-thirds of the renicula (9-11.5 mm). The sporta measured 0.3-0.5 mm in thickness (Fig 13- 115).

When a renicula was serially sectioned transversely starting at the surface of the cortex and proceeding to the level of the corticomedullary junction, it was evident that the connective tissue of the sporta started about 0.5 mm from the surface as a thickening of the stroma of the central zone of the cortex. It was perforated by ascending and descending renal tubules (medullary rays). Deeper sections demonstrated further expansion of the sporta which was perforated by larger bundles of tubules. At the corticomedullary junction it became a wavy connective tissue circle with thickenings accommodating arcuate vessels (Fig 13-119).

The calyx of each renicula had a wall that measured 0.3 mm in thickness; however, it got thicker by blending with walls of neighboring calyces, or by being continuous with the walls of veins in the vicinity (Figs 13-110, 13-120). The wall of the calyx was continuous with the sporta at the corticomedullary junction.

Calyces became continuous with an expansion of a ureteral branch or infundibulum (Figs 13-109, 13-110, 13-114, 13-115). Sometimes more than one calyx shared an infundibulum (Fig 13-118). Ureteral branches draining several clusters joined to form larger branches. This pattern of union was repeated through the specimen and terminated in the formation of two or three ureteral branches draining each piece.

On examination of kidney tissue under the light microscope, it was obvious that the renicula was the morphological unit of the whale kidney. Each renicula was covered by a very thin 20  $\mu$ m capsule made of loose connective tissue. Deep to the capsule, the parenchyma was divided into cortical and medullary regions with an obvious corticomedullary zone of collagenous connective tissue, the sporta perimedullaris. The renal papilla of each renicula was surrounded by a calyx. The wall of the calyx either blended with the wall of a neighboring one or with the wall of a vein that surrounded it (Fig 13- 120).

#### Cortex

The cortex of the bowhead kidney renicula is of the typical mammalian type consisting of renal corpuscles and

tubules. Renal corpuscles were scattered among the tubules just under the capsule in the middle of the cortex, and were partially embedded in or very close to the corticomedullary connective tissue. Measurements of the corpuscles ranged from 120 x 100 to 170 x 110  $\mu\text{m}$ . Some corpuscles abutted each other to form clusters (Fig 13-121). Parietal epithelial cells of Bowman's capsule, podocytes and glomerular capillaries were easily demonstrated (Fig 13-122). Juxtaglomerular structures were well developed. Maculae densae, afferent arterioles, efferent arterioles and polar cushions were observed. Afferent arterioles were different from efferent arterioles in that they had thicker walls, wider lumina and the majority of smooth muscle cells in their walls were modified. Instead of the normal smooth muscle cell size and staining properties, these cells were stouter and had optically clear, lighter staining cytoplasm. They measured 18 x 8  $\mu\text{m}$  while regular smooth muscle cells measured 25 x 5  $\mu\text{m}$ . The transformation from the normal smooth muscle cell type began as these arterioles originated from interlobular arteries far from the juxtaglomerular areas (Fig 13-123). They also branched toward different glomeruli with their walls already modified (Fig 13-124).

In all the specimens studied (79B1, 79B2, 80B1, 80B2, 80B7, 80B8), no periodic acid-Schiff reaction (PAS) positive renin granules occurred in the juxtaglomerular cells of the afferent arterioles. The diameter of afferent arterioles ranged from 17.5-20  $\mu\text{m}$ . Efferent arterioles emerged from the glomeruli and acquired a smooth muscle wall. They had a comparatively narrower lumen (Fig 13-125).

#### Macula Densa

The part of the distal convoluted tubule that participates in the juxtaglomerular apparatus, the macula densa, was made of light staining, cuboidal epithelial cells with cytoplasm containing fine granules. The part of the tubule next to the glomerulus and its arterioles was characterized by crowding of the cuboidal cells forming a linear cluster of up to 19 cells (Figs 13-125, 13-126). The cells on the other side of the tubule were widely spaced. The polar cushion, or extraglomerular mesangial cells, were represented by a stratification of flattened cells with oval to round nuclei. They filled the triangular area formed by the macula densa, afferent arteriole, and efferent arteriole, and were continuous with the glomerular mesangium (Fig 13-125).

#### Glomerulus

The afferent arteriole entered the renal corpuscle and joined a maze of capillary-like channels lined by endothelial cells. They rested on a basal lamina that was continuous around the channels

in the glomerulus. The channels were arranged into three to five units which were clearly separated from each other. Each unit represented a glomerular lobule. These were easier to observe if the tissue was stained for PAS reaction, owing to the positive reaction of the basal laminae surrounding these channels (Fig 13-127). Glomerular mesangial cells represented connective tissue cells that were an extension of the polar cushion. They were located in the central or axial area of the glomerulus between vascular channels and had an abundant light staining cytoplasm and rounded nuclei (Figs 13-122, 13-125).

Parietal epithelium of the renal corpuscle was made of simple squamous epithelium with large oval nuclei that protruded into the urinary space. The epithelium rested on a complete basal lamina that surrounded the corpuscle except at the vascular and urinary poles (Fig 13-128). The visceral cells, or podocytes, had thicker nuclei and their cytoplasm rested on the basal lamina of the glomerular capillaries. They had more abundant cytoplasm than parietal cells and they stained more darkly than mesangial cells (Figs 13-122, 13-125).

At the ultrastructural level, the renal glomerulus and capsule were similar to those seen in other mammals. The parietal epithelium of Bowman's capsule was simple squamous while the visceral epithelium consisted of podocytes with numerous primary and secondary (foot) processes. The foot processes rested on the basal lamina of the capillaries of the glomerulus and interdigitated to form 25-50 nm filtration slits (Figs 13-129, 13-130, 13-131). Diaphragms bridging filtration slits were not observed (Figs 13-130, 13-131). The basal lamina extending between the foot processes and the capillary endothelium measured approximately 0.18  $\mu\text{m}$  in thickness. The parietal epithelium rested against a basal lamina which separated the capsule from the connective tissue between nephrons (Figs 13-129, 13-132). Mesangial cells were also evident on the capillary side of the basal lamina (Fig 13-129).

Renal Tubules (uriniferous tubules) Due to poor preservation, the study of cellular detail was not possible. Proximal, distal, ascending and descending limbs, and collecting tubules could be identified, however.

Proximal convoluted tubules were identifiable throughout the cortex from just under the capsule to the corticomedullary junction. The epithelium in these tubules was dark staining, granular columnar cells (Fig 13-123). The brush border was not fixed well and was not visible even after the PAS reac-

tion, although the basal lamina was easily demonstrated (Fig 13-127). The tubules measured 30-50  $\mu\text{m}$  in diameter. The lumen of the tubules was the narrowest among those seen in the cortex.

Distal convoluted tubules had a wider lumen because the lining epithelium was cuboidal in shape. The cells stained lighter, were less granular (Fig 13-123) and the lumen measured 30-40  $\mu\text{m}$  in diameter. Descending and ascending thick limbs of Henle's loop formed the medullary rays. The descending one resembled proximal convoluted tubules, while ascending limbs resembled distal convoluted tubules. The only difference was their straight course through the cortex (Fig 13-121).

Collecting tubules or ducts were lined by optically clear cuboidal epithelial cells. The cells bulged into the lumen, almost occluding it. Proximal and distal tubules as well as the collecting ducts were poorly preserved, making fine structural observations with the electron microscope impossible (Figs 13-133, 13-134).

Interlobular arteries were easily recognized in the cortex and averaged 75  $\mu\text{m}$  in diameter. An obvious morphological feature of the kidney cortex of the bowhead whale was the presence of large, thin walled subcapsular veins that had large lumina. These were easily demonstrated by subgross and microscopic means (Figs 13-111, 13-112, 13-113). These subcapsular veins drained the capillary networks of the outer cortex, then led into interlobular veins which traversed the cortex to join larger arcuate veins in the sporta perimedullaris. The arcuate veins then left the renicula and drained into the veins that surrounded the renicular structures (Fig 13-135).

#### Connective Tissue Stroma

The cortex of the kidney of the bowhead had a well developed dense connective tissue stroma that surrounded all structures. It was most abundant around arteries and renal corpuscles in the cortex (Fig 13-136) and ranged from 2.5-7.5  $\mu\text{m}$  around tubules, and from 10-20  $\mu\text{m}$  around corpuscles. As described above in macroscopic studies, the connective tissue that formed the sporta perimedullaris actually had its origin in the middle layer of the cortex. It was a connective tissue sheet through which medullary rays ascended and descended between cortex and medulla (Fig 13-119B). Close to the corticomedullary junction, more connective tissue stroma surrounded the cortical elements (Figs 13-119C, 13-119E).

The corticomedullary junction was characterized by this well developed sheet of connective tissue that physically separated the cortex from the medulla except where tubules and blood vessels descended and ascended between

them. The corticomedullary tissue was made of dense white fibrous connective tissue with very few elastic fibers. No smooth muscle fibers were identified as part of this tissue, even with such differentiating stains as Masson's and Milligan's techniques (Figs 13-137, 13-138). The only muscle fibers observed in the corticomedullary tissue belonged to the walls of blood vessels. At the periphery of the reniculus, the corticomedullary tissue, or sporta perimedullaris, became continuous with the wall of the calyx. Blood vessels entered and exited through this junction between the sporta and calyx wall (Fig 13-120). When two adjacent calyces shared the same wall, usually the sportae of both renicules were continuous at the junction of the combined calyx wall (Figs 13-139, 13-143).

#### Medulla

The medulla consisted of outer and inner zones. The outer zone was composed mainly of medullary rays and vasa rectae among the straight tubules of Henle's loop. It is important to differentiate between thin segments of Henle's loop and vasa rectae. In the bowhead the arterial segments of the vasa rectae had the thickest walls with simple squamous endothelial lining and one smooth muscle layer. The venous segment had a very thin wall made of endothelial cells and looked like a large lumened capillary. Both of these frequently contained blood elements which made the identification easy.

Henle's thin loop was intermediate in size. It was made of very flat, low cuboidal or even simple squamous epithelium. In the latter type, it was very difficult to differentiate between it and the venous segments of the vasa rectae. The only clue was that the nuclei of the thin segment epithelium did not bulge into the lumen as much as in the venous segments. The thick segments of Henle's loop had the same morphology as their related convoluted tubules (Figs 13-140, 13-141). Collecting ducts were easily differentiated from the rest of the medullary structures. They were lined with optically clear cuboidal epithelial cells with sharply demarcated cellular membranes and centrally located nuclei (Figs 13-140, 13-141). Close to the tip of the renal papilla only collecting ducts and thin segments prevailed (Fig 13-142). It was difficult to differentiate interstitial medullary cells in light microscopic observations. The surface of the medulla and papilla that faces the calyx was covered by a very low transitional epithelium.

Two renal papillae may be fused and open into a common calyx that leads to a common infundibulum (Fig 13-143) without fusion of the cortices. In other renicules, the cortices may be fused but the papillae and calyces

remained separate (Fig 13-144). A third variation was the presence of separate cortices, papillae and calyces, but the calyces communicated to empty into a common infundibulum (Fig 13-145). The calyx wall was made of dense white fibrous connective tissue which was rich in capillaries. There were no smooth muscle fibers in the wall of the calyx or infundibulum. Smooth muscle fibers were present in the walls of ureteral branches only. The calyx, infundibulum and ureteral branches were lined with transitional epithelium (Figs 13-145, 13-146, 13-147).

The ureteral branch wall had a lamina propria-submucosa which was combined peripheral to the transitional epithelium. An outer circular smooth muscle layer and a tunica adventitia completed the wall. A unique feature in the bowhead was the presence of large thin walled veins that surrounded and sometimes shared walls with ureteral branches (Fig 13-148).

## Urinary Bladder

### Macroscopic Dissection

Two samples of urinary bladder were received from whales 79B1 and 80B7. The lining mucous membrane was smooth and highly folded in an irregular manner. The outer surface was covered by a loose tunica serosa that measured 4 mm in thickness. The complete thickness of the wall of the bladder was 3.7 cm in 79B1, a 8.7 m male Ingutuk variant and 6.5 cm in 80B7, a 10.0 m female ordinary bowhead. Other than the mucosal lining and tunica serosa, the rest of the wall was made of a very tough and vascular fibromuscular tissue. Due to the highly folded mucous membrane it was presumed that the samples were taken from contracted bladders.

### Microscopic Anatomy

The tunica mucosa had a lamina epithelialis of transitional epithelium. It varied between four and nine cell layers in thickness. Epithelial cells were missing from parts of the lining surface as a result of handling and processing of the specimens (Fig 13-150). In both specimens, a fine capillary network occurred adjacent to the basal cell layer (Figs 13-149, 13-150). The lamina propria was vascular, reasonably dense, fibroelastic connective tissue (Figs 13-149, 13-150). It terminated with a lamina muscularis mucosae of circularly arranged bundles of smooth muscle fibers in the male Ingutuk (79B1) (Fig 13-151). Peripheral to these bundles, the tunica submucosa consisted of highly vascular, much looser, fibroelastic connective tissue. Bundles of circularly arranged smooth muscle fibers were scattered with some longitudinally arranged fibers located around large thin walled veins (Fig 13-151). In sections taken from the bladder of the female



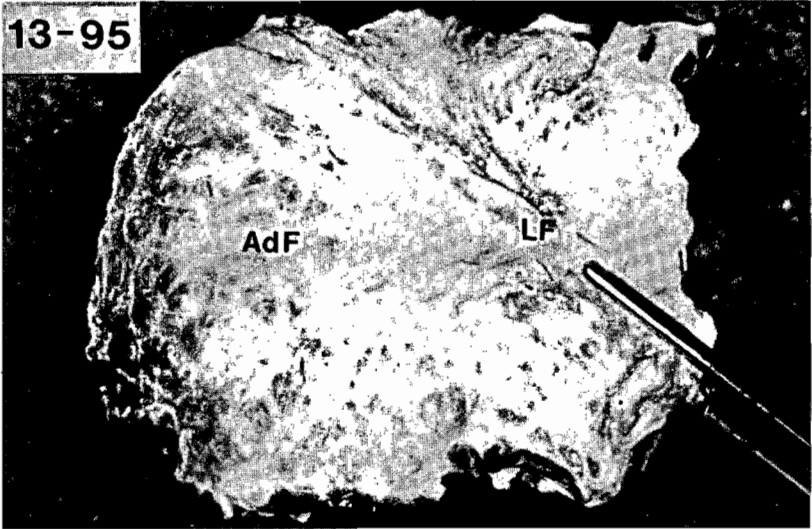
bowhead (80B7), the wall had a propria-submucosa without intervening muscularis mucosae. Bundles of smooth muscle fibers were scattered among the vascular connective tissue of both layers of the wall. The tunica muscularis was made of thick multidirectionally arranged bundles of smooth muscle fibers very loosely connected by loose connective septa in 79B1. In 80B7 the bundles were thicker and tightly packed together. Bundles of nerve fibers (Fig 13-152), autonomic nerve ganglia and blood vessels were also present within the tunica muscularis. The tunica adventitia consisted of loose fibroelastic connective tissue.

Figure 13-95. Photograph of a kidney sample covered with fascia, 80B7. Loose fascia (LF) is pulled away to expose a thin layer of fascia (AdF) adherent to renicules. X0.5

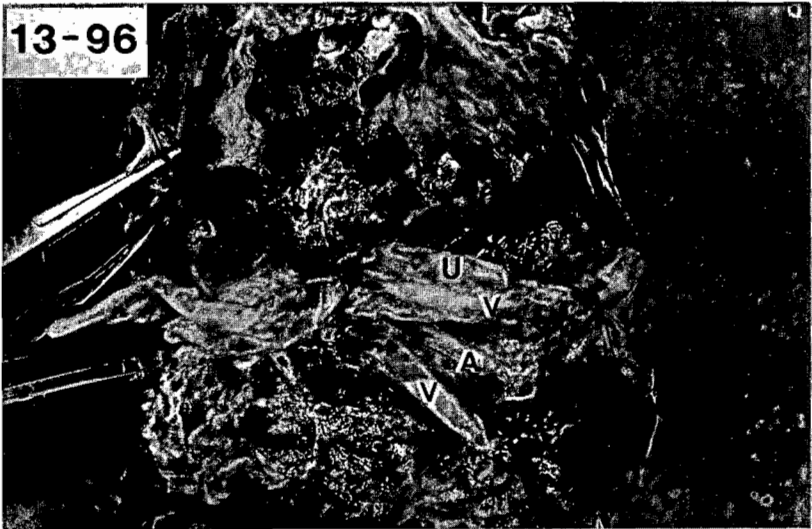
Figure 13-96. Photograph of a specimen from the margin of the left kidney, 80B7. The renal artery (A) and vein (V) branches and ureteral branch (U) are located in an indentation on the surface of the specimen. Structures are invested with loose fascia. X0.5

Figure 13-97. Photograph of the same specimen in Fig 13-96 with vessels and ureteral branch pulled away to expose indentation (H) on the surface of the kidney. This indentation probably represents the tip of the renal sinus. The part of this sinus where the blood vessels enter and leave the kidney is the hilus. X0.5

13-95



13-96



13-97

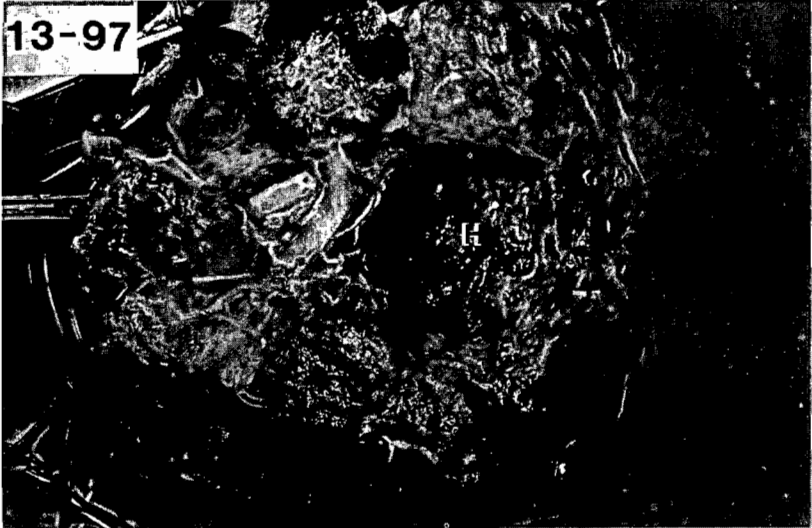


Figure 13-98. Photograph of a kidney specimen after removal of surface fascia, 80B7. Renucles are arranged in clusters (C). Only the bases of renucles represented by cortex surfaces are showing. X1

Figure 13-99. Photograph of fascial compartments (arrows) surrounding individual renucles of a cluster after removing the renucles, 80B7. X4.5

Figure 13-100. Photograph of the cortical surface of a cluster made of four renucles (R), 80B1. X4.5

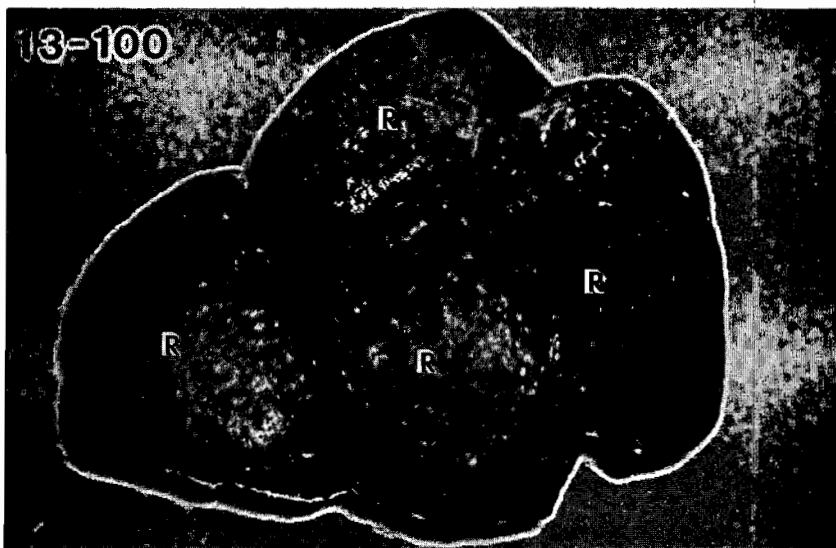
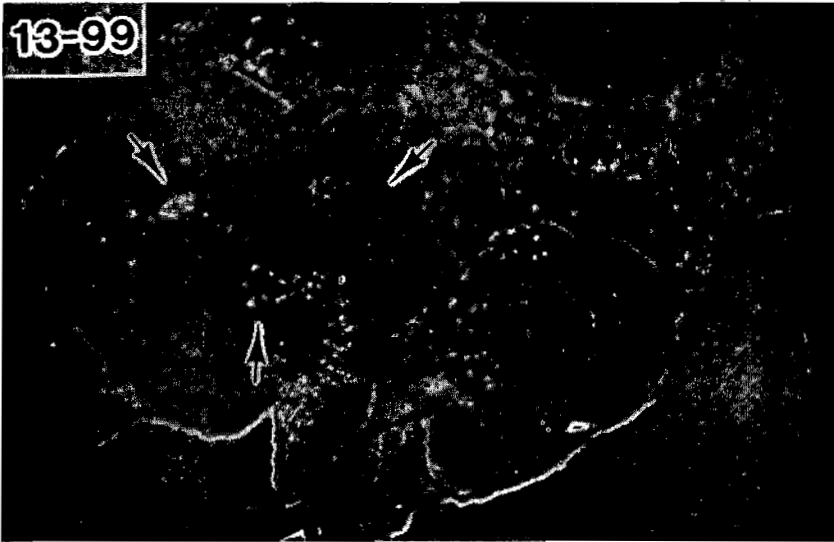
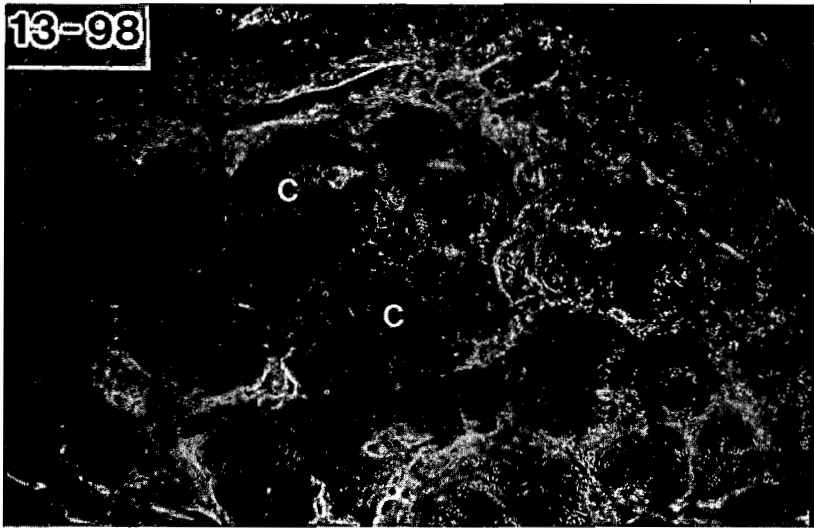
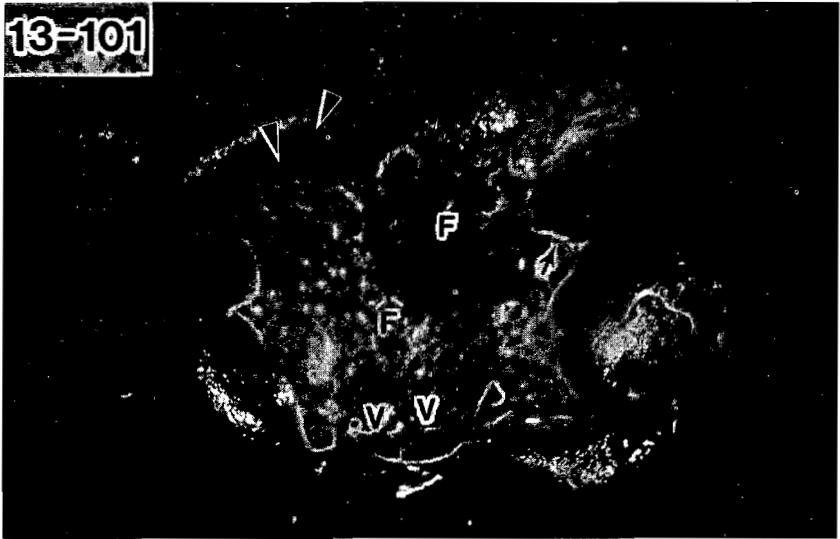


Figure 13-101. Photograph of the deep surface of same cluster in Fig 13-100. The minor calyces are completely hidden by fascia (F) and thin walled veins (V). A small artery (arrow) is entering the renicula at the corticomedullary junction. Superficial sub-capsular veins are seen under cortical capsule (arrowheads). X7.5

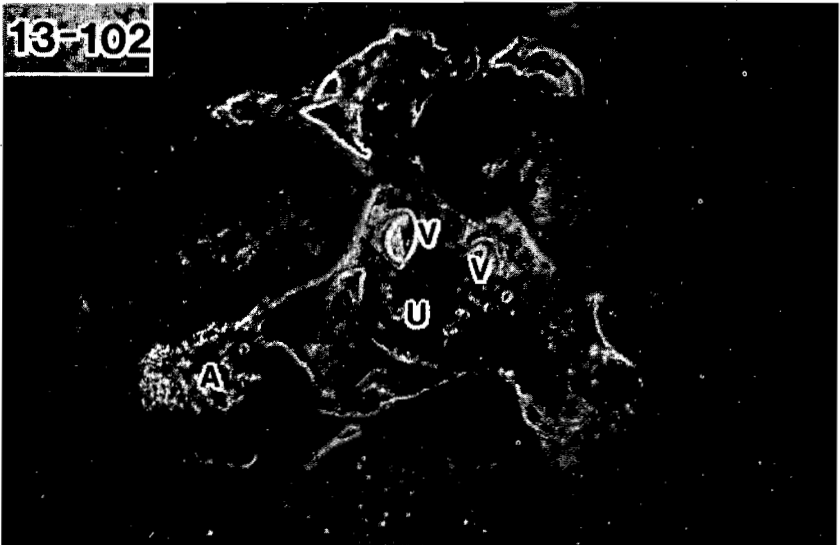
Figure 13-102. Photograph of the deep surface of same cluster in Fig 13-101 with fascia cleaned. Ureteral branch (U), renal artery (A) and veins (V) are exposed. Veins and ureter are cut transversely. One vein contains Microfil (white) mass that was injected into larger vein in the specimen. X5

Figure 13-103. Photograph of the deep surface of a cluster of renicula, 79B1. Fascia is cleaned away very carefully to expose very large thin walled vein (V) that fills the space (arrows) between renicula and hides an artery and ureteral branch. A cannula inserted through a hole in the venous wall is directed towards the renicula. X6

13-101



13-102



13-103



Figure 13-104. Photograph of the same specimen in Fig 13-103. The cannula in the vein is directed away from the renicule to show how extensive the veins (V) are. X4

Figure 13-105. Photograph of a microdissection of the deep surface of a cluster of renicules (80B1). Most of the fascia is cleaned away. A ureteral branch (U) is surrounded by large thin walled veins (V) while an artery (unopened) (A) crosses the area. Other thin walled veins (V) can be seen. X4

Figure 13-106. Higher magnification photograph of specimen in Fig 13-102 (80B1). It demonstrates how smaller veins open into larger ones on raised folds of the tunica intima (arrow). U = ureter; V = vein; A = artery X20



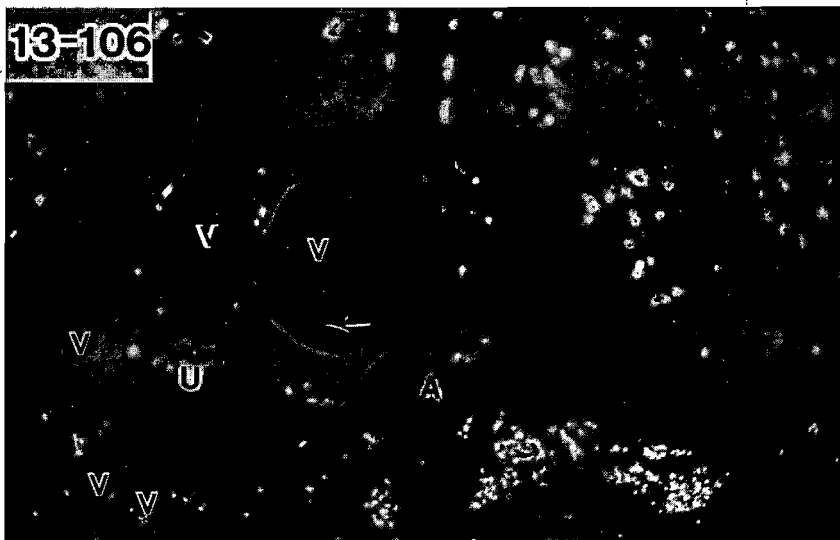


Figure 13-107. Photograph of a small artery (arrow) injected with latex entering a renicule at the corticomedullary junction, 79B1. The medulla is covered by cortex (C). The calyx is covered by fascia and thin walled veins (FV). X7.5

Figure 13-108. Drawing of the distribution of arterial branches to a cluster of renicules. 79B2.

A = artery; V = veins; U = ureteric branch; R = renicule

Figure 13-109. Photograph of a vertical section of a renicule to demonstrate how a calyx (Cl) leads into an infundibulum (I) at the tip of the renicule (arrow), 80B8. Notice that the papilla (P) protrudes into infundibulum. Cortex (C), medulla (M), and sporta perimedullaris (Sp) are demonstrated in this photograph. Cortex is shown to cover calyx on right side. X7.5

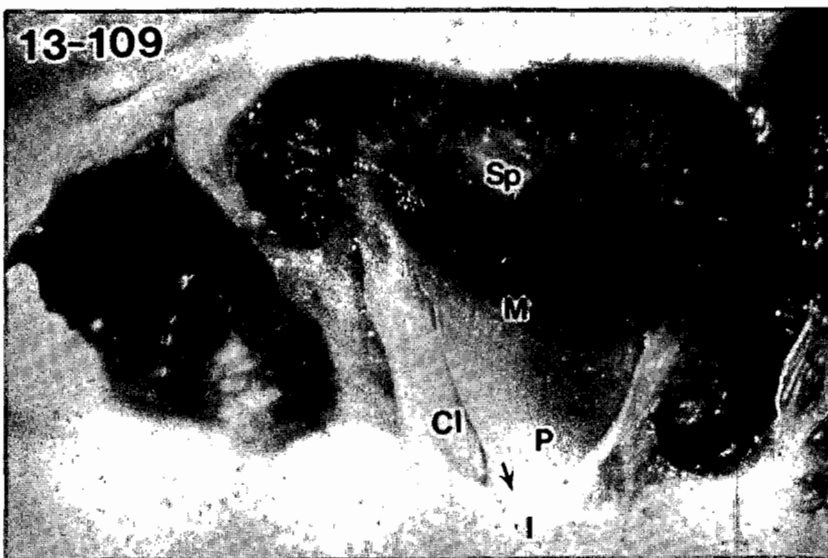
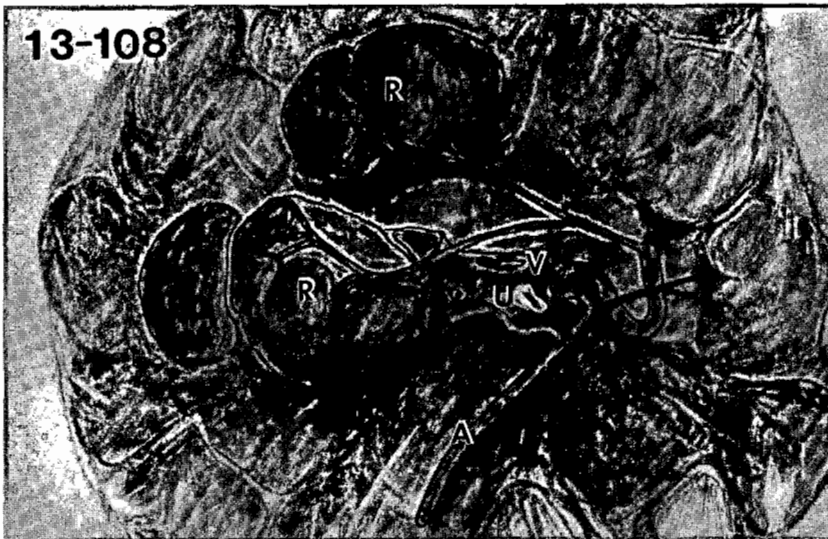


Figure 13-110. Photograph of a vertical section of a renicule from 79B2 demonstrates the cut surfaces of cortex (C) and medulla (M). The cortex is superficial and caps the medulla covering about half of its lateral surface. The thickness of the cortex is about 1/4 that of the medulla. Cortex and medulla are separated at the corticomedullary junction by a sheet of connective tissue, the sporta perimedullaris (arrowheads). An arcuate vessel (AV) is embedded in the sporta. The medulla tapers and forms a renal papilla (P). A calyx (Cl) surrounds the medulla and leads into an infundibulum (I). Large veins (V) surround the calyx and infundibulum. X20

Figure 13-111. Photograph of the outer surface of cortex of a renicule from 80B1. Subcapsular veins show under the thin reflective capsule as a dark network (arrowheads). X20

Figure 13-112. Photograph of the surface of the cortex of a renicule from 80B1. After an injection of yellow colored Microfil, a subcapsular vein is well demonstrated (arrowhead). X20

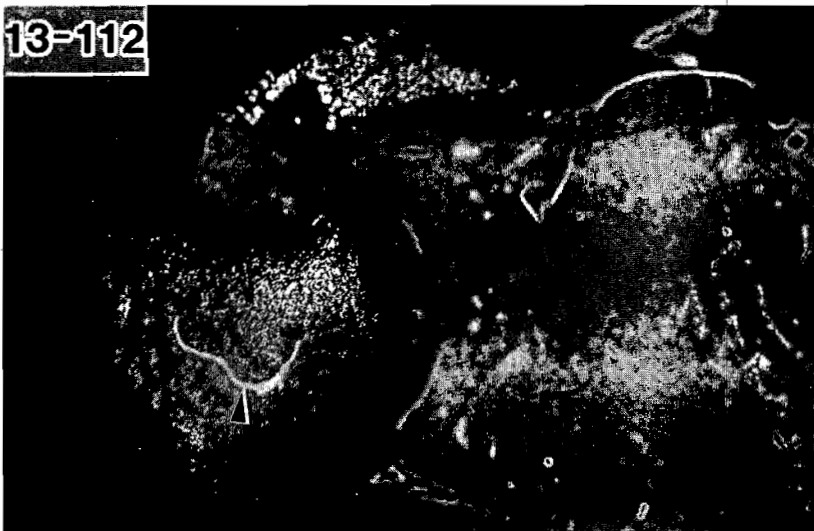
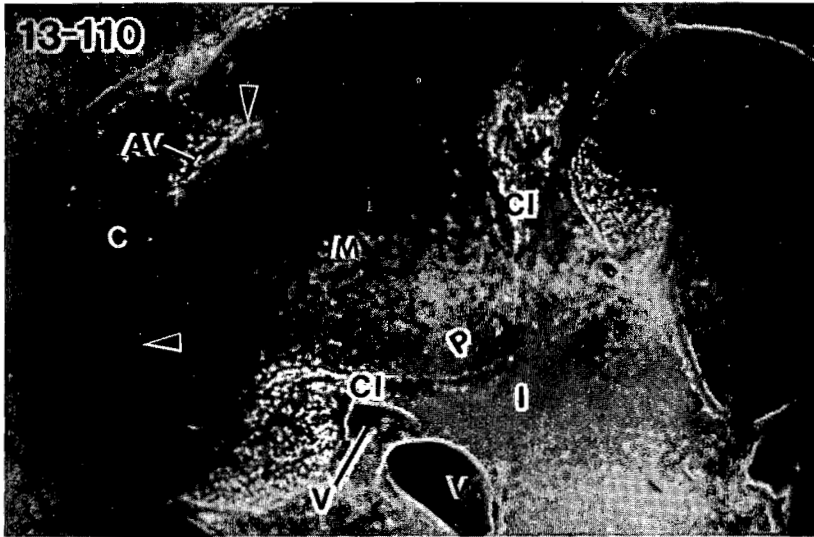
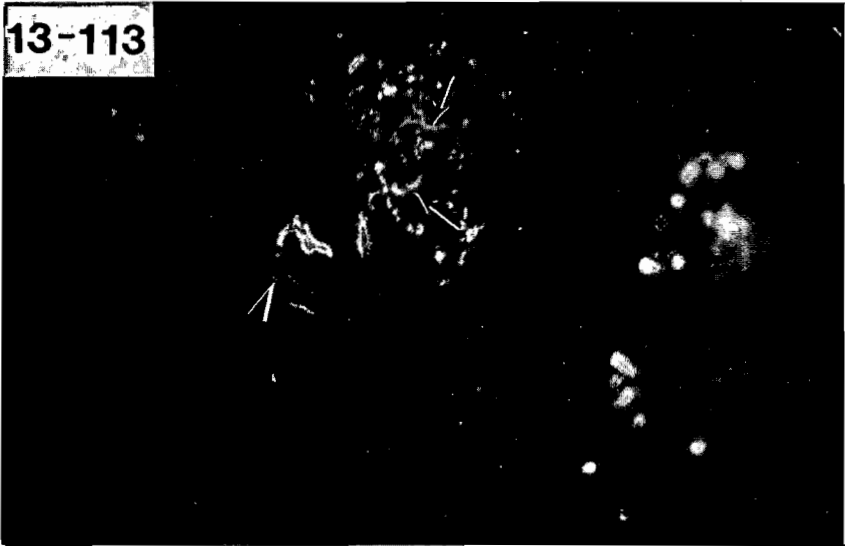


Figure 13-113. Higher magnification photograph of the subcapsular area of a sectioned cortex from 80B1. Microfil was injected into one of the veins leading from the renicule. Subcapsular veins are demonstrated on the outer surface of the cortex (arrowhead). Deeper veins filled with Microfil can be seen on the cut surface of the cortex (arrows). X20

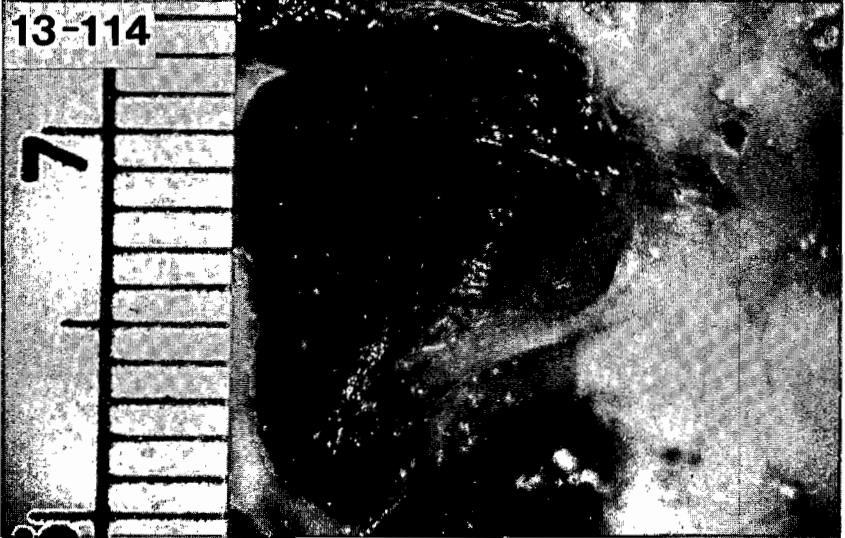
Figure 13-114. Photograph of a vertical section of a renicule from 80B8. The millimeter scale demonstrates measurement of the longest diameter at the base of renicule. It measures 13 mm.

Figure 13-115. Photograph of a vertical section of a renicule from 80B8. The millimeter scale demonstrates measurement of the shortest diameter of the renicule which extends from the tip of the medulla to the surface of the cortex. It measures 10 mm.

13-113



13-114



13-115

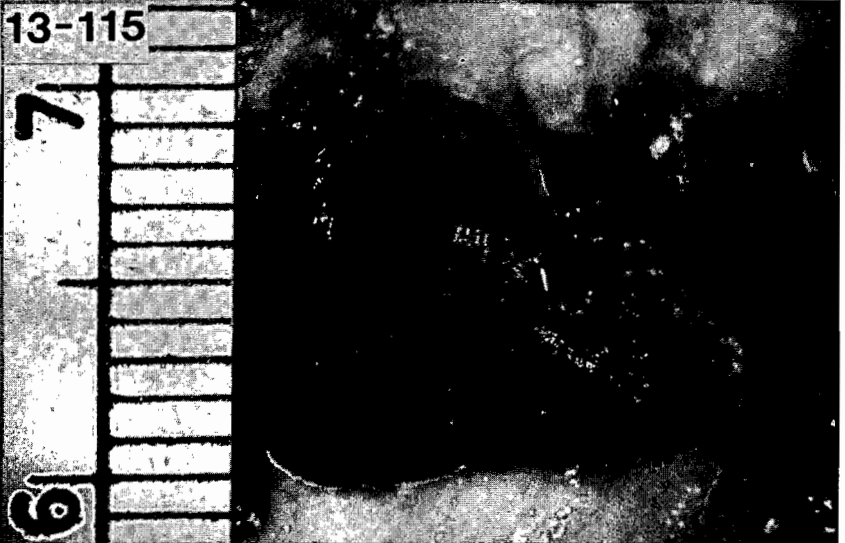


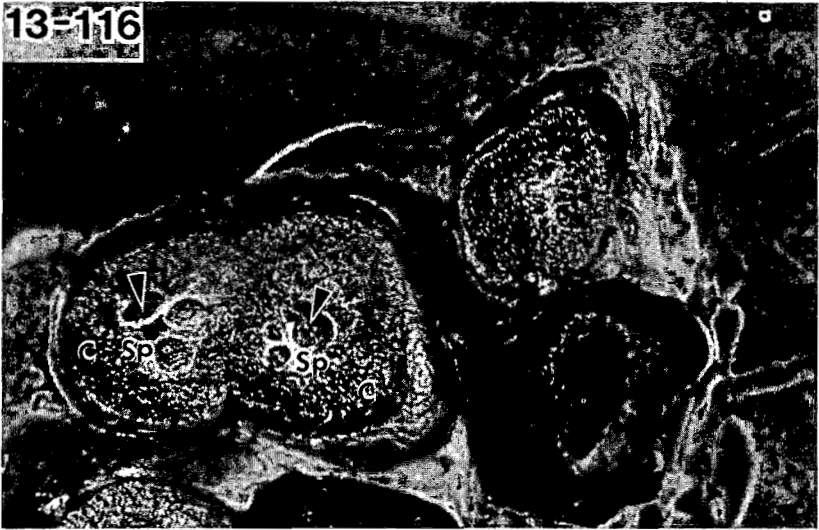
Figure 13-116. Photograph of a transverse section of two renicules in a cluster from 79B2. The cortices (C) of the two renicules are fused at this level. The fibrous sporta perimedullaris (Sp) is represented by a white sheet perforated by medullary rays (arrowheads). X7.5

Figure 13-117. Photograph of a latex cast of calyces from the renicule clusters from 79B1. The chalice shape of the calyces (C1) is well represented. Infundibula (arrowheads) lead into ureteral branches. X15

Figure 13-118. Photograph of a dissection of renicules demonstrates two renal papillae (A) and (B) protruding from two calyces which lead into one common infundibulum (arrows), 79B1. Notice large veins (V) surrounding calyces and infundibulum. Some of the veins' walls are fused with the wall of the calyx (C1). X4



13-116



13-117



13-118

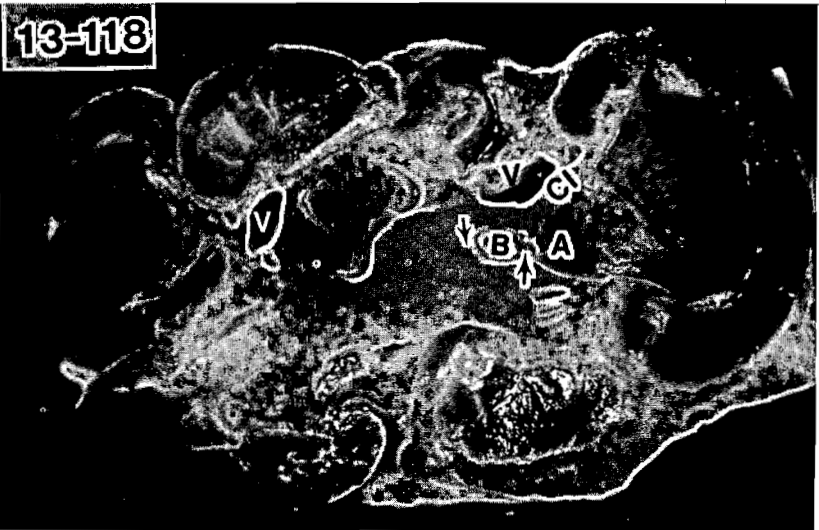
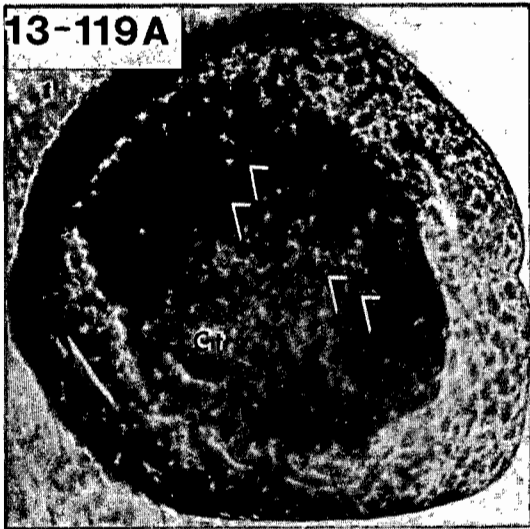


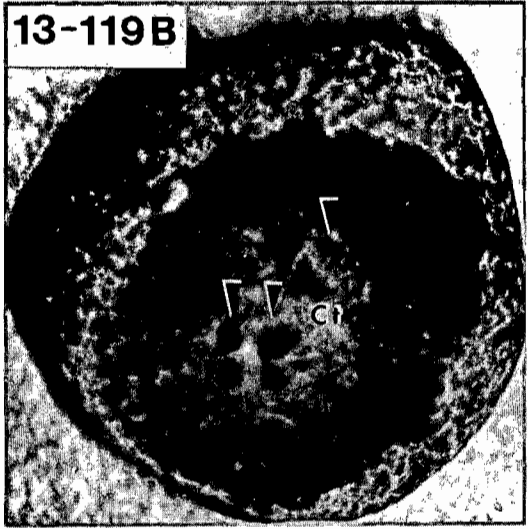
Figure 13-119. Photographs of a renicule isolated and serially sectioned transversely at one millimeter thick slices starting at the surface of the cortex inward toward the medulla, 79B1. X7.5

- A. About 0.5 mm of the cortex is sliced away. Increase of connective tissue stroma among cortical parenchyma is evidenced by increase of pale whitish tissue (Ct). Medullary rays are also evident as small rounded areas (arrowheads) that penetrate through the connective tissue stroma.
- B. One millimeter deep into the cortex, the connective tissue (Ct) becomes more dense with more obvious medullary rays (arrowheads).
- C. About two millimeters deep into the cortex, a definite sheet of connective tissue (Ct) is formed with larger medullary rays penetrating it. This is definitely part of the sporta perimedullaris. At this level or at the above levels there is no evidence of arcuate vessels.
- D. At the corticomedullary junction, the sporta (Sp) is broken down into an interrupted line of connective tissue with medullary tissue in between. Arcuate vessels are shown embedded in the tissue of the sporta (arrowheads).
- E. Deepest layer of the sporta (Sp) bordering on the medulla (M). Cortical tissue (C) at this level represents the lateral extension of the cortex down onto the outer surface of the medulla. The arcuate vessels (arrowheads) are definitely in the deepest layer of the sporta.

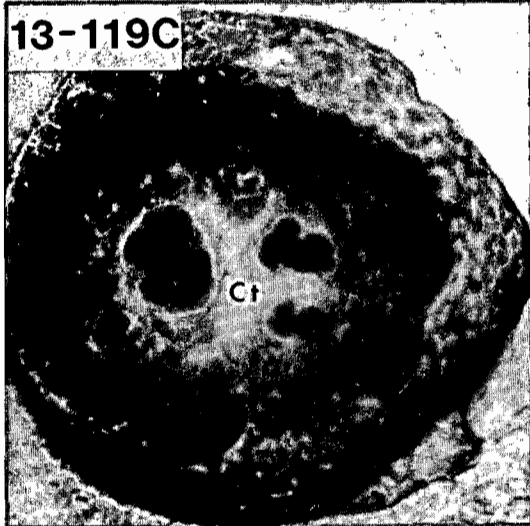
13-119A



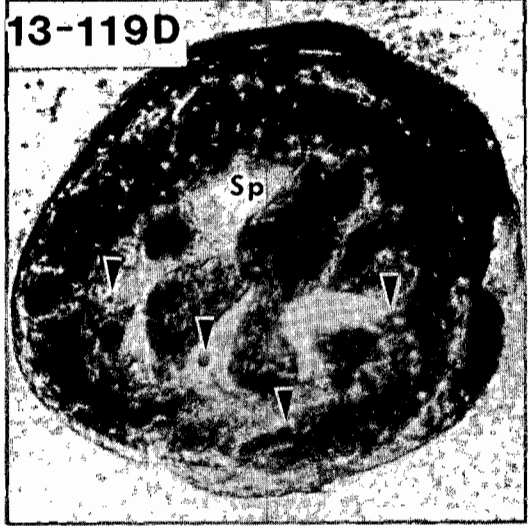
13-119B



13-119C



13-119D



13-119E

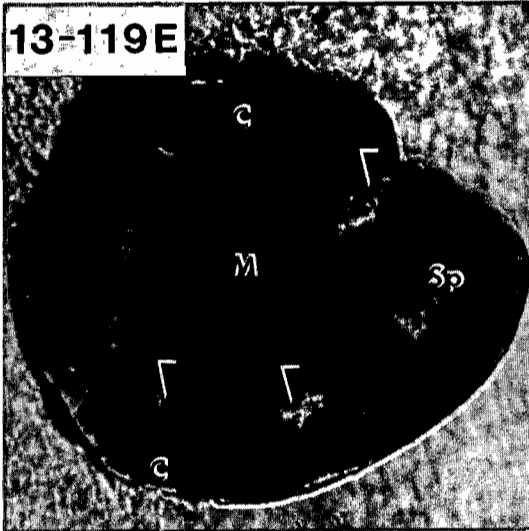


Figure 13-120. Photomicrograph of a parasagittal section of a reniculate, 79B1. Cortex (C) is on top of a part of medulla (M) and the renal papilla (P) is surrounded by the calyx (Cl). The calyx wall in the top part of the field joins the wall of another calyx. The other side of the calyx shares the wall of large lumen veins (V). An artery (A) enters the reniculate at the cortico-medullary junction. The sporta perimedullaris (Sp) is broken into five segments separated by medullary rays. L.S., Verhoeff stain. X7.5

Figure 13-121. Photomicrograph of the renicular cortex, 79B1. Three renal corpuscles (Rc) are clustered together in midcortex. PAS reaction stains the basal lamina around tubules. The proximal convoluted tubule (Pt) epithelium is not well preserved. Distal convoluted tubules (Dt) have wider lumina. A medullary ray (Mr) made of ascending and descending thick parts of Henle's loops is well demonstrated. L.S., PAS stain, X300

Figure 13-122. Photomicrograph of a semi-thin section of reniculate cortex, 80B1. A renal corpuscle demonstrates Bowman's capsule (Bc) lined with parietal simple squamous epithelial cells. Urinary space (Us) surrounds the glomerulus. Podocytes (arrows) representing the visceral layer of Bowman's capsule are next to glomerular capillaries. Mesangial cells (M) have lighter staining cytoplasm and roundish nuclei. Epon, X.S., Azure blue-methylene blue stain, X300

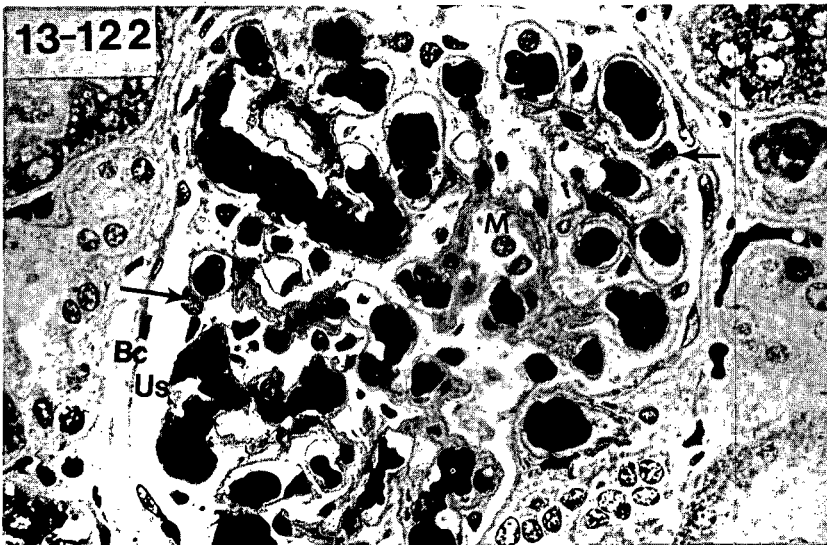
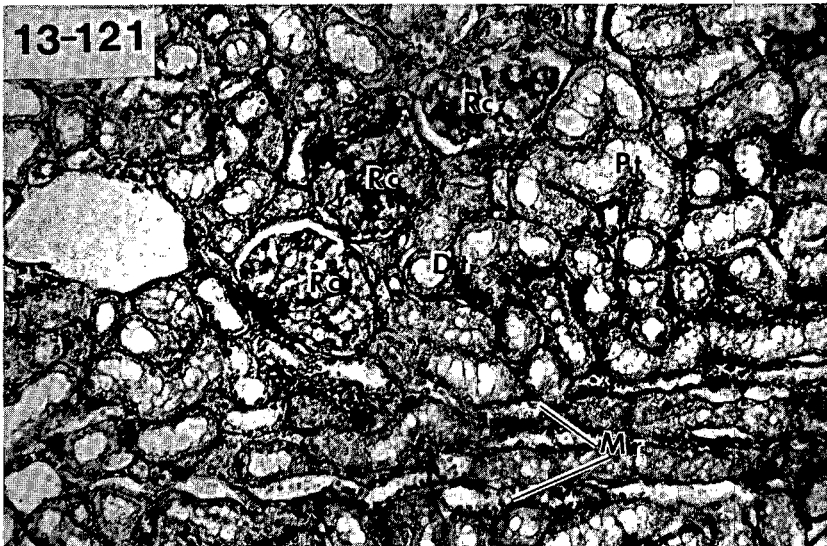
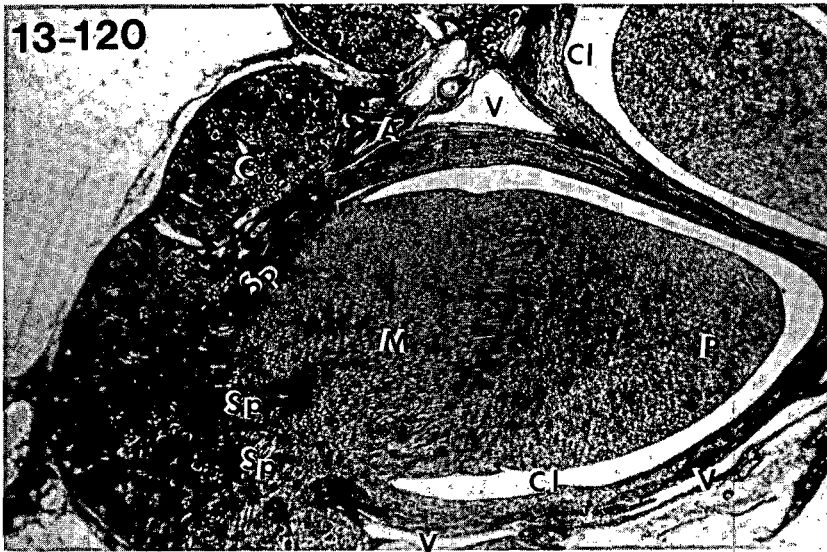


Figure 13-123. Photomicrograph of a semi-thin section of renicular cortex, 80B1. An afferent arteriole (Aa) branches off an interlobular artery (IL). The smooth muscle fibers in the afferent arteriole are optically clear and stouter than those in the wall of the interlobular artery. The lumen of the arteriole is also wide. Proximal convoluted tubules (Pc) (poorly fixed) are lined with darker staining cells as compared with the lighter staining cells lining the distal convoluted tubules (Dc). Epon, X.S., Azure blue-methylene blue stain, X470

Figure 13-124. Photomicrograph of a semi-thin section of renicular cortex, 80B1. Two arterioles (A) branch from a common trunk (T). Each arteriole is directed toward a renal corpuscle becoming its afferent arteriole. Arteriolar trunk and branch arterioles have modified muscle cells in their walls. Epon, X.S., Azure blue-methylene blue stain, X470

Figure 13-125. Photomicrograph of a semi-thin section of a renal corpuscle with a complete juxtaglomerular apparatus, 80B1. The afferent arteriole (Aa) is on the right side of the corpuscle. Its wall is made of modified smooth muscle cells and has a wide lumen as it enters the glomerulus. The efferent arteriole (Ea) is on the left side and has regular smooth muscle cells in its walls and a narrower lumen. A polar cushion (Pc) and a macula densa (Md) complete the J.G. apparatus. A mesangial cell is easily seen in the center of the glomerulus (arrow). Epon, X.S., Azure blue-methylene blue stain, X470

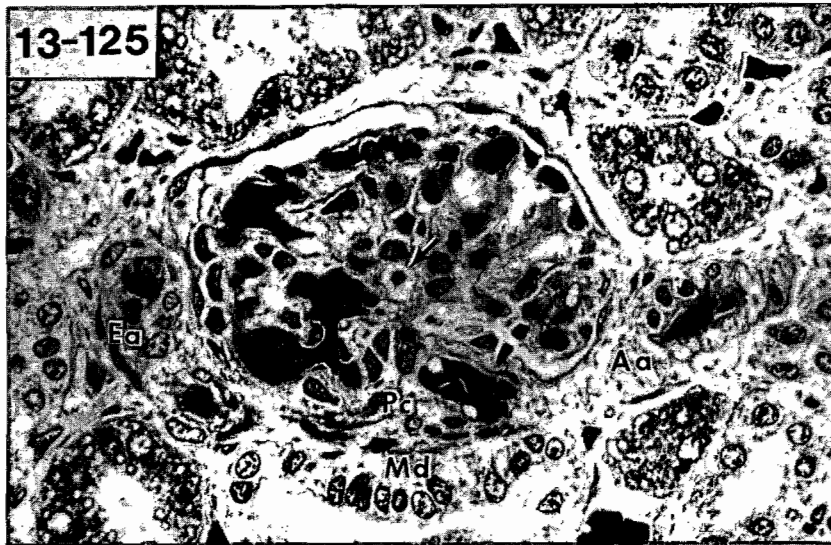
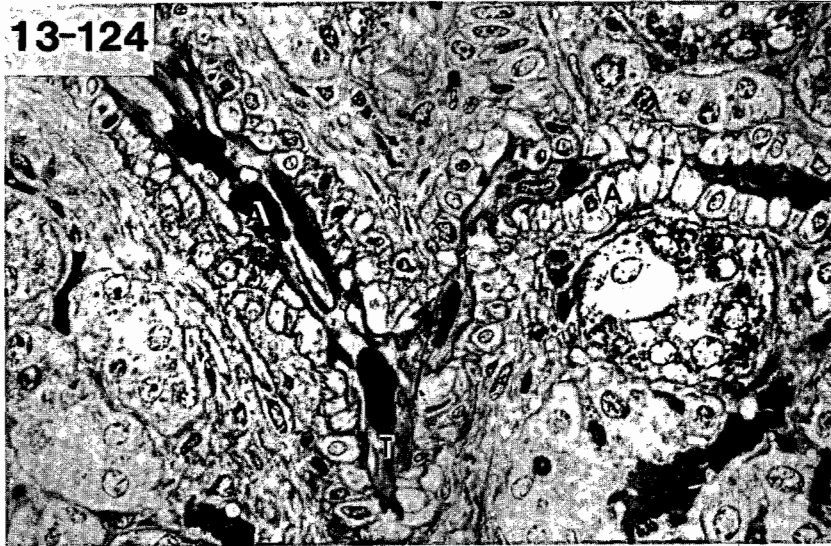
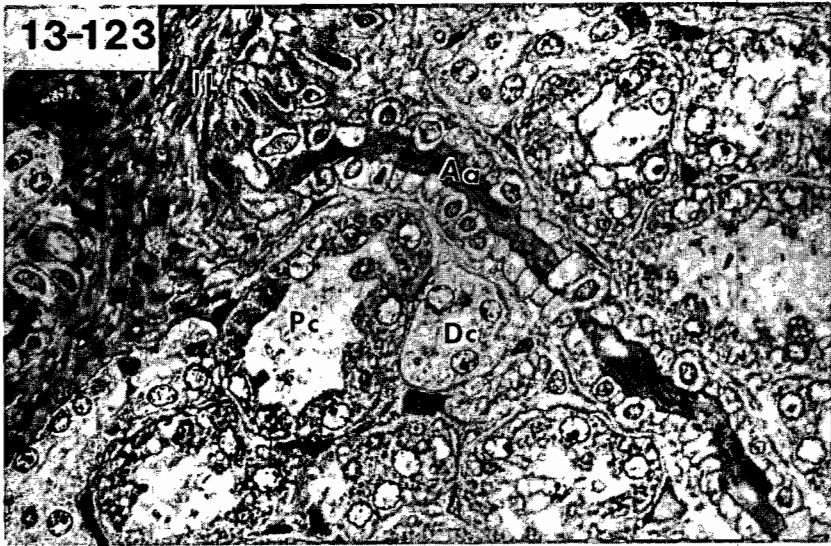


Figure 13-126. Photomicrograph of a semi-thin section of a renal corpuscle (Rc), 80B1. The macula densa (Md) is the part of the distal convoluted tubule that is in contact with the glomerulus. The nuclei of the lining epithelium are crowded in this part of the wall of the tubule. Epon, X.S., Azure blue-methylene blue stain, X470

Figure 13-127. Photomicrograph of renicular cortex, 79B1. A renal corpuscle has three glomerular lobules (arrowheads). Part of the capsule of the cortex (Cp) is showing. Small, thin walled tubules (T) are located directly under the capsule and represent connecting tubules that connect distal convoluted tubules to collecting ducts. X.S., PAS, X375

Figure 13-128. Photomicrograph of renicular cortex, 79B1. Renal corpuscles show a thin dark staining basal lamina (arrowheads) positive for the periodic acid-Schiff reaction. The vascular pole (Vp) and urinary pole (Up) of one corpuscle are demonstrated. X.S., PAS, X375



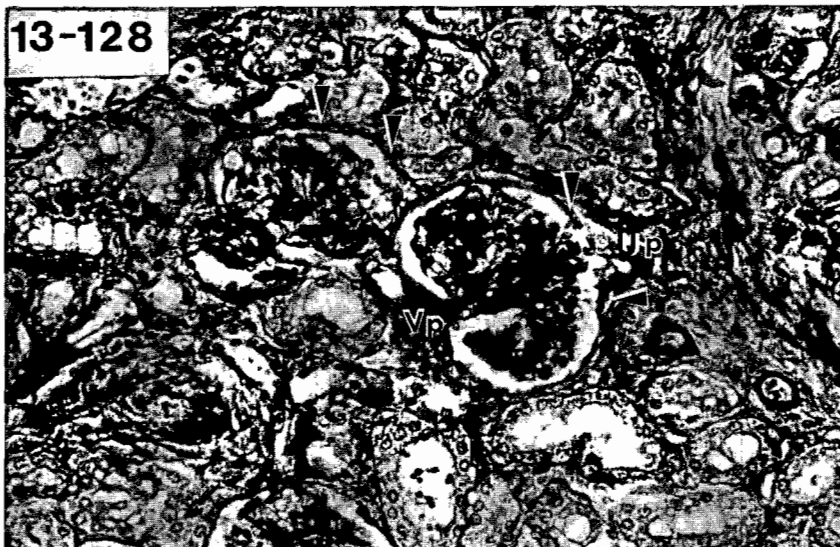
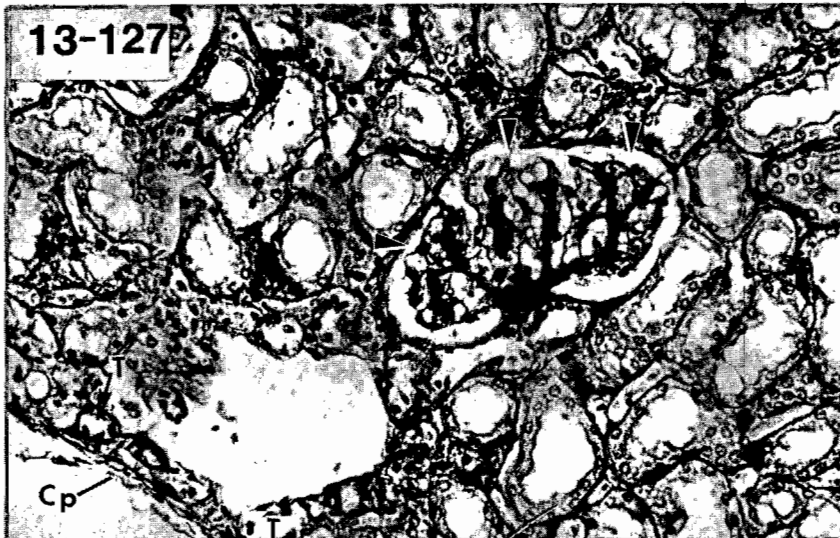
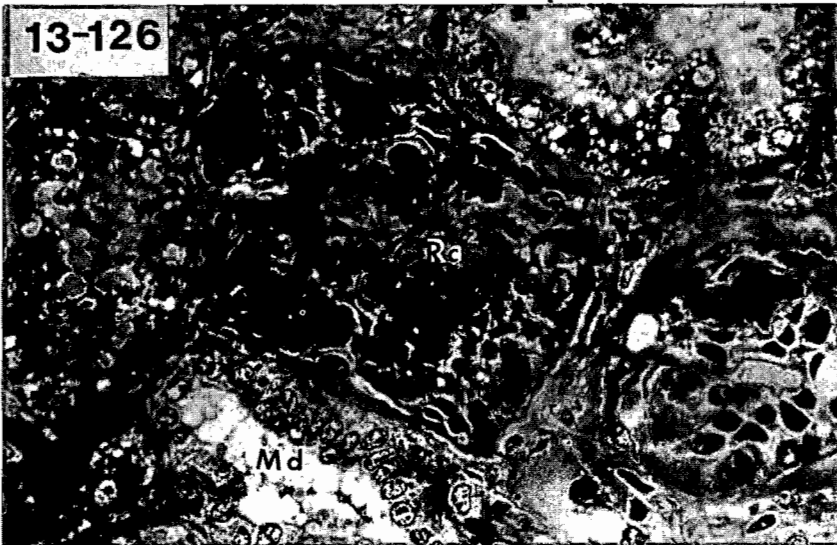
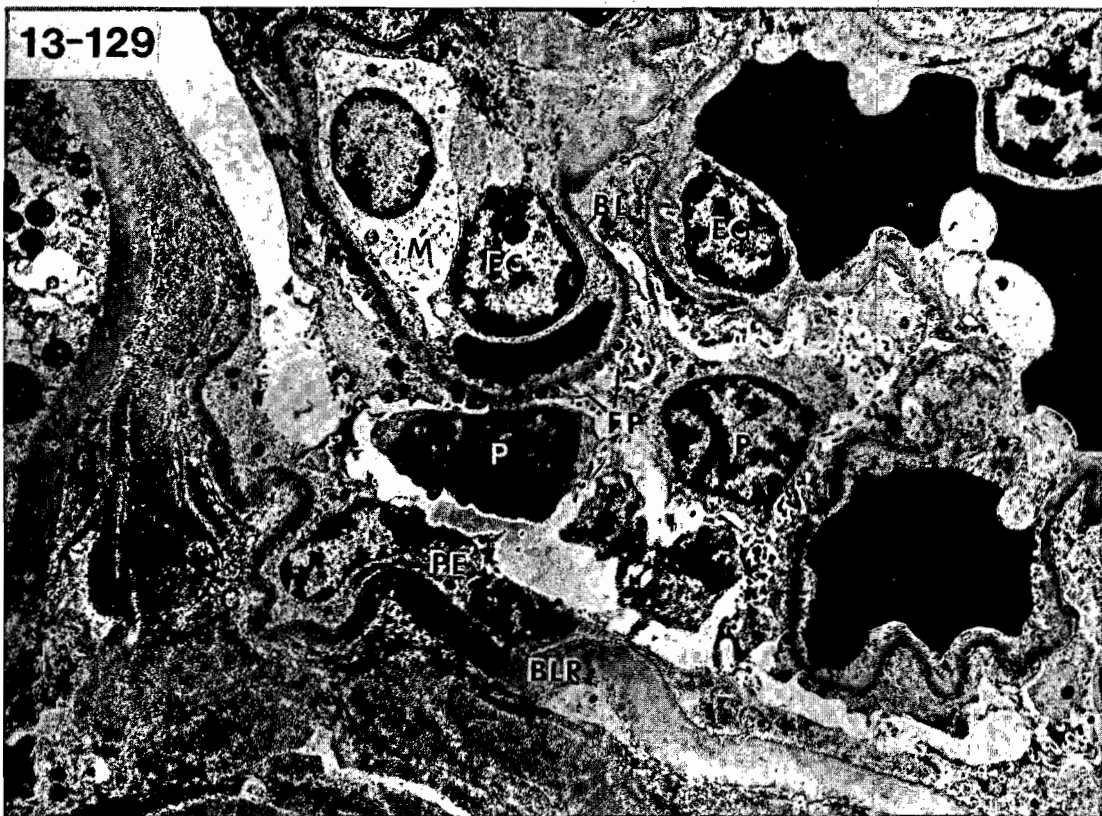


Figure 13-129. Transmission electron photomicrograph of a portion of a renal corpuscle, 80B1. Endothelial cells (EC) of capillaries are evident resting on their basal lamina (BL). The foot processes (FP) of podocytes (P) are seen on the opposite surface of the basal lamina. A mesangial cell (M) is seen within the basal lamina surrounding a capillary. Cells of the parietal epithelium (PE) are seen resting on the basal lamina of the renal corpuscle (BLR). Outside the renal corpuscle a heavy concentration of collagen (C) is seen. X4,400

Figure 13-130. Higher magnification transmission electron photomicrograph of a glomerular capillary and associated podocyte from the renal corpuscle shown in Fig 13-129. A red blood cell (RBC) may be seen closely appressed to the surface of an endothelial cell (EC). The basal lamina (BL) separates the endothelial cell from the foot processes (FP) of a podocyte (P). X30,000

13-129



13-130

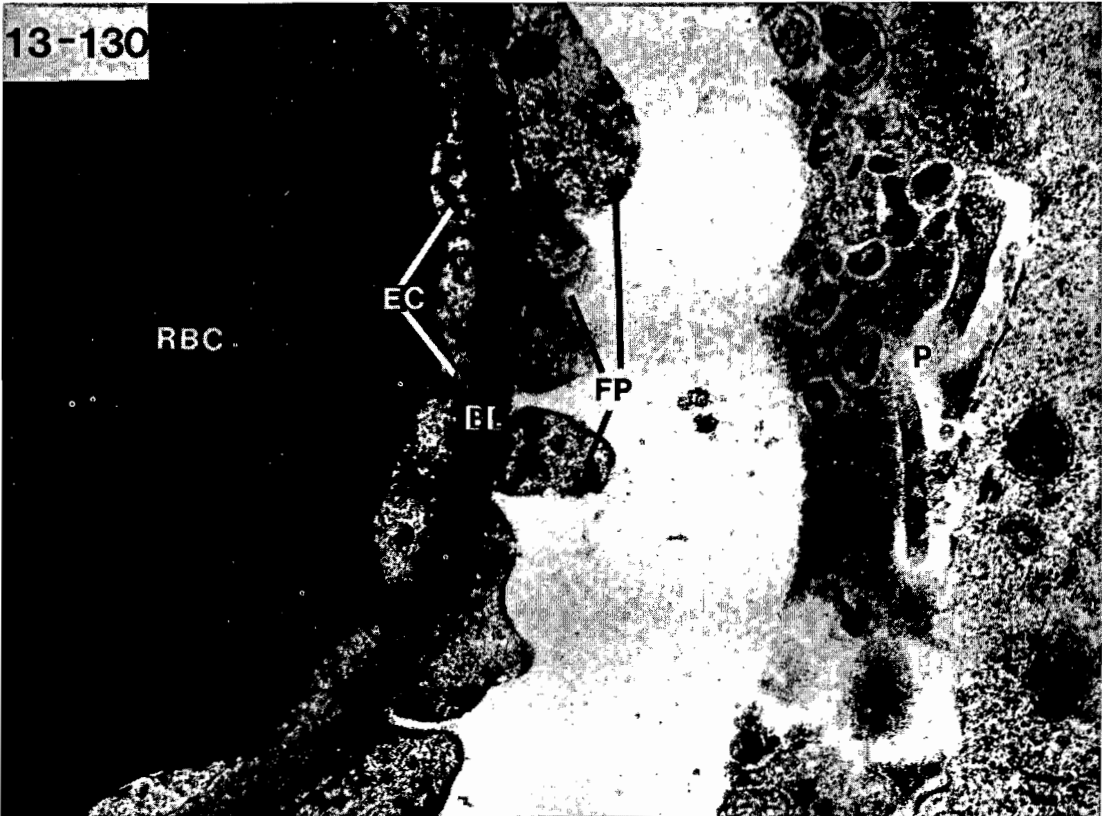


Figure 13-131. Very high magnification transmission electron photomicrograph of a region of podocyte-basal lamina contact from the renal corpuscle shown in Fig 13-129. Podocyte foot processes (FP) may be seen resting on the basal lamina (BL) of a glomerular capillary. The foot processes are separated from each other by a filtration slit (FS). No diaphragm across the filtration slit is evident. Mitochondria (M), microfilaments (MF) and a microtubule (MT) are evident in the foot process. X90,900

Figure 13-132. High magnification transmission electron photomicrograph of a region near the edge of the renal corpuscle seen in Fig 13-129. The basal lamina of the renal corpuscle (BLR) is evident as is the cytoplasm of a parietal cell (PC) on the interior of the corpuscle. Concentrations of collagen (C) may be seen exterior to the BLR. A fibroblast (F) is also evident. X36,000

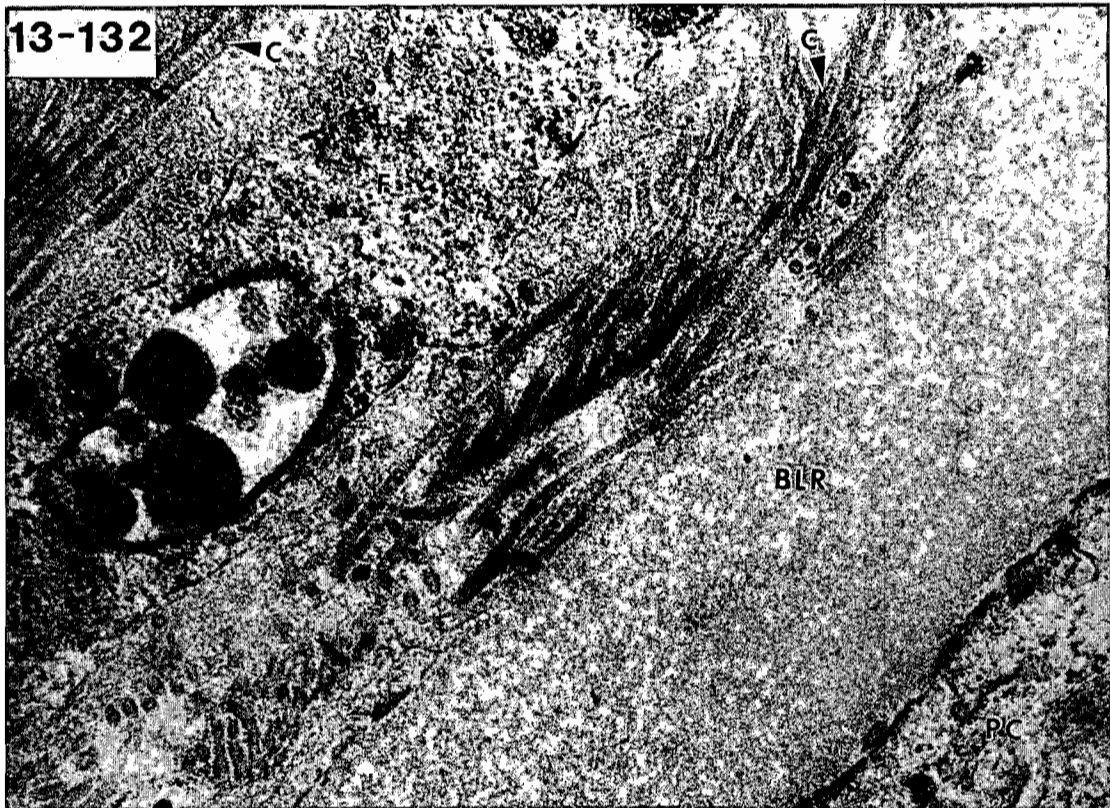
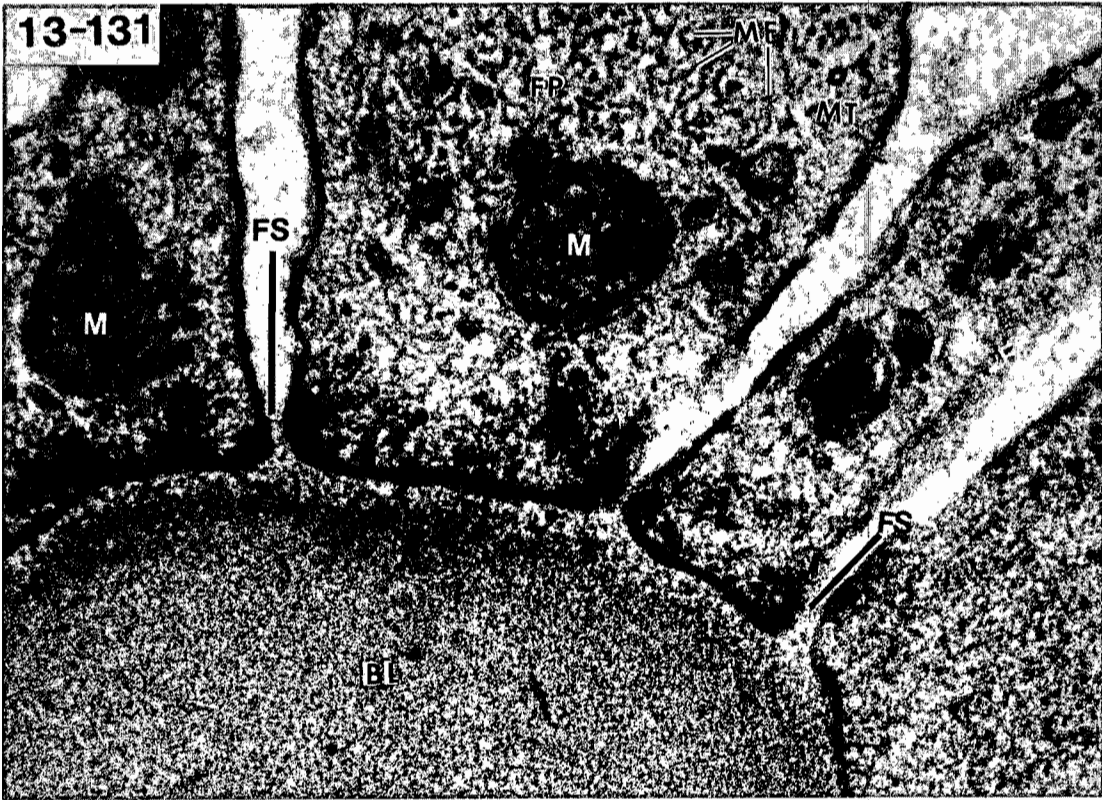


Figure 13-133. Transmission electron photomicrograph of a typical renal tubule taken from a kidney of 80B1. The basal lamina (BL), mitochondria (M) and nuclei (N) are visible but preservation is poor. X4,600

Figure 13-134. Higher magnification electron photomicrograph of the edge of the tubule shown in Fig 13-133. The fibrous structure of the basal lamina (BL) is evident but cytoplasmic constituents other than mitochondria (M) are not discernable. X36,600

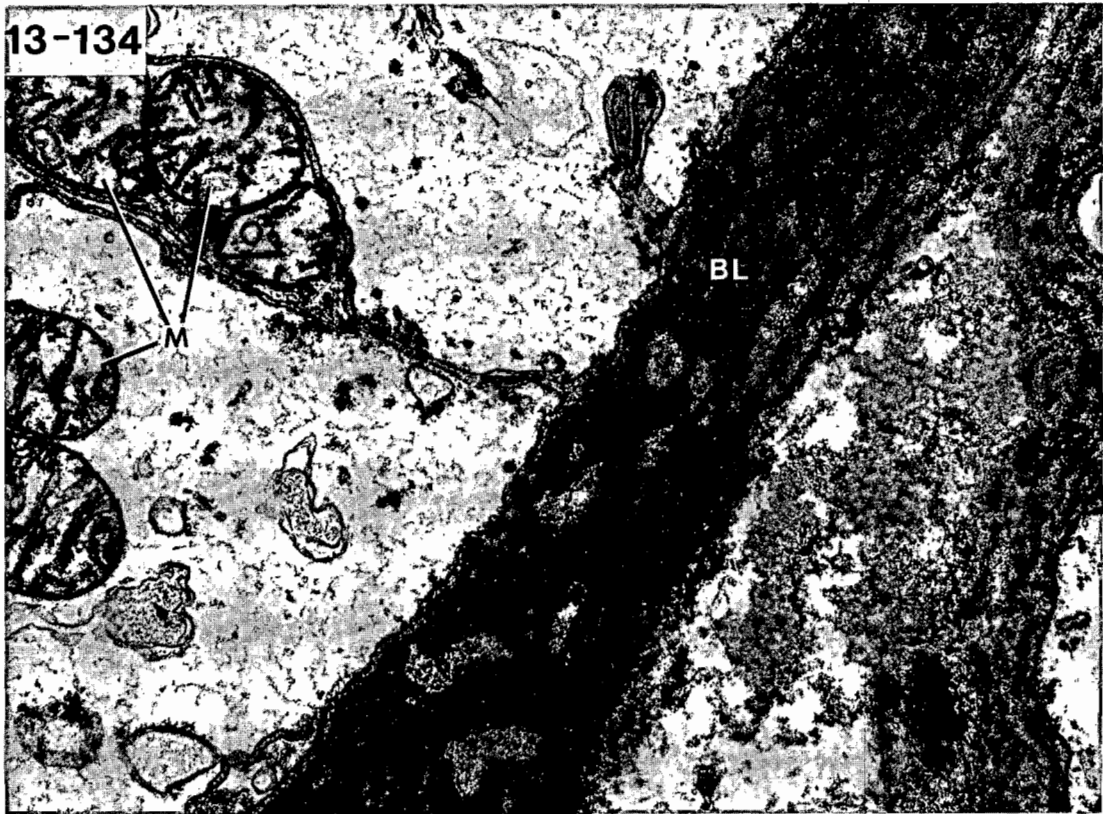


Figure 13-135. Photomicrograph of the cortices of two renicules, 79B1. Cortical veins are very well demonstrated (ScV and ILV). The flow of venous return from the cortex to the corticomedullary junction and then outside the renicule can be followed in the left renicule. Subcapsular veins (ScV) continue as a straight interlobular vein (ILV) across the cortex to larger veins at corticomedullary junction (CmV), to the renicular vein (Rv) between renicules. X.S., Verhoeff stain, X9

Figure 13-136. Photomicrograph of a renal corpuscle, tubules and connective tissue stroma, 80B1. The stroma (Ct) is most abundant around the corpuscle. This is typical of the bowhead kidney. Epon, X.S., Azure blue-methylene blue stain, X470

Figure 13-137. Photomicrograph of the sporta perimedullaris (Sp) at lower magnification, 80B1. The tissues were stained with Milligan's trichrome technique which stains white fibrous connective tissue green and smooth muscle fibers purplish red. In this photograph the smooth muscle fibers in the arterial wall (A) are dark while the connective tissue sporta is lighter in color. There is no evidence of smooth muscle fibers in the sporta in this preparation or from other samples. Cortical tubules (T) indicate that the sporta extends into the cortex and is not limited to the corticomedullary junction. L.S., Milligan's stain, X19





- Figure 13-138. High magnification photomicrograph of tissue of the spota perimedullaris, 79B1. The spota is composed of dense white fibrous connective tissue with collagenous fibers (Cf) irregularly arranged, elastic fibers (not obvious with this staining technique) and connective tissue cells (mainly fibroblasts) whose nuclei only are showing (arrows). There are no smooth muscle fibers. If there were any, they would have stained darker and their nuclei would be larger and with more open chromatin than those of the fibroblasts. A lymphatic vessel (Lv) crosses through the tissue. L.S., Masson's stain, X375
- Figure 13-139. Photomicrograph of sections of two renicules to demonstrate the continuation between calyx wall (Clw) and the spota perimedullaris (Sp), 79B1. Arteries (A) enter and veins (V) leave the renicule at the level of the spota. This photomicrograph demonstrates the presence of large vessels (arcuate in the spota). L.S., Verhoeff's stain, X30
- Figure 13-140. Photomicrograph of a semi-thin longitudinal section of outer medulla (medullary rays), 79B2. It demonstrates descending thick segment (Dt), ascending thick segment (At), thin segment of Henle's loop (Tht), collecting ducts (Cd), arterial vasa rectae (Avr) and venous vasa rectae (filled with dark staining red blood corpuscles) (Vvr). Epon, L.S.. Azure blue-methylene blue stain, X300

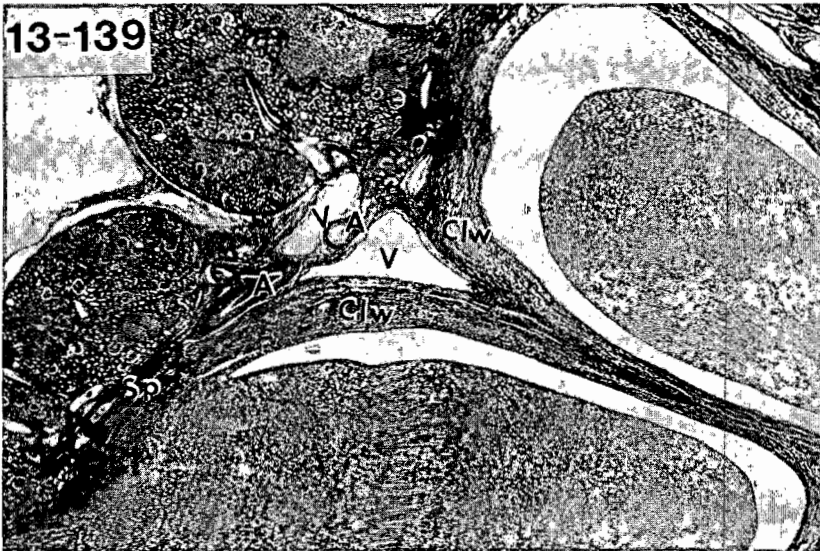
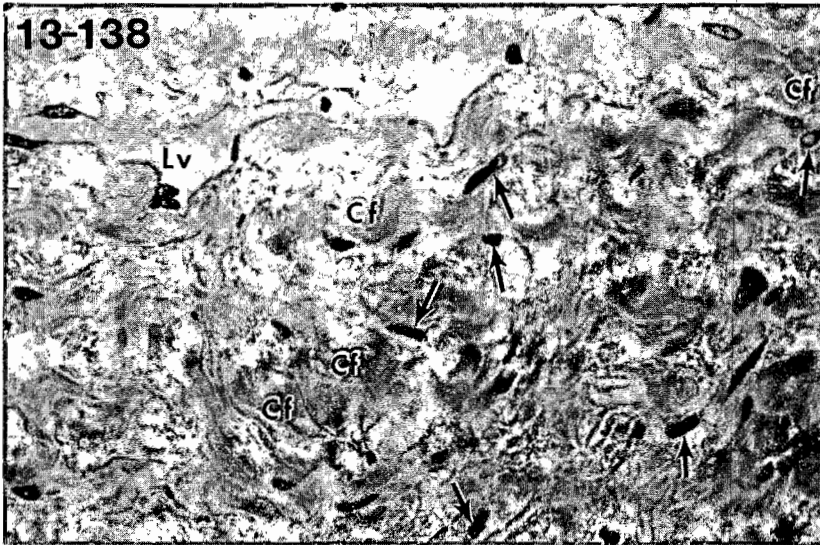


Figure 13-141. Photomicrograph of a semi-thin transverse section of outer medulla (medullary rays), 79B2. It demonstrates descending thick segment (Dt), ascending thick segment (At), thin segment of Henle's loop (Tht), arterial vasa rectae (Avr) and venous vasa rectae (Vvr). X.S., Azure blue-methylene blue stain, X300

Figure 13-142. Photomicrograph of a renicular renal papilla, 79B2. It mainly consists of cross sections of collecting ducts (Cd) and thin segments of Henle's loop (Tht). It is covered at the calyx (Cl) surface by a low transitional epithelium (Te). X.S., H and E, X300

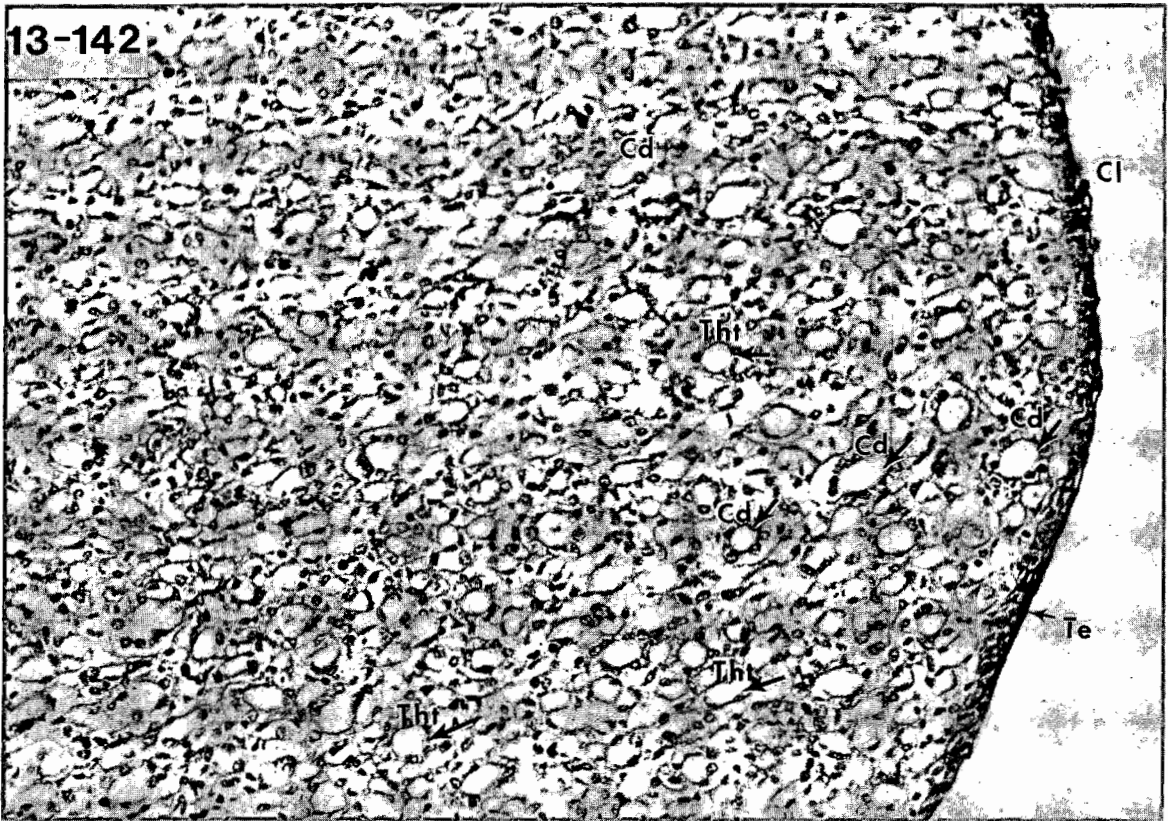
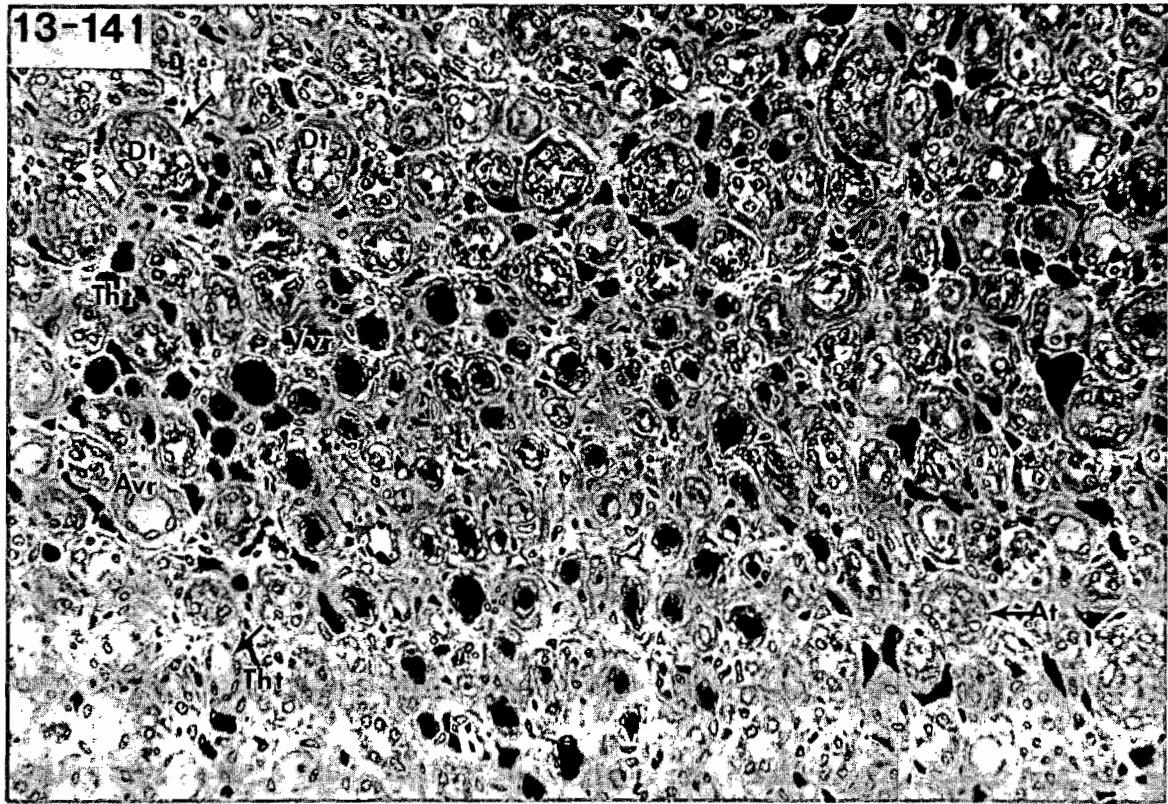


Figure 13-143. Photomicrograph of a section of two reniculi with fused papillae (P), 80B1. They share a common calyx (Cl) and infundibulum (In). The sporta (Sp) is continuous across the two renicules. L.S., Milligan's stain, X19

Figure 13-144. Photomicrograph of two renicules with fused cortices (C) but separate renal papillae (P) and calyces (Cl), 80B1. The two calyx walls are fused with the sporta (Sp) which is continuous from one renicule to the other. L.S., Milligan's stain, X19

Figure 13-145. Photomicrograph of two renicules, 79B2. The two calyces (Cl) communicate to empty into the same infundibulum (arrow). Om-outer medulla; P-papilla. Calyx walls are fused. L.S., H and E, X30

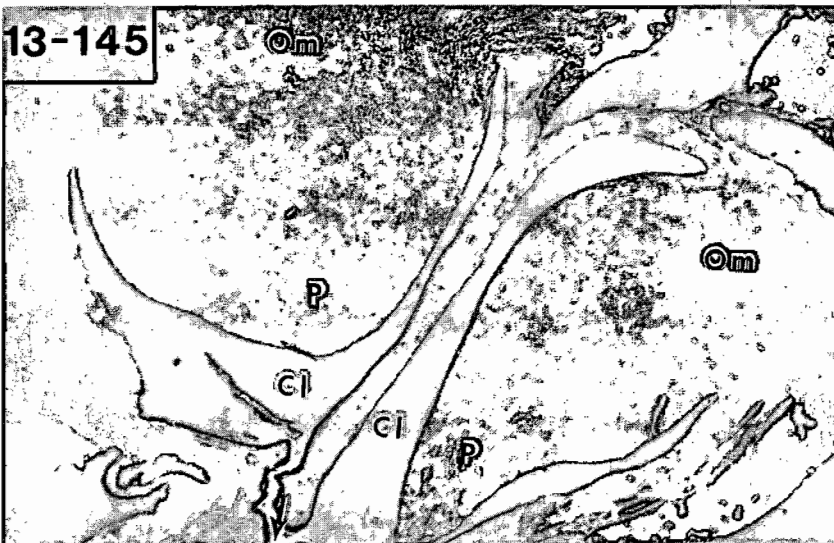
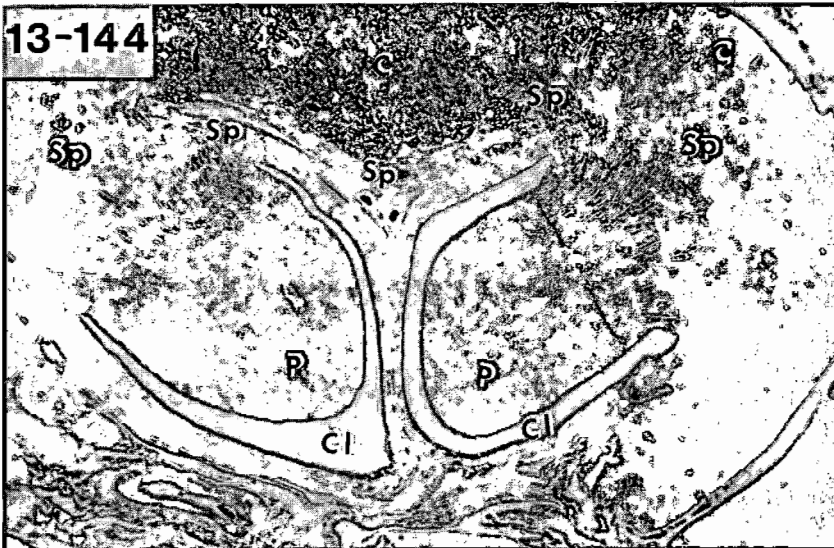
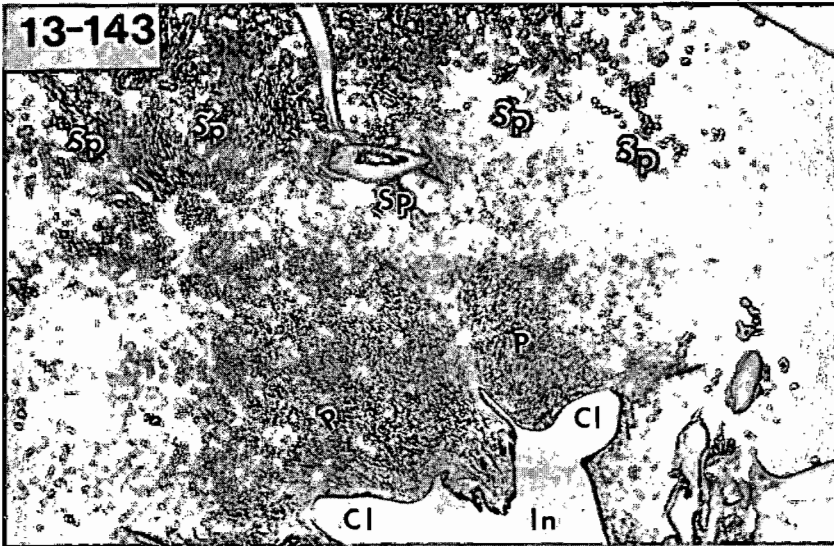


Figure 13-146. Photomicrograph of a section through part of a calyx wall (Clw) and part of renal papilla (P) with the cavity of the calyx (Cl) separating them, 79B1. The wall of the calyx is composed of dense white fibrous connective tissue. Capillaries (Cap) filled with red blood corpuscles show the vascularity of the tissue. The wall contains no smooth muscle. L.S., H and E, X1000

Figure 13-147. Higher magnification photomicrograph of structures in Fig 13-146. Transitional epithelium lining the calyx (Cl) has optically clear ballooned superficial cells (arrows). The remainder of the calyx wall (Clw) is made of fibrous connective tissue. The papilla (P) consists mainly of collecting ducts (Cd) and thin tubules of Henle's loop (Tht). X1,000



13-146



13-147



Figure 13-148. Photomicrograph of a ureteral branch, 79B1. The lining transitional epithelium (Te), propria-submucosa layer (Ps), and smooth muscle layer (M) form the wall. The tunica adventitia (Ta) blends with the walls of surrounding veins (V). X.S., Verhoeff's stain, X30

Figure 13-149. Photomicrograph of the wall of the urinary bladder, 79B1. The lining epithelium is of the transitional type (Te). Small and large blood capillaries (Cap) lie next to the basal lamina of the epithelium. The lamina propria (Lp) is composed of dense white fibrous connective tissue and contains large veins (V). X.S., Verhoeff's stain, X475

Figure 13-150. Photomicrograph demonstrating the same structures described in Fig 13-149, 80B7. Transitional epithelium (Te), lamina propria (Lp), and blood capillaries (Cap) are labelled. In this photomicrograph lymphatics (L) are shown instead of veins. X.S., H and E, X475

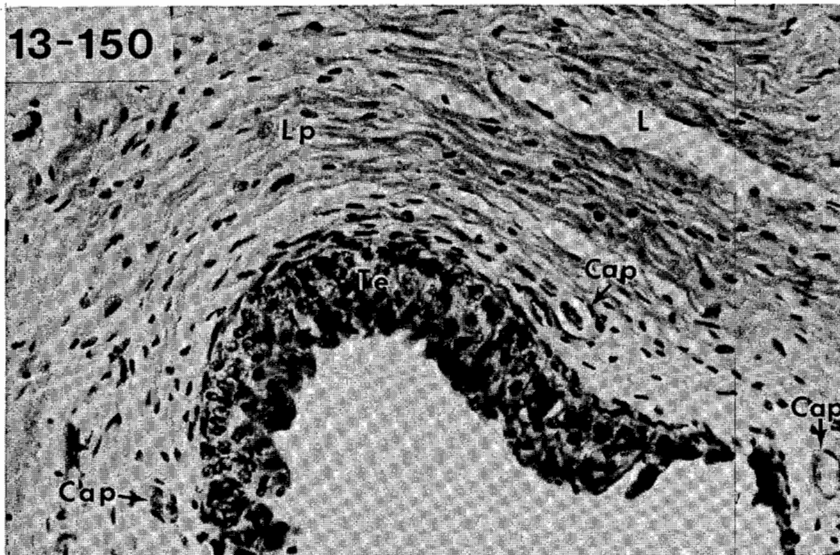
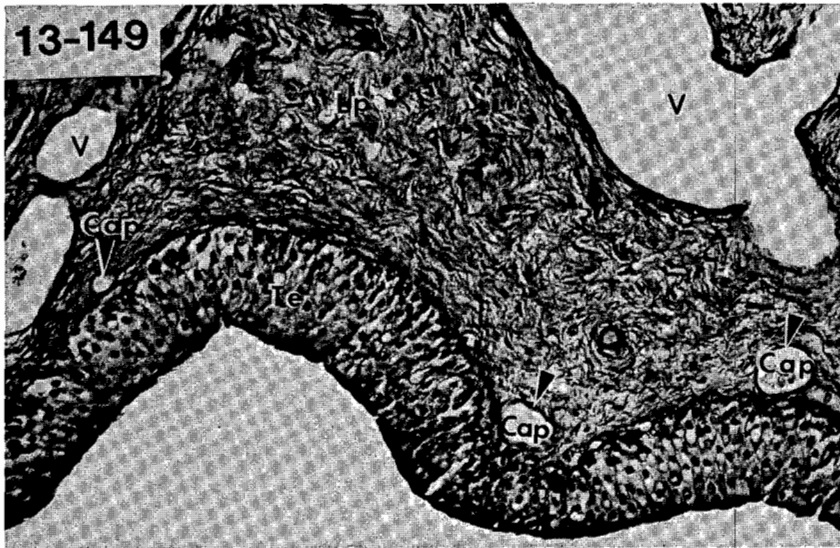
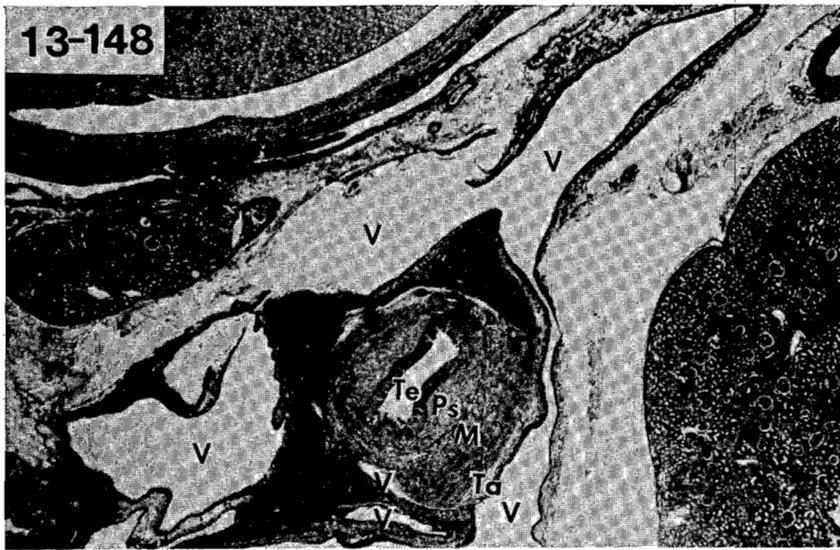
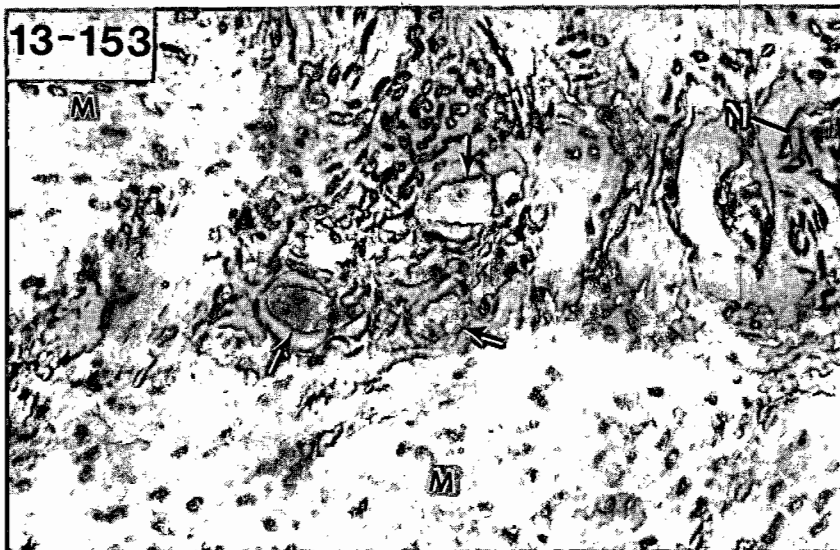
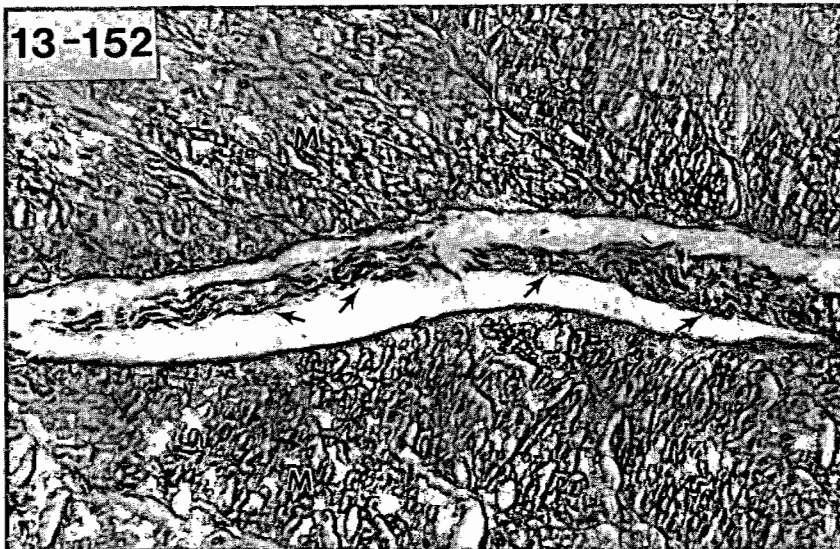
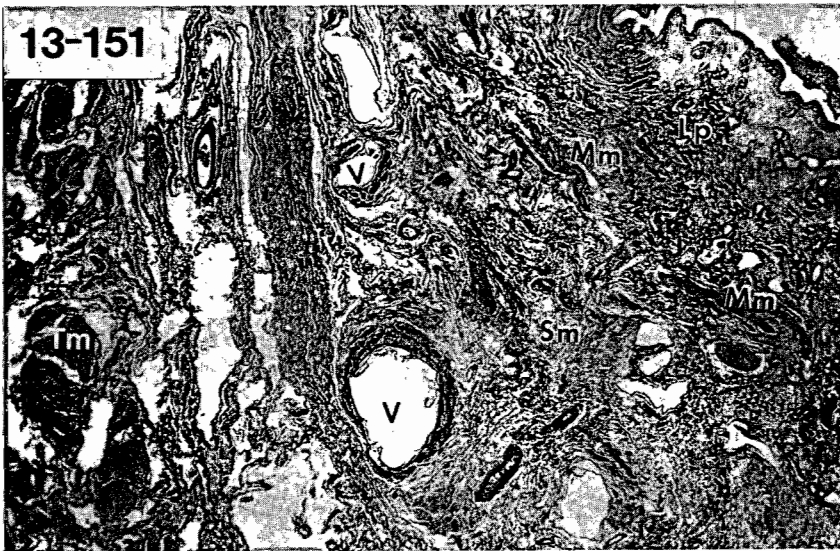


Figure 13-151. Photomicrograph of a section in the wall of the urinary bladder, 79B1. The transitional epithelial lining is missing in the section. The lamina propria (LP), lamina muscularis mucosae (Mm), tunica submucosa (Sm), veins (V) and beginning of tunica muscularis (Tm) are well demonstrated. The submucosa consists of a looser connective tissue than that of the lamina propria and is also more vascular. X.S., Verhoeff's stain, X19

Figure 13-152. Photomicrograph of a section through the tunica muscularis (M) of urinary bladder, 80B7. A nerve fiber bundle (arrows) is located between muscle bundles. X.S., H and E, X300

Figure 13-153. Photomicrograph of a section of the tunica muscularis of the wall of the urinary bladder, 80B7. An autonomic nerve ganglion is located between muscle bundles (M). Ganglion cells (arrows) exhibit the typical eccentric location of nuclei. Bundles of nerve fibers (N) are nearby. X.S., H and E, X475



### III. Brain

Cetacean brains retain their embryonic cervical, pontine, and mesencephalic flexures in the definitive state, whereas only the mesencephalic flexure is retained in the human brain, and all three flexures are lost in the course of development in the brains of domestic mammals (McFarland et al 1969, Morgane et al 1980). By means of these flexures, the brain is shortened by a sort of "accordian folding" and is widened laterally so that it presents a globoid appearance. The basal forebrain lies close to the intercrural fossa and the optic tract forms a very acute angle with the crus cerebri. The usual directional terms used for terrestrial mammals hardly apply. The "frontal lobe" is directed more ventrally than rostrally, the "occipital" area is directed more dorsally than caudally, and the temporal pole is directed more ventrally than rostrally. The lateral (Sylvian) fissure is oriented almost vertically (Morgane et al 1972, 1980).

The cerebral hemispheres of the bowhead brain exhibited deep sulci and convoluted gyri as is characteristic of cetacean brains (Figs 13-154, 13-155). Since no intact bowhead brains were received, no attempt was made to identify sulci and gyri either in comparison to those of ungulates and carnivores or according to the scheme of Morgane et al (1980). Ridgway has observed that there are fewer sulci and gyri in the hemispheres of the bowhead brain than in brains of some toothed whales (Appendix IV).

The "rhinic lobe" or rhinencephalon has been defined by Morgane et al (1980) as the portion of the telencephalon limited by the "rhinic cleft." Their rhinic cleft is a continuous sulcus made up by the rostral (anterior), and caudal (posterior) rhinal sulci, rhinohippocampal sulcus, hippocampal sulcus, the sulcus of the corpus callosum, and the caudal (posterior) parolfactory sulcus. The rhinic lobe is described as consisting of archicortical and paleocortical parts which meet in the median plane through the septal area and bilaterally through the unci.

The paleocortex (olfactory) is separated from the neocortex by the rhinal sulcus. Olfactory peduncles and olfactory bulbs have been described on brains from other mysticete whales, but none were observed on the bowhead brains examined, probably because of the method of removal. The lateral olfactory gyrus, which lies just medial to the rhinal sulcus on some cetacean brains, was not identified on the bowhead brains. The most prominent feature of the bowhead paleocortex was the olfactory tubercle (Fig 13-156). This region overlies the head of the caudate nucleus (Breathnach 1955). Caudal and

medial to the olfactory tubercle is the diagonal area which extends from the septum to the periamygdalar area. Its caudolateral part is perforated by blood vessels. The uncus, consisting of the gyrus semilunaris medially and the gyrus ambiens laterally, lies medial to the temporal pole (parahippocampal gyrus) separated from the latter by the caudal rhinal sulcus. The rostral part of the uncus is the periamygdalar area and is essentially identical with the corticomедial complex of the amygdalar nuclei (Morgane et al 1972). The stria terminalis, which arises from the amygdaloid nuclei, could be easily identified medial to the caudate nucleus (Figs 13-158, 13-160, 13-166).

The archicortex (hippocampal formation) began as the subcallosal gyrus under the rostrum and genu of the corpus callosum in the septal area (Fig 13-162). It continued dorsal to the corpus callosum, limited laterally by the sulcus of the corpus callosum, as the indusium griseum (Figs 13-162, 13-158) and around the splenium of the corpus callosum as the fasciola cinerea. At this point began the hippocampus major (or proper). Part of the temporal lobe was missing on the brain of 80B1, so its full extent was not observed (Fig 13-158). The temporal part of the hippocampus did protrude into the temporal horn of the lateral ventricle in the bowhead brain (Fig 13-165). Note in this figure that there is no occipital horn of the lateral ventricle.

The septum lay between the rostral horns of the lateral ventricles below the rostrum of the corpus callosum. Caudally it was traversed by the rostral commissure, which is characteristically small in cetaceans. It was separated from the neocortical parolfactory area (of Broca) by the caudal parolfactory and rostral rhinal sulci. It can be seen in Fig 13-162.

Several of the basal nuclei were identified on the bowhead brains. The caudate nucleus can be seen in Figs 13-158, 13-160, 13-164. The putamen is also seen in Figs 13-164 and 13-166. The claustrum is seen between the external and extreme capsules in Fig 13-166.

The caudolateral part of the thalamus was very well developed. The medial geniculate body was very large compared to domestic terrestrial mammals, but not necessarily so for cetaceans (Figs 13-156, 13-158). The lateral geniculate body could be identified easily but was not large compared to the medial geniculate body. The stria habenularis was easily identified but the habenula was not easily seen grossly (Fig 13-160). The pineal body was not seen and may not have been present. The interthalamic adhesion (massa intermedia) was not present in the bowhead thalamus. The rostral thalamic tubercle was recognizable, but was not prominent (Figs 13-166, 13-161).

The hypothalamus in cetacean brains is short rostrocaudally and deep dorsoventrally. The mammillary bodies are usually not readily identifiable grossly, and this was true of the bowhead. Most of the hypothalamus remained with the meninges when they were separated from the brain of 80B1 prior to its arrival at our lab. The optic chiasm and proximal parts of the optic tracts can be seen in Figs 13-167 and 13-168.

In many cetaceans, the adenohypophysis and neurohypophysis are not closely associated distally. This must be true of the bowhead, because the neurohypophysis came out with the meninges of 80B1 and can be seen in Figs 13-169 and 13-170, but the adenohypophysis apparently remained in the dura mater in the skull. See RU 580 also.

One of the most remarkable features of the brain of cetaceans is the great size of the cerebellum, particularly the paraflocculus. The ratio of the cerebellar weight to the total brain weight for the bowhead brain is at the upper end of the range given for cetacean brains (Ridgway, Appendix IV). To a veterinary anatomist, the cerebellum of the bowhead brain is comparable to the cerebellum of domestic terrestrial mammals and has been labeled accordingly in this report. This does not coincide with the designations given by Jansen (1950) for the cerebellum of the fin whale (Balaenoptera rostratus) and the bottle nose whale (Hyperoodon rostratus). Most authors describing the cerebellum of cetacean brains have followed the format used by Jansen in 1950. The cerebellum of the bowhead whale is shown in the accompanying figures. One could substitute the labels most frequently used for cetaceans if preferred.

Like the rest of the brain, the cerebellum was very fragile. The only picture that shows it completely intact is Fig 13-167, which was taken before the leptomeninges were removed. The nomenclature for the mammalian cerebellar vermis and hemispheres was established by Larsell (1970). The numbered hemispheric lobules are continuous with like-numbered vermal lobules. However, in these bowhead specimens the connections which were deep within sulci could not be investigated in detail because of the fragility of the brains, so the designations given the hemispheric lobules were based only on their appearance.

The cerebellum is shown from the dorsal aspect in Figs 13-171 and 13-172. The primary fissure is relatively far forward, so most of the cerebellum is the caudal lobe, as is true for other cetaceans. The culmen of the rostral lobe is rostral to the primary fissure. The lobulus simplex and declive are limited by the primary fissure rostrally and the posterior super-



ior or preansiform fissure caudally. The large region of the cerebellum limited rostrally by the posterior superior or preansiform fissure, laterally by the parafloccular fissure, and caudally by the ansoparamedian fissure is the ansiform lobule. The ansoparamedian fissure appears as a dark line in Fig 13-167, where the meninges extend down into it, and as a wide cleft in Fig 13-172. Most authors describing the cerebellum of cetaceans have designated only the oval-shaped rostral portion of this area as the ansiform lobule and the remainder as the paramedian lobule even though it is not near the median plane. The vermis separated where the ansoparamedian fissure crosses it. The vermal portion between this fissure and the posterior superior fissure is thought to be the folium vermis, which is supposed to be continuous with the ansiform lobule.

The prominent lobule caudal to the ansoparamedian fissure is the paramedian lobule. These lobules resemble the paramedian lobules of domestic terrestrial mammals and lie on either side of the median plane next to the vermis. The paramedian lobules are supposed to be attached to the tuber vermis and the rostral part of the pyramis, but this could not be confirmed on these specimens.

The ventral part of the hemisphere of the caudal lobe of the cerebellum consists of the dorsal and ventral parafloccular lobules. The dorsal paraflocculus can be seen in Figs 13-167, 13-171, and 13-175 from the caudal view. The division between the paramedian lobule and the dorsal paraflocculus is hard to determine in Fig 13-175 but is readily seen in Fig 13-167 on the right side. Here the parafloccular fissure can be followed passing ventral to the paramedian lobule.

The ventrolateral aspect of the cerebellum is presented in Figs 13-176 and 13-177. The convoluted dorsal paraflocculus, which is separated from the ansiform and paramedian lobules by the parafloccular fissure, can be traced around to the rostral aspect of the cerebellum, where it can also be seen in Fig 13-173 on the right side of the picture (left side of the cerebellum). The ventral paraflocculus is separated from the dorsal paraflocculus by the intraparafloccular fissure and lies ventromedial to the dorsal paraflocculus (Figs 13-176, 13-177, 13-178, and 13-179). It too, is convoluted. Various portions of it have been designated as the accessory paraflocculus by authors describing the cerebellum of other cetaceans.

The caudolateral (posterolateral) fissure and the flocculonodular lobe were not identified on these specimens. The caudal vermis was in pieces, so that the pyramis, uvula, and nodule could not be identified.

The rostral lobe of the cerebellum of cetaceans is small compared to the caudal lobe and also compared to the rostral lobe of domestic terrestrial mammals, especially carnivores. Most of the rostral lobe is seen in the rostroventral views of the cerebellum in Figs 13-180, 13-181, 13-182, and 13-183. The hemispheres of the rostral lobe were more extensive laterally than in most domestic mammals.

The sagittally sectioned cerebellum of 80B1 is shown in Figs 13-181, 13-182, and 13-183. The vermis disintegrated caudal to the folium vermis, so the caudal lobules could not be identified. The primary fissure and the posterior superior or preansiform fissure were determined by comparison with the surface, where they limit the very obvious lobulus simplex and declive. The other lobules were determined by the branching of the arbor vitae and by the depth of the fissures.

Almost all of the available brains appeared to have been rather violently separated through the mesencephalon with resulting distortions, so not too much can be said about this region. In other cetaceans the mesencephalic (cerebral) aqueduct is said to be voluminous caudally at the level of the caudal colliculus. This is probably true for the bowhead brain, so the aqueduct is depicted as expanding caudally in Fig 13-160. The only brain stem fragment that included both the rostral and caudal colliculi is pictured in Fig 13-184. Superficially, the rostral and caudal colliculi appeared to be about the same size. The rostral colliculi did not appear as massive as in domestic ruminants, but would not be regarded as small. The caudal colliculi appeared somewhat larger relative to other brain stem structures in the bowhead brain than is the case in carnivores, but were probably not larger than the caudal colliculi of other cetaceans. The lateral lemniscus was very prominent and so was the brachium of the caudal colliculus (Fig 13-184 and 13-185). The large medial geniculate body has already been mentioned with the thalamus.

The rhombencephalon appeared to be wide and shallow, especially in the brain of 80B1 (Figs 13-186, 13-187, 13-188, and 13-189). The transverse fibers of the pons formed a massive structure, as would be expected with the large cerebellum (Figs 13-188 and 13-189). The middle cerebellar peduncle (brachium pontis) was twice as large as the rostral or caudal cerebellar peduncle, but neither of the latter two structures appeared to be particularly small (Figs 13-186, 13-187). The large trigeminal nerve (V) exited through the transverse fibers of the pons, as in the human brain and unlike the

arrangement in domestic mammals, where it exits caudal to the transverse fibers or middle cerebellar peduncle (Figs 13-188, 13-189). The vestibulocochlear nerve (VIII) can be seen caudal to the cerebellar peduncles in Figs 13-186 and 13-187 and at the lateral border of the trapezoid body (CT) in Figs 13-188 and 13-189. It was not larger than the trigeminal nerve in the bowhead, which is typical for baleen whales, although the vestibulocochlear nerve has been reported to be larger than the trigeminal nerve in some toothed whales (Pilleri and Gahr 1970).

The superficial origins of some other cranial nerves can be seen on the ventral surface of the brain stem in Figs 13-188 and 13-189. The facial nerve (VII) exited between the trigeminal and vestibulocochlear nerves (V and VIII). The glossopharyngeal nerve (IX) exited caudal to the vestibulocochlear nerve (VIII). The rootlets of the hypoglossal nerve (XII) could be seen exiting lateral to the pyramids. The rootlets of the vagus nerve (X) and the accessory nerve (XI) were not identified on the bowhead brain stems, but on other cetacean brains, both motor and sensory rootlets of the vagus nerve have been described caudal to the glossopharyngeal nerve, with the rootlets of the accessory nerve continuing in line with the vagal motor rootlets (Breathnach 1955, 1960, Pilleri 1964, 1966a).

The oculomotor nerve (III), trochlear nerve (IV) and abducent nerve (VI), which innervate the extraocular muscles, have been described for most cetacean brains (Pilleri and Gahr 1970), but were not identified with certainty on these bowhead specimens. The band of fibers drawn in ventral to the mesencephalic aqueduct in Fig 13-160, but not labeled, may be the oculomotor nerve. This band can be seen on the other half of the brain of 80B1 in Fig 13-159, but is not depicted in Fig. 13-158. A smaller band of fibers was seen exiting the brain stem of 79B1 between the rostral cerebellar peduncle and the lateral lemniscus which may have been the trochlear nerve, since this is the site of superficial origin given for it in the humpback whale by Breathnach (1955). The abducent nerve is always pictured in its normal location exiting through the trapezoid body just lateral to the pyramid, but it was not identified on any of the bowhead brain stems examined.

The olives are seen on either side of the ventral median fissure in Figs 13-188 and 13-189. This protuberance, which is characteristic of cetacean brains, was the surface representation of the very large medial accessory olivary nucleus. The pyramids emerged caudal to the pontine transverse fibers

and passed ventral to the trapezoid body and around the lateral sides of the olives and decussated caudal to them.

The dorsal median sulcus and the dorsolateral sulcus can be seen on the dorsal surface of the brain stem in Figs 13-186 and 13-187. The fasciculus cuneatus and the cuneate tubercle could be seen. The nucleus gracilis was visible at the caudal extremity of the fourth ventricle, but a fasciculus gracilis was not visible on the dorsal surface. The bulge lateral to the dorsolateral sulcus in the caudal part of the medulla oblongata was probably the spinal tract of the trigeminal nerve.

The pontine flexure was at the level of the vestibulocochlear nerve and trapezoid body, and the cervical flexure was approximately at the junction between the brain stem and spinal cord.

#### Abbreviations Used for Labeling Figures 13-154 through 13-189

AC	Commissura rostralis
ALC	Ala lobuli centralis
APB	Area parolfactoria (Brocae)
Aq	Aqueductus mesencephali (A. cerebi)
AS	Area septalis (Area subcallosa)
BCdC	Brachium colliculi caudalis
Cl	Clastrum
Cu	Culmen
CC	Corpus callosum
CdC	Colliculus caudalis
CrC	Crus cerebri
CE	Capsula externa
CEm	Capsula extrema
CI	Capsula interna
CT	Corpus trapezoideum

D	Declive
F	Fornix
FAPM	Fissura ansoparamediana
FC	Fasciculus cuneatus
FD	Fascia dentata
FH	Fimbria hippocampi
FIPf	Fissura intraparafloccularis
FP	Fissura prima
FPf	Fissura parafloccularis
FPS	Fissura preansiformis (F. posterior superior)
FPrC	Fissura preculminata
FoV	Folium vermis
GA	Gyrus ambiens
GD	Gyrus diagonalis
GS	Gyrus semilunaris
H	Hippocampus
I	Infundibulum
IG	Indusium griseum
L	Lingula (cerebelli)
LA	Lobulus ansiformis
LC	Lobulus centralis
LG	Corpus geniculatum laterale
LL	Lemniscus lateralis
LPM	Lobulus paramedianus
LQ	Lobulus quadrangularis
LS	Lobulus simplex
MG	Corpus geniculatum mediale

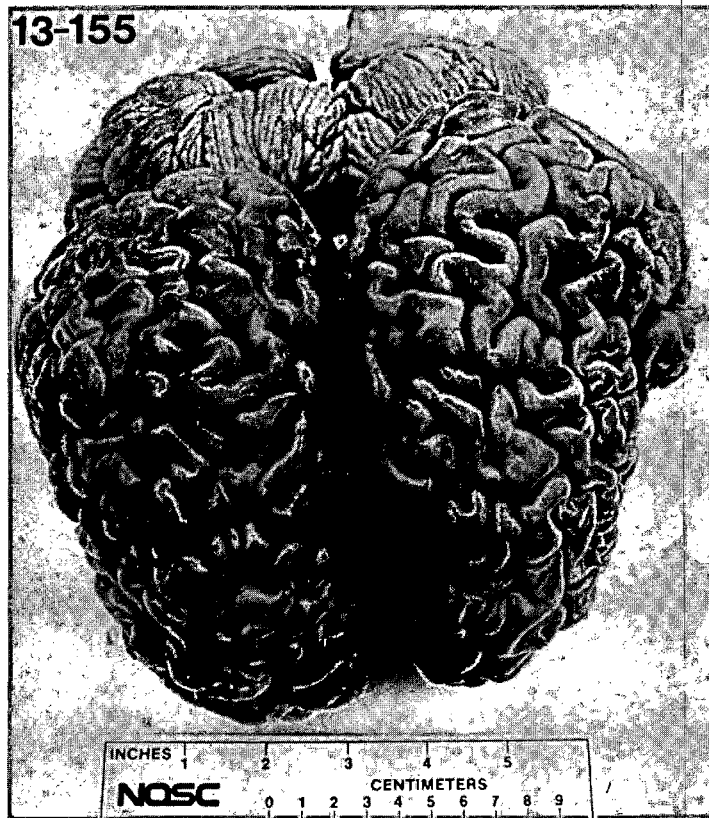
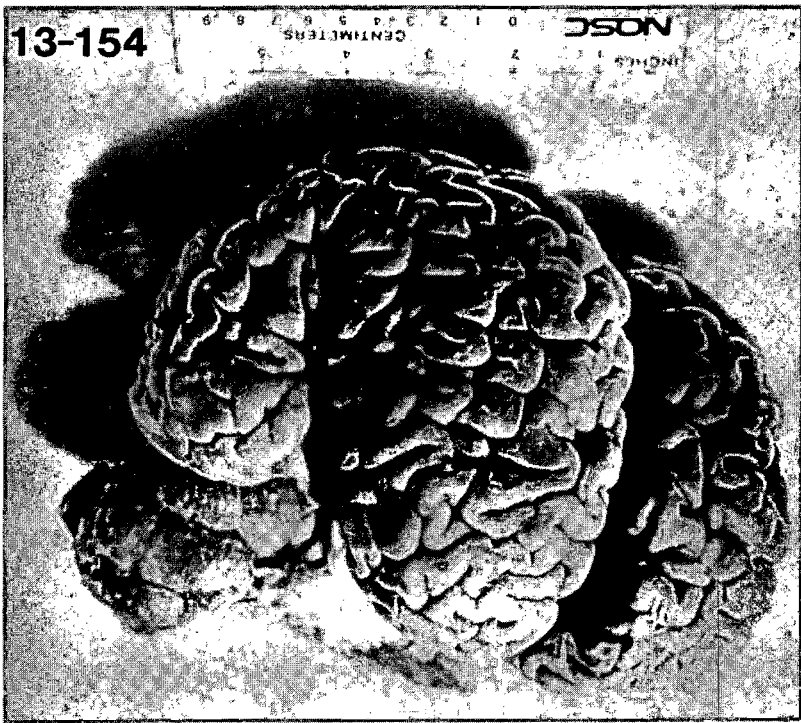
NC	Nucleus caudatus
NH	Neurohypophysis
N II	Nervus opticus
N V	Nervus trigeminus
N VII	Nervus facialis
N VIII	Nervus vestibulocochlearis
N IX	Nervus glossopharyngeus
N XII	Nervus hypoglossus
O	Oliva
OC	Chiasma optica
OT	Tractus opticus
PCC.	Pedunculus cerebellaris caudalis
PCM	Pedunculus cerebellaris medius
PCR	Pedunculus cerebellaris rostralis
PfD	Paraflocculus dorsalis
PfV	Paraflocculus ventralis
Pul	Pulvinar
Put	Putamen
Py	Pyramis (medullae oblongatae)
RC	Colliculus rostralis
RTT	Tuberculum rostrale thalami
SH	Sulcus hippocampi
SLD	Sulcus lateralis dorsalis
SMD	Sulcus medianus dorsalis
SP	Septum telencephali (pellucidum)
SPfA	Substantia perforata rostralis (anterior)
SRhA	Sulcus rhinalis rostralis (anterior)
SpCC	Splenium corporis callosi
StH	Stria habenularis thalami
StT	Stria terminalis

TC	Tuberculum nuclei, cuneati
TO	Tuberculum olfactorium
V	Vinculum lingulae
VL	Ventriculus lateralis

Figure 13-154. Photograph of an intact brain of bowhead whale. Photograph obtained from Dr. Sam Ridgway, NOSC. It is purposely mounted upside down to facilitate comparison with brains of other species.

Figure 13-155. Photograph of the dorsal aspect of the intact brain of 80B2. Photograph obtained from Dr. Sam Ridgway, NOSC.





13-156

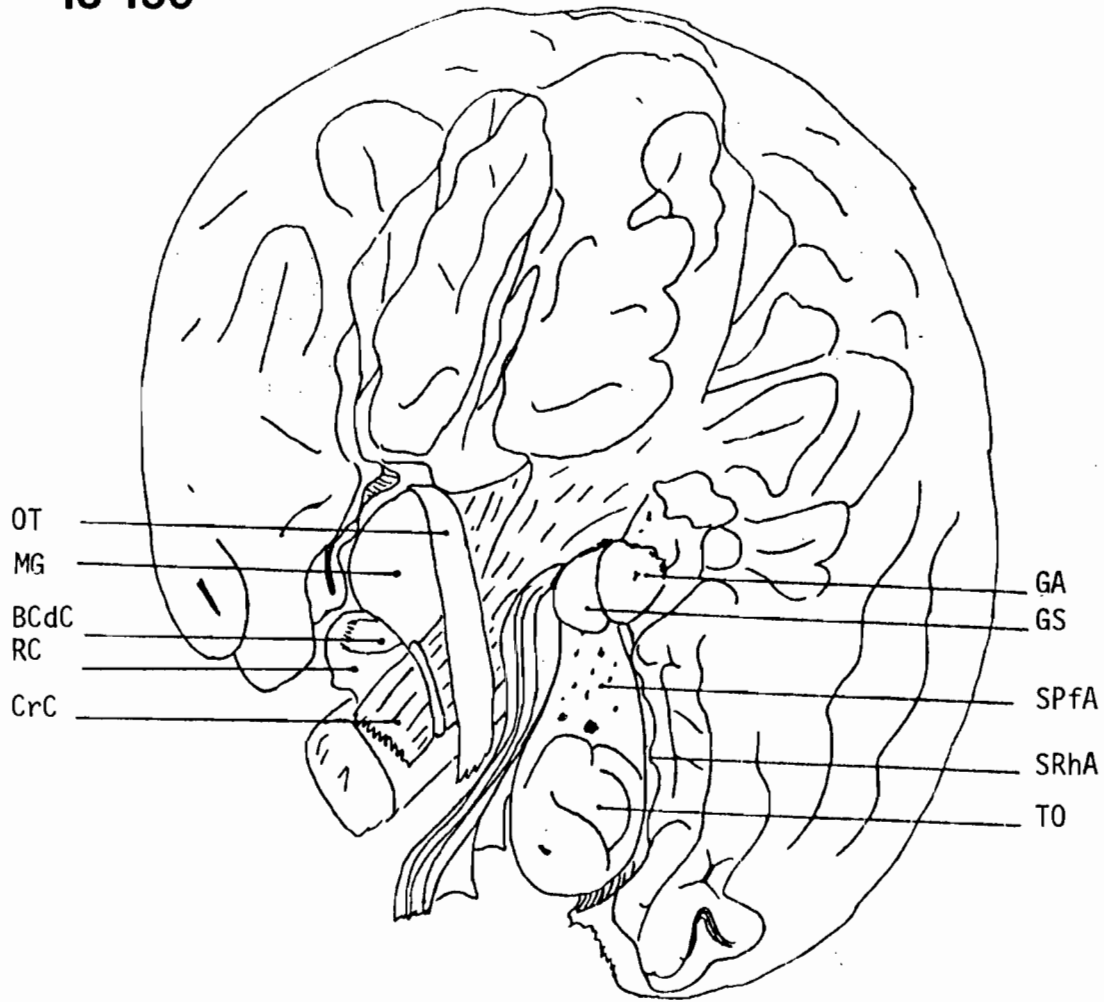


Figure 13-156. Sketch of the ventrolateral aspect of the "forebrain" of 80B1 ("damaged in removal"). Compare to Fig 13-157. Drawn from the same brain fragment shown in Fig 13-157, but not from the photograph. BCdC - Brachium colliculi caudalis; CrC - Crus cerebri; GA - Gyrus ambiens; GS - Gyrus semilunaris; MG - Corpus geniculatum mediale; OT - Tractus opticus; RC - Colliculus rostralis; SPfA - Substantia perforata rostralis (anterior); SRhA - Sulcus rhinalis rostralis (anterior); TO - Tuberculum olfactorium.

13-157

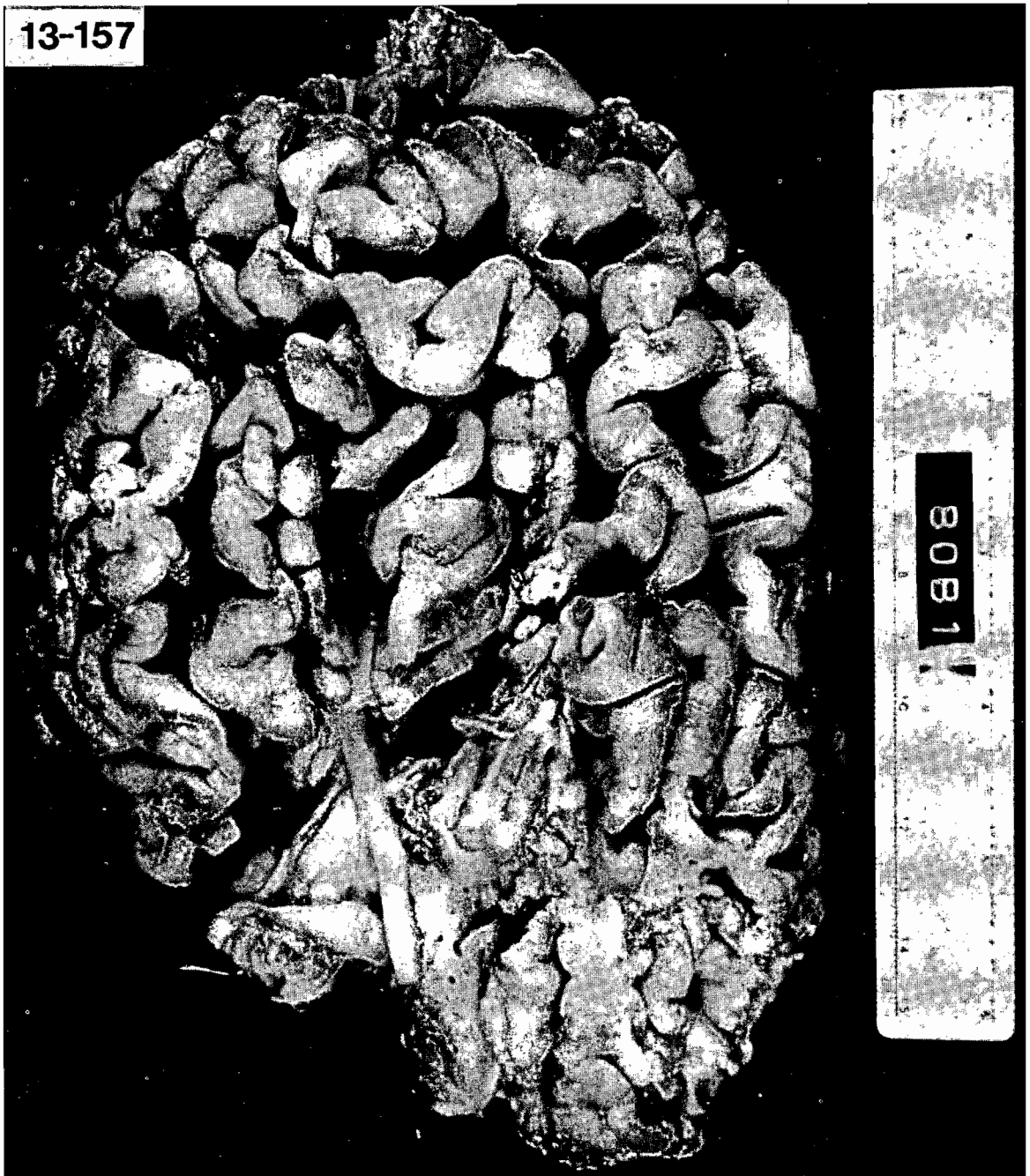


Figure 13-157. Photograph of the ventrolateral aspect of the forebrain of 80B1 (right side). Compare to Fig 13-156.

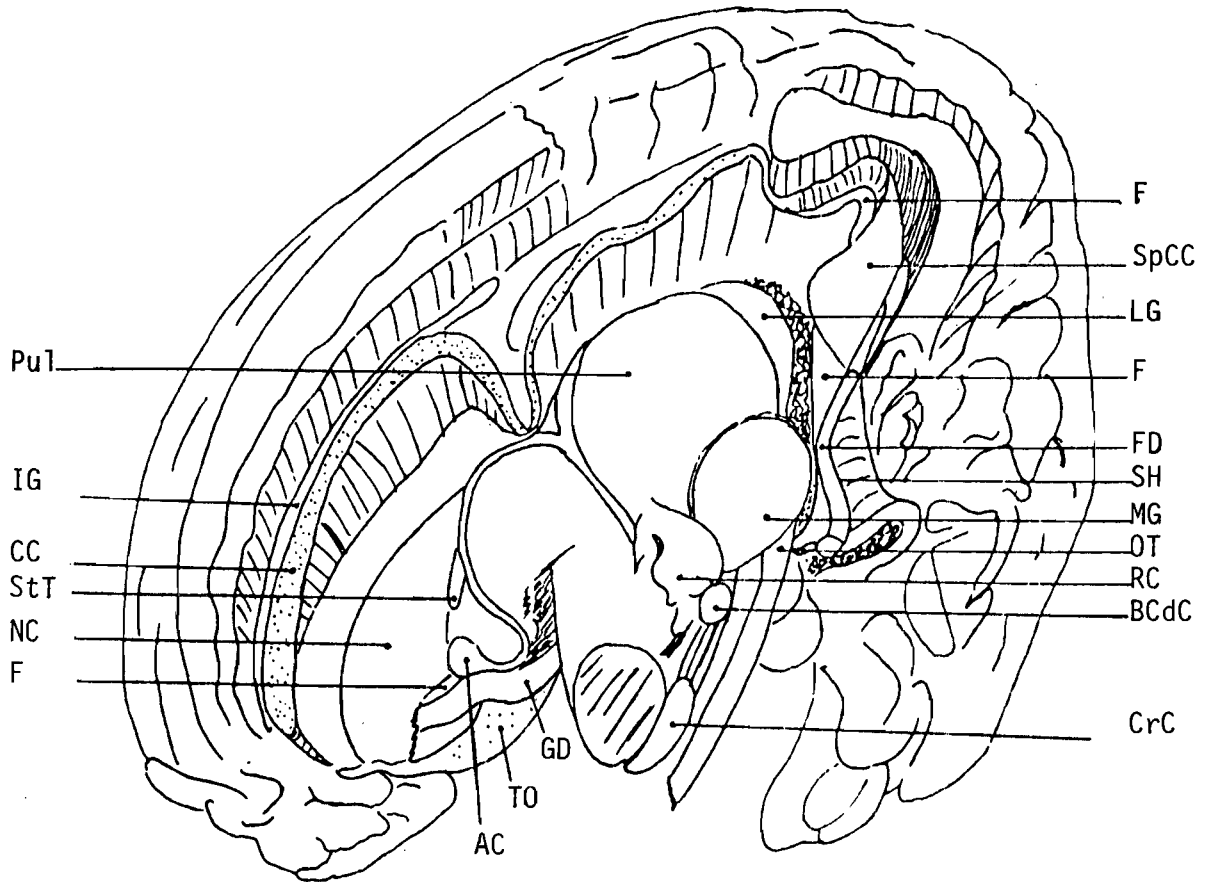


Figure 13-158. Sketch of the ventromedial view of the right "half" of the forebrain of 80B1. Compare to Fig 13-159. Orientation not exactly the same as in the photograph. AC - Commissura rostralis; BCdC - Brachium colliculi caudalis; CC - Corpus callosum; CrC - Crus cerebri; F - Fornix; FD - Fascia dentata; GD - Gyrus diagonalis; IG - Induseum griseum; LG - Corpus geniculatum laterale; MG - Corpus geniculatum mediale; NC - Nucleus caudatus; OT - Tractus opticus; Pul - Pulvinar; RC - Colliculus rostralis; SH - Sulcus hippocampi; SpCC - Splenium corporis callosi; StT - Stria terminalis; TO - Tuberculum olfactorium.



Figure 13-159. Photograph of the medial aspect of the right half of the forebrain of 80B1. Compare to Fig 13-158. Orientation not exactly the same as in the sketch.

13-160

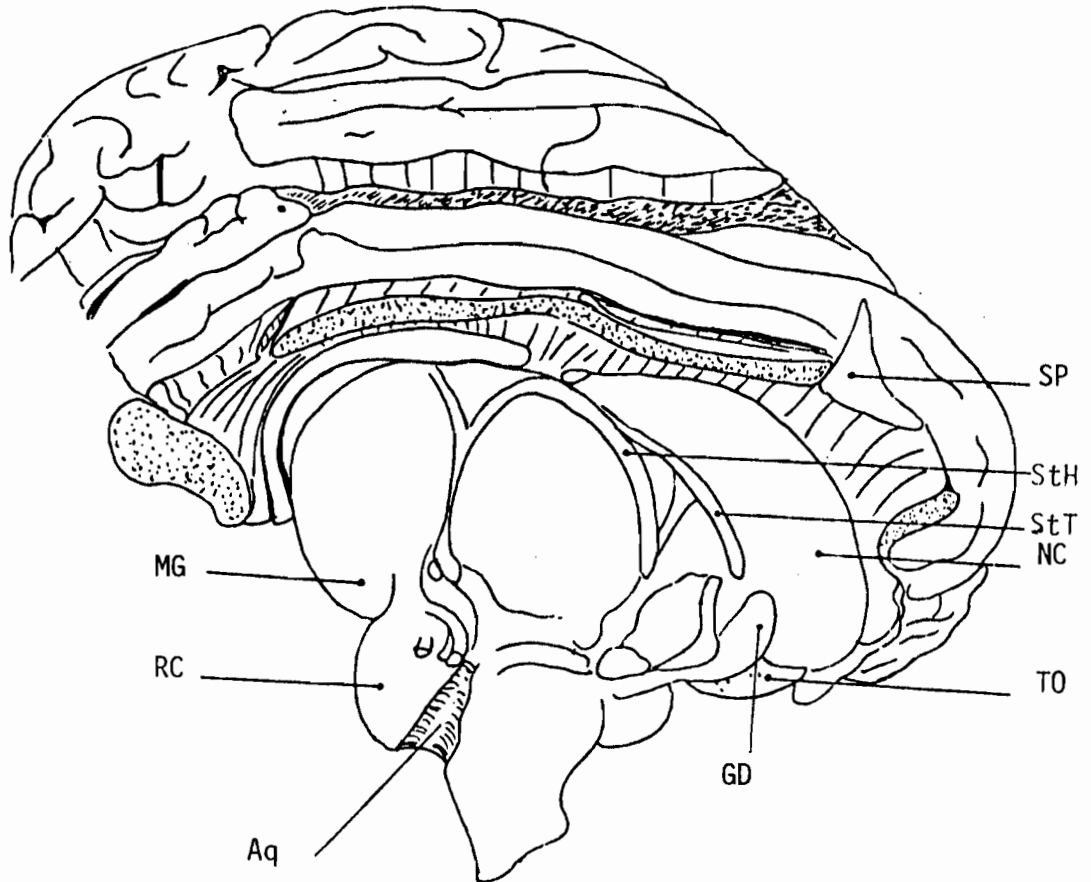


Figure 13-160. Sketch of the ventromedial aspect of the left "half" of the "forebrain" of 80B1. Compare to Fig 13-161. Drawn from the same brain fragment shown in Fig 13-161, but not from the same orientation. Aq - Aqueductus mesencephali (A. cerebri); GD - Gyrus diagonalis; MG - Corpus geniculatum mediale; NC - Nucleus caudatus; RC - Colliculus rostralis; SP - Septum telencephali (pellucidum); StH - Stria habenularis; StT - Stria terminalis; TO - Tuberculum olfactorium.



Figure 13-161. Photograph of the medial aspect of the left "half" of the "forebrain" of 80B1. Compare to Fig 13-160.

Figure 13-162. Photograph of the medial aspect of a slice of the right cerebral hemisphere of 80B2, showing the septal area. AC - Commissura rostralis; APB - Area parolfactoria (Brocae); AS - Area septalis; CC - Corpus callosum; F - Fornix; IG - Indusium griseum.

Figure 13-163. Photograph of the reapproximated slices of the left half of the "forebrain" of 79KK2.



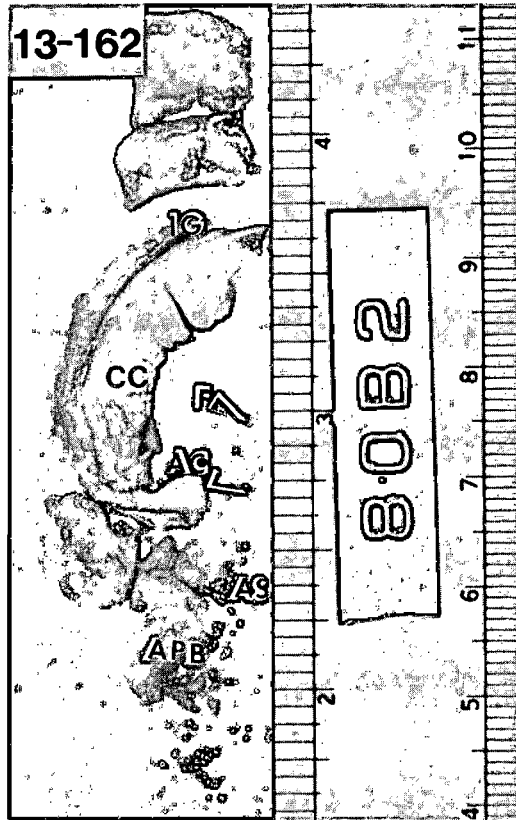
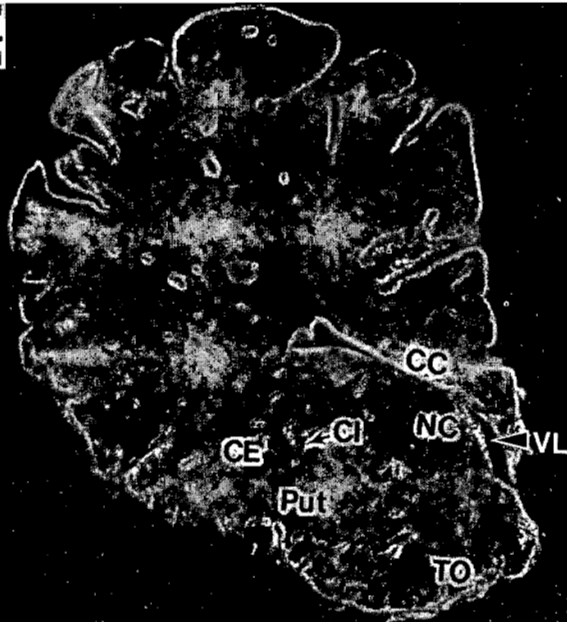


Figure 13-164. Photograph of the caudal surface of the fourth slice from the "frontal" pole of the left hemisphere of 79KK2. See Fig 13-163. CC - Corpus callosum; CE - Capsula externa; CI - Capsula interna; NC - Nucleus caudatus; Put - Putamen; TO - Tuberculum olfactorium; VL - Ventriculus lateralis.

Figure 13-165. Photograph of the rostral surface of the tenth slice from the "frontal" pole of the left hemisphere of 79KK2 (through the temporal horn of the lateral ventricle). Compare to Fig 13-163. The hippocampus does protrude into the lateral ventricle. FH - Fimbria hippocampi; H - Hippocampus; VL - Ventriculus lateralis.

13-164



79KK2

13-165



79KK2

Figure 13-166. Photograph of the rostral surface of a slice of the left hemisphere of 79KK4 at the interventricular foramen. The plane of sectioning is different than in 79KK2. CC - Corpus callosum; CE - Capsula externa; CEm - Capsula extrema; CI - Capsula interna; Cl - Claustrum; NC - Nucleus caudatus; Put - Putamen; RTT - Tuberculum rostrale thalami; StT - Stria terminalis.

13-166

CC

RTT

ST

NC

CT

Pu

CE

CI

CEm

79KK4

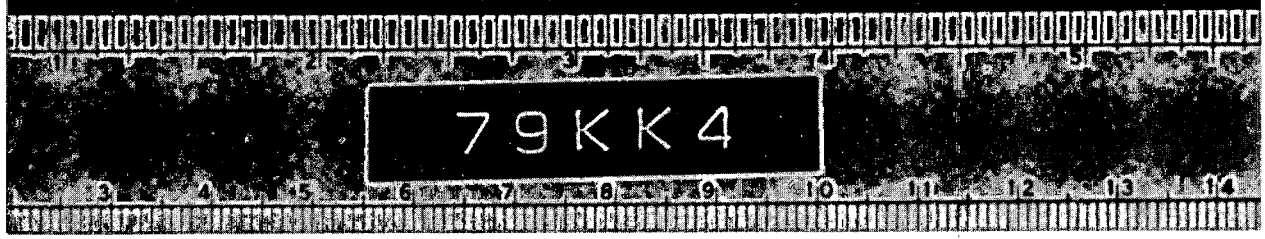


Figure 13-167. Photograph of a dorsal view of the detached leptomeninges of the forebrain and the cerebellum and brain stem of 80B1 still covered by leptomeninges. The optic chiasm and parts of the optic tracts are visible. Compare to Fig 13-168. LPM - Lobulus paramedianus; OC - Chiasma optica; PFD - Paraflocculus dorsalis.

Figure 13-168. Photograph of a closer view of the optic chiasm, optic tracts, and ventral hypothalamus of 80B1 in the leptomeninges. I - Infundibulum; OC - Chiasma optica; OT - Tractus opticus.



Figure 13-169. Photograph of a ventral view of the leptomeninges, cerebellum and brain stem of 80B1. The optic nerves (N II) and neurohypophysis (NH) are visible. Compare to Fig 13-170.

Figure 13-170. Photograph of a closer view of the optic nerves and neurohypophysis of 80B1. N II - Nervus opticus; NH - Neurohypophysis.





13-171

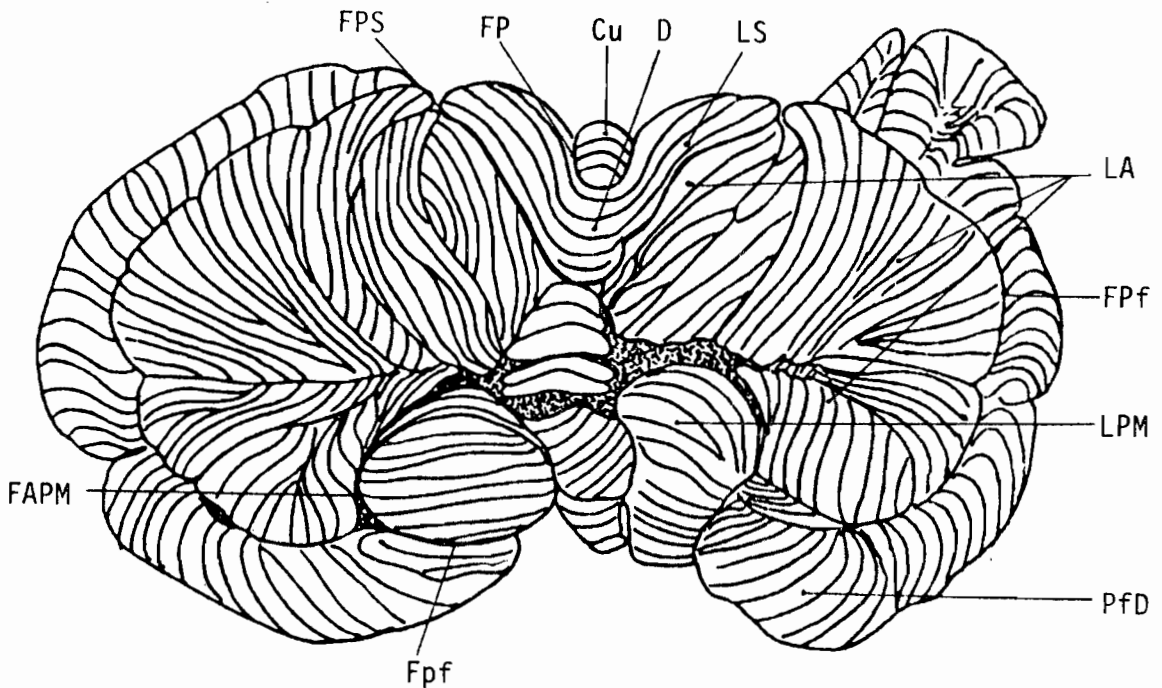


Figure 13-171. Sketch of the dorsal aspect of the cerebellum of 80B1. Note the ansiform lobule (LA). Cu - Culmen; D - Declive; FAPM - Fissura ansoparamediana; FP - Fissura prima; FPS - Fissura preansiformis (F. posterior superior); FPf - Fissura parafloccularis; LA - Lobulus ansiformis; LPM - Lobulus paramedianus; LS - Lobulus simplex; PFD - Paraflocculus dorsalis.



Figure 13-172. Photograph of the dorsal aspect of the cerebellum of 80B1.  
Compare to Fig 13-171. X0.85

13-173

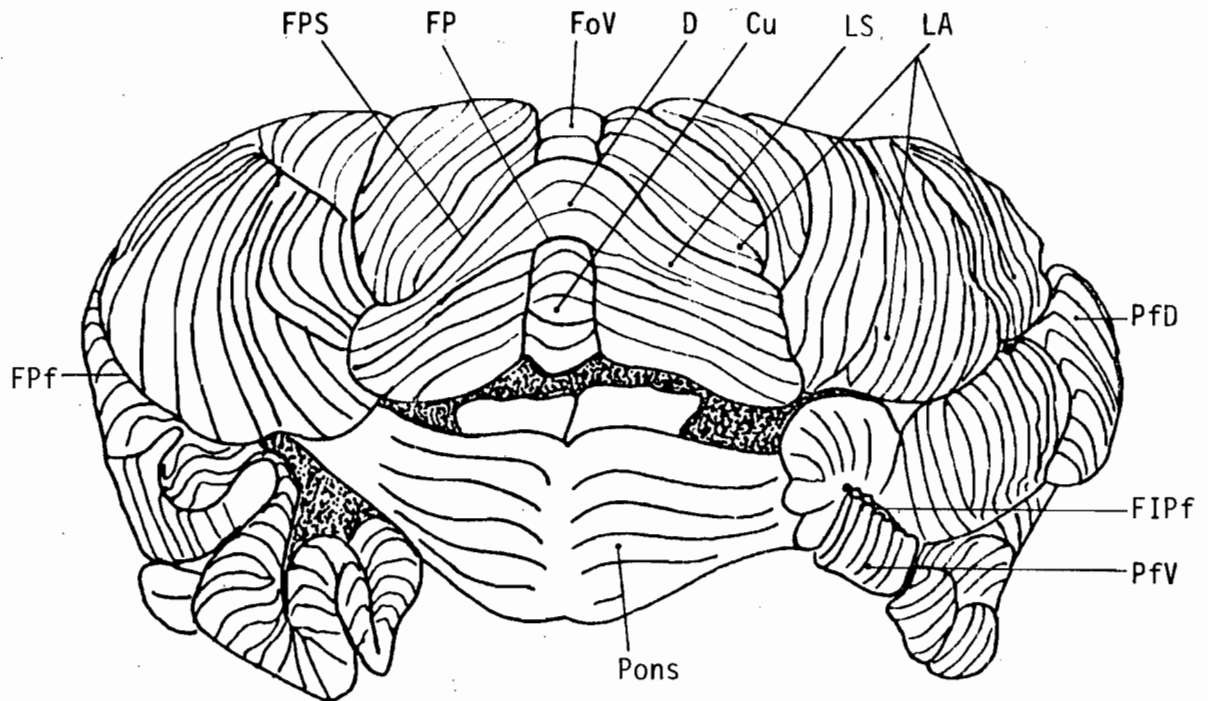


Figure 13-173. Sketch of the rostral aspect of the cerebellum of 80B1 (still attached to the brain stem). Cu - Culmen; D - Declive; FIPf - Fissura intraparafloccularis; FP - Fissura prima; FPF - Fissura parafloccularis; FPS - Fissura preansiformis (F. posterior superior); FoV - Folium vermis; LA - Lobulus ansiformis; LS - Lobulus simplex; PFD - Paraflocculus dorsalis; PfV - Paraflocculus ventralis.

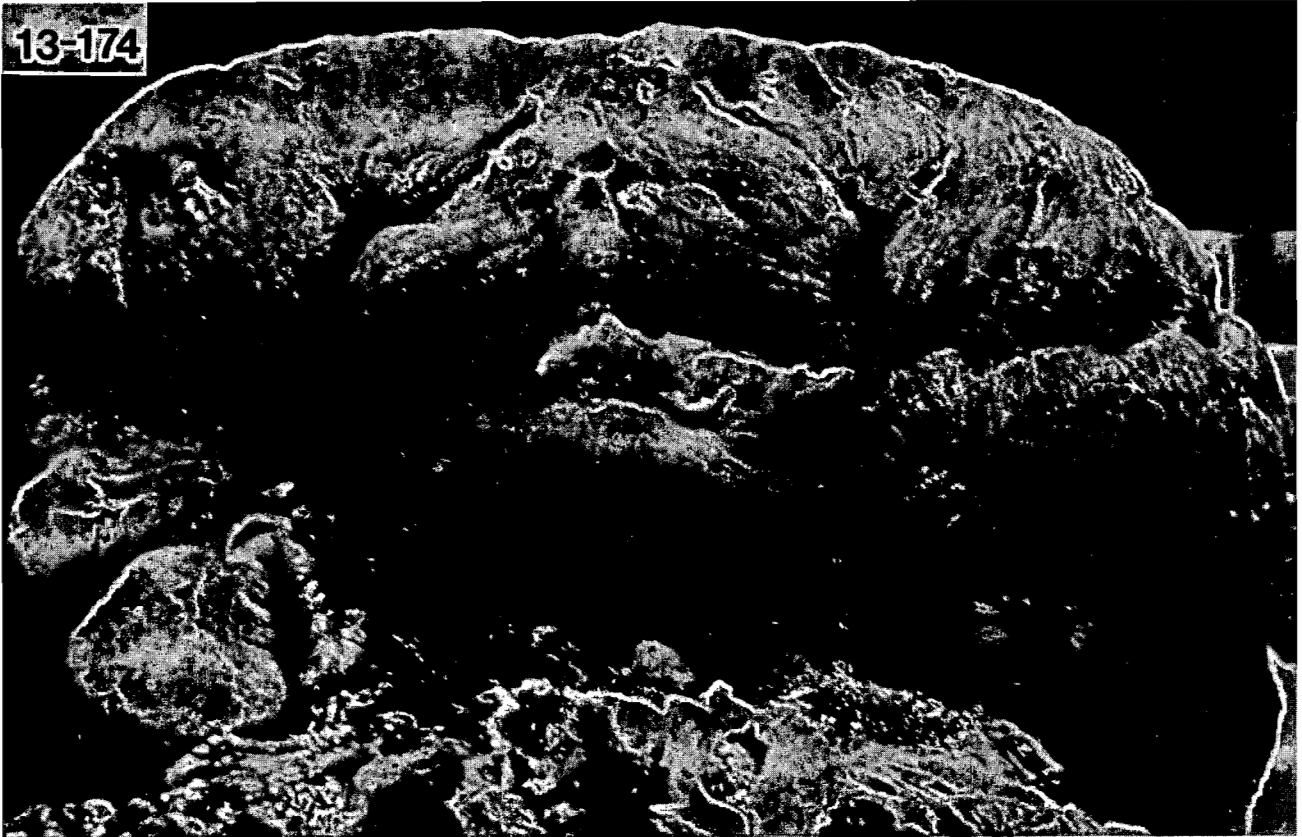
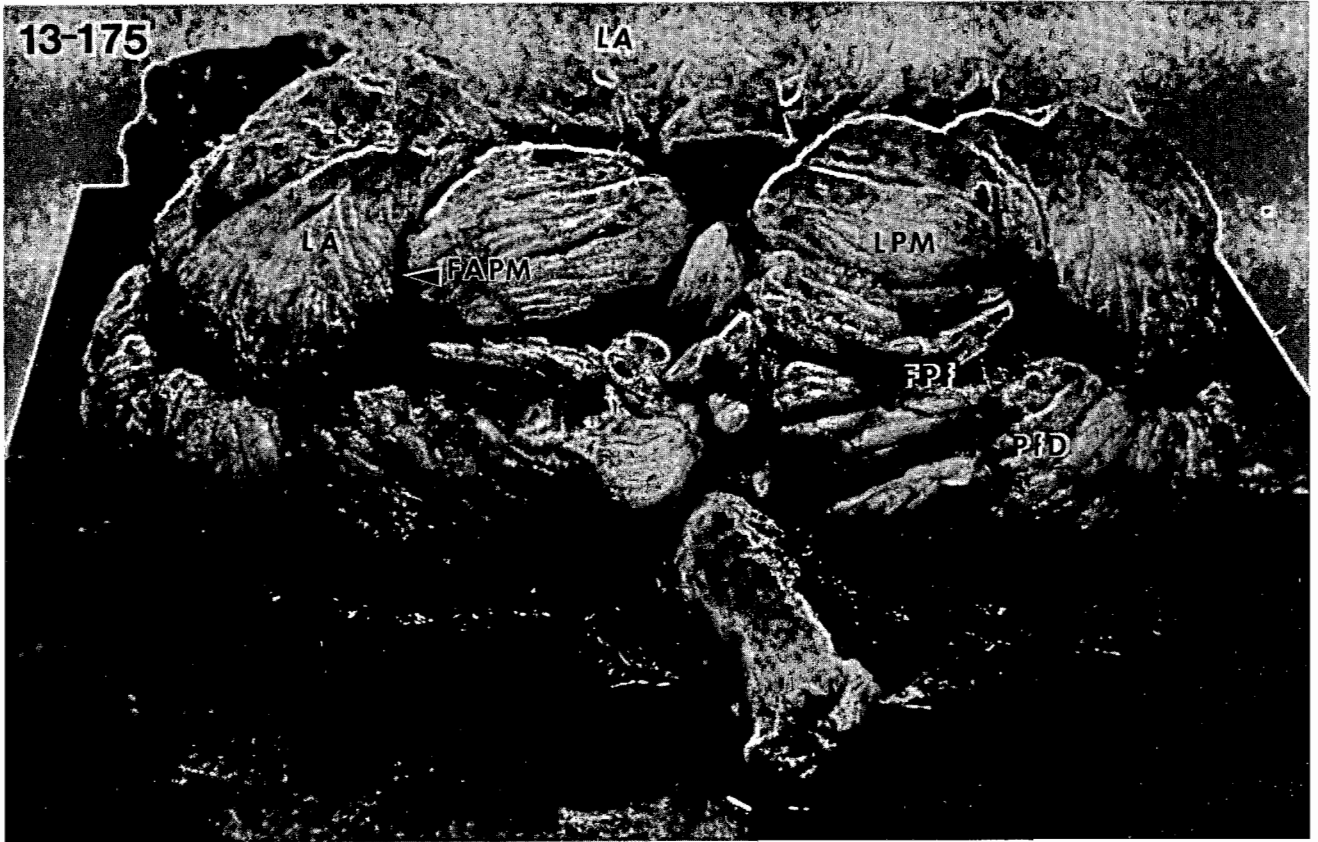


Figure 13-174. Photograph of the rostral aspect of the cerebellum of 80B1.  
Compare to Fig 13-173. X1

Figure 13-175. Photograph of the caudal aspect of the cerebellum of 80B1. Note the paramedian lobules (LPM) on either side of the vermis and the dorsal paraflocculus (PFD). FAPM - Fissura ansoparamediana; FPf - Fissura parafloccularis; LA - Lobulus ansiformis. X0.85



13-176

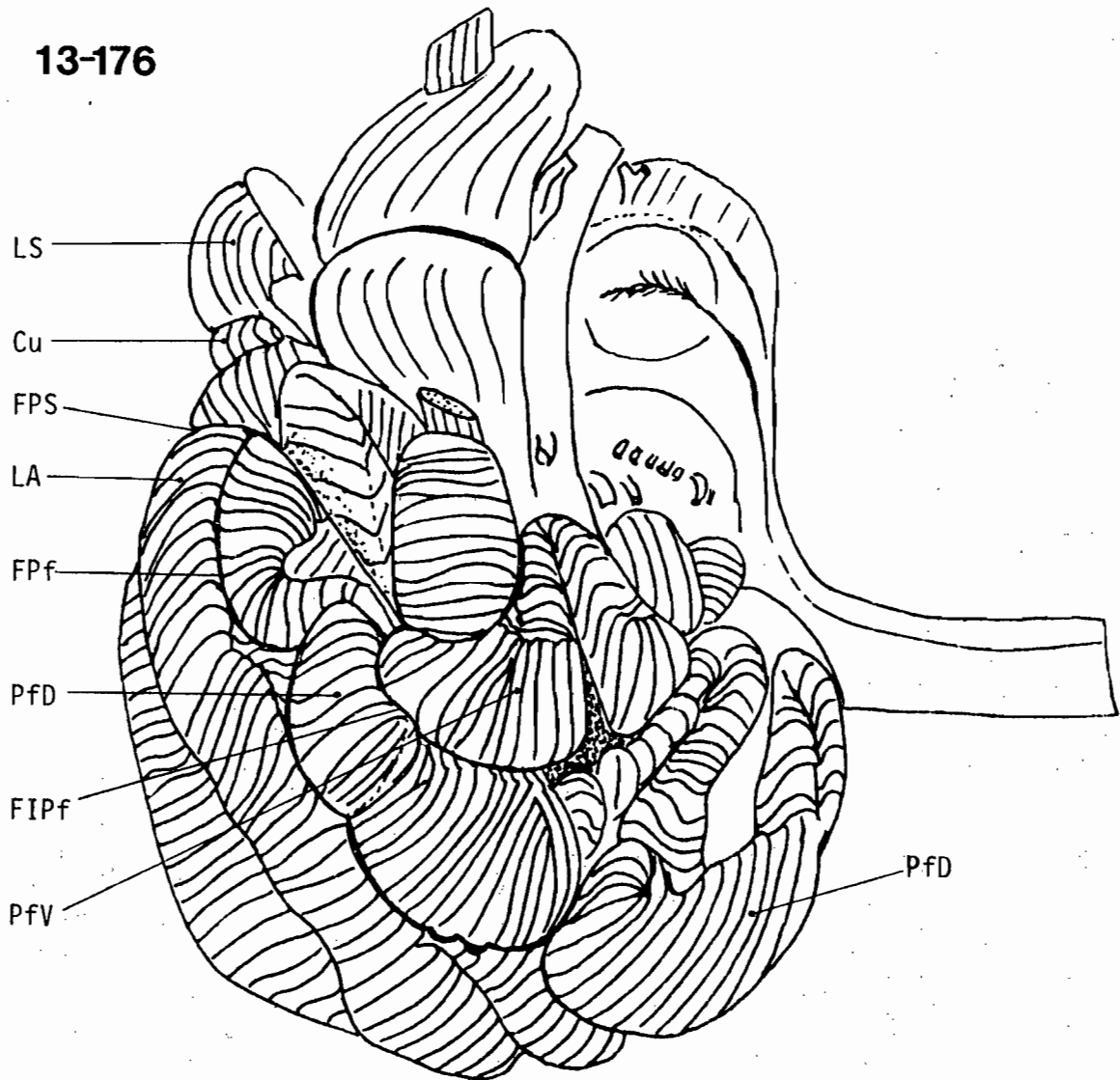


Figure 13-176. Sketch of the ventrolateral aspect of the cerebellum of 80B1. Note the dorsal paraflocculus (PFD). Cu - Culmen; FIPf - Fissura intraparafloccularis; FPf - Fissura parafloccularis; FPS - Fissura preansiformis (F. posterior superior); LA - Lobulus ansiformis; LS - Lobulus simplex; PFD - Paraflocculus dorsalis; Pfv - Paraflocculus ventralis.





Figure 13-177. Photograph of the ventrolateral aspect of the cerebellum of 80B1. Compare to Fig 13-176. X1



Figure 13-178. Photograph of the rostroventral aspect of the cerebellum of 80B1. Note the intraparafloccular fissure (FIPf). Fpf - Fissura parafloccularis; LA - Lobulus ansiformis; LS - Lobulus simplex; Pfd - Paraflocculus dorsalis; Pfv - Paraflocculus ventralis. X1

13-179



Figure 13-179. Photograph of the ventral aspect of the right cerebellar hemisphere of 80B1. Note the ventral paraflocculus (PfV). FIPf - Fissura intraparafloccularis; PfD - Paraflocculus dorsalis. X1.55

**13-180**

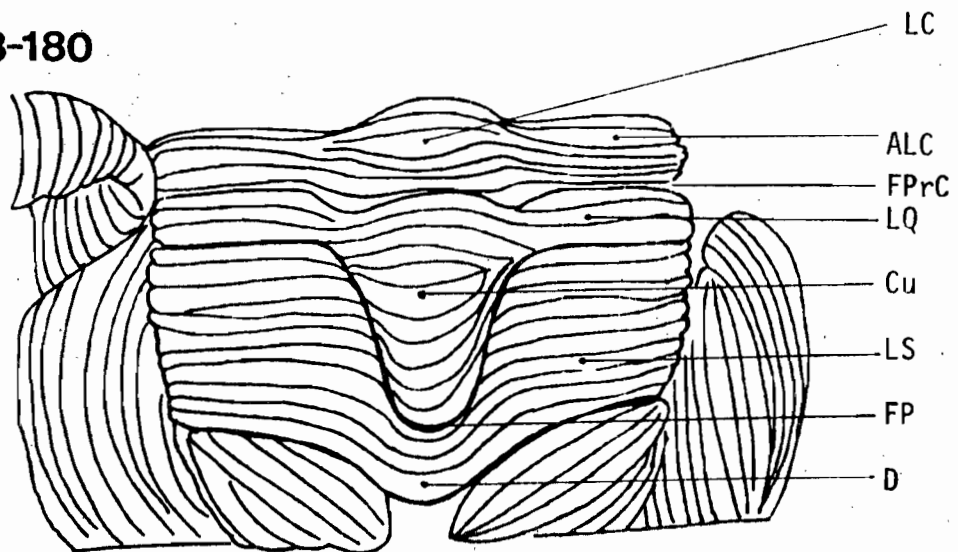


Figure 13-180. Sketch of the rostral aspect of the cerebellum of 80B1 with the brain stem removed. ALC - Ala lobuli centralis; Cu - Culmen; D - Declive; FP - Fissura prima; FPrC - Fissura preculminata; LC - Lobulus centralis; LQ - Lobulus quadrangularis; LS - Lobulus simplex.



Figure 13-181. Photograph of the rostroventral aspect of the cerebellum of 80B1. The cerebellum has been sectioned sagittally. Note the lateral extent of the rostral lobules. Compare to Figs 13-180 and 13-182. ALC - Ala lobuli centralis; Cu - Culmen; FP - Fissura prima; LC - Lobulus centralis; LQ - Lobulus quadrangularis; LS - Lobulus simplex. X1.83

13-182

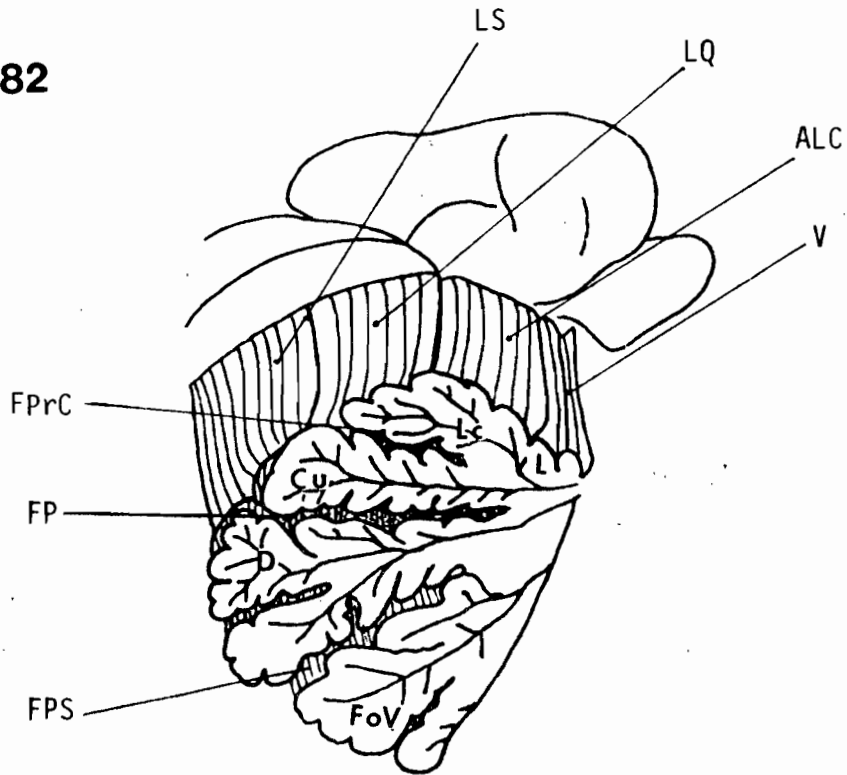


Figure 13-182. Sketch of the sagittal section of the cerebellum of 80B1 oriented as in Figs 13-181 and 13-183. ALC - Ala lobuli centralis; Cu - Culmen; D - Declive; FP - Fissura prima; FPrC - Fissura preculminata; FPS - Fissura preansiformis (F. posterior superior); FoV - Folium vermis; L - Lingula; LC - Lobulus centralis; LQ - Lobulus quadrangularis; LS - Lobulus simplex; V - Vinculum lingulae.

13-183

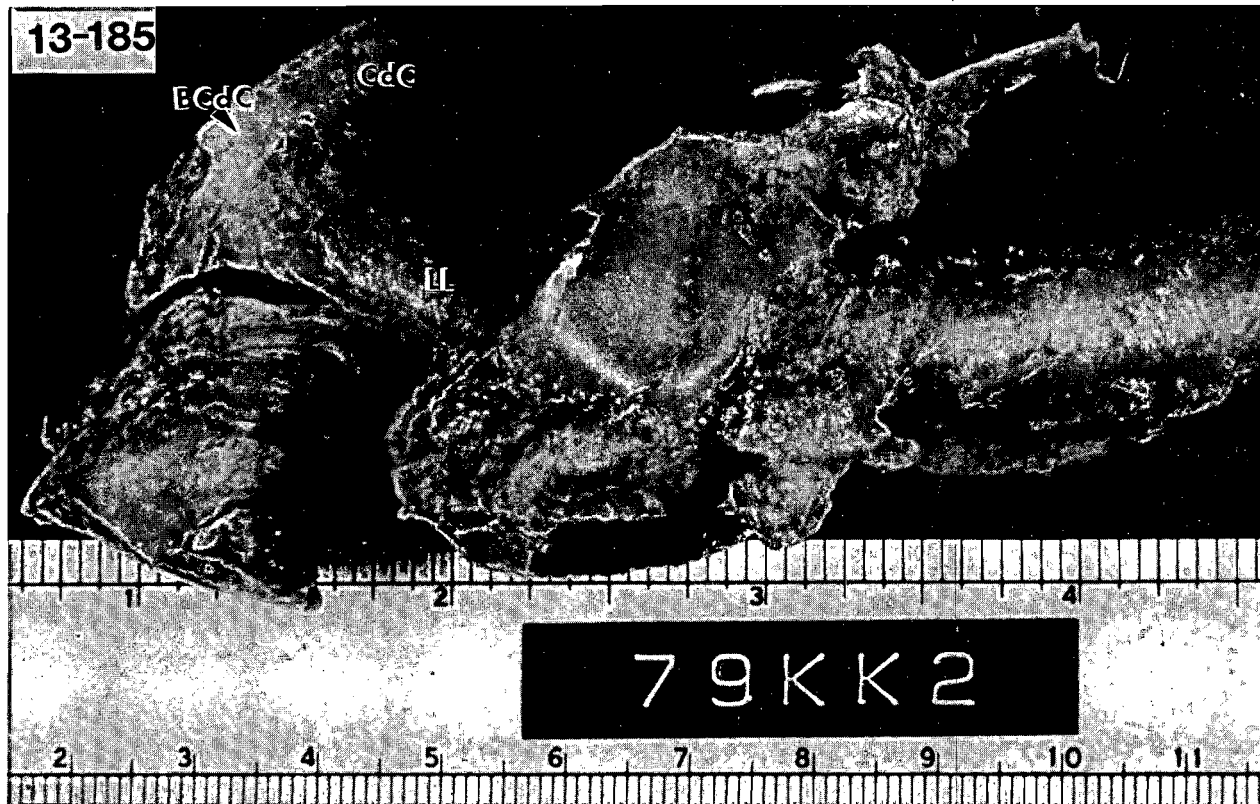


Figure 13-183. Photograph of the sagittal section of the cerebellum of 80B1.  
Compare to Fig 13-182. X1.83

Figure 13-184. Photograph of the dorsal aspect of the brain stem of 79KK3, showing the rostral colliculi, and lateral lemniscus, caudal colliculus and the brachium colliculi caudalis on the right side. The left caudal colliculus is also present. BCdC - Brachium colliculi caudalis; CdC - Colliculus caudalis, LL - Lemniscus lateralis; RC - Colliculus rostralis.

Figure 13-185. Photograph of the lateral aspect of the left half of the brain stem of 79KK2, showing the lateral lemniscus and caudal colliculus. BCdC - Brachium colliculi caudalis; CdC - Colliculus caudalis; LL - Lemniscus lateralis.





13-186

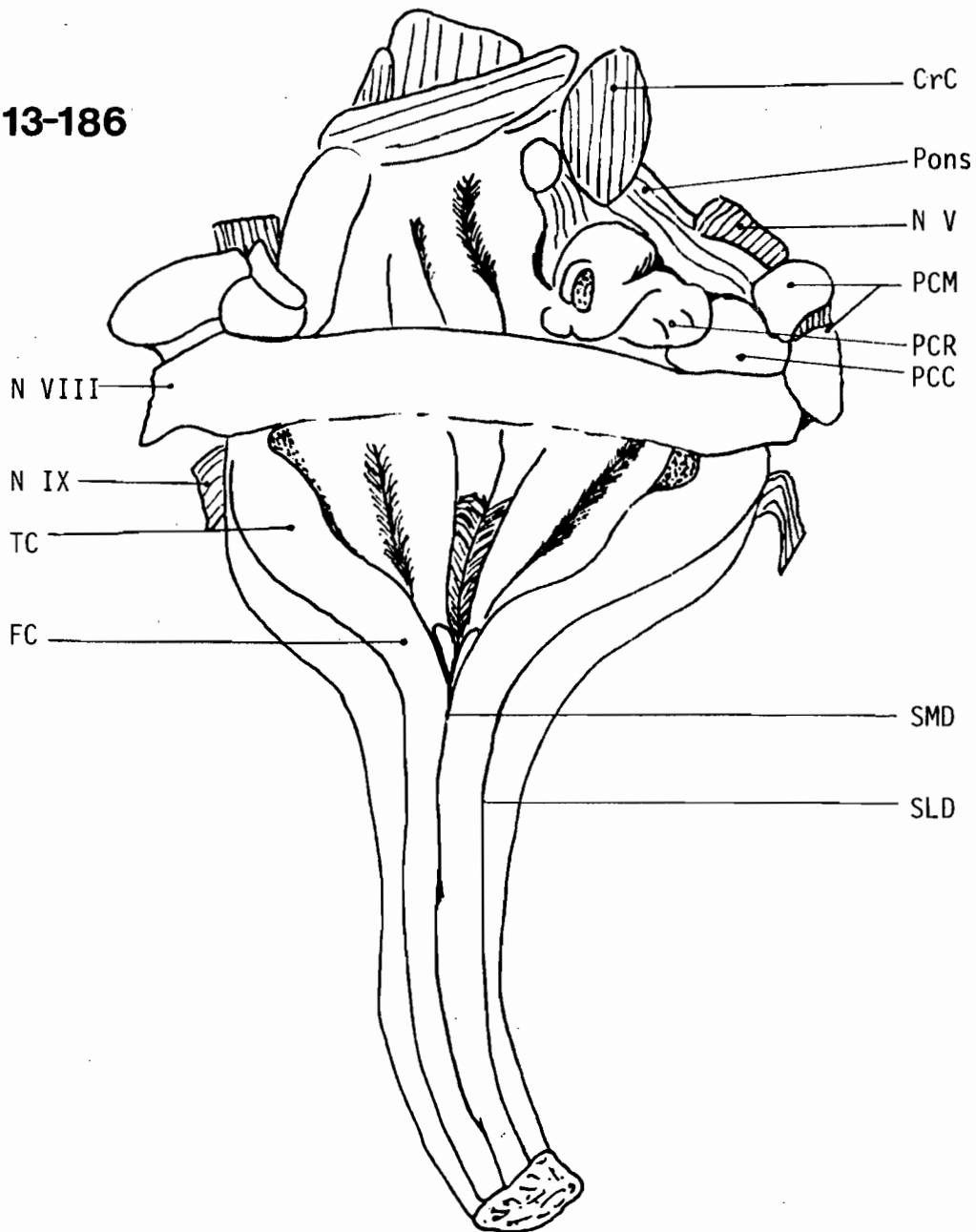


Figure 13-186. Sketch of the dorsal aspect of the brain stem of 80B1. CrC - Crus cerebri; FC - Fasciculus cuneatus; N V - Nervus trigeminus; N VIII - Nervus vestibulocochlearis; N IX - Nervus glossopharyngeus; PCC - Pedunculus cerebellaris caudalis; PCM - Pedunculus cerebellaris medius; PCR - Pedunculus cerebellaris rostralis; SLD - Sulcus lateralis dorsalis; SMD - Sulcus medianus dorsalis; TC - Tuberculum nuclei cuneati.

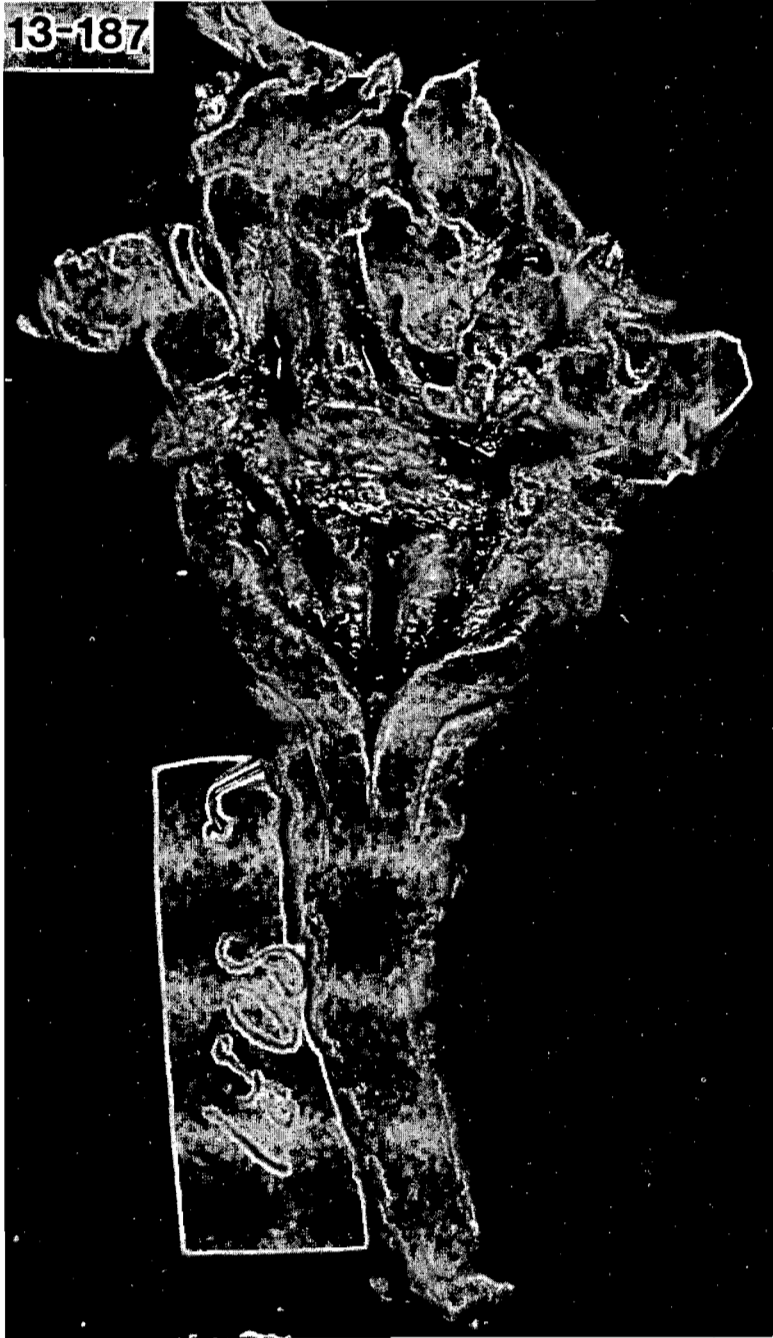


Figure 13-187. Photograph of the dorsal aspect of the brain stem of 80B1. Compare to Fig 13-186. X1.14

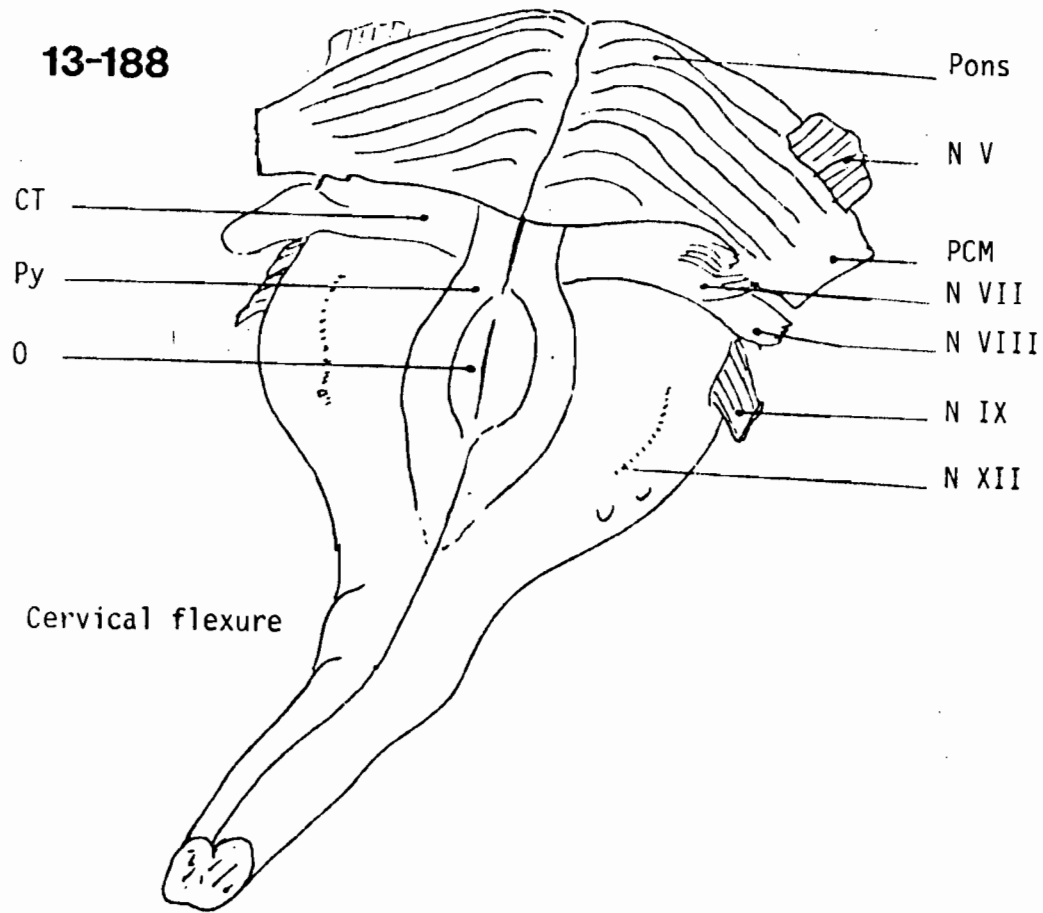


Figure 13-188. Sketch of the ventral aspect of the brain stem of 80B1. Note the trigeminal (V) and vestibulocochlear (VIII) nerves and the olive (O). CT - Corpus trapezoideum; N V - Nervus trigeminus; N VII - Nervus facialis; N VIII - Nervus vestibulocochlearis; N IX - Nervus glossopharyngeus; N XII - Nervus hypoglossus; O - Oliva; PCM - Pedunculus cerebellaris medius; Py - Pyramis (medullae oblongatae).

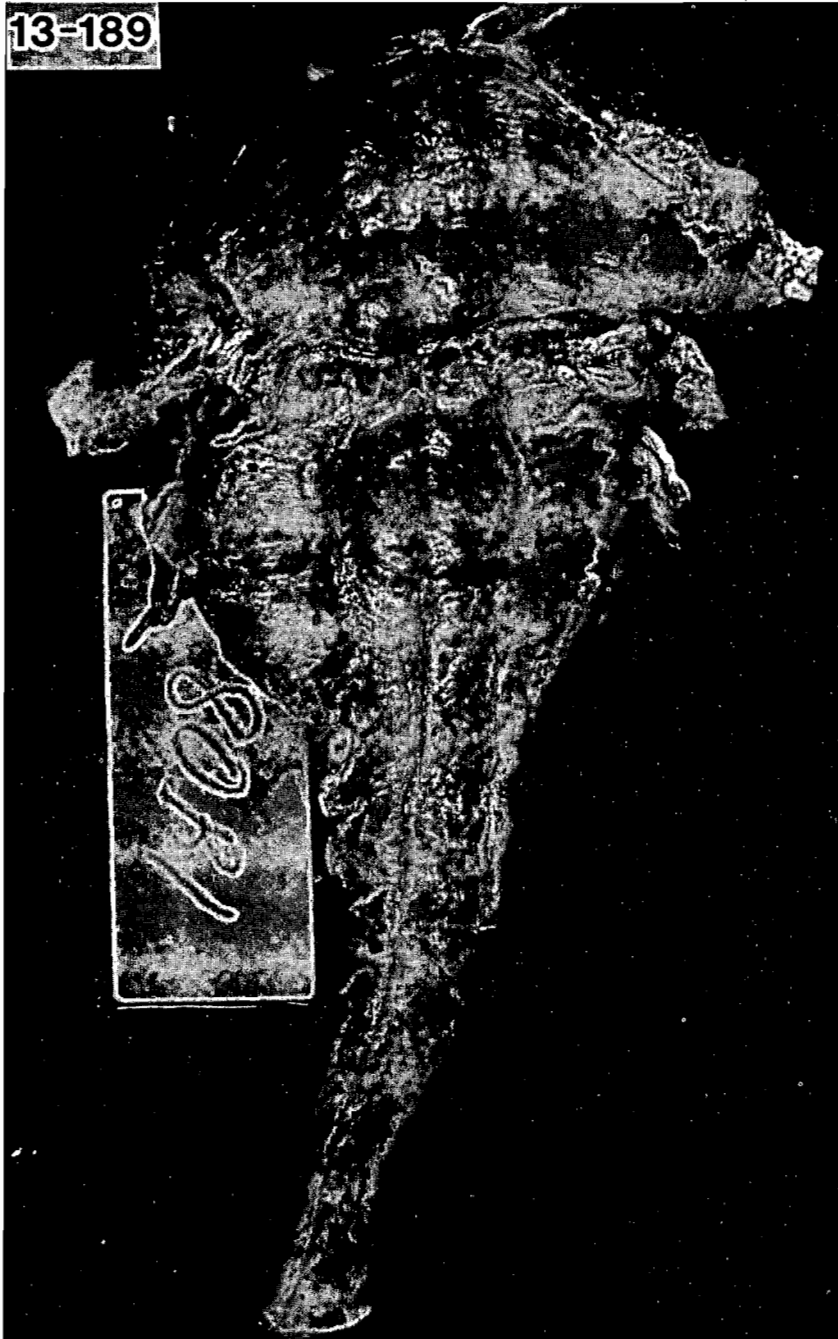


Figure 13-189. Photograph of the ventral aspect of the brain stem of 80B1. Compare to Fig 13-188. X1.14

#### IV. Skin

##### General Characteristics

The ordinary bowhead skin samples collected and supplied by RU 180 (79B3, 80B1, 80B2, 80B7) represented most of the various body regions (Fig 13-190). Samples obtained from Ingutuk variants (79B1, 79B2, 80B8) were also from most body regions (Fig 13-191), but more limited in quantity. The areas sampled included: the lower jaw; lower lip (inner and outer surfaces); upper lip (inner and outer surfaces); upper and lower eyelids; flipper (dorsal and ventral surfaces); fluke (dorsal and ventral surfaces); and dorsal, lateral, and ventral body wall regions. Most samples of the hard palate included parts of the gums (gingivae) containing many rows of baleen hairs and a very few small baleen plates. The surface area of the samples ranged between 1-7 cm by up to 15 cm. The dermis and some blubber of variable thicknesses were also present.

The formalin fixed skin of the bowhead whale was shiny and black over the dorsal surface and gradually changed to dark gray ventrally (Fig 13-192). Cream colored skin was present around the chin and to a variable extent on the ventral surface of the body (Fig 13-193) extending to near the urogenital orifice in some individuals. The preserved epidermis was thick with a rubbery consistency and ranged from 1 mm thick at the eyelid to 24 mm thick on the dorsal midline (Figs 13-190, 13-191). A yellowish coating of diatoms was present on most samples.

The skin samples obtained from the lower jaw showed rounded epidermal depressions between 1-3 mm in diameter at the surface (Fig 13-194) which extended inward about 4-8 mm. The apex of each funnel-shaped depression was directed toward the dermis (Fig 13-195) with a simple tactile hair emerging from the center. The tactile hairs were few in number with distances of 3-20 mm between them. Tactile hairs were present only on the margins of the upper and lower jaws, the chin, and in a V-shaped arrangement just caudal to the blowhole. They always emerged from black epidermis areas even in generally cream colored regions (Fig 13-196).

The epidermis of the bowhead was covered by a macroscopic, thin superficial layer of cells between 0.25 and 1 mm thick (the parakeratotic stratum corneum). This layer was present on both creamy and black skin and also on the mucosa of the hard palate and inner lips although thinner.

The epidermis of the flippers and the flukes varied in thickness in the various regions of their dorsal and of their ventral surface (Figs 13-

197, 13-198; Table 13-4). Deep macroscopic dermal papillae were visible on cut surfaces.

The epidermis of bowheads varied slightly in thickness (Table 13-5) and color in different regions. In general the trunk had the thickest epidermis. The epidermis of the head region was mostly a black to dark gray color with a variably sized area of cream colored skin on the chin (Figs 13-193, 13-194) caudally. Epidermal thickness also varied in different regions of the head (Table 13-6).

Variable numbers and sizes of epidermal lesions occurred in the skin of the various body regions. At least six morphological types were present on the samples received: (1) elevated smooth areas (79B2 chin), (2) even granular areas (80B8, Tag 96 dorsal midline), (3) elevated granular areas (80B2 lower eyelid), (4) shallow depressions (80B7, Tag 12A, chin ventral midline), (5) granular deep depressions (80B8, Tag 84 ventral midline), (6) smooth deep depressions (80B8, Tag 3A outer upper lip). Table 13-7 lists the approximate sizes and morphological types. The data are biased by the large number of samples from one whale which was indicative only of the cooperation of one whaling captain and his crew in sampling. Data concerning the abundance of lesions on other whales was not available.

The gross appearance of the various lesions was distinct. Fig 13-200 shows both a depression lesion and a depression lesion with a granular raised central mass. Depression lesions also occurred in areas with even granular lesions (Fig 13-201). A granular depression lesion is shown in Fig 13-202 with an adjacent depression lesion with raised center. Shallow depression lesions are most noticeable in the cream colored areas (Fig 13-203) since they were frequently darker in color. The eyelids were also subject to lesions (Figs 13-204, 13-205). Scanning electron microscopy showed that the simple depression lesions actually had a slightly elevated rim with a rather smooth interior (Figs 13-206, 13-207) which was occupied by an extensive and varied microflora of bacteria and diatoms (Cocconeis and Navicula). Depression lesions with raised centers (Fig 13-208) had a totally different group of microorganisms (bacteria, Stauroneis and Navicula diatoms) present (Fig 13-209). Some lesions were fuzzy or filamentous in appearance (Fig 13-210). Increased magnification showed that the filaments were primarily chains of diatoms and bacteria (Fig 13-211). The smooth areas in the floor of some depression lesions (Fig 13-212) proved to be primarily chains of large bacilli with a few filamentous diatoms (Fig 13-213). Finally, the granular depression

TABLE 13-4 AVERAGE PRESERVED EPIDERMAL THICKNESS OF THE SKIN OF THE FLIPPERS AND FLUKES OF BOWHEADS

Region	Sample Numbers	Average Preserved Epidermal Thickness (mm)
Dorsal Flipper	80B1: Tag 57, Tag 60, Tag 64, Tag 68, Tag 70, Tag 71, Tag 73	12.57
	80B7: Tag 1A, Tag RF3, Tag 5A, Tag 7A Tag 10A, Tag TRF, Tag RF1	12.14
Ventral Flipper	80B1: Tag 57, Tag 64, Tag 68. Tag 70, Tag 71, Tag 73	11.16
Dorsal Fluke	79B3; 80B2: Tag 11, Tag 30, Tag 32, Tag 34, Tag 35, Tag 38, Tag 40	11.86
	80B7: Tag 2A, Tag 4A, Tag 3A	
Ventral Fluke	80B2: Tag 35, Tag 40	9.66
	80B7: Tag 4A	



TABLE 13-5 AVERAGE PRESERVED EPIDERMAL THICKNESS OF THE BODY SKIN OF BOWHEADS

Region	Sample Numbers	Average Preserved Epidermal Thickness (mm)
Dorsal 1/3 *	80B7 Tag 1/3 D 80B8 Tag 87	20
Dorsal 2/3	80B7 Tag 2/3 D 80B8 Tag 85	18
Lateral 1/3	80B6 Tag 1/3 L 80B8 Tag 86	20.5
Lateral 2/3	80B7 Tag 2/3 L 80B8 Tag 93	20.5
Ventral 1/3	80B7 Tag 1/3 V 80B8 Tag 98	20.75
Ventral 2/3	80B7 Tag 2/3 V 80B8 Tag 84	18
Ventral 1/2	80B8 Tag 27, Tag 98	21.25
Lower Jaw	80B8 Tag 25, Tag 26	20.5

\* 1/3 = 1/3 the distance from flipper to fluke.

1/2 = 1/2 the total body length.

2/3 = 2/3 the distance from flipper to fluke.

TABLE 13-6 AVERAGE PRESERVED EPIDERMAL THICKNESS OF THE SKIN OF HEADS  
OF BOWHEADS

Region	Sample Numbers	Average Preserved Epidermal Thickness(mm)
Blowhole	79KK1 80B8 Tag 96	20
Outer Upper Lip	79B3 80B7 Tag 1 80B8 Tag 3A, Tag 9	15.5
Outer Lower Lip	80B1 Tag 42, Tag 43, Tag 44, Tag 53, Tag 66 80B7 Tag 5, Tag 38 80B8 Tag 20, Tag 35, Tag 37, Tag 42	12.77
Eyelids	80B2 80B7 Tag LLEL, Tag LUEL 80B8-Tag 8	11.75
Lower Jaw	79B1 79B2 80B1 Tag 45, Tag 54 80B7 Tag 8A, Tag 12A, Tag 13A 80B8 Tag 22, Tag 28, Tag 30	17.55

TABLE 13-7 RELATIVE SIZES AND TYPES OF EPIDERMAL LESIONS ON BOWHEAD SKIN SAMPLES

Region	Sample Number	Lesion	
		Size*	Type
Lower Lip	80B1 Tag 53	Medium	Depression
Chin	80B7 Tag 11A	Small	Depression
Chin	80B7 Tag 12A	Small	Depression
Chin	79B1 Tag 1	Large	Elev Smooth
Chin	79B1 Tag 2	Large	Elev Smooth
Chin	79B1 Tag 2	Small	Elev Smooth
Lower Jaw 1' Caudally	80B8 Tag 22	Very Small	Depression
Lower Jaw 6' Caudally	80B8 Tag 28	Medium	Depression
Lower Jaw 6' Caudally	80B8 Tag 28	Large	Depression
Lower Jaw 4' Caudally	80B8 Tag 30	Very Large	Depression
Outer Lower Lip	80B8 Tag 37	Large	Deep Depression
Outer Upper Lip	80B8 Tag 3A	Large	Depression
Blowhole	79KK1	Large	Irregular Depression
Blowhole	79KK1	Large	Raised Granular
Blowhole	79KK1	Very Large	Raised Granular
Blowhole	79KK1	Very Large	Raised Granular
Blowhole	79KK1	Very Large	Raised Granular
Blowhole	79KK1	Very Large	Raised Granular
Blowhole	79KK1	Very Large	Raised Granular
(continued)			

TABLE 13-7 RELATIVE SIZES AND TYPES OF EPIDERMAL LESIONS ON BOWHEAD SKIN SAMPLE (continued)

Region	Sample Number	Lesion	
		Size*	Type
Lower Eyelid	80B2	Small	
Dorsal Eyelid	80B8 Tag 11	Very Large	Depress w/ Raised Center
1/2 <sup>a</sup> Ventral Body Wall	80B8 Tag 27	Medium	Even
1/2 <sup>a</sup> Ventral Body Wall	80B8 Tag 27	Small	Even
1/2 <sup>a</sup> Ventral Body Wall	80B8 Tag 27	Medium	Depression
2/3 Dorsal Body Wall	80B8 Tag 85	Large	Depress w/ Raised
2/3 Dorsal Body Wall	80B8 Tag 85	Medium	Depress w/ Raised
2/3 Dorsal body Wall	80B8 Tag 85	Small	Depression
1/3 Dorsal Body Wall	80B8 Tag 87	Large	Depression Gran
1/3 Dorsal Body Wall	80B8 Tag 87	Medium	Depression
Dorsal Midline 1 m Caudal of Blowhole	80B8 Tag 96	Very Large	Even Granular
Dorsal Midline 1 m Caudal of Blowhole	80B8 Tag 96	Large	Even Granular
Dorsal Midline 1 m Caudal of Blowhole	80B8 Tag 96	Large	Even Granular
Dorsal Midline 1 m Caudal of Blowhole	80B8 Tag 96	Medium	Even Granular
1/3 Dorsal Body Wall	80B8 Tag 87	Large	Granular Depression
2/3 Dorsal Body Wall	80B8 Tag 85	Small	Depress w/ Raised Center

(continued)

TABLE 13-7 RELATIVE SIZES AND TYPES OF EPIDERMAL LESIONS ON BOWHEAD SKIN SAMPLES (continued)

Region	Sample		Lesion	
	Number	Type	Size*	Type
2/3 Lateral Body Wall	80B8 Tag 93		Large	Depression
2/3 Lateral Body Wall	80B8 Tag 93		Small	Granular Depression
2/3 Lateral Body Wall	80B8 Tag 84		Large	Granular Depression
2/3 Ventral Body Wall	80B8 Tag 84		Small	Granular Depression
2/3 Ventral Body Wall	80B8 Tag 84		Large	Granular Depression
2/3 Ventral Body Wall	80B8 Tag 84		Small	Granular Depression
2/3 Ventral Body Wall	80B9 Tag 84		Medium	Granular Depression
1/3 Ventral Body Wall	80B9 Tag 88		Very Small	Depression
Dorsal Fluke	80B2 Tag 32		Very Large	Irregular Depression

\* Very Small - about 1 mm; Small - 2-4 mm; Medium = 5-8 mm; Large = 10-15 mm; Very Large = 20 mm or more.

a 1/3 = 1/3 the distance from flipper to fluke.

1/2 = 1/2 the total body length

2/3 = 2/3 the distance from flipper to fluke.

TABLE 13-8 QUALITATIVE ESTIMATES AND TYPES OF MICROORGANISMS OCCURRING ON AND IN BOWHEAD UNBLEMISHED SKIN

Region	Sample Number	Organisms*	Abundance
Inner Upper Lip	80B8 Tag 9	None	-
Inner Upper Lip	80B8 Tag 37	None	-
Inner Upper Lip	80B8 Tag 34	None	-
Outer Upper Lip	80B8 Tag 9	Gom or Staur	few
Outer Upper Lip	80B8 Tag 37	Bac, Coc and Gom or Staur	many, few, several
Inner Lower Lip	80B8 Tag 42	None	-
Outer Lower Lip	80B8 Tag 42	Coc and Gom or Staur	few, several
Outer Lower Lip	80B1 Tag 53	Gom or Staur	few
Outer Lower Lip	80B1 Tag 66	None	-
Lower Jaw	80B1 Tag 43	Bac and Pro	many, few
Upper Eyelid	80B9 Tag 11	None	-
Lower Eyelid	80B8 Tag 11	None	-

(continued)

TABLE 13-8 QUALITATIVE ESTIMATES AND TYPES OF MICROORGANISMS OCCURRING ON AND IN BOWHEAD UNBLEMISHED SKIN  
(continued)

Region	Sample Number	Organisms*	Abundance
1/3 Dorsal Body Wall	80B8 Tag 87	Coc and Gom or Staur	few, many
1/3 Dorsal Body Wall	80B8 Tag 1/3D	None	-
1/3 Lateral Body Wall	80B7 Tag 1/3L	Coc and Gom or Staur	few, several
1/3 Ventral Body Wall	80B7 Tag 1/3V	Gom or Staur	several
2/3 Dorsal Body Wall	80B7 Tag 2/3D	Gom or Staur	few
2/3 Dorsal Body Wall	80B7 Tag 85	Coc and Gom or Staur	few, several
2/3 Lateral Body Wall	80B7 Tag 2/3L	None	-
2/3 Lateral Body Wall	80B8 Tag 93	None	-
Cranial Dorsal Fluke	80B2 Tag 17	Coc and Nav	
Caudal Dorsal Fluke	80B2 Tag 35	Coc and Nav	

\* Bac = Bacteria - unknown; Coc = Cocconeis sp.; Gom = Gomphonema sp.; Nav = Navicula sp.;

Pro = Protozoan - possible; Staur = Stauroneis sp.

TABLE 13-9 QUALITATIVE ESTIMATES AND TYPES OF MICROORGANISMS OCCURRING ON AND IN BOWHEAD SKIN EPIDERMAL LESIONS

Lesion Type	Sample Number	Organisms*	Abundance
Depression with Raised Center	80B8 Tag 85	Bac and Poss Pro	many, few
Depression with Raised Center	80B8 Tag 84	Bac and Gom or Staur	many, several
Shallow Depression	80B8 Tag 84	Bac	many
Granular Depression	80B8 Tag 87	Nav and Bac	many, many

\* Bac = Bacteria - unknown; Coc = Cocconeis sp.; Gom = Gomphonema sp.; Nav = Navicula sp.;  
 Pro = Protozoan - possible; Staur = Stauroneis sp.



TABLE 13-10 NUMBER OF DERMAL PAPILLAE PER mm<sup>2</sup> IN DIFFERENT REGIONS OF BOWHEAD WHALE SKIN

Regional	Sample Number	Ordinary Bowheads		Ingutuk Variant		Sample Number
		Dermal	Sensory	Dermal	Sensory	
Inner Upper Lip	80B1 Tag 100	8	4	4	1	80B8 Tag 9
Outer Upper Lip				5		80B8 Tag 9
Inner Lower Lip	80B1 Tag 43	5	1	22	3	80B8 Tag 34
Inner Lower Lip	80B1 Tag 53	11	1	4	1	80B8 Tag 37
Inner Lower Lip	80B1 Tag 66	5		16		80B8 Tag 42
Outer Lower Lip	80B1 Tag 43	7		9		80B8 Tag 20
Outer Lower Lip	80B1 Tag 53	6		7		80B8 Tag 37
Outer Lower Lip	80B1 Tag 66	8		9		80B8 Tag 42
Caudal Dorsal Flipper	80B1 Tag 57	5				
Caudal Ventral Flipper	80B1 Tag 57	9				
1/3a Dorsal Body Wall	80B7 Tag 1/3D	6		10		80B8 Tag 87
1/3 Lateral Body Wall	80B7 Tag 1/3L	7		5		80B8 Tag 86
1/3 Ventral Body Wall	80B7 Tag 1/3V	5		6		80B8 Tag 88
2/3b Dorsal Body Wall	80B7 Tag 2/3D	5		5		80B8 Tag 85
2/3 Lateral Body Wall	80B7 Tag 2/3L	6		7		80B8 Tag 93
2/3 Ventral Body Wall	80B7 Tag 2/3V	5		5		80B8 Tag 84
Cranial Ventral Fluke	80B2 Tag 17	7				
Upper Eyelid					10	80B8 Tag 11
Lower Eyelid					6	80B8 Tag 11

a 1/3 the distance from flipper to fluke.

b 2/3 the distance from flipper to fluke.

TABLE 13-11 REGIONAL VARIATION OF DISTANCE OF DERMAL PAPILLAE TIPS FROM THE BOWHEAD EPIDERMAL SURFACE

Region	Sample Number	Papilla Type	Distance (mm)
Lower Eyelid Skin	80B8 Tag 11LL	Sensory	0.070
Lower Eyelid Conjunctiva	80B8 Tag 11LL	Dermal	0.005
Upper Eyelid Skin	80B8 Tag 11LU	Sensory	0.090
Upper Eyelid Conjunctiva	80B8 Tag 11LU	Dermal	0.010
Inside Upper Lip	80B7 Tag 12	Sensory	0.100
Outside Upper Lip	80B7 Tag 12	Sensory	0.170
Chin	80B7 Tag 1L	Dermal	7.5
Caudal Dorsal Flipper	80B1 Tag 57	Dermal	5.0
Caudal Ventral Flipper	80B1 Tag 57	Dermal	4.375
Cranial Dorsal Fluke	80B2 Tag 17	Dermal	4.750
Cranial Ventral Fluke	80B2 Tag 17	Dermal	3.750
1/3 Dorsal Body Wall <sup>a</sup>	80B8 Tag 87	Dermal	10.250
2/3 Dorsal Body Wall	80B8 Tag 85	Dermal	9.0
2/3 Ventral Body Wall	80B8 Tag 84	Dermal	15.625*
2/3 Ventral Body Wall	80B8 Tag 84	Dermal	13.5**

\* Adjacent to shallow depression lesion.

\*\* Adjacent to depression lesion with raised center.

<sup>a</sup> 1/3 or 2/3 the distance from flipper to fluke.

lesions also had a rim, but the interior was rough (Fig 13-214). High magnification revealed a still different floral composition of Cocconeis only (Fig 13-215). Based on the limited sampling that was possible from most of the bowheads of this study, it appeared that epidermal lesions occurred on all regions of the body with higher concentrations located on the lower lips, chin, and jaw caudally onto the ventral body wall (Fig 13-216). See RU 780 for description of the general pathology of lesions of the head.

The epithelium of the hard palate was about 1 mm thick, black to gray in color and appeared granular with very small rounded elevations. The baleen hairs and plates extended from the right and left sides of the upper jaws (Fig 13-217) lateral to the narrow hard palate. The baleen emerged from smooth gray tissue which represented the gums (gingivae) of the whale. The epithelium which bore the baleen was much thicker than the epithelium of the hard palate. The baleen at the medial epithelial elevation of the gingiva consisted of many rows of fine white baleen hairs which ranged from 6-30 mm in length. This type of baleen resembled the coarse hair of some mammals in being simple with one small baleen hair emerging from each orifice in the gingiva. Toward the upper lip (laterad), the baleen became denser, coarser and darker in color (Fig 13-217). This second type of baleen was both longer and compound, i.e., several simple baleen hairs fused into one large hair emerged from each orifice in the gingiva. Such compound baleen hairs were 0.5-1 mm in diameter at the gum line. Further laterad the fusion of the compound hairs produced baleen plates (Fig 13-217).

In front of the baleen, the upper lips and snout had a restricted area of well defined, elevated, light colored, papillae about 1 mm in diameter and about 0.5 mm tall (Fig 13-218). The epidermis thickened rostrad and laterad to the papillary area becoming similar to the skin of other body regions.

Dermal papillae were abundant throughout the integument and interdigitated with the epidermis (Figs 13-193, 13-219). The superficial (reticular) dermis was dense irregular white fibrous connective tissue which varied from 2-4 mm in thickness. The underlying hypodermis or blubber was largely adipose connective tissue laced with distinct strands of more regularly arranged dense white fibrous connective tissue and blood vessels (see RU 480). The blubber between the dorsal and ventral epidermises of the flippers and flukes possessed more abundant coarse white fibers than other regions (Fig 13-

220) with the flukes having more than the flippers (Figs 13-196, 13-220, 13-221).

#### Microscopic Characteristics

The epidermis of bowhead skin was covered by a continuous layer of stratified squamous epithelial cells, the stratum corneum, consisting of between 12-60 rows of flattened to oval cells (Fig 13- 222). Their long axes were parallel to the skin surface. For the most part, they retained their nuclei and their cytoplasm contained abundant keratin. Their nuclei were varied in shape, but were generally flattened and oval with the cytoplasm containing small amounts of fibrillar material. The stratum corneum showed keratinization, but was parakeratotic. The parakeratotic stratum corneum was thinnest on the inner surface of the lips and outer eyelids and was thickest on the epidermis of the chin. The stratum corneum which extended into the funnel-shaped depressions around the tactile hairs showed several rows of cells with few nuclei (Fig 13-223) and was more typically keratinized. Most regions of the parakeratotic stratum corneum showed concentrations of epidermal rods arising from the stratum basale cells around the tips of the dermal papillae. Most of the cells of the parakeratotic stratum corneum also exhibited variable numbers of melanin granules within the pigmented epidermis.

Although the gross appearance of bowhead skin was smooth and shiny, scanning electron microscopy clearly showed flaking of the surface squamous cells. One of the most highly keratinized regions was the inner lip epithelium (Figs 13-224, 13-225). The surface cells apparently were desquamating individually with the cells showing close apposition to each other and surface ridges similar to those seen in terrestrial mammals. The epidermal surface of the outer lip (Fig 13-226) showed more flaking with aggregates of desquamating cells. Fig 13-227 illustrates some of the normal inhabitants of the minute cracks and crevices that occur in normal whale skin exposed to the marine environment. The epidermis on the dorsal, lateral and ventral aspects of the body trunk (Figs 13-228 through 13-233) had a somewhat rougher texture with a more varied population of microorganisms (see Table 13-8). See RU 1280 also for diatom analysis. The epidermal rods that arose from the stratum basale cells covering the ends of the dermal papillae maintained their rodlike configuration through the stratum corneum and showed on the surface as rosettes of squamous cells.

The epidermal cells deep to the parakeratotic stratum corneum comprised a typical stratum spinosum. The cells were rounded, oval, or poly-

hedral with oval to round nuclei (Fig 13-234). The nuclei showed scanty, marginally placed, clumped chromatin. Many of the cells had melanin granules in their cytoplasm (Fig 13-234). All cells of this region had a distinct fibrous texture with cell boundaries appearing thick under the light microscope. This "thickness" was the result of highly folded cell membranes and desmosomes, clearly demonstrated by transmission electron microscopy (Fig 13-235). All cells in the stratum spinosum contained tonofilaments arranged in parallel bundles as well as large numbers of ribosomes and polyribosomes (Fig 13-235). Keratohyalin granules of variable diameter were scattered throughout the cytoplasm (Figs 13-236, 13-237). At the ultrastructural level, the nuclei of the spinosal cells were large and irregular (Fig 13-237) with eccentric to centrally located nucleoli and marginal heterochromatin. Some cells contained melanin granules near the nucleus (Figs 13-237, 13-238). The deeper cells of the stratum spinosum were rounder and smaller than the more superficial cells. More cellular fibrous elements were seen in the cells of the stratum spinosum of flukes and flippers than elsewhere.

The number of keratohyalin granules in the epidermis decreased in the spinosal cells as they were pushed toward the stratum corneum. The number of keratohyalin granules varied in different body regions, being most abundant in the stratum spinosum of the chin and outer lip. The cytoplasm of most spinosal cells contained a considerable number of melanin granules (Fig 13-239). Melanin granules were most abundant in the stratum basale, but were also present in cells of the parakeratotic stratum corneum (Fig 13-222).

The stratum basale consisted of a single layer of columnar cells with basally located oval nuclei. The PAS reaction showed a basement membrane between the dermis and the epidermis. Melanocytes were present between the basal cells and occasionally in the first layers of the stratum spinosum. They were very well developed, large and possessed dendritic processes (Figs 13-239, 13-240). Numerous cytoplasmic undulations of the basal cells interdigitated with the superficial layer of the dermis (Fig 13-241) and maintained contact with the basal lamina that separated epidermis from dermis (Fig 13-242). The basal cells also had lateral interdigitations with adjacent cells which produced wide areas of apparent intercellular space. These wide areas were merely the interfolding of the undulating adjacent cell membranes with more desmosomes than occurred in the other two strata (Fig 13-243).

Histologic examination of a shallow depression lesion 13 mm diameter X 1.875 mm deep showed that the parakeratotic stratum corneum was intact

and 375  $\mu\text{m}$  thick. The parakeratotic layer had small Gram positive bacilli between cells and on the surface. Occasional bacteria and diatoms (Stauroneis and/or Gomphonema) were present in the parakeratotic stratum corneum around the lesion (Fig 13-244). A granular depression lesion 6 mm in diameter X 2.75 mm deep showed the parakeratotic layer missing and a V-shaped area of the stratum spinosum also gone (Fig 13-245). The outer 875  $\mu\text{m}$  of spinosal cells on the depression surface were different in appearance than those located deeper below the depression. The modified layer was penetrated to its full depth in several loci by chains of large Gram positive bacilli. The surface of the depression was also coated with bacilli, some Stauroneis and/or Gomphonema, and many spherical cells about 3.74-7.5  $\mu\text{m}$  in diameter. Some of the spherical cells were in between the cell layers with the bacilli. Flaking of the modified spinosal layer in the depression resulted in exposure of the tips of the epidermal rods. A depression lesion of 11 mm diameter X 3.6 mm deep with a raised center 3.2 mm high X 2.5 mm in diameter undercut all around except at the attached basal area, is shown in Fig 13-246. The central mass sat upon a small pedestal-like, 0.5 mm diameter portion of the spinosum which maintained contact with the underlying spinosal layers. No exposed epithelial rods were present within the lesion. The depression surface and, particularly, the raised mass had several foci of Stauroneis and/or Gomphonema and small Gram positive bacilli which extended inward penetrating most of the raised mass. Occasional 21 x 55  $\mu\text{m}$  nucleated protozoan-like cells were also on the central mass surface with concentrations of these cells in the clefts of the parakeratotic mass as well. A 6 mm diameter X 2 mm deep lesion with raised center had the central mass permeated with chains of large Gram positive bacilli and Stauroneis and/or Gomphonema between the cells with some bacteria inside the cells. No exposure of epithelial rods was visible. The central mass was also undercut almost completely around except at the small pedestal-like basal attachment to the underlying spinosal layers (Fig 13-247). Cocconeis and Navicula (diatoms) also occurred in some of the other types of lesions, either separately or in conjunction with other diatoms or bacteria (Table 13-9).

Long dermal papillae (Fig 13-239, 13-240) interdigitated with the epidermis exhibiting definite regional variations in number of papillae per square millimeter (Table 13-10). The regions with the greatest numbers were the upper lip where the majority were large and sensory and the lower lip where fewer sensory papillae were mixed with ordinary papillae. The eyelids

possessed an intermediate number of both types of papillae. The general body wall had the lowest number, all of which were of the non-sensory type. The ordinary dermal papillae varied in basal diameter and tended to be oval in cross section. Secondary papillae arose from the basal portions of large dermal papillae. Above the origin of the secondary papillae, the main dermal papilla became smaller and smoother resembling the secondary papillae. All papillae within a given area ended at about the same level, but the level of papillary termination varied in distance from the epidermal surface according to epidermal thickness (Table 13-11).

Blood vessels occurred in all dermal papillae, but consisted of only arterioles, capillaries, and venules at the most distal levels. Even the smallest secondary papillae contained capillaries. Nerve fibers also occurred in the basal portions of the dermal papillae with the papillae of the inner lips and eyelids possessing numerous nerve fibers (Fig 13-248) and Herbst-like encapsulated sensory nerve endings.

The reticular dermis consisted of dense irregular connective tissue with collagen fibers continuing into the loose connective tissue of the dermal papillae (Figs 13-222, 13-239). Elastic fibers were present throughout this tissue which also contained many arteries, veins, large venous sinuses and nerve fiber bundles (Fig 13-240).

#### Tactile hair structure

Tactile hairs were present in specimens from 79KK1 (blowhole); 79B1, 79B2, 80B1, and 80B7 (chin); and 80B7 (upper lip). The tactile hairs extended above the surrounding epidermal surface 1-1.5 cm after exiting the epidermis in the center of a funnel-shaped depression which was 4 mm in depth. Some hairs among our specimens appeared to be broken off which may have introduced errors into our measurements. The dermal sheath surrounding the tactile hair follicle continued into the hypodermis for 20-30 mm (Figs 13-194, 13-196). The hairs emerged singularly, but occasionally split above the epidermal surface into two or three small units.

Longitudinal and frontal serial sections through tactile hairs and follicles from 80B1 and 80B7 were examined. The hair follicle had the usual components: a central shaft (tactile hair) surrounded by an epidermal sheath which was enveloped in a dermal sheath (Fig 13-249). In longitudinal sections the hairs were seen exiting through the center of the funnel-shaped depression of the epidermis. Midway between the rim of the funnel and the base of the funnel (Fig 13-250), the typically mammalian stratum corneum thinned. Close

to the shaft the stratum corneum became thinner resembling stratum disjunctum and housed bacteria, diatoms and possibly protozoa (Fig 13-251). The free shaft extended through the epidermal layer and 3-3.2 cm below the superficial dermis level into the hypodermis (Fig 13-252). The epidermis surrounded the free shaft down through the superficial dermis and was in turn surrounded by a dense, vascular dermal sheath. The dense irregular connective tissue of the dermal sheath contained numerous nerve fibers and what appeared to be receptor organs. These structures were seen lying 2.8-4.1 mm below the general dermal-epidermal junction (Fig 13-253). A few nerve fiber bundles were seen surrounding the follicle as well as near the base of the follicle. The receptor organs appeared similar to the Herbsti-type. The majority of these structures lay 0.5 mm superficial to the sinus area. Arteries and nerves appeared to enter the follicle at its base in the hypodermis (Fig 13-254). The nerves coursed superficially and branched within the dermal sheath. The blood vessels entered sinuses which formed a complete sinusoidal network surrounding the epidermal portion of the tactile hair follicle (Fig 13-255). The sinuses extended only three-fifths of the way up the follicle toward the dermal-epidermal junction. The hair shaft originated at the bulb which surrounded the dermal papilla of the follicle (Fig 13-254). No glands were seen associated with the follicle.

Serial frontal sections near the dermal-epidermal junction of the surrounding skin showed the hair shaft with a thin cortex and solid medulla (Fig 13-249). The epidermal layer of the follicle had a heavily keratinized stratum corneum adjacent to the shaft. The epidermis of the funnel shaped depression extended below the surrounding dermal-epidermal junction forming an extension of the epidermis into the hypodermis (Fig 13-252). Frontal sections through this depressed area showed the same epidermal-hair shaft relationship (Fig 13-249).

### Baleen

Serial sections of the baleen hairs showed that individual hairs started as single tube-like structures arising from the epithelial cells in contact with the connective tissue papillae. Each single tubule consisted of a medulla of vascularized loose connective tissue surrounded by the stratum basale. Spinosal cells produced hard keratin peripherally around the tubule (Fig 13-256) forming several layers which increased in number as the tubules extended beyond the papillae to approach the surface of the gingiva (Fig-257). The medulla of a baleen hair consisted



of an outer cellular zone and an inner highly vascular zone (Fig 13-258) with little loose connective tissue. The medulla continued into the free shaft of the baleen hairs occupied with a reticulum of dead avascular connective tissue (Fig 13-258).

Further laterad in the gingiva, single baleen hairs arising in clusters joined each other with fusion of their cortices to form compound baleen hairs consisting of three to twelve tubules (Fig 13-259). As compound baleen hairs approached the gingival surface, their common, hard keratin, outer cortex became more circular forming a single layer of hard keratin around several originally single tubules (Fig 13-260) which emerged from the gingival surface as a large compound baleen hair with several medullary spaces (Fig 13-261).

#### Skin-oil Interactions

Prudhoe Bay crude oil was cohesive enough at room temperature that the oil formed a thick film on a nonagitated artificial sea water surface. This cohesiveness permitted only a portion of the aquarium surface to be coated. After slow cooling to 3°C, the oil slick was 4 mm thick and covered 3/4 of the water surface. When a piece of preserved whale skin cooled to 3°C at the clear end of the aquarium was lifted through the cold oil slick, the film of oil remained intact over the entire piece until the skin surface was lifted more than 10 mm above the water surface after which the oil film separated and drooped over the sides of the piece of skin. Submerging the oil coated skin back through the oil film left most of the oil film on the water surface or it floated free of the skin shortly after full submergence leaving small patches of oil on all preserved skin samples tested. This minor agitation of the oil slick broke up the film leaving oil patches on the water surface surrounded by the undisturbed film. Oil globules of varying sizes were carried beneath the surface with the skin samples, but did not remain suspended beneath the water surface of the undisturbed aquarium. They floated upward beneath the surface oil film and patches making them thicker (up to 10 mm) producing an undulating water-oil interface while the oil-air interface remained smooth. Alternatively they created additional oil patches on the water surface that was clear. No globs or globules remained suspended within the water column after a few minutes.

The number and size of the small patches of oil adhering to the various types of preserved skin samples after a simulated breathing cycle of 3 surfacings and submergences (breathing rolls) seemed to be in direct propor-

tion to (1) the number of cycles and (2) the roughness of the skin sample. Oil adhered to the vibrissae and their surrounding epidermal depressions (Figs 13-262, 13-263) and various other rough areas (Figs 13-264, 13-265). The epidermal lesions and abrasion (Figs 13-266, 13-267, 13-268) showed variable degrees of oil adhesion. Diatom covered regions around vibrissal depressions, and in some cases even the normal smooth appearing skin seemed to show oil adhesion. The least amount of oil adherence seemed to occur in the smoothest areas, i.e., those areas where the sea water film tended to be maintained with the least disruption as contact was made with the oil slick. These results are only valid for formalin fixed skin samples in an undisturbed cold artificial sea water situation in a laboratory.

13-190

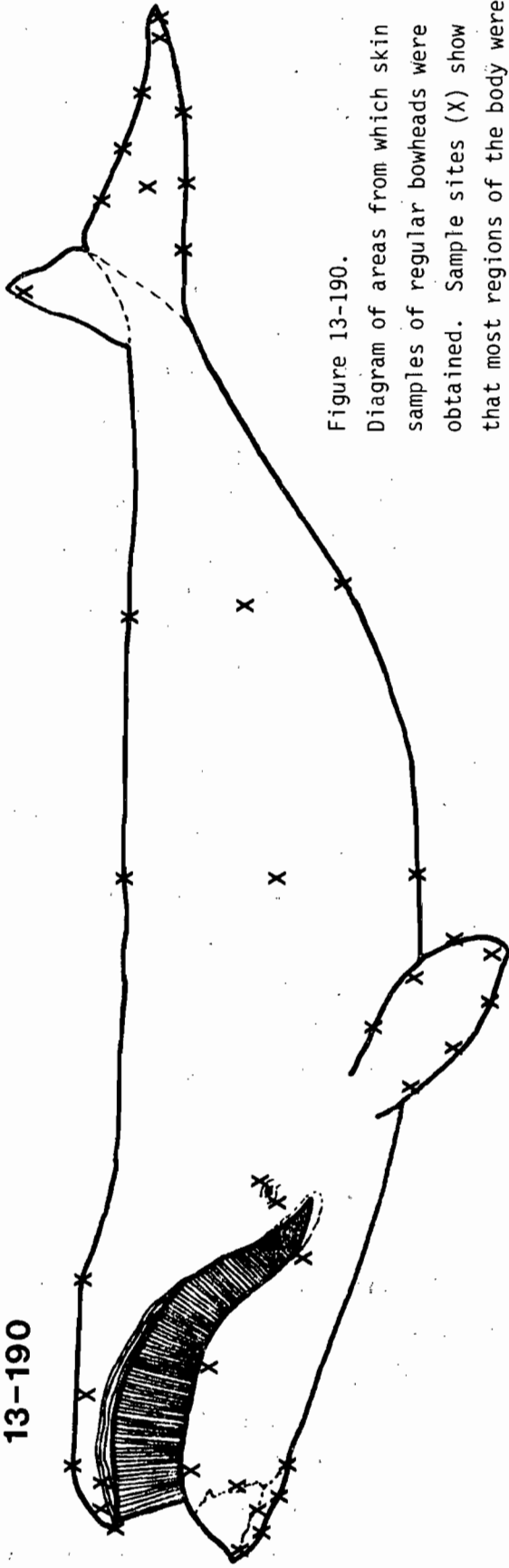


Figure 13-190.

Diagram of areas from which skin samples of regular bowheads were obtained. Sample sites (X) show that most regions of the body were sampled.

13-191

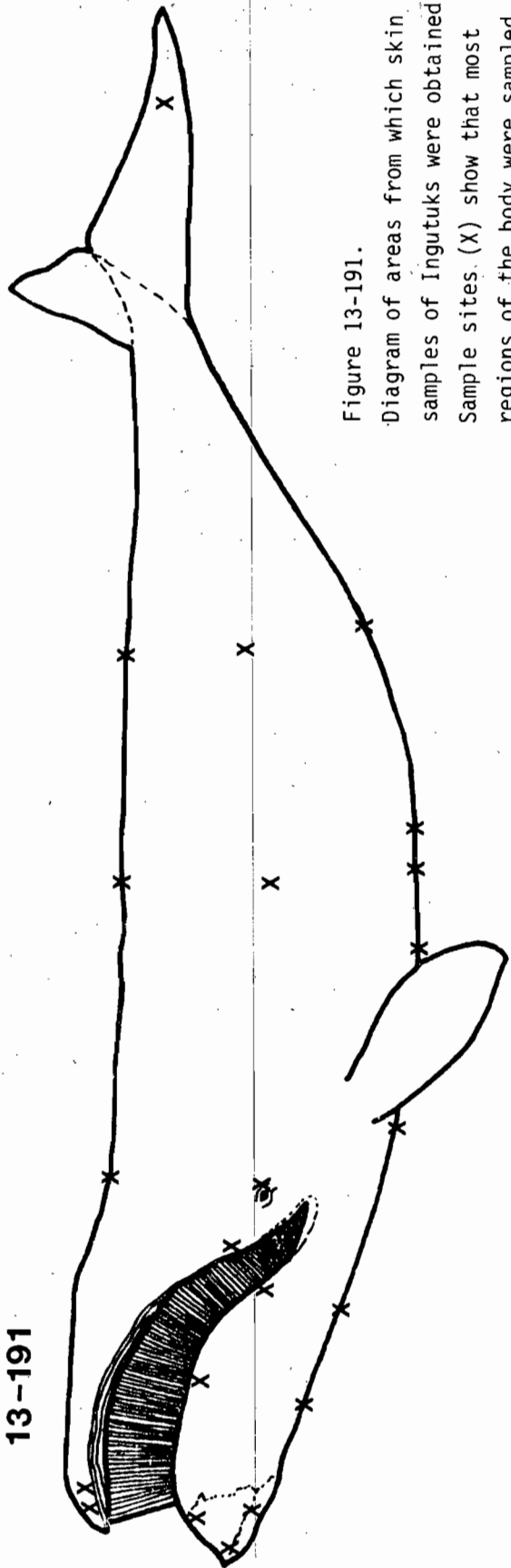


Figure 13-191.

Diagram of areas from which skin samples of Ingutuks were obtained. Sample sites (X) show that most regions of the body were sampled.

- Figure 13-192. Photograph of the upper lip, 79B3. The cut edge slightly visible toward the ruler shows the thin epithelium of the inner lip (left) with the gradual change to thicker epidermis of the outer surface (right).
- Figure 13-193. Photograph of the cut edge of chin skin, 80B1. The nonpigmented areas of the chin are creamy in color. Without pigment in the epidermis, the pigmentation in the vascular dermal papillae clearly shows the extent of the papillary interdigitation with the epidermis (arrows). Immediately beneath the epidermis is the dense irregular connective tissue of the dermis (D) and beneath this the hypodermis (H) or blubber. The surface of this sample is more desquamated (flaky) than usual.
- Figure 13-194. Photograph of a skin sample with vibrissa from the upper lip, 79B2. The outer upper lip, the outer lower lip, and the chin have distinct regions in which vibrissae are located. Each vibrissa emerges from a funnel shaped depression (arrowheads) which is surrounded by a slightly elevated portion of the epidermis. The elevations are not light colored as they appear here, but are as dark as the surrounding epidermis. The white area (Sc) is an apparent healed scar (See RU 780).
- Figure 13-195. Photograph of the cut surface of the same sample in Fig 13-194 showing extent of a tactile hair follicle. The funnel shaped depression from which the hair shaft emerges shows as a triangular black area at the epidermal surface. The epidermis dips below the normal dermal-epidermal junction (arrow) extending ultimately to the base of the hair follicle. The hair shaft and follicle were cut off with only the edge of the dermal sheath (DS) surrounding the follicle indicating the extent of the follicle penetration into the hypodermis (H).